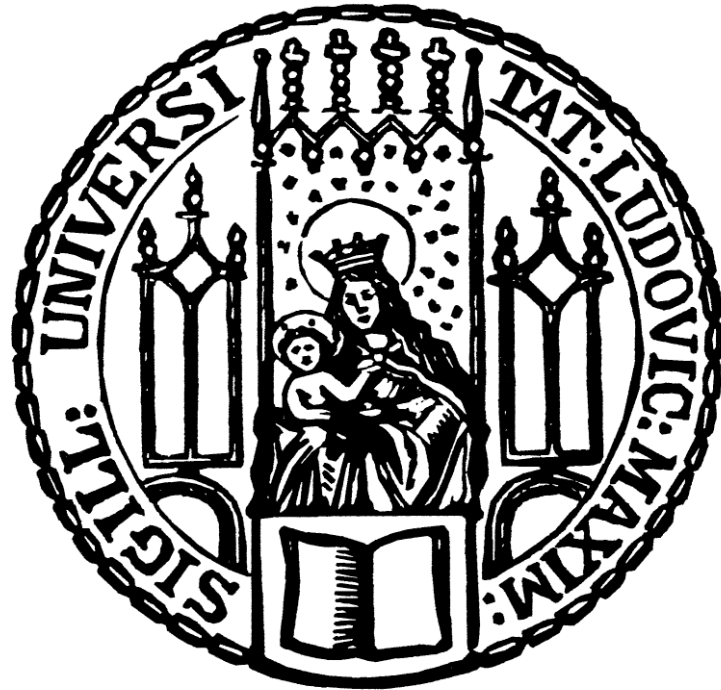**Dissertation zur Erlangung des Doktorgrades der Fakultät für Chemie und Pharmazie der Ludwig-Maximilians-Universität München**

Estradiol derivatives and analogs as blockers of TRPML1 cation channels

Philipp Rühl

aus

Eggenfelden

2024

Erklärung

Diese Dissertation wurde im Sinne von § 7 der Promotionsordnung vom 28. November 2011 von Herrn Prof. Dr. Franz Bracher betreut.

Eidesstattliche Versicherung

Diese Dissertation wurde eigenständig und ohne unerlaubte Hilfe erarbeitet.

München, den 07.06.2024

_____

Philipp Rühl

Dissertation eingereicht am 11.06.2024

1. Gutachter: Prof. Dr. Franz Bracher

2. Gutachter: Prof. Dr. Dr. Christian Grimm

Mündliche Prüfung am 14.08.2024

Publications

Rühl P., Scotto Rosato A., Urban N., Gerndt S., Tang R., Abrahamian C., Leser C., Sheng J., Jha A., Vollmer G., Schaefer M., Bracher F., Grimm C., Estradiol analogs attenuate autophagy, cell migration and invasion by direct and selective inhibition of TRPML1 *Scientific Reports* **2021**, 11 (1) 8313

Rühl P., Bracher F., Aza analogs of the TRPML1 inhibitor estradiol methyl ether (EDME) *Molecules* **2023**, 28 (21) 7428

Poster

Rühl P., Bracher F., Estradiol derivatives and analogs as blockers of TRPML1 cation channels, Frontiers in Medicinal Chemistry 2024 (GDCH), 17.03.2024 - 20.03.2024, Munich

Table of contents

1. Introduction

1.1 Lysosomes

The lysosome is a field of research that has long been underestimated but is now receiving more and more attention. The growing interest in lysosomes and the endolysosomal system (ELS) can be attributed to the numerous processes they regulate, which in turn affect human health and disease.

Lysosomes are membrane-bound organelles found in eukaryotic cells. With an intraluminal pH of < 5, their interior milieu is acidic. They were first discovered by CHRISTIAN DE DUVE[1], who eventually received the Nobel Prize in Physiology or Medicine for his findings in 1974. Lysosomes are equipped with a comprehensive set of hydrolytic enzymes that can break down various biomolecules like peptides, nucleic acids, lipids and polysaccharides. The lumen of the lysosome is encircled by a cholesterol-poor and heavily glycosylated membrane, which segregates the aggressive acidic environment from the rest of the cell. The membrane is traversed by various ion channels (**Figure 1**). Autodigestion of the membrane by the hydrolytic enzymes is prevented by the glycocalix[2, 3]. The enzymes work best in a specific, acidic environment, which is maintained in the lysosomal lumen by an ATP-consuming proton pump (VATPase)[4].
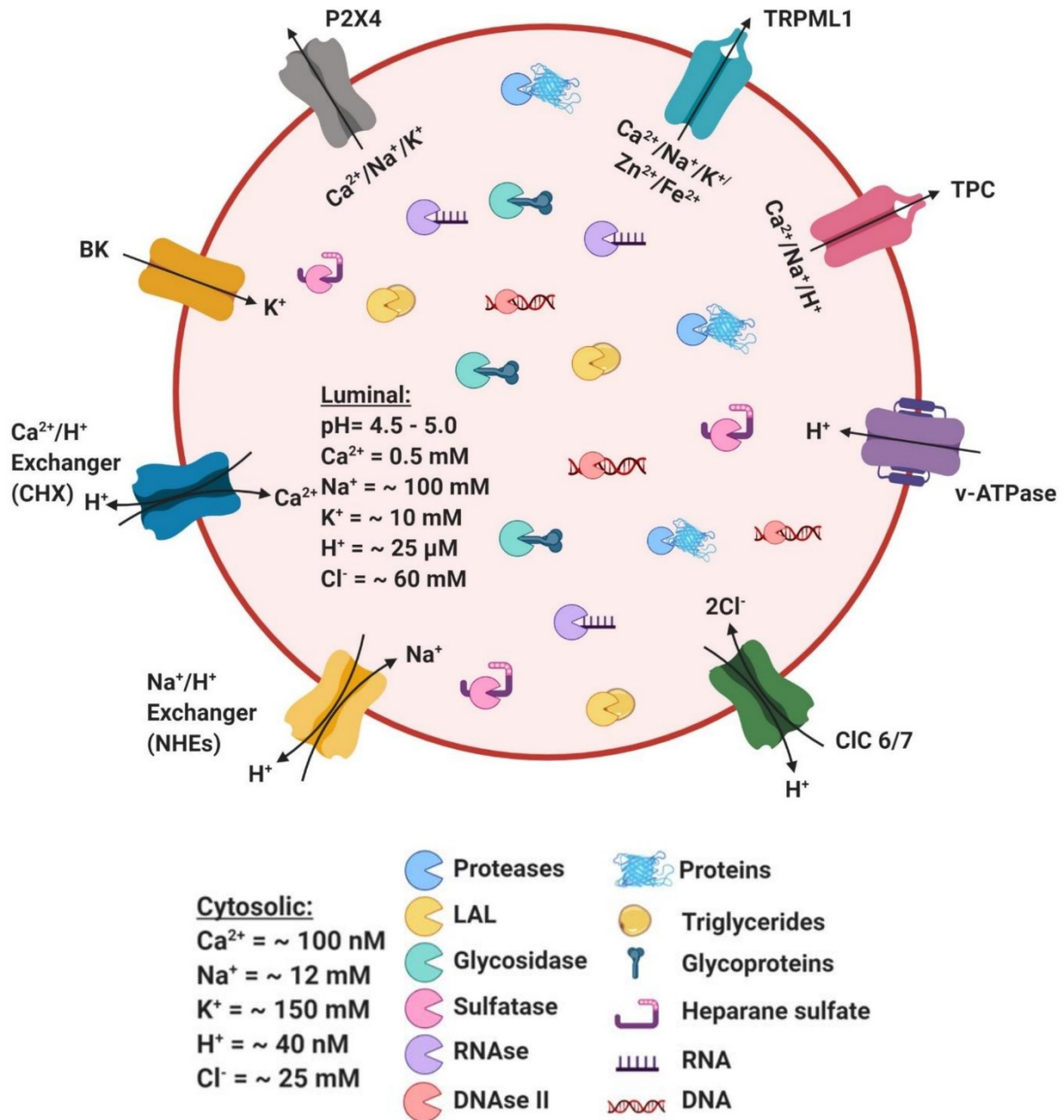
Figure 1: Depiction of the lysosome with selected digestive enzymes and ion channels (cf. lit.[5])

One of the main functions of lysosomes is the digestion of macromolecules. These macromolecules reach the lysosomes by various routes, including the endocytotic and the autophagic pathway[6]. Both itineraries mainly lead to the fusion of cargo loaded vesicles with the lysosomes to form hybrid organelles.

In the endocytotic pathway, in brief, extracellular molecules or surface proteins are internalized by endocytosis and then delivered to early endosomes (EE) where they are efficiently sorted. For recycling, the cargo can be transported back to the plasma membrane through recycling

endosomes (RE). For degradation, the EE matures to a late endosome (LE), which can fuse with a lysosome to form an endolysosome, where the eventual degradation takes place[7-10].

The autophagic pathway is divided into three different types: macroautophagy, microautophagy and chaperone-mediated autophagy. In the following, the focus is on macroautophagy and the term autophagy refers to this subject. Succinctly, the autophagy process consists of the sequestration of cytoplasmic material like macromolecules, organelles and misfolded proteins into an autophagosome that is delivered to a lysosome. The fusion of the two vesicles creates an autolysosome in which the cargo is finally degraded and recycled[11] (**Figure 2**). Autophagy is a pivotal catabolic process associated with the maintenance of cellular and tissue homeostasis[12, 13].
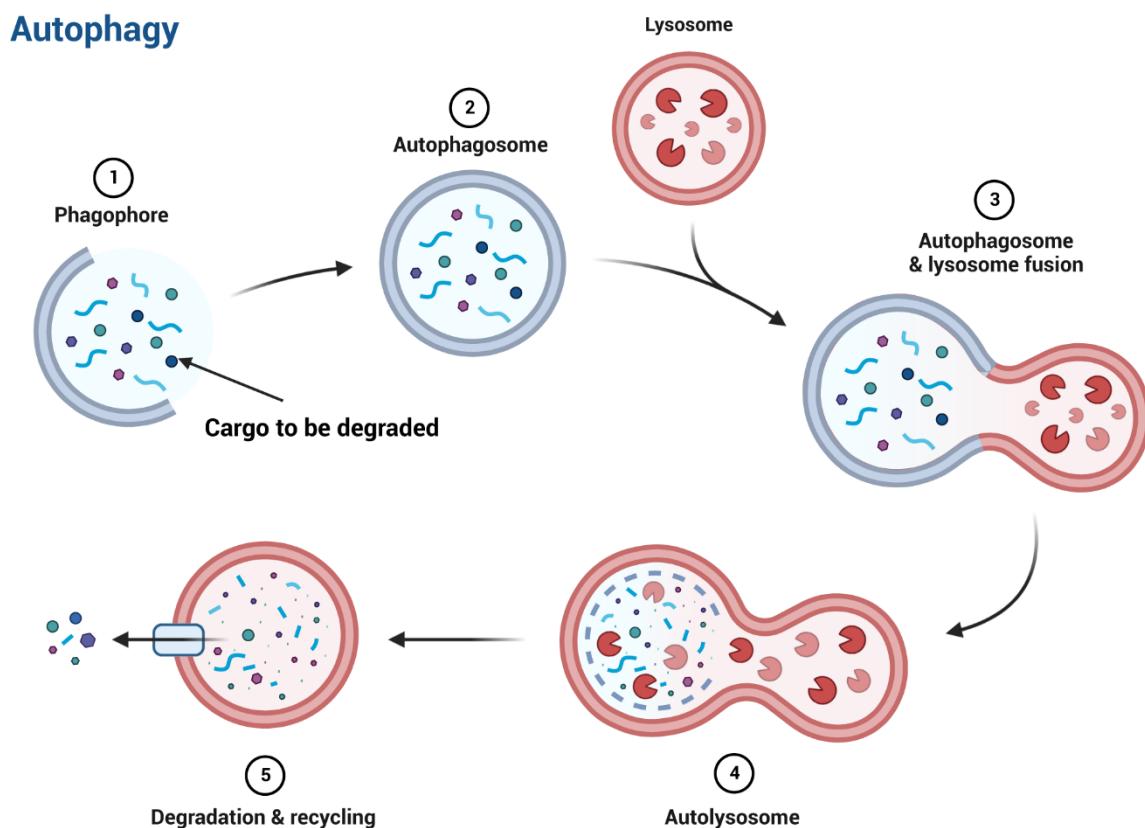
Figure 2: The process of macroautophagy (cf. lit.[14])

Lysosomes have emerged as an important subject of research, involved in various biochemical processes and diseases. For a long time merely recognized as the trash can or the recycle bin of the cell, in recent years lysosomes have been shown to transcend this role by far[15, 16]. They possess several functions within the cell: They participate in immunity, plasma-membrane repair, cell adhesion and cell migration. Furthermore, they act as a sophisticated regulatory and signaling hub that is responsive to environmental cues as well as cellular and organismal needs[6]. They are also involved in nutrient sensing, metabolic signal transduction[17] and cell

death[18]. With a Ca^{2+} concentration which is 5000 fold higher than in the cytosol (~ 0.5 mM in the lysosome vs ~ 100 nM in the cytosol) lysosomes are small Ca^{2+} stores in the cell[19].

In particular, the role of autophagy in health and disease has arisen as a substantial topic of scientific investigations over the last two decades. Several studies have emphasized the role of autophagy in longevity[20, 21], cancer[22, 23], neurodegeneration[24, 25] and a myriad of other biochemical processes.

A master transcriptional regulator of autophagy and lysosomal biogenesis is transcription factor EB (TFEB). In brief, the regulatory function of this protein works by translocation from the cytosol to the nucleus, resulting in the activation of genes including those of the CLEAR (Coordinated Lysosomal Expression and Regulation) network[26-28]. The cellular localization and the activity of TFEB are primarily controlled by its phosphorylation status. The two main kinases known to phosphorylate TFEB are mechanistic target of rapamycin complex 1 (mTORC1) and extracellular signal-regulated kinase 2 (ERK2), both master regulators of cellular growth. Phosphorylated TFEB is kept inactive in the cytosol[29]. Dephosphorylation by the phosphatase calcineurin initiates its nuclear translocation and thus promotes activation[30] (**Figure 3**). A crucial element in the process of autophagy and in the ELS is the endolysosomal ion channel TRPML1.
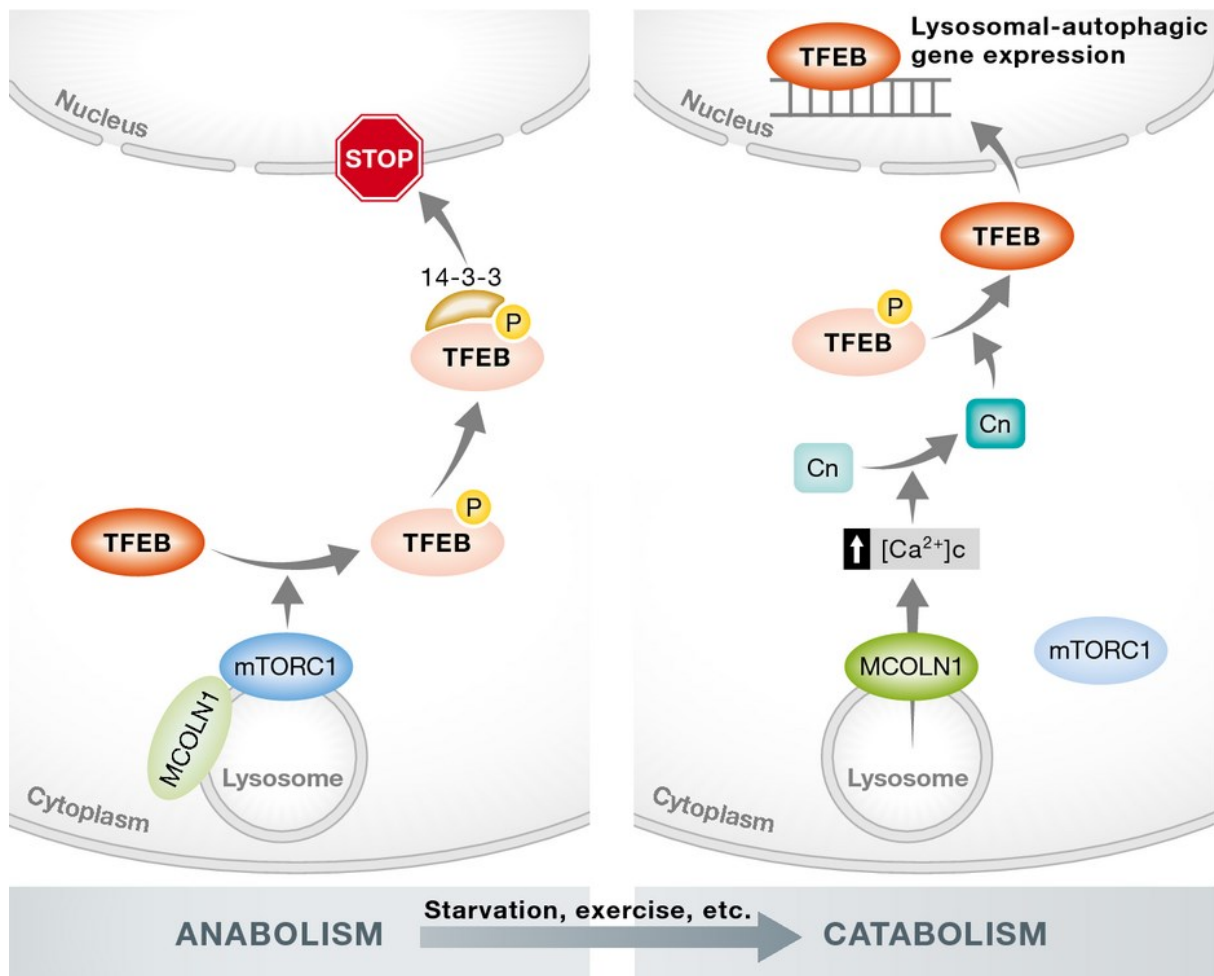
Figure 3: Regulation of autophagy and gene expression by TFEB and lysosomal signaling, Cn = Calcineurin, MCOLN1=TRPML1 (cf. lit.[31])

1.2 TRPML1

TRPML (transient receptor potential mucolipin) is a sub-family within the transient receptor potential (TRP) cation channel superfamily. The TRP group comprises the seven members TRPML, TRPA, TRPC, TRPM, TRPV, TRPP and TRPN, whereby the first six are found in mammals. TRPML in turn is composed of the three isoforms TRPML1, TRPML2 and TRPML3. TRPML1, encoded by the MCOLN1 gene and often also referred as Mucolipin-1 (MCOLN1), is an unselective, inwardly rectifying cation channel predominantly localized in the membrane of late endosomes and lysosomes in all mammalian cell types. Mainly known as a Ca^{2+} release channel in the lysosome, it is also permeable for Na^+, Fe^{2+}, Zn^{2+} and other cations. The channel is a tetrameric protein with six transmembrane domains[32] whose trafficking to lysosomes and late endosomes is regulated by two di-leucine motifs at the cytosolic N- and C-terminal tails (**Figure 4**)[33].
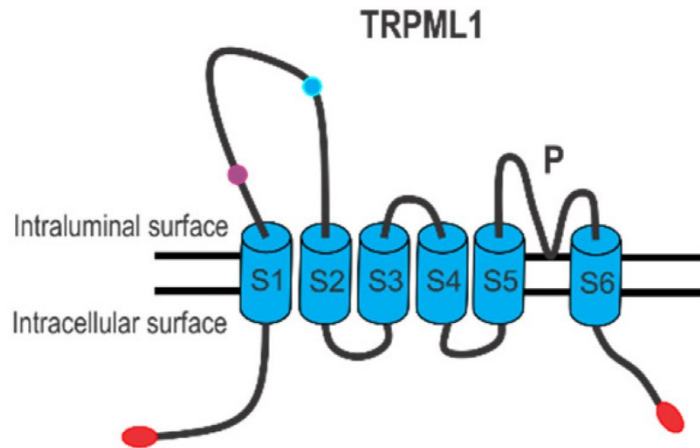
Figure 4: The TRPML1 ion channel with its six transmembrane domains, **red**: di-leucin motif, **purple**: proline rich domain, **blue**: serine lipase motif, P: pore region cf. lit[34]

The endolysosomal inositol lipid phosphatidylinositol 3,5-bisphosphate (PI(3,5)P_2), a major constituent of the lysosomal membrane, has been described as an endogenous activator of all TRPML channels. In contrast, phosphatidylinositol 4,5-bisphosphate (PI(4,5)P_2), which is mainly found in the plasma membrane, has been identified as endogenous inhibitor of TRPML1[35] (**Figure 5**). A study by ZHANG *et al.* suggests that reactive oxygen species (ROS) are also capable of activating TRPML1 and that the channel acts as a ROS sensor in lysosomes[36].

PI(3,5)P_2   **PI(4,5)P_2**
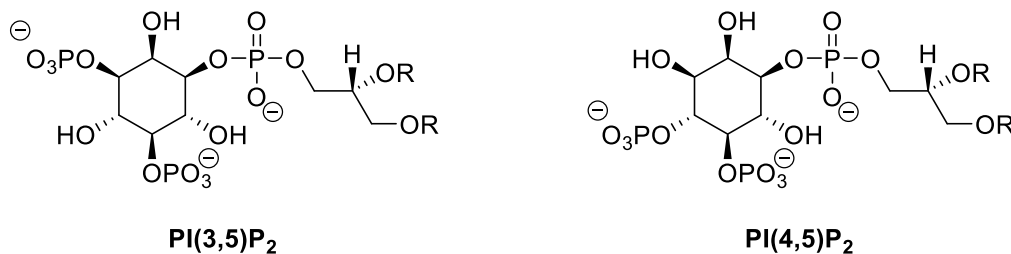
Figure 5: Endogenous ligands of TRPML1, left: phosphatidylinositol 3,5-bisphosphate (activator), right: phosphatidylinositol 4,5-bisphosphate (inhibitor)

Moreover, the regulation of TRPML1 by Ca^{2+} and pH has been described[37]. Although the channel has been shown to be impermeable for protons, TRPML1-mediated currents are potentiated by low luminal pH[38, 39] and loss of TRPML1 reportedly affects the lysosomal luminal pH[40, 41]. Loss or mutation of TRPML1 with dysfunction causes Mucolipidosis Type IV (ML-IV), a neurodegenerative lysosomal storage disorder. Most ML-IV patients suffer from psychomotor delay, progressive visual impairment and achlorhydria[42].

TRPML1 exhibits several functions in different physiological processes, albeit its role in many of them is still not fully understood. It is involved in membrane trafficking, fission and fusion of

vesicles, lysosomal exocytosis and regulates mTORC1 activity as well as lysosomal motility and positioning[43-47]. Autophagy is mediated by TRPML1 through activation of calcineurin and the resulting induction of TFEB (see **Figure 3**) as well as *via* a pathway independent of TFEB[30, 48]. The ion channel is involved in sarcolemma repair, osteoclastogenesis and bone remodeling[49, 50]. In the immune system, TRPML1 controls the migration of dendritic cells[51] and is implicated in the education of natural killer (NK) cells[52, 53]. These processes are mainly mediated by the channel through calcium signaling, whereby recent studies also emphasize the relevance of TRPML1 in governing the flux and homeostasis of Fe^{2+} and Zn^{2+}[38, 54-56].

Likewise, TRPML1 is associated with various human diseases. Its role in different neurodegenerative diseases is discussed. It has been shown that TRPML1 affects the clearance of accumulated tau in Alzheimer's disease by lysosomal exocytosis through regulation of TFEB[57]. Recent studies revealed that activating the channel with a synthetic, subtype-unselective agonist rescues Alzheimer related alterations[58] and protects human dopaminergic neurons from *α*-synuclein toxicity, which is part of the pathogenesis of Parkinson's disease[59]. TRPML1 is also linked to infectious diseases: It is involved in viral infections such as HIV[60] and the bacterial *Helicobacter pylori* infection[61]. Finally, one of the most investigated subjects in the research on TRPML1 is its role in cancer. It has been shown that the loss of TRPML1 function impairs growth of melanoma cells[62] and suppresses the growth of triple negative breast cancer (TNBC)[63, 64]. Moreover, TRPML1 regulates cancer cell migration[65] and cancer cells driven by the small GTPase HRAS are vulnerable to TRPML1 inhibition[66]. In contrast, activation of TRPML1 was found to reduce cell viability and induce apoptosis in glioma cells[67].

In conclusion, TRPML1 contributes to a myriad of physiological processes and diseases. Due to its intricate and elusive role in many of them, chemical tools for studying TRPML1 as a vital component of lysosomes and the ELS are highly sought after. Chemical tools in general are essential for research on a biological target, in particular if the functions and the mechanisms of the addressed target are not yet fully explored. Potent and selective modulators of TRPML1 as chemical tools would not only provide the opportunity for further investigation of the channel but may also evolve into attractive lead structures and drug candidates in clinical pharmacology. They could then represent potential options for pharmacotherapy in the future[68-70].

The endogenous ligands PI(4,5)P$_2$ and PI(3,5)P$_2$ are too polar and therefore not suitable chemical tools apart from their use in selected biological experiments like endolysosomal patch-clamp. Hence, several low-molecular activators and inhibitors of TRPML1 with better pharmacokinetic properties have been developed in recent years. The field of agonists includes the unselective TRPML activators **MK6-83**[71], **SF-51** and **ML-SA1**[72] as well as the

TRPML1 selective activator **ML1-SA1**[73] (**Figure 6**), most of them developed by the BRACHER group. With the not specifically named tetrazole compounds **1** and **2** very recently described by PENG *et al.*, more activators have been added to the toolbox[74]. Regarding synthetic inhibitors, only the indoline derivative **ML-SI1**, an inhibitor with undisclosed structure named **ML-SI2** and the 1,2-diaminocyclohexane derivative **ML-SI3** were known, but poorly characterized examples in the literature[75, 76]. SAMIE *et al.* and WANG *et al.* who described **ML-SI1** and **ML-SI3** in their publications did not provide any information regarding stereochemistry, although both molecules possess two stereocenters. Recent work by members of the BRACHER group shed light on the stereochemistry of **ML-SI3** and identified (-)-(R,R)-trans-**ML-SI3** as the most potent enantiomer[77, 78]. Given that all **ML-SI** compounds lack TRPML isoform-selectivity, there remained an evident need for selective TRPML1 inhibitors.
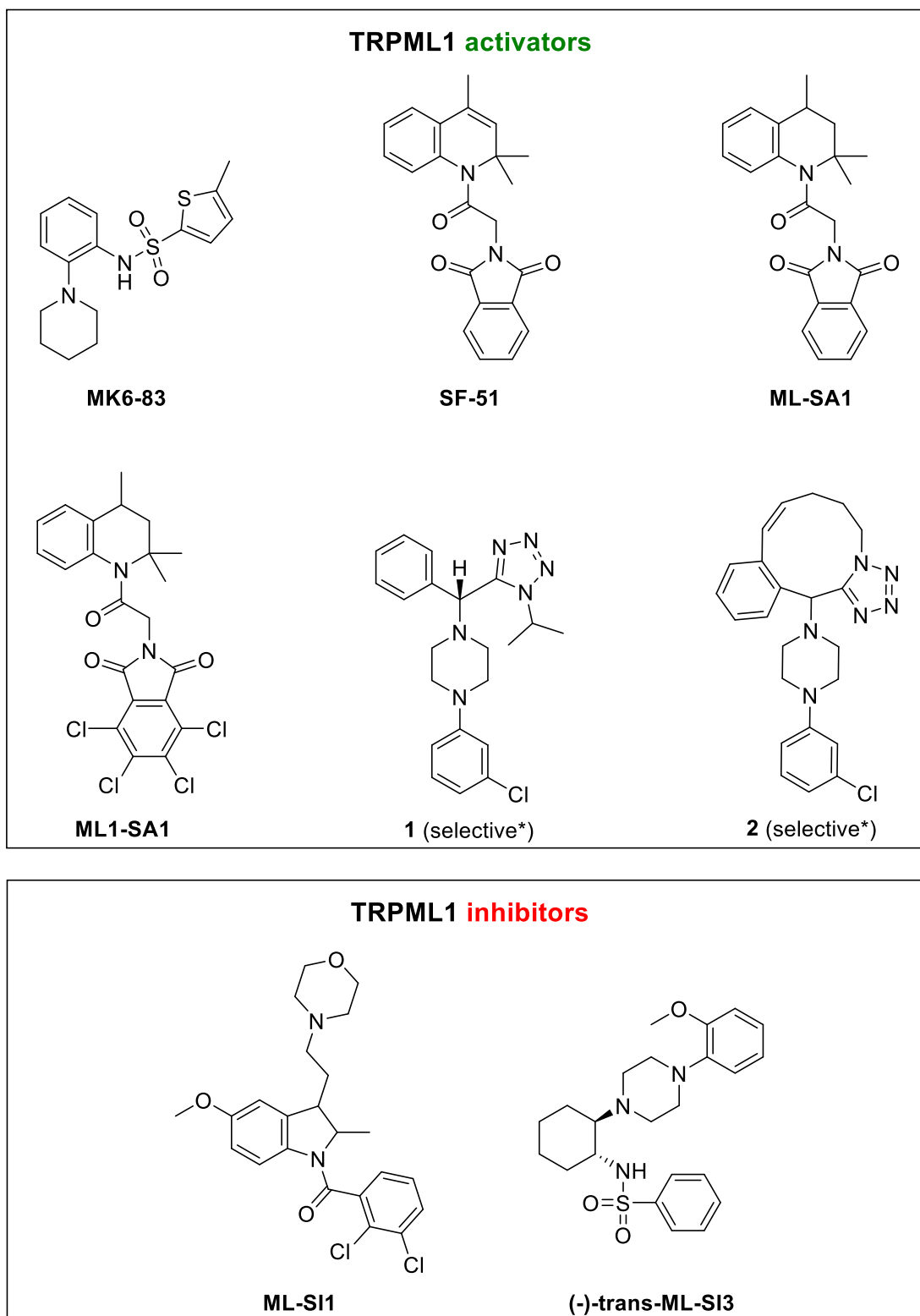
Figure 6: Selection of literature known TRPML1 modulators, *: selectivity only confirmed by TRPML1 knock-out experiments, effect on other channels was not determined

With this in mind, our cooperation partners Prof. Dr. Dr. CHRISTIAN GRIMM from the Walther-Straub-Institut in Munich and Prof. Dr. MICHAEL SCHAEFER from the Rudolf-Boehm-Institut in

Leipzig together with their respective groups conducted a high-throughput screening (HTS) of a library of 2430 drug-like small molecules, including numerous FDA approved drugs, to identify TRPML isoform-selective inhibitors. The screening and the subsequent retesting revealed one promising hit: The steroidal compound 17β-estradiol methyl ether (**EDME**) (**Figure 7**), which showed an IC_{50} value of 0.5 µM for TRPML1 inhibition and a good isoform-selectivity. **EDME** is not only selective, but also much more potent than the two literature known unselective inhibitors **ML-SI1** (IC_{50}: 15 µM) and (-)-trans-**ML-SI3** (IC_{50}: 1.6 µM)[77]. The inhibitory effect of **EDME** was confirmed by both whole-cell and endolysosomal patch-clamp experiments performed by the group of Prof. Dr. Dr. CHRISTIAN GRIMM. Taken together, this molecule was identified as the first potent and selective TRPML1 inhibitor.
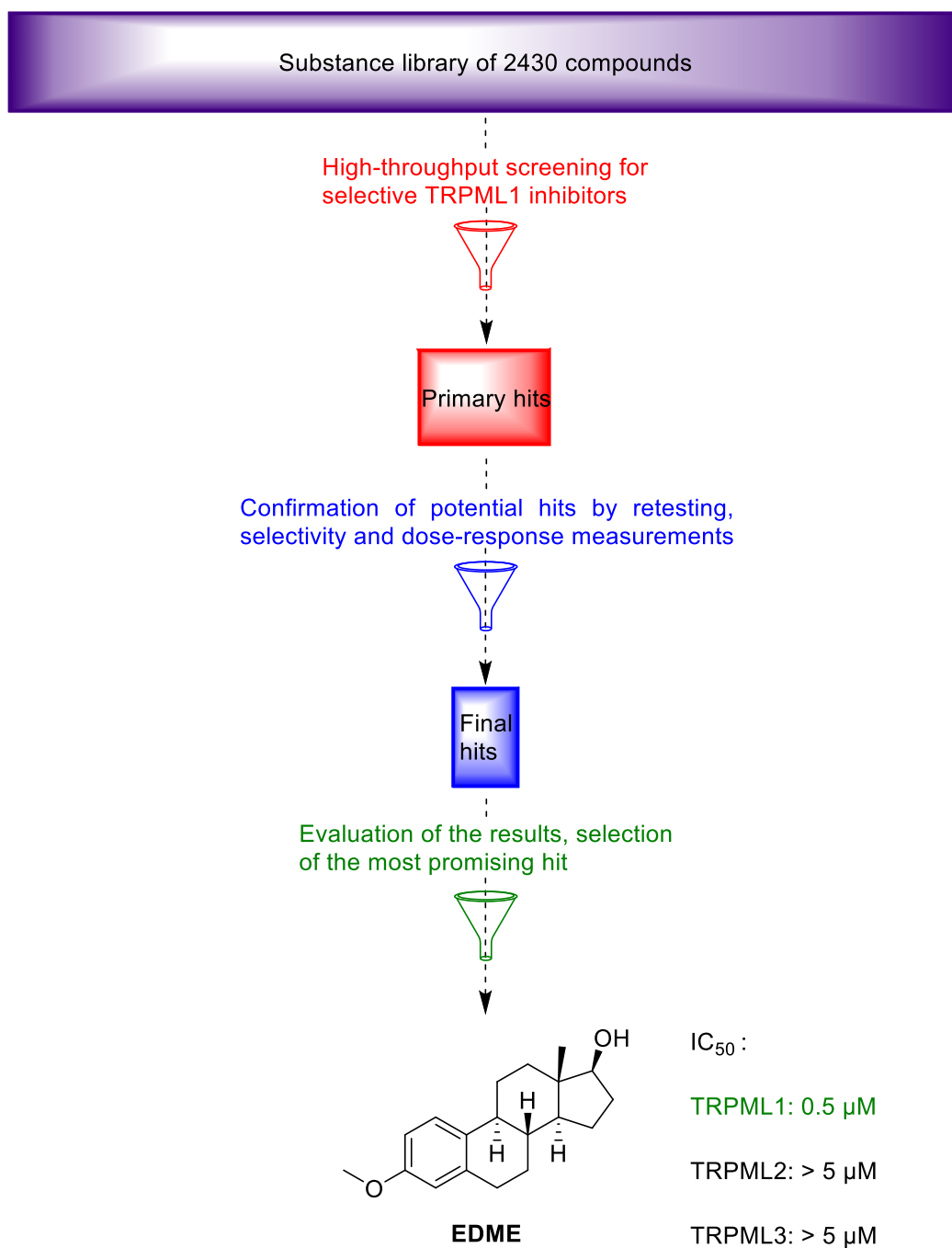
Figure 7: HTS and the resulting hit **EDME**. For the HTS, substances were analyzed by a fluorimetric Ca^{2+} influx assay. Primary hits were subsequently retested to be confirmed or falsified. Dose-response measurements and evaluation of TRPML isoform-selectivity revealed the final hits, of which **EDME** was by far the most promising compound due to its high potency and selectivity.

2. Objectives

As the molecule **EDME** has been identified as a potent TRPML1 inhibitor with a decent isoform-selectivity, its general suitability as a pharmacological tool or even as a future drug candidate had to be investigated. Due to the structural similarity to 17*β*-estradiol a possible activity on estrogen receptors was expectable. Furthermore, the phenolic methyl ether moiety is known to be cleaved *in vivo* by CYP enzymes to give the free phenol. In the case of **EDME**, a study has shown that this process leads to 17*β*-estradiol[79], which is not only exceedingly less active on TRPML1 but also the endogenous ligand for estrogen receptors. Consequently, **EDME** can't be considered as a drug candidate for this target.

Rather, the systematic structural variation of this molecule was a promising strategy to gain access to better eligible TRPML1 inhibitors. The aim of this approach was to minimize or, if possible, eliminate estrogenic activity while simultaneously maintaining or even improving potency and selectivity on the desired target. In order to gather first insights into structure-activity relationships, a second screening campaign was initiated in which several other pharmacologically active synthetic estrogens and antiestrogens as well as natural steroidal compounds were tested for their TRPML1 inhibitory activity. It was found that molecules without aromaticity in ring A (sterols e.g. cholesterol, pregnanes e.g. pregnenolone), which is the distinctive structural motif for steroidal estrogens, lacked notable activity. Only melengestrol acetate, a synthetic progestogen, and testosterone showed very weak inhibition of TRPML1. Antiestrogens (e.g. tamoxifene) were inactive. Among the estrogens tested, estradiol (**3**) showed a much weaker inhibitory effect, while only Mestranol, the 3-methyl ether of ethinylestradiol and 17*α*-ethynyl analog of **EDME**, showed a noteworthy inhibition. Moreover, estrogens bearing esters or a ketone instead of an alcohol at C-17 were found to be virtually inactive (**Figure 8**).
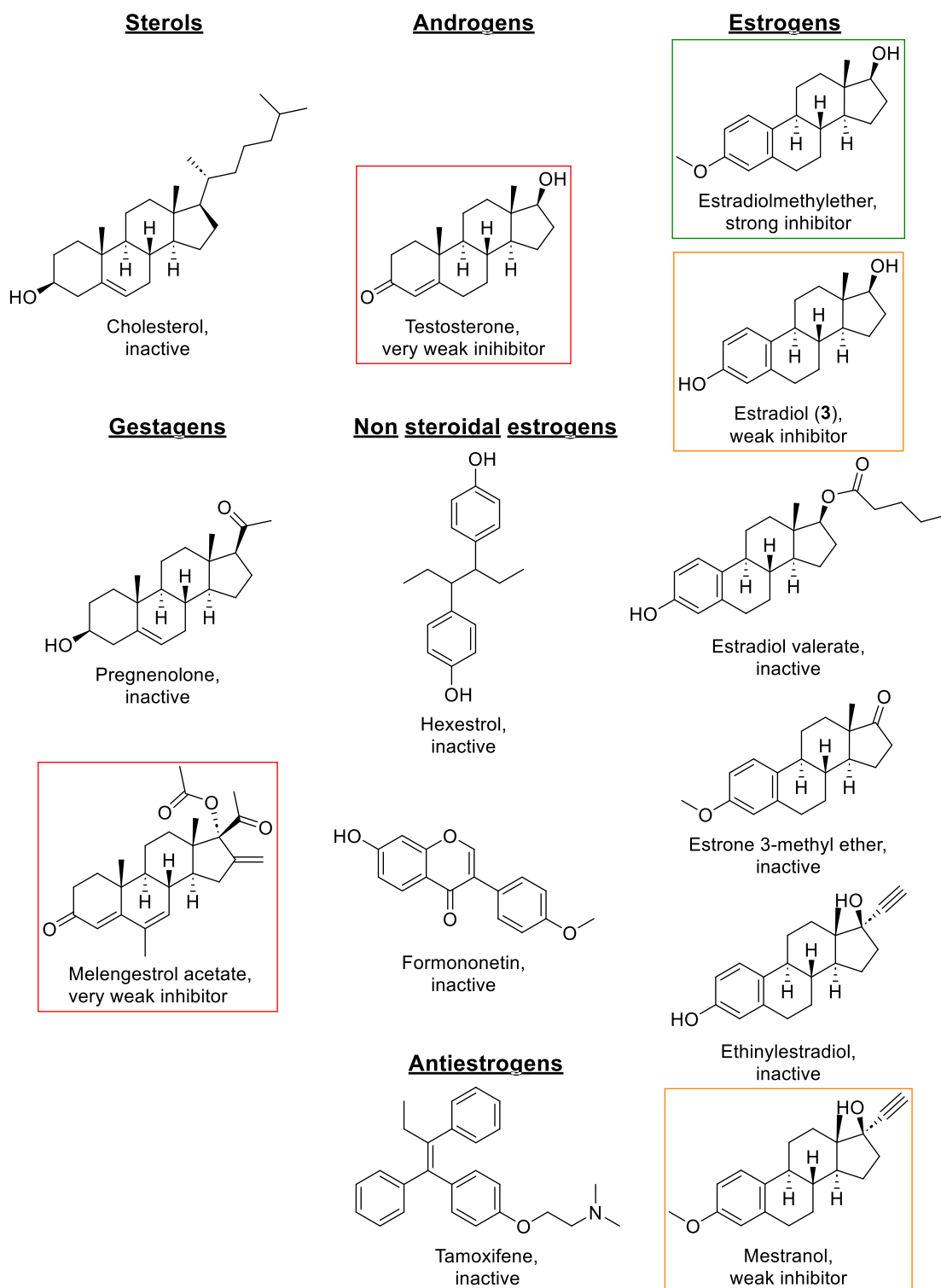
Figure 8: Results of the screening and the consecutive tests. Selected substances and their activity on TRPML1 are shown

As none of these substances could match the TRPML1 inhibitory activity of **EDME**, the preliminary structure-activity relationship derived from these results can be resumed as follows: Aromaticity in ring A is crucial for the activity and variations at ring D are most likely critical. Since ring B and C are hardly accessible for synthetic variations, the most favorable positions for structural modifications were C-2 and C-3 of ring A. Furthermore, inversion of the

configuration of the secondary alcohol at C-17 had to be considered to elucidate whether the stereochemistry at this position is essential. In addition, substitution of the phenyl ring by suitable bioisosteres was a promising strategy of structural modification to alter the physicochemical and pharmacological properties of the molecule. In general, the design and synthesis of potential new inhibitors was limited by the availability of appropriate synthetic precursors.
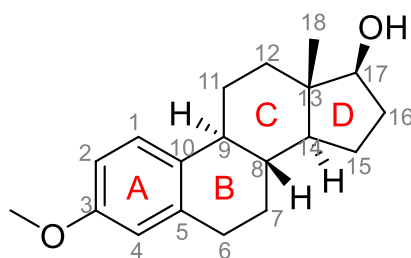
Figure 9: EDME, numbering and ring annotation

On these premises, the aim of this work was to synthesize and biologically evaluate systematically modified analogs of **EDME** in order to get access to new potent and isoform-selective TRPML1 inhibitors that are less active on estrogen receptors than the initial screening hit.

3. Strategy of synthesis

The principle structure of potential inhibitors, as determined by the results of the preceding tests, is composed of an estrane-type scaffold with an aromatic ring A and a secondary alcohol at C-17. Taking all the information into account, the most reasonable structural modifications can be displayed as follows:
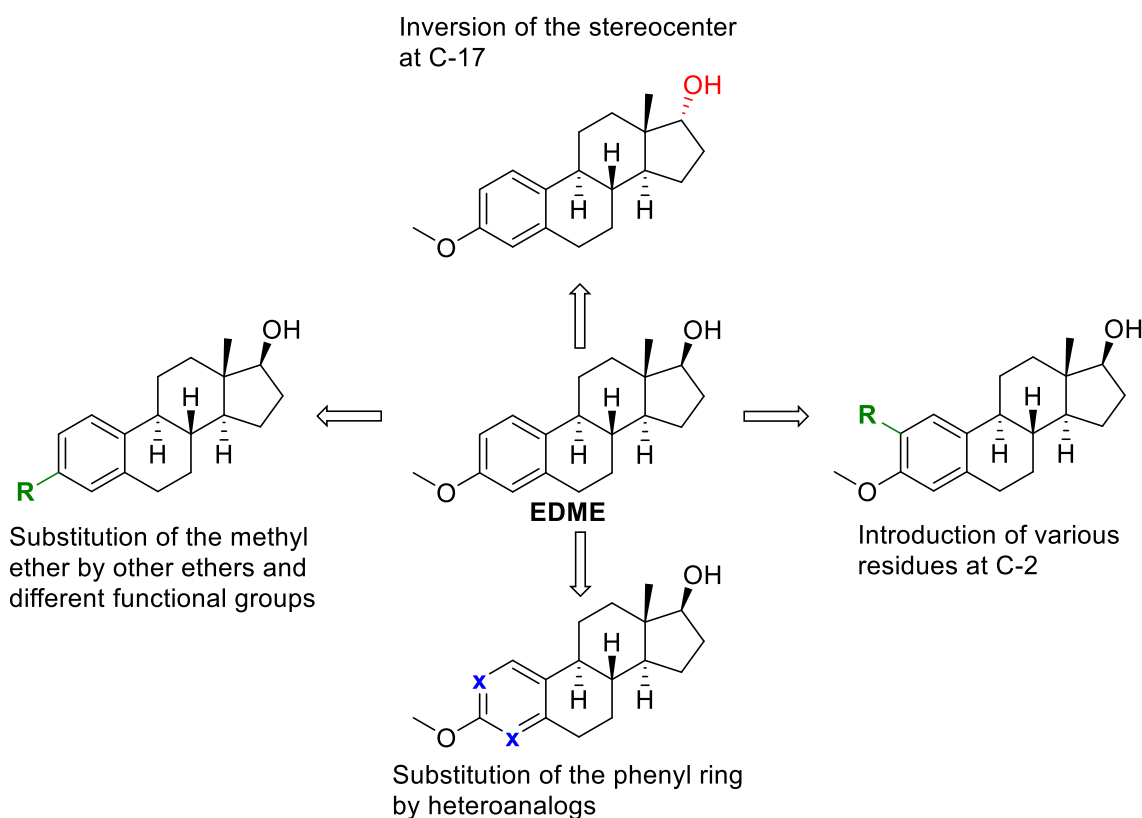
Figure 10: Potential structural modifications of **EDME**

Since the stereochemistry of potential new inhibitors was predefined by the estrane-type scaffold and the intention was to synthesize each compound in an enantiomerically pure form, the starting material generally had to be chosen in accordance with a "chiral pool"[80] synthesis approach. *De novo* synthesis was not considered a favorable option as it was too inefficient due to the complexity of the steroidal structure and the large number of possible stereoisomers formed during the process.

The first idea was to synthesize the 17α-epimer of **EDME**, since molecules with this configuration were not included in the previous tests. It is known that the configuration at this position has a strong impact on estrogen receptor activity. In the case of estradiol, its 17α-epimer alfatradiol shows a significantly lower binding affinity to estrogen receptors[81] and is recognized to have much weaker estrogenic effects[82]. Given that a change in configuration at

this position was seen as a opportunity to diminish effects on estrogen receptors, it was of great relevance how this modification affects the activity on TRPML1.

All other planned novel analogs can essentially be divided into two sets of substances: Firstly, molecules with ammended, deleted and/or additional side chains and secondly, molecules with a heteroaromatic ring A. This distinction is made because each set requires a separate strategy of synthesis starting from completely different starting materials.

The strategy for the first group was to modify the decoration of ring A. Estradiol (**3**) was selected as the perfect starting material for this approach as it has the required stereochemical properties, is commercially available and relatively inexpensive. Since it's a phenol, it is accessible for various synthetic procedures and therefore a promising synthetic precursor for most of the above-mentioned approaches (see **Figure 10**). Substitution of the methyl ether with other ethers of different chain length and composition can be accomplished by etherification of estradiol (**3**). With regard to a possible *in vivo* use of the substances, metabolic stability was also a criterion for the design of potential analogs. As regular phenol ethers would presumably be cleaved by metabolic enzymes, it was also intended to synthesize compounds that are most likely not affected by this process. Examples for this type of molecules would be diaryl ethers or fluorinated alkyl ethers. Besides and also with this aspect in mind, it was planned to replace the methyl ether by other functional groups. Since this is not feasible with phenols directly, it was necessary to derivatize the starting material estradiol (**3**) in order to create a new useful building block that is accessible for this type of modification. The most promising option was to convert the phenol to a reasonable leaving group, preferably an aryl halide or aryl triflate, which could then undergo palladium-catalyzed cross-coupling or similar reactions. This would allow the introduction of a wide variety of functional groups at C-3. Lastly, it was planned to attach different substituents at C-2 of the phenyl ring. Analogous to the approach above, the preferred strategy was to first create an aryl halide or aryl triflate that could then be employed for palladium-catalyzed coupling reactions. In this case, halogenation of estradiol (**3**) at C-2 should provide the appropriate building block. This systematic modification of substituents should furnish further insights into the structure-activity relationships.
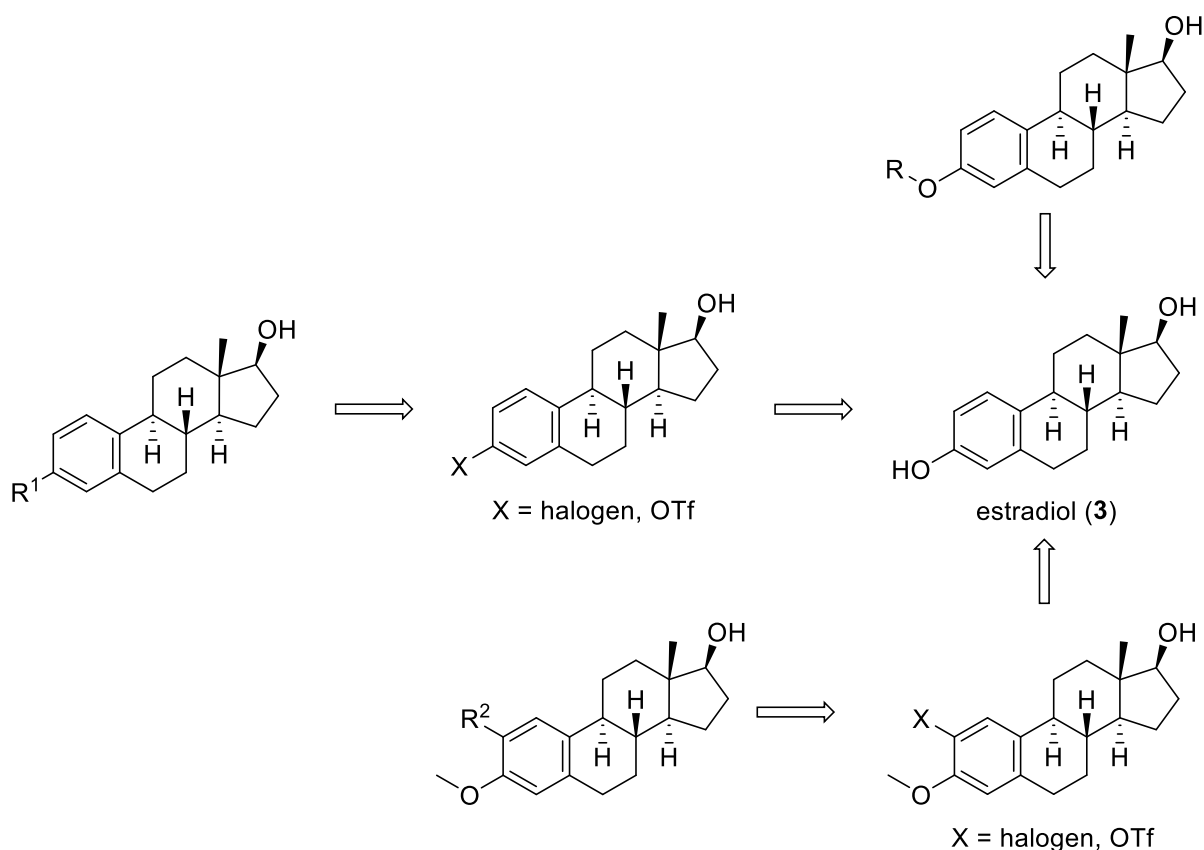
Scheme 1: Retrosynthesis of the first set of compounds

The idea behind the second group of compounds was to exchange the phenyl motif of ring A with adequate bioisosteres. The principle of "bioisosteres"[83] is a well-established strategy in medicinal chemistry to alter physicochemical and pharmacological properties of a bioactive molecule by replacing single atoms or functional groups by more or less similar moieties. This change affects toxicity, metabolism and pharmacokinetic and can at best enhance potency and improve selectivity. There are two different categories for the bioisosteric replacement of phenyl rings. The classical option is to implement neutral aromatic rings (thiophene, furan) or azaarenes (pyridine, pyrimidine). Besides, also non-classical bioisosteres (acetylene, bridged aliphatic ring systems) have been developed. For this work, the azaarene bioisosteres pyridine (4-aza analog of **EDME**) and pyrimidine (2,4-diaza anlalog of **EDME**) were chosen as the most favorable options as they can introduce basicity as well as H-bond donor and/or H-bond acceptor properties. This could lead to either an increase or a decrease in the interaction with the target protein and thus further elucidate the structure-activity relationships. For the synthesis of these compounds neither estradiol (**3**) nor **EDME** were suitable starting materials due to the lack of synthetic methods to convert phenols or phenol ethers into heterocyclic compounds. Instead, the also commercially available and affordable compound 19-nortestosterone (nandrolone, **4**) was chosen as the starting point for this set of analogs. As a homochiral molecule, it already possesses the required configurations at the stereocenters in

17

rings C and D, and above all its ring A is a cyclohexenone which can be cleaved by oxidation. This allows the introduction of nitrogen moieties. In addition, unlike testosterone and similar molecules, it does not bear a methyl group at C-10, which would prevent aromatization of ring A. Hence, it could later be recyclized to obtain the desired azaarenes.

19-nortestosterone (**4**)

4-aza analog

2,4-diaza analog
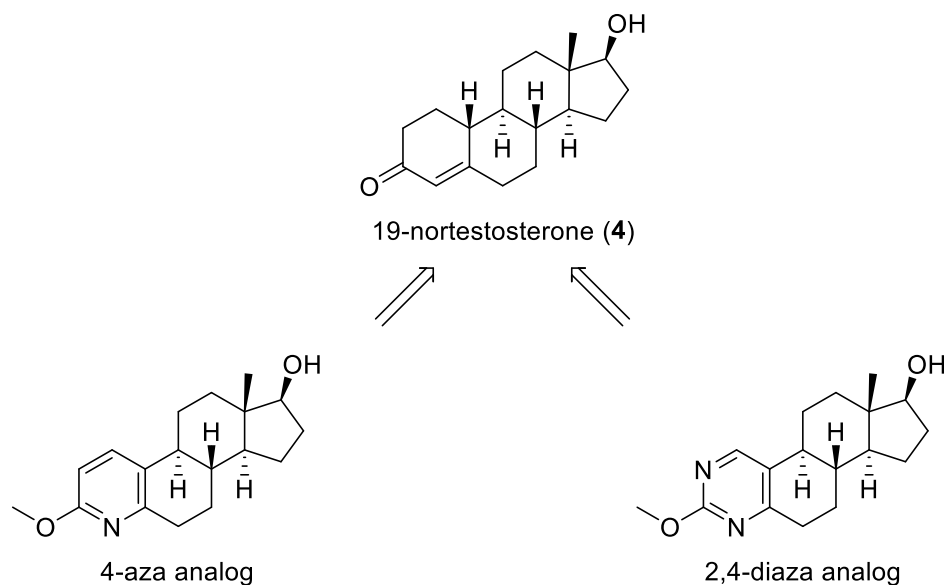
Scheme 2: Starting material 19-nortestosterone (**4**) and the two azaarenes

All in all, comprehensive modifications of **EDME** were designed under the aspects of feasibility and reasonability. The successful and unsuccessful synthesis attempts for all analogs derived from the above strategies as well as the biological evaluation of the resulting compounds are described and analyzed in the following chapters.

4. Results and discussion

In this section, the experiments performed in the course of this work are shown and discussed. The first segment contains all conducted synthetic procedures and the results that have been published in scientific journals. In the second segment, the biological tests (mostly done by cooperation partners) and their individual outcome are presented.

4.1 Synthesis

As outlined above, the original synthesis concept was divided in separate parts based on the different type of modification. Further, the molecules can be categorized by their "generation". The first generation is defined as all compounds that were synthesized and biologically evaluated in the course of the first publication in Scientific Reports in 2021[84]. All compounds prepared thereafter are classified as analogs of the second generation.

4.1.1 First generation of analogs

The first part of the investigations was the synthesis of analogs by substitution of residues at C-3 and the variation of stereochemistry at C-17 of the estrane-type scaffold. The synthesis and biological evaluation of **EDME** and the first 10 analogs are described in the publication in Scientific Reports in 2021[84], which is displayed in Chapter **4.1.3**. The substances contained in this paper are published and referred as **PRU**-compounds.

As the focus of this publication is more on the biological evaluation of the compounds, the design and synthesis concept of the analogs could not be presented in full detail. In the following two chapters, the synthesis routes to **EDME** and two of the analogs of the first generation are explicitly shown in detail in order to illustrate the specific contexts of their design and preparation. The design and synthesis of the other eight analogs does not require additional context and is therefore sufficiently covered in the publication.

4.1.1.1 Synthesis of EDME and 17α-EDME

Due to its combination of high selectivity and activity, **EDME** was in great demand by our cooperation partners for use in various biological experiments. Even though it is commercially available, due to its high price it was more reasonable to find a practical and effective synthesis protocol to produce the required quantities. **EDME** was successfully prepared in 69 % yield by O-methylation of estradiol (**3**) with dimethyl sulfate under alkaline conditions[85] (**Scheme 3**).

The same protocol was applied to alfatradiol (**5**), the 17α-epimer of estradiol, to obtain the 17 α-analog **PRU-2** in 51 % yield[85].
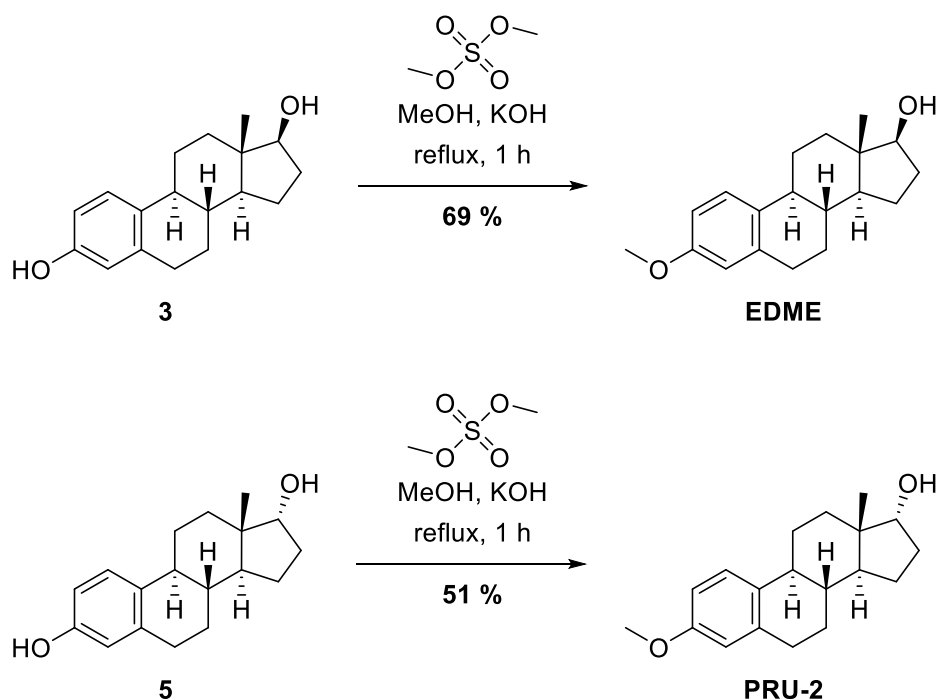
Scheme 3: Preparation of **EDME** and **PRU-2**

Unfortunately, reaction conditions for this method could not be optimized, as neither prolongation of the reaction time nor a higher amount of the alkylating agent led to better results. Because of the rather unsatisfying yield for this simple phenol methylation, the difficult handling and the high quantities of dimethylsulfate required, an alternative approach described by MUDDANA *et al.* was carried out with estradiol (**3**)[86] (**Scheme 4**). In this case, iodomethane was used as the alkylating agent and potassium carbonate as the base. With this protocol, the yield could be increased to 96 %.
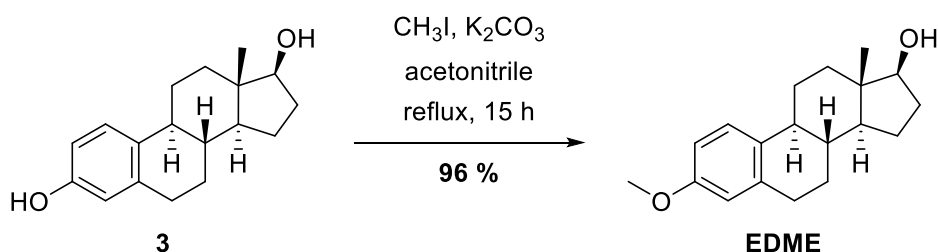
Scheme 4: Alternative, high-yielding preparation of **EDME**

The target for the next series of syntheses was to substitute the methyl ether with other ethers of different chain lengths and/or different physicochemical properties.

4.1.1.2 Synthesis of fluorinated ethers

As mentioned above, a big concern regarding **EDME** was the probable metabolic cleavage of its methyl ether group *in vivo* by CYP enzymes. To address this issue, it was intended to exchange this moiety by a metabolically stable bioisosteric group. Examples for such bioisosteres are the trifluoromethoxy group[87-90] as contained in the drug riluzole, and the difluoromethoxy group[91-93], as contained in the proton pump inhibitor pantoprazole and in roflumilast, an inhibitor of the enzyme phosphodiesterase-4. The rate-limiting step in an *O*-demethylation reaction is the abstraction of a hydrogen atom from the CH_3O group[87]. Since the C-F bond is much stronger than the C-H bond, such modifications should impede metabolic cleavage of this type.

The first approach was to prepare estradiol-3-trifluoromethyl ether (**6**) by silver-catalyzed *O*-trifluoromethylation of estradiol with the Ruppert–Prakash reagent (CF_3SiMe_3) and a mixture of various oxidants following the procedure of Liu *et al.*[94] (**Scheme 5 A**). In contrast to the findings of Liu *et al.* (56 % yield), in our case only traces of a substance which possesses the appropriate mass could be found, but the amount was too low for a proper NMR analysis. TLC reaction control indicated complete consumption of the starting material, but due to the many employed reagents, most of them detectable on the TLC plate under UV irradiation, it was arduous to identify potential pro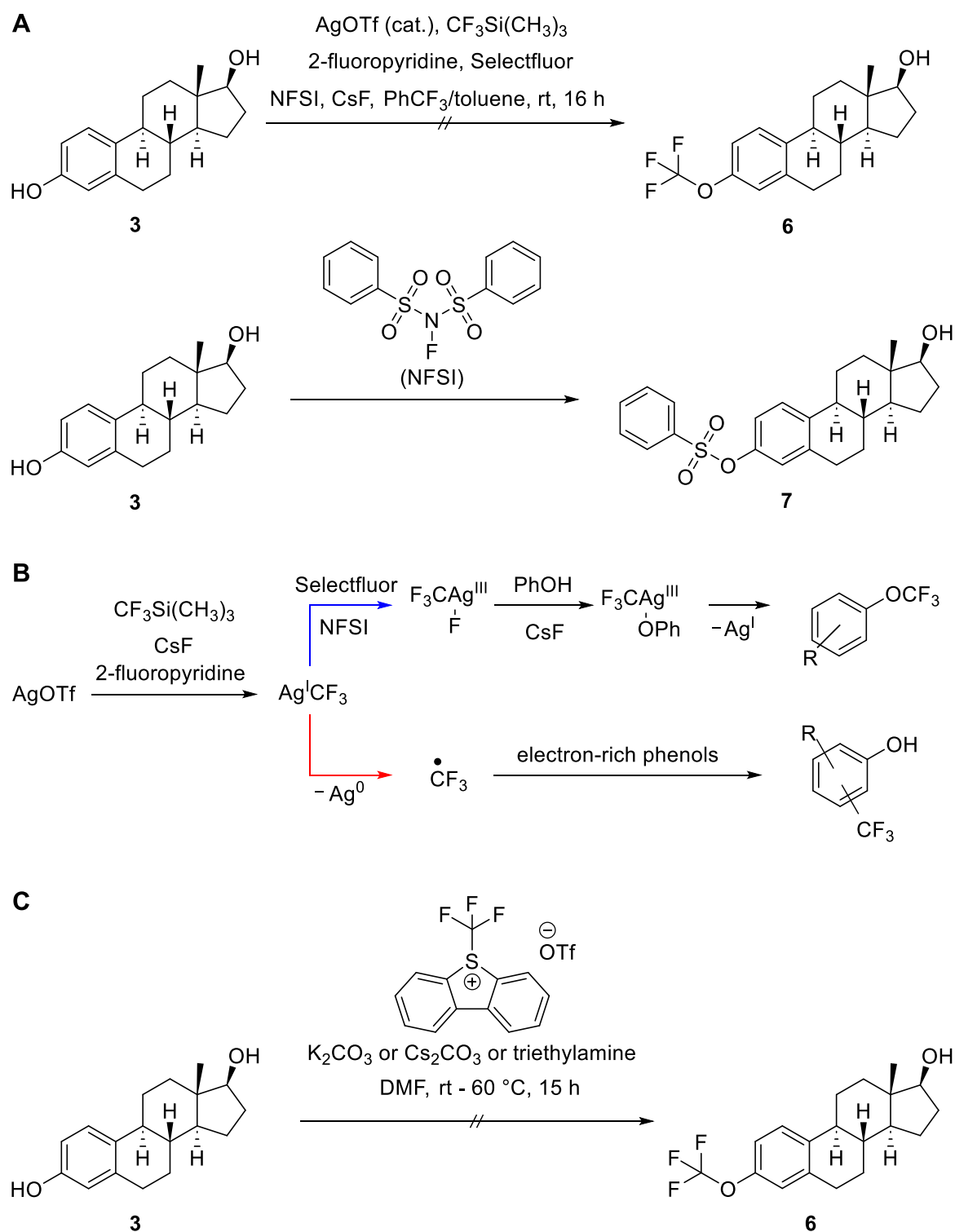ducts. The number of partially overlapping spots on TLC as well as complicated flash column chromatography hampered the isolation and purification process. Beside the substance above mentioned, small amounts of one other product could be obtained. The detected mass corresponds to the mass of a molecule with two CF_3 groups, albeit this could not be confirmed by NMR-analysis, since sufficient purity could not be reached for this product. Variation of the order in which the components were added or variations in temperature or reaction time failed to provide better results. In their publication, Liu *et al.* propose a possible mechanism of the reaction including a competitive side pathway, which leads to the formation of trifluoruoromethylated arenes by a radical mechanism (**Scheme 5 B**). The key step for this is the homolytic cleavage of intermediate Ag-CF_3. Another mentioned side product is the respective benzenesulfonate (**7**), which could be created by reaction of the phenol with *N*-fluorobenzenesulfonimide (NFSI). To impede these two pathways, the protocol of Liu *et al.* was slightly amended by carrying out the reaction under exclusion of light and with the addition of antioxidant 2,4-di-*tert*-butylphenol (2,4-DTBP). In the paper, Liu *et al.* stated that for phenols bearing electron-donating substituents, the addition of this antioxidant inhibited side product formation and increased the yield of the desired trifluoromethyl ethers, but in the case of estradiol they refrained from adding 2,4-DTBP. However, none of these measures changed the outcome of the reaction in our case. A possible explanation could be lacking robustness of this method. Liu *et al.* did not only perform all reactions under an inert argon atmosphere but also used a glovebox for addition of all components. In our case, the reaction

was only carried out under a nitrogen atmosphere, which may not be sufficient for a successful reproduction of their results. After this approach failed, an alternative protocol for trifluoromethylation was explored. Usage of a method for the trifluoromethylation of phenols with 5-(trifluoromethyl)dibenzothiophenium trifluoromethanesulfonate under alkaline conditions[95] left **3** untouched (**Scheme 5 C**). Higher temperature (60°C – 100 °C) and a change of the base (K_2CO_3, Cs_2CO_3, triethylamine) did not lead to a different result.

A

AgOTf (cat.), CF$_3$Si(CH$_3$)$_3$
2-fluoropyridine, Selectfluor
NFSI, CsF, PhCF$_3$/toluene, rt, 16 h

3 → 6

(NFSI)

3 → 7

B

CF$_3$Si(CH$_3$)$_3$
CsF
2-fluoropyridine

AgOTf → Ag^{I}CF$_3$

Selectfluor / NFSI → F$_3$CAg^{III}F → PhOH / CsF → F$_3$CAg^{III}OPh → −Ag^I → R—OCF$_3$

−Ag^0 → •CF$_3$ → electron-rich phenols → R—OH / CF$_3$

blue: desired pathway, red: undesired pathway

C

K$_2$CO$_3$ or Cs$_2$CO$_3$ or triethylamine
DMF, rt - 60 °C, 15 h

3 → 6

Scheme 5: Attempted *O*-trifluoromethylations of estradiol (3), **A**: Attempt following the protocol of LIU *et al.*[94] **B**: Possible competitive reaction with NFSI and mechanism proposed by LIU *et al.*[94] blue: desired pathway, red: undesired pathway (own depiction) **C**: Attempt using 5-(trifluoromethyl)dibenzothiophenium trifluoromethanesulfonate

Since the preparation of the 3-trifluoromethoxy analog of **EDME 6** was not successful, the alternative approach was to synthesize the 3-difluoromethoxy analog. Therefore, the method

for direct difluoromethylation of phenols under alkaline conditions described by ZAFRANI *et al*.[96] was applied to estradiol (**3**) to give 3-difluoromethoxy analog **PRU-4** in 35 % yield. In this procedure, diethyl bromodifluoromethylphosphonate is used as a precursor for difluorocarbene. According to ZAFRANI *et al*., the key step of this process is the hydrolysis-based P-C bond cleavage which leads to the bromodifluoromethyl anion. After elimiation of bromide, the carbene is formed which then reacts with the respective phenolate to form the difluoromethyl ether (**Scheme 6**).
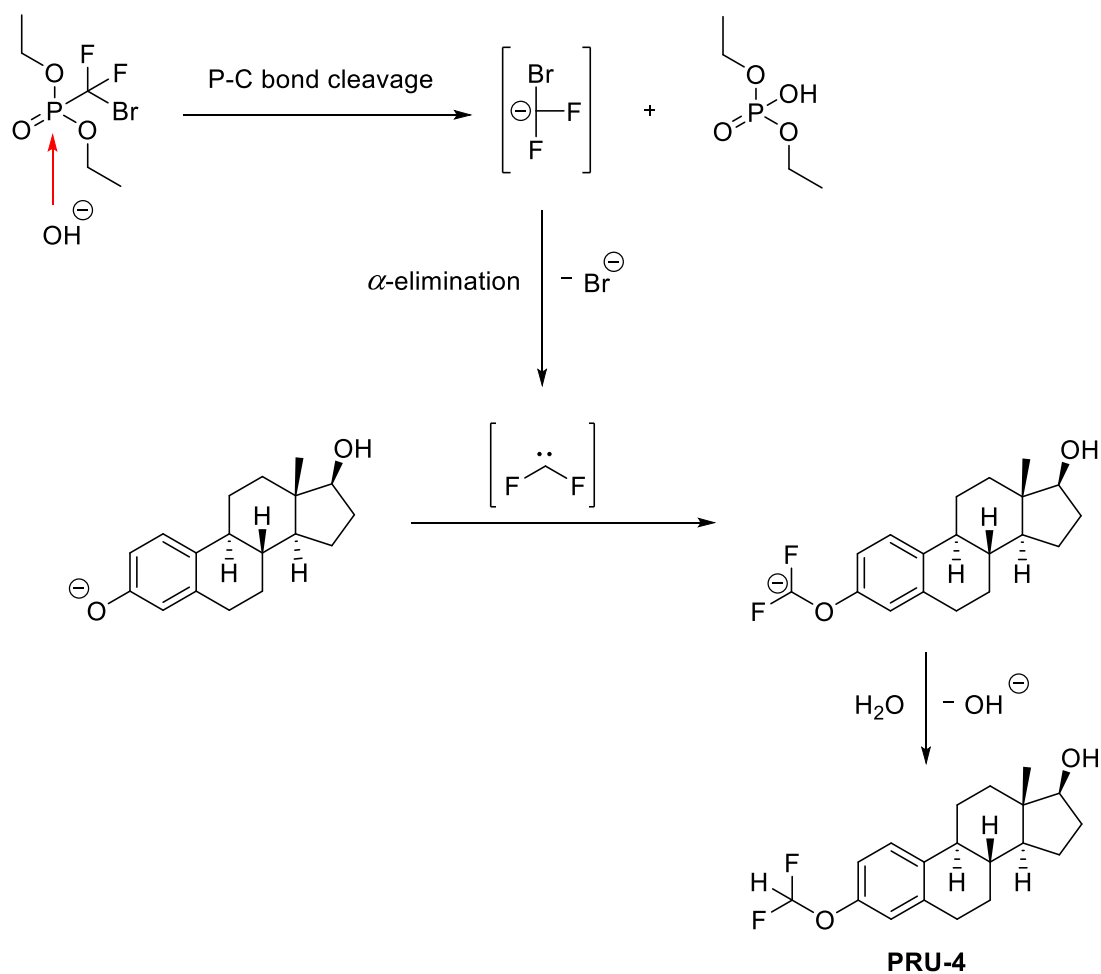
Scheme 6: Mechanism of the difluoromethylation proposed by ZAFRANI *et al*.[96] applied to estradiol (**3**) (own depiction)

4.1.1.3 Estradiol analogs attenuate autophagy, cell migration and invasion by direct and selective inhibition of TRPML1

Rühl P., Scotto Rosato A., Urban N., Gerndt S., Tang R., Abrahamian C., Leser C., Sheng J., Jha A., Vollmer G., Schaefer M., Bracher F., Grimm C., *Scientific Reports* **2021**, 11 (1) 8313

Summary

During this study, a substance library of 2430 drug-like small-molecule compounds was screened for TRPML1 isoform-selective inhibitors. Screening hit 17β-estradiol methyl ether (**EDME**) is described as the first highly potent and subtype-selective antagonist of TRPML1. The inhibitory effect of **EDME** and its superiority over the literature known inhibitor **ML-SI3** was confirmed by whole cell patch-clamp experiments. TRPML1 inhibition of **EDME** was additionally demonstrated by endolysosomal patch-clamp. Further, **EDME** was chemically modified. In addition to the aforementioned analogs **PRU-2** and **PRU-4**, eight more analogs with different substitution at C-3 were synthesized (**Figure 11**) in order to improve characteristics and explore structure-activity relationships. **EDME** and the prepared analogs were tested and biologically evaluated. This evaluation includes single cell Fura-2 Ca^{2+} imaging and fluorescence imaging plate reader (FLIPR) assisted Fluo-4 Ca^{2+} imaging for determination of TRPML1 activity and subtype-selectivity and a yeast estrogen screen (YES) assay with *saccharomyces cerevisiae*, stably transfected with estrogen receptor α, for the assessment of effects at ERα. Taking all results of these tests together, 3-vinylestrane **PRU-10** and methyl ketone **PRU-12** were identified as the analogs with the best characteristics, offering a better selectivity profile and lower effects at ERα compared to **EDME**. **EDME** and these two analogs were shown to inhibit TFEB translocation to the nucleus and block autophagy by direct and selective inhibition of TRPML1. In addition, **EDME** was found to reduce cell migration and invasion in human estrogen receptor (ER-) negative breast cancer cells (MDA-MB-231). This result confirms that these compounds can effectively interfere with cancer hallmarks by inhibiting TRPML1, but independently of estrogen receptors.
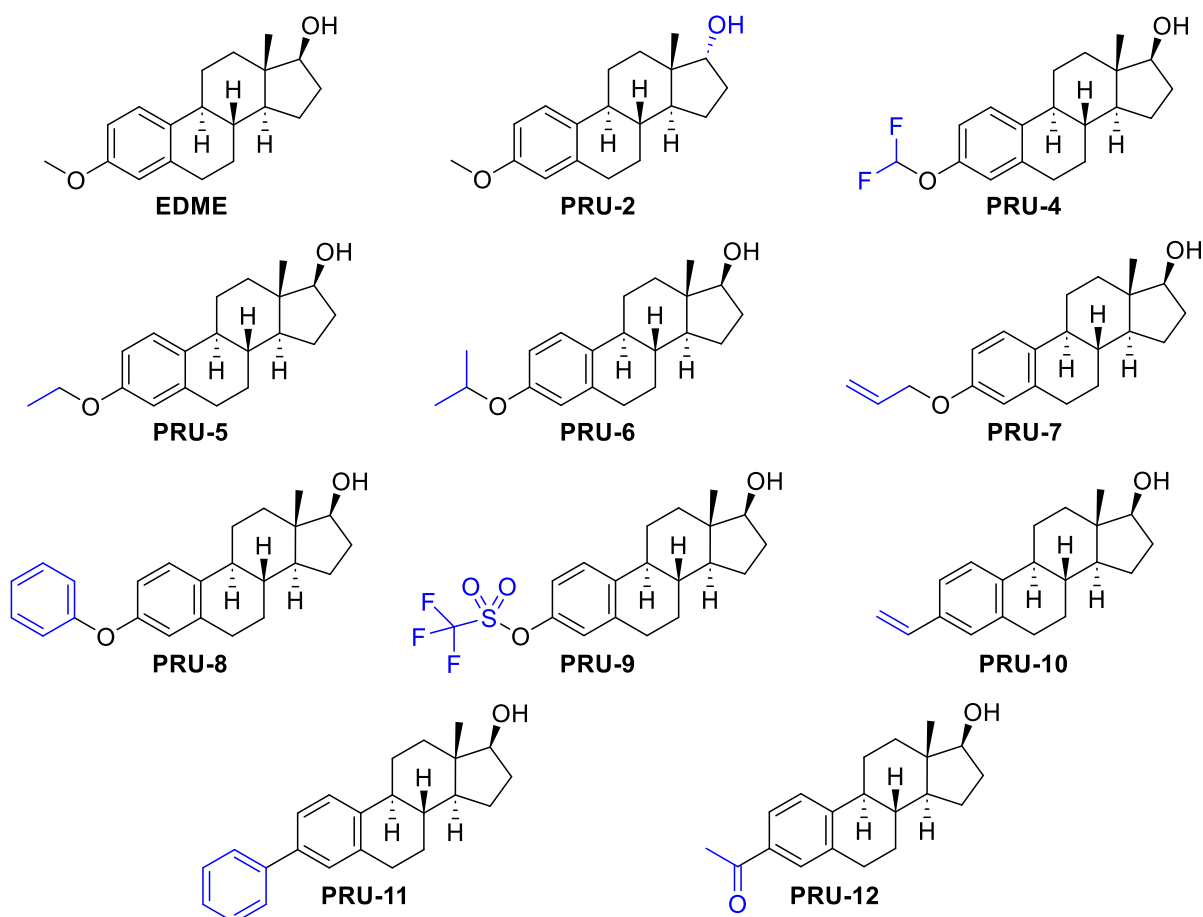
Figure 11: **EDME** and the first ten synthesized analogs (first generation of analogs)

Personal contribution

My personal contribution for the manuscript was the synthesis of all **PRU** compounds and **EDME**, the planning, execution and analysis of all Fura-2 Ca^{2+} imaging experiments as well as visualization of these experiments and graphical illustration of the results of the YES assay. Regarding the Supporting Information, I was responsible for Table S1, Figure S2, Suppl. Scheme 1 and the Synthetic Procedures part.

ANNA SCOTTO ROSATO performed and analyzed the autophagy experiments and contributed to reviewing and editing the original draft.

NICOLE URBAN performed, analyzed and visualized the screening and Fluo-4 Ca^{2+} imaging experiments.

SUSANNE RAUTENBERG (née GERNDT) performed, analyzed and visualized the screening experiments and contributed to reviewing and editing the original draft.

CARLA ABRAHAMIAN created the CRISPR/Cas9 human MCOLN1 KO for MDA-MB-231 breast cancer lines and performed invasion and migration experiments.

ARCHANA JHA, JIANSONG SHENG and RACHEL TANG performed and analyzed patch-clamp experiments.

CHARLOTTE LESER synthesized **ML-SI3**.

GÜNTHER VOLLMER planned, performed and analyzed the YES assay experiments.

CHRISTIAN GRIMM designed the study, analyzed data, wrote the manuscript and provided funding.

FRANZ BRACHER designed the study, created the concept, analyzed data, wrote the manuscript, provided funding and supervised and supported design and synthesis of all compounds.

Article

Reproduction of this article is in accordance with Springer Nature. It is printed in the original wording. Formatting may differ slightly compared to the original article.

Check for updates

scientific reports

OPEN

Estradiol analogs attenuate autophagy, cell migration and invasion by direct and selective inhibition of TRPML1, independent of estrogen receptors

Philipp Rühl[1,7], Anna Scotto Rosato[2,7], Nicole Urban[3,7], Susanne Gerndt[1], Rachel Tang[2], Carla Abrahamian[2], Charlotte Leser[1], Jiansong Sheng[4], Archana Jha[5], Günter Vollmer[6], Michael Schaefer[3✉], Franz Bracher[1✉] & Christian Grimm[2✉]

The cation channel TRPML1 is an important regulator of lysosomal function and autophagy. Loss of TRPML1 is associated with neurodegeneration and lysosomal storage disease, while temporary inhibition of this ion channel has been proposed to be beneficial in cancer therapy. Currently available TRPML1 channel inhibitors are not TRPML isoform selective and block at least two of the three human isoforms. We have now identified the first highly potent and isoform-selective TRPML1 antagonist, the steroid 17β-estradiol methyl ether (EDME). Two analogs of EDME, PRU-10 and PRU-12, characterized by their reduced activity at the estrogen receptor, have been identified through systematic chemical modification of the lead structure. EDME and its analogs, besides being promising new small molecule tool compounds for the investigation of TRPML1, selectively affect key features of TRPML1 function: autophagy induction and transcription factor EB (TFEB) translocation. In addition, they act as inhibitors of triple-negative breast cancer cell migration and invasion.

TRPML1 is a lysosomal cation channel of the transient receptor potential (TRP) superfamily permeable for Ca^{2+}, Na^+, Fe^{2+}, Zn^{2+}, and other cations. TRPML1 is involved in a number of physiological processes and human diseases. Loss or mutation of TRPML1 causes the neurodegenerative lysosomal storage disorder mucolipidosis type IV[1]; vice versa activation of TRPML1 clears intraneuronal Aβ in preclinical models of HIV infection[2] and protects human dopaminergic neurons from α-synuclein toxicity through increased lysosomal exocytosis[3]. TRPML1 is also essential for sarcolemma repair to prevent muscular dystrophy[4], and small molecule activation of TRPML1 ameliorates Duchenne muscular dystrophy[5]. TRPML1 further plays a role in gastric acid secretion and may represent a therapeutic target for chronic Helicobacter pylori infection[6–8]. TRPML1 also acts as ROS (reactive oxygen species) sensor in lysosomes[9], it regulates autophagy through calcineurin and transcription factor EB (TFEB)[10] or in a TFEB-independent manner[11,12], it regulates lysosomal motility and lysosomal positioning[13], and it plays a role in osteoclastogenesis and bone remodeling[14]. Furthermore, TRPML1 has functions in the immune system, e.g. it controls the migration of dendritic cells[15] and it plays a role in the education process of natural killer (NK) cells[16]. Finally, HRAS-driven cancer cells, i.e. cells containing mutations in HRAS, a small GTPase of the Ras superfamily, are vulnerable to TRPML1 inhibition[17]. Loss of TRPML1 impairs the growth of melanoma[18] and reduces cell proliferation, cell viability and tumor growth in the MDA-MB-231 breast cancer cell line, a highly aggressive, invasive and poorly differentiated triple-negative breast cancer (TNBC) cell line lacking estrogen and progesterone receptor expression as well as HER2 (human epidermal growth factor receptor 2) amplification[18].

[1]Department of Pharmacy – Center for Drug Research, Ludwig-Maximilians University, Munich, Germany. [2]Walther Straub Institute of Pharmacology and Toxicology, Faculty of Medicine, Ludwig-Maximilians University, Munich, Germany. [3]Rudolf-Boehm-Institute for Pharmacology and Toxicology, University of Leipzig, Leipzig, Germany. [4]CiPA LAB, LLC, Gaitherburg, MD, USA. [5]Casma Therapeutics Inc, Cambridge, MA, USA. [6]Institute of Zoology, Molecular Cell Physiology and Endocrinology, University of Dresden, Dresden, Germany. [7]These authors contributed equally: Philipp Rühl, Anna Scotto Rosato, and Nicole Urban. ✉email: Michael.Schaefer@medizin.uni-leipzig.de; franz.bracher@cup.uni-muenchen.de; christian.grimm@med.uni-muenchen.de
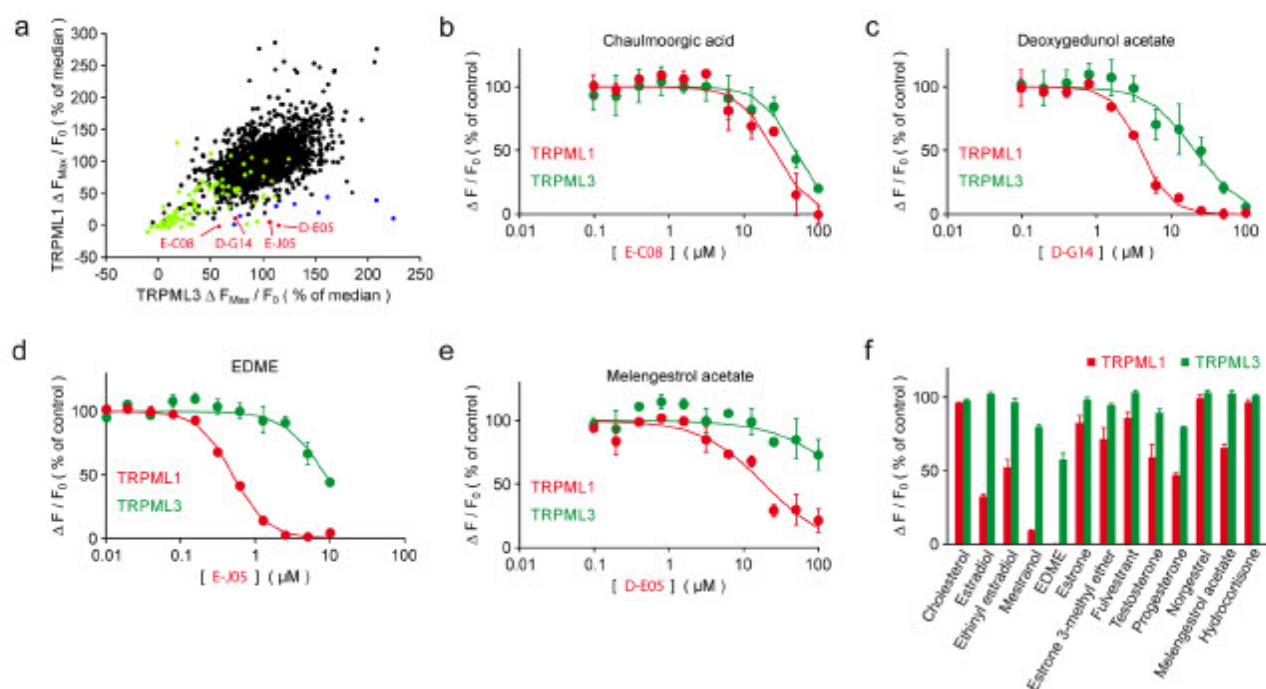
Figure 1. Compound screening and hit validation. (**a**) Dot plot showing the inhibitory effects of 2430 bioactive compounds (20 µM) on fluo4-loaded HEK293 cell lines stably expressing hTRPML1ΔNC-YFP and hTRPML3-YFP after activation of the cells with 5 µM ML-SA1. Peak fluorescence intensities after stimulation were normalized to the median response in the respective screening plate. Black dots indicate compounds with no discernible effect on either TRPML1 or TRPML3. Green dots represent fluorescent compounds that were not further considered. Blue dots are notoriously positive hits previously identified in several other screened targets. Red dots indicate TRPML1-selective hits. (**b–e**) Representative concentration–response curves of the 4 specific hits in (A) for TRPML1 (red dots and lines) and TRPML3 (green dots and lines). (**f**) Effect of retested and pharmacologically relevant steroids on TRPML1 and TRPML3 at a concentration of 12.5 µM, which in the case of EDME completely blocks TRPML1. Shown is the inhibition of Fluo-4 fluorescence responses to stimulation with 5 µM ML-SA1 and normalization to an untreated control. Aggregated data sets from 3 to 5 independent experiments, each performed in duplicates, are displayed (means ± SEM).

In recent years several TRPML channel activators have been developed by different groups, e.g. SF-22, MK6-83, ML-SA1, or ML-SA5[5,19–21]. In addition, TRPML isoform-selective agonists have been discovered recently such as a TRPML2-selective agonist, ML2-SA1[22] or TRPML3-selective agonists, SN-2 and EVP-21[20,22]. TRPML1-selective agonists are currently not available, neither are TRPML1-selective antagonists. Only inhibitors without isoform-selectivity, e.g. ML-SI1 and ML-SI3 have been described so far[23,24]. TRPML channel isoforms can occur not only in the same cell type, e.g. in certain types of macrophages and other immune cells, but also in the same type of organelle, e.g. in early endosomes (EE), late endosomes (LE), or lysosomes (LY). In particular, TRPML1, 2, and 3 in LE/LY and TRPML2 and 3 in EE. Isoform-selective agonists and antagonists are therefore highly desired as chemical tools to decipher channel functions in endogenously expressing cell systems and organelles with TRPML isoform-heterogeneity; and therapeutically to exclude potential side effects mediated by inhibition or activation of the other TRPML isoforms. We have screened a library of 2430 drug-like small molecule compounds, the majority of which from the Spectrum Collection compound library (MS Discoveries; 2000 compounds) containing numerous FDA-approved drugs, to identify TRPML isoform-selective inhibitors. In the following we describe the first highly potent and subtype-selective antagonist of TRPML1, 17β-estradiol methyl ether (EDME), which we further modified chemically to improve its characteristics. Thus, analogs of EDME were generated with reduced estrogen receptor alpha (ERα) activity. Functionally, we found that EDME and its analogs inhibit autophagy and translocation of TFEB, a master regulator of autophagy and lysosomal biogenesis, to the nucleus by direct and selective inhibition of TRPML1. In human estrogen receptor negative (ER-) breast cancer cells (MDA-MB-231) EDME was found to reduce migration and invasion, corroborating the efficacy of these compounds to interfere with cancer hallmarks in a TRPML1-dependent but estrogen receptor independent manner.

Results

### Identification of EDME as selective TRPML1 antagonist.
Initially, 2430 compounds were tested on hTRPML1ΔNC-YFP, a plasma membrane variant of wild-type TRPML1 lacking N- and C-terminal lysosomal targeting sequences as reported previously[22], and hTRPML3-YFP, both stably expressed in HEK293 cells. TRPML1 and TRPML3 were activated with 5 µM ML-SA1, respectively (Fig. 1a), a concentration which

showed no effect in the parental control cell line. Four TRPML1 selective hit compounds [the synthetic gestagen melengestrol acetate (D-E05; MGA), 17β-estradiol methyl ether (E-J05; EDME), the natural triterpene deoxygedunol acetate (D-G14; DGA), and the fatty acid derivative chaulmoorgic acid (E-C08)] were initially identified and subsequently retested by performing concentration–response measurements (Fig. 1b–e, S1). MGA and EDME were thus confirmed as highly TRPML1-selective with IC_{50} values of 18.6 µM (MGA) and 0.5 µM (EDME). EDME showed the lowest IC_{50} for TRPML1. Subsequently, other pharmacologically relevant steroidal compounds were tested. Of those, estradiol, ethinylestradiol, and mestranol which is the 3-methyl ether of ethinylestradiol also showed stronger inhibitory effects on TRPML1 than on TRPML3 with mestranol showing the strongest effect. However, none of these reached the TRPML1-inhibitory activity of EDME. Other steroid hormones like progesterone and testosterone showed much weaker inhibitory effects compared to EDME or mestranol while cholesterol, hydrocortisone, estrone, estrone 3-methyl ether, norgestrel, and fulvestrant, the latter one used to treat hormone receptor positive metastatic breast cancer, had no effect on either TRPML1 or TRPML3 (Figs. 1f, S1). TRPML channels belong to the superfamily of transient receptor potential (TRP) channels. Those are the channels TRPMLs are most closely related with. Hence, we have counter screened EDME against a plethora of other members of the TRP superfamily, namely TRPC3, 4, 5, 6, and 7 of the canonical or classical TRP subfamily, members of the melastatin subfamily, TRPM2, 3, and 8 as well as members of the vanilloid subfamily, TRPV1, 2, 3, and 4. We further repeated testing against TRPML2 and TRPML3 as well as the functionally related endolysosomal two-pore cation channel TPC2. Channels were activated with previously reported activation concentrations of known ligands, respectively (Fig. 2a). While no meaningful IC_{50}s were obtained for EDME for most channels including TPC2, activated by either TPC2-A1-P or TPC2-A1-N as reported recently[25], the following IC_{50}s were determined for TRPML1, 2 and 3: 0.6 µM, 5.9 µM, and 19.5 µM (Table S1). To further corroborate these data we performed whole-cell patch-clamp experiments with EDME using stable cell lines expressing either the plasma membrane variant hTRPML1[L15/16A, 1577/578A], hTRPML2, or hTRPML3. While no block for TRPML3 was found, TRPML2 was blocked with an IC_{50} of 3.8 µM. The IC_{50} measured for TRPML1 was 0.22 µM (Fig. 2b,d). For comparison, we also tested the recently described TRPML inhibitor ML-SI3 which blocked TRPML1 with an IC_{50} of 4.7 µM and TRPML2 with an IC_{50} of 1.7 µM, suggesting that ML-SI3 has an almost threefold stronger effect on TRPML2 compared to TRPML1 and is >20-fold weaker on TRPML1 than EDME (Fig. 2c,e). Next, we confirmed the inhibitory effect of EDME in endolysosomal patch-clamp experiments by isolating vacuolin-enlarged endo-lysosomes from hTRPML1 WT expressing HEK293 cells (Fig. 2f–h). Finally, we used TRPML1 endogenously expressing murine alveolar macrophages to confirm inhibition of TRPML1 activation by EDME (Fig. 2i).

Systematic modification of EDME. Initial structure–activity relationships (SAR) were detected by analyzing the structures of the screening hits and other steroidal compounds tested in either the random screening or the consecutive experiments. From these data it was evident that natural and synthetic steroids lacking an aromatic ring A (typical for estrogens) have virtually no (cholesterol, phytosterols, glucocorticoids, mineralocorticoids, antiestrogens, antiandrogens, 5α-reductase inhibitors) or only weak TRPML1-inhibitory activity (some androgens and gestagens) (Fig. 1f). In the class of gestagens progesterone and melengestrol acetate (MGA) had shown modest TRPML1 inhibition (IC_{50} = 12 µM and 19 µM, respectively). Further, stilbene-type synthetic estrogens and plant phytoestrogens were inactive in the primary screen. In the class of estrogens, the native hormone 17β-estradiol was significantly weaker (IC_{50} = 5.3 µM) than EDME. Likewise, the synthetic 17-ethinyl derivative ethinylestradiol was only weakly active. Modification of 17β-estradiol at 3-OH with an ionic residue (estradiol-3-sulfate sodium salt) eliminated TRPML1-inhibitory activity. Only mestranol, a congener of EDME bearing an additional ethinyl group at C-17, showed considerable activity. From these structures of mainly weakly active or inactive steroidal and related compounds it was evident that there is a very steep structure–activity relationship: only estrane-type compounds are promising and variations at ring D are most likely critical; the most obvious position for further modifications was position 3 at the aromatic ring A. Therefore we synthesized 10 modified versions of EDME, most of which have in common a replacement of the methoxy group at C-3 with a lipophilic residue. One single variation was performed on ring D by conversion of alfatradiol, the 17α epimer of physiological 17β-estradiol, into its 3-methoxy derivative PRU-2 by simple O-methylation[26]. A couple of ethers of 17β-estradiol were obtained by various etherification protocols: known O-alkyl derivatives like ethyl ether PRU-5[27], isopropyl ether PRU-6[28], and allyl ether PRU-7[29] were obtained under standard Williamson conditions. Since for these trivial alkyl ethers undesired oxidative O-dealkylation by CYP enzymes to give free 17β-estradiol cannot be excluded[25], we prepared two estradiol ethers with presumably high metabolic stability. Difluoromethyl ether PRU-4[30] was obtained from 17β-estradiol using Zafrani's diethyl (bromodifluoromethyl)phosphonate reagent[31], and phenyl ether PRU-8 was prepared by O-phenylation with benzyne generated from 2-(trimethylsilyl)phenyl trifluoromethanesulfonate with fluoride ions[32]. In order to obtain lipophilic 17β-estradiol analogs without a C,O-bond at C-3, for which metabolism into the parent hormone should be fully excluded, we converted the phenolic group into the O-triflate to give the useful building block PRU-9[33]. Suzuki–Miyaura cross-coupling of PRU-9 with phenylboronic acid gave the 3-phenylestrane PRU-11, Stille cross-coupling with tributyl(vinyl)tin under Pd(II) catalysis[34] the 3-vinylestrane PRU-10. Methyl ketone PRU-12[34] was obtained via Stille cross-coupling of PRU-9 with tributyl(1-ethoxyvinyl)tin, followed by aqueous hydrolysis of the formed enol ether (Scheme S1). These EDME analogs were tested for TRPML1 inhibition in single cell Fura-2 calcium imaging experiments at a concentration of 10 µM (Figs. 3a–l and S2). Surprisingly, in these experiments all compounds showed strong efficacy in blocking TRPML1 with the exception of 17α-epimer PRU-2. In a next series of experiments, we performed concentration–response measurements with 17β-estradiol (E2), EDME and the 10 analogs. For analysis of subtype selectivity, we further tested all compounds on TRPML1, 2, and 3 as well as the related endolysosomal cation channel TPC2 (Fig. 4a–l). Again, 17α-epimer PRU-2 showed only poor activity,
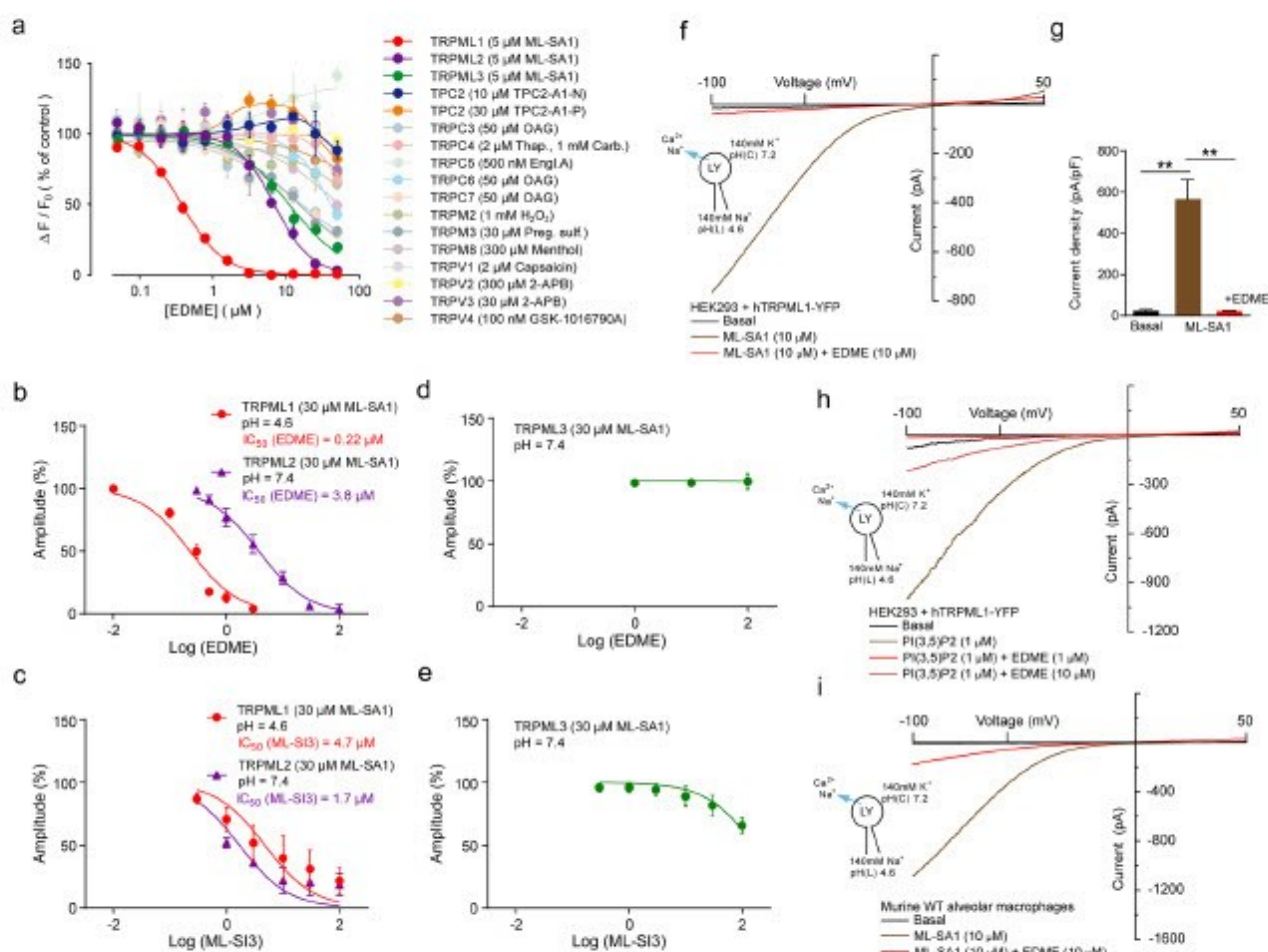
Figure 2. EDME is a potent and selective blocker of TRPML1. (**a**) Representative concentration-effect relationships for Ca²⁺ increases (Fluo-4) in response to different concentrations of EDME on HEK293 cells stably expressing different TRP channels including hTRPML1ΔNC, 2, 3, or TPC2, respectively. Corresponding activators for each TRP channel are listed in parentheses. (**b–e**) Concentration-effect relationships obtained from whole-cell patch-clamp measurements showing effect of EDME (**b, d**) and the previously described non-selective TRPML blocker ML-SI3 (**c, e**) on hTRPML1L15/16A, L577/578A (pH 4.6; n = 6, each), hTRPML2 (pH 7.4; n = 4, each), and hTRPML3 (pH 7.4; n = 3, each) in the presence of 30 μM ML-SA1. Current recording was done with WinWCP5.2.7 (University of Strathclyde, UK) software, and analysis was done with the help of a customized Igor pro program (WaveMetrics). (**f**) Endolysosomal patch-clamp experiment showing effect of EDME on WT hTRPML1 after activation with ML-SA1 (10 μM). (**g**) Statistical analysis for experiments as shown in (**f**) (luminal pH 4.6; n = 3, each). P-values were calculated by one-way ANOVA followed by Tukey's post hoc test. **p-value < 0.01. (**h**) Endolysosomal patch-clamp experiment showing effect of EDME on WT hTRPML1 after activation with the endogenous ligand PI(3,5)P₂ (1 μM). (**i**) Endolysosomal patch-clamp experiment showing effect of EDME (10 μM) on TRPML1 endogenously expressed in mouse alveolar macrophages after activation with ML-SA1 (10 μM). All endolysosomal patch-clamp experiments were analyzed using PatchMaster acquisition software (https://www.heka.com/) and OriginPro 6.1 (https://www.originlab.com/). All statistical analysis was done using GraphPadPrism software (https://www.graphpad.com/scientific-software/prism/).

whereas all other EDME analogues with a 17β hydroxyl group were identified as potent inhibitors of TRPML1 with IC₅₀ values below 1 μM (Table S1). PRU-8, PRU-9, PRU-10, and PRU-12 showed a further improved selectivity profile compared to EDME (Fig. 4h–j,l).

Effect of EDME and analogs at estrogen receptor alpha. To assess the effect of EDME and its synthetic analogs at ERα, we performed a yeast estrogen receptor assay used to determine the relative transactivation activity of the human ERα in response to test substances as previously described[35]. Briefly, Saccharomyces cerevisiae stably transfected with a human ERα construct and an estrogen responsive element fused to the reporter gene lacZ encoding for β-galactosidase were treated with the test substances. We found that PRU-2, PRU-10 and PRU-12 had relatively low efficacy at ERα while EDME and the other analogs had comparably strong effects (Fig. 5). PRU-2, the 17α-epimer of EDME, showed the desired low efficacy at ERα, but since it had a much higher
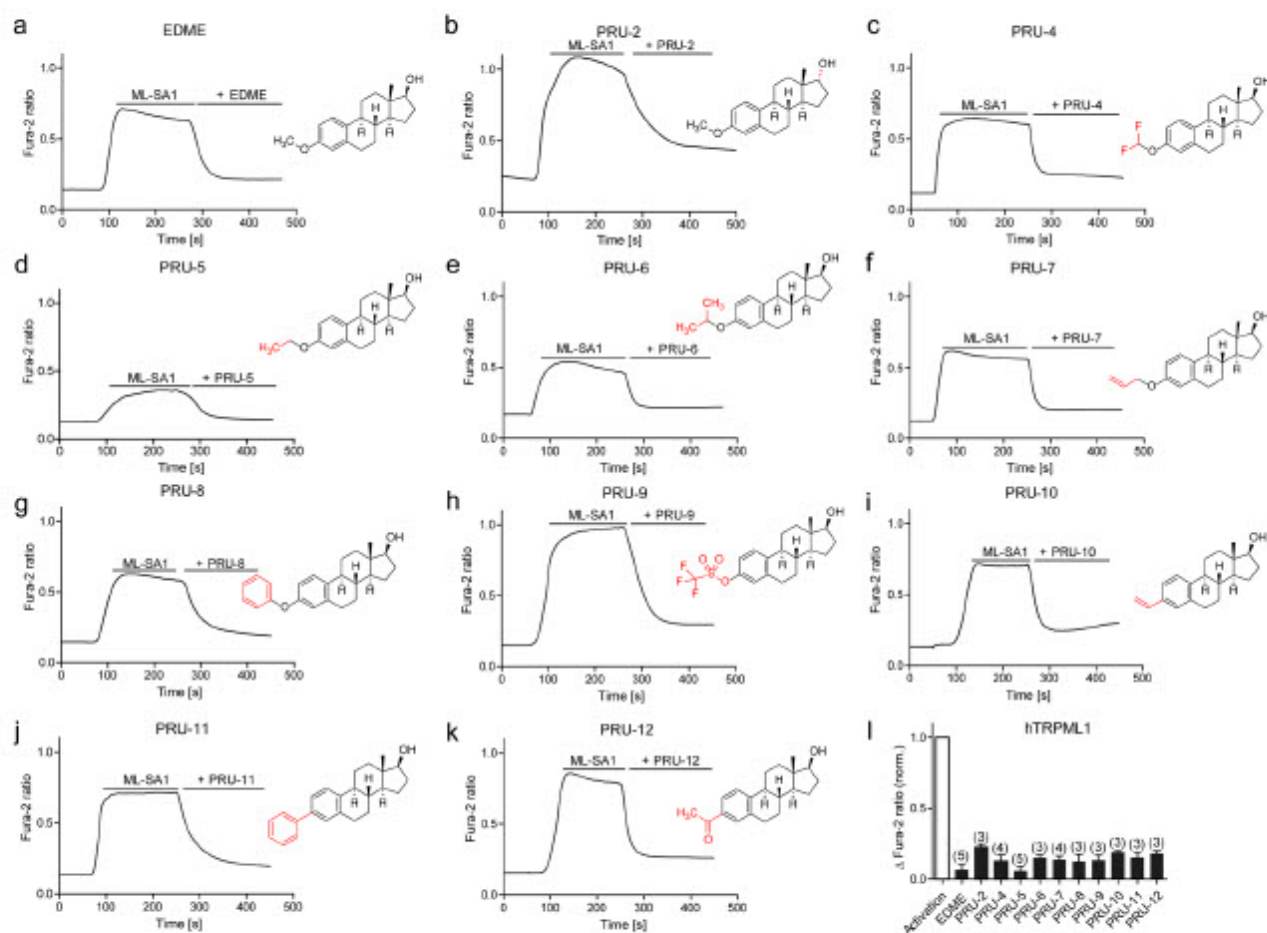
Figure 3. EDME and analogs in Fura-2 single cell calcium imaging experiments. (**a–k**) Representative Fura-2 calcium signals recorded from HEK293 cells stably expressing hTRPML1ΔNC-YFP. Cells were stimulated with ML-SA1 (10 μM), then treated with EDME and analogs (10 μM, each). Characteristic structural motifs of the EDME analogs are highlighted in red in the structures. (**l**) Statistical analysis of the maximal change in Fura-2 ratio (mean ±SEM) with the number of independent experiments in parentheses (with 5–12 cells in each experiment). Data were normalized to the maximal effect of the agonist ML-SA1.

IC_{50} (14 μM) for TRPML1 compared to EDME this compound was not further considered. PRU-8 showed a very good selectivity profile for TRPMLs, but unfortunately a strong effect at ERα, whereas PRU-10 and PRU-12 showed both a low ERα activity and a good TRPML isoform selectivity profile. In the following experiments, we therefore focused on EDME, PRU-10, and PRU-12.

Effect of EDME and selected analogs on autophagy and TFEB translocation. TRPML1 plays a major role in autophagy and starvation-stimulated TFEB nuclear translocation[10,11]. Indeed, cells from Mucolipidosis type IV (MLIV) patients show a delayed fusion of autophagosomes with late endosomes/lysosomes and alterations in TFEB shuttling[10,36,37]. In order to evaluate the efficacy of the novel compounds on TRPML1 functions we tested their effects on TFEB dephosphorylation and autophagic flux. As previously demonstrated for other, non-selective inhibitors, treatment with EDME reduced TFEB molecular downshift induced by nutrient starvation (Figs. 6a,b and S3). In order to evaluate lysosome-dependent degradation of autophagic material, we treated cells with EDME, PRU-10, and PRU-12 in combination with bafilomycin A1, a potent V-ATPase inhibitor[38]. Cells treated with TRPML1 inhibitors behaved similarly to MLIV patient fibroblasts which lack functional TRPML1 (Figs. 6c and S3). No increase in LC3 compared to vehicle (DMSO) was found, suggesting an impairment in the induction of autophagy upon starvation (Figs. 6d–f and S3). EDME and PRU-12 had the strongest effects, showing efficacy at as low as 1 μM. For PRU-10 a higher effective concentration was needed (3 μM). Estradiol showed effects when a concentration of 10 μM was applied. Concentrations of 10 nM or 1 μM showed no effect (Figs. 6g–h and S3). Taken together, these results demonstrate functional efficacy of EDME and analogs in blocking endogenous TRPML1 activity in intact cells, establishing them as suitable tools for cellular assays.
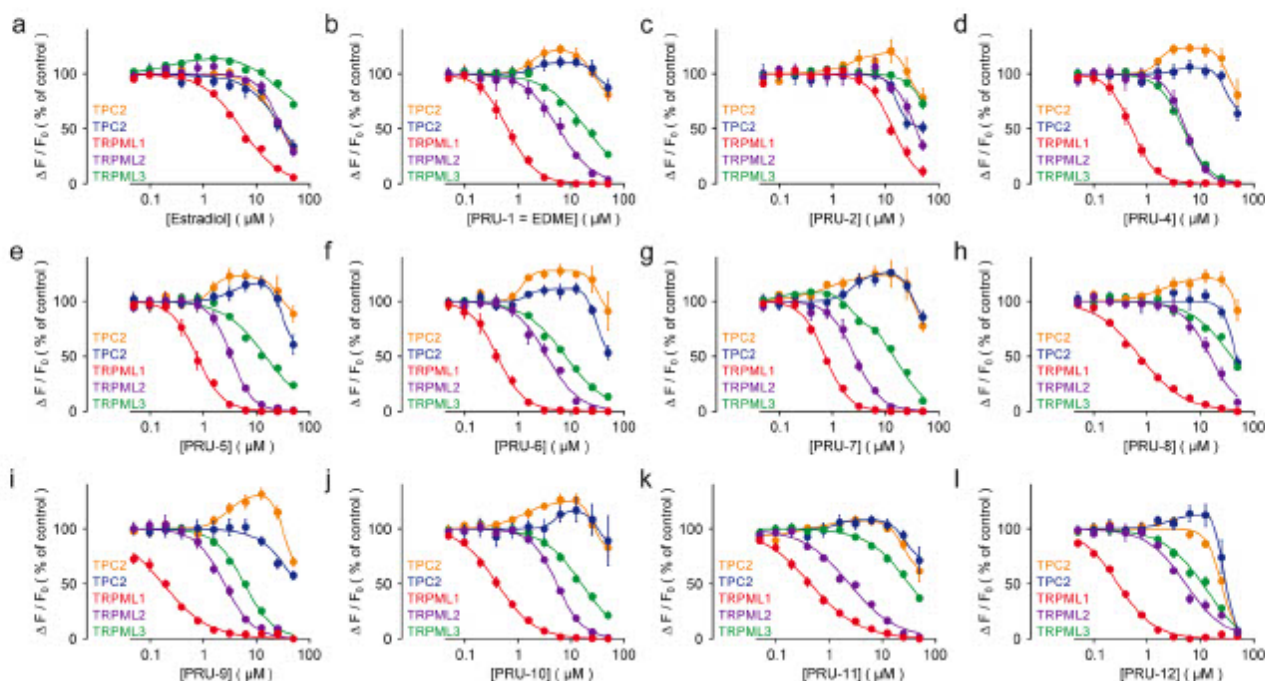
Figure 4. Estradiol, EDME and analogs in Fluo-4 calcium imaging experiments. (a–l) Concentration-effect relationships for Ca^{2+} increases (Fluo-4) in response to different concentrations of EDME, estradiol and analogs on HEK293 cells stably expressing hTRPML1ΔNC-YFP, hTRPML2-YFP, hTRPML3-YFP or hTPC2L11A/L12A-RFP[22,34]. Cells were activated with ML-SA1 (5 μM) for TRPMLs or TPC2-A1-N (10 μM; blue) and TPC2-A1-P (30 μM; orange) for hTPC2. Data are calculated from 3 to 5 independent experiments, each, and represented as means ± SEM. IC$_{50}$ values are presented in Table S1.

Effect of EDME and selected analogs on breast cancer cell migration and invasion. The MDA-MB-231 human breast cancer cell line is one of the most commonly used breast cancer cell lines in medical research. MDA-MB-231 is a highly aggressive, invasive and poorly differentiated triple-negative breast cancer (TNBC) cell line. It lacks estrogen and progesterone receptor expression as well as HER2 (human epidermal growth factor receptor 2) amplification. Knockdown of TRPML1 has been reported before to result in reduced migration and invasion of MDA-MB-231 cells[35]. We used EDME to show reduction in migration and invasion, and we generated TRPML1 KO cell lines using CRISPR/Cas9 to confirm involvement of TRPML1 and on-target effect of EDME. At the same time the lack of estrogen receptor was used to confirm estrogen receptor independent efficacy of EDME. Two TRPML1 KO cell lines (KO1 and KO2) were generated and loss of TRPML1 was confirmed by qRT-PCR and by endolysosomal patch-clamp experimentation (Fig. 7a–d). As shown before in overexpressing HEK293 cells and in endogenously expressing alveolar macrophages, EDME inhibits TRPML1 activation with ML-SA1. Both KO cell showed complete lack of activation by ML-SA1, suggesting absence of TRPML1 but also TRPML2 and TRPML3, which would likewise be activated by the non-selective TRPML-agonist ML-SA1. This was further confirmed by qRT-PCR analysis (Fig. 7e). We next assessed the effect of EDME on migration and invasion of MDA-MB-231 cells. Invasion was found to be significantly reduced after application of EDME at various concentrations (Fig. 7f–h). Effects were comparable to those seen in MDA-MB-231 TRPML1 KO cells (KO1 and KO2). Importantly, the effect was not further reduced in KO cells, indicating on-target activity of EDME (Fig. 7f,g). Like invasion migration was also reduced significantly after application of EDME at various concentrations (Fig. 7i,j). In sum these experiments confirmed estrogen receptor independent and TRPML1-mediated activity of EDME.

Discussion

We describe here the first in-class TRPML1-selective inhibitors, which are blocking endogenously expressing TRPML1 and efficiently interfere with major functional activities of TRPML1, autophagy regulation and TFEB translocation to the nucleus. Autophagy is a vital process, involved in various diseases such as neurodegenerative, metabolic and infectious diseases as well as cancer. Both reduced and increased autophagy can impact disease. Autophagy is regulated by many factors including glucose, growth factors, amino acids, or starvation and energy status. The elimination of unwanted protein aggregates and damaged organelles is essential to avoid cell damage, e.g. damage to neurons and other brain cells, resulting eventually in a neurodegenerative processes. Pharmacological activation of autophagy processes has been propagated for the treatment of metabolic diseases such as obesity (activation of liver autophagy) or neurodegenerative diseases caused by the accumulation of inclusions or aggregates of different proteins as in the case of Parkinson's, Huntington's, or Alzheimer's disease to enhance clearance and to prevent cell death. In cancer, autophagy seems to function as a tumor suppressor
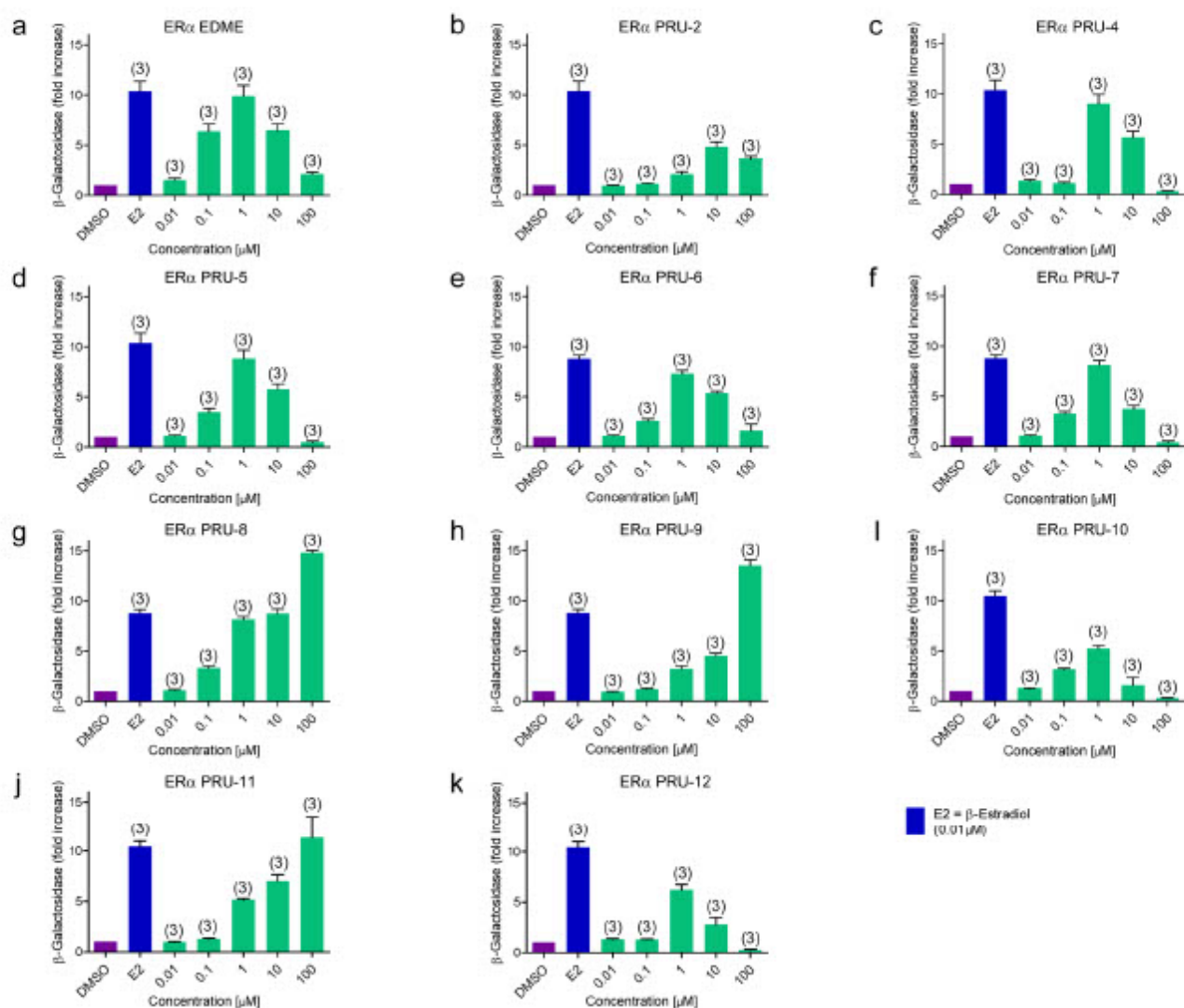
Figure 5. Activity at ERα of EDME and analogs. (**a–k**) Shown are effects of EDME and analogs at the estrogen receptor alpha (ERα) in *Saccharomyces cerevisiae* stably transfected with ERα, with the number of independent experiments in parentheses. The weakest effects at ERα were found for PRU-2, PRU-10, and PRU-12.

that prevents tumor initiation but also as a pro-survival factor helping tumor cells to endure metabolic stress and to avoid cell death triggered by chemotherapeutics[39]. Despite this diametrically opposed role autophagy might play in cancer, several inhibitors of the autophagic machinery are in preclinical development[40]. TFEB is a master regulator of autophagy by promoting expression of genes involved in autophagy, it also regulates lysosomal biogenesis, lysosomal exocytosis, lysosomal positioning and energy metabolism. Lysosomal Ca^{2+} release through TRPML1 activates calcineurin, which binds and dephosphorylates TFEB, thus promoting its nuclear translocation[10] while phosphorylated TFEB remains inactive in the cytosol. Here, we demonstrate efficacy of the estradiol-derived TRPML1 antagonist EDME and analogs, which were rationally designed based on a profound SAR analysis of numerous tested steroidal compounds, on autophagy and TFEB translocation as well as breast cancer cell migration and invasion. To confirm that these effects were estrogen receptor independent we used the estrogen receptor negative MDA-MB-231 human breast cancer cell line. In sum, we identified novel potent and selective inhibitors for TRPML1, which effectively block autophagy and TFEB translocation as well as migration and invasion of TRPML1 endogenously expressing cells. Despite some activity of EDME at ERα, the experiments in ER negative MDA-MB-231 breast cancer cells demonstrate estrogen receptor independent effects of EDME similar to effects seen in TRPML1 KO MDA-MB-231 cells. Furthermore, we have generated the EDME analogs PRU-10 and PRU-12, which show comparable TRPML isoform selectivity but further reduced efficacy at ERα.

Materials and methods

Compound screening and generation of concentration response curves.

To identify inhibitors of TRPML1 and TRPML3, the Spectrum Collection compound library (MS Discoveries; 2000 compounds) and additional 430 bioactive compounds were screened. To this end, fluorometric Ca^{2+} influx assays were performed
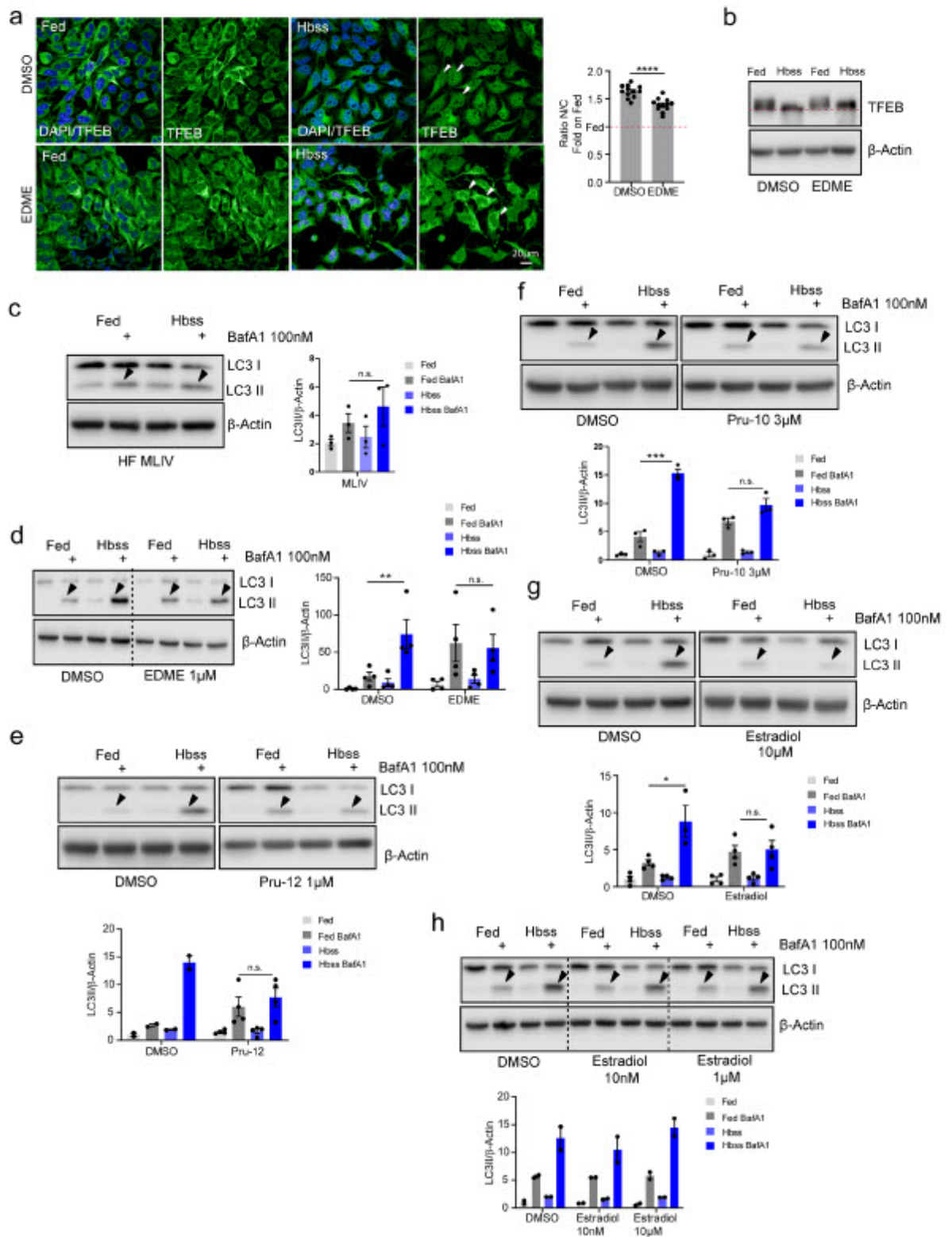
◄**Figure 6.** Effect of EDME and selected analogs on autophagy and TFEB nuclear translocation. (**a**) Representative confocal images of endogenous TFEB in HeLa cells treated with DMSO and EDME (1 µM) in complete media (Fed) or Hbss (nutrient starved media). The plot represents the TFEB nuclear to cytosol ratio and values are expressed as fold induction on Fed. Values are means ± SEM of n = 300 cells per condition, pooled from two independent experiments. (**b**) Representative image of immunoblot analysis of endogenous TFEB in human fibroblasts treated with DMSO and EDME (1 µM) in Fed and Hbss. The red dashed line highlights TFEB molecular downshift. (**c**) Representative image of immunoblot analysis of endogenous LC3 in MLIV patients' fibroblasts treated with Fed and Hbss alone or in the presence of BafA1 (bafilomycin A1). Plot shows the densitometry of LC3II band normalized to actin. The data in the graphs are mean values ± SEM, n = 3 lysates per condition pooled from 3 independent experiments. (**d–h**) Representative image of immunoblot analysis of endogenous LC3 in human fibroblasts wild type treated with DMSO, EDME 1 µM, PRU-12 1 µM, PRU-10 3 µM and estradiol (10 µM, 1 µM, and 10 nM) in Fed and Hbss alone or in the presence of BafA1. Plot shows the densitometry of LC3II band normalized to actin. The data in the graphs are mean values ± SEM, n = 2–4 lysates per condition pooled from 2 to 4 independent experiments. P-values were calculated by two-tailed Student's t-test. *p-value < 0.05; **p-value < 0.01. All statistical analysis was done using GraphPadPrism software (https://www.graphpad.com/scientific-software/prism/).

by using the calcium dye Fluo-4/AM (Invitrogen, Thermo Fisher Scientific, Waltham, MA, USA) and a custom-made fluorescence imaging plate reader built into a robotic liquid handling station (Freedom Evo 150, Tecan, Männedorf, Switzerland). All measurements were done in a HEPES buffered solution (HBS), containing 132 mM NaCl, 6 mM KCl, 1 mM $MgCl_2$, 1 mM $CaCl_2$, 5.5 mM D-glucose, 10 mM HEPES, pH 7.4. Screening compounds dissolved in DMSO (10 mM) were prediluted in 150 mM NaCl, 20 mM HEPES, pH 7.4, to a concentration of 200 µM. For primary screens, HEK293 stably expressing plasma membrane-targeted TRPML1 or TRPML3 were trypsinized and resuspended in cell culture medium supplemented with 4 µM Fluo-4/AM. After incubation at 37 °C for 30 min, the cell suspension was briefly centrifuged resuspended in HBS, and dispensed into black pigmented, clear-bottom 384-well microwell plates (Greiner µClear, Frickenhausen, Germany). Plates were placed into the FLIPR and fluorescence signals (excitation 470 nm, emission 515 nm) were recorded with a Zyla 5.5 camera (Andor, Belfast, UK) and the µManager software like previously described[41]. In a first video, compound libraries were successively added to the cells with the Tecan 96-tip multichannel arm to a final concentration of 20 µM to map unspecific effects like autofluorescence or toxicity. In a second step the agonist ML-SA1 was pipetted in each well and fluorescence signals were recorded for 10 min. Analyses were done by calculating fluorescence intensities for each well and background areas with ImageJ (National Institutes of Health, Bethesda, MD, USA). Finally, the background was subtracted and the fluorescence intensities were normalized to initial intensities (F/F0). Concentration response curves were generated by the same procedure but compounds were manually prediluted in 96-well plates containing HBS, now supplemented with 0.1% bovine serum albumin. Here data was fitted to a four-parameter Hill equation to obtain Imin, Imax, IC_{50}), and the Hill coefficient n.

Synthesis of compounds. EDME analogs were prepared starting from commercially available 17β-estradiol (E2) and 17α-estradiol (alfatradiol) as described in detail in the Supporting Information. All compounds were fully characterized by ^{1}H- and ^{13}C-NMR, IR and HRMS data.

Whole-cell patch-clamp experiments. For whole-cell patch-clamp experiments tetracycline-inducible hTRPML1L15/16A, L577/578A, hTRPML2 and TRPML3 HEK293 cell lines were used, generated by ICAGEN Inc. using the FLP-in-Tet-On system. Experiments were performed as described previously[20,42]. In brief, cells were cultured on coverslips (Fisherbrand, Fisher Scientific) in complete DMEM medium with 10% FBS (Thermo Fisher). HEK293 cells expressing the desired channel protein were patch-clamped after overnight induction with tetracycline (1 µg/mL). Patch-clamp pipettes were pulled from glass capillaries (Sutter Instrument) using a micropipette puller (P-87; Sutter Instrument) and had a resistance of 3–5 MΩ when filled with the pipette solution. The pipette solution contained (mM) 122 Cs-methanosulfonate, 4 NaCl, 10 EGTA, 2 Na-ATP, 2 $MgCl_2$ and 20 HEPES, pH 7.2 (with CsOH). The standard bath solution contained (mM) 153 NaCl, 5 KCl, 2 $CaCl_2$, 1 $MgCl_2$, 20 HEPES and 10 Glucose (pH 7.4 with NaOH). The low pH bath solution contained (mM) 150 Na-Gluconate, 5 KCl, 2 $CaCl_2$, 1 $MgCl_2$, 10 glucose, 10 HEPES and 10 MES (pH 4.6). Whole-cell currents were recorded using a Multiclamp 700B amplifier (Molecular Devices) with low-pass filtering at 3 kHz. The currents were digitized at a sampling frequency of 10 kHz using BNC-2110 and PCI-6221 with NI-DAQmx (National Instruments) and stored directly to a hard drive. Current recording was done with WinWCP5.2.7 (University of Strathclyde, UK) software, and analysis was done with the help of a customized Igor pro program (WaveMetrics). The current was recorded by 1 s rapid alterations of membrane potential (RAMP) from − 100 to + 100 mV from a holding potential of 0 mV. RAMPs were spaced at 4-s intervals. The current recorded at − 100 mV was used for current measurement. Concentration–response curves were fitted by using the model where X is the concentration and Y is the normalized response $Y = 100/(1 + 10^{(X-LogIC50)})$.

Endolysosomal patch-clamp experiments. For whole-LE/LY manual patch-clamp recordings, cells were treated with 1 µM vacuolin-1 (>2 h) at 37 °C and 5% CO_2 and experiments performed as described previously[19,25]. Compound was washed out before patch-clamp experimentation. Currents were recorded using an EPC-10 patch-clamp amplifier (HEKA, Lambrecht, Germany) and PatchMaster acquisition software (https://www.heka.com/). Data were digitized at 40 kHz and filtered at 2.8 kHz. Fast and slow capacitive transients were cancelled by the compensation circuit of the EPC-10 amplifier. All recordings were obtained at room tem-
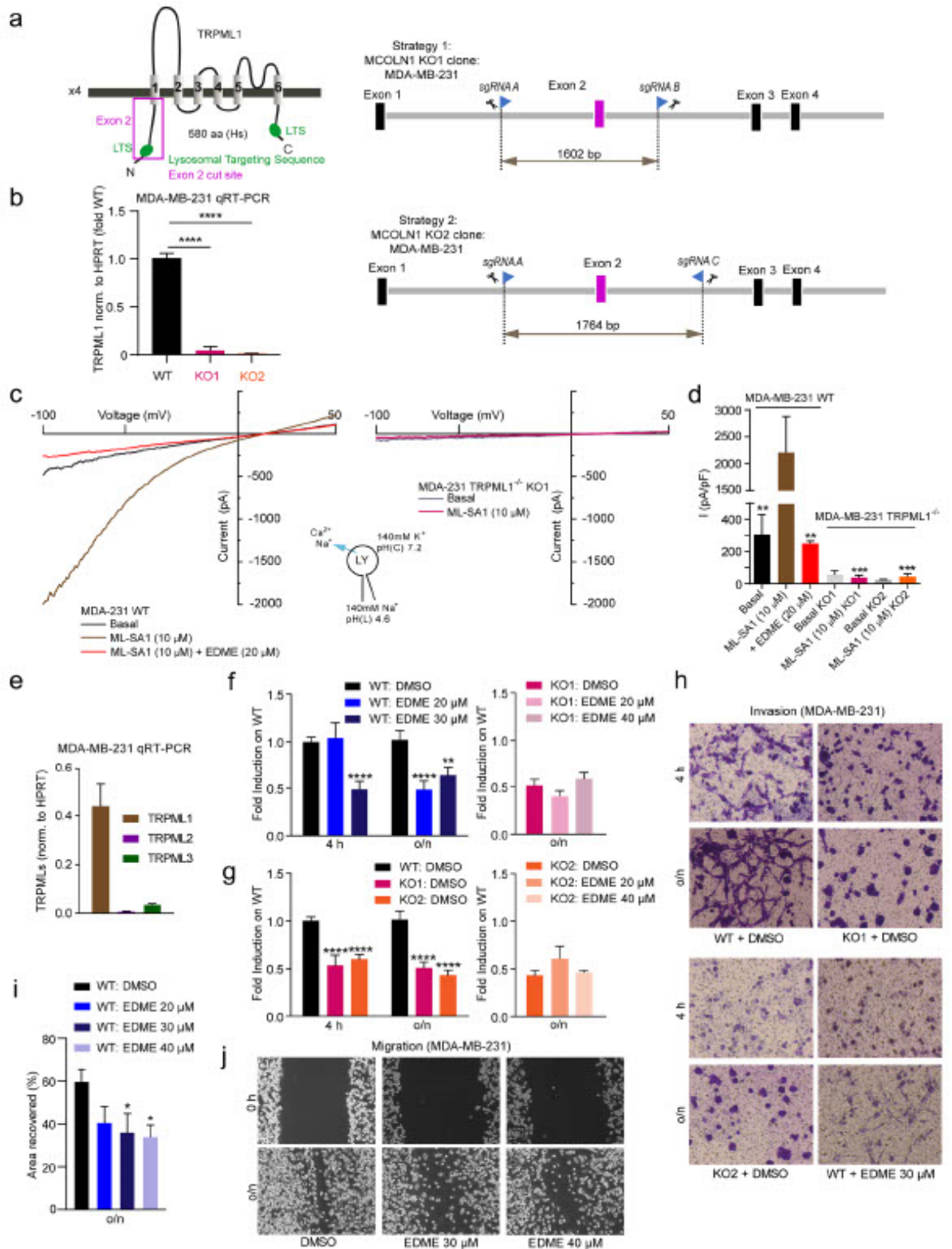
◄**Figure 7.** Effect of EDME on ER- breast cancer (MDA-MB-231) cell migration and invasion. (**a**) Genetic ablation of human MCOLN1 (TRPML1) in MDA-MB-231 cells was created by using two CRISPR/Cas9 strategies targeting Exon 2, resulting in KO1 and KO2. For further details see Methods section. Validation was performed by endolysosomal patch-clamp experimentation and by quantitative PCR analysis. (**b**) qRT-PCR results showing expression levels of TRPML1 in WT, KO1, and KO2 MDA-MB-231 cell lines. (**c**) Representative current densities measured from vacuolin-enlarged endo-lysosomes isolated from WT and KO1 MDA-MB-231 cells. (**d**) Statistical analysis for experiments as shown in c (n = 3, each). (**e**) qRT-PCR results showing expression levels of TRPML1, 2, and 3 in WT MDA-MB-231 cells. (**f–g**) Invasion assay using transwell chambers. Statistical analysis of experiments as presented in (**h**) (n = 3, each). Statistical significance was determined by two-way ANOVA followed by Bonferroni multiple comparison test. **p-value < 0.01; ***p-value < 0.0001. (**h**) Shown are representative images for WT MDA-MB-231 cells and the two TRPML1$^{-/-}$ MDA-MB-231 cell lines KO1 and KO2 at 4 h and after o/n treatment, treated with either DMSO (control vehicle) or EDME at different concentrations. (**i, j**) Migration/wound healing scratch assay experiments. Shown in i is the statistical analysis of experiments as presented in (**j**) at various concentrations of EDME compared to DMSO (n = 3, each). Statistical significance was determined by one-way ANOVA followed by Bonferroni multiple comparison test. *p-value < 0.05. Shown in j are representative images for WT MDA-MB-231 cells at 0 h and after o/n incubation post scratch, treated with either the control vehicle (DMSO) or EDME at different concentrations. All statistical analysis was done using GraphPadPrism software (https://www.graphpad.com/scientific-software/prism/).

perature and were analyzed using PatchMaster acquisition software (https://www.heka.com/) and OriginPro 6.1 (https://www.originlab.com/). Recording glass pipettes were polished and had a resistance of 4–8 MΩ. For all experiments, salt-agar bridges were used to connect the reference Ag–AgCl wire to the bath solution to minimize voltage offsets. Liquid junction potential was corrected. For the application of the small molecule inhibitors/flavonoids, cytoplasmic solution was completely exchanged by cytoplasmic solution containing compound. The current amplitudes at − 100 mV were extracted from individual ramp current recordings. Unless otherwise stated, cytoplasmic solution contained 140 mM K-MSA, 5 mM KOH, 4 mM NaCl, 0.39 mM CaCl$_2$, 1 mM EGTA and 10 mM HEPES (pH was adjusted with KOH to 7.2). Luminal solution contained 140 mM Na-MSA, 5 mM K-MSA, 2 mM Ca-MSA, 1 mM CaCl$_2$, 10 mM HEPES and 10 mM MES (pH was adjusted with methanesulfonic acid to 4.6). In all experiments, 500-ms voltage ramps from -100 to + 100 mV were applied every 5 s. All statistical analysis was done using GraphPadPrism software.

Transfection, cell culture and calcium imaging.   Single cell Ca^{2+} imaging experiments were performed using Fura-2 as previously described[42]. HEK293 cells stably expressing hTRPML1ΔNC-YFP, hTRPML2-YFP, hTPPML3-YFP or hTPC2L11A/L12A-RFP (22, 24) were cultured at 37 °C with 5% of CO$_2$ in Dulbecco's modified Eagle medium (Thermo Fisher), supplemented with 10% fetal bovine serum, 100 U/mL penicillin, and 0.1 mg/mL streptomycin. Cells were plated onto poly-L-lysine (sigma)-coated glass coverslips and grown for 2–3 days. For Ca^{2+} imaging experiments cells were loaded for 1 h at room temperature with Fura-2 AM (4.0 μM) and 0.005% (v/v) pluronic acid (both from Thermo Fisher) in HEPES-buffered solution (HBS) comprising 138 mM NaCl, 6 mM KCl, 2 mM MgCl$_2$, 2 mM CaCl$_2$, 10 mM HEPES, and 5.5 mM D-glucose (adjusted to pH 7.4 with NaOH). After loading, cells were washed with HBS and mounted in an imaging chamber. All recordings were performed in HBS. Ca^{2+} imaging was performed using a Leica DMi8 live cell microscope. Fura-2 was excited at 340 nm/380 nm. Emitted fluorescence was captured using 515 nm long-pass filter. Compounds were pre diluted in DMSO and stored as 10 mM stock solutions at − 20 °C, not exceeding three months. Working solutions were prepared directly before using by dilution with HBS.

For endolysosomal patch-clamp experiments murine alveolar macrophages were prepared and cultured as described recently[22,25]. The human TRPML2-YFP stable cell line was generated as described previously[42].

MDA-MB-231 cell culture and genetic ablation of human MCOLN1 (TRPML1).   MDA-MB-231 cells were grown in high glucose DMEM, supplemented with 10% FBS (Thermo Fisher), and 1% penicillin–streptomycin (Sigma-Aldrich). Cell lines were maintained at 37 °C in a 5% CO$_2$ incubator. The following guide RNAs (Metabion) were designed to target Exon 2 of the human MCOLN1 gene using CRISPOR software (http://crispor.tefor.net/): sgRNA A: 5′-GGGTCCCAGCTACTAACTAC-3′; sgRNA B: 5′-GTGCAGCCATTGGGT CAACA-3′; sgRNA C: 5′-GAAAAGGGACCCAATTGTCC-3′. Approximately 3 × 105 MDA-MB-231 cells were seeded in 6-well plates (Sarstedt). The cells were co-transfected with two combinations of sgRNAs: A + B and A + C, using Lipofectamine 3000 (Themo Fisher) reagent, according to the manufacturer's instructions. Antibiotic selection with Puromycin and Blasticidin (Gibco) was carried out for 72 h, followed by single cell dilution and clonal expansion of cells in collagen-coated 96-well plates (Sarstedt). The clones were screened and validated through several methods: first, gDNA isolation (PureLink Genomic DNA Mini Kit, Thermo Fisher), PCR (Q5 High-Fidelity DNA Polymerase, NEB) and agarose gel electrophoresis; second, isolation of RNA (Rneasy Mini Kit, Qiagen), cDNA synthesis (RevertAid First Strand cDNA synthesis kit, Thermo Fisher) and qPCR (LightCycler 480 SYBR Green I Master, Roche Life Science); third, measuring TRPML1 channel activity via the endolysosomal patch clamp technique. The strategy insured the genetic knockout of Exon 2 of human MCOLN1, its first transmembrane domain, the lysosomal targeting sequence (LTS), and a pre-mature stop codon creating a frameshift mutation.

Estrogen receptor assay.   The yeast estrogen receptor assay (YES-assay) was provided by Dr. J.P. Sumpter (Brunel University, Uxbridge, UK; Routledge & Sumpter, 1996) and was used to determine the relative trans-

activation activity of the human ERα in response to test substances as previously described[35]. Briefly, *Saccharomyces cerevisiae* stably transfected with a human ERα construct and an estrogen responsive element fused to the reporter gene lacZ encoding for β-galactosidase were treated with the test substances for 48 h. The β-galactosidase enzymatic activity was measured in a colorimetric assay using the substrate chlorophenol red β-D-galactopyranoside (Roche Diagnostics, Mannheim Germany). Formation of chlorophenol red was measured at 540 nm. For the test, all compounds were diluted in DMSO. 17β-estradiol (10 nM; Sigma, Deisenhofen, Germany) served as positive control and DMSO was used as vehicle control. All compounds, were dose dependently tested in a concentration range of 0.01–100 µM, using technical quadruplicates and biological triplicates.

Autophagy assays and TFEB shift. 5×10^4 wild-type human fibroblasts were seeded in a 12-well plate and treated overnight with DMSO or different TRPML1 inhibitors (EDME, PRU-10, PRU-12). The day after, cells were treated for 3 h in full media (Fed) or HBSS supplemented with 10 mM HEPES (nutrient starved) in presence of DMSO or different TRPML1 inhibitors (EDME, PRU-10, PRU-12). For autophagic flux experiments, cells were co-treated with 100 nM of bafilomycin A1 (Sigma).

Total cell lysates were prepared using TRIS HCl 10 mM pH 8.0 and 0.2% SDS supplemented with protein and phosphatase inhibitors (Sigma). Protein concentration was determined using the Bradford method. After SDS–polyacrylamide gel electrophoresis (PAGE) and immunoblotting, the protein recognized by the specific antibody was visualized by chemiluminescence methods (Luminata Crescendo Western HRP substrate, Millipore) using HRP-conjugated anti-rabbit or anti-mouse secondary antibodies (Cell Signalling). Images were acquired using Li-Cor Odyssey Fc Imaging System and densitometric quantification of unsaturated images was performed using ImageJ software (NIH). Uncropped and unprocessed western blot scans are provided as Fig. S1. The following primary antibodies were used: LC3 (Novus Cat. No. NB100-2220, 1:1000 in 5% milk), TFEB (Cell Signaling Cat. No. 4240, 1:1000 in 5% BSA) and β-actin (Santa Cruz Cat. No. Sc-47778, 1: 1000 in 5% BSA).

Wound healing/migration and invasion assays. Wound healing assay was performed using 12-well plates (Sarstedt) at full confluency. Cells were incubated overnight (serum-free), and a scratch was performed using a yellow pipet tip. Pictures were taken at 0 h and after over night (o/n) incubation using an inverted microscope (Leica DM IL LED) and using a microscope camera (Leica DFC 3000 G). The wounded cell area was quantified using ImageJ 1.52a software and was subtracted from 0 h values.

For invasion measurements transwell chambers in 24-well permeable support plates (Corning, #3421) were coated with Corning Matrigel basement membrane matrix (Corning, #354234) for 1.5 h. A total of 4×10^4 MDA-MB-231 WT and TRPML1 KO cells were seeded on top of the chambers in serum-free medium, and direct stimulation with EDME was performed. The lower compartment contained the chemotactic gradient, medium with 10% FBS. Cells were allowed to migrate for 4 h and o/n, and were then fixed and stained with crystal violet containing methanol. Non-invaded cells were removed with Q-tips and pictures were taken of the bottom side of the membrane using an inverted microscope (Olympus CKX41) and an Olympus SC50 camera (Olympus). The number of invaded cells was quantified using ImageJ 1.52a software.

RNA isolation and quantitative PCR. Total RNA was isolated from cells using the RNeasy Mini Kit (Qiagen). Reverse Transcription was performed using the Revert First Strand cDNA Synthesis Kit (Thermo Fisher). Real-time quantitative Reverse Transcription PCR (qPCR) was performed in triplicates for each sample using LightCycler 480 SYBR Green I Master and using the LightCycler 480 II machine (Roche Life Science), following the recommended parameters. HPRT was used as the housekeeping gene. The following human primer sets were used: HPRT; fw: 5′-TGGCGTCGTGATTAGTGATG-3′, rev: 5′-AACACCCTTTCCAAATCCTCA-3′; MCOLN1: fw: 5′-TCTTCCAGCACGGAGACAAC-3′, rev: 5′-GCCACATGAACCCCACAAAC-3′; MCOLN2: fw: 5′-AACGGTGTTTCCTGTTCCGA-3′, rev: 5′-GCCATTGCATTTCTGACG GTTA-3′; MCOLN3: fw: 5′-TGCTTCTGTGGATGGATCG-3′, rev: 5′-GAGACCATGTTC AGAGAACG-3′; TPCN1: fw: 5′-TCCCAA AGCGCTGAGATTAC-3′, rev: 5′-TCTGGTTTGAG CTCCCTTTC-3′; TPCN2: fw: 5′-GTACCCCTCTTGTGT GGACG-3′, rev: 5′-GGCCCTGACA GTGACAACTT-3′.

TFEB immunofluorescence. 3.5×10^4 HeLa cells were seeded in a 24-well plate and treated overnight with DMSO or EDME 1 µM. The day after, cells were treated for 3 h in full media (Fed) or HBSS supplemented with 10 mM HEPES (nutrient starved) in presence of DMSO or EDME 1 µM. Cells were fixed in PFA 4% 10′ and permeabilized 7′ with PBS 1X and 0.02% Triton-X. TFEB antibody (Cell Signaling Cat. No. 4240, 1:100 overnight) and Goat anti-Rabbit IgG (H + L) Secondary Antibody, Alexa Fluor 488 (ThermoFisher, 1:400 45′) were applied in blocking buffer saponin (1% BSA, 0.05% saponin and 50 mM NH4Cl in PBS1X). Samples were examined under a Zeiss LSM 880 confocal microscope. Optical sections were obtained under a 40× immersion objective at a definition of 1024 × 1024 pixels (average of 8 scans), adjusting the pinhole diameter to 1 Airy unit for each emission channel to have all the intensity values between 1 and 254 (linear range). TFEB nuclear and cytoplasmic intensity was measured on unsaturated images using ImageJ software (NIH). The value reported is a ratio value resulting from the average intensity of nuclear TFEB fluorescence divided by the cytosolic intensity of TFEB fluorescence.

Statistical analysis. Details of statistical analyses and n values are provided in the Materials and Methods or the Figures or Figure legends. Statistical analyses were carried out using GraphPadPrism software (https://www.graphpad.com/scientific-software/prism/). All error bars are depicted as mean ± SEM. Statistical significance is denoted on Figures as outlined in the legends.

Data availability

All data generated or analyzed during this study are included in this published article and its additional files.

References

1. Bargal, R. et al. Identification of the gene causing mucolipidosis type IV. Nat. Genet. 26, 118–123 (2000).
2. Bae, M. et al. Activation of TRPML1 clears intraneuronal Abeta in preclinical models of HIV infection. J. Neurosci. 34, 11485–11503 (2014).
3. Tsunemi, T. et al. Increased lysosomal exocytosis induced by lysosomal Ca(2+) channel agonists protects human dopaminergic neurons from alpha-synuclein toxicity. J. Neurosci. 39, 5760–5772 (2019).
4. Cheng, X. et al. The intracellular Ca(2)(+) channel MCOLN1 is required for sarcolemma repair to prevent muscular dystrophy. Nat. Med. 20, 1187–1192 (2014).
5. Yu, L. et al. Small-molecule activation of lysosomal TRP channels ameliorates Duchenne muscular dystrophy in mouse models. Sci. Adv. 6, e2736 (2020).
6. Capurro, M. I. et al. VacA generates a protective intracellular reservoir for Helicobacter pylori that is eliminated by activation of the lysosomal calcium channel TRPML1. Nat. Microbiol. 4, 1411–1423 (2019).
7. Chandra, M. et al. A role for the Ca²⁺ channel TRPML in gastric acid secretion, based on analysis of knockout mice. Gastroenterology 140, 857–867 (2011).
8. Sahoo, N. et al. Gastric acid secretion from parietal cells is mediated by a Ca²⁺ efflux channel in the tubulovesicle. Dev. Cell. 41, 262-273.e6 (2017).
9. Zhang, X. et al. MCOLN1 is a ROS sensor in lysosomes that regulates autophagy. Nat. Commun. 7, 12109 (2016).
10. Medina, D. L. et al. Lysosomal calcium signalling regulates autophagy through calcineurin and TFEB. Nat. Cell Biol. 17, 288–299 (2015).
11. Scotto Rosato, A. et al. TRPML1 links lysosomal calcium to autophagosome biogenesis through the activation of the CaMKKbeta/VPS34 pathway. Nat. Commun. 10, 5630 (2019).
12. Zhang, X. et al. Rapamycin directly activates lysosomal mucolipin TRP channels independent of mTOR. PLoS Biol. 17, e3000252 (2019).
13. Li, X. et al. A molecular mechanism to regulate lysosome motility for lysosome positioning and tubulation. Nat. Cell. Biol. 18, 404–417 (2016).
14. Erkhembaatar, M. et al. Lysosomal Ca(2+) signaling is essential for osteoclastogenesis and bone remodeling. J. Bone Miner. Res. 32, 385–396 (2017).
15. Bretou, M. et al. Lysosome signaling controls the migration of dendritic cells. Sci. Immunol. 2, 9573 (2017).
16. Goodridge, J. P. et al. Remodeling of secretory lysosomes during education tunes functional potential in NK cells. Nat. Commun. 10, 514 (2019).
17. Jung, J. et al. HRAS-driven cancer cells are vulnerable to TRPML1 inhibition. EMBO Rep. 20, e47953 (2019).
18. Kasitinon, S. Y. et al. TRPML1 promotes protein homeostasis in melanoma cells by negatively regulating MAPK and mTORC1 signaling. Cell Rep. 28, 2293–2305 (2019).
19. Chen, C. C. et al. A small molecule restores function to TRPML1 mutant isoforms responsible for mucolipidosis type IV. Nat. Commun. 5, 4681 (2014).
20. Grimm, C. et al. Small molecule activators of TRPML3. Chem. Biol. 17, 135–148 (2010).
21. Shen, D. et al. Lipid storage disorders block lysosomal trafficking by inhibiting a TRP channel and lysosomal calcium release. Nat. Commun. 3, 731 (2012).
22. Plesch, E. et al. Selective agonist of TRPML2 reveals direct role in chemokine release from innate immune cells. Elife 7, e39720 (2018).
23. Wang, W. et al. Up-regulation of lysosomal TRPML1 channels is essential for lysosomal adaptation to nutrient starvation. PNAS 112, E1373-1381 (2015).
24. Leser, C. et al. Chemical and pharmacological characterization of the TRPML calcium channel blockers ML-SI1 and ML-SI3. Eur J Med Chem. 24, 112966 (2020).
25. Gerndt, S. et al. Agonist-mediated switching of ion selectivity in TPC2 differentially promotes lysosomal function. Elife 9, e54712 (2020).
26. Pindur, U. & Schall, T. Proton acid-catalysed transformations of estrogen derivatives: New results and some mechanistic aspects of the Kober colour reaction. Arch. Pharm. 327, 637–642 (1994).
27. Triggle, D. J., Ridley, H. F. & DeMaio, D. M. Some 3-alkoxyestra-1,3,5(10)-trien-17-beta-ols. J. Med. Chem. 12, 346 (1969).
28. Tedesco, R., Thomas, J. A., Katzenellenbogen, B. S. & Katzenellenbogen, J. A. The estrogen receptor: A structure-based approach to the design of new specific hormone–receptor combinations. Chem. Biol. 8, 277–287 (2001).
29. Santra, S. & Guin, J. Enhanced reactivity of aerobic diimide olefin hydrogenation with arylboronic compounds: An efficient one-pot reduction/oxidation protocol. Eur. J. Org. Chem. 2015, 7253–7257 (2015).
30. Lin, X., Hou, C., Li, H. & Weng, Z. Decarboxylative trifluoromethylating reagent [Cu(O2 CCF3)(phen)] and difluorocarbene precursor [Cu(phen)2][O2 CCF2 Cl]. Chem. Eur. J. 22, 2075–2084 (2016).
31. Zafrani, Y., Sod-Moriah, G. & Segall, Y. Diethyl bromodifluoromethylphosphonate: A highly efficient and environmentally benign difluorocarbene precursor. Tetrahedron 65, 5278–5283 (2009).
32. Himeshima, Y., Sonoda, T. & Kobayashi, H. Fluoride-induced 1,2-elimination Ofo-trimethylsilylphenyl triflate to benzyne under mild conditions. Chem. Lett. 12, 1211–1214 (1983).
33. Hostetler, E. D., Jonson, S. D., Welch, M. J. & Katzenellenbogen, J. A. Synthesis of 2-[(18)F]Fluoroestradiol, a potential diagnostic imaging agent for breast cancer: strategies to achieve nucleophilic substitution of an electron-rich aromatic ring with [(18)F]F(-). J. Org. Chem. 64, 178–185 (1999).
34. Shi, Y. & Koh, J. T. Functionally orthogonal ligand-receptor pairs for the selective regulation of gene expression generated by manipulation of charged residues at the ligand-receptor interface of ER alpha and ER beta. J. Am. Chem. Soc. 124, 6921–6928 (2002).
35. Zierau, O. et al. Estrogenic activity of the phytoestrogens naringenin, 6-(1,1-dimethylallyl)naringenin and 8-prenylnaringenin. Planta Med. 68, 449–451 (2002).
36. Curcio-Morelli, C. et al. Macroautophagy is defective in mucolipin-1-deficient mouse neurons. Neurobiol. Dis. 40, 370–377 (2010).
37. Vergarajauregui, S., Connelly, P. S., Daniels, M. P. & Puertollano, R. Autophagic dysfunction in mucolipidosis type IV patients. Hum. Mol. Genet. 17, 2723–2737 (2008).
38. Ohkuma, S. et al. Inhibition of cell growth by bafilomycin A1, a selective inhibitor of vacuolar H(+)-ATPase. In Vitro Cell. Dev. Biol. Anim. 29A, 862–866 (1993).

39. Rubinsztein, D. C., Codogno, P. & Levine, B. Autophagy modulation as a potential therapeutic target for diverse diseases. *Nat. Rev. Drug. Discov.* 11, 709–730 (2012).
40. Perez-Hernandez, M. *et al.* Targeting autophagy for cancer treatment and tumor chemosensitization. *Cancers* 11, 1599 (2019).
41. Urban, N. & Schaefer, M. Direct activation of TRPC3 channels by the antimalarial agent artemisinin. *Cells* 9, 202 (2020).
42. Grimm, C., Jörs, S., Guo, Z., Obukhov, A. G. & Heller, S. Constitutive activity of TRPML2 and TRPML3 channels versus activation by low extracellular sodium and small molecules. *J. Biol. Chem.* 287, 22701–22708 (2012).

Acknowledgements

Author contributions

P.R. synthesized the compounds and performed calcium imaging experiments. A.S.R. performed autophagy experiments. N.U. and S.G. performed and analyzed screening experiments. C.A. created the CRISPR/Cas9 human MCOLN1 KO for MDA-MB-231 breast cancer lines and performed invasion and migration experiments. A.J., J.S. and R.T. performed patch-clamp experiments. C.L. synthesized ML-SI3. G.V. performed testing on the estrogen receptor. C.G. and F.B. designed the study, analyzed data, wrote the manuscript and provided funding. M.S. edited the manuscript and provided funding. All of the authors discussed the results and commented on the manuscript.

Funding

Competing interests

The authors declare no competing interests.

Additional information

Supplementary Information The online version contains supplementary material available at https://doi.org/10.1038/s41598-021-87817-4.

Correspondence and requests for materials should be addressed to M.S., F.B. or C.G.

Reprints and permissions information is available at www.nature.com/reprints.

Publisher's note Springer Nature remains neutral with regard to jurisdictional claims in published maps and institutional affiliations.

Supplementary Information

Estradiol analogs attenuate autophagy, cell migration and invasion by direct and selective inhibition of TRPML1, independent of estrogen receptors

Philipp Rühl[1#], Anna Scotto Rosato[2#], Nicole Urban[3#], Susanne Gerndt[1], Rachel Tang[2], Carla Abrahamian[2], Charlotte Leser[1], Jiansong Sheng[4], Archana Jha[5], Günter Vollmer[6], Michael Schaefer[3*], Franz Bracher[1*], Christian Grimm[2*]

[1]Department of Pharmacy – Center for Drug Research, Ludwig-Maximilians University, Munich, Germany
[2]Walther Straub Institute of Pharmacology and Toxicology, Faculty of Medicine, Ludwig-Maximilians University, Munich, Germany
[3]Rudolf-Boehm-Institute for Pharmacology and Toxicology, University of Leipzig, Germany
[4]CiPA LAB, LLC, Gaitherburg, MD, USA
[5]Casma Therapeutics Inc., Cambridge, MA, USA
[6]Institute of Zoology, Molecular Cell Physiology and Endocrinology, University of Dresden, Germany

Supplementary Tables: 1

Supplementary Figures: 3
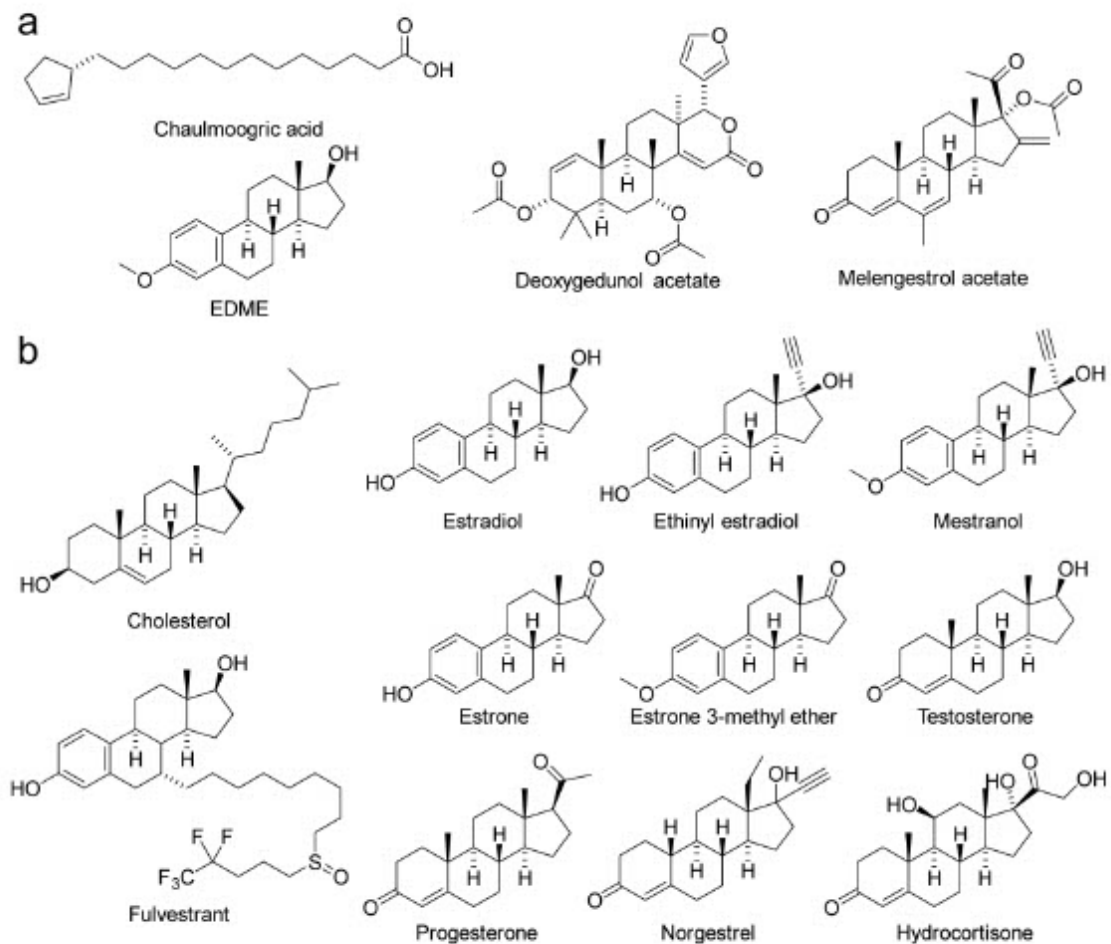
Supplementary Schemes: 1

Synthetic Procedures

Table S1

Potency and selectivity of PRU compounds and estradiol.

|	TRPML1	TRPML2	TRPML3	TRPML1:TRPML2	TRPML1:TRPML3
	IC_{50} (µM)	IC_{50} (µM)	IC_{50} (µM)	fold selectivity	fold selectivity
Estradiol	5.3	30.43	>50	5.77	n.c.
PRU-1 = EDME	0.6	5.85	19.5	9.14	30.47
PRU-2	13.8	37.02	>50	2.67	n.c.
PRU-4	0.5	5.23	4.78	10.25	9.37
PRU-5	0.8	3.38	14.88	4.45	19.58
PRU-6	0.41	3.57	7.87	8.71	19.2
PRU-7	0.73	2.64	15.2	3.62	20.82
PRU-8	0.72	15.32	38.65	21.28	53.68
PRU-9	0.17	2.53	5.96	14.88	35.06
PRU-10	0.41	5.4	15.83	13.17	38.61
PRU-11	0.44	2.4	32.11	5.45	72.98
PRU-12	0.28	5.28	14.08	18.86	50.29

Fig. S1

Structures of the noteworthy compounds of the high-throughput screening. (a) Structures of the four specific screening hits (b) Structures of retested and pharmacologically relevant steroids.


a

Chaulmoogric acid

EDME

Deoxygedunol acetate

Melengestrol acetate

b

Cholesterol

Estradiol

Ethinyl estradiol

Mestranol

Estrone

Estrone 3-methyl ether

Testosterone

Fulvestrant

Progesterone

Norgestrel

Hydrocortisone

Fig. S2

Effects of PRU-10 and PRU-12 on hTPC2. Representative Fura-2 calcium signals recorded from HEK293 cells stably expressing hTPC2$^{L11A/L12A}$-RFP. Cells were either stimulated with PRU-10 or PRU-12 alone (a-b) or they were sequentially stimulated with TPC2 agonist TPC2-A1-N (10 µM) and then treated with EDME analogs (10 µM, each) (c-d). Neither an activating nor a blocking effect on TPC2 was found for PRU-10 and PRU-12.
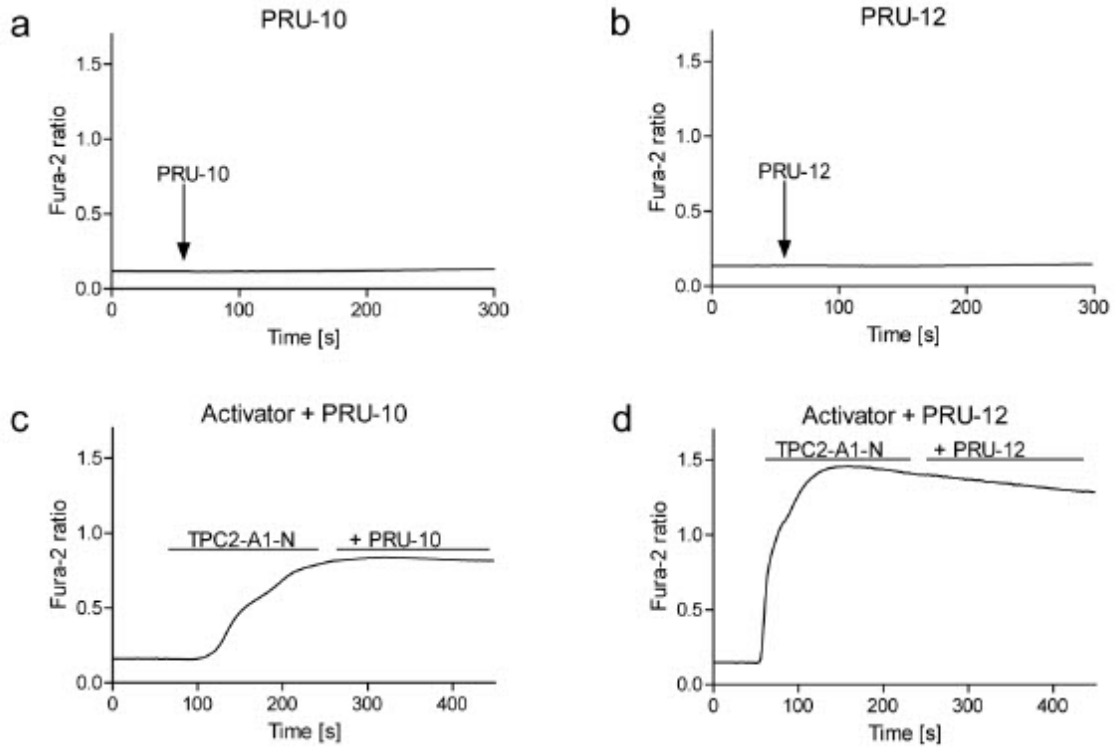
Fig. S3

Western blots uncropped. Shown are the Western blots from Fig. 6 in uncropped format.
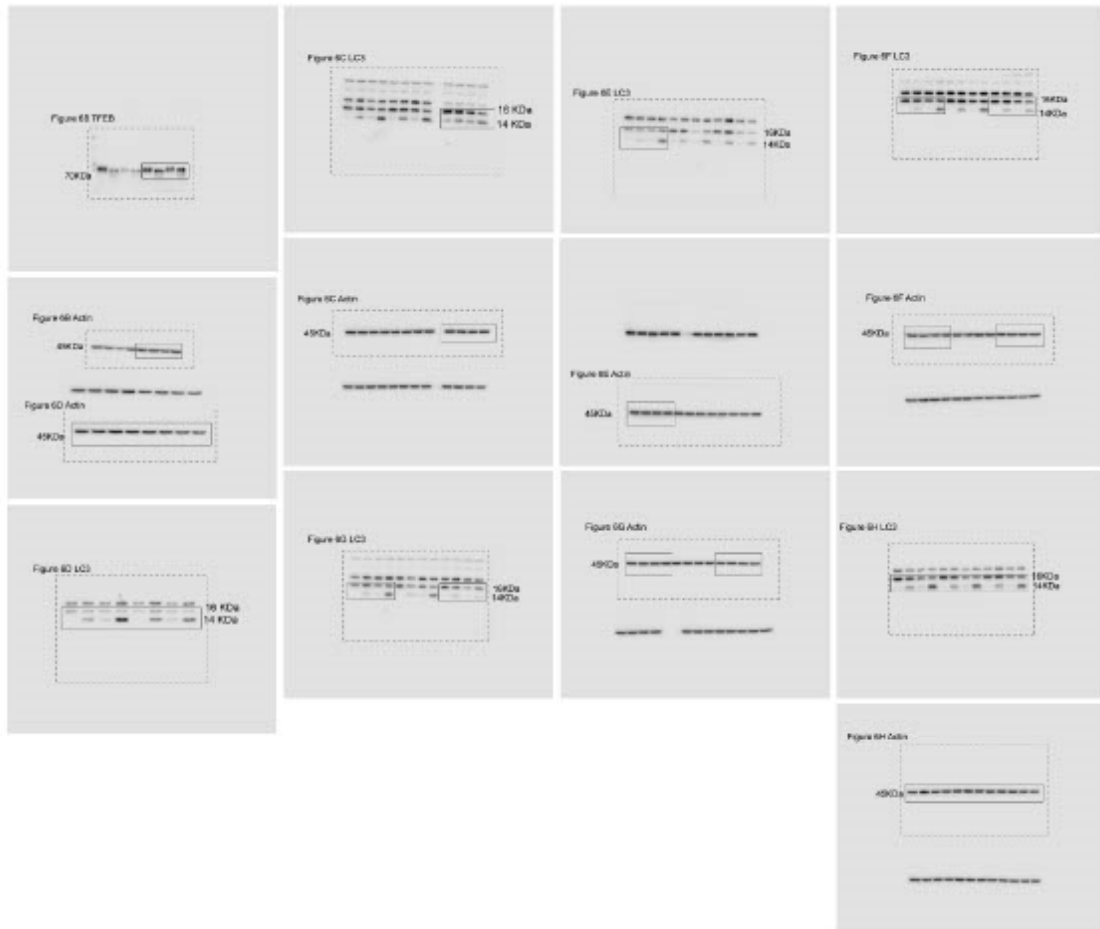
Suppl. Scheme 1

Synthesis of EDME analogs. Reaction conditions: a) for **PRU-2**: dimethyl sulfate, KOH, water/methanol, 65 °C, 1 h (51 %); b) for **PRU-4**: diethyl (bromodifluoromethyl) phosphonate, acetonitrile/water, 0 to 20 °C, 15 min (35 %); c) for **PRU-5**: bromoethane, NaOH, THF/water, reflux, 7 h (71%); d) for **PRU-6**: 2-bromopropane, NaOH, THF/water, reflux, 7 h (32 %); e) for **PRU-7**: 3-bromopropene, K$_2$CO$_3$, acetone, 50 °C, 40 h (89 %); f) for **PRU-8**: 2-(trimethylsilyl)phenyl trifluoromethanesulfonate, CsF, acetonitrile, 20 °C, 24 h (39 %); g) for **PRU-9**: 4-nitrophenyl trifluoromethanesulfonate, K$_2$CO$_3$, DMF, 20 °C, 2 h (74 %); h) for **PRU-10**: tributyl(vinyl)tin, cat. bis(triphenylphosphine)palladium(II)chloride, LiCl, 2,6-di-*tert*-butyl-4-methylphenol, DMF, N$_2$ atmosphere, 90 °C, 4 h (88 %); i) for **PRU-11**: phenylboronic acid, K$_3$PO$_4$, cat. Pd(OAc)$_2$, cat. SPhos, dioxane, N$_2$ atmosphere, 100 °C, 20 h (50 %); j) for **PRU-12**: tributyl(1-ethoxyvinyl)tin, cat. bis(triphenylphosphine) palladium(II)chloride, LiCl, DMF, N$_2$ atmosphere, 110 °C, 14 h, then water (54 %).
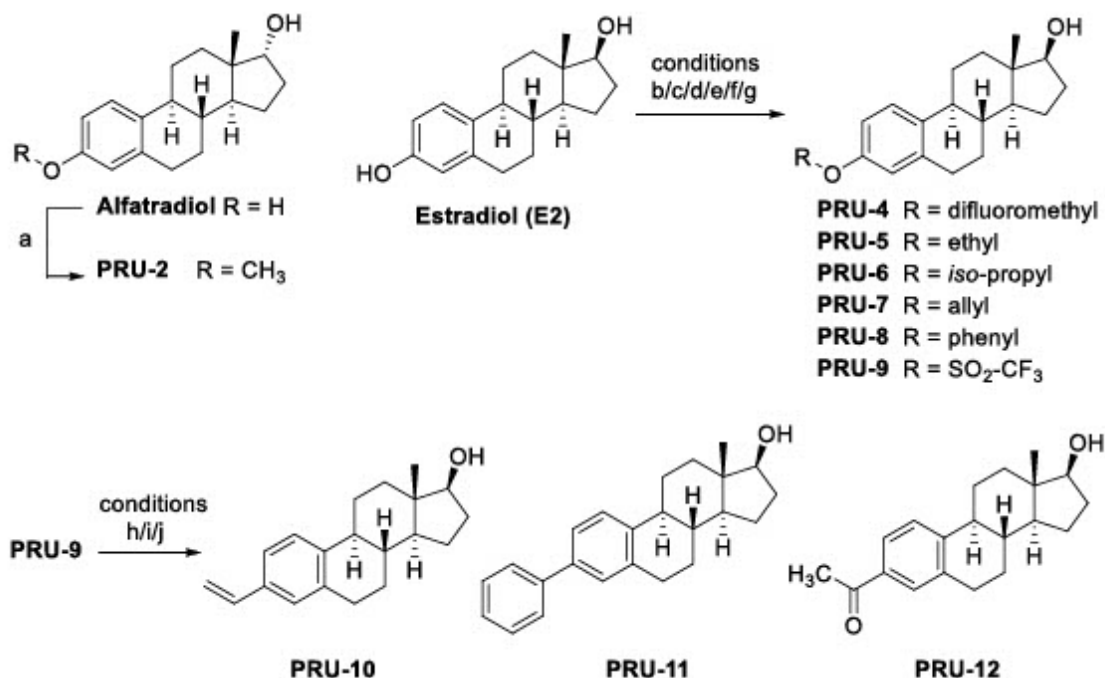
Synthetic procedures

Synthesis details and analytical data

All NMR spectra (^{1}H, ^{13}C, DEPT, H-H-COSY, HSQC, HMBC) were recorded at 23 °C on an Avance III 400 MHz Bruker BioSpin or Avance III 500 MHz Bruker BioSpin instrument unless otherwise specified. Chemical shifts δ are stated in parts per million (ppm) and are calibrated using residual protic solvents as an internal reference for proton (CDCl$_3$: δ = 7.26 ppm, DMSO: δ = 2.50 ppm) and for carbon the central carbon resonance of the solvent (CDCl$_3$: δ = 77.16 ppm, DMSO: δ = 39.52 ppm). Multiplicity is defined as s = singlet, d = doublet, t = triplet, q = quartet, m = multiplet. NMR spectra were analyzed with NMR software MestReNova, version 12.0.1-20560 (Mestrelab Research S.L.). High resolution mass spectra were performed by the LMU Mass Spectrometry Service applying a Thermo Finnigan MAT 95 or Joel MStation Sektorfeld instrument at a core temperature of 250 °C and 70 eV for EI or a Thermo Finnigan LTQ FT Ultra Fourier Transform Ion Cyclotron Resonance device at 250 °C for ESI. IR spectra were recorded on a Perkin Elmer FT-IR Paragon 1000 instrument as neat materials. Absorption bands were reported in wave number (cm^{-1}) with ATR PRO450-S. Melting points were determined by the open tube capillary method on a Büchi melting point B-540 apparatus and are uncorrected. HPLC purities were determined using an HP Agilent 1100 HPLC with a diode array detector and an Agilent Poroshell column (120 EC-C18; 3.0 × 100 mm; 2.7 micron) with acetonitrile/water as eluent (70:30 acetonitrile/water). All chemicals used were of analytical grade. 17β-Estradiol was purchased from TCI Deutschland GmbH (Eschborn, Germany), 17α-estradiol (alfatradiol, Ph. Eur. quality) from EDQM (Strasbourg, France). Isohexane, ethyl acetate and methylene chloride were purified by distillation. All reactions were monitored by thin-layer chromatography (TLC) using pre-coated plastic sheets POLYGRAM® SIL G/UV254 from Macherey-Nagel (Düren, Germany). Flash column chromatography was performed on Merck silica gel Si 60 (0.015 – 0.040 mm).
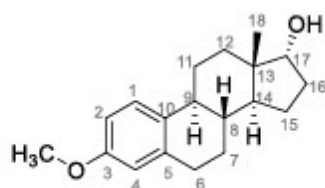
17β-Estradiol-3-methylether (EDME)
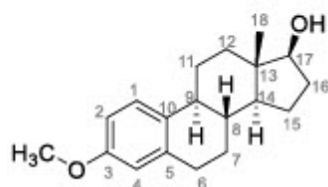
17β-Estradiol (222 mg, 0.815 mmol) was dissolved in 20 mL methanol. After addition of 5 mL of aqueous KOH (10%) and 0.50 mL (5.3 mmol) dimethyl sulfate, the solution was stirred at 65 °C for 30 min before another 0.50 mL (5.3 mmol) of dimethyl sulfate was added. After further 30 min, the solution was allowed to cool to room temperature and diluted with 20 mL of water. The precipitated solid was collected by filtration, washed with water, dried and purified by silica

gel column chromatography (isohexane/ethyl acetate 3:1) to give the methyl ether **EDME** as a colorless solid (160 mg, 0.559 mmol, 69%). m.p.: 121°C[1]: 119-120°C]. ^{1}H NMR (400 MHz, CDCl$_3$) δ/ppm = 7.21 (d, J = 8.4 Hz, 1H, 1-H), 6.71 (dd, J = 8.6 Hz, 2.8 Hz,1H, 2-H), 6.63 (d, J = 2.7 Hz, 1H, 4-H), 3.78 (s, 3H, 3-OCH$_3$), 3.73 (dd, J = 9.0 Hz, 8.0 Hz, 1H, 17α-H), 2.85 (m, 2H, 6-α-H, 6-β-H), 2.32 (m, 1H, 11-H), 2.19 (m, 1H, 9-H), 2.12 (m, 1H, 16-H), 1.95 (m, 1H, 12-H), 1.88 (m, 1H, 7-H), 1.70 (m, 1H, 15-H), 1.51 (m, 1H, 11-H), 1.46 (m, 1H, 16-H), 1.43 (m, 1H, 8-H), 1.39 (m, 1H, 15-H), 1.33 (m, 1H, 7-H), 1.29 (m, 1H, 12-H), 1.20 (m, 1H, 14-H), 0.71 (s, 3H, 18-H). ^{13}C NMR (100 MHz, CDCl$_3$) δ/ppm = 157.6 (C3), 138.1 (C5), 132.8 (C10), 126.5 (C1), 114.0 (C4), 111.6 (C2), 82.1 (C17), 55.4 (3-OCH$_3$), 50.2 (C14), 44.1 (C13), 43. (C9), 39.0 (C8), 36.9 (C12), 30.8 (C16), 30.0 (C6), 27.4 (C7), 26.5 (C11), 23.3 (C15), 11.2 (C18). IR (ATR): $\tilde{v}_{max}$/cm^{-1} = 3410, 2920, 2866, 1605, 1574, 1500, 1477, 1444, 1390, 1344, 1310, 1281, 1254, 1232, 1182, 1158, 1133, 1115, 1075, 1055, 964, 947, 862, 846, 818, 777, 572, 486, 442. HRMS (EI): calcd. for C$_{19}$H$_{26}$O$_2$ (M)$^{\cdot+}$: 286.1927; found: 286.1927. Purity (HPLC): >96% (λ = 210 nm), 93% (λ = 254 nm).

17α-Estradiol-3-methylether (PRU-2)

Prepared from 17α-estradiol (alfatradiol) (179 mg, 0.657 mmol) in the same manner as described above for the 17β epimer **EDME**. 17α-Estradiol-3-methylether (**PRU-2**) was obtained as a colorless solid (95.5 mg, 0.333 mmol, 51 %). m.p.: 109°C[2]: 106-107°C]. ^{1}H NMR δ/ppm = 7.18 (d, J = 8.6 Hz, 1H, 1-H), 6.67 (dd, J = 8.6 Hz, 2.8Hz,1H, 2-H), 6.59 (d, J = 2.8 Hz, 1H, 4-H), 4.34 (d, J = 4.2 Hz, 1H, OH) 3.68 (s, 3H, OCH$_3$), 3.57 (dd, J = 5.8 Hz, 4.1 Hz, 1H, 17β-H), 2.78 (m, 2H, 6α-H, 6β-H), 2.30 (m, 1H, 11-H), 2.10 (m, 1H, 9-H), 2.04 (m, 1H, 16-H), 1.83 (m, 1H, 7-H), 1.76 (m, 1H, 12-H), 1.71 (m, 1H, 15-H), 1.55 (m, 1H, 14-H), 1.44 (m, 1H, 12-H), 1.38 (m, 1H, 16-H), 1.34 (m, 1H, 11-H), 1.31 (m, 1H, 7-H), 1.27 (m, 1H, 8-H), 1.16 (m, 1H, 15-H), 0.61 (s, 3H, 18-H). ^{13}C NMR δ/ppm = 157.0(C3), 137.4 (C5), 132.3 (C10), 126.2 (C1), 113.4 (C4), 111.4 (C2), 78.0(C17), 54.8 (OCH$_3$), 47.2 (C14), 45.0(C13). 43.4 (C9), 38.8 (C8), 32.1 (C16), 31.5 (C12), 29.4 (C6), 27.8 (C7), 26.0 (C11), 23.9 (C15), 17.0 (C18). IR (ATR): $\tilde{v}_{max}$/cm^{-1} = 3599, 3513, 3324, 2910, 2862, 1608, 1576, 1499, 1467, 1378, 1280, 1254, 1235, 1155, 1119, 1104, 1075, 1037, 970, 941, 683, 663, 441. HRMS (EI): calcd. for C$_{19}$H$_{26}$O$_2$ (M)$^{\cdot+}$: 286.1927; found: 286.1920. Purity (HPLC): >96% (λ = 210 nm), >96% (λ = 254 nm)

The PRU numbers arise from consecutive numbering of synthesis experiments in our electronic lab book. Experiment **PRU**-3 did not lead to an identifiable product. We attempted here to prepare an EDME analogue in which the metabolically labile methoxy group is replaced by a trifluoromethoxy group. Since (based on clear evidence from literature) the same stability can as well be achieved by a difluoromethoxy analogue (= PRU-4), compound PRU-3 was no longer persued.

17β-Estradiol-3-(difluoromethyl)ether (PRU-4)
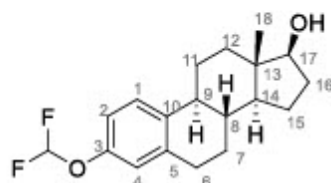
17β-Estradiol (300 mg, 1.10 mmol, 1.00 eq) and KOH (1.27 g, 22.6 mmol, 20.5 eq) were combined in a round-bottom flask following the addition of 30 mL of an acetonitrile/ water mixture (1:1). After cooling down to 0°C, diethyl (bromodifluoromethyl)phosphonate (600 mg, 2.25 mmol, 2.05 eq) was added and the biphasic mixture was allowed to reach room temperature over 15 minutes. The reaction mixture was diluted with 10 mL of diethyl ether, the layers were separated and the aqueous layer was further extracted with diethyl ether (3 × 10 mL). The combined organic layers were dried over anhydrous Na_2SO_4 and concentrated *in vacuo*. Purification was accomplished by silica gel column chromatography (isohexane/ethyl acetate 3:1) to yield **PRU-4** as a colorless oil (125 mg, 0.388 mmol, 35%). Analytical data are in accordance with literature[3]. ^1H NMR δ/ppm = 7.30 (d, J = 8.50 Hz, 1H, 1-H), 7.14 (t, J = 74.50 Hz,1H, CHF_2), 6.90 (dd, J = 8.5, 2.7 Hz, 1H, 2-H), 6.85 (d, J = 2.7 Hz,1H, 4-H), 4.50 (d, J = 4.8 Hz,1H, OH), 3.52 (m, 1H, 17-α-H), 2.80 (m, 2H, 6-α-H, 6-β-H), 2.28 (m, 1H, 11-H), 2.13 (m, 1H, 9-H), 1.88 (m, 1H, 16-H), 1.83 (m, 1H, 12-H), 1.79 (m, 1H, 7-H), 1.59 (m, 1H, 15-H), 1.38 (m, 1H, 16-H), 1.35 (m, 1H, 11-H), 1.32 (m, 1H, 8-H), 1.29 (m, 1H, 7-H), 1.26 (m, 1H, 15-H), 1.20 (m, 1H, 12-H), 1.14 (m, 1H, 14-H), 0.66 (s, 3H, 18-H). ^{13}C NMR δ/ppm= 148.7 (C3), 138.4 (C5), 137.2 (C10), 126.8 (C1), 118.7 (C4), 116.5 (t, J = 257 Hz, CHF_2), 116.0 (C2), 80.0 (C17), 49.5 (C14), 43.6 (C9), 42.8 (C13), 38.2 (C8), 36.5 (C12), 29.9 (C16), 29.0(C6), 26.6 (C7), 25.9 (C11), 22.8 (C15), 11.2 (C18). IR (ATR): $\tilde{v}_{max}$/cm^{-1} =3410, 2929, 2870, 1611, 1496, 1452, 1382, 1356, 1233, 1165, 1128, 1047, 934, 878, 821, 792, 763, 575, 449. HRMS (EI): calcd. for $C_{19}H_{24}F_2O_2$ (M)$^{+}$: 322.1739; found: 322.1749. Purity (HLPC): >96% (λ = 210 nm), >96% (λ = 254 nm).

17β-Estradiol-3-ethylether (PRU-5)
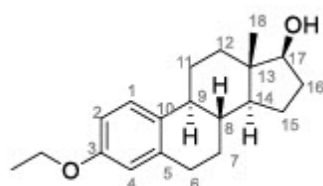
Bromoethane (118 mg, 1.08 mmol, 1.35 eq) was added to a solution of 17β-estradiol (217 mg, 0.797 mmol, 1.00 eq) and NaOH (44 mg, 1.1 mmol, 1.4 eq) in THF (20 mL) and water (5 mL). The reaction mixture was heated under reflux for 7 h and then diluted with water (10 mL). The mixture was extracted with diethyl ether (3 × 10 mL), the combined organic layers were dried over anhydrous Na_2SO_4 and concentrated *in vacuo*. The crude product was purified by column chromatography (isohexane/ethyl acetate 3:1) to yield **PRU-5** as a colorless solid (171 mg, 0.571 mmol, 71%). m.p.: 120°C[4]: 124-125°C]. ^{1}H NMR δ/ppm = 7.14 (d, J = 8.2 Hz, 1H, 1-H), 6.64 (dd, J = 8.6 Hz, 2.8 Hz, 1H, 2-H), 6.57 (d, J = 2.8 Hz, 1H, 4-H), 4.48 (d, J = 4.8, 1H, OH), 3.94 (q, J = 6.9 Hz, 2H, OCH_2), 3.51 (td, J = 8.5 Hz, 4.8 Hz 1H, 17-α-H), 2.75 (m, 2H, 6-α-H, 6-β-H), 2.25 (m, 1H, 11-H), 2.10 (m, 1H, 9-H), 1.86 (m, 1H, 16-H), 1.82 (m, 1H, 12-H), 1.78 (m, 1H, 7-H), 1.58 (m, 1H, 15-H), 1.37 (m, 1H, 16-H), 1.32 (m, 1H, 11-H), 1.29 (t, J = 7.0 Hz, 3H, ethyl CH_3), 1.27 (m, 1H, 8-H), 1.24 (m, 1H, 7-H), 1.21 (m, 1H, 15-H), 1.16 (m, 1H, 12-H), 1.10 (m, 1H, 14-H), 0.66 (s, 3H, 18-H). ^{13}C NMR δ/ppm = 156.3 (C3), 137.4 (C5), 132.1 (C10), 126.2 (C1), 114.1 (C4), 112.0(C2), 80.1 (C17), 62.7 (OCH_2), 49.6 (C14), 43.6 (C9), 42.9 (C13), 38.6 (C8), 36.6 (C12), 29.9 (C16), 29.3 (C6), 26.9 (C7), 26.1 (C11), 22.8 (C15), 14.8 (ethyl CH_3), 11.3 (C18). IR (ATR): $\tilde{v}_{max}$/cm^{-1} = 3410, 2920, 2866, 1605, 1500, 1477, 1390, 1344, 1310, 1254, 1232, 1182, 1157, 1133, 1054, 947, 862, 818, 777, 572. HRMS (EI): calcd. for $C_{20}H_{28}O_2$ (M)$^{·+}$: 300.2089; found: 300.2082. Purity (HPLC): >96% (λ = 210 nm), >96% (λ = 254 nm).

17β-Estradiol-3-isopropylether (PRU-6)
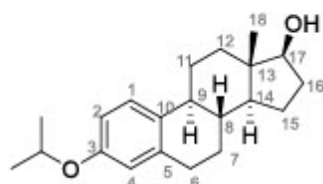
2-Bromopropane (128 mg, 1.03 mmol, 1.40 eq) was added to a solution of 17β-estradiol (200 mg, 0.734 mmol, 1.00 eq) and NaOH (41 mg, 1.10 mmol, 1.50 eq) in THF (20 mL) and water (5 mL). The solution was heated under reflux for 7 h and then diluted with water. The reaction mixture was extracted with diethyl ether (3 × 10 mL) and the combined organic layers

were dried over Na_2SO_4, filtered and concentrated *in vacuo*. Purification was accomplished by column chromatography (isohexane/ethyl acetate 3:1) to yield **PRU-6** as a colorless solid (74.9 mg 0.238 mmol, 32%). m.p.: 124°C[5]:119-122°C]. ^{1}H NMR δ/ppm = 7.13 (d, *J* = 8.5 Hz,1H, 1-H)), 6.63 (dd, J = 8.5 Hz, 2.7 ,1H, 2-H)), 6.56 (d, *J* = 2.7 Hz, 1H, 4-H), 4.50 (sept, *J* = 6.1 Hz, 1H, isopropyl CH), 4.48 (d, *J* = 4.8 Hz, 1H, OH), 3.51 (td, *J* = 8.5 Hz, 4.8 Hz,1H, 17-H), 2.74 (m, 2H, 6-α-H, 6-β-H), 2.24 (m, 1H, 11-H), 2.07 (m, 1H, 9-H), 1.87 (m, 1H, 16-H), 1.83 (m, 1H, 12-H), 1.77 (m, 1H, 7-H), 1.57 (m, 1H, 15-H), 1.38 (m, 1H, 16-H), 1.32 (m, 1H, 11-H), 1.29 (m, 1H, 8-H), 1.26 (m, 1H, 15-H), 1.23 (m, 1H, C7), 1.21 (2 d, *J* = 6.0 Hz, 2 x 3H, 2 isopropyl CH_3), 1.17 (m, 1H, 12-H), 1.11 (m, 1H, 14-H), 0.66 (s, 3H, 18-H). ^{13}C NMR δ/ppm = 155.1 (C3), 137.4 (C5), 132.0 (C10), 126.1 (C1), 115.4 (C4), 113.1 (C2), 80.0 (C17), 68.8 (isopropyl CH), 49.5 (C14), 43.5 (C9), 42.8 (C13), 38.6 (C8), 36.6 (C12), 29.9 (C16), 29.2 (C6), 26.9 (C7), 26.0 (C11), 22.8 (C15), 21.9 and 21.9 (2 isopropyl CH_3), 11.3 (C18). IR (ATR): $\tilde{v}_{max}$/cm^{-1} = 3478, 2914, 2863, 1610, 1494, 1378, 1333, 1279, 1252, 1109, 1052, 1008, 970, 874, 808, 774, 572. HRMS (EI): calcd. for $C_{21}H_{30}O_2$ (M)$^{+\cdot}$: 314.2240; found: 314.2241. Purity (HPLC): >96% (λ = 210 nm), >96% (λ = 254 nm).

17β-Estradiol-3-allylether (PRU-7)
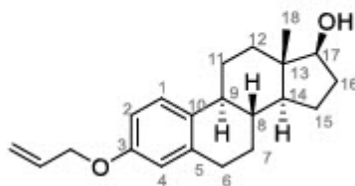
17β-Estradiol (136 mg, 0.499 mmol, 1.00 eq), 3-bromopropene (121 mg, 1.00 mmol, 86.0 µL, 2.00 eq), K_2CO_3 (248 mg, 1.50 mmol, 3.00 eq) and acetone (7.5 mL) were combined in a round bottom flask and stirred at 50 °C for 40 h. Then the mixture was diluted with water (5 mL) and extracted with CH_2Cl_2 (3 × 10 mL). The combined organic layers were dried over anhydrous Na_2SO_4 and concentrated *in vacuo*. The crude product was purified by silica gel column chromatography (isohexane/ethyl acetate 3:1) to afford **PRU-7** as a colorless solid (138 mg, 0.443 mmol, 89%). Analytical data are in accordance with literature[6]. m.p.: 64°C. ^{1}H NMR δ/ppm = 7.15 (d, *J* = 8.9 Hz ,1H, 1-H), 6.68 (dd, J = 8.6 Hz, 2.8 Hz,1H, 2-H), 6.61 (d, *J* = 2.7 Hz, 1H, 4-H), 6.01 (ddt, *J* = 17.4 Hz, 10.5 Hz, 5.2 Hz,1H, allyl CH), 5.36 (dq, *J* = 17.2 Hz, 1.8 Hz, 1H, allyl $=CH_2$), 5.22 (dq, *J* = 10.5 Hz, 1.6 Hz, 1H, 21-H), 4.49 (m, 3H, OH, OCH_2), 3.52 (td, *J* = 8.5 Hz, 4.9 Hz, 1H, 17-H), 2.75 (m, 2H, 6-H), 2.25 (m, 1H, 11-H), 2.09 (m, 1H, 9-H), 1.88 (m, 1H, 16-H), 1.84 (m, 1H, 12-H), 1.79 (m, 1H, 7-H), 1.58 (m, 1H, 15-H), 1.38 (m, 1H, 16-H), 1.32 (m, 1H, 11-H), 1.29 (m, 1H, 8-H), 1.26 (m, 1H, 15-H), 1.23 (m, 1H, 7-H), 1.18 (m, 1H, 12-H), 1.12 (m, 1H, 14-H), 0.66 (s, 3H, 18-H). ^{13}C NMR δ/ppm = 155.9 (C3), 137.4 (C5), 134.0 (allyl CH), 132.3 (C10), 126.1 (C1), 117.0 (allyl $=CH_2$), 114.3 (C4), 112.1 (C2), 80.0

(C17), 68.0(OCH$_2$), 49.5 (C14), 43.5 (C9), 42.8 (C13), 38.5 (C8), 36.6 (C12), 29.9 (C16), 29.2 (C6), 26.8 (C7), 26.0(C11), 22.8 (C15), 11.2 (C18). IR (ATR): $\tilde{v}_{max}$/cm^{-1} = 3399, 2923, 2359, 1606, 1498, 1455, 1381, 1345, 1309, 1282, 1230, 1158, 1133, 1053. 1023, 917, 861, 818, 788, 569. HRMS (EI): calcd. for C$_{21}$H$_{28}$O$_2$ (M)$^{+}$: 312.2084; found: 312.2083. Purity (HPLC): >96% (λ = 210 nm), >96% (λ = 254 nm).

17β-Estradiol-3-phenylether (PRU-8)
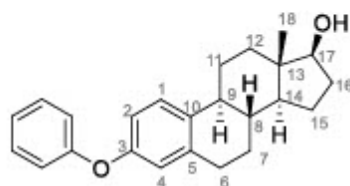

17β-Estradiol (202 mg, 0.741 mmol, 1.00 eq) and CsF (337 mg, 2.22 mmol, 3.00 eq) were suspended in acetonitrile (6.2 mL), then 2-(trimethylsilyl)phenyl trifluoromethanesulfonate (270 µL, 1.11 mmol, 1.50 eq) was added and the suspension was stirred for 24 h at room temperature. The resulting mixture was washed with brine (20 mL) and extracted with diethyl ether (3 × 10 mL). The combined ether fractions were dried over Na$_2$SO$_4$ and concentrated under reduced pressure. Purification was accomplished by column chromatography (isohexane/ethyl acetate 3:1) to yield **PRU-8** as a colorless oil (100 mg, 0.29 mmol, 39%). ^{1}H NMR δ/ppm = 7.36 (m, 2H), 7.27 (d, J = 8.5 Hz, 1H), 7.1 (m, 1H), 6.96 (m, 2H), 6.75 (dd, J = 8.5 Hz, 2.6 Hz, 1H, 2-H), 6.69 (d, J = 2.7 Hz, 1H, 4-H), 4.50 (d, J = 4.9Hz, 1H, OH), 3.53 (td, J = 8.5 Hz, 4.8 Hz, 17-H), 2.76 (m, 2H, 6-H), 2.28 (m, 1 H, 11-H), 2.15 (m, 1H, 9-H). 1.88 (m, 1H, 16-H), 1.85 (m, 1H, 12-H), 1.79 (m, 1H, 7-H), 1.59 (m, 1H, 15-H), 1.38 (m, 1H, 11-H), 1.35 (m, 1H, 16-H), 1.33 (m, 1H, 8-H), 1.29 (m, 1H, 7-H), 1.25 (m, 1H, 15-H), 1.19 (m, 1H, 12-H), 1.12 (m, 1H, 14-H), 0.68 (s, 3H, 18-H). ^{13}C NMR δ/ppm = 157.1, 154.1, 138.3, 135.4, 129.9, 126.8, 123.0, 118.6, 118.7, 116.1 (C2), 80.0 (C17), 49.6 (C14), 43.6 (C9), 42.8 (C13), 38.4 (C8), 36.6 (C12), 29.9 (C16), 29.1 (C6), 26.7 (C7), 25.9 (C11), 22.77 (C15), 11.2 (C18). HRMS (EI): calcd. for C$_{24}$H$_{28}$O$_2$ (M)$^{+}$: 348.2084, found: 348.2089. Purity (HPLC): >91% (λ = 210 nm), >91% (λ = 254 nm).

17β-Estradiol-3-trifluoromethanesulfonate (PRU-9)
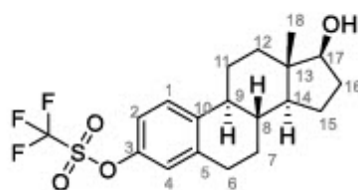
17β-Estradiol (1.00 g, 3.68 mmol, 1.00 eq) was dissolved in DMF (12 mL). K_2CO_3 (1.20 g, 7.34 mmol, 2.00 eq) was added, followed by 4-nitrophenyl trifluoromethanesulfonate (1.04 g, 3.85 mmol, 1.05 eq), and the resulting suspension was stirred for 2 h at room temperature. Then water (12 mL) and diethyl ether (5 mL) were added, the aqueous layer was separated and extracted with diethyl ether (3 × 5 mL). The combined organic layers were washed with cold 1M hydrochloric acid (10 mL), 1M NaOH solution (3 × 10 mL), water (3 × 10 mL), brine (10 mL) and 1M aqueous LiCl solution and dried over anhydrous Na_2SO_4. After evaporation the crude product was purified by column chromatography (isohexane/ethyl acetate 2:1) to yield **PRU-9** as a colorless solid (1.10 g, 2.72 mmol, 74%). m.p.: 79°C[7]: 123-125°C]. ^{1}H NMR δ/ppm = 7.34 (d, J = 8.7 Hz, 1H, 1-H), 7.02 (dd, J = 8.7 Hz, 2.7 Hz, 1H, 2-H), 6.97 (d, J = 2.7 Hz, 1H, 4-H), 3.74 (t, J = 8.7 Hz, 1H, 17-H), 2.89 (m, 2H, 6-H), 2.32 (m, 1H, 11-H), 2.24 (m, 1H, 9-H), 2.13 (m, 1H, 16-H), 1.98 (m, 1H, 12-H), 1.92 (m, 1H, 7-H), 1.71 (m, 1H, 15-H), 1.55 (m, 1H, 11-H), 1.49 (m, 1H, 16-H), 1.44 (m, 1H, 8-H), 1.38 (m, 1H, 15-H), 1.34 (m, 7-H), 1.30 (m, 1H, 12-H), 1.20 (m, 1H, 14-H), ^{13}C NMR δ/ppm = 147.6 (C3), 141.0 (C5), 139.7 (C10), 127.3 (C1), 121.3 (C4), 119.3 (q, J = 322.6 Hz, CF_3), 118.3 (C2), 81.9 (C17), 50.2 (C14), 44.2 (C9), 43.3 (C13), 38.4 (C8), 36.7 (C12), 30.7 (C16), 29.7 (C6), 26.9 (C7), 26.2 (C11), 23.3 (C15), 11.2 (C18). IR (ATR): $\tilde{v}_{max}$/cm^{-1} = 3400, 2958, 1489, 1418, 1250, 1206, 1142, 1049, 1002, 928, 976, 856, 718, 618, 499. HRMS (EI): calcd. for $C_{19}H_{23}F_3O_4S$ (M)$^{+}$: 404.1264, found: 404.1269. Purity (HPLC) >96% (λ = 210 nm), >96% (λ = 254 nm).

## (8R,9S,13S,14S,17S)-13-Methyl-3-ethenyl-7,8,9,11,12,13,14,15,16,17-decahydro-6H-cyclopenta[a]phenanthren-17-ol (PRU-10)
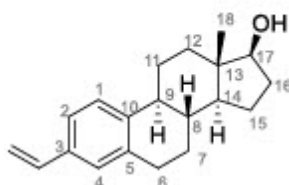
A flame-dried Schlenk flask was evacuated and backfilled with nitrogen 5 times prior to the addition of 300 mg (0.742 mmol, 1.00 eq) of 17β-estradiol-3-trifluoromethanesulfonate (PRU-9), 135 mg (3.15 mmol, 4.26 eq) lithium chloride, 1.6 mg of 2,6-di-*tert*-butyl-4-methylphenol and 52 mg (0.074 mmol, 0.10 eq) of bis(triphenylphosphine)palladium(II)chloride. After addition of 4.5 mL DMF, 0.28 mL (305 mg, 0.962 mmol, 1.30 eq) tributyl(vinyl)tin were added dropwise. The resulting suspension was stirred for 4 h at 90 °C under nitrogen atmosphere, then cooled to room temperature and treated with 0.3 mL of pyridine and 0.6 mL of hydrogen fluoride pyridine (Olah's reagent). The resulting mixture was stirred at room temperature overnight and then diluted with 20 mL diethyl ether, filtered and washed with 10 mL of water, 10 mL of 10% hydrochloric acid, again 10 mL of water and 10 mL of brine. The organic layer was dried over anhydrous Na_2SO_4 and concentrated under reduced pressure. The crude

product was suspended in cold isohexane and left in the fridge overnight. The precipitated solid was collected by filtration and purified by silica gel column chromatography (isohexane/ethyl acetate 4:1) to yield **PRU-10** as a colorless solid (184 mg, 0.651 mmol, 88%). Analytical data are in accordance with literature[8]. m.p.: 104°C. ^{1}H NMR δ/ppm = 7.24 (d, J = 8.2 Hz, 1H, 1-H), 7.2 (dd, J = 8.1 Hz, 1.8 Hz, 1H, 2-H), 7.12 (d, J = 1.8 Hz, 1H, 4-H), 6.64 (dd, J = 17.6 Hz, 10.9 Hz, 1H, vinyl CH), 5.73 (dd, J = 17.7 Hz, 1.2 Hz, 1H, vinyl CH_2), 5.17 (dd, J = 17.7 Hz, 1.2 Hz, 1H, vinyl CH_2), 4.50 (d, J = 4.8 Hz, 1H, 17-OH), 3.53 (td, J = 8.5 Hz, 4.8 Hz, 1H, 17α-H), 2.79 (dd, J = 8.8 Hz, 4.1 Hz, 2H, 6α-H, 6β-H), 2.29 (m, 1H, 11-H) 2.16 (m, 1H, 9-H) 1.89 (m, 1H, 16-H) 1.85 (m, 1H, 12-H) 1.81 (m, 1H, 7-H) 1.59 (m,1H, 11-H) 1.38 (m, 1H, 16-H), 1.35 (m, 1H, 11-H), 1.33 (m, 1H, 9-H), 1.28 (m, 1H, 7-H) 1.26 (m, 1H, 15-H), 1.19 (m, 1H, 12-H), 1.14 (m, 1H, 14-H), 0.67 (s, 3H, 18-H). ^{13}C NMR δ/ppm = 140.0 (C10), 136.6 (C19), 136.4 (C5), 134.3 (C3), 126.5 (C4), 125.4 (C1), 123.3 (C2), 113.1 (C20), 80.0 (C17), 49.6 (C8), 44.0(C14), 42.8 (C13), 38.5 (C9), 36.6 (C12), 29.9 (C16), 28.9 (C6), 26.8 (C7), 25.8 (C11), 22,8 (C15), 11.2 (C18). IR (ATR): $\tilde{v}_{max}$/cm^{-1} = 3410, 2930, 2864, 1629, 1562, 1496, 1445, 1385, 1335, 1250, 1134, 1074, 1052, 1021, 988, 898, 823, 787, 727, 567, 443. HRMS (EI): calcd. for $C_{20}H_{26}O$ (M)$^{+}$: 282.1978, found: 282.1984. Purity (HPLC): >96% (λ = 210 nm), >96% (λ = 254 nm).

(8*R*,9*S*,13*S*,14*S*,17*S*)-13-Methyl-3-phenyl-7,8,9,11,12,13,14,15,16,17-decahydro-6*H*-cyclopenta[a]phenanthren-17-ol (PRU-11)
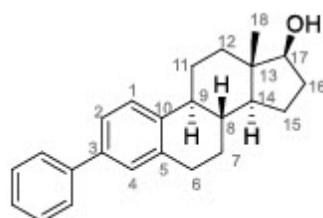
A flame dried Schlenk flask was evacuated and backfilled with nitrogen 5 times prior to the addition of 17β-estradiol-3-trifluoromethanesulfonate (PRU-9), 209 mg, 0.50 mmol, 1.00 eq), phenylboronic acid (122 mg, 1.00 mmol, 2.00 eq), K_3PO_4 (212 mg, 1.00 mmol, 2.00 eq), Pd(OAc)$_2$ (5.7 mg, 0.025 mmol, 0.05 eq), SPhos (20.5 mg, 0.0500 mmol, 0.100 eq) and dioxane (8 mL). The resulting suspension was heated at 100 °C for 20 h under nitrogen atmosphere and then quenched with water (15 mL) and diluted with ethyl acetate (15 mL). The organic phase was separated and the aqueous phase was extracted with ethyl acetate (3 × 10 mL). The combined organic phases were filtered, washed with brine and dried over anhydrous Na_2SO_4. The crude product was purified by column chromatography (hexane/ethyl acetate 4:1) to yield **PRU-11** as a colorless solid (174 mg, 0.501 mmol, 50%). m.p.: 172°C. ^{1}H NMR δ/ppm = 7.58 (m, 2H), 7.42 (m, 2H), 7,39 (m, 2H, 1-H, 2-H), 7.33 (m, 2H), 3.76 (dd, J = 9.0 Hz, 7.9 Hz ,1H, 17α-H), 2.96 (m, 2H, 6-H), 2.40 (m, 1H, 11-H), 2.30 (m,1H, 9-H), 2.15 (m, 1H, 16-H),

1.99 (m,1H, 12-H), 1.94 (m, 1H, 7-H), 1.74 (m, 1H, 15-H), 1.58 (m, 1H, 11-H), 1.52 (m, 1H, 16-H), 1,50 (m, 1H, 8-H), 1,43 (m, 1H, 7-H), 1.40 (m, 1H, 15-H), 1.35 (m, 1H, 12-H), 1.27 (m, 1H, 14-H), 0.81 (s, 3H, 18-H). ^{13}C NMR δ/ppm = 141.3, 139.7 (C10), 138.7 (C3), 137.3 (C5), 128.8, 127.9 (C4), 127.2, 127.1, 126.0(C1), 124.6 (C2), 82.1 (C17), 50.3 (C14), 44.5 (C9), 43.4 (C13), 38.8 (C8), 36.9 (C12), 30.8 (C16), 29.8 (C6), 27.4 (C7), 26.3 (C11), 23.3 (C15), 11.2 (C18). IR (ATR): $\tilde{v}_{max}$/cm^{-1} = 3563, 2935, 2898, 1484, 1376, 1127, 1067, 1028, 1008, 889, 849, 762, 713, 698, 529. HRMS (EI): calcd. for C$_{24}$H$_{28}$O (M)$^{+}$: 332.2135, found: 332.2132. Purity (HPLC): >95% (λ = 210 nm), >95% (λ = 254 nm)

1-((8R,9S,13S,14S,17S)-17-Hydroxy-13-methyl-7,8,9,11,12,13,14,15,16,17-decahydro-6H-cyclopenta[a]phenanthren-3-yl)ethan-1-one (PRU-12)
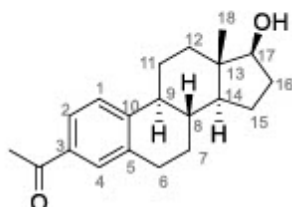
A flame dried Schlenk flask was evacuated and backfilled with nitrogen 5 times prior to the addition of 202 mg (0.50 mmol, 1.00 eq) 17β-estradiol-3-trifluoromethane-sulfonate (PRU-9), 64.2 mg (1.50 mmol, 3.00 eq) lithium chloride and 35.1 mg (0.0500 mmol, 0.100 eq) bis(triphenylphosphine)palladium(II)chloride. After addition of 3 mL of DMF, tributyl(1-ethoxyvinyl)tin (0.170 mL, 181 mg, 0.503 mmol, 1.00 eq) was added dropwise and the resulting suspension was stirred at 110 °C for 14 h under nitrogen atmosphere. After cooling, the mixture was treated with 5 mL of water and diluted with 5 mL of ethyl acetate. The organic phase was separated and washed with cold water (3 × 10 mL), brine and aqueous 1M LiCl solution, dried over anhydrous Na$_2$SO$_4$ and concentrated *in vacuo*. The crude product was purified by flash column chromatography (isohexane/ ethyl acetate 4:1) to yield PRU-12 as a colorless solid (80.2 mg, 0.27 mmol, 54%). m.p.: 180°C^8:170-172°C]. ^{1}H NMR δ/ppm = 7.72 (dd, J = 8.1 Hz, 2.0 Hz, 1H, 2-H), 7.68 (d, J = 1.9 Hz, 1H, 4-H), 7.38 (d, J = 8.3Hz, 1H, 1-H), 3.74 (dd, 9.0 Hz, 8.0 Hz, 17α-H), 2.92 (m, 2H, 6α-H, 6β-H), 2.57 (s, 3H, acetyl CH$_3$), 2.37 (m, 1H, 11-H), 2.28 (m, 1H, 9-H), 2.13 (m, 1H, 16-H), 1.98 (m, 1H, 12-H), 1.93 (m, 1H, 7-H), 1.72 (m, 1H, 15-H), 1.55 (m, 1H, 11-H), 1.50 (m, 1H, 16-H), 1.46 (m, 1H, 8-H), 1.39 (m, 1H, 15-H), 1.35 (m, 1H, 7-H), 1.30 (m, 1H, 12-H), 1.22 (m, 1H, 14-H), 0.79 (s, 3H, 18-H). ^{13}C NMR δ/ppm = 198.4 (C=O), 146.3 (C10), 137.3 (C5), 134.8

(C3), 129.1 (C4), 125.8 (C2), 125.7 (C1), 81.9 (C17), 50.3 (C14), 44.9 (C9), 43.3 (C13), 38.5 (C8), 36.8 (C12), 30.7 (C16), 29.6 (C6), 27.1 (C7), 26.7 (acetyl CH_3), 26.1 (C11), 23.3 (C15), 11.2 (C18). IR (ATR): $\tilde{v}_{max}$/cm^{-1} = 3507, 2917, 2868, 1664, 1605, 1562, 1363, 1267, 1171, 1056, 898, 834, 592. HRMS (EI): calcd. for $C_{20}H_{26}O$ (M)$^{\cdot+}$: 298.1927, found: 298.1926. Purity (HPLC): >96% (λ = 210 nm), >96% (λ = 254 nm).

**Supporting Information References:**

1. Muddana, S.S., Price, A.M., MacBride, M.M., and Peterson, B.R. (2004). 11beta-alkyl-Delta9-19-nortestosterone derivatives: high-affinity ligands and potent partial agonists of the androgen receptor. J Med Chem *47*, 4985-4988.
2. Pindur, U., and Schall, T. (1994). Proton Acid-Catalysed Transformations of Estrogen Derivatives: New Results and Some Mechanistic Aspects of the Kober Colour Reaction. Arch Pharm *327*, 637-642.
3. Lin, X., Hou, C., Li, H., and Weng, Z. (2016). Decarboxylative Trifluoromethylating Reagent [Cu(O2 CCF3)(phen)] and Difluorocarbene Precursor [Cu(phen)2][O2 CCF2 Cl]. Chemistry *22*, 2075-2084.
4. Triggle, D.J., Ridley, H.F., and DeMaio, D.M. (1969). Some 3-alkoxyestra-1,3,5(10)-trien-17-beta-ols. J Med Chem *12*, 346.
5. Tedesco, R., Thomas, J.A., Katzenellenbogen, B.S., and Katzenellenbogen, J.A. (2001). The estrogen receptor: a structure-based approach to the design of new specific hormone–receptor combinations. Chem Biol *8*, 277-287.
6. Santra, S., and Guin, J. (2015). Enhanced Reactivity of Aerobic Diimide Olefin Hydrogenation with Arylboronic Compounds: An Efficient One-Pot Reduction/Oxidation Protocol. Eur J Org Chem *2015*, 7253-7257.
7. Hostetler, E.D., Jonson, S.D., Welch, M.J., and Katzenellenbogen, J.A. (1999). Synthesis of 2-[(18)F]Fluoroestradiol, a Potential Diagnostic Imaging Agent for Breast Cancer: Strategies to Achieve Nucleophilic Substitution of an Electron-Rich Aromatic Ring with [(18)F]F(-). J Org Chem *64*, 178-185.
8. Shi, Y., and Koh, J.T. (2002). Functionally orthogonal ligand-receptor pairs for the selective regulation of gene expression generated by manipulation of charged residues at the ligand-receptor interface of ER alpha and ER beta. J Am Chem Soc *124*, 6921-6928.

4.1.2 Second generation of analogs

4.1.2.1 Insertion of different functional groups at C-3 of the estrane scaffold

The plan for the next series of compounds was to build on the results of the biological evaluation of the first generation and introduce other functional groups with different physico-chemical properties at C-3 of the estrane scaffold.

Since 3-vinylestrane **PRU-10** and methyl ketone **PRU-12** (**Scheme 7**) showed the best characteristics of all substances of the first generation, the first task for the next generation of compounds was to synthesize more analogs with a C-C instead of a C-O bond at C-3. One idea was to introduce lipophilic alkyl residues that would prevent the molecule from building H-bonds at this site but, unlike **PRU-10**, would not carry a double bond. The first approach of this concept was the catalytic hydrogenation of the above described olefin **PRU-10** in methanol, which gave ethyl analog **8** in excellent yield[97].
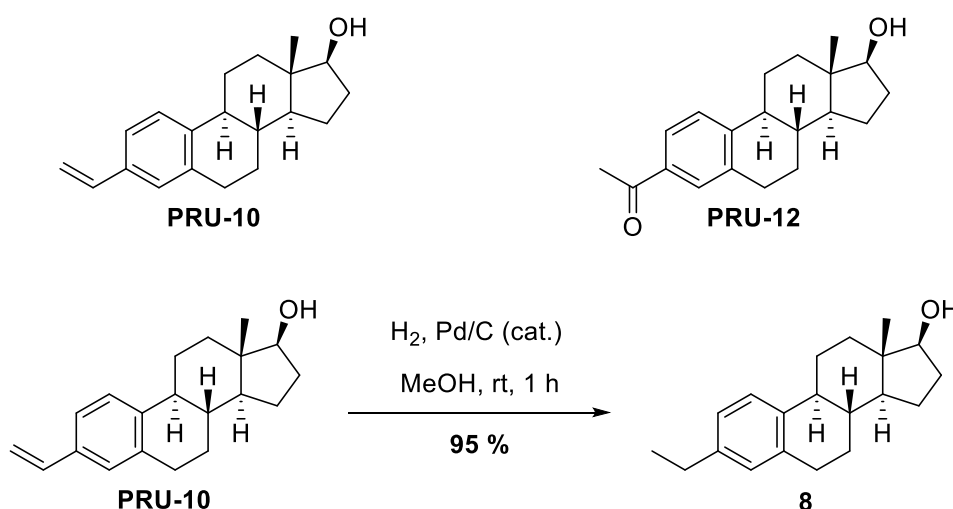

Scheme 7: Best analogs of the first generation and synthesis of ethyl analog **8**

To get access to more analogs with comparable or also completely different structural features at C-3, the basic plan was to perform various palladium-catalyzed cross-couplings or similar reactions using estradiol 3-triflate (**PRU-9**) as the key intermediate.

Following this principle, the 3-methyl analog of **EDME 9**, bearing a truncated alkyl chain compared to **8**, should be prepared according to a procedure for palladium-catalyzed methylation of aryl halides and pseudohalides developed by COOPER *et al.*[98]. In this protocol, the (AlMe₃)₂·DABCO adduct (DABCO = 1,4-diazabicyclo[2.2.2]octane) is used as a transmitter of methyl carbanions (**Scheme 8**). In our case, the methyl analog could not be obtained as this approach merely led to decomposition of the reactant. Even though the authors pointed out that this method is applicable to a wide range of aryl halides and pseudohalides and that alcohols are tolerated, more complex and bigger molecules have not been investigated. Only

one example for a primary alcohol (4-bromobenzyl alcohol) was shown, secondary and tertiary alcohols were not included. Most likely, the utilized reagent is too reactive and decomposes the reactant **PRU-9** before it can undergo the desired reaction.
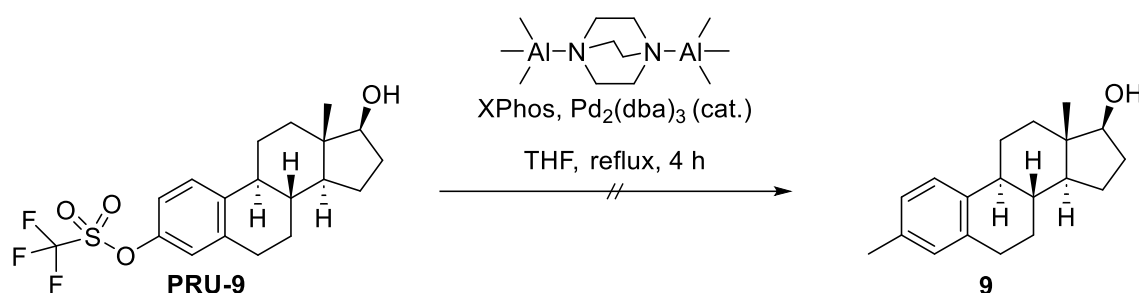
Scheme 8: Failed attempt to synthesize the 3-methyl analog **9**

After preparation of the vinyl analog **PRU-10** and the ethyl analog **8** (see **Scheme 7**), the next reasonable modification in this series was the corresponding alkyne. Like alkene and alkane, the alkyne moiety is lipophilic, but it also brings in various other effects. The alkyne bond is shorter than a C-C single or double bond and its hyperconjugated π-system provides donor-acceptor interactions similar to those observed with the phenyl ring[99]. Therefore, it is classified as a bioisostere of a phenyl group[100], but can also mimic a variety of other functional groups including chloro, iodo and carboxamide[99]. Moreover, it is a weak electron withdrawing function and thus slightly changes electron density in ring A.

The classic method for the synthesis of arylalkynes is SONOGASHIRA coupling. Coupling of estradiol 3-triflate (**PRU-9**) with trimethylsilylacetylene[101] led to the intermediate **10**. Subsequent splitting of the trimethylsilyl group with tetrabutylammonium fluoride (TBAF) gave the aryl alkyne **11** with 61 % yield over two steps (**Scheme 9**). These two molecules have already been described by WANG *et al.*[102], however, their approach necessitates an additional reduction step as they used estrone 3-triflate as reactant.
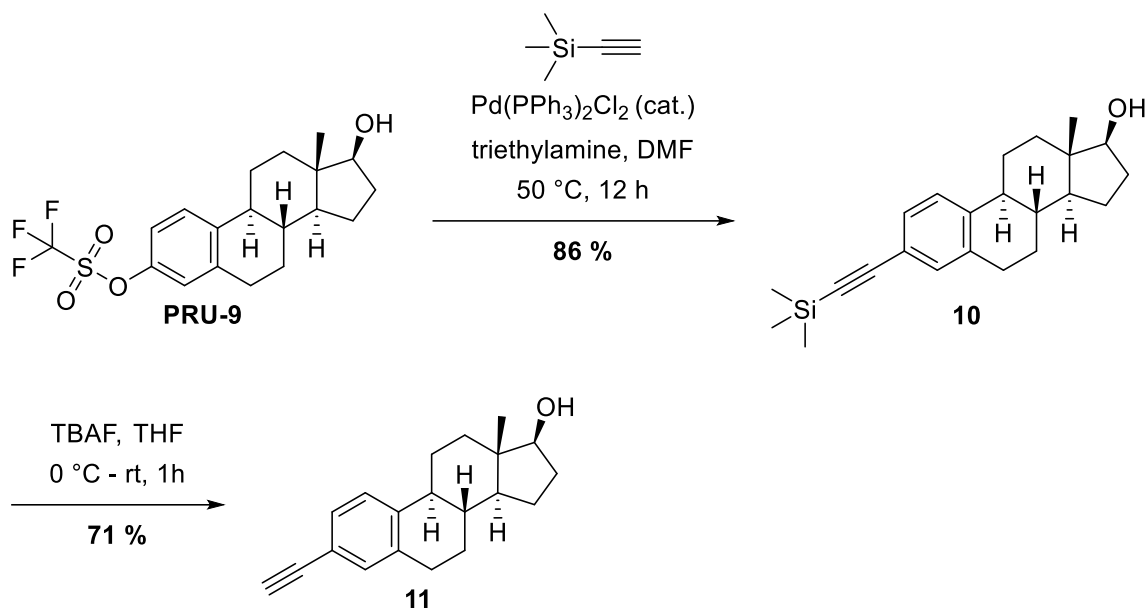
Scheme 9: Preparation of **11** *via* trimethylsilyl intermediate **10**

Since 3-acetyl analog **PRU-12** provided good biological results, the synthesis of an analog bearing an aldehyde function at C-3 was also of great interest. This aldehyde would not only form similar hydrogen bonds like ketone **PRU-12**, but could in principle also act as reversible covalent inhibitor.

The concept of covalent inhibition of enzymes or other target proteins is well established in medicinal chemistry as multiple approved drugs act as covalent inhibitors. The mode of action of these inhibitors is the creation of covalent bonds with nucleophilic amino acid residues or nucleobases. This principle of drug design can provide several advantages. Covalent inhibitors might require lower doses due to their high biochemical efficiency, which could result in decreased off-target effects. Due to the covalent binding, even high concentrations of endogenous substrate can't easily displace the inhibitor from the binding site and the prolonged duration of action at the target might enable less-frequent drug dosing[103-105]. Covalent inhibitors can be divided into two classes: The irreversible covalent inhibitors and the reversible covalent inhibitors.

The irreversible covalent inhibitors form permanent bonds with the target protein, which results in complete disactivation thereof. Prominent approved drugs belonging to this category are the NSAR ASS, the propargylamine rasagilin, the epoxide carfilzomib and the nitrogen mustard derivative bendamustin. The main disadvantage of these drugs is their high reactivity, which can lead to unwanted side effects and drug-induced toxicity like hepatotoxicity, mutagenicity or carcinogenicity[105]. The covalent modification of host proteins can also trigger an immune response, leading to idiosyncratic drug toxicity (IDT)[106]. Another issue of these inhibitors is

that the function of the biological target can only be restored by *de novo* synthesis of the affected protein, which strongly differs from target to target. If the affected protein is rapidly turned over by protein biosynthesis, the benefits of these drugs are limited, if the turnover occurs extremely slow, the long lasting time could again lead to toxicity[107]. Mechanism-based inhibitors like esomeprazol, fluoruracil, clopidogrel, clavulanic acid and finasteride are more specific as they are only converted into their active form by the target protein itself or at certain conditions that prevail almost exclusively in the target compartment (i.e. activation of esomeprazol in the highly acidic conditions of the canaliculi of parientel cells)[108]. The problem in drug design of these inhibitors is that such transformations only occur at particular targets, mainly enzymes, and are hard to predict. Additionally, dependence on the protein turnover is still a drawback. Above all, this mechanism of action is often only discovered retrospectively[109]. Hence, this principle is merely applicable in particular cases.

The reversible covalent inhibitors also form covalent bonds with the target protein, the decisive difference to the irreversible inhibitors is that this bond is rather labile and can be cleaved to restore the affected protein, resulting in an equilibrium between the bound and unbound form. At the target protein, this bound form is stabilized by complex molecular interactions (i.e. H-bounds) with the inhibitor, whereas the inhibitor can rather easily be released from off-target proteins due to the minor strength or absence of this effect. Thereby, enhanced selectivity and a reduced risk of off-target effects und undesirable activation of the immune system can be achieved[110]. The principle of reversible covalent inhibition is gaining more and more interest in medicinal chemistry and the number of approved drugs possessing this mechanism is increasing. Outstanding examples of these are the lactone orlistat (inhibitor of pancreatic lipase), the carbamate rivastigmine (AChE inhibitor), the nitriles saxagliptine and vildagliptine (DPP IV inhibitors) and the boronic acid bortezomib (proteasome inhibitor). One of the most important functional groups accessible for reversible covalent binding are aldehydes. Despite no approved covalent reversible inhibitor with an aldehyde as active warhead currently on the market, the ability of aldehydes to form these bonds is well known and widely utilized in pharmaceutical research. Especially in the field of proteasome inhibitors, aldehydes play an important role and were the first compounds investigated for this purpose, Calpain Inhibitor I (CAL I) being the most prominent example. The clinical drug candidate roblitinib (FGFR4 inhibitor) is another covalent reversible inhibitor with an aldehyde as the active function. The reversible covalent inhibition of aldehydes works by the formation of a hemiacetal with a serine or threonine residue, or a hemithioacetal with a cysteine residue (**Figure 12**)[111, 112].
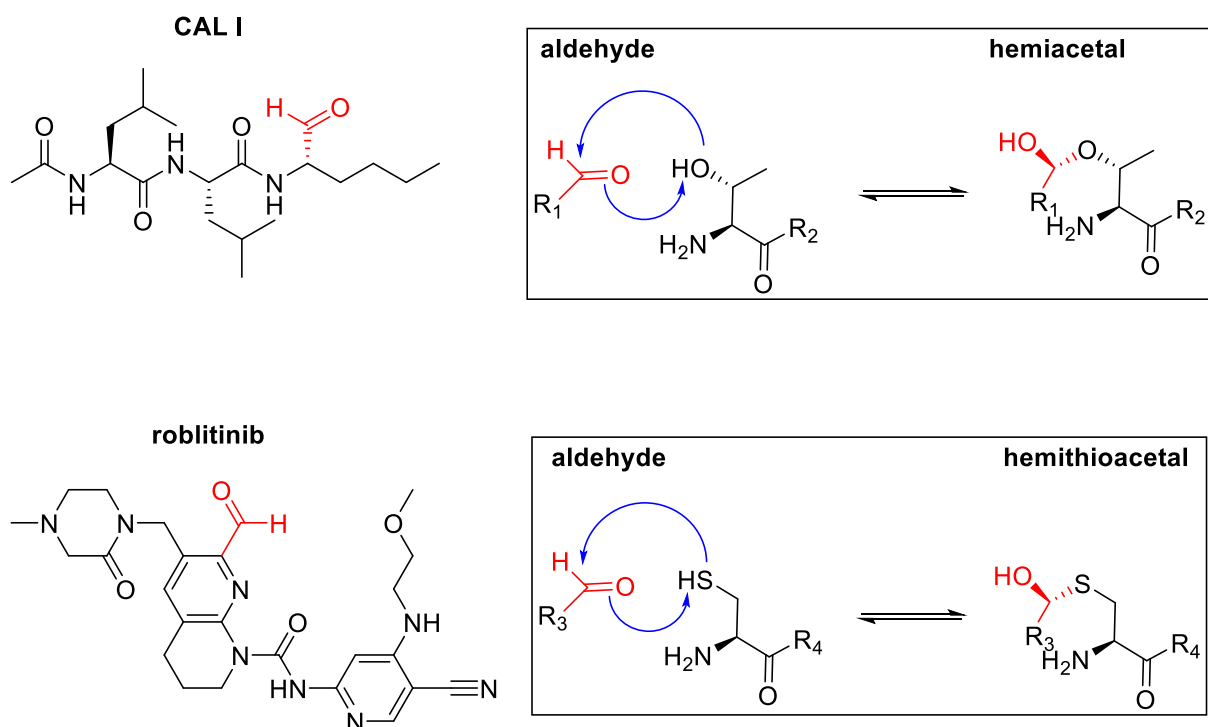
Figure 12: CAL I and roblitinib, mechanisms of reversible covalent binding
Aldehyde-R1 = CAL 1, Aldehyde-R3 = roblitinib

With this in mind, the **EDME**-derived aromatic aldehyde **12** (**Scheme 10**) was considered as an interesting compound for our project.

The preparation of this analog was performed according to a method for palladium-catalyzed reductive carbonylation using *N*-formylsaccharine as a carbon monoxide surrogate, as published by KONISHI *et al.*[113]. Aldehyde **12** was obtained from aryl triflate **PRU-9** in 20 % yield.
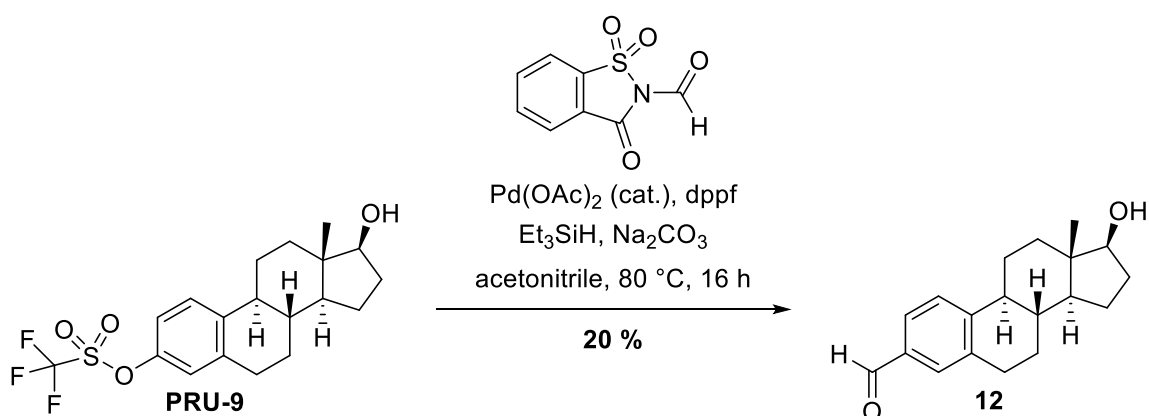
Scheme 10: Synthesis of aldehyde analog **12**

The advantage of this method is that it avoids working with carbon monoxide gas, which is extremely toxic and difficult to handle. Instead, the stable, inexpensive and easy-to-handle solid *N*-formylsaccharine is used as a CO source. The proposed mechanism of this formylation is depicted in **Scheme 11**.
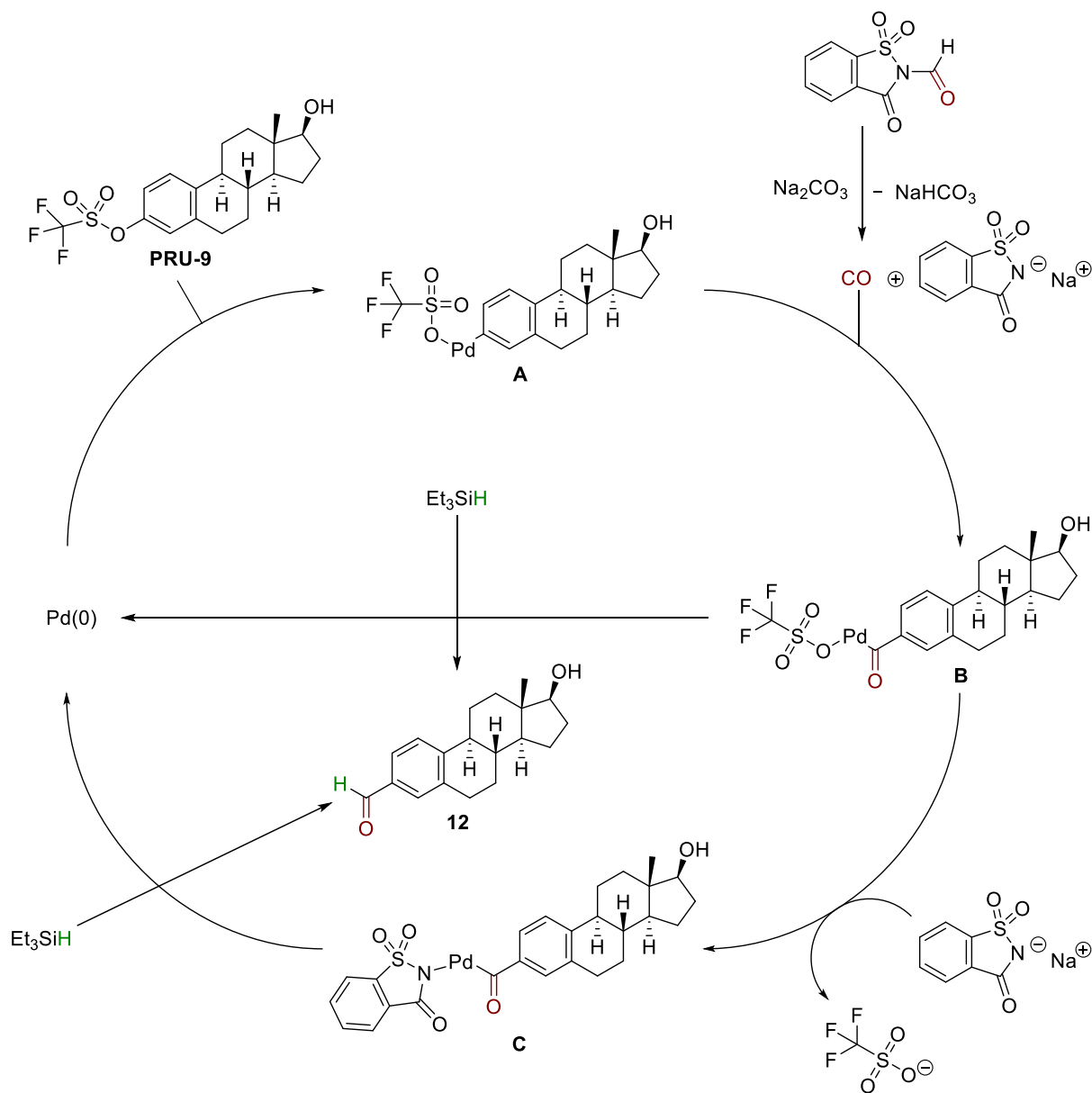

Scheme 11: Proposed mechanism according to KONISHI *et al.*[113] applied to **PRU-9** (own depiction)

According to KONISHI *et al.*, a plausible mechanism involves reaction of *N*-formylsaccharine with a base to produce carbon monoxide (CO) and saccharinate. Oxidative addition of the substrate (in our case **PRU-9**) to Pd (0) generates Pd (II) intermediate **A**, which is followed by coordination and migratory insertion of CO to form intermediate **B**. From this stage, the authors suggest two possible paths to afford the desired aldehyde product (in our case **12**): Intermediate **B** could either react directly with triethylsilane to produce the aldehyde and

recover palladium (0), or it could first exchange the triflate with saccharinate to form intermediate **C**, which then reacts with triethylsilane to generate the desired product.

Even though TLC monitoring suggested a high conversion rate, the final yield was unexpectedly low. Since aromatic aldehydes are known to be sensitive molecules, the most plausible explanation is that the formed product decomposes partly during the work up or the purification process. The aromatic aldehyde function could be oxidized under the influence of oxygen and temperature (rotary evaporator) or react with the free silanol groups of the silica gel in the column during flash column chromatography. As sufficient purity could not be achieved with column chromatography, a bisulfite extraction protocol, which is used as a specific method for the purification of aldehydes[114] was also employed. By combination of these two procedures, a purity of 92 % could be attained.

After successful preparation of the aldehyde compound, the next target was the synthesis of nitrile analogs. As mentioned above, some nitriles are also able to act as reversible covalent inhibitors, with the DPP IV inhibitors vildagliptine and saxagliptine being the most prominent representatives. Nitriles can undergo reversible PINNER reactions, in the case of vildagliptine and saxagliptine reaction with an active site serine generates an imidate[105, 107]. The investigational drug odanacatib (inhibitor of cathepsin K) reversibly forms a thioimidate ester with a cysteine residue[115] (**Figure 13**).
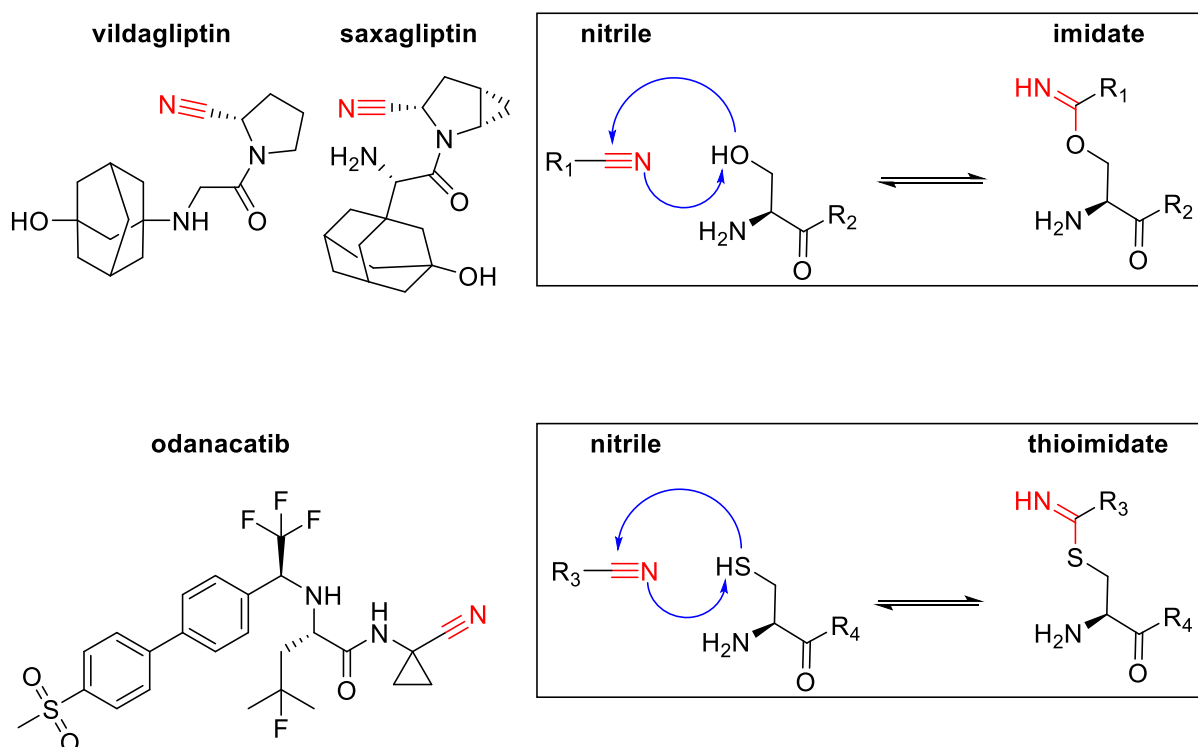
Figure 13: DPP IV inhibitors vildagliptin and saxagliptin and cathepsin K inhibitor odanacatib, mechanisms of reversible covalent binding

In order to obtain the desired nitrile analogs of **EDME**, palladium-catalyzed coupling approaches were again conducted with **PRU-9**. Two protocols from a publication by Sнı *et al.* afforded the nitriles **13** and **14**[97]. Compound **13** was prepared by palladium-catalyzed cyanation with potassium cyanide in *N*-methyl-2-pyrrolidinone (NMP) with good yield (80 %). A Heck reaction of **PRU-9** with 2-propenenitrile gave the vinylogous nitrile **14** as an inseparable mixture of *E*- and *Z*-isomers in moderate yield (34 %) (**Scheme 12**).
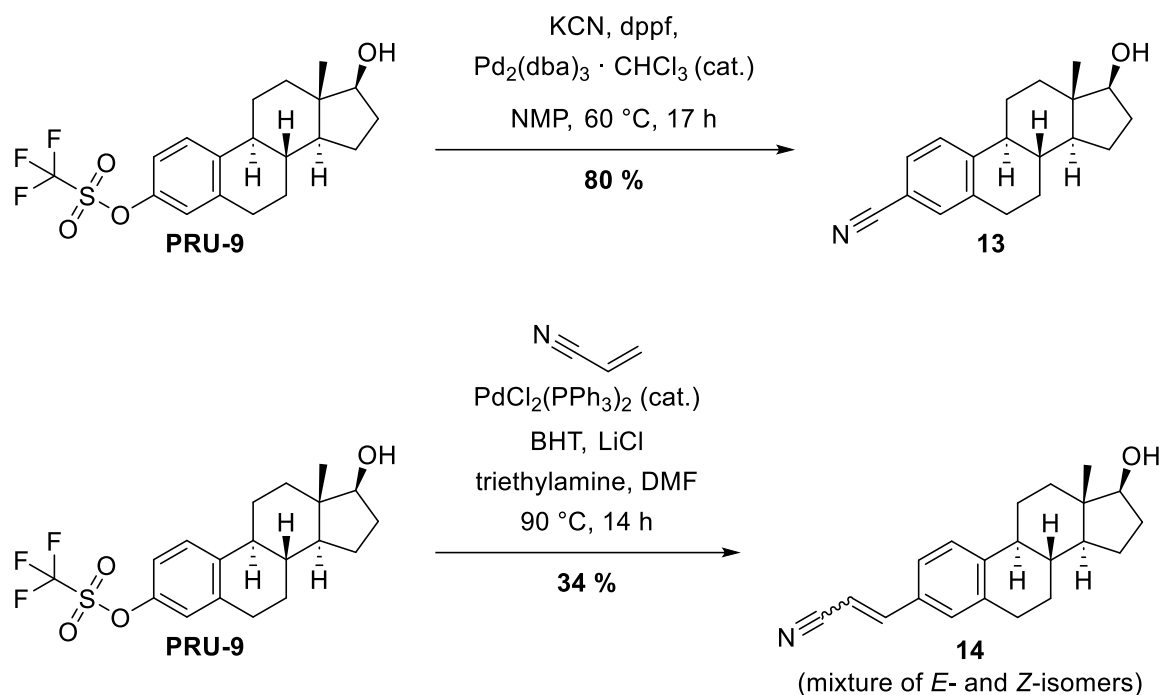
**Scheme 12**: Preparation of the nitriles **13** and **14**

With these two nitriles and the aldehyde **12**, three compounds were synthesized which could possibly act as reversible covalent inhibitors.

The next envisaged modification was to substitute the oxygen of the original screening hit **EDME** by a nitrogen and thus generate amino analogs. These analogs would bring different physicochemical properties and also possess a basic character. Through systematic modification of the substitution of these analogs, different H-bond donor and/or H-bond acceptor properties can be implemented. The plan was to synthesize the unsubstituted aniline analog **15** and the *N*-methyl aniline analog **16**, which would be both H-bond donors and acceptors and as well as the *N,N*-dimethylaniline analog **17** (**Figure 14**), which would only act as H-bond acceptor, but carry two methyl groups at the nitrogen. The favored strategy was to establish one pathway to get access to all three analogs.
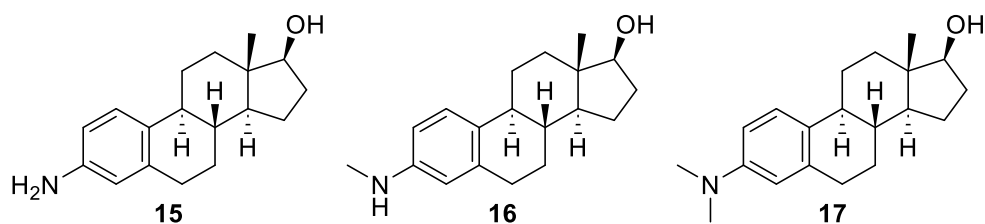
Figure 14: Structure of the aniline analogs of **EDME**

WEIDNER *et al.* described a method for the preparation of 3-aminoestratrienes starting from 19-nortestosterone (**4**) by a optimized SEMMLER-WOLFF rearrangement[116]. This protocol should be reproduced as described in order to receive the 3-amino analogs of **EDME**. The first step was the condensation of the ketone function of 19-nortestosterone with hydroxylamine, which gave in our case a mixture of the *syn-* and *anti-*oximes **18** and **19** in 83 % yield. SEMMLER-WOLFF rearrangement of these oximes by heating in acetic anhydride at 110 °C for 39 hours and subsequent hydrolysis with hydrochloric acid gave the *N-* and *O-*acetylated estrane **20** (**Scheme 13**). This process proved to be problematic for a number of reasons. Firstly, the results of this key step were highly inconsistent. In three approaches with different batch sizes, the yields ranged from 11 % to 37 %. Secondly, purification of the crude product could not be done as described in the paper, as recrystallization was not successful. Instead, two runs of elaborate column chromatography were performed to obtain the substance in at least moderate purity. The high amount of resulting side products and impurities aggravated the process.
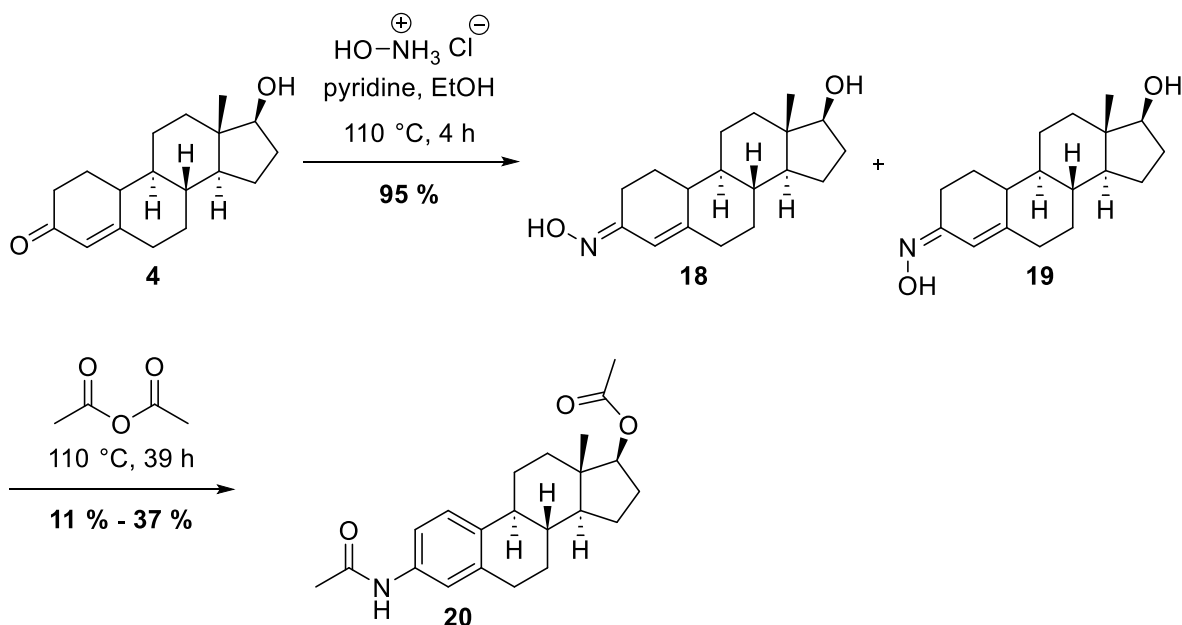
Scheme 13: Preparation of **20** following the protocol of WEIDNER *et al.*[116]

The inconvienience of this step could be caused by the harsh conditions and possible side reactions. The BECKMANN rearrangement is known as a competing reaction under comparable

conditions[117, 118]. Albeit strong acids are normally used for this method, it is quite plausible that the reaction can also take place under these conditions, since the used acetic anhydride could not only contain acetic acid as an impurity, but also produces it in the course of the SEMMLER-WOLFF reaction. As depicted in **Scheme 14** the SEMMLER-WOLFF reaction starts with *O*-acetylation of the employed oxime **A** to generate **B**. This molecule is protonated to afford **C**. This protonation is usually done with strong acids like hydrochloric acid, in the protocol of WEIDNER *et al*. exclusively acetic acid is used. Formal abstraction of acetic acid from tautomer **D** generates intermediate **E** which can subsequently be deprotonated by the resulting acetate to produce acetic acid and the desired aniline (**F**)[119]. In the BECKMANN rearrangement, starting material **A** is protonated to generate species **G** which subsequently proceeds to split off water. Nitrilium ion **H** is formed due to the migration of one alkyle residue to the nitrogen. Nucleophilic attack of a water molecule is followed by the abstraction of a proton to produce imidate **J**. Tautomerization of **J** finally generates amide **K** as the final product[120].
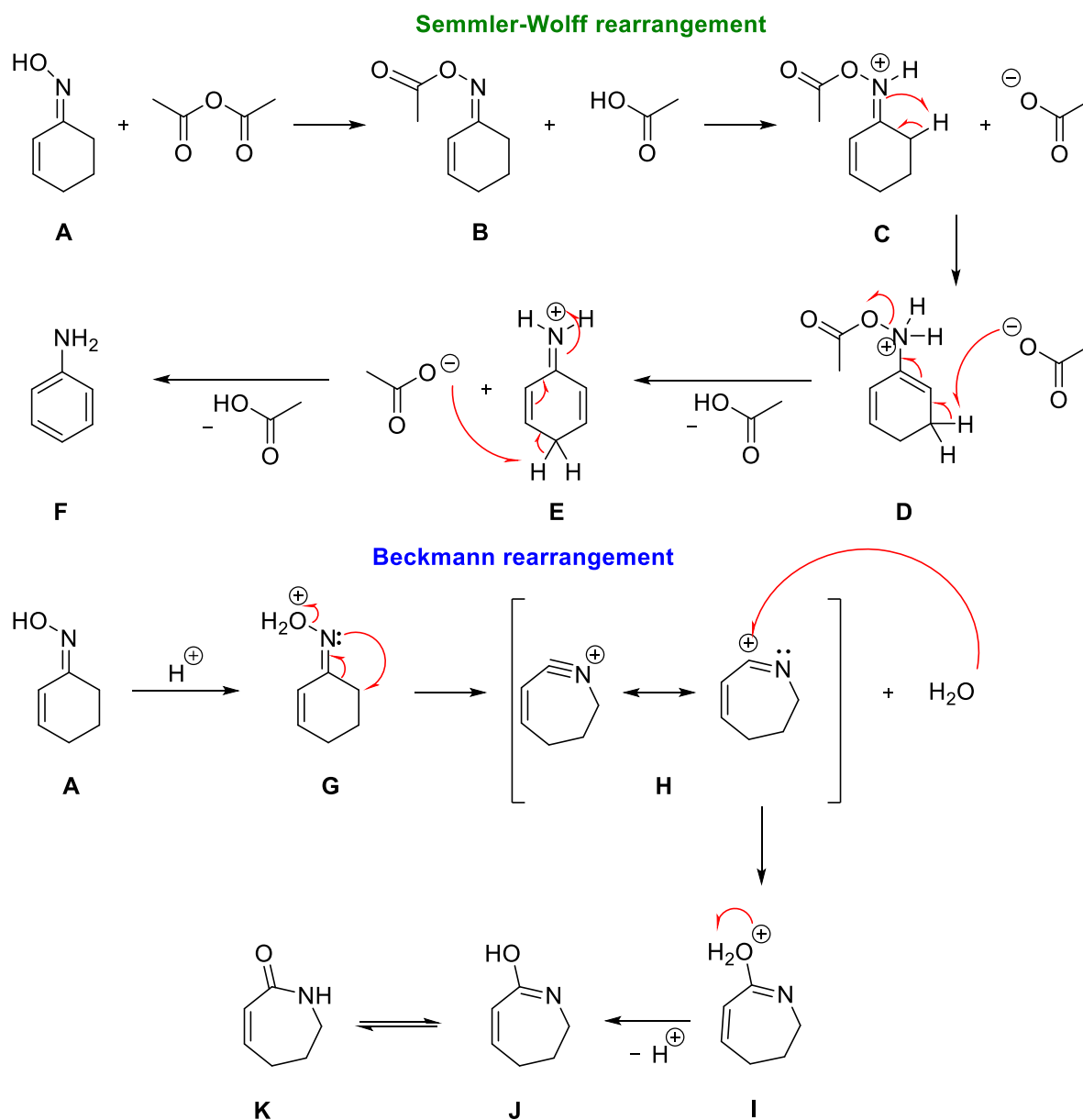
Scheme 14: Proposed mechanisms for desired SEMMLER-WOLFF rearrangement and competing BECKMANN rearrangement shown on cyclohexenone oxime[119, 120] (own depiction)

Acetylated aniline **20** (see **Scheme 13**) as product of the SEMMLER-WOLFF rearrangement was considered as a possible synthetic precursor for the preparation of the *N*-monomethylated amino analog **16** (see **Figure 14**). The preparation of *N*-monomethyl anilines in general is often challenging. In most cases, it is not possible to start from unsubstituted anilines since classic methylation using alkylating agents as well as reductive alkylation with formaldehyde usually provide the *N,N*-dimethyl aniline exclusively, since the intermediate *N*-monomethyl anilines are stronger nucleophiles than the unsubstituted anilines and thus directly continue to react again. Hence, the preferred strategy for the synthesis of *N*-monomethyl anilines is to start from single

protected anilines. The protective group prevents the second methylation and can subsequently be cleaved to obtain the desired *N*-monomethyl aniline.

Consequently, two small scale (10 mg) experiments for *N*-methylation of *N*-arylacetamide compound **20** were carried out. Treatment with sodium hydride and iodomethane led to decomposition of the molecule, mainly because the ester at C-17 interferes with this reaction. Although this outcome was to be expected, an attempt was made since there are examples in literature in which comparable esters were left untouched under these conditions [121, 122]. An alternative monoselective *N*-methylation method for amides[123] using phenyl trimethylammonium iodide as donor of a methyl group and cesium carbonate as base did not result in any conversion (**Scheme 15**). After failure of these approaches this strategy was no longer pursued.
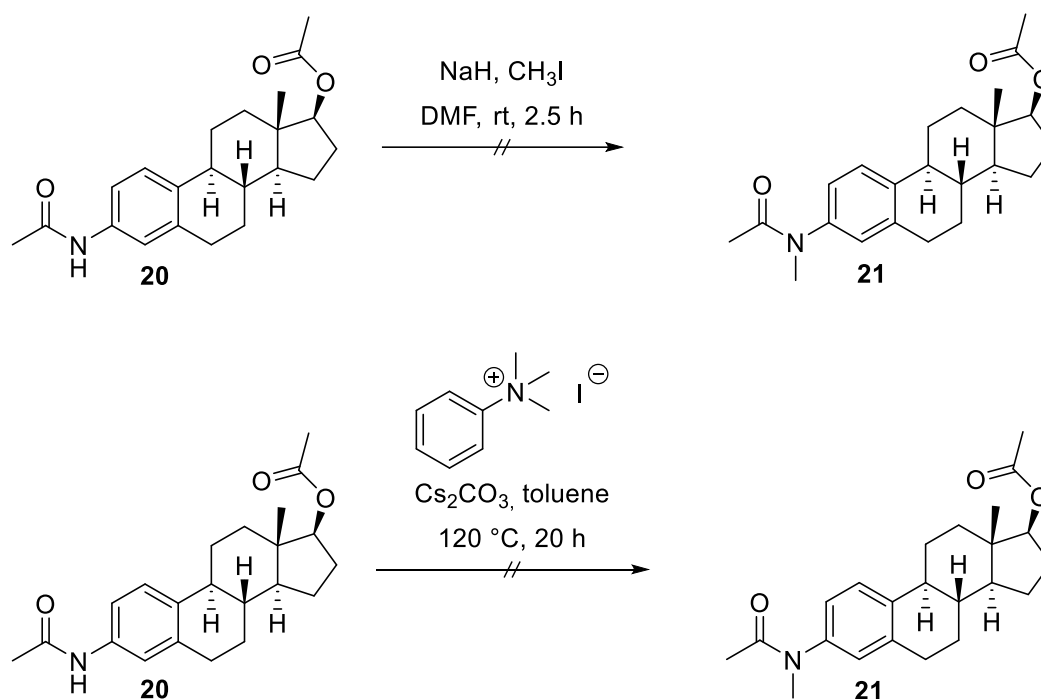
Scheme 15: Failed attempts for *N*-methylation of *N*-arylacetamide **20**

To continue this route nonetheless, **20** was treated with aqueous hydrochloric acid in ethanol to hydrolyze the acetate and the amide generating the hydrochloride salt **22**, which was obtained in 70 % yield. (**Scheme 16**). Just like its precursor, this compound could not be isolated completely pure.
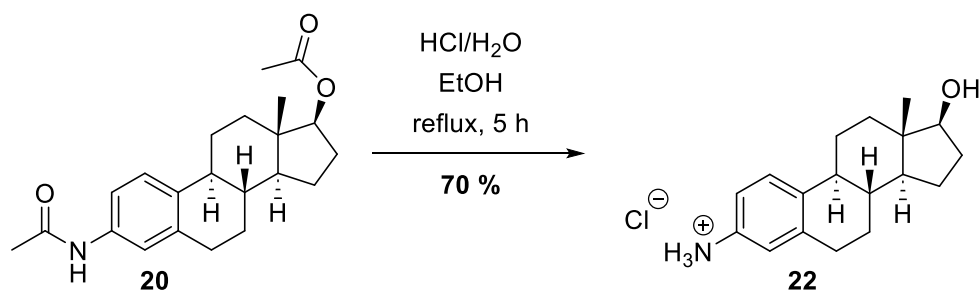
Scheme 16: Preparation of primary aromatic amine **22**

Due to bad atom economy, difficult purification caused by concomitant side-products as well as impurities and poor reproducibility, this SEMMLER-WOLFF method was not deemed a promising route for the synthesis of the three targeted amino analogs.

Consequently, an alternative strategy for the synthesis of these molecules had to be developed. A standard method for preparation of aromatic amines is the BUCHWALD-HARTWIG coupling. It belongs to the palladium-catalyzed coupling reactions and is widely used in medicinal chemistry. The main difference to SUZUKI, NEGISHI, STILLE or similar cross-couplings is that BUCHWALD-HARTWIG reactions form C-N bonds instead of C-C bonds. To realize this, the usage of special and complex phosphane ligands, highly dependent of the individual substrate, is necessary. The choice of bases is also limited, in most cases very strong and bulky bases like sodium *tert*-butoxide (NaOtBu) or lithium bis(trimethylsilyl)amide (LiHMDS) are required to achieve the amination[124, 125]. Since it is applicable to aryl halides and aryl pseudohalides, trifluoromethanesulfonate **PRU-9** was again chosen as a suitable reactant. The substance should be converted with the two corresponding alkylamines under classical BUCHWALD-HARTWIG conditions to obtain *N*-monomethyl- and *N,N*,-dimethylamines **16** and **17** (**Scheme 17**). Unfortunately, both attempts failed. Neither with *N*-methylamine nor with *N,N*-dimethylamine the desired product was formed. Tris(dibenzylideneacetone)dipalladium (0) with 2-(dicyclohexylphosphino)-2',4',6'-triisopropyl-1,1'-biphenyl (XPhos)[126] and palladium (II) acetate with 2,2′-bis(diphenylphosphino)-1,1′-binaphthyl (BINAP)[127] were used as catalysts. Since the secondary alcohol function at C-17 could be deprotonated by the frequently used base sodium *tert*-butoxide and thus consume one equivalent thereof, the usage of two equivalents was tested as well. To exclude a negative influence of the alcoholate function, the weaker bases cesium carbonate and potassium phosphate were also tried as alternatives to sodium *tert*-butoxide[128]. In all cases, either no conversion, decomposition or hydrolysis of the trifluoromethanesulfonate, which led to the formation of the original starting material estradiol (**3**), was observed.
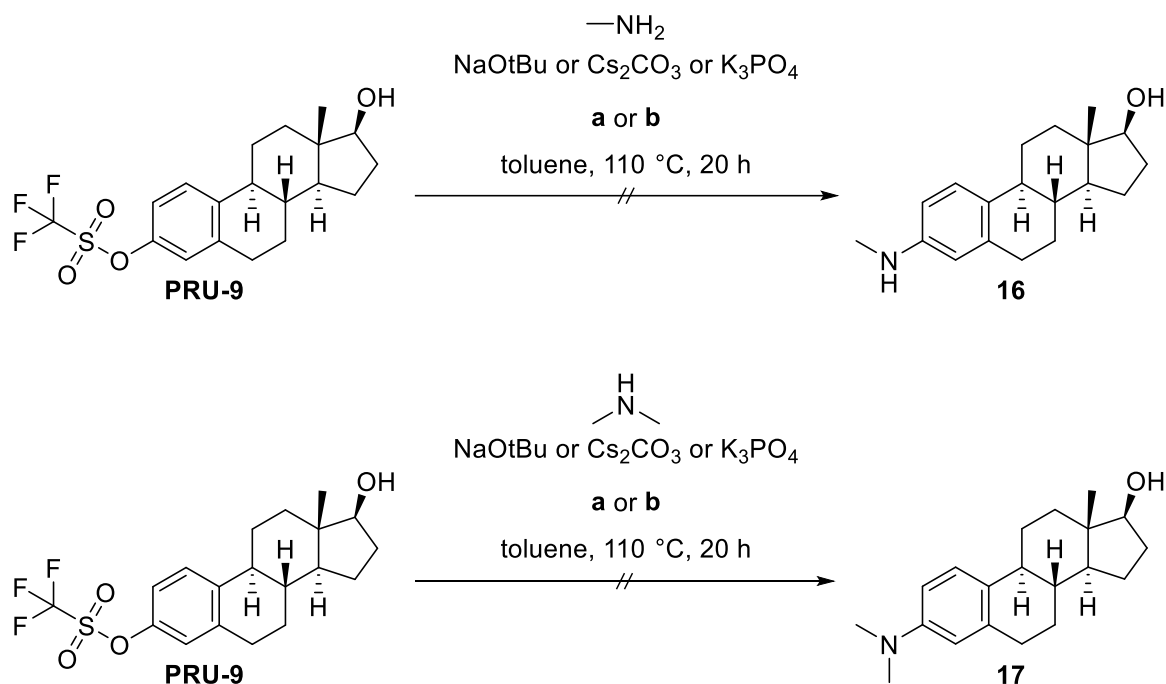
Scheme 17: Failed attempts of BUCHWALD-HARTWIG amination, **a**: Pd$_2$(dba)$_3$ and XPhos **b**: Pd(OAc)$_2$ and BINAP

Since the conditions and catalyst systems used are well established[126-128], the failure of this approach could be determined by two components: The amine and the reactant. Regarding the amine, it has to be noted that the BUCHWALD-HARTWIG coupling is markedly superior for cyclic amines and benzyl amines. Even though many protocols and catalyst systems for application of various amines have been described in recent years, the coupling of acyclic and especially primary amines tends to be more critical. The major problem in this case is the β-hydride elimination as a possible side reaction. The mechanism of the BUCHWALD-HARTWIG amination and the competing β-hydride elimination are shown in **Scheme 18**. After oxidative addition of the aryl halide or aryl pseudohalide (Ar-X) to a Pd (0) species and the following addition of the employed amine, an intermediate of the formula "L$_n$Pd (II)-NCH$_3$(R^2)" is formed. If the BUCHWALD-HARTWIG amination proceeds correctly, this species undergoes reductive elimination to afford the desired aryl amine, regenerating the Pd (0) catalyst concurrently. However, this intermediate can also be subjected to β-hydride elimination. In this process, a hydrogen of the alkyl group in β-position to the palladium gets transferred to the metal center as a hydride, forming an imine and a "Ar-Pd (II)-H" species which can reductively eliminate and thus produce the Ar-H side product, whereby the Pd (0) catalyst is regenerated[124]. Over time, more complex ligands have been developed to diminish the reaction rate of this unwanted pathway and make primary and secondary alkyl amines accessible for the BUCHWALD-HARTWIG amination. Among them, especially chelating (i.e. BINAP[127, 129] and more bulky (i.e. Xphos[126, 130]) ligands increased the yields, when primary and secondary amines were

employed. Nevertheless, this method still has limitations, since the result of the reaction is heavily substrate-dependent, as can be seen in our case.
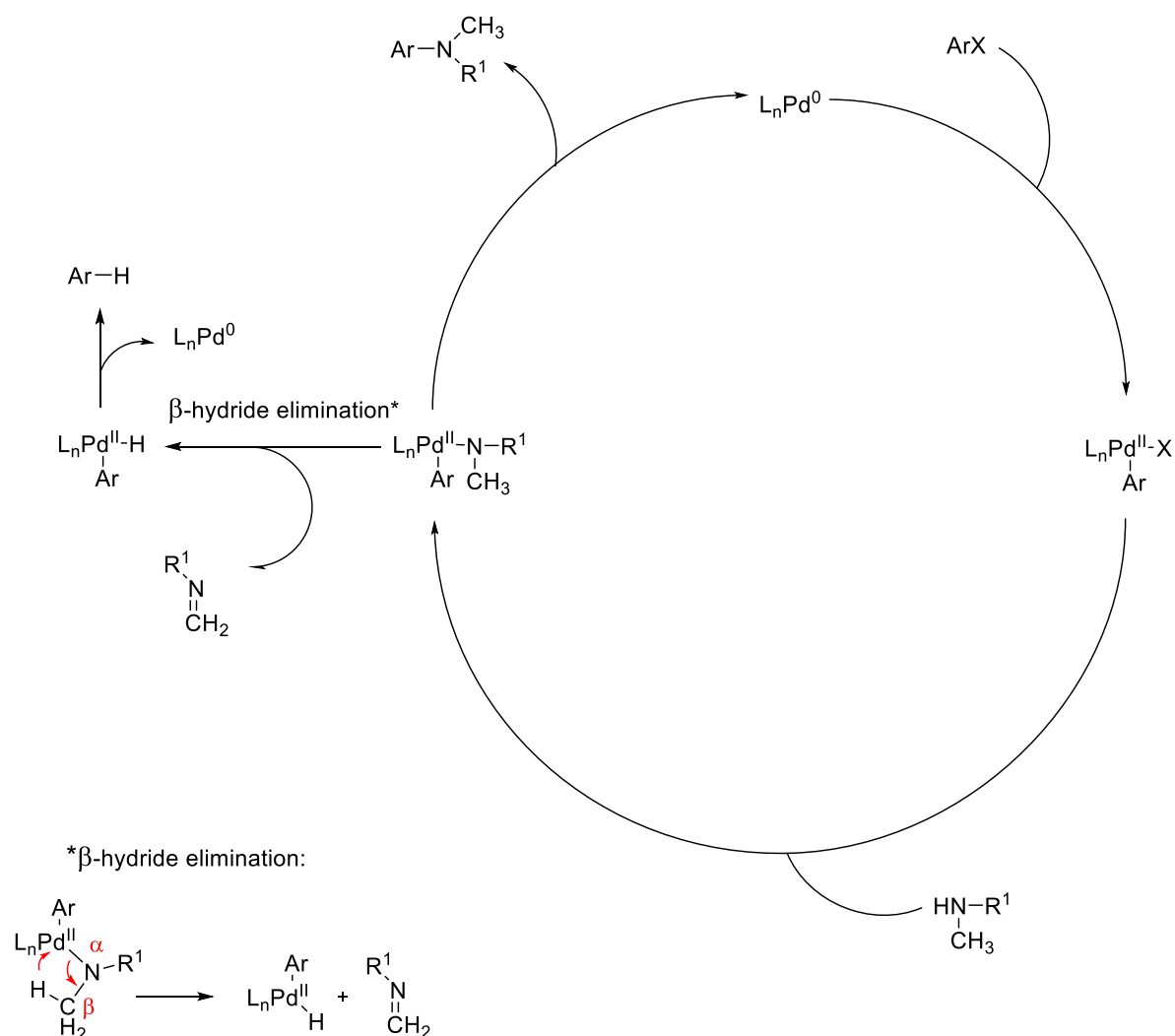

Scheme 18: Reaction mechanism of the BUCHWALD-HARTWIG coupling including β-hydride elimination as unproductive side reaction as proposed by the group of BUCHWALD[124] transferred to a acyclic primary or secondary amine (own depiction), Ar: aryl, X: halide or pseudohalide, R^1: H or methyl, L: Ligand

Regarding the reactant **PRU-9**, one of the problems could be the secondary alcohol function at C-17. The classical procedure involves usage of strong bases like sodium *tert*-butoxide or lithium bis(trimethylsilyl)amide, which may not be compatible with the alcohol. The employment of weaker bases such as carbonates and phosphates is also well established [128, 131], but in most cases leads to a lower conversion rate. The sole product that could be isolated was identified as estradiol (**3**), indicating that triflate hydrolysis is a major side reaction. This process can take place when triflates are treated with bases at higher temperatures. Stronger bases promote hydrolysis[132], but the weaker base cesium carbonate is also known to be capable of triflate hydrolysis[133]. Since this reaction competes with the desired conversion, the outcome of the approach is determined by the kinetics of both reactions. For a good result, it would be

crucial that the BUCHWALD-HARTWIG coupling proceeds faster than the hydrolysis as the emerging estradiol can not take place in this reaction and as a phenol with a pK$_a$ value of about 10 also consumes one more equivalent of base. These circumstances together may have led to the failure of this approach.

To address these issues, two changes had to be made. The first concerned the choice of the amine used. This had to fulfill two criteria: The amine should be more reactive under the applied conditions than those previously used and, at the same time, offer feasible synthetic possibilities for conversion to the unsubstituted aniline, *N*-monomethyl- and *N,N*-dimethylaniline. Regarding these aspects, benzylamine emerged as the most promising option. As already mentioned, it is a well established building block for BUCHWALD-HARTWIG couplings. In addition, the generated *N*-benzylaniline compound could serve as a precursor for all three analogs, since the benzyl group should allow *N*-monomethylation of the nitrogen and can usually be easily split off. The second change is the introduction of a suitable protective group for the secondary alcohol at C-17. This group should sustain the conditions of the coupling step and ideally also subsequent *N*-methylation or reductive alkylation of the amine in order to obtain *N*-monomethylamine analog **16**. Since the theoretical product of the BUCHWALD-HARTWIG reaction would already carry a benzyl group at the nitrogen, the plan was to protect the alcohol (17-OH) with a benzyl group beforehand in order to obtain the benzyl protected triflate **23**, and after the coupling step ultimately cleave off both benzyl groups in one single step (**Scheme 19**).
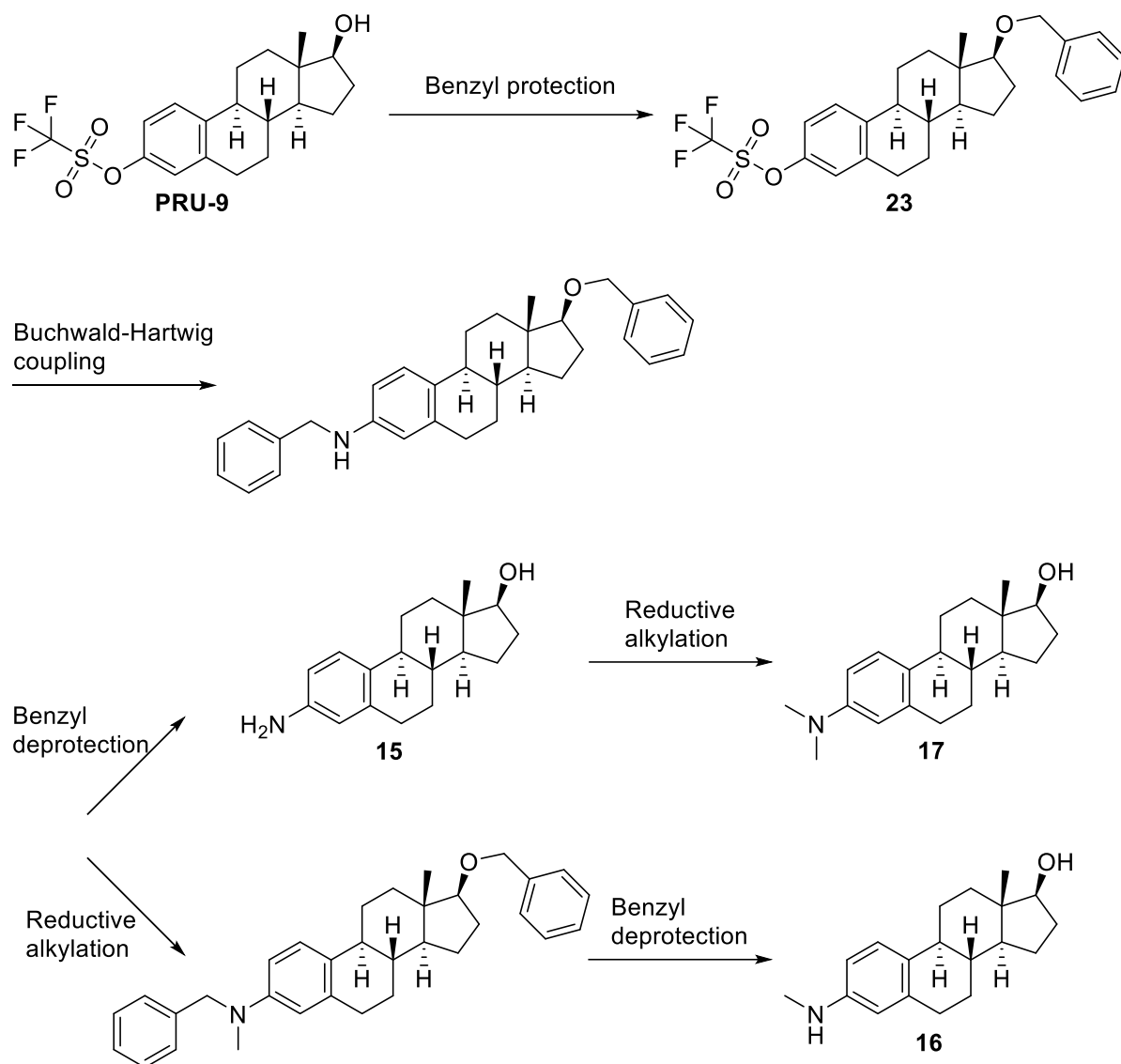
Scheme 19: Planned synthesis route to amines **15**, **16** and **17** *via* benzyl protection of the C-17 alcohol and BUCHWALD-HARTWIG coupling with benzylamine

Excursus: Investigation on suitable benzylation methods for the benzyl protection of estradiol derivatives and 19-nortestosterone

In the course of this project, the introduction of appropriate protective groups played an important role. All starting materials used for the synthesis of **EDME** analogs carried a secondary alcohol at C-17. In many cases, protection of this group was decisive for the success of the subsequent reactions.

The benzyl group is one of the most favored and most utilized protective groups for alcohols. Besides the triflate **PRU-9**, two more compounds were planned to be converted into their corresponding benzyl ethers: carbamate **24** and 19-nortestosterone (**4**) (**Scheme 20**). The two latter substances and the associated reactions are part of the following chapters. Despite this, they are also included in this excursus, since the investigation on the most effective benzylation

method contained experiments with these compounds. The goal was to find one general procedure which is applicable to all three substances. Since 19-nortestosterone (**4**) was readily available in high amounts, pilot reactions were mostly conducted with this substance as starting material.
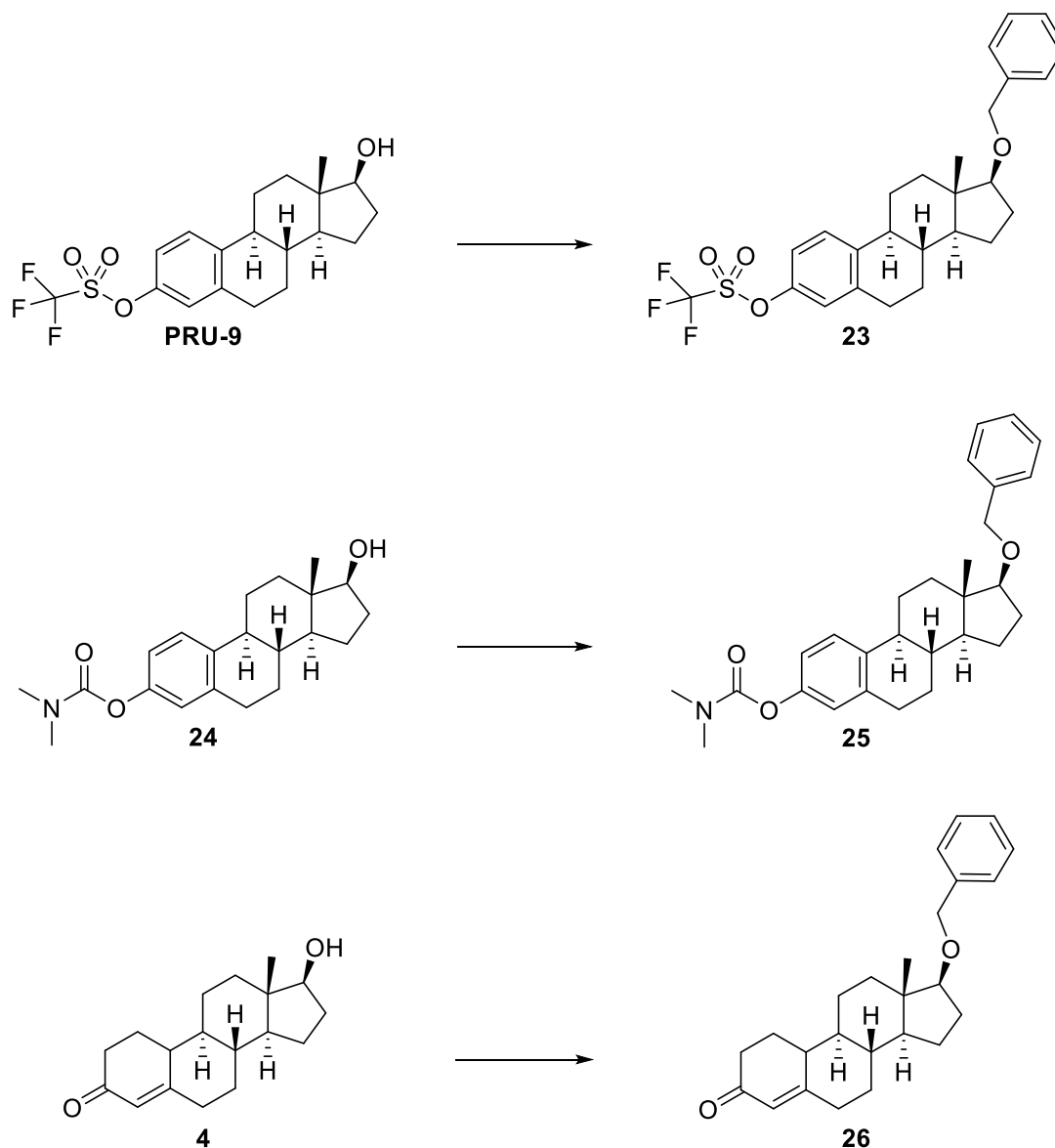

Scheme 20: Depiction of the three compounds and their potential benzylation products

The standard method for the benzyl protection of aliphatic alcohols is using the WILLIAMSON ether synthesis. Deprotonation with strong bases like sodium hydride generates an alcoholate, which subsequently undergoes a nucleophilic substitution reaction with a benzyl halide or benzyl triflate to form the desired benzyl ether. In the case of the three shown compounds, small scale test reactions indicated that none of the substances is suitable for this protocol. In all three cases, treatment of the respective starting material in DMF with sodium hydride led to its decomposition (**Scheme 21**).
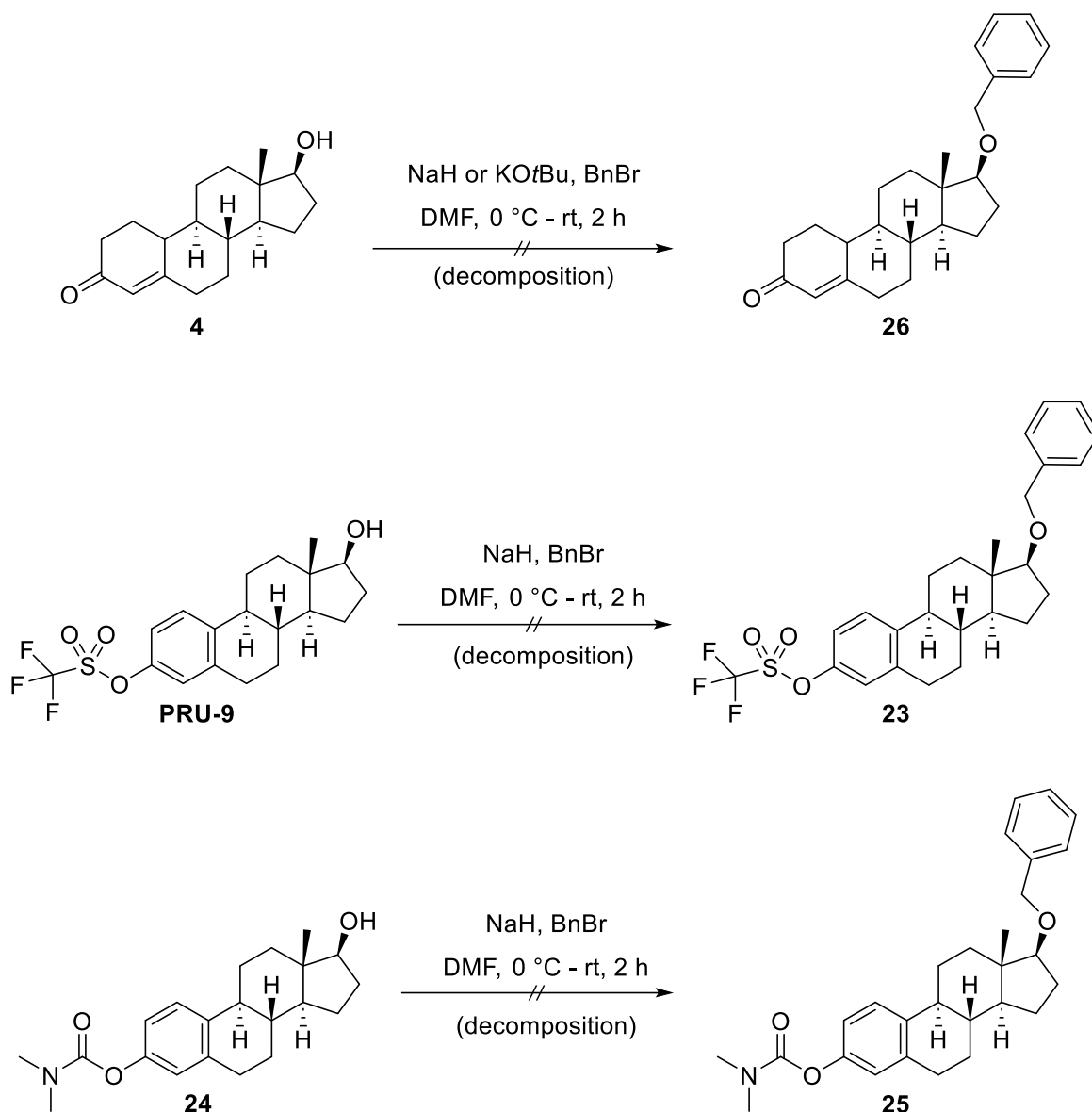
Scheme 21: First benzylation approach with a classic WILLIAMSON ether synthesis

Since sodium hydride was deemed to be too reactive for our purpose, an alternative option was to use the milder base silver (I) oxide[134, 135]. Consequently, two small scale experiments in DMF and DCM were conducted under a nitrogen atmosphere using 19-nortestosterone (**4**), benzyl bromide (1.1 eq) and silver (I) oxide (1.5 eq) as base (**Scheme 22**). After stirring for 15 hours at ambient temperature, TLC monitoring showed no conversion in either solvent. Even after increase of the temperature to 80 °C and gradual addition of another two equivalents of base and benzyl bromide, the starting material remained untouched.
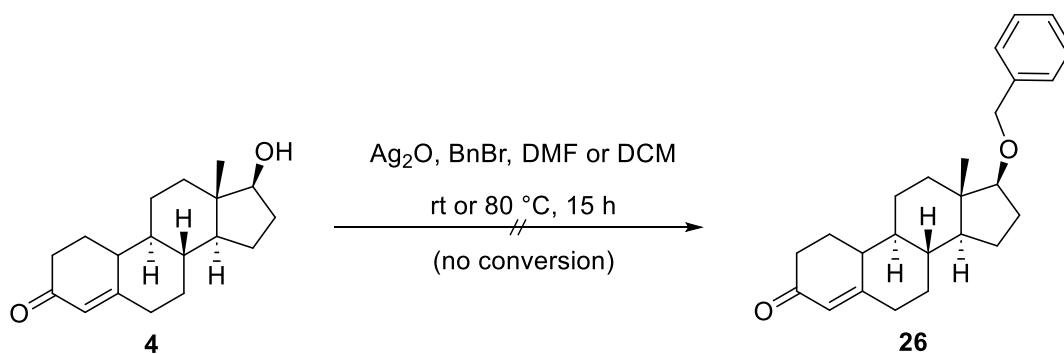
Scheme 22: Attempt with silver(I) oxide

After failure of these approaches under basic conditions, benzyl protection under acidic conditions should be examined. Benzyl 2,2,2-trichloroacetimidate is a reagent which allows acid-catalyzed benzylation of alcohols[136, 137]. To judge suitability of this reagent, a method published by SKAANDERUP *et al.*[138] using the LEWIS acid zinc trifluoromethanesulfonate as catalyst was tested on 19-nortestosterone (**4**) (**Scheme 23**). Generation of the potential product could be observed by TLC monitoring, but the reaction did not run until completion. The yield could not be accurately determined because a large amount of by-product trichloroacetamide (**27**) was produced, which could not be effectively separed by flash column chromatography.
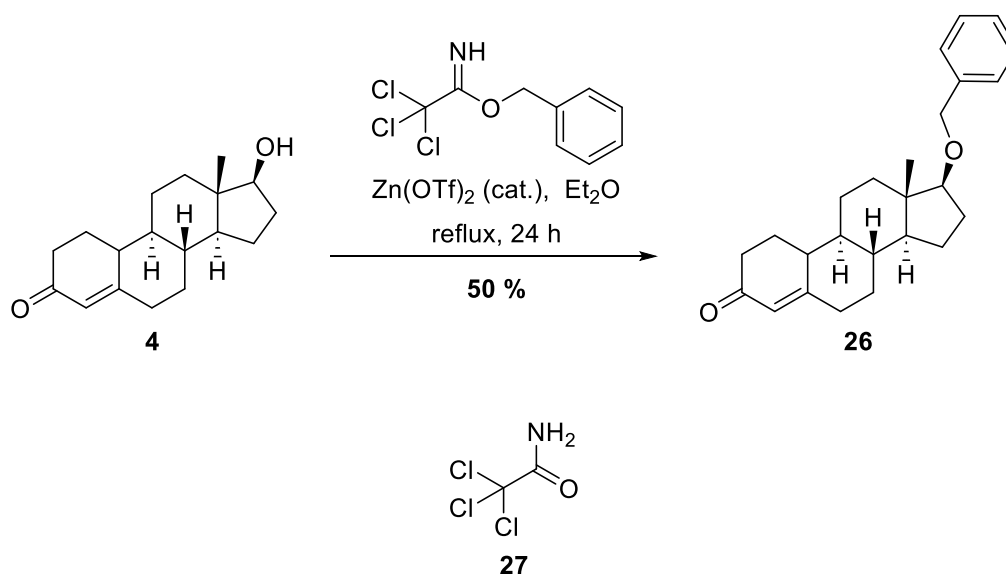
Scheme 23: Benzylation of **4** with benzyl 2,2,2-trichloroacetimidate and the generated by-product **27**

Nevertheless, identity of **26** could be confirmed by NMR and mass spectrometry analysis. The estimated yield based on NMR data was 50 %. Since the conversion rate was only moderate, the same reaction was again carried out using higher amounts of benzyl 2,2,2-

77

trichloroacetimidate. Unfortunately, addition of more equivalents of the reagent did not lead to a significant increase of the yield. Improved dissolution of the starting material could be reached by changing the solvent from diethyl ether to THF, but had no effect on the yield. Further on, another approach to receive a better result was usage of a BRØNSTED acid as catalyst. Hence, a protocol published by TARIQ RIAZ *et al.* conducting the reaction with trifluoromethanesulfonic acid and a 1:1 mixture of DCM and hexanes as solvent[139] was applied to **4** (**Scheme 24**). The outcome of this change was an even lower yield (20 % based on NMR data), while at the same time more side products were formed.
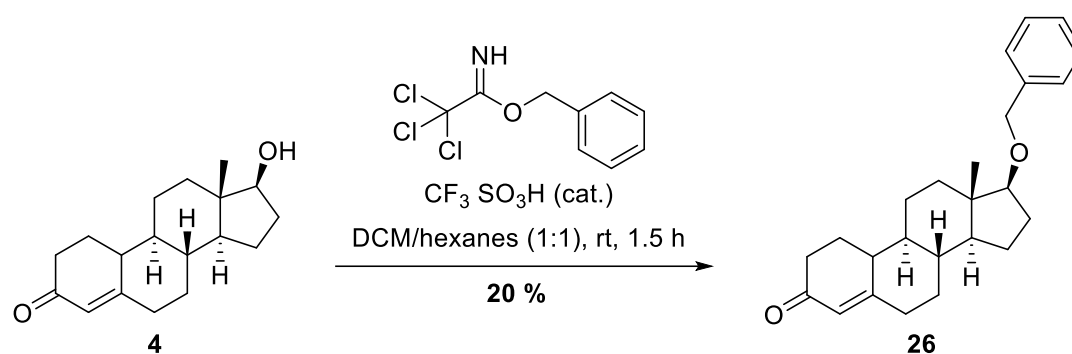
**Scheme 24**: Benzylation attempt with trifluoromethanesulfonic acid catalysis

In order to assess transferability of the more successful LEWIS acid protocol with zinc trifluoromethanesulfonate, this reaction was also conducted with carbamate **24** (**Scheme 25**). Since the reaction could not be carried out in diethyl ether due to the extremely low solubility of **24** in this solvent, a mixure of diisopropyl ether (DIPE) and chloroform (7:1) was used instead. Benzyl ether **25** was obtained in 30 % yield (estimated based on NMR data), but again separation from by-product **27** could not be fully achieved. Due to the only moderate yields and the separation issue, this method was not considered ideal for our purposes and was correspondingly not pursued further.
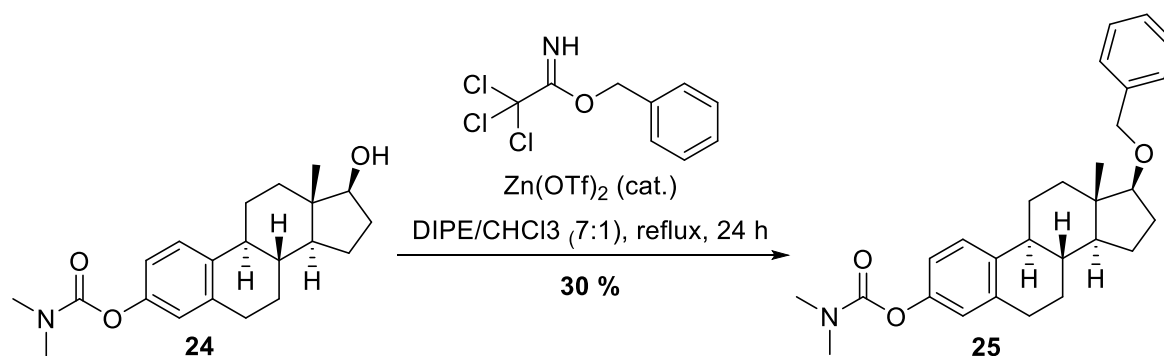
**Scheme 25**: Benzylation of **24** using the method by SKAANDERUP *et al.*[138]

In addition to benzylation under basic and acidic conditions, new methods have been developed in the last two decades that enable benzyl protection under neutral conditions. The group of DUDLEY described the benzylation of alcohols using pyridinium salt 2-benzyloxy-1-methyl-pyridinium triflate (Dudley's reagent) as donor of a benzyl group and magnesium oxide as acid scavenger[140]. The authors showed that several different substrates could be converted into their corresponding benzyl ethers in predominantly high yields. To investigate whether this protocol could provide better results than the method by SKAANDERUP *et al.*, it should first be applied to **4** (**Scheme 26**). Heating the steroid **4**, benzyl group donor 2-benzyloxy-1-methyl-pyridinium triflate, which was previously prepared according to the method described in the paper[140] and magnesium oxide in trifluorotoluene gave the desired benzyl ether **26** in 82 % yield (shown in the later displayed publication in *Molecules* in 2023[141], substance number **7** in the paper). After this success, carbamate **24** and triflate **PRU-9** were also subjected to this procedure yielding the desired benzyl ethers **25** (57 %) and **23** (90 %).
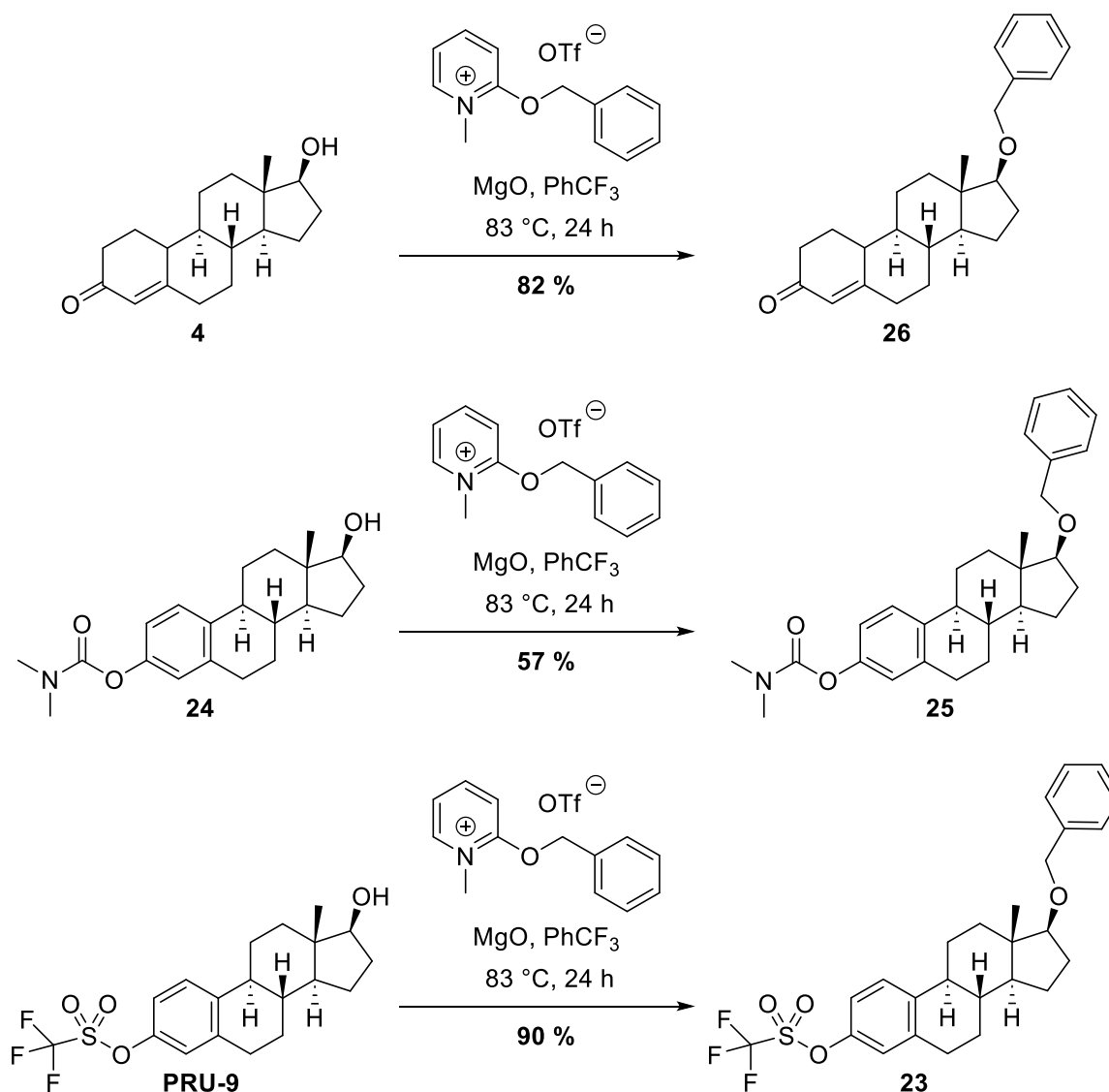
Scheme 26: Successful strategy for the benzylation of the three compounds using the method by the group of DUDLEY[140]

The mechanism proposed in the publication assumes either a S_N2 or a S_N1 type pathway (**Scheme 27**), whereby the authors consider a S_N1 mechanism to be more likely. Benzylation reagent 2-benzyloxy-1-methyl-pyridinium triflate reacts with an alcohol to produce the respective benzylether and 1-methyl-2-pyridone. Magnesium oxide is used as an acid scavenger to trap the released protons.
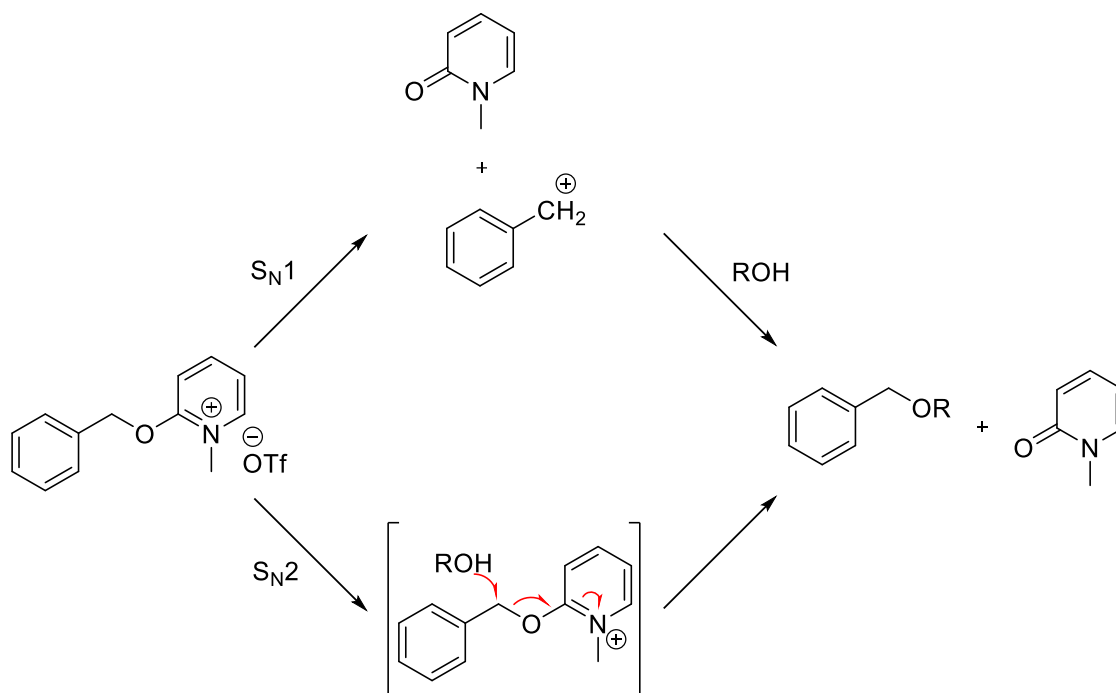
Scheme 27: Mechanism of the benzylation with 2-benzyloxy-1-methyl-pyridinium triflate proposed by the group of DUDLEY[140] (own depiction)

In conclusion, the *O*-benzylation method developed by the group of DUDLEY has proven to be suitable for the benzyl protection of all three compounds. The three resulting benzyl ethers could later be used for different synthesis approaches. The synthesis and characterization of **26** is shown in detail in the publication in Molecules in 2023[141] which is depicted in Chapter **4.1.2.3** (substance **7** in the paper).

With benzyl protected triflate **23** now in hand, the BUCHWALD-HARTWIG coupling route could be proceeded. Compound **23** should be converted into amine **28** *via* coupling with benzylamine (**Scheme 28**). For the determination of the ideal reaction conditions for the BUCHWALD-HARTWIG coupling, five test approaches were performed using varying combinations of temperature, base and catalyst (**Table 1**). All reactions were carried out with triflate **23** and benzylamine as reactants.

| Method	Catalyst	Base	Time, temperature	Solvent	Result/Yield of 28
1	Pd$_2$(dba)$_3$, XPhos	K$_3$PO$_4$	100 °C, 24 h	dioxane	19 %
2	Pd(OAc)$_2$, XPhos	Cs$_2$CO$_3$	160 °C, 10 min (microwave)	DMF	Hydrolysis to estradiol 17-benzyl ether (28)
3	Pd(OAc)$_2$, XPhos	Cs$_2$CO$_3$	100 °C, 24 h	DMF	68 %
4	Pd(OAc)$_2$, BINAP	NaOtBu	80 °C, 24 h	toluene	27 %

Table 1: Conditions of the test approaches of the BUCHWALD-HARTWIG coupling with **23** and benzylamine

Methods 1[142] and 4[143] provided rather low yields with **23**. Microwave-assisted method 2[144] resulted in nearly quantitative hydrolysis of the triflate to give estradiol 17-benzyl ether (**29**). The same procedure, carried out at a lower temperature in an oil bath without microwave assistance (method 3), provided the key intermediate **28** in good yield (68 %).
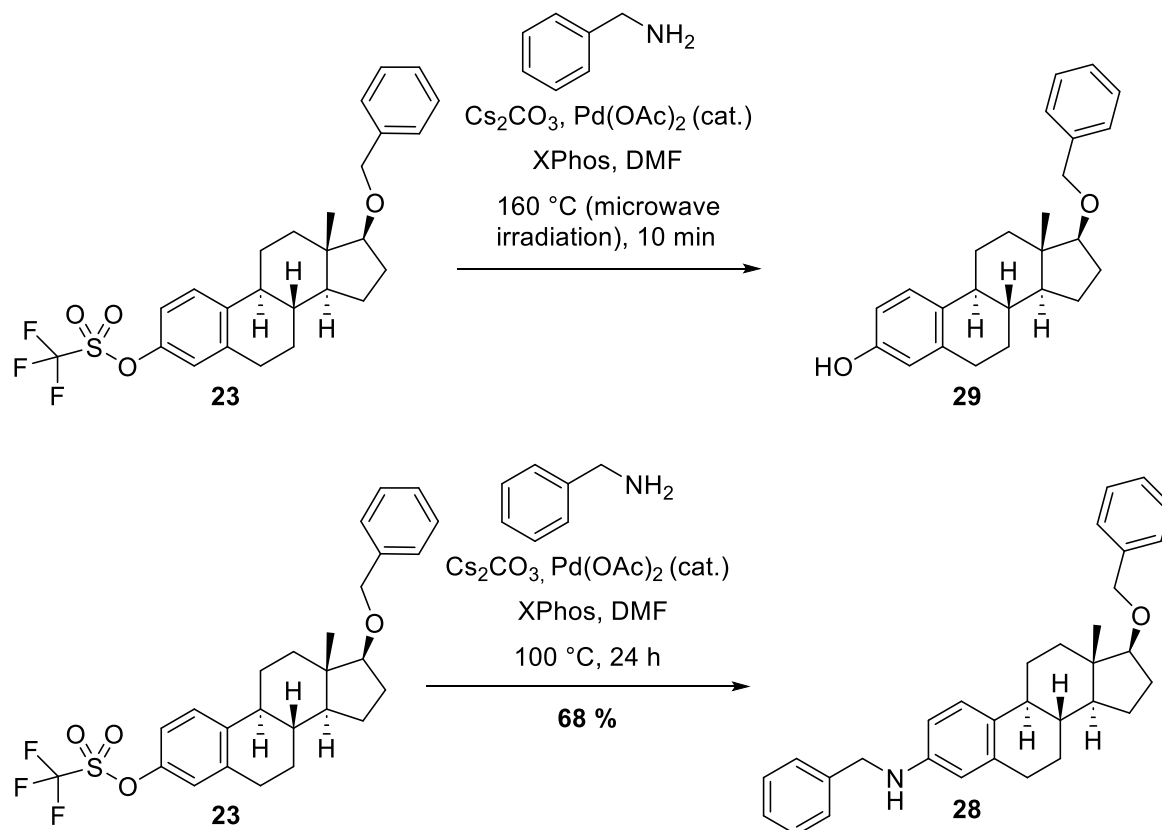

Scheme 28: BUCHWALD-HARTWIG coupling with benzylamine: Hydrolysis of **23** and most successful method 3 using an oil bath instead of microwave irradiation

Reductive *N*-methylation with formaldehyde and sodium cyanoborohydride in acetonitrile and acetic acid[145] gave **30** in 53 % yield. The subsequent catalytic hydrogenation merely cleaved the benzyl group bound to the nitrogen, while the benzyl ether at C-17 remained untouched. To accomplish the second debenzylation, the formed product **31** was treated with boron trichloride[146] giving the desired *N*-methyl aniline **16** in 70 % yield (**Scheme 29**).
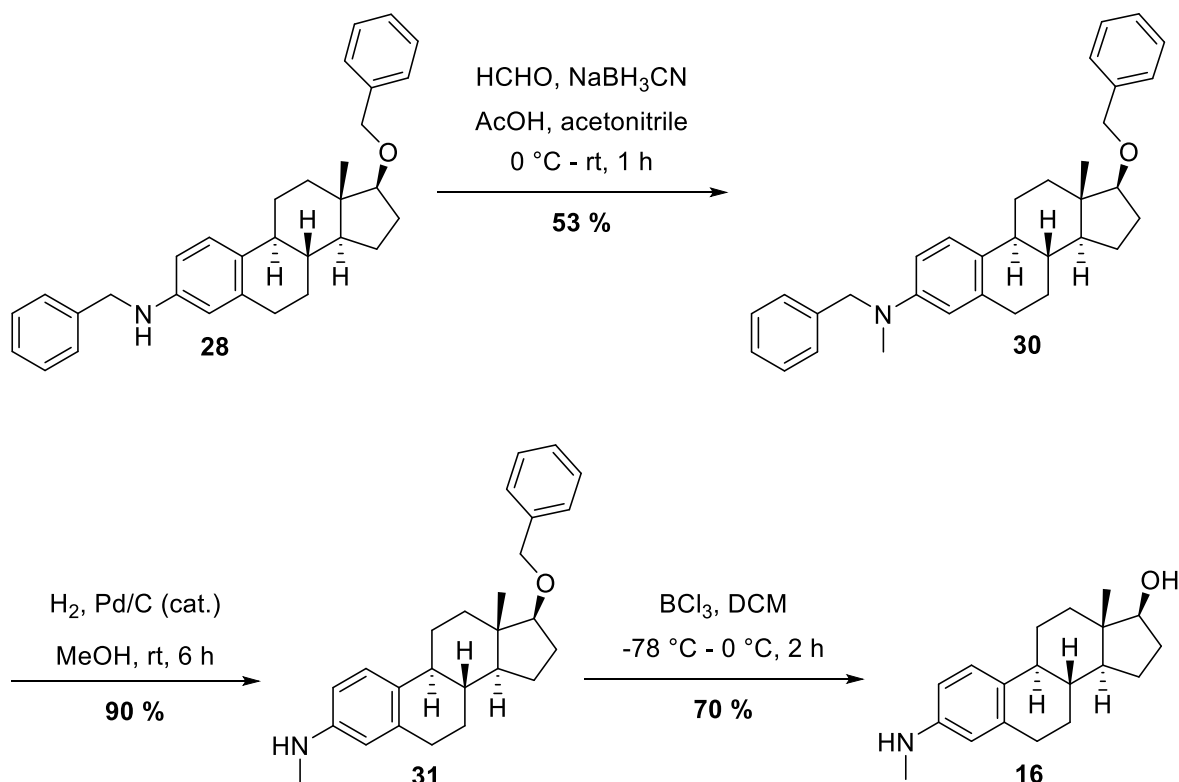

Scheme 29: Preparation of *N*-methyl aniline analog **16**

For the synthesis of the primary aromatic amine **15** (see **Figure 14**, **Scheme 19**), BUCHWALD-HARTWIG product **28** had to be debenzylated in the same manner. In contrast to the previous debenzylation sequence, **28** was first treated with boron trichloride, which resulted in selective cleavage of the benzyl ether to form benzyl amine **32** in 86 % yield. This time, the benzyl group bound to the nitrogen was left untouched. Subsequent catalytic hydrogenation of **32** finally yielded primary aromatic amine analog **15** (90 %). Reductive alkylation of this compound with formaldehyde and sodium cyanoborohydride[145] gave the *N*,*N*-dimethylamino analog **17** in 56 % yield (**Scheme 30**).
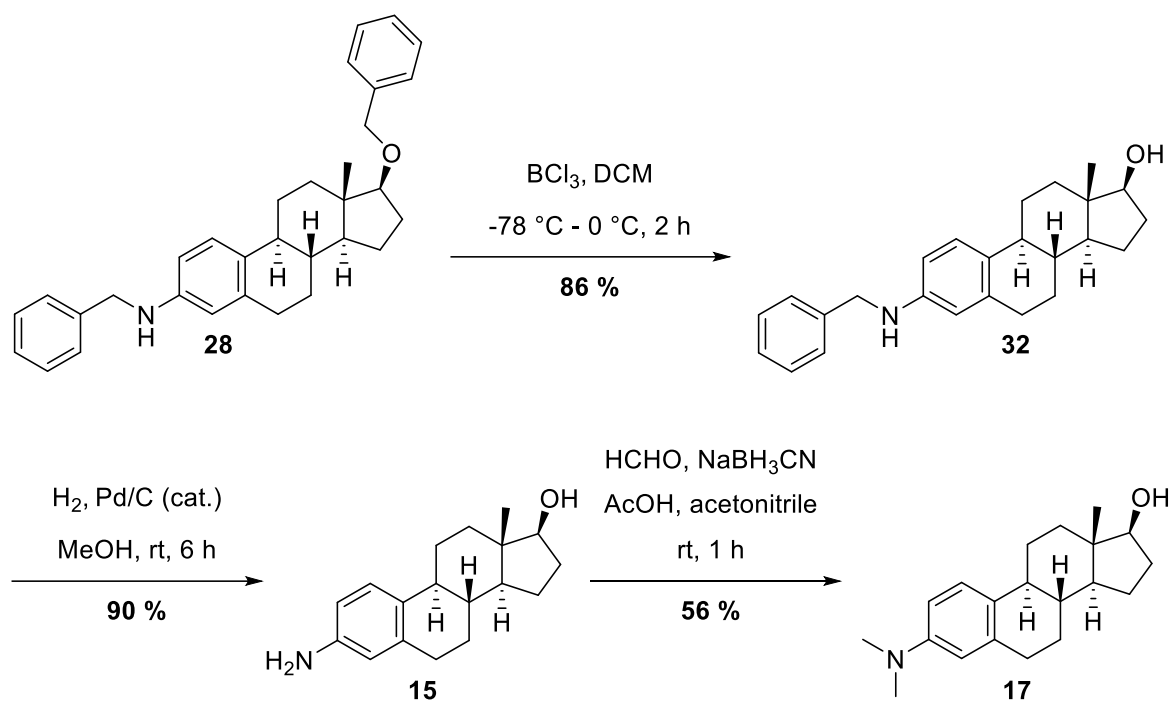
Scheme 30: Synthesis of primary aromatic amine **15** and its *N,N*-dimethyl derivative **17**

Since the cleavage of the two benzyl groups in this procedure again takes two steps, another approach was made with the goal to achieve this in one single step. While treatment with boron trichloride turned out to be selective for *O*-benzyl cleavage, catalytic hydrogenation can normally accomplish both *N*-benzyl and *O*-benzyl deprotection. Therefore, catalytic hydrogenation of **28** was attempted. As cleavage of the benzyl ether was not observed under classical conditions with the similar amine **30** (see **Scheme 29**), a few changes were implemented to the method. The first one was the degasification of the solvent with the Freeze-Pump-Thaw method (FPT). In this procedure, the solvent is cooled to -78 °C in a dry ice/acetone bath and the headspace of the then frozen solvent is evacuated. The solvent is allowed to warm and thaw in order to draw the dissolved gases into the headspace. The entire process is repeated three times to achieve proper degassing. After that, the catalytic hydrogenation was done using the analogous method as with **30**. The idea behind this pretreatment is to saturate the solvent with hydrogen. As indicated by TLC, one benzyl group was removed while the other one again remained intact. Addition of acetic acid did also not change the result, thus after a short work-up, the crude product was combined with palladium on charcoal and triethylsilane according to a procedure published by MANDAL *et al.*[147]. The principle of this hydrogenation method is the *in situ* generation of hydrogen from triethylsilane, though this strategy was not successful either since only substance **33** with an intact benzyl ether at C-17 could be isolated (**Scheme 31**). In conclusion, the synthesis route to **15** and **17** (see **Scheme 30**) could not be abridged as still two steps were required for the removal of both benzyl groups.
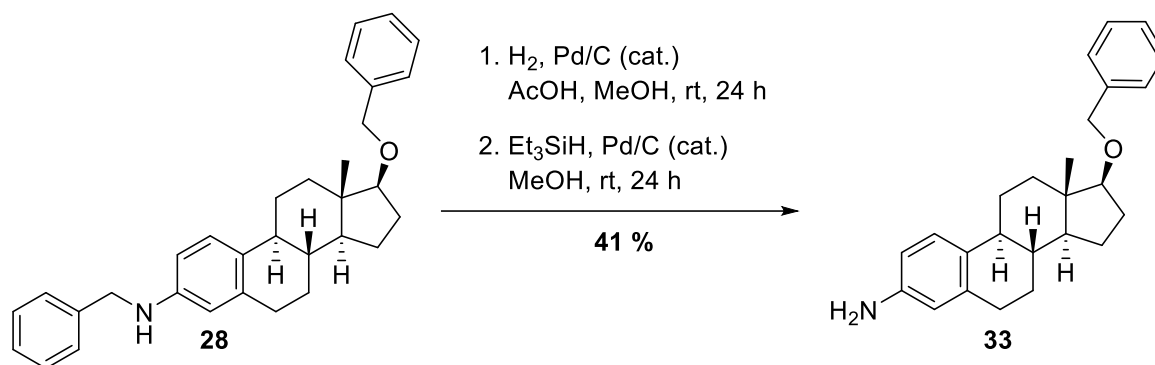
Scheme 31: Alternative unsuccessful approach for simultaneous cleavage of both benzyl groups leading to single debenzylated compound **33**

After successful exchange of the oxygen at C-3 of the estrane scaffold by a nitrogen atom, one more interesting structural modification at C-3 was the construction of a thio analog of **EDME**. Sulfur as a chalcogen possesses similar physicochemical properties compared to oxygen but is a weaker hydrogen bond acceptor and has a bigger atom radius. These differences could influence binding and interaction of the molecule with the target protein and estrogen receptors. YOU *et al.*[148] described a palladium-catalyzed coupling reaction with potassium thioacetate starting from estrone 3-triflate to give the corresponding thioacetate, which could then be hydrolyzed to yield the 3-thio analog of estrone. However, application of this protocol to estradiol 3-triflate (**PRU-9**) did not lead to the formation of the desired product **34**, but instead to the decomposition of the starting material in the first step (**Scheme 32**).
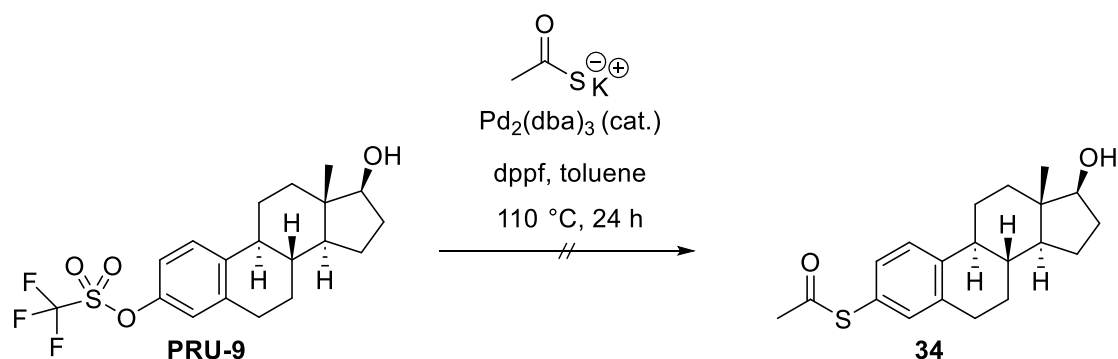
Scheme 32: Unsuccessful approach to a thio analog of **EDME** using the procedure by YOU *et al.*[148]

In general, palladium-catalyzed reactions with sulfur containing reagents rarely proceed smoothly due to the catalyst poisoning effect of sulfur[149]. An alternative approach for the synthesis of the target substance was the NEWMAN-KWART rearrangement. This reaction is used as a standard method for the synthesis of thiophenols starting from their corresponding phenols. The first step of this process is the conversion of a phenol into the *O*-aryl thiocarbamate. This is followed by the actual rearrangement step which usually takes place at

very high temperatures (250 - 300 °C) and leads to the *S*-aryl thiocarbamate. Hydrolysis thereof then yields the thiophenol. Following a procedure published by BROESE *et al.*, estradiol (**3**) was converted into thiocarbamate **35** in 76 % yield by addition of *N,N*-dimethylthiocarbamoyl chloride after deprotonation with sodium hydride[150] (**Scheme 33**).
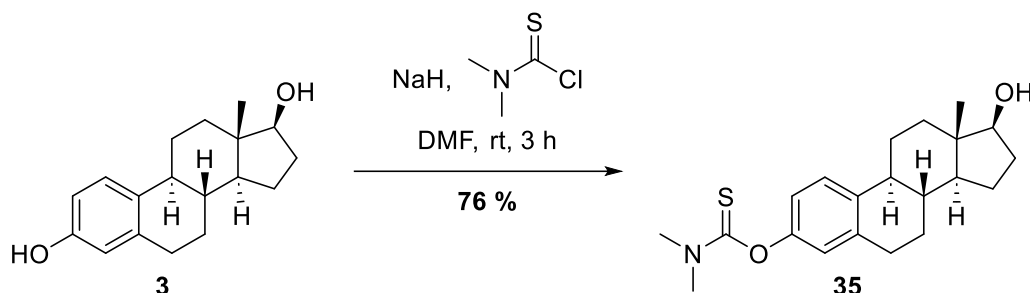

Scheme 33: Preparation of *O*-aryl thiocarbamate **35** using the protocol by BROESE *et al.*[150]

In order to realize the subsequent rearrangement step, it was crucial to select practicable conditions for this reaction. The NEWMAN-KWART rearrangement can basically be classified as an intramolecular aromatic nucleophilic substitution (see **Scheme 34**). Substrates bearing electron withdrawing groups in *para*- or *ortho*- position provide better results at lower temperatures because of the lower electron density on the aromatic ring, whereas electron-rich aromatic substrates require harsher conditions[151].
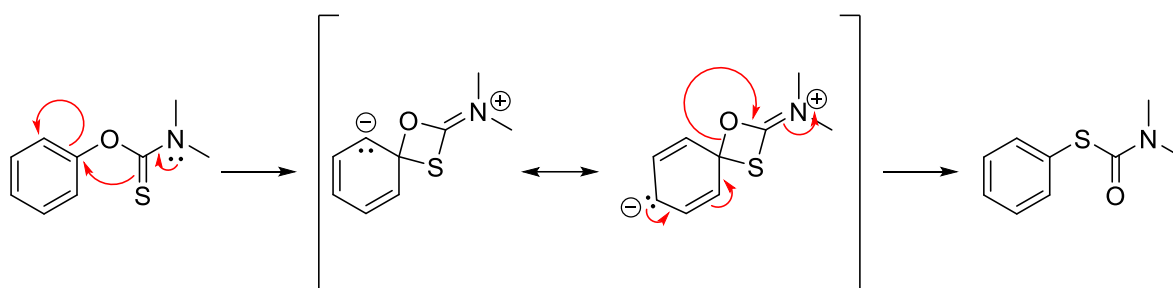
Scheme 34: Proposed mechanism of the NEWMAN-KWART rearrangement[151] (own depiction)

Due to the +I effect of the alkyl substituents in *para*- and *meta*-position to the estradiol-derived thiocarbamate, **35** belongs to the second category of substrates. Therefore, the thermic rearrangement would demand temperatures up to 300 °C. LI *et al.* described the NEWMAN-KWART rearrangement of the 17-keto analog of **36**, which they prepared from estrone. They heated a suspension of this compound in mineral oil at 280 °C for 5 hours to obtain *S*-aryl thiocarbamate **37**[152] (**Scheme 35**).
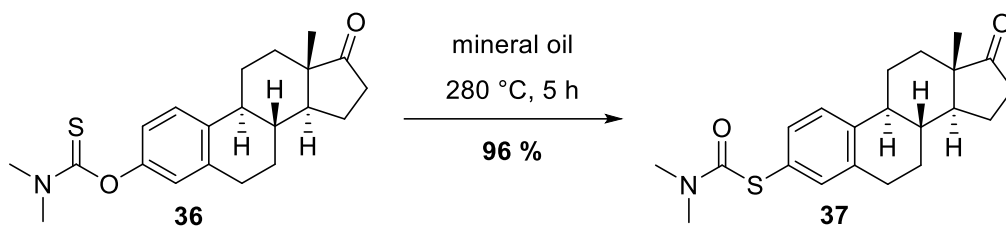
Scheme 35: NEWMAN-KWART rearrangement described by LI *et al.*[152] (own depiction)

One disadvantage of this method is the challenging removal of the high boiling solvent. Furthermore, due to technical limitations, this exceptionally high temperature cannot be easily reached using convenient laboratory equipment such as a magnetic stirrer with heating plate and oil bath. Most importantly, an analogous treatment of **35** could lead to degradation of the molecule or isomerization of the secondary alcohol function at C-17.

HARVEY *et al.* described a method for palladium-catalyzed NEWMAN-KWART rearrangement[153]. The addition of a palladium catalyst allows a significant decrease of the reaction temperature to 100 °C and the utilization of the lower boiling solvent toluene. NEWMAN-KWART rearrangement product **38** was prepared according to this protocol in moderate yield (**Scheme 36**).
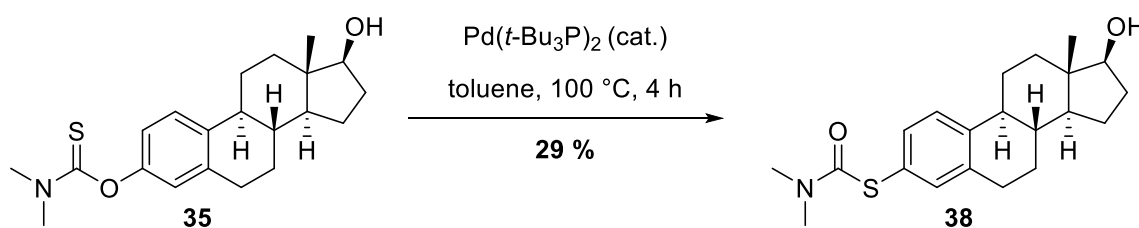

Scheme 36: Synthesis of *S*-aryl thiocarbamate **38** using the NEWMAN-KWART rearrangement method of HARVEY *et al.*[153]

To review the issues regarding the thermal NEWMAN-KWART rearrangement conditions, two additional attempts were made applying these classical conditions to **35**. The highest reachable temperature using a magnetic stirrer with heating plate and a metal heating block or an oil bath in our case was 260 °C. After 24 hours, small amounts of potential product could be detected, but not characterized or quantified as the resulting residue could not be purified sufficiently for a proper NMR analysis. This result confirms that **35** is not suitable for the application of these harsh conditions with convenient laboratory equipment.

Thiophenol **39** was obtained by hydrolysis of previously prepared *S*-aryl thiocarbamate **38** with aqueous sodium hydroxide in ethanol. This intermediate was *S*-methylated with iodomethane after deprotonation with sodium hydride to obtain the 3-methylthio analog of **EDME 40** in poor yield (**Scheme 37**).
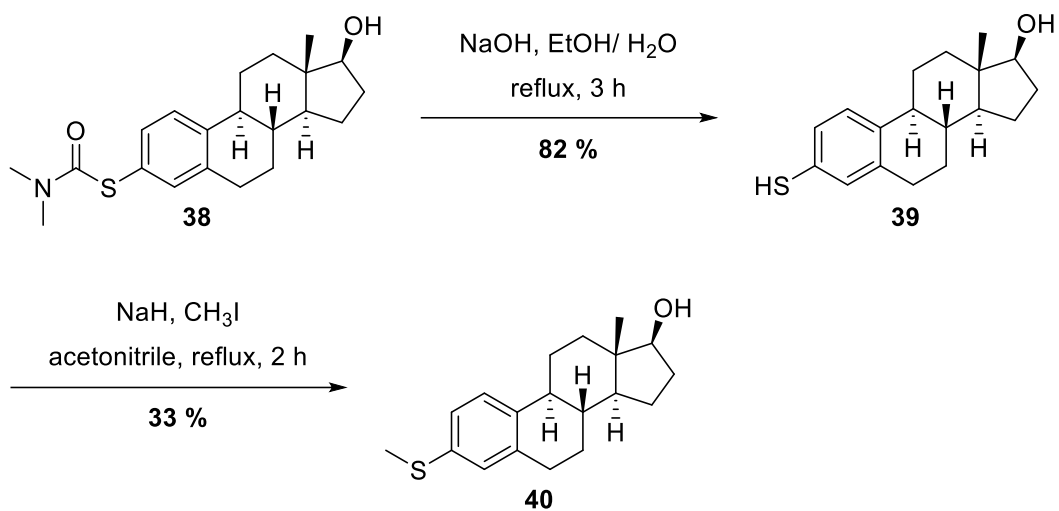
**Scheme 37**: Synthesis of 3-methylthio analog **40**

In summary, nine more analogs were designed and synthesized by structural modification at C-3 of the estrane scaffold. These represent one of three series of compounds that together constitute the second generation of **EDME** analogs (**Figure 15**).
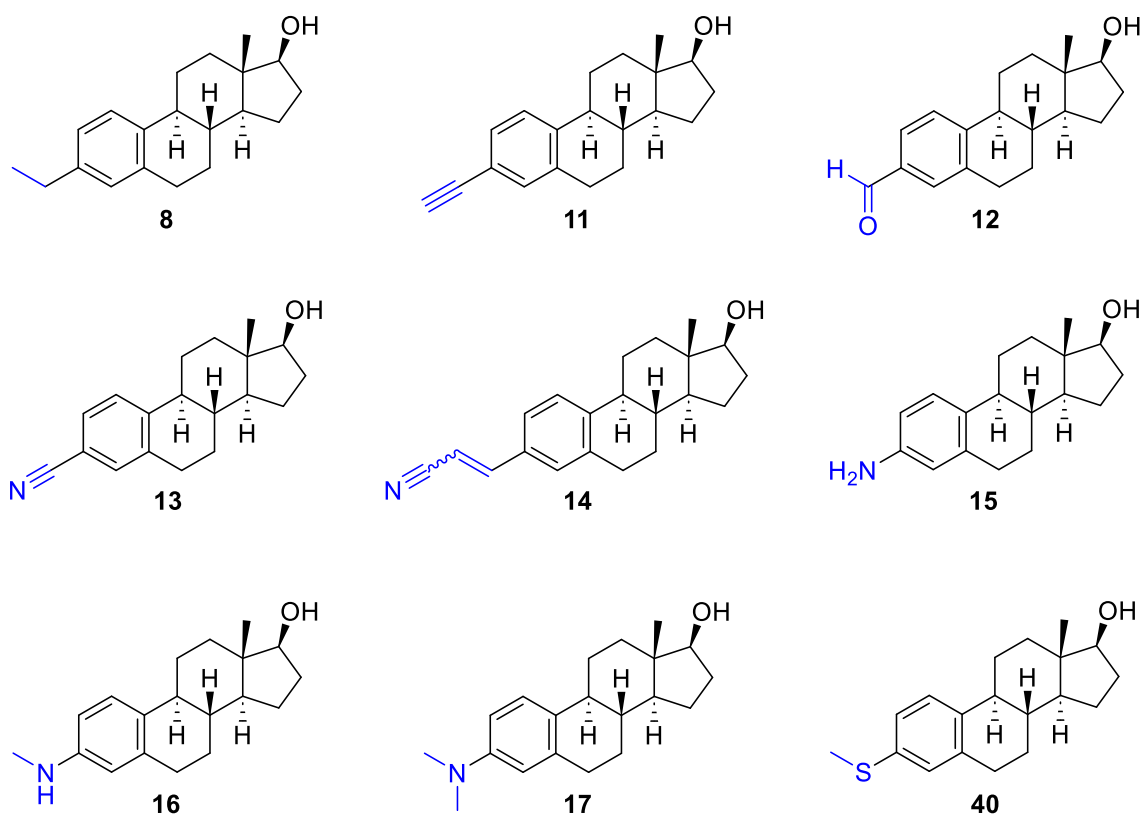
Figure 15: Overview of the new analogs carrying various substituents at C-3

4.1.2.2 Insertion of substituents at C-2 of the estrane scaffold

The next series of analogs is characterized by introduction of substituents at C-2. Since none of the substances tested up to this point carried substituents at this position, it was of utmost interest to introduce this mode of structural alteration. The intention was to construct molecules of this type by first synthesizing a building block bearing a halide or a pseudohalide at this position and then, similar to the procedure conducted with the triflate at C-3 (**PRU-9**), submitting this building block to various palladium-catalyzed coupling reactions. Thereby it should be possible to implement different functional groups and residues. Hence, the first step was to design and synthesize this building block. The most auspicious starting material for this strategy was again estradiol (**3**). A halogen can easily be introduced at C-2 by means of an electrophilic substitution reaction. To assure monoselective halogenation at C-2, it was crucial to select suitable conditions. ZHOU *et al.* published a method for the mild iodination of arenes with *N*-iodosuccinimide and indium (III) trifluoromethanesulfonate[154]. Among their examples, the authors showed that estradiol could be monoselectively iodinated at C-2. Consequently, this method was used to convert estradiol (**3**) into aryl iodide **41** (**Scheme 38**). The desired product **41** and the double iodinated side product **42** could be isolated in 63 % and 8 % yield, respectively. Since the formation of 4-iodoestradiol could not be observed, **42** must have been generated from **41** by further halogenation.
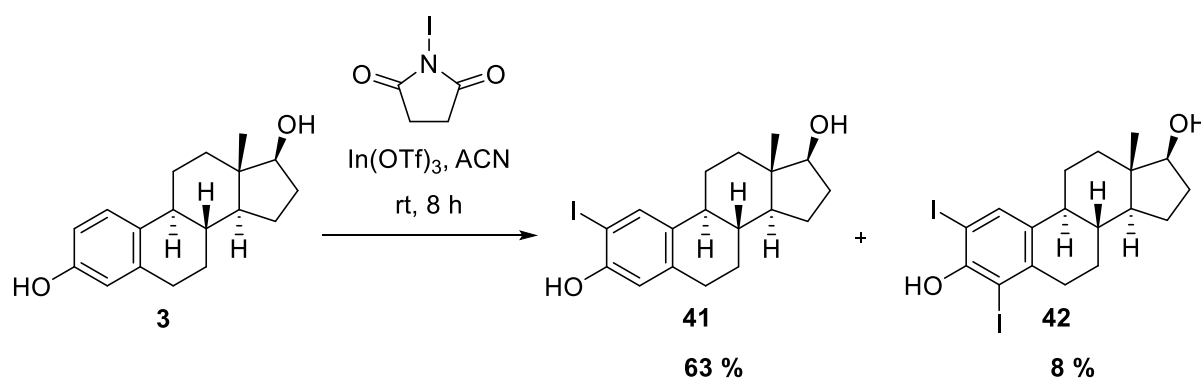

Scheme 38: Preparation of aryl iodide **41** and its 2,4-diiodo derivative **42**[154]

With this building block in hand, different substitutions at C-2 could be approached.

The first type of modification was to retain the methyl ether moiety at C-3 while inserting simple residues at C-2 to learn if additional substituents at this position are beneficial in inhibiting TRPML1 and/or reducing estrogenic effects. Additional substituents at C-2 could possibly allow more interaction with the target protein but also change the geometry of the molecule and exhibit steric effects. The envisaged substituents were functional groups accessible by cross-coupling protocols analogous to the modifications performed at C-3. To acquire a suitable synthetic precursor for this plan, it was advisable to first convert phenol **41** (see **Scheme 38**)

into the aryl methyl ether, as this structure motif of **EDME** should be conserved and the phenol could impede the subsequent steps. Consequently, a standard phenol ether synthesis protocol[155] was applied to 2-iodoestradiol (**41**) to obtain the desired *O*-methylated 2-iodoarene compound **43** in high yield (**Scheme 39**). This is not only a useful building block for the next reaction, but also the 2-iodo analog of **EDME** and thus itself represents an interesting compound.
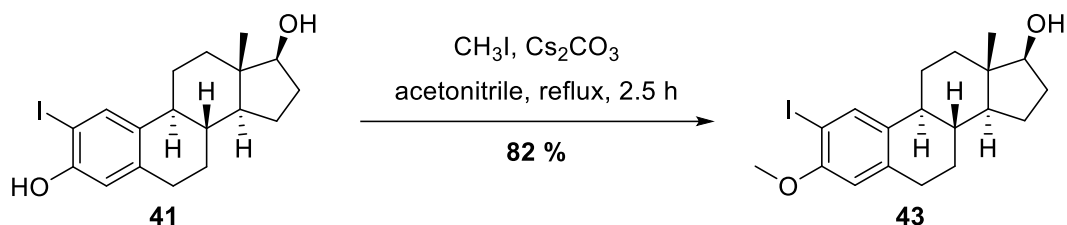
**Scheme 39**: Synthesis of the 2-iodo analog of **EDME 43**

The first two designated molecules accessible with the aid of 2-iodoarene **43** were the 2-vinyl analog **44** and the 2-acetyl analog **46**, which could be synthesized by two STILLE cross-coupling protocols (**Scheme 40**). For the preparation of 2-vinyl analog **44**, a method of SHI *et al.*[97], which was originally used for the synthesis of 3-vinyl analog **PRU-10**, was conducted with **43** to give the desired product in 77 % yield. Another STILLE protocol by CARRO *et al.*[156] employing tributyl(1-ethoxyvinyl)tin was applied to **43** to first form enol ether **45**. Subsequent hydrolysis, which occurred during the aqueous work-up process, gave 2-acetyl analog **46** in 43 % yield.
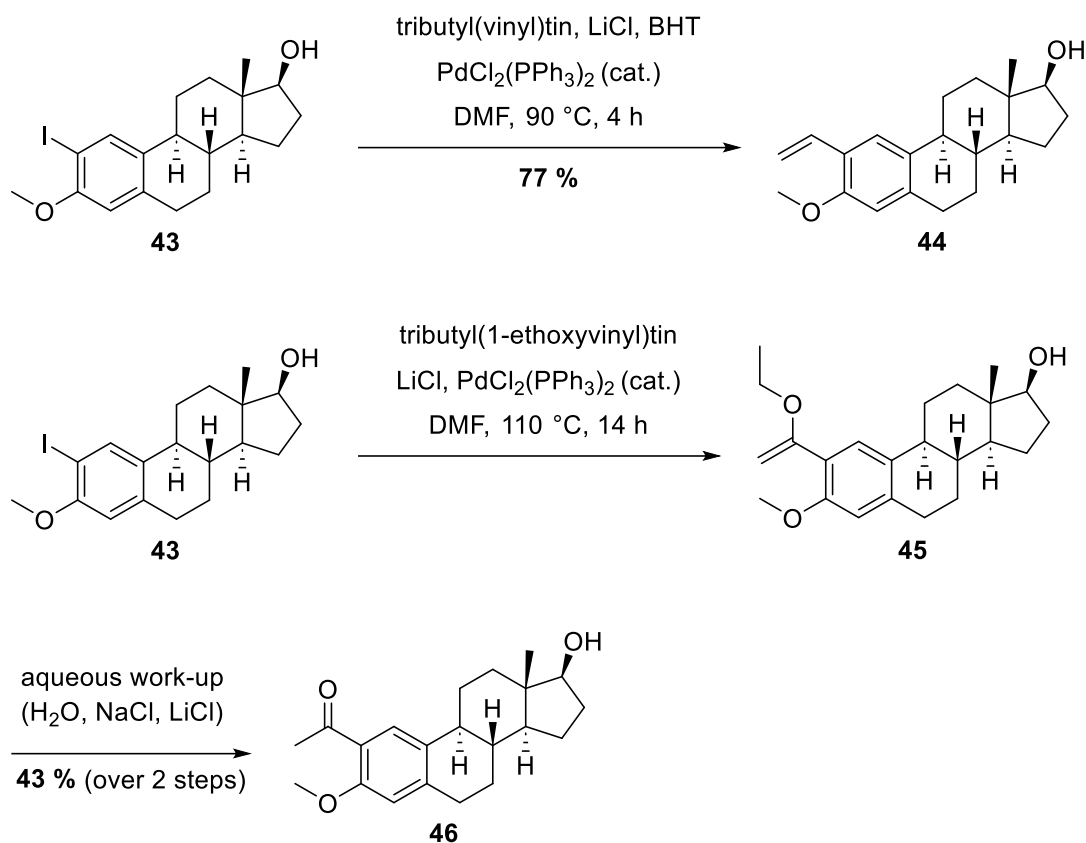
Scheme 40: Preparation of 2-vinyl analog **44** and 2-acetyl analog **46** by means of STILLE coupling with 2-iodoarene **43**

The next goal was the preparation of the 2-phenyl substituted analog **47**, which was intended to be achieved by means of SUZUKI coupling. Consequently, 2-iodinated **EDME** (**43**) was subjected to a classic SUZUKI protocol[157] using phenylboronic acid, bis(triphenylphosphine)palladium (II) chloride and triethylamine to afford the desired product **47** (**Scheme 41 A**). Due to the similar polarity of reactant **43**, product **47** and another unidentified side product, repeated flash column chromatography did not lead to a complete separation and 2-phenyl substituted analog **47** could not be retrieved in pure form. Recrystallization attempts in various solvents were equally fruitless. To avoid this separation issue, an alternative approach was taken: The idea was to first conduct the SUZUKI coupling with 2-iodo phenol **41** and subsequently attach the methyl group to obtain the phenol ether **47** (**Scheme 41 B**). The purpose of this twist was to facilitate purification in anticipation that 2-iodo phenol **41** and the SUZUKI product **48** are separable. The biaryl coupling was accomplished using the same SUZUKI method[157] to give 2-phenyl substituted compound **48** in 74 % yield. This time the purification proceeded smoothly, as the reactant and the product could be easily separated by column chromatography. Downstream methylation under standard conditions[155] led to the formation of the target compound **47**. Unexpectedly, **47** could again not be isolated in analytically pure form. Although only one spot was visible on standard

TLC plates, NMR and HPLC analysis indicated the presence of an unknown impurity (ratio product:impurity estimated on basis of NMR data = 3-4:1). As separation could not be attained even by repeated column chromatography with common silica gel, an additional attempt of column chromatography was conducted using C_{18}-reversed phase silica gel (Merck, Darmstadt, Germany). This minimized the amount of the unknown impurity. Accordingly, a purity of 92 % was achieved for 2-phenyl analog **47**.
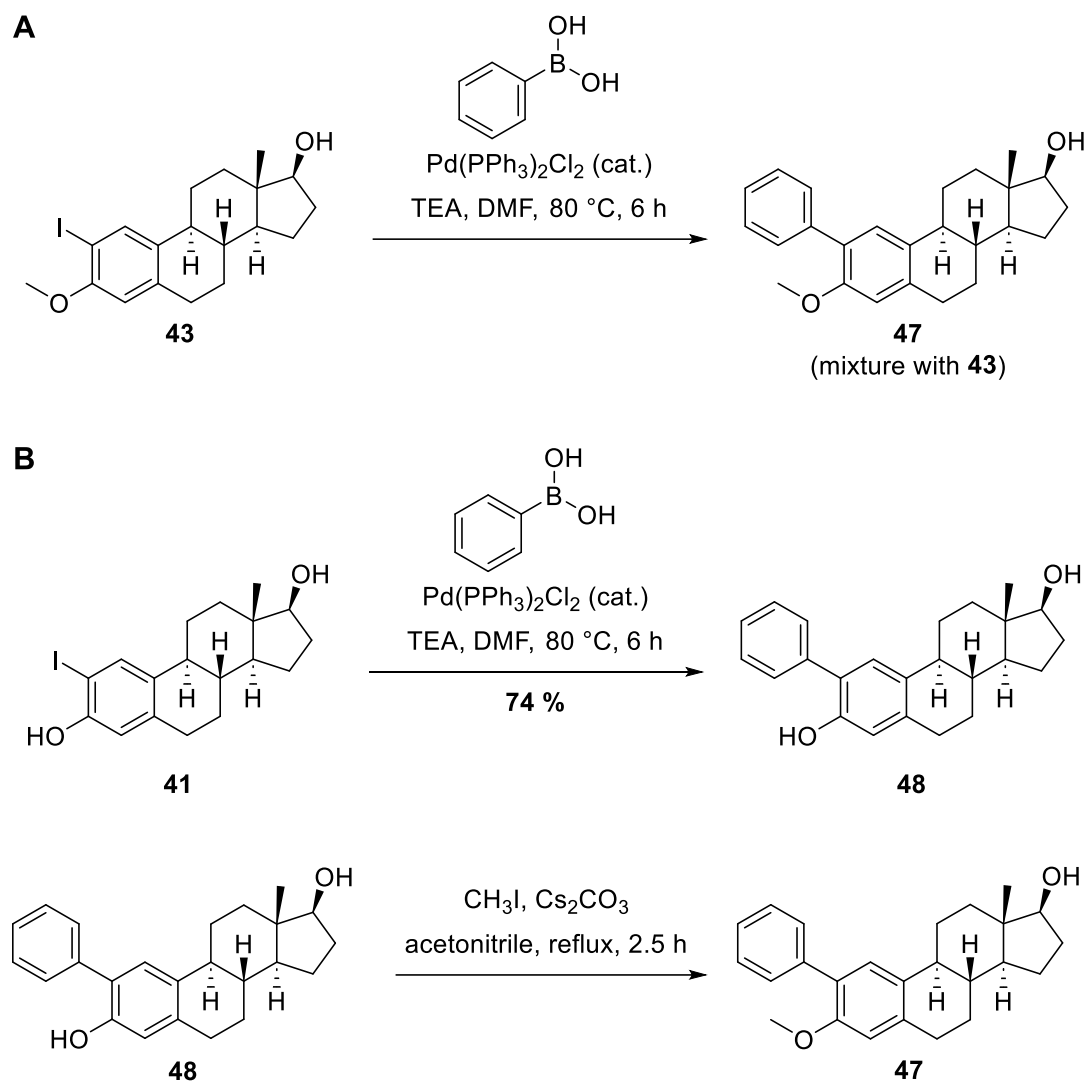

Scheme 41: Synthesis routes to the 2-phenyl analog of **EDME 47**, **A**: SUZUKI coupling of 2-iodinated **EDME 43**, **B**: SUZUKI coupling of 2-iodinated estradiol **41** and subsequent *O*-methylation

Another objective was the preparation of annulated benzofuran analog **53** (**Scheme 42**). This molecule differs from all previous ones in that the construction of the furan moiety entails modification of both C-2 and C-3.

The substance has already been synthesized and described by CUSHMAN *et al.*[158] and TEDESCO *et al.*[159]. Interestingly, TEDESCO *et al.* investigated on the relative binding affinity

(RBA) of this compound to the wild type estrogen receptor (ER). They found a RBA value of 1.6 % compared to estradiol (100 %). Since this indicates a strongly decreased estrogenic effect, **53** was a valuable target compound for our purposes. CUSHMAN *et al.* started from double TBDMS protected compound **49** (**Scheme 42**), which then underwent a SONOGASHIRA coupling with pure propyne gas to form **50** in poor yield (12 %). They treated this compound with TBAF to obtain double deprotected compound **51** in 15 % yield and single deprotected phenol **52** in 38 % yield. They finally afforded benzofuran compound **53** by another TBAF treatment at high temperature and a reaction time of 22 hours. TEDESCO *et al.* also first introduced two TBDMS protective groups to produce **49** and obtained 2-propynyl compound **50** by NEGISHI coupling of this compound with the *in situ* generated propynyl zinc halide. They afforded benzofuran **53** by deprotection and cyclization using TBAF. The combined yield over these three steps was 54 %.
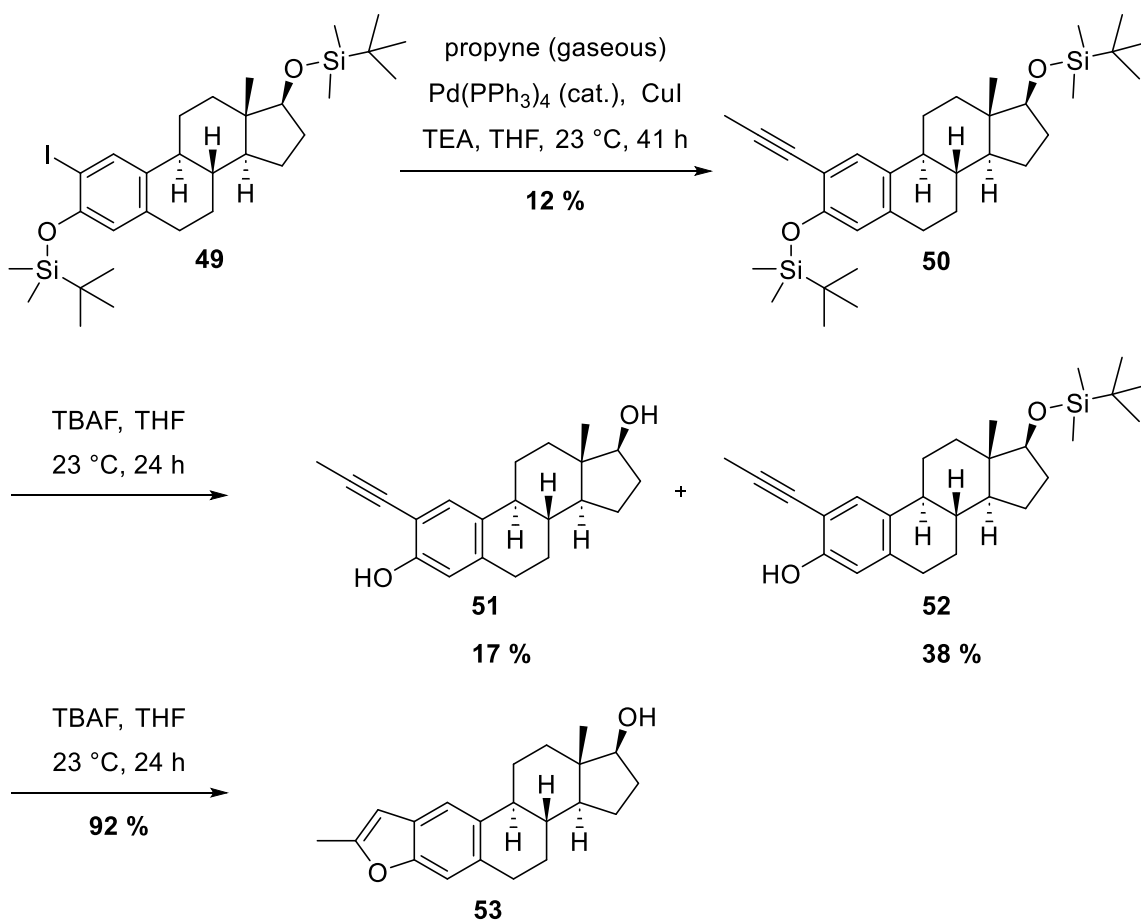
Cushman *et al.*:
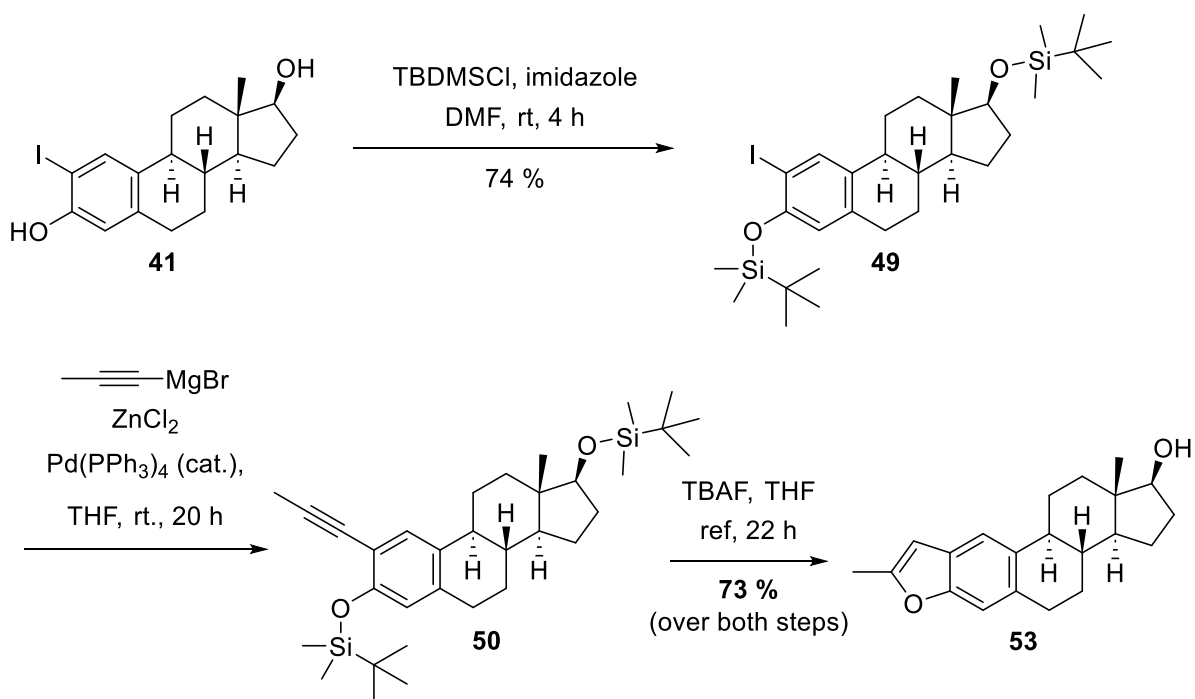
Scheme 42: Synthesis of **53** published by Cushman *et al.*[158] and Tedesco *et al.*[159]

As the synthesis protocols in both publications contain at least three steps, the target was to find an abbreviated route for the preparation of **53**. Notably, both groups used the double TBDMS protected compound **49** for the palladium-catalyzed coupling step. The idea was to omit the TBDMS protection step and directly conduct SONOGASHIRA coupling with building block 2-iodoestradiol (**41**). Consequently, **41** was subjected to a standard SONOGASHIRA coupling protocol published by OHNO et al.[160] to create 2-propynyl substituted steroid **51**. The advantage of this method compared to the method of CUSHMAN et al. is the utilization of a commercially available solution of propyne in DMF instead of the explosive and highly flammable propyne gas. A proper characterization of substance **51** and the determination of the yield were not possible because separation from reactant **41** could not be accomplished. The reaction did not run until completion and the two substances showed the same R_f value on TLC with several mixtures of eluents, thus they are eluted simultaneously during flash column chromatography. Recrystallization attempts in different solvents also failed to deliver good results. The formation of the desired product could only be confirmed by NMR analysis of the obtained mixture. The preserved spectrum consists of two sets of coherent peaks, one of which contains the characteristic methyl peak of the propynyl group. Analysis of the mixture by mass spectrometry provided no further evidence for the presence of **51**. Independent of the applied ionization technique, only the mass of **41** was found, presumably the mass peaks of **51** were superimposed or suppressed by the mass signal of the reactant and the associated fragment signals. Because of these circumstances, the inseparable mixture of both substances was used for the following cyclization step. This was accomplished by intramolecular condensation of the phenol with the alkyne using a solution of KOH in a mixture of water and methanol. Benzofuran analog **53** could be easily separated from **41** and was obtained in 36 % yield over these two steps (**Scheme 43**). All in all, the synthesis pathway to **53** was successfully shortened, with the overall yield being only slightly lower (this protocol 36% vs 54% of TEDESCO et al.).
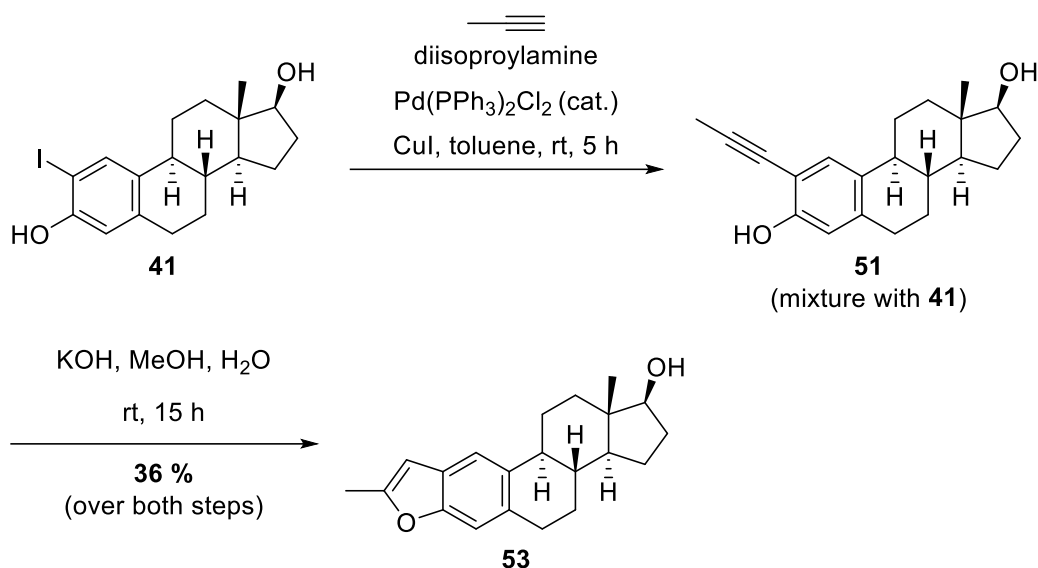
**Scheme 43**: Preparation of benzofuran analog **53**

The next envisaged analog was the 2-methoxy estrane **54** (**Scheme 44**). This molecule carries, in contrast to **EDME**, the methoxy group at C-2 instead of C-3, changing the geometry of the molecule and the location of possible interactions between the molecule and amino acid residues. This could affect activity on the three TRPML channels as well as on estrogen receptors. The first step was to find a suitable synthetic precursor. This precursor would ideally bear a hydroxy group or any other group which can be converted into a methoxy group at C-2 and contain the required estrane scaffold with the secondary alcohol function at C-17. Unfortunately, most molecules fulfilling these criteria are hardly accessible in the required amounts and extraordinary expensive to purchase. Among these, only 2-methoxyestradiol (**55**) was a considerable option. It is a natural metabolite of 17β-estradiol, which is built in the human body by biochemical hydroxylation by cytochrome enzymes and subsequent methylation by the enzyme catechol-O-methyl transferase (COMT)[161]. It is commercially available, albeit only small quantities of this substance are orderable and the price is still pretty high. For these reasons, it was more rational to first attempt synthesis of a suitable building block. In general, appropriate and feasible synthetic precursors for **54** would be 2-hydroxy or 2-methoxy substituted 17β-estradiol triflates (**Scheme 44 A**), since the triflate group could be exchanged by a hydrogen using a palladium-catalyzed reduction procedure. The key step was to insert a hydroxy or methoxy group at C-2 of the estrane scaffold. Temporary protection of both hydroxy groups at C-3 and C-17 also had to be considered. The big advantage of this route would be that it could start from readily available and inexpensive 17β-estradiol (**3**).
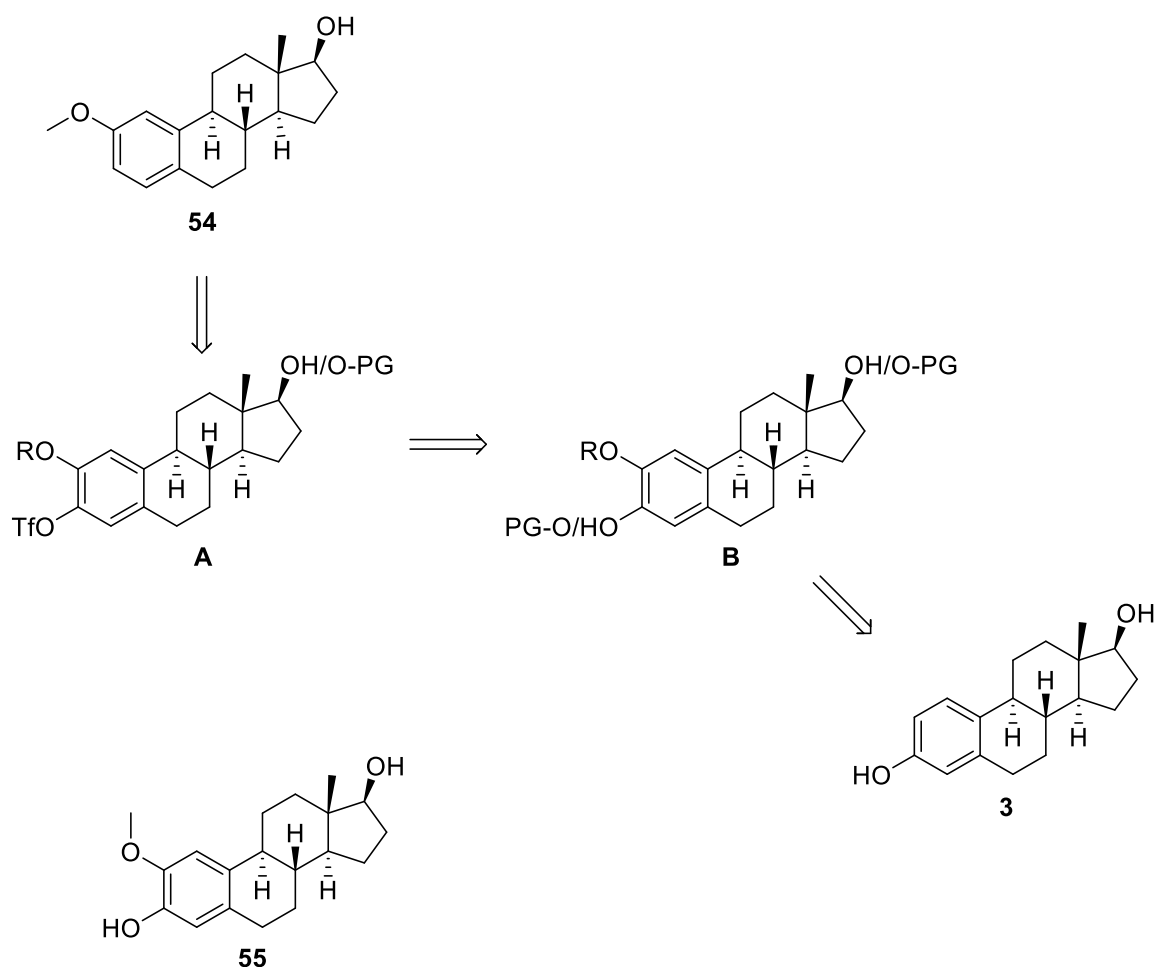
Scheme 44: Potential precursor 2-methoxyestradiol (**55**) and retrosynthesis of **54**, R =H or CH₃

B_A *et al.* described the synthesis of above mentioned 2-methoxyestradiol (**55**)[162]. The protocol of B_A *et al.* also started from 17β-estradiol (**3**) which was converted into carbamate **24** (**Scheme 45**). The subsequent synthesis proceeded *via* a ruthenium-catalyzed C-2 hydroxylation to form 2-hydroxylated compound **56**. Since **56** could act as intermediate **B** and the synthesis route of B_A *et* al. seemed favorable and efficient, the procedure should be reproduced. Carbamate **24** was successfully prepared in quantitative yield by treatment of estradiol (**3**) with *N*,*N*-dimethylcarbamoyl chloride, using potassium carbonate as an auxiliary base to neutralize the generated hydrochloric acid. The carbamate should act as directing group for the crucial subsequent ring hydroxylation step, establishing a weak coordination of the ruthenium catalyst with the carbonyl oxygen[163]. For this key reaction, catalyst dichloro(p-cymene) ruthenium (II) dimer and oxidant iodobenzene diacetate were added to carbamate **24** in a 1:1 mixture of trifluoroacetic acid and trifluoroacetic anhydride. Unfortunately, the results of this step were not identical to the findings of B_A *et al.*, who described a pretty good yield (65 %). In our case, multiple products were formed. The main product was assumed to be trifluoroacetic ester **57**. As it could not be obtained in pure form and the NMR and mass data

were ambiguous, identity of the substance could not be confirmed. Attempts of alkaline hydrolysis with aqueous sodium hydroxide in methanol both at ambient and higher temperature left the material unchanged. Thus, this product could neither be characterized nor was useful for further synthetic approaches. The desired product **56** was indeed found in small quantities, albeit purification and NMR analysis turned out to be complicated. Only after tedious flash column chromatography it was possible to obtain sufficiently pure samples for NMR analysis.
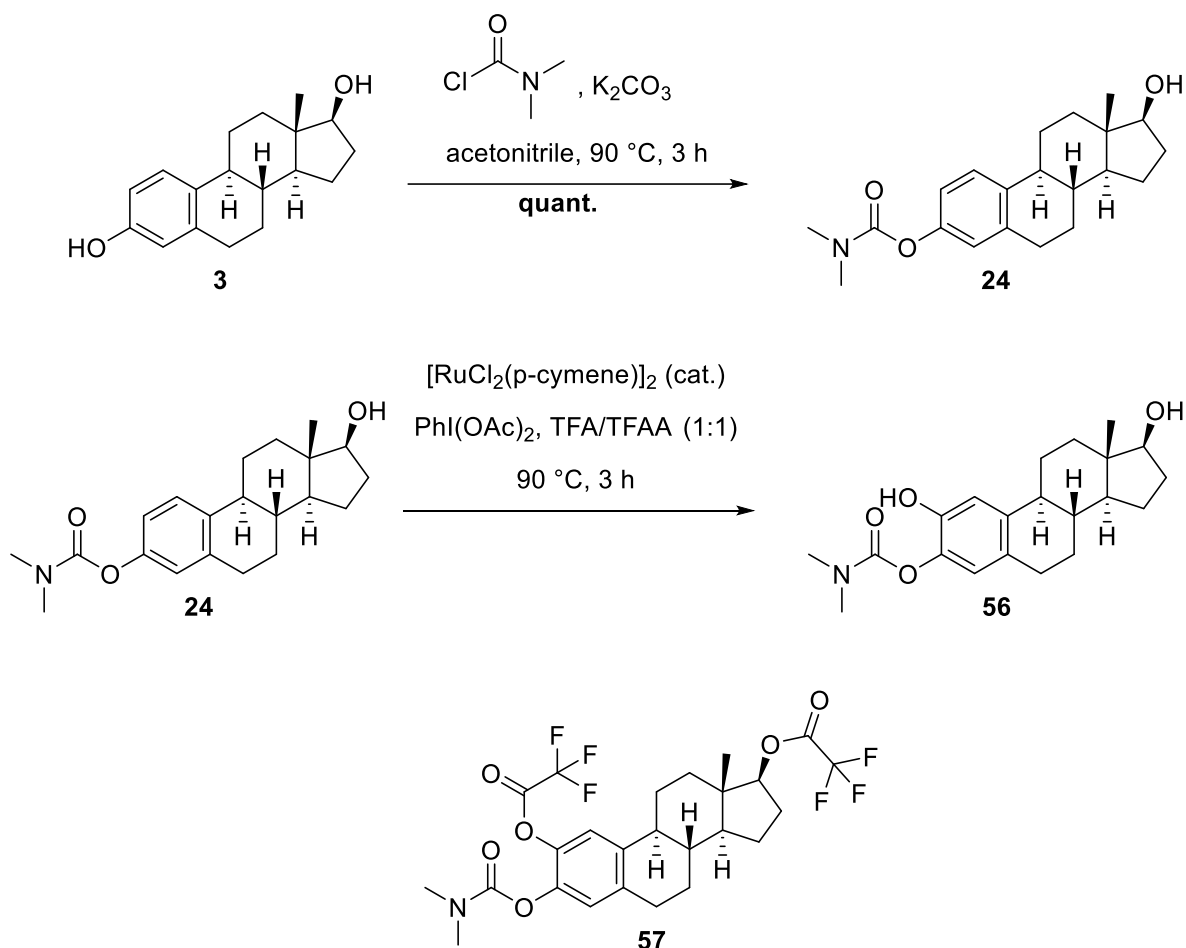
Scheme 45: Attempted synthesis of 2-hydroxylated compound **56** and potential structure of substance **57**

Depending on the concentration and minor impurities, two different NMR spectra of the same product were received. Excerpts of the two spectra are depicted in **Figure 16**. On the upper side, the spectrum corresponds to the expected peak split. In contrast, there is a double set of peaks on the spectrum on the lower side. The regioselectivity of the hydroxylation could be approved by the obtained NMR spectra, since hydroxylation at C-4 alongside the desired hydroxylation at C-2 would lead to different peaks with varying multiplicity instead of a homogenous double set. The most likely explanation is that the carbamate forms different types and extents of hydrogen bonds with the phenolic hydroxyl group depending on the

surroundings. Due to the restricted rotatability of the carbonyl bond, this might result in the formation of two conformational isomers, which split differently in the NMR spectrum.
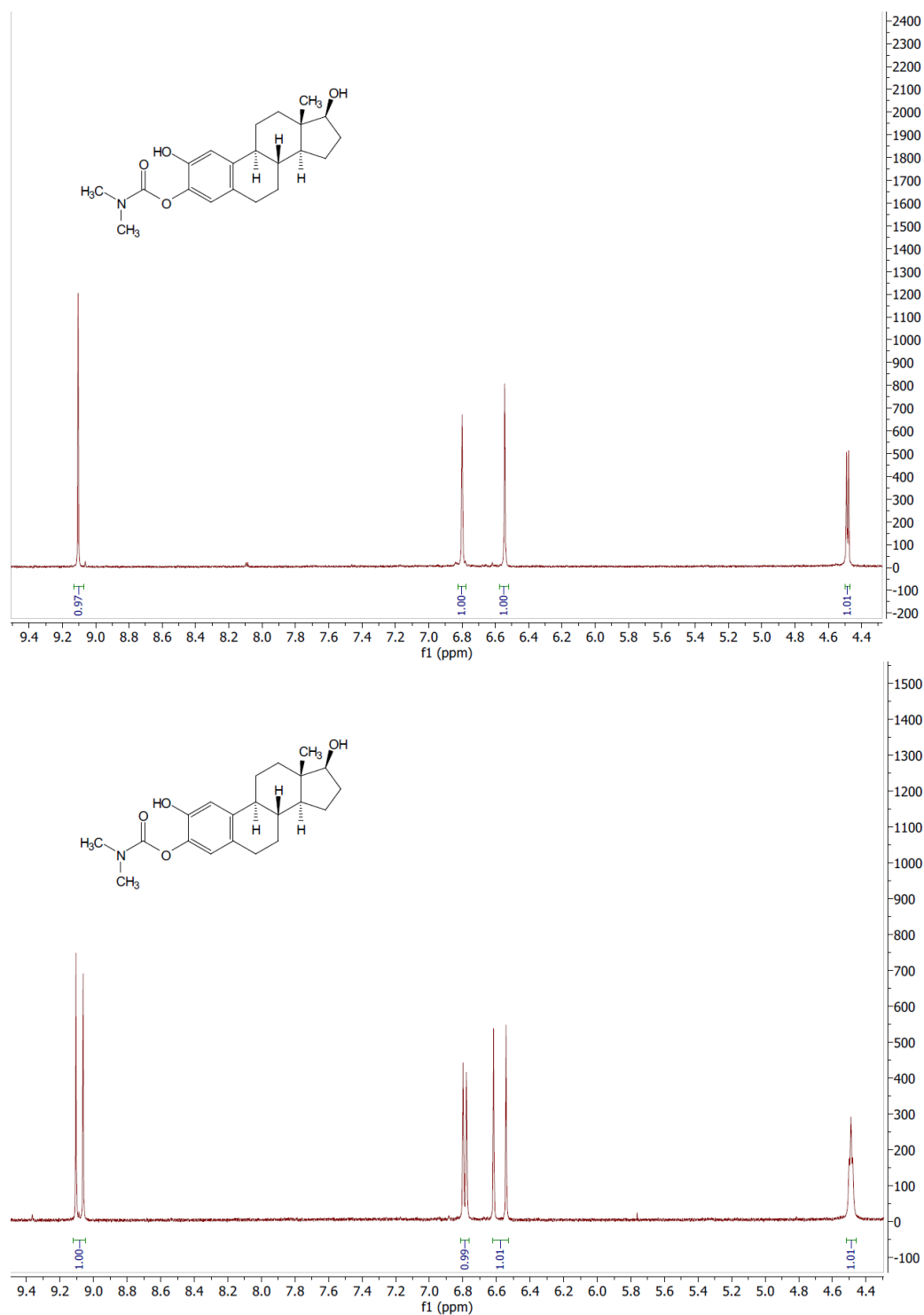

Figure 16: Excerpts of the two different NMR spectra of **56**. The region between 9.50 ppm to 4.29 ppm is depicted. Left peak: phenolic OH, middle peaks: aromatic Hs, right peak: aliphatic OH

Under the circumstances of the reaction, the stability and reactivity of the aliphatic alcohol at C-17 was pondered to be a factor for the generation of side products. One strategy for mitigating the risk of side reactions was thus the introduction of a suitable protective group on the C-17 alcohol. Due to the aforementioned acidic conditions and the applied high temperature, the selection of practicable protective groups was limited, since they were required to sustain these. With that in mind, two protective groups were considered: An acetic ester and a benzyl group. The conversion of **24** into its corresponding benzyl ether **25** was previously shown (see **Scheme 26**). The hydroxylation procedure by Bᴀ *et al.* conducted with this compound led to the cleavage of the benzyl ether and in consequence again to the formation of numerous side products, among them the previously discussed unidentified substance **57** (see **Scheme 45**). Introduction of the acetic ester could be accomplished by treatment of carbamate **24** with acetic anhydride in pyridine (**Scheme 46**), leading to the formation of acetic ester **58** in 76 % yield. Ester **58** was then also subjected to the hydroxylation procedure, resulting in the formation of 2-hydroxylated compound **59**. It could be observed that the generation of side products was significantly decreased compared to the analogous reaction conducted with **24**. Nevertheless, the product was still hard to purify and the NMR spectrum showed a double set of peaks, making it hard to estimate the yield and characterize the substance. Above all, the yield of the reaction was still too low to pursue this route further.
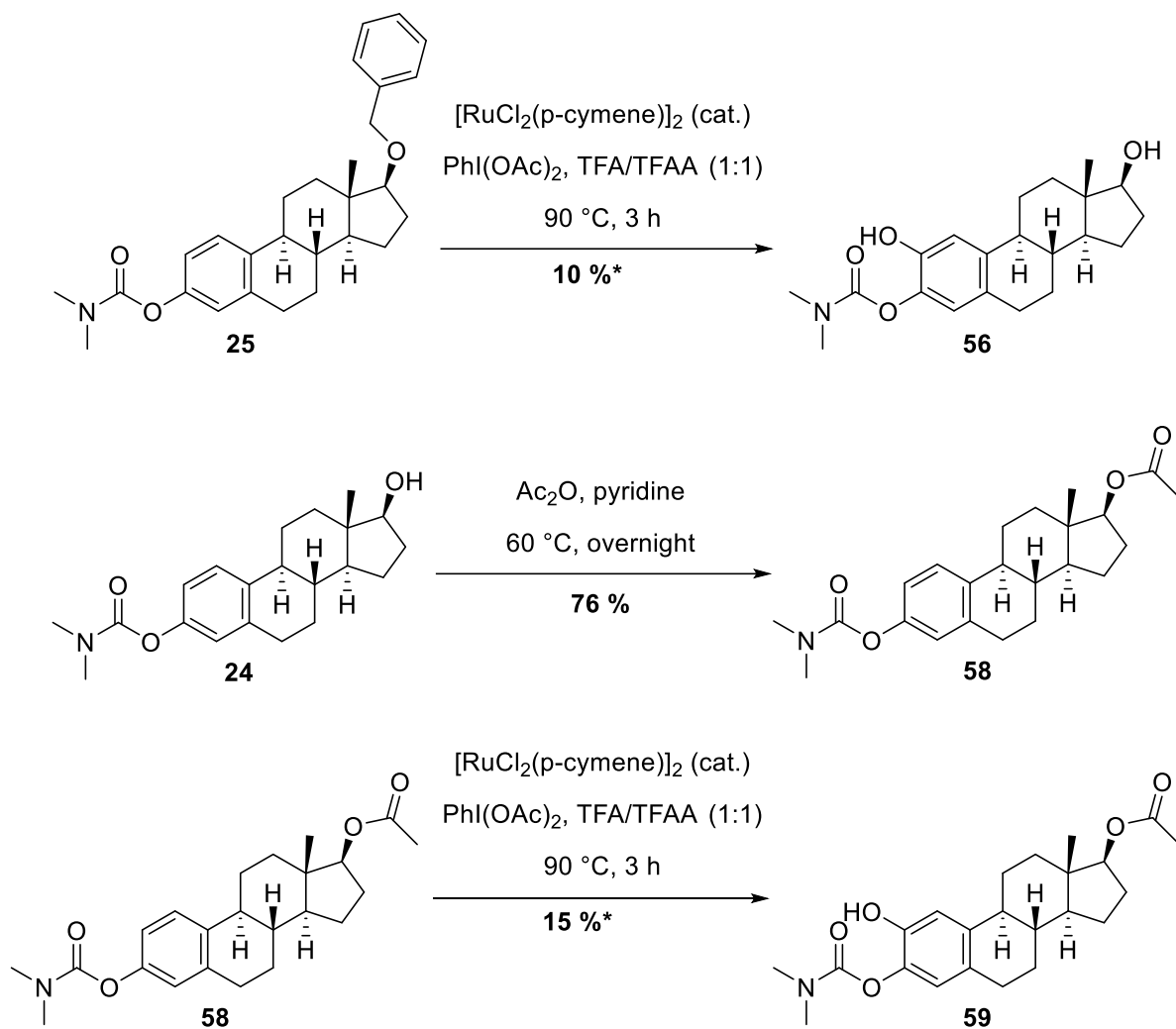
Scheme 46: Attempts with the acetyl and benzyl protected compounds. *Yields of **56** and **59** were estimated

In summary, all approaches utilizing the protocol of BA *et al.* failed to provide reasonable amounts of the desired product in pure form. Alternative methods for hydroxylation of 17β-estradiol (**3**) like formylation followed by DAKIN oxidation[164, 165] (**Scheme 47 A**) or methoxy methyl (MOM) directed lithiation and subsequent oxidation[166] (**Scheme 47 B**) were not deemed attractive. Method **A** lacks regioselectivity and contains multiple steps, method **B** requires stringent conditions and the usage of highly flammable *sec*-butyllithium (*s*-BuLi) as well as expensive and toxic chloromethyl methyl ether.

A

B
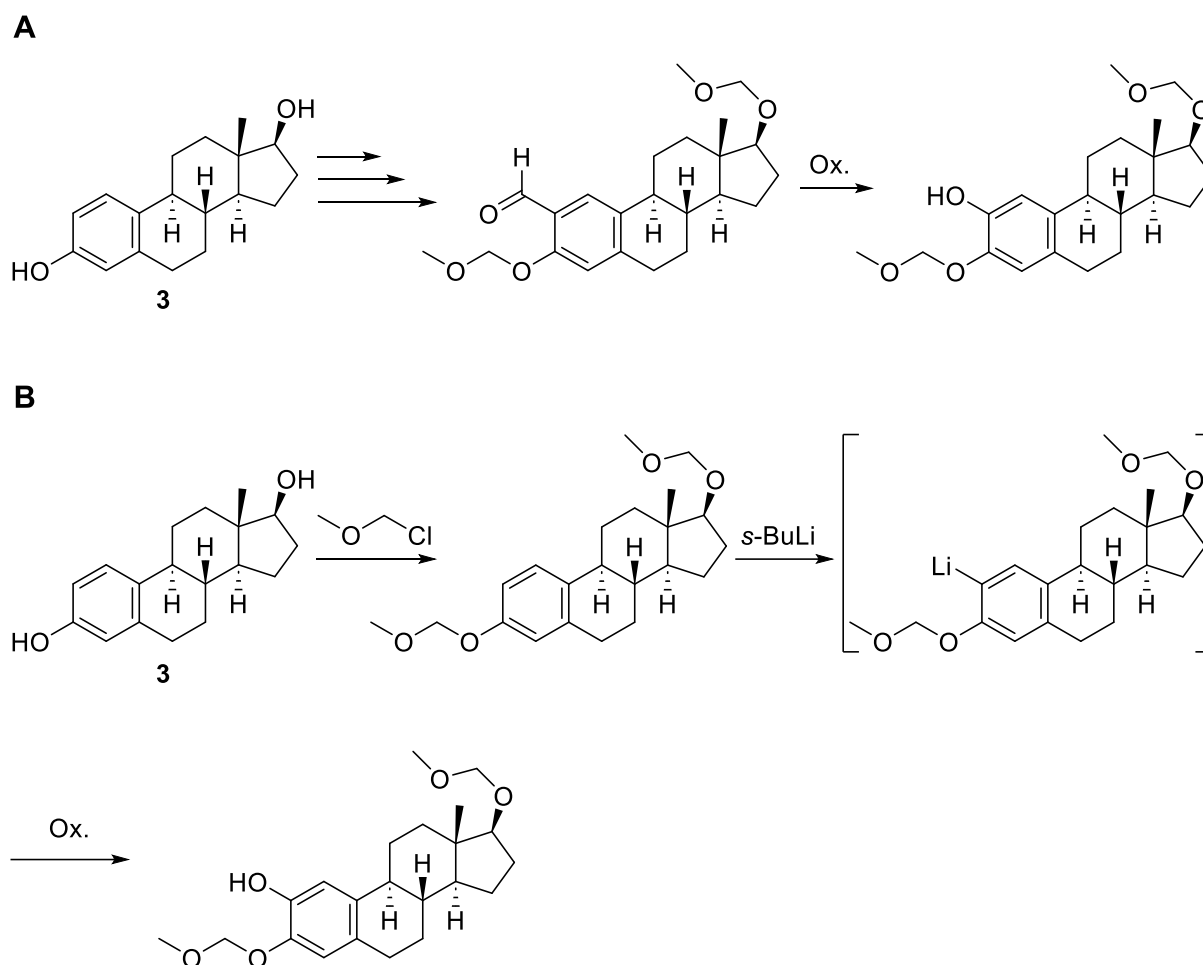
Scheme 47: Examples of alternative methods for C-2 hydroxylation of 17β-estradiol (**3**)

Since only 100 mg of 2-methoxyestradiol (**55**, see **Scheme 44**) were estimated to be sufficient for the synthesis of **54**, the purchase of **55** was regarded as more economical than further elaborate synthesis attempts. With **55** now in hand, the envisaged synthesis pathway could be progressed. Phenol **55** was smoothly converted into triflate **60** in 77 % yield by reaction with 4-nitrophenyl trifluoromethanesulfonate and potassium carbonate in DMF (**Scheme 48**). The used method was originally published for the synthesis of estradiol triflate (**PRU-9**)[167]. A standard protocol for palladium-catalyzed reduction of aryl triflates[168] using formic acid, triethylamine (TEA), palladium (II) acetate and triphenylphosphine enabled conversion of **60** into the desired 2-methoxy analog **54**, whereby 27.7 mg (57 % yield) of the product could be isolated.
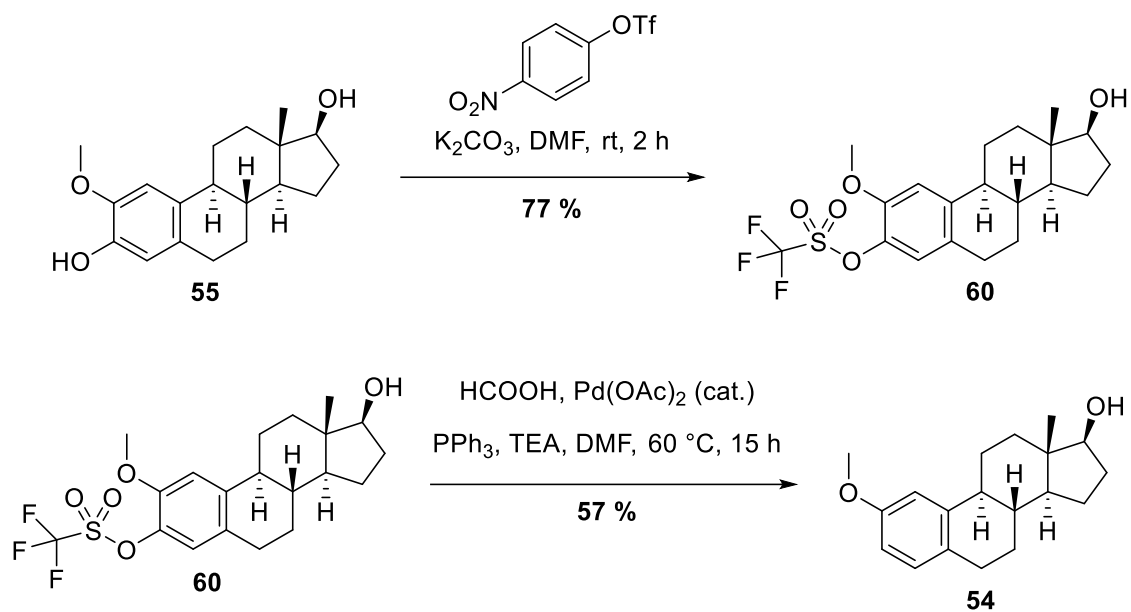
Scheme 48: Preparation of 2-methoxy analog **54** starting from commercially acquired 2-methoxyestradiol (**55**)

Altogether, six analogs could be successfully prepared by introduction of various substituents at C-2 of the estrane scaffold. With annulated benzofuran **53** and 2-methoxy compound **54**, two among them simultaneously contain modifications at C-3.
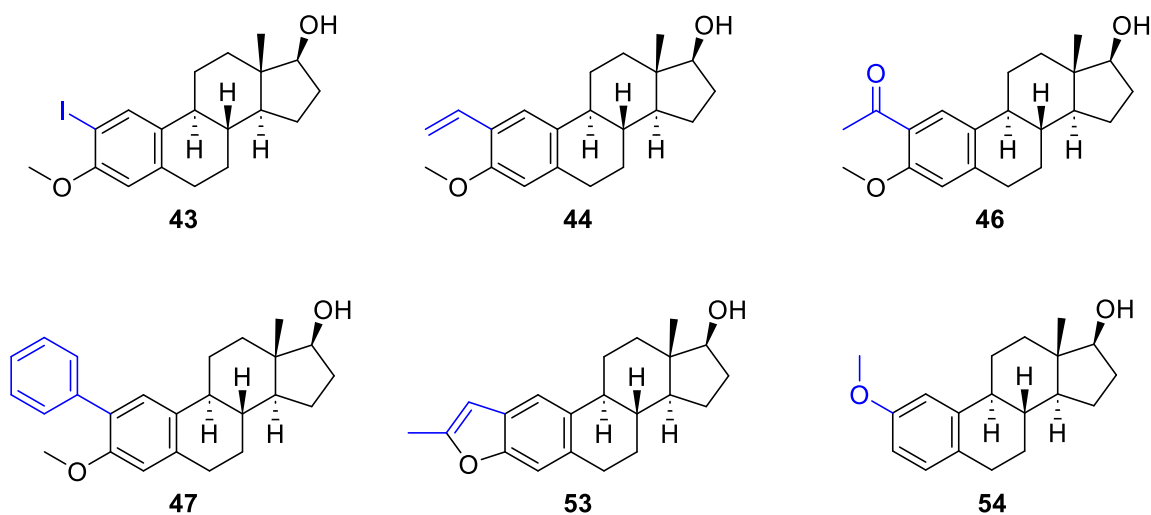
**Figure 17**: Overview of the synthesized C-2 substituted analogs

4.1.2.3 Aza analogs of the TRPML1 inhibitor estradiol methyl ether (EDME)

Rühl P., Bracher F., *Molecules* **2023**; 28 (21) 7428

Summary

Building on our preliminary findings[84], the target of this study was to further elucidate the effect of different modifications of ring A of the estrane scaffold and expand our knowledge on structure-activity relationships. Whilst our previous work focused on the variation of substituents at C-3, this study covers structural alteration of ring A by bioisosteric replacement of the benzenoid ring. Specifically, the azaarenes pyridine and pyrimidine as bioisosteres of the phenyl group were of great interest, since the incorporated nitrogen atoms implement basic as well as H-bond acceptor and/or H-bond donor properties and can thus influence the interactions with the target protein. Starting from commercially available 19-nortestosterone (**4**), the 4-aza (pyridine) analog **61** (compound number **1** in the publication) and the 2,4-diaza (pyrimidine) analog **62** (compound number **2** in the publication) were successfully synthesized in an enantiomerically pure form in six and eight steps, respectively. Well-considered selection of suitable protective groups and the oxidative cleavage of the cyclohexenone-type ring A of 19-nortestosterone (**4**) were the basis for the development of two practical synthesis routes that provided the two analogs *via* different intermediates. In addition, pyridone analog **63** (compound number **6** in the publication) could be isolated as a side product generated in the course of one synthesis pathway. Biological testing of the three analogs by Fluo-4 Ca^{2+} imaging revealed an IC_{50} value of 1.0 µM for the 4-aza analog **61** and 8.8 µM for the 2,4-diaza analog **62**. Compared to **EDME** (0.60 µM), TRPML1 inhibitory activity of **61** is slightly reduced, whereas **62** showed only very weak TRPML1 inhibition. The pyridone analog **63** was virtually inactive.
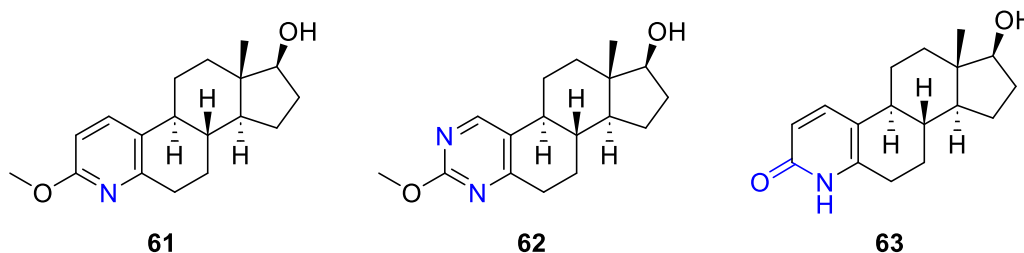
Figure 18: Synthesized aza analogs of **EDME**

Personal contribution

My contribution was the synthesis of all compounds. I further contributed to the development of the methodology, the data curation and visualization, writing of the original draft and reviewing and editing the manuscript.

FRANZ BRACHER created the concept, contributed to the development of the methodology, the data curation and visualization, writing of the original draft and reviewing and editing the manuscript. He provided the resources and supervised and supported all chemical work.

Article

Reproduction of this article is in accordance with MDPI. It is printed in the original wording. Formatting may differ slightly compared to the original article.

molecules

Article

Aza Analogs of the TRPML1 Inhibitor Estradiol Methyl Ether (EDME)

Philipp Rühl and Franz Bracher *

Department of Pharmacy, Center for Drug Research, Ludwig-Maximilians University, 80539 Munich, Germany;
philipp.ruehl@cup.lmu.de
* Correspondence: franz.bracher@cup.uni-muenchen.de

Abstract: Estradiol methyl ether (EDME) has recently been described by us as a very potent and subtype-specific inhibitor of the lysosomal cation channel TRPML1. Following the principle of bioisosteres, we worked out efficient synthetic approaches to ring-A aza-analogs of EDME, namely a methoxypyridine and a methoxypyrimidine analog. Both target compounds were obtained in good overall yields in six and eight steps starting from 19-nortestosterone via the oxidative cleavage of ring A followed over several intermediates and with the use of well-selected protective groups by re-cyclization to provide the desired hetero-analogs. The methoxypyridine analog largely retained its TRPML1-inhibitory activity, whereas the methoxypyrimidine analog significantly lost activity.

Keywords: cation channels; TRPML1; bioisostere; steroids; estrogens; ring cleavage; protective groups; pyridines; pyrimidines; cyclization

1. Introduction

TRPML1 is one of three members (TRPML1-3) of the TRPML cation channels group, a subfamily within the transient receptor potential (TRP) superfamily. As a non-selective lysosomal channel permeable to Ca^{2+}, Na^+, Fe^{2+}, Zn^{2+} and other cations, it plays an important role in multiple physiological processes but also in several human diseases. A mutation with loss of function of TRPML1 causes Mucolipidosis Type IV, a neurodegenerative lysosomal storage disorder [1]. Furthermore, TRPML1 has gained interest as it is associated to be involved in various processes in different cancers, e.g., melanoma [2] and non-small lung cancer [3], and its influence on cardiovascular [4] and neurodegenerative diseases has been discussed [5].

Therefore, obtaining access to inhibitors and activators for this target as pharmacological tools or even as possible future therapeutic options is of great interest.

Phosphatidylinositol 3,5-bisphosphate (PI(3,5)P2), a major constituent of the lysosomal membrane, has been described as an endogenous activator of all TRPML channels, while phosphatidylinositol 4-5-bisphosphate (PI(4,5)P2), which is mainly found in the plasma membrane, has been identified as endogenous inhibitor of TRPML1 and TRPML3 [6]. Due to their structural characteristics (polarity), these two molecules are not suitable as pharmacological tools as they cannot permeate cell membranes.

As a consequence, several low-molecular activators and inhibitors of TRPML1 with suitable pharmacokinetic properties have been developed in recent years. While MK6-83 [7], SF-51 and ML-SA1 [8] are examples of unselective TRPML activators, the only known selective activator of TRPML1 is ML1-SA1 [9]. Despite the evident need for potent TRPML1 inhibitors, the number of these is still limited.

While the indoline derivative **ML-SI1** and the 1,2-diaminocyclohexane derivative **ML-SI3** are known examples in the literature for isoform-unselective inhibitors [10–12], we described the steroidal compound estradiol methyl ether (EDME) as the first highly potent (IC_{50} 0.6 μM) and subtype-selective TRPML1 inhibitor in our previous work (Figure 1) [13].

This inhibitor was identified by random screening of 2,430 compounds on hTRPML1ΔNC-YFP, a plasma membrane variant of wild-type TRPML1. Subsequently, we tested other pharmacologically relevant steroidal compounds and found that natural and synthetic steroids lacking aromaticity in ring A (the typical structure motif of estrogens) are virtually inactive (cholesterol, phytosterols, glucocorticoids, mineralocorticoids, antiestrogens, antiandrogens, 5α-reductase inhibitors). In the class of estrogens, the native hormone 17β-estradiol showed significantly reduced inhibition (IC_{50} 5.3 μM) and only mestranol, a congener of EDME bearing an additional ethinyl group at C-17, showed considerable activity. Inversion of the configuration of the 17α-hydroxy group eliminated inhibitory activity in all cases. Finally, we synthesized ten modified versions of EDME, most of which have a replacement of the methoxy group at C-3 in common with a lipophilic residue. Out of these, the 3-vinylestrane **PRU-10** (IC_{50} 0.41 μM) and the 3-acetyl derivative **PRU-12** (IC_{50} 0.28 μM) (Figure 1) showed stronger TRPML1 inhibition, an improved selectivity profile compared to **EDME**, and reduced estrogenic activity.
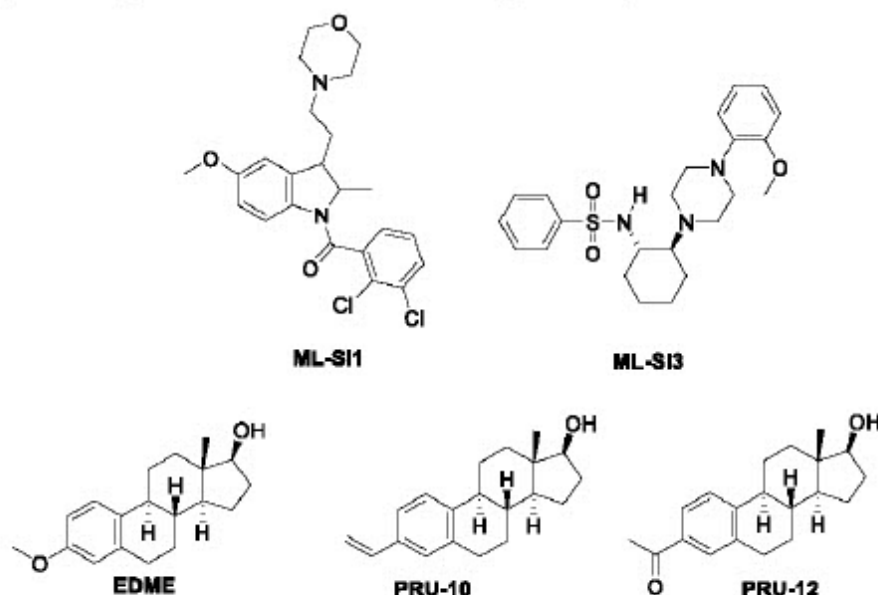

Figure 1. Structures of published TRPML inhibitors.

Based on this preliminary evidence on structure–activity relationships, we focussed on additional modifications of ring A of **EDME**. Due to our own positive experience with the synthesis of aza analogs of steroidal lead structures for improving or modulating biological activities [14,15], we decided to investigate a pyridine-type 4-aza analog (**1**) and a pyrimidine-type 2,4-diaza analog (**2**) of **EDME**.

Following the well-established principle of "bioisosteres" [16], single functional groups in a bioactive molecule can be replaced by other, more or less similar groups in order to extend or improve potency, enhance selectivity, alter the physicochemical properties or metabolism, or improve pharmacokinetics or toxicity. The bioisosteric replacement of phenyl rings can be performed in a classical manner with the introduction of neutral aromatic rings (thiophene, furan) or azaarenes (pyridine, pyrimidine, pyrazine) [17], further "nonclassical" biosisosteres (acetylene, bridged aliphatic ring systems) have been developed [18]. The azaarene bioisosteres have gained significant interest since they can introduce basic properties as well as H-bond acceptor and/or H-bond donor properties and thus improve (or reduce) the interaction with the target protein.

2. Results and Discussion

2.1. Chemistry

As we intended to synthesize both target compounds in an enantiomerically pure form, we selected a "chiral pool" approach [19] for our syntheses. Estradiol or **EDME** were not suitable starting materials for this approach due to the lack of feasible synthetic methods for the conversion of phenols/phenol ethers into pyridines and pyrimidines. The same holds for non-estrogenic sterols bearing a methyl group (C-19) at C-10 since this residue would prevent aromatization of ring A. For our purposes, 19-nortestosterone (nandrolone; 3) was identified as the best precursor for a couple of reasons: this (commercially available and affordable) homochiral compound already has the required configurations at the stereocenters in rings C and D, its ring A is a cyclohexenone that can be cleaved by oxidation, and, last but not least, there is no methyl group at C-10. The published oxidative degradation of 19-nortestosterone (3) under the cleavage of the C-4,C-5 bond and decarboxylation yields a ketocarboxylic acid of type **A** [20]. The formal integration of ammonia and oxidative aromatization should provide a ring A pyridone, which was then to be *O*-methylated to provide the desired 4-aza analog **1** of **EDME**.

Oxidative degradation of the propionate side chain in **A** [20] would provide a ketoaldehyde of type **B**, which, upon treatment with *O*-methylisourea, should provide the methoxypyrimidine target compound **2**. In both series, temporary protection of the 17-OH group had to be considered (Figure 2).
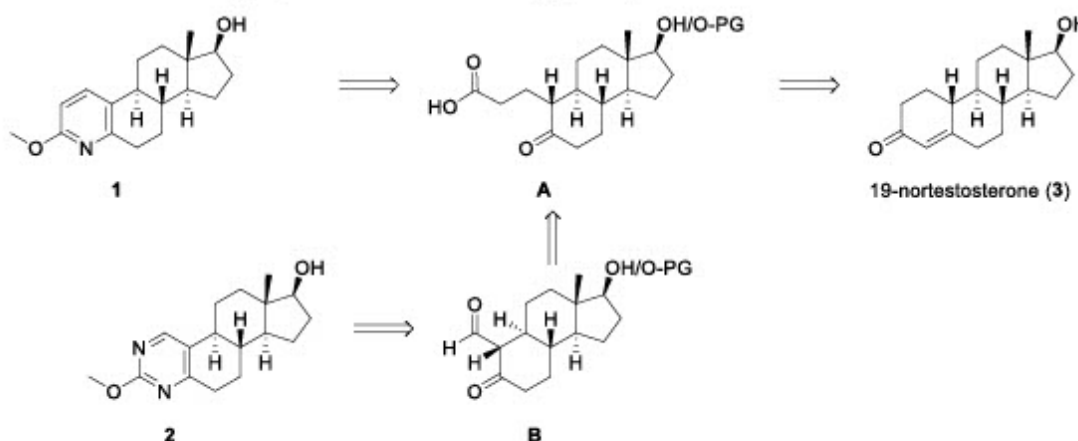

Figure 2. Retrosynthesis of the target compounds **1** and **2** (PG—protective group).

2.1.1. 4-Aza Analog of EDME

Our chiral pool approach started with the oxidative cleavage of ring A of 19-nortestosterone (3) to provide ketocarboxylic acid **4**. While Holt et al. [20] described an ozonolysis protocol with a yield of 50%, we obtained **4** in a yield of 94.5% by using NaIO$_4$/KMnO$_4$ as the oxidant, a method established for a related degradation of a 19-methyl steroid in the course of the synthesis of the drug finasteride [21]. Subsequent treatment with ammonium acetate in acetic acid under reflux [22] resulted in ring closure to two poorly separable unsaturated lactams, **5a** with a Δ5,10- and **5b** with a Δ5,6 double bond (yield: 87.4%, ratio **5a**:**5b**: 15:85). Unfortunately, we could not find a suitable oxidant for direct dehydrogenation of these lactams to the ring A pyridone **6** (Scheme 1). Most likely, the unprotected 17-OH group interfered with the examined oxidants (DDQ, iodine-based reagents, and others). As a consequence, we examined protective groups for 17-OH.
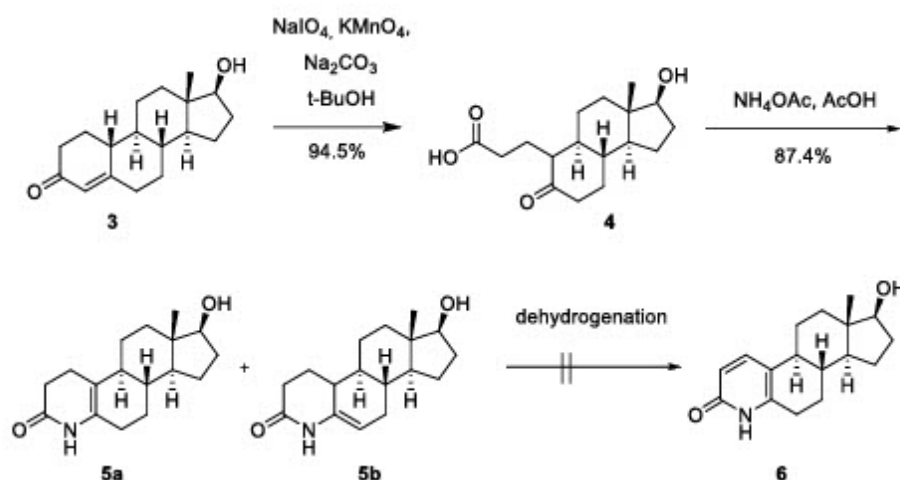
Scheme 1. First attempt for the synthesis of the 4-aza analog **1** of EDME.
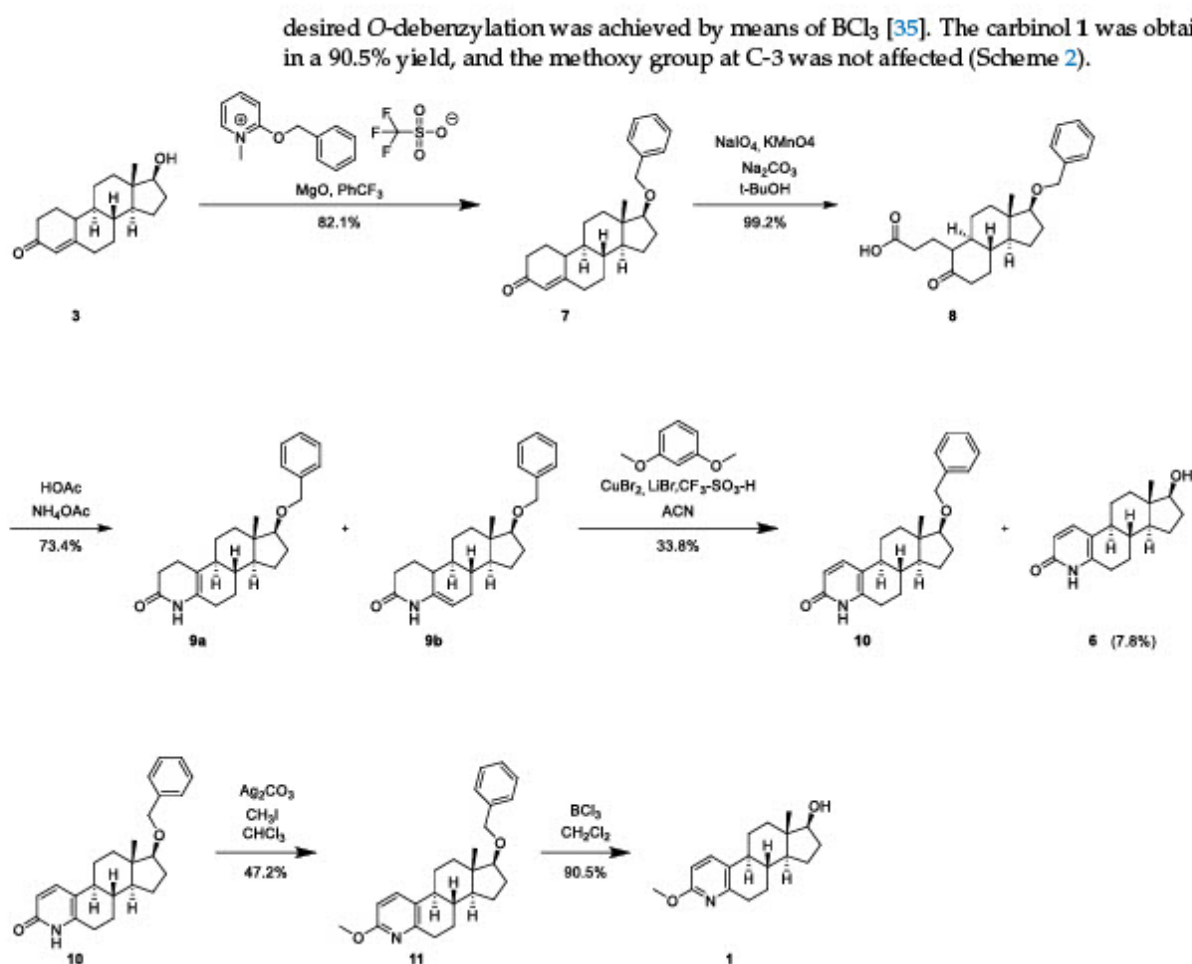
Our first attempts to utilize MOM protection of the starting material 19-nortestosterone (**3**) failed early due to problems with introducing this protective group. The following experiments using TBDMS protection gave promising results in the early steps (for details, see Supporting Information) but failed due to the instability of the TBDMS ether as soon as experiments were performed under acidic conditions (no details shown).

Finally, we turned to benzyl protection of 17-OH. Surprisingly, standard protocols for the protection of this secondary alcohol under alkaline (NaH/benzyl halides) or acidic conditions [23] (benzyl trichloroacetimidate/TFA) failed to provide acceptable yields. However, Dudley's protocol [24] utilizing 2-benzyloxy-1-methylpyridinium triflate/MgO gave the desired benzyl ether **7** in 82.1% yield. Following the general strategy described above, oxidative ring A degradation with $NaIO_4$/$KMnO_4$ yielded ketocarboxylic acid **8** in a 99.2% yield. Subsequent treatment with ammonium acetate in acetic acid under reflux resulted in ring closure to two (still poorly separable) unsaturated lactams, **9a** with a Δ5,10- and **9b** with a Δ5,6 double bond (73.4% yield of the mixture, ratio **9a**:**9b**: 15:85).

With this mixture of isomers in hand, we again investigated numerous reagents used in previous publications to dehydrogenate dihydropyridines. These included treatment with MnO_2 [25] (result: no conversion), $Pb(OAc)_4$ [26] (result: decomposition), air oxidation [27] (result: no conversion), and treatment with $KMnO_4$ (result: decomposition).

As all of these experiments failed, we attempted formal dehydrogenation via halogenation at the methylene group next to the lactam carbonyl, followed by dehydrohalogenation utilizing published reagents from the pyridone and related fields (SO_2Cl_2 [28], iodotrimethylsilane [29], $CuBr_2$ [30]). Neither of these reagents gave noteworthy amounts of the dehydrogenation product. Finally, treating **9a**/**9b** with a combination of reagents ($CuBr_2$, LiBr, 1,3-dimethoxybenzene, trifluoromethanesulfonic acid in acetonitrile) that was originally used for a cyclohexenone-to-phenol conversion in 19-norandrost-4-en-3-ones [31] gave the desired pyridone **10** in 33.8% yield. This product was accompanied by small amounts (7.8%) of the 17-*O*-deprotected pyridone **6** (see Scheme 1).

O-Methylation of **10** to provide the methoxypyridine derivative **11** was achieved in 47.2% yield using iodomethane/Ag_2CO_3 [32]. As the final step, the benzyl protective group at 17-OH had to be removed without affecting the methoxypyridine unit. This step turned out to be more difficult than expected. Under standard *O*-debenzylation conditions (hydrogenolysis under Pd catalysis), no conversion was achieved; an alternative Pd-catalyzed method using Et_3SiH as the reductant [33] failed as well. A published method for the selective cleavage of benzyl ethers utilizing $CrCl_2$/LiI [34] surprisingly led to the cleavage of the methyl ether at the pyridine ring and left the benzyl ether untouched. Pyridone **10** (the precursor of **11**) was obtained in a 90% yield. Finally, the

desired *O*-debenzylation was achieved by means of BCl$_3$ [35]. The carbinol **1** was obtained in a 90.5% yield, and the methoxy group at C-3 was not affected (Scheme 2).


Scheme 2. Successful approach to the 4-aza analog **1** utilizing benzyl protection at 17-OH.

2.1.2. 2,4-Diaza (pyrimidine) Analog of **EDME**

As mentioned above (Figure 2), the methoxy pyrimidine motif of the target compound **2** should be built up by cyclocondensation of a ketoaldehyde of type **B** with *O*-methylisourea. This approach has, in principle, been published before in a French patent claimed by Roussel Uclaf in 1967 [36]; however, this route started with a fully synthetic precursor [37] of undefined stereochemistry (most likely racemic), and neither full experimental details nor acceptable spectroscopic data on the characterization of intermediates and the final product were presented.

Our chiral pool approach started once again with 19-nortestosterone (**3**). For this new purpose, the ketocarboxylic acid **4** obtained by oxidative cleavage of ring A (Scheme 1) needed to be degraded further in order to convert the propionate side-chain into a formyl group (see Figure 2) following, in general, a poorly detailed protocol published by Holt et al. [20]. For this purpose, ketocarboxylic acid **4** was first converted into its methyl ester **12** via a higher-yielding protocol utilizing iodomethane/Cs$_2$CO$_3$ (96.9% yield), followed by conversion of the keto group into the dioxolane **13** (67.5% yield). Next, and distinct from the Holt protocol, the 17-OH group was protected by conversion into the TBDS ether **14** (74.4% yield), in order to circumvent interference of the acidic 17-OH group with the strong base LDA required for the following step. Then, the methyl propionate side chain was converted into the α,β-unsaturated ester **15** in 72.2% yield by a selenation-selenoxide elimination protocol including treatment with LDA/diphenyldiselenide and oxidation with H$_2$O$_2$ [38], followed by spontaneous elimination. Two-carbon degradation was then per-

formed by ozonolysis followed by work-up with dimethyl sulfide to provide the aldehyde **16** in 75.8% yield. The treatment of **16** with acetic acid in THF-water resulted in simultaneous deprotection of the dioxolane and the TBDS ether to provide the ketoaldehyde **17** in 79.2% yield. Finally, treatment with *O*-methylisourea gave the target methoxypyrimidine **2** in 37.7% yield (Scheme 3).
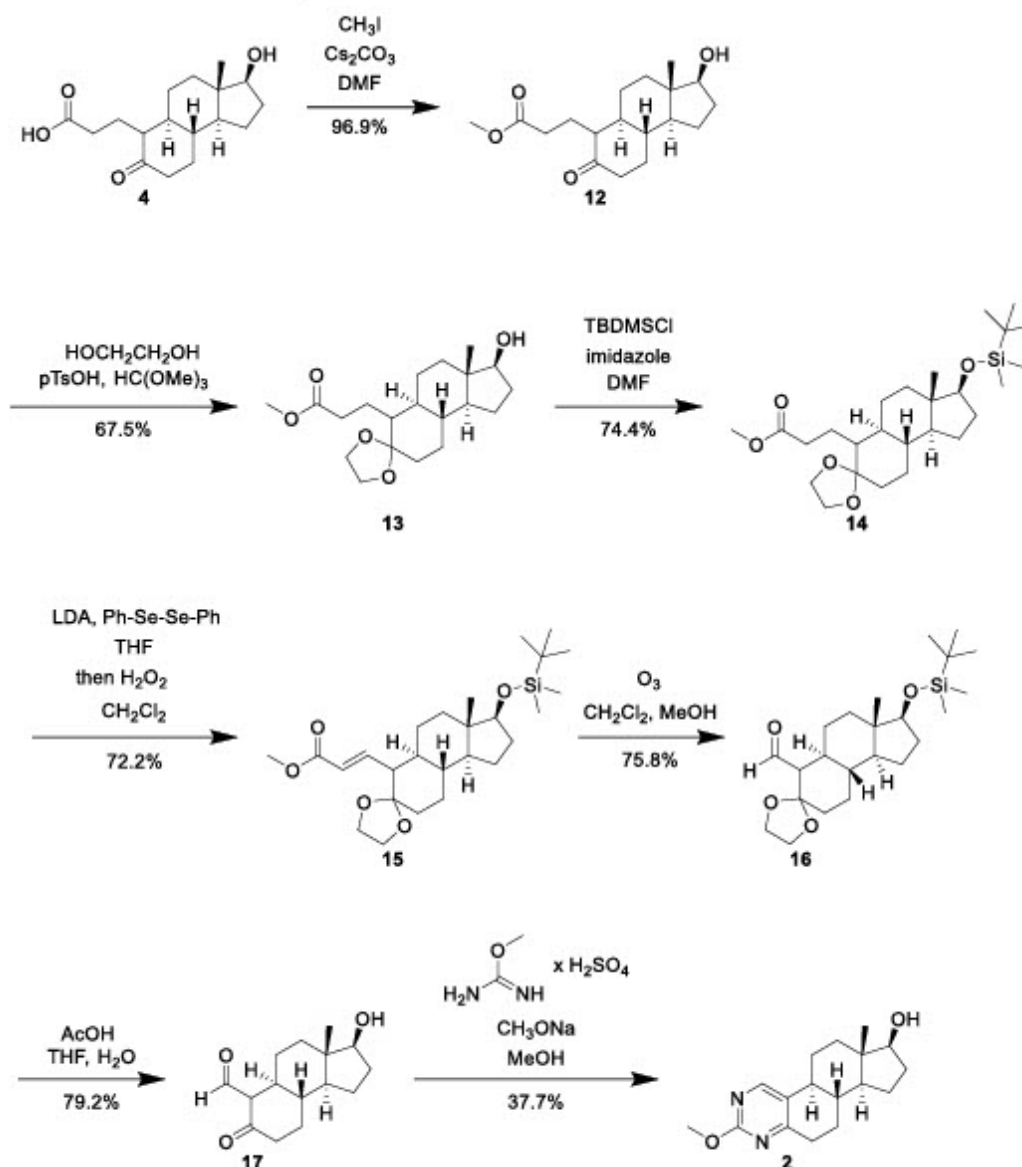
Scheme 3. Synthesis of the 2,4-diaza analog **2** of EDME.

2.2. Biological Testing

The two target compounds, pyridine analog **1** and pyrimidine analog **2**, as well as the inadvertently obtained pyridone analog **6** were submitted to our previously described [13] test for inhibition of TRPML1 on hTRPML1ΔNC-YFP, a plasma membrane variant of wild-type TRPML1 by means of a fluorimetric Ca²⁺ influx assay. The results are shown in Table 1.

Table 1. TRPML1-inhibitory activities of lead structure **EDME** and the three synthesized aza analogs.

Compound	IC$_{50}$ for TRPML1 Inhibition
EDME	0.60 µM
1	1.0 µM
2	8.8 µM
6	40 µM

Compared to EDME, the 4-aza analog **1** showed slightly reduced TRPML1-inhibitory activity (factor <2 less potent), the 2,4-diaza analog **2**; however, it is only a very weak inhibitor, and the pyridone analog **6** is virtually inactive.

3. Materials and Methods

3.1. Chemistry

All NMR spectra (^{1}H, ^{13}C, DEPT, H-H-COSY, HSQC, HMBC) were recorded at 23 °C on an Avance III 400 MHz Bruker BioSpin or Avance III 500 MHz Bruker BioSpin instrument (Bruker, Billerica, MA, USA) unless otherwise specified. Chemical shifts δ are stated in parts per million (ppm) and are calibrated using residual protic solvents as an internal reference for proton (CD$_2$Cl$_2$: δ = 5.32 ppm, MeOD δ = 3.31 ppm, DMSO: δ = 2.50 ppm) and for carbon the central carbon resonance of the solvent (CD$_2$Cl$_2$: δ = 53.84 ppm, MeOD δ = 49.00 ppm, DMSO: δ = 39.52 ppm). Multiplicity is defined as s—singlet, d—doublet, t—triplet, q—quartet, and m—multiplet. NMR spectra were analyzed with the NMR software MestReNova, version 12.0.1-20560 (Mestrelab Research S.L., Santiago de Compostela, Spain). Numbering of the carbon atoms in seco-steroids: For the sake of comparability, we kept using the numbering the single carbon atoms had in the intact steroids, since, in the following, the seco-steroidal intermediates were cyclized to the azasteroids later. High-resolution mass spectra were performed by the LMU Mass Spectrometry Service applying a Thermo Finnigan MAT 95 (Thermo Fisher Scientific, Waltham, MA, USA) or Joel MStation Sektorfeld instrument (Peabody, MA, USA) at a core temperature of 250 °C and 70 eV for EI or a Thermo Finnigan LTQ FT Ultra Fourier Transform Ion Cyclotron Resonance device (Thermo Fisher Scientific, Waltham, MA, USA) at 250 °C for ESI. IR spectra were recorded on a Perkin Elmer FT-IR Paragon 1000 instrument (Perkin Elmer, Hong Kong, China) as neat materials. The absorption bands were reported in wave number (cm^{-1}) with ATR PRO450-S. Melting points were determined by the open tube capillary method on a Büchi melting point B-540 apparatus and are uncorrected. The HPLC purities were determined using an HP Agilent 1100 HPLC (Agilent, Santa Clara, CA, USA) with a diode array detector at 210 nm and an Agilent Poroshell column (120 EC-C18; 3.0 × 100 mm; 2.7 micron) with acetonitrile/water as eluent. Values for specific rotation (α) were measured at 23 °C at a wavelength of λ = 589 nm (Na-D-line) using a Perkin Elmer 241 Polarimeter instrument (Perkin Elmer, Hong Kong, China). All samples were dissolved in dichloromethane (layer thickness l = 10 cm, concentration c = 0.1 mg/100 mL). All chemicals used were of analytical grade. Isohexane, ethyl acetate and methylene chloride were purified by distillation. All reactions were monitored by thin-layer chromatography (TLC) using pre-coated plastic sheets, POLYGRAM® SIL G/UV 254 from Macherey-Nagel (Düren, Germany). Flash column chromatography was performed on Merck silica gel Si 60 (0.015–0.040 mm). Ozonolysis was performed on an Ozonova Type OG700-10WC (Jeske Ozontechnik, Ruderserg, Germany).

3-((3S,3aS,5aS,6R,9aR,9bS)-3-Hydroxy-3a-methyl-7-oxododecahydro-1H-cyclopenta[a]naphthalen-6-yl)propanoic acid (**4**): To a solution of 19-nortestosterone (**3**; 3.01 g, 10.9 mmol, 1.00 eq) in 60 mL of *tert*-butanol were added 19.5 mL of a saturated aqueous Na$_2$CO$_3$ solution. The mixture was heated at reflux, and a solution of NaIO$_4$ (23.4 g, 110 mmol, 10.00 eq) and KMnO$_4$ (0.130 g, 0.821 mmol, 7.50 mol%) in water (66 mL), preheated to 80 °C, was added via a dropping funnel over a time period of 30 min. After cooling, the reaction mixture was filtered, and the filter cake was washed with 10 mL of water. The filtrate

was acidified with 6M HCl to pH 2 and then extracted with dichloromethane (4×20 mL). The organic phase was washed with water (20 mL) and dried over anhydrous sodium sulfate. After filtration and removal of the solvent, the crude product was purified by flash column chromatography (isohexane/ethyl acetate 1:1) to yield a colorless oil (3.08 g, 10.4 mmol, 95.4%). ^{1}H NMR (400 MHz, DMSO-d_6) δ/ppm = 11.95 (s, 1H, COOH), 4.48 (d, J = 4.8 Hz, 1H, OH), 3.46 (td, J = 8,5 Hz, 4,7 Hz, 1H, 17-H), 2.42 (m, 1H, 6-H$_a$), 2.29 (ddd, J = 11.2 Hz, 7.8 Hz, 2.5 Hz, 1H, 10-H), 2.21 (m, 1H, 6-H$_b$), 2.17 (m, 1H, 2-H$_a$), 2.09 (m, 1H, 2-H$_b$), 1.88 (m, 1H, 7-H$_a$), 1.75 (m, 1H, 1-H$_a$), 1.72 (m, 1H, 12-H$_a$), 1.69 (m, 1H, 15-H$_a$), 1.63 (m, 1H, 1-H$_b$), 1.57 (m, 1H, 8-H), 1.52 (m, 1H, 11-H$_a$), 1.36 (m, 1H, 16-H$_a$), 1.30 (m, 1H, 15-H$_b$), 1.24 (m, 1H, 11-H$_b$ or 16-H$_b$), 1.22 (m, 1H, 11-H$_b$ or 16-H$_b$), 1.15 (m, 1H, 7-H$_b$), 1.04 (m, 1H, 9-H), 1.00 (m, 1H, 12-H$_b$), 0.95 (m, 1H, 14-H), 0.72 (s, 3H, 18-H) ^{13}C NMR (101 MHz, DMSO-d_6) δ/ppm = 211.41 (C-5), 174.6 (C-3), 79.84 (C-17), 52.85 (C-10), 49.08 (C-14), 47.50 (C-9), 42.69 (C-13), 41.19 (C-6), 40.19 (C-8), 36.16 (C-12), 30.96 (C-2), 30.77 (C-7), 29.73 (C-16), 26.59 (C-15), 22.96 (C-11), 20.57 (C-1), 11.25 (C-18) IR (ATR): ν_{max}/cm^{-1} = 2921, 2359, 1698, 1636, 1455, 1385, 1261, 1127, 1055, 805, 696 HRMS (EI): m/z = [M$^{\bullet+}$] calculated for $C_{17}H_{26}O_4^{\bullet+}$: 294.1826; found: 294.1825.

(4bS,6aS,7S,9aS,9bR)-7-Hydroxy-6a-methyl-1,3,4,4a,4b,5,6,6a,7,8,9,9a,9b,10-tetradecahydro-2H-indeno[5,4-f]quinolin-2-one (**5a**) and *(4bS,6aS,7S,9aS,9bR)-7-hydroxy-6a-methyl-1,3,4,4b,5,6,6a,7,8,9,9a,9b,10,11-tetradecahydro-2H-indeno[5,4-f]quinolin-2-one* (**5b**): A mixture of compound **4** (0.795 g, 2.70 mmol, 1.00 eq) and ammonium acetate (0.728 g, 9.45 mmol, 3.50 eq) in glacial acetic acid (20 mL) was stirred and heated at reflux for 4 h. After cooling, the mixture was concentrated under reduced pressure and the residue was poured into water. The precipitate was collected by filtration, washed with water (10 mL) and dissolved in dichloromethane (20 mL). The resulting solution was washed with NaOH (1M, 3×10 mL), water (10 mL) and brine (10 mL), filtered over a hydrophobic filter, and concentrated in vacuo. The crude product was purified by flash column chromatography (isohexane/ethyl acetate 3:1) to yield 0.650 g (2.36 mmol, 87.4%) of a mixture of lactams **5a** and **5b** (ratio **5a**/**5b**: 15:85) as a beige solid.

5a: m.p.: 209 °C ^{1}H NMR (500 MHz, CD$_2$Cl$_2$) δ/ppm = 6.88 (s, 1H, NH), 3.65 (t, J = 8.5 Hz, 1H, 17-H), 2.38 (m, 2H, 2-H), 2.32 (m, 1H, 1-H$_a$), 2.20 (m, 1H, 1-H$_b$), 2.15 (m, 1H, 6-H$_a$), 2.04 (m, 1H, 16-H$_a$), 1.95 (m, 1H, 6-H$_b$), 1.87 (m, 1H, 11-H$_a$ or 15-H$_a$), 1.81 (dt, J = 12.3 Hz, 3.1 Hz, 1H, 12-H$_a$), 1.75 (m, 1H, 7-H$_a$), 1.71 (m, 1H, 9-H), 1.60 (m, 1H, 11-H$_a$ or 15-H$_a$), 1.43 (m, 1H, 16-H$_b$), 1.34 (m, 1H, 8-H or 11-H$_b$ or 15-H$_b$), 1.31 (m, 1H, 8-H or 11-H$_b$ or 15-H$_b$), 1.26 (m, 1H, 11-H$_b$ or 15-H$_b$), 1.22 (m, 1H, 7-H$_b$), 1.17 (m, 1H, 12-H$_b$), 1.11 (m, 1H, 14-H$_b$), 0.75 (s, 3H, 18-H) ^{13}C NMR (126 MHz, CD$_2$Cl$_2$) δ/ppm = 171.03 (C-3), 128.63 (C-5), 112.88 (C-10), 81.99 (C-17), 49.70 (C-14), 44.31 (C-9), 44.00 (C-13), 39.50 (C-8), 37.16 (C-12), 31.11 (C-2), 30.92 (C-16), 27.34 (C-6), 26.33 (C-7), 25.68 (C-11 or C-15), 23.30 (C-11 or C-15), 22.21 (C-1), 11.46 (C-18) IR (ATR): ν_{max}/cm^{-1} = 3465, 2913, 2868, 1683, 1668, 1542, 1507, 1473, 1456, 1388, 1319, 1284, 1224, 1186, 1133, 1055, 1027, 894, 842 HRMS (EI): m/z = [M$^{\bullet+}$] calculated for $C_{17}H_{25}NO_2^{\bullet+}$: 275.1880; found: 275.1880.

5b: m.p.: 218 °C ^{1}H NMR (500 MHz, CD$_2$Cl$_2$) δ/ppm = 7.34 (s, 1H, NH), 4.86 (dt, J = 5.1 Hz, 2.3 Hz, 1H, 6-H), 3.63 (t, J = 8.6 Hz, 1H, 17-H), 2.47 (m, 1H, 2-H$_a$), 2.37 (m, 1H, 2-H$_b$), 2.10 (m, 1H, 7-H$_a$), 2.05 (m, 1H, 16-H$_a$), 2.02 (m, 1H, 10-H), 1.92 (m, 1H, 1-H$_a$), 1.81 (dt, J = 12.6 Hz, 3.4 Hz, 1H, 12-H$_a$), 1.65 (m, 1H, 11-H$_a$), 1.60 (m, 1H, 15-H$_a$), 1.46 (m, 1H, 7-H$_b$ or 11-H$_b$), 1.43 (m, 1H, 16-H$_b$), 1.40 (m, 1H, 8-H), 1.31 (m, 1H, 1-H$_b$), 1.29 (m, 1H, 15-H$_b$), 1.26 (m, 1H, 7-H$_b$ or 11-H$_b$), 1.15 (m, 1H, 12-H$_b$), 1.04 (m, 1H, 14-H), 1.00 (m, 1H, 9-H), 0.76 (s, 3H, 18-H) ^{13}C NMR (126 MHz, CD$_2$Cl$_2$) δ/ppm = 169.77 (C-3), 136.46 (C-5), 102.48 (C-6), 82.05 (C-17), 50.71 (C-14), 43.79 (C-9), 43.35 (C-13), 39.98 (C-10), 37.08 (C-8), 36.66 (C-12), 32.36 (C-2), 30.78 (C-16), 29.18 (C-11), 26.60 (C-1), 25.29 (C-7), 23.47 (C-15), 11.10 (C-18) IR (ATR): ν_{max}/cm^{-1} = 2920, 2308, 1636, 1558, 1541, 1507, 1457, 1386, 1055, 735 HRMS (EI): m/z = [M$^{\bullet+}$] calculated for $C_{17}H_{25}NO_2^{\bullet+}$: 275.1880; found: 275.1880.

(8R,9S,13S,14S,17S)-17-(Benzyloxy)-13-methyl-1,2,6,7,8,9,10,11,12,13,14,15,16,17-tetradecahydro-3H-cyclopenta[a]phenanthren-3-one (7): 19-Nortestosterone (3; 2.47 g, 9.00 mmol, 1.00 eq), 2-benzyloxy-1-methylpyridinium triflate (6.29 g, 18.0 mmol, 2.00 eq) and magnesium oxide (vacuum-dried, 0.744 g, 18.0 mmol, 2.00 eq) were combined in a round bottom flask. Benzotrifluoride (20 mL) was added, and the resulting suspension was heated under stirring at 83 °C for 24 h. After cooling to room temperature, the reaction mixture was diluted with dichloromethane (20 mL) and filtered through Celite. After evaporation of the solvent, the crude product was purified by flash column chromatography (isohexane/ethyl acetate 10:1) to yield 2.69 g (7.39 mmol, 82.1%) of compound 7 as a white solid. m.p.: 176 °C ^{1}H NMR (400 MHz, DMSO-d_6) δ/ppm = 7.31 (m, 4H, benzyl aromatic ortho and meta Hs), 7.26 (m, 1H, benzyl aromatic para H), 5.72 (s, 1H, 4-H), 4.50 (s, 2H, benzyl CH$_2$), 3.41 (t, J = 8.2 Hz, 1H, 17-H), 2.42 (m, 6-H$_a$), 2.26 (m, 6-H$_b$), 2.22 (m, 1H, 1-H$_a$), 2.20 (m, 1H, 2-H$_a$), 2.16 (m, 1H, 10-H), 1.97 (m, 1H, 16-H$_a$), 1.87 (dt, J = 12.2 Hz, 3.2 Hz, 1H, 2-H$_b$), 1.78 (m, 1H, 15-H$_a$), 1.73 (m, 1H, 7-H$_a$), 1.55 (m, 1H, 11-H$_a$), 1.48 (m, 1H, 16-H$_b$), 1.43 (m, 1H, 12-H$_a$), 1.37 (m, 1H, 1-H$_b$ or 15-H$_b$), 1.30 (m, 1H, 8-H), 1.26 (m, 1H, 11-H$_b$), 1.21 (m, 1H, 1-H$_b$ or 15-H$_b$), 1.12 (m, 1H, 12-H$_b$), 1.01 (m, 1H, 14-H), 0.95 (m, 1H, 7-H$_b$), 0.81 (s, 3H, 18-H), 0.77 (m, 1H, 9-H) ^{13}C NMR (101 MHz, DMSO-d_6) δ/ppm = 198.41 (C-3), 166.76 (C-5), 139.18 (benzyl, quaternary carbon), 128.15 (benzyl, aromatic para), 127.15 (4C, benzyl aromatic ortho and meta), 123.75 (C-4), 87.59 (C-17), 70.74 (benzyl CH$_2$), 49.27 (C-14), 48.95 (C-9), 42.69 (C-13), 41.67 (C-10), 37.09 (C-12), 36.16 (C-2), 34.60 (C-6), 30.28 (C-7), 27.49 (C-16), 26.13 (C-1 or C-15), 25.64 (C-1 or C-15), 22.81 (C-11), 11.68 (C-18). IR (ATR): ν_{max}/cm^{-1} = 2927, 2870, 2350, 2307, 1717, 1653, 1558, 1541, 1507, 1489, 1473, 1456, 1388, 1339, 1067 HRMS (EI): m/z = [M$^{\bullet+}$] calculated for C$_{25}$H$_{32}$O$_2$$^{\bullet+}$ 364.2397; found: 364.2396.

3-((3S,3aS,5aS,9aR,9bS)-3-(Benzyloxy)-3a-methyl-7-oxododecahydro-1H-cyclopenta[a]naphthalen-6-yl)propanoic acid (8): To a solution of compound 7 (2.63 g, 7.20 mmol, 1.00 eq) in 75 mL of *tert*-butanol were added 13.5 mL of a saturated aqueous Na$_2$CO$_3$ solution. The mixture was heated at reflux, and a solution of NaIO$_4$ (15.4 g, 72.0 mmol, 10.00 eq) and KMnO$_4$ (85.3 mg, 0.540 mmol, 7.50 mol%) in water (45 mL), preheated to 80 °C, was added via a dropping funnel over a time period of 30 min. After cooling, the reaction mixture was filtered, and the filter cake was washed with 10 mL of water. The filtrate was acidified with 6M HCl to pH 2 and then extracted with dichloromethane (4 × 20 mL). The organic phase was washed with water (20 mL) and dried over anhydrous sodium sulfate. After filtration and removal of the solvent, the crude product was purified by flash column chromatography (isohexane/ethyl acetate 3:1) to yield compound 8 as a colorless oil (2.86 g, 7.44 mmol, 99.2%) ^{1}H NMR (500 MHz, CD$_2$Cl$_2$) δ/ppm = 7.33 (2s, 4H, benzyl aromatic ortho and meta Hs) 7.26 (hept, J = 3.8 Hz, 1H, benzyl aromatic para H), 4.51 (s, 2H, benzyl CH$_2$), 3.45 (td, J = 7.5 Hz, 6.8 Hz, 2.5 Hz, 1H, 17-H), 2.41 (m, 1H, 2-H$_a$), 2.37 (m, 1H, 6-H$_a$), 2.35 (m, 1H, 6-H$_b$), 2.30 (m, 1H, 2-H$_b$), 2.26 (m, 1H, 7-H$_a$), 2.23 (m, 1H, 10-H), 2.05 (m, 1H, 16-H$_a$), 2.01 (m, 1H, 7-H$_b$), 1.96 (m, 1H, 12-H$_a$), 1.91 (m, 1H, 1-H$_a$), 1.80 (m, 1H, 15-H$_a$), 1.77 (m, 1H, 1-H$_b$), 1.62 (m, 1H, 11-H$_a$), 1.59 (m, 1H, 8-H), 1.55 (m, 1H, 16-H$_b$), 1.39 (m, 1H, 15-H$_b$), 1.35 (m, 1H, 11-H$_b$), 1.20 (m, 1H, 12-H$_b$), 1.08 (m, 1H, 9-H), 1.03 (m, 1H, 14-H), 0.90 (s, 3H, 18-H) ^{13}C NMR (126 MHz, CD$_2$Cl$_2$) δ/ppm = 212.32 (C-5), 178.14 (C-3), 139.84 (benzyl, quaternary carbon), 128.57 (benzyl, aromatic para), 127.74 (4C, benzyl aromatic ortho and meta), 88.66 (C-17), 72.00 (benzyl CH$_2$), 54.17 (C-10), 50.17 (C-14), 48.71 (C-9), 43.59 (C-13), 42.21 (C-6), 40.72 (C-8), 37.81 (C-12), 31.76 (C-7), 31.34 (C-2), 28.17 (C-16), 27.51 (C-15), 23.64 (C-11), 21.08 (C-1), 11.98 (C-18). IR (ATR): ν_{max}/cm^{-1} = 2927, 2871, 2349, 2307, 1868, 1705, 1653, 1558, 1541, 1521, 1507, 1497, 1456, 1418, 1362, 1279, 869 HRMS (EI): m/z = [M$^{\bullet+}$] calculated for C$_{24}$H$_{32}$O$_4$$^{\bullet+}$: 384.2295; found: 384.2294.

(4bS,6aS,7S,9aS,9bR)-7-(Benzyloxy)-6a-methyl-1,3,4,4a,4b,5,6,6a,7,8,9,9a,9b,10-tetradecahydro-2H-indeno[5,4-f]quinolin-2-one (9a) and *(4bS,6aS,7S,9aS,9bR)-7-(benzyloxy)-6a-methyl-1,3,4,4b,5,6,6a,7,8,9,9a,9b,10,11-tetradecahydro-2H-indeno[5,4-f]quinolin-2-one* (9b): A mixture of compound 8 (2.54 g, 6.60 mmol, 1.00 eq) and ammonium acetate (1.78 g, 23.1 mmol, 3.50 eq)

in glacial acetic acid (60 mL) was stirred and heated at reflux for 4 h. After cooling, it was concentrated under reduced pressure and the remaining residue was poured into water. The precipitate was filtered, washed with water (20 mL) and dissolved in dichloromethane (40 mL). The resulting solution was washed with NaOH (1M, 3 × 20 mL), water (20 mL) and brine (20 mL), filtered over a hydrophobic filter and concentrated in vacuo. The crude product was purified by flash column chromatography (isohexane/ethyl acetate 5:1) to provide a total of 1.77 g (4.85 mmol, 73.4%) of fractions containing compounds **9a/9b** (ratio **9a:9b**: ca. 15:85) as beige solids (pure **9a**: 0.150 g, 0.420 mmol, 6.3%, pure **9b**: 0.870 g, 2.37 mmol, 35.9%, mixed fraction: 0.750 g, 2.05 mmol, 31.1%; ratio **9a:9b**: ca. 15:85).

9a: m.p.: 207 °C ^{1}H NMR (400 MHz, CD_2Cl_2) δ/ppm = 7.32 (m, 4H, benzyl aromatic ortho and meta Hs), 7.26 (m, 1H, benzyl aromatic para H), 6.69 (s, 1H, NH), 4.51 (s, 2H, benzyl CH_2), 3.47 (m, 1H, 17-H), 2.39 (m, 2H, 2-H), 2.32 (m, 1H, 1-H_a), 2.20 (m, 1H, 1-H_b), 2.14 (m, 1H, 6-H_a), 2.04 (m, 1H, 16-H_a), 1.98 (m, 1H, 12-H_a), 1.92 (m, 1H, 6-H_b), 1.85 (m, 1H, 7-H_a), 1.75 (m, 1H, 11-H_a), 1.69 (m, 1H, 9-H), 1.63 (m, 1H, 15-H_a), 1.55 (m, 1H, 16-H_b), 1.34 (m, 1H, 15-H_b), 1.30 (m, 1H, 8-H), 1.26 (m, 1H, 12-H_b), 1.24 (m, 1H, 11-H_b), 1.20 (m, 1H, 7-H_b), 1.14 (m, 1H, 14-H), 0.84 (s, 3H, 18-H) ^{13}C NMR (101 MHz, CD_2Cl_2) δ/ppm = 170.75 (C-3), 139.95 (benzyl, quaternary carbon), 128.61 (C-5), 128.56 (2C, benzyl aromatic ortho or meta), 127.72 (2C, benzyl aromatic ortho or meta), 127.60 (benzyl, aromatic para), 112.82 (C-10), 88.88 (C-17), 72.00 (benzyl CH_2), 49.88 (C-14), 44.31 (C-9), 44.18 (C-13), 39.29 (C-8), 38.36 (C-12), 31.17 (C-2), 28.39 (C-16), 27.38 (C-6), 26.33 (C-11), 25.81 (C-7), 23.32 (C-15), 22.24 (C-1), 12.21 (C-18). IR (ATR): ν_{max}/cm^{-1} = 3087, 2925, 2870, 2348, 2307, 1868, 1698, 1558, 1542, 1521, 1507, 1490, 1455, 1387, 1338 HRMS (EI): m/z = [M$^{\bullet+}$] calculated for $C_{24}H_{31}NO_2$ $^{\bullet+}$: 365.2349; found: 365.2354.

9b: 207 °C ^{1}H NMR (400 MHz, CD_2Cl_2) δ 7.52 (s, 1H, NH), 7.33 (2s, 4H, benzyl aromatic ortho and meta Hs), 7.26 (ddt, J = 5.7 Hz, 3.7 Hz, 2.2 Hz, 1H, benzyl aromatic para H), 4.87 (dt, J = 5.1 Hz, 2.3 Hz, 1H, 6-H), 4.52 (s. 2H, benzyl CH_2), 3.45 (dd, J = 8.7 Hz, 7.6 Hz, 1H, 17-H), 2.47 (ddd, J = 17.8 Hz, 5.2 Hz, 2.0 Hz, 1H, 2-H_a), 2.35 (ddd, J = 18.0 Hz, 13.0 Hz, 5.9 Hz, 1H, 2-H_b), 2.12 (m, 1H, 7-H_a), 2.07 (m, 1H, 7-H_b), 2.03 (m, 1H, 16-H_a), 2.00 (m, 1H, 10-H), 1.97 (m, 1H, 12-H_a), 1.92 (m, 1H, 11-H_a or 15-H_a), 1.58 (m, 1H, 1-H_a), 1.55 (m, 1H, 16-H_b), 1.48 (m, 1H, 8-H), 1.42 (m, 1H, 11-H_a or 15-H_a), 1.32 (m, 1H, 1-H_b), 1.29 (m, 1H, 12-H_b), 1.25 (m, 1H, 11-H_b or 15-H_b), 1.22 (m, 1H, 11-H_b or 15-H_b), 1.05 (m, 1H, 14-H), 1.01 (m, 1H, 9-H), 0.85 (s, 3H, 18-H) ^{13}C NMR (101 MHz, CD_2Cl_2) δ/ppm = 169.91 (C-3), 139.93 (benzyl, quaternary carbon), 136.45 (C-5), 128.56 (2C, benzyl aromatic ortho or meta), 127.73 (2C, benzyl aromatic ortho or meta), 127.61 (benzyl, aromatic para), 102.56 (C-6), 88.92 (C-17), 72.02 (benzyl CH_2), 50.89 (C-14), 43.81 (C-9), 43.53 (C-13), 39.97 (C-10), 37.86 (C-12), 36.87 (C-8), 32.35 (C-2), 29.20 (C-7), 28.23 (C-16), 26.70 (C-15), 25.27 (C-11), 23.51 (C-1), 11.85 (C-18). IR (ATR): ν_{max}/cm^{-1} = 3195, 3062, 2920, 2872, 1716, 1569, 1355, 1332, 1317, 1190, 1139, 1070, 1045, 843, 800, 737, 695, 647 HRMS (EI): m/z = [M$^{\bullet+}$] calculated For $C_{24}H_{31}NO_2$ $^{\bullet+}$: 365.2349; found: 365.2349.

(4bS,6aS,7S,9aS,9bR)-7-(Benzyloxy)-6a-methyl-1,4b,5,6,6a,7,8,9,9a,9b,10,11-dodecahydro-2H-indeno[5,4-f]quinolin-2-one (**10**) and *(4bS,6aS,7S,9aS,9bR)-7-hydroxy-6a-methyl-1,4b,5,6,6a,7,8, 9,9a,9b,10,11-dodecahydro-2H-indeno[5,4-f]quinolin-2-one* (**6**): A mixture of compounds **9a/9b** (0.256 g, 0.700 mmol, 1.00 eq) was suspended in acetonitrile (2 mL). 1.3-Dimethoxybenzene (0.2 mL), a suspension of copper (II) bromide (87.6 mg, 0.392 mmol, 0.560 eq) and lithium bromide (78.6 mg, 0.896 mmol, 1.28 eq) in acetonitrile (2 mL) and a solution of methanesulfonic acid (23.2 μL, 0.350 mmol, 0.500 eq in 1.2 mL acetonitrile) were added. The resulting mixture was stirred and heated at reflux for 5 h. Then water (5 mL) was added, and the mixture was extracted with dichloromethane (3 × 10 mL). The organic layers were combined, washed with brine (10 mL), and filtered through a hydrophobic filter. After evaporation of the solvent, the crude product was purified by flash column chromatography to yield 86.0 mg (0.237 mmol, 33.8%) of **10** (eluated first with

dichloromethane/methanol 100:3) as a beige solid and 14.9 mg (0.0546 mmol, 7.8%) of **6** (eluated second with dichloromethane/methanol 10:1) as a beige solid.

10: m.p.: 302 °C ^{1}H NMR (400 MHz, CD$_2$Cl$_2$) δ/ppm = 12.78 (br s, 1H, NH), 7.44 (d, J = 9.4 Hz, 1H, 1-H), 7.33 (m, 4H, benzyl aromatic ortho and meta Hs), 7.27 (dq, J = 7.4, 2.8 Hz, 1H, benzyl aromatic para H), 6.28 (d, J = 9.3 Hz, 1H, 2-H), 4.53 (s, 2H, benzyl CH$_2$), 3.50 (t, J = 8.2 Hz, 1H, 17-H), 2.70 (m, 2H, 6-H), 2.14 (m, 1H, 11-H$_a$), 2.08 (m, 1H, 16-H$_a$), 2.05 (m, 1H, 12-H$_a$), 2.02 (m, 1H, 9-H), 1.89 (m, 1H, 7-H$_a$), 1.68 (ddd, J = 12.4 Hz, 6.8 Hz, 2.8 Hz, 1H, 15-H$_a$), 1.57 (ddd, J = 13.4 Hz, 7.8 Hz, 3.0 Hz, 1H, 16-H$_b$), 1.43 (m, 1H, 8-H), 1.39 (m, 1H, 11-H$_b$), 1.36 (m, 1H, 15-H$_b$), 1.34 (m, 1H, 12-H$_b$), 1.29 (m, 1H, 7-H$_b$), 1.19 (td, J = 11.4 Hz, 6.9 Hz, 1H, 14-H), 0.85 (s, 3H, 18-H). ^{13}C NMR (101 MHz, CD$_2$Cl$_2$) δ/ppm = 164.69 (C-3), 143.70 (C-5), 140.66 (C-1), 139.91 (benzyl, quaternary carbon), 128.57 (2C, benzyl aromatic ortho or meta), 127.73 (2C, benzyl aromatic ortho or meta), 127.62 (benzyl, aromatic para), 118.06 (C-10), 116.73 (C-2), 88.82 (C-17), 72.02 (benzyl CH$_2$), 49.85 (C-14), 43.91 (C-13), 42.35 (C-9), 38.74 (C-8), 38.01 (C-12), 28.30 (C-16), 27.46 (C-6), 26.53 (C-11), 26.07 (C-7), 23.35 (C-15), 12.05 (C-18) IR (ATR): v_{max}/cm^{-1} = 3087, 2933, 2869, 2348, 2307, 1869, 1845, 1716, 1614, 1542, 1522, 1508, 1496, 1456, 1420 HRMS (EI): m/z = [M$^{\bullet+}$] calculated for C$_{24}$H$_{29}$NO$_2$ $^{\bullet+}$: 363.2193; found: 363.2192.

6: m.p.: 306 °C ^{1}H NMR (500 MHz, MeOD-d$_4$) δ/ppm = 7.61 (d, J = 9.4 Hz, 1H, 1-H), 6.36 (d, J = 9.3 Hz, 1H, 2-H), 3.66 (m, 1H, 17-H), 2.70 (m, 2H, 6-H), 2.24 (dq, J = 12.7 Hz, 3.7 Hz, 1H, 11-H$_a$), 2.09 (m, 1H, 9-H), 2.04 (m, 1H, 16-H$_a$), 1.97 (m, 1H, 12-H$_a$), 1.93 (m, 1H, 7-H$_a$), 1.69 (dddd, J = 12.3 Hz, 9.6 Hz, 7.1 Hz, 3.3 Hz, 1H, 15-H$_a$), 1.53 (dddd, J = 13.1 Hz, 11.6 Hz, 8.2 Hz, 3.3 Hz, 1H, 16-H$_b$), 1.44 (m, 1H, 8-H), 1.40 (m, 1H, 11-H$_b$ or 15-H$_b$), 1.38 (m, 1H, 11-H$_b$ or 15-H$_b$), 1.35 (m, 1H, 7-H$_b$), 1.28 (m, 1H, 12-H$_b$), 1.22 (m, 1H, 14-H), 0.79 (s, 3H, 18-H) ^{13}C NMR (126 MHz, MeOD-d$_4$) δ/ppm = 165.20 (C-3), 144.55 (C-5), 142.44 (C-1), 120.32 (C-10), 117.12 (C-2), 82.28 (C-17), 50.50 (C-14), 44.51 (C-13), 43.27 (C-9), 39.87 (C-8), 37.72 (C-12), 30.65 (C-16), 27.92 (C-6), 27.13 (C-11), 26.77 (C-7), 23.86 (C-15), 11.70 (C-18) IR (ATR): v_{max}/cm^{-1} = 3399, 2929, 2869, 1651, 1606, 1550, 1507, 1449, 1375, 1338, 1293, 1253, 1196, 1136, 1100, 1081, 1057, 1022, 960 HRMS (EI): m/z = [M$^{\bullet+}$] calculated for C$_{17}$H$_{23}$NO$_2$ $^{\bullet+}$: 273.1723; found: 273.1724.

(4bS,6aS,7S,9aS,9bR)-7-(Benzyloxy)-2-methoxy-6a-methyl-4b,6,6a,7,8,9,9a,9b,10,11-decahydro-5H-indeno[5,4-f]quinoline (**11**): To a solution of compound **10** (83.6 mg, 0.230 mmol, 1.00 eq) in chloroform (3.5 mL), silver carbonate (320 mg, 1.15 mmol, 5.00 eq) and iodomethane (0.859 mL, 13.8 mmol, 60.0 eq) were added and the mixture was stirred for 40 h at ambient temperature under exclusion of light. Thereafter, the mixture was filtered through Celite, which was washed with chloroform (5 mL), and the filtrate was concentrated in vacuo. The crude product was purified by flash column chromatography (isohexane/ethyl acetate 4:1) to yield 41.0 mg (0.109 mmol, 47.2%) of compound **11** as a colorless solid. m.p.: 102 °C ^{1}H NMR (500 MHz, CD$_2$Cl$_2$) δ/ppm = 7.48 (d, J = 8.5 Hz, 1H, 1-H), 7.34 (m, 4H, benzyl aromatic ortho and meta Hs), 7.26 (ddt, J = 8.6 Hz, 5.5 Hz, 2.5 Hz, 1H, benzyl aromatic para H), 6.49 (d, J = 8.5 Hz, 1H, 2-H), 4.54 (benzyl CH$_2$), 3.84 (OCH$_3$), 3.52 (t, J = 8.3 Hz, 1H, 17-H), 2.84 (m, 2H, 6-H), 2.23 (m, 1H, 11-H$_a$), 2.18 (m, 1H, 9-H), 2.10 (m, 1H, 16-H$_a$), 2.06 (m, 1H, 12-H$_a$), 1.95 (dtd, J = 10.6 Hz, 4.6 Hz, 2.2 Hz, 1H, 7-H$_a$), 1.71 (dddd, J = 12.4 Hz, 9.7 Hz, 7.0 Hz, 3.3 Hz, 1H, 15-H$_a$), 1.59 (dddd, J = 13.2 Hz, 11.5 Hz, 7.9 Hz, 3.4 Hz, 1H, 16-H$_b$), 1.49 (m, 1H, 11-H$_b$), 1.44 (m, 1H, 8-H), 1.41 (m, 1H, 15-H$_b$), 1.39 (m, 1H, 7-H$_b$), 1.36 (m, 1H, 12-H$_b$), 1.22 (m, 1H, 14-H), 0.85 (s, 3H, 18-H) ^{13}C NMR (126 MHz, CD$_2$Cl$_2$) δ/ppm = 161.97 (C-3), 154.62 (C-5), 139.96 (benzyl, quaternary carbon), 136.57 (C-1), 128.57 (2C, benzyl aromatic ortho or meta), 128.21 (C-10), 127.74 (2C, benzyl aromatic ortho or meta), 127.61 62 (benzyl, aromatic para), 107.59 (C-2), 88.93 (C-17), 72.02 (benzyl CH$_2$), 53.32 (OCH$_3$), 50.36 (C-14), 43.81 (C-13), 43.67 (C-9), 38.70 (C-8), 38.17 (C-12), 32.94 (C-6), 28.33 (C-16), 27.42 (C-7), 26.77 (C-11), 23.45 (C-15), 12.00 (C-18). IR (ATR): v_{max}/cm^{-1} = 2928, 2871, 2348, 2306, 1869, 1716,

1698, 1670, 1654, 1596, 1558, 1541, 1507, 1474, 1457, 1419 HRMS (EI): m/z = [M$^{\bullet+}$] calculated for $C_{25}H_{31}NO_2{}^{\bullet+}$: 377.2349; found: 377.2354.

(4bS,6aS,7S,9aS,9bR)-2-Methoxy-6a-methyl-4b,6,6a,7,8,9,9a,9b,10,11-decahydro-5H-indeno[5,4-f]quinolin-7-ol (**1**): Under a nitrogen atmosphere compound **11** (18.9 mg, 0.0500 mmol, 1.00 eq) was dissolved in dichloromethane (1.0 mL) and cooled to −78 °C. Then, boron trichloride solution (1M in dichloromethane, 0.15 mL, 0.150 mmol, 3.00 eq) was added dropwise, and the resulting solution was allowed to warm to 0 °C and stirred at this temperature for 2 h. Thereafter, the mixture was quenched with methanol (1 mL) and filtered through Celite. After evaporation of the solvent, the crude product was purified by flash column chromatography (isohexane/ethyl acetate 3:1 with 1% triethylamine) to yield 13.0 mg (0.0452 mmol, 90.5%) of compound **1** as a white solid m.p. 157 °C $[\alpha]_D^{23}$ = 2.5° (CH$_2$Cl$_2$) ^{1}H NMR (400 MHz, CD$_2$Cl$_2$) δ/ppm = 7.48 (d, J = 8.5 Hz, 1H, 1-H), 6.49 (d, J = 8.5 Hz, 1H, 2-H), 3.84 (s, 3H, OCH$_3$), 3.69 (t, J = 8.4 Hz, 1H, 17-H), 2.85 (td, J = 7.0 Hz, 5.8 Hz, 2.6 Hz, 2H, 6-H), 2.25 (m, 1H, 11-H$_a$), 2.20 (m, 1H, 9-H), 2.08 (m, 1H, 16-H$_a$), 1.95 (m, 1H, 7-H$_a$), 1.92 (m, 1H, 12-H$_a$), 1.71 (m, 1H, 15-H$_a$), 1.49 (m, 1H, 11-H$_b$), 1.44 (m, 1H, 1H, 16-H$_b$), 1.42 (m, 1H, 1H, 8-H), 1.38 (m, 1H, 7-H$_b$), 1.34 (m, 1H, 15-H$_b$), 1.26 (m, 1H, 12-H$_b$), 1.19 (m, 1H, 14-H), 0.76 (s, 3H, 18-H) ^{13}C NMR (101 MHz, CD$_2$Cl$_2$) δ/ppm = 161.98 (C-3), 154.63 (C-5), 136.59 (C-1), 128.20 (C-10), 107.59 (C-2), 82.08 (C-17), 53.35 (OCH$_3$), 50.20 (C-14), 43.68 (C-13), 43.65 (C-9), 38.93 (C-8), 37.00 (C-12), 32.93 (C-6), 30.92 (C-16), 27.43 (C-7), 26.67 (C-11), 23.42 (C-15), 11.25 (C-18). IR (ATR): ν_{max}/cm^{-1} = 2928, 2870, 2349, 2307, 1715, 1654, 1596, 1542, 1507, 1475, 1420, 1385, 1309, 1286, 1257, 1309, 1257, 1080 HRMS (EI): m/z = [M$^{\bullet+}$] calculated for $C_{18}H_{25}NO_2{}^{\bullet+}$: 287.1880; found: 287.1888 Purity (HPLC, acetonitrile/water 70:30): >95% (λ = 210 nm), >95% (λ = 254 nm).

Methyl 3-((3S,3aS,5aS,9aR,9bS)-3-Hydroxy-3a-methyl-7-oxododecahydro-1H-cyclopenta[a]naphthalen-6-yl)propanoate (**12**): Ketocarboxylic acid **4** (3.06 g, 10.4 mmol, 1.00 eq), Cs$_2$CO$_3$ (6.78 g, 20.8 mmol, 2.00 eq) and dry DMF (34 mL) were added to an oven-dried round-bottom flask and the mixture was stirred for 30 min at room temperature. Then, iodomethane (2.37 mL, 15.6 mmol, 1.50 eq) was added, and the reaction mixture was stirred overnight at room temperature. After quenching with H$_2$O (30 mL), the mixture was extracted with diethyl ether (3 × 30 mL). The combined organic phases were washed with water (30 mL) and brine (30 mL), dried over anhydrous sodium sulfate, filtered and concentrated in vacuo. The residue was purified by flash column chromatography (isohexane/ethyl acetate 2:1) to obtain methyl ester **12** as a colorless oil (3.11 g, 10.1 mmol, 96.9%) ^{1}H NMR (400 MHz, DMSO-d_6) δ/ppm = 4.49 (d, 1H, J = 4.9 Hz, OH), 3.45 (td, 1H, J = 8.5 Hz, 4.9 Hz, 17-H), 2.41 (m, H, 6-H$_a$), 2.29 (m, 1H, 10-H), 2.24 (m, 1H, 6-H$_b$), 2.20 (m, 1H, 2-H$_a$), 2.13 (m, 1H, 2-H$_b$), 1.88 (m, 1H, 7-H$_a$), 1.81 (m, 1H, 1-H$_a$), 1.73 (m, 1H, 12-H$_a$), 1.68 (m, 1H, 15-H$_a$), 1.64 (m, 1H, 1-H$_b$), 1.58 (m, 1H, 8-H), 1.51 (m, 1H, 11-H$_a$), 1.37 (m, 1H, 16-H$_a$), 1.30 (m, 1H, 15-H$_b$), 1.24 (m, 1H, 16-H$_b$), 1.19 (m, 1H, 11-H$_b$), 1.12 (m, 1H, 7-H$_b$), 1.04 (m, 1H, 9-H), 0.99 (m, 1H, 12-H$_b$), 0.93 (m, 1H, 14-H), 0.71 (s, 3H, 18-H) ^{13}C NMR (101 MHz, DMSO-d_6): δ/ppm = 211.39 (C-5), 173.49 (C-3), 79.86 (C-17), 52.75 (C-10), 51.22 (OCH$_3$), 49.09 (C-14), 47.41 (C-9), 42.70 (C-13), 41.17 (C-6), 40.19 (C-8), 36.17 (C-12), 30.75 (C-2), 30.66 (C-7), 29.73 (C-16), 26.58 (C-15), 22.97 (C-11), 20.58 (C-1), 11.25 (C-18). IR (ATR): ν_{max}/cm^{-1} = 2943, 2308, 1733, 1715, 1647, 1542, 1457, 1387, 1055 HRMS (EI): m/z = [M$^{\bullet+}$] calculated for $C_{18}H_{28}O_4{}^{\bullet+}$: 308.1982; found: 308.1982.

Methyl 3-((3S,3aS,5aS,6R,9aR,9bS)-3-Hydroxy-3a-methyldodecahydrospiro[cyclopenta[a]naphthalene-7,2'-[1,3]dioxolan]-6-yl)propanoate (**13**): A mixture of ketone **12** (3.09 g, 10.0 mmol, 1.00 eq), trimethyl orthoformate (24.1 mL, 220.0 mmol, 22.0 eq), ethylene glycol (24 mL, 430 mmol, 43.0 eq) and p-toluenesulfonic acid (0.194 g, 1.00 mmol, 0.100 eq) in a round bottom flask was stirred overnight at room temperature. The mixture was diluted with ethyl acetate, and the solution was washed with saturated aqueous sodium bicarbonate solution. The organic phase was dried over anhydrous sodium sulfate, filtered, and concentrated. The

residue was purified by flash column chromatography (isohexane/ethyl acetate 2:1) to obtain the dioxolane **13** as a colorless solid (2.38 g, 6.75 mmol, 67.5%). m.p.: 84 °C ^{1}H NMR (400 MHz, DMSO-d_6) δ/ppm = 4.44 (d, 1H, J = 4.8 Hz, OH), 3.88 (m, 2H, ethylene), 3.81 (m, 2H, ethylene), 3.56 (2s, 3H, OCH$_3$) 3.43 (td, 1H, J = 8.4 Hz, 4.9 Hz, 17-H), 2.38 (ddd, J = 16.7 Hz, 10.0 Hz, 6.6 Hz, 1H, 2-H$_a$), 2.24 (ddd, J = 16.0 Hz, 10.0 Hz, 6.1 Hz, 1H, 2-H$_b$), 1.82 (m, 1H, 16-H$_a$), 1.76 (m, 1H, 6-H$_a$), 1.70 (m, 1H, 12-H$_a$), 1.64 (m, 1H, 15-H$_a$), 1.61 (m, 1H, 1-H$_a$), 1.57 (m, 1H, 1-H$_b$), 1.47 (m, 1H, 11-H$_a$ or 7-H$_a$), 1.44 (m, 1H, 11-H$_a$ or 7-H$_a$), 1.38 (m, 1H, 10-H), 1.31 (m, 1H, 16-H$_b$), 1.21 (m, 1H, 6-H$_b$), 1.16 (m, 1H, 11-H$_b$ or 15-H$_b$), 1.13 (m, 1H, 11-H$_b$ or 15-H$_b$), 1.06 (m, 1H, 8-H), 1.01 (m, 1H, 9-H or 12-H$_b$), 0.97 (m, 1H, 9-H or 12-H$_b$), 0.95 (m, 1H, 7-H$_b$), 0.91 (m, 1H, 14-H), 0.63 (s, 3H, 18-H) ^{13}C NMR (101 MHz, DMSO-d_6) δ/ppm = 173.76 (C-3), 110.55 (C-5), 79.99 (C-17), 63.88 (ethylene), 63.86 (ethylene), 51.14 (OCH$_3$), 49.41 (C-14), 47.32 (C-10), 44.90 (C-9), 42.71 (C-13), 40.22 (C-8), 36.58 (C-12), 33.91 (C-6), 32.68 (C-2), 29.82 (C-16), 27.17 (C-7), 25.92 (C-15), 22.93 (C-11), 21.13 (C-1), 11.35 (C-18). IR (ATR): ν_{max}/cm^{-1} = 1868, 2307, 1732, 1698, 1647, 1635, 1321 HRMS (EI): m/z = [M$^{\bullet+}$] calculated for C$_{20}$H$_{32}$O$_5$$^{\bullet+}$: 352.2244; found: 352.2244.

Methyl 3-((3S,3aS,5aS,6R,9aR,9bS)-3-((tert-butyldimethylsilyl)oxy)-3a-methyl dodecahydro spiro[cyclopenta[a]naphthalene-7,2'-[1,3]dioxolan]-6-yl)propanoate (**14**): Compound **13** (2.38 g, 6.75 mmol, 1.00 eq) was dissolved in dimethylformamide (14 mL). Then imidazole (0.957 g, 14.1 mmol, 3.80 eq) and tert-butyldimethylsilyl chloride (1.06 g, 7.03 mmol, 2.00 eq) were added, and the resulting mixture was stirred overnight at room temperature. After addition of water (10 mL), the mixture was extracted with ethyl acetate (3 × 10 mL). The combined organic layers were washed with 1M hydrochloric acid (30 mL), water (20 mL) and brine (20 mL), dried over anhydrous sodium sulfate, filtered and concentrated in vacuo. The crude product was purified by flash column chromatography (isohexane/ethyl acetate 9:1) to obtain a colorless solid (2.35 g, 5.02 mmol, 74.4%). m.p.: 86 °C ^{1}H NMR (400 MHz, CD$_2$Cl$_2$) δ/ppm = 3.94 (m, 2H, ethylene), 3.89 (m, 2H, ethylene), 3.61 (s, 3H, ester CH$_3$), 3.58 (m, 1H, 17-H), 2.43 (m, 1H, 2-H$_a$), 2.31 (m, 1H, 2-H$_b$), 1.88 (m, 1H, 12-H$_a$), 1.80 (m, 1H, 6-H$_a$), 1.74 (m, 1H, 7-H$_a$), 1.71 (m, 1H, 1-H$_a$), 1.69 (m, 1H, 10-H), 1.56 (m, 1H, 16-H$_a$), 1.54 (m, 1H, 11-H$_a$ or 15-H$_a$), 1.51 (m, 1H, 11-H$_a$ or 15-H$_a$), 1.44 (m, 1H, 12-H$_b$), 1.39 (m, 1H, 16-H$_b$), 1.29 (m, 1H, 6-H$_b$), 1.25 (m, 1H, 1-H$_b$), 1.21 (m, 1H, 11-H$_b$), 1.14 (m, 1H, 15-H$_b$), 1.09 (m, 1H, 8-H or 9-H), 1.06 (m, 1H, 8-H or 9-H), 1.02 (m, 1H, 7-H$_b$), 0.97 (m, 1H, 14-H), 0.87 (s, 9H, tert-butyl), 0.72 (s, 3H, 18-H), 0.01 (s, 3H, dimethylsilyl), 0.01 (s, 3H, dimethylsilyl). ^{13}C NMR (101 MHz, CD$_2$Cl$_2$) δ/ppm = 175.01 (ester carbonyl), 111.91 (C-5), 82.36 (C-17), 64.89 (ethylene), 51.69 (methyl ester), 49.96 (C-14), 48.53 (C-10), 45.93 (C-9), 43.99 (C-13), 41.33 (C-8), 37.70 (C-12), 34.93 (C-6), 33.69 (C-2), 31.44 (C-16), 27.97 (C-7), 27.04 (C-15), 26.18 (tert-butyl CH$_3$), 23.89 (C-11), 21.96 (C-1), 18.54 (tert-butyl C), 11.77 (C-18), −4.25 (dimethylsilyl), −4.54 (dimethylsilyl). IR (ATR): ν_{max}/cm^{-1} = 2926, 2885, 2854, 2307, 1735, 1472, 1162, 1093, 899, 885 HRMS (EI): m/z = [M$^{\bullet+}$] calculated for C$_{26}$H$_{46}$O$_5$Si$^{\bullet+}$: 466.3109; found: 466.3102.

Methyl (E)-3-((3S,3aS,5aS,6R,9aR,9bS)-3-((tert-butyldimethylsilyl)oxy)-3a-methyl dodecah ydrospiro[cyclopenta[a]naphthalene-7,2'-[1,3]dioxolan]-6 yl)acrylate (**15**): Dry THF (1.2 mL) and lithium diisoproylamide (2M in in THF, 3.76 mL, 7.53 mmol, 1.25 eq) were added to a flame-dried Schlenk flask under nitrogen. The solution was cooled down to -78 °C, and after 10 min, a solution of compound **14** (2.34 g, 5.02 mmol, 1.00 eq) in 8.5 mL of dry THF was added dropwise via a syringe. After stirring for 25 min, a solution of diphenyldiselenide (0.888 g, 2.84 mmol, 1.25 eq) in 8.8 mL dry THF was added quickly. The mixture was stirred at −78 °C for 30 min and then gradually warmed up to room temperature over a 2 h period. The reaction mixture was then quenched by adding a saturated ammonium chloride solution (50 mL). After extraction with ethyl acetate (3 × 5 mL), the combined organic layers were washed with 1M hydrochloric acid (50 mL), water (50 mL), saturated aqueous sodium bicarbonate solution (50 mL) and brine (50 mL), dried over anhydrous sodium sulfate and filtered. After the evaporation of the solvent, an orange solid was obtained.

Dichloromethane (15 mL) was added to this solid, and the resulting solution was cooled to 0 °C. The temperature of the solution was monitored throughout the whole reaction. Then, a solution of hydrogen peroxide (30%, 4.4 mL, 131 mmol, 26.0 eq) in water (4.4 mL) was added dropwise. After the addition was complete, the temperature of the reaction mixture rose quickly to about 30 °C, dropping thereafter. The mixture was allowed to come to room temperature and stirred until the reaction was complete (TLC control). The reaction mixture was transferred to a separation funnel containing saturated aqueous sodium bicarbonate solution (50 mL) and extracted with dichloromethane (3 × 25 mL). The combined organic layers were dried over anhydrous sodium sulfate, filtered and concentrated in vacuo. The crude product was purified by flash column chromatography (isohexane/ethyl acetate 9:1) to yield compound **15** (1.69 g, 3.63 mmol, 72.2%) as a colorless solid. m.p.: 96 °C
^{1}H NMR (400 MHz, CD$_2$Cl$_2$) δ/ppm = 6.72 (dd, 1H, J = 15.7 Hz, 10.0 Hz, 1-H), 5.82 (d, 1H, J = 15.7 Hz, 2-H), 3.90-3.70 (m, 4H, ethylene), 3.68 (s, 3H, ester CH$_3$), 3.58 (dd, 1H, J = 8.8 Hz, 7.8 Hz, 17-H), 2.21 (t, J = 10.6 Hz, 1H, 10-H), 1.89 (dtd, J = 13.1 Hz, 9.1 Hz, 5.7 Hz, 1H, 16-H$_a$), 1.79 (dt, J = 13.5 Hz, 3.0 Hz, 1H, 6-H$_a$), 1.66 (dt, J = 12.2 Hz, 2.9 Hz, 1H, 12-H$_a$), 1.60 (m, 1H, 7-H or 11-H), 1.56 (m, 1H, 15-H$_a$), 1.45 (m, 1H, 6-H$_b$), 1.41 (m, 1H, 16-H$_b$), 1.38 (m, 1H, 7-H or 11-H), 1.30 (m, 1H, 7-H or 11-H), 1.26 (m, 1H, 15-H$_b$), 1.24 (m, 1H, 9-H), 1.12 (m, 1H, 8-H), 1.08 (m, 1H, 7-H or 11-H), 1.02 (m, 1H, 12-H$_b$), 0.98 (m, 1H, 14-H), 0.87 (s, 9H, tert-butyl), 0.71 (s, 3H, 18-H), 0.00 (s, 6H, dimethylsilyl) ^{13}C NMR (101 MHz, CD$_2$Cl$_2$) δ/ppm = 167.04 (ester carbonyl), 148.73 (C-1), 124.24 (C-2), 110.53 (C-5), 82.26 (C-17), 65.78 (Ethylen), 65.50 (ethylene), 55.39 (C-10), 51.72 (OCH$_3$), 49.86 (C-14), 45.00 (C-9), 44.15 (C-13), 40.48 (C-8), 37.38 (C-12), 35.68 (C-6), 31.37 (C-16), 28.03 (C-7 or C-11), 28.02 (C-7 or C-11), 26.17 (tert-butyl CH$_3$), 23.83 (C-15), 18.52 (tert-butyl C), 11.72 (C-18), −4.25 (dimethylsilyl), −4.25 (dimethylsilyl). IR (ATR): ν_{max}/cm^{-1} = 2952, 2928, 2858, 1718, 1652, 1472, 1435, 1163, 900, 772 HRMS (EI): m/z = [M$^{•+}$] calculated for C$_{26}$H$_{44}$O$_5$Si$^{•+}$: 464.2953; found: 464.2951.

(3S,3aS,5aS,9aR,9bS)-3-((tert-Butyldimethylsilyl)oxy)-3a-methyldodecahydrospiro[cyclopenta[a] naphthalene-7,2'-[1,3]dioxolane]-6-carbaldehyde (**16**): Compound **15** (1.44 g, 3.10 mmol) was dissolved in a mixture of dichloromethane (18 mL) and methanol (10 mL). The solution was cooled to −78 °C and then treated with ozone (5 min, flow: 50 L/h, 55 W). Progress of the reaction was monitored via TLC. After excess ozone had been removed by a stream of nitrogen, dimethyl sulfide (18.0 mL, 243 mmol) was added, and the reaction mixture was allowed to warm gradually. It was then stirred overnight at room temperature. The mixture was diluted with dichloromethane (18 mL) and washed with saturated aqueous sodium bicarbonate solution (2 × 50 mL) and brine (50 mL). The organic layer was dried over anhydrous sodium sulfate filtered, and the solvent was evaporated to obtain a colorless solid (0.960 g, 2.35 mmol, 75.8%), which was used as such in the next step. m.p.: 135 °C
^{1}H NMR (500 MHz, CD$_2$Cl$_2$; pure compound obtained by tedious flash chromatography) δ/ppm = 4.01(m, 4H, ethylene), 3.61 (s, 3H, OCH$_3$), 3.59 (t, J = 8.3 Hz, 17-H), 2.54 (d, J = 11.5 Hz, 1H, 10-H), 1.92 (m, 1H, 16-H$_a$), 1.89 (m, 1H, 6-H$_a$), 1.72 (m, 1H, 12-H$_a$), 1.62 (m, 1H, 7-H$_a$ or 11-H$_a$), 1.56 (m, 1H, 15-H$_a$), 1.49 (m, 1H, 7-H$_a$ or 11-H$_a$), 1.45 (m, 1H, 16-H$_b$), 1.41 (m, 1H, 8-H), 1.39 (m, 1H, 6-H$_b$), 1.36 (m, 1H, 7-H$_b$ or 11-H$_b$), 1.28 (m, 1H, 15-H$_b$), 1.15 (m, 1H, 9-H), 1.14 (m, 1H, 7-H$_b$ or 11-H$_b$), 1.05 (m, 1H, 12-H$_b$), 1.01 (m, 1H, 14-H), 0.87 (s, 9H, (CH$_3$)$_3$), 0.73 (s, 3H, 18-H), 0.01 (s, 3H, dimethylsilyl), 0.01 (s, 3H, dimethylsilyl) ^{13}C NMR (126 MHz, CD$_2$Cl$_2$) δ/ppm = 172.18 (C-1), 109.88 (C-5), 82.11 (C-17), 64.98 (ethylen), 64.95 (ethylen), 57.16 (C-10), 49.55 (C-14), 44.20 (C-13), 44.20 (C-8) 40.33 (C-9), 37.06 (C-12), 34.11 (C-6), 31.29 (C-16), 27.58 (C-7 or C-11), 27.34 (C-7 or C-11), 26.15 (tert-butyl CH$_3$), 23.75 (C-15), 18.51 (tert-butyl quaternary carbon), 11.68 (C-18), −4.26 (dimethylsilyl), −4.57 (dimethylsilyl). IR (ATR): ν_{max}/cm^{-1} = 2927, 2308, 1733, 1717, 1653, 1558, 1261, 900 HRMS (EI): m/z = [M$^{•+}$] calculated for C$_{23}$H$_{40}$O$_4$Si$^{•+}$: 408.2690; found: 408.2658.

(3S,3aS,5aS,9aR,9bS)-3-Hydroxy-3a-methyl-7-oxododecahydro-1H-cyclopenta[a]naphthalene-6-carbaldehyde (**17**): Crude compound **16** (0.899 g, about 2.20 mmol) was suspended in a mixture of glacial acetic acid (22.0 mL), THF (7.5 mL) and water (7.5 mL) and stirred

overnight at room temperature. After the addition of 16.4 mL of a 50% solution of acetic acid in water, the mixture was refluxed for 1 h. After cooling to room temperature, brine (20 mL) was added, and the mixture was extracted with ethyl acetate (4 × 50 mL). The combined organic extracts were washed with saturated aqueous sodium bicarbonate solution (50 mL), dried over anhydrous sodium sulfate and filtered. After evaporation of the solvent, compound **17** was obtained as a colorless oil (0.436 g, 1.74 mmol, about 79.2%), which was used as such in the next step. ^{1}H NMR (400 MHz, CD$_2$Cl$_2$; pure compound obtained by tedious flash chromatography) δ/ppm = 15.45 (d, J = 6.2 Hz, 0.41H, enol OH), 9.60 (dd, J = 4.6 Hz, 2.2 Hz, 1H, 0.26H, aldehyde, keto tautomer), 8.28 (d, J = 5.7 Hz, 0.46H, aldehyde, enol tautomer), 3.90 (m, 1H), 3.66 (m, 1H, 17-H), 2.46 (m, 1H), 2.04 (m, 1H), 1.97 (m, 1H), 1.84 (m, 1H), 1.68 (m, 1H), 1.61 (m, 1H), 1.57 (m, 1H), 1.45 (m, 1H), 1.40 (m, 1H), 1.36 (m, 1H), 1.31 (m, 1H), 1.27 (m, 1H), 1.20 (m, 1H), 1.15 (m, 1H), 1.09 (m, 1H), 0.80-0.73 (3s, 3H, 18-H). ^{13}C NMR (101 MHz, CD$_2$Cl$_2$) δ/ppm = 204.59 (aldehyde, keto tautomer), 200.93 (C-5, keto tautomer) 194.50 (C-5, enol tautomer), 178.27 (aldehyde, enol tautomer), 113.83 (C-10, enol tautomer), 81.98 (C-17), 62.51 (C-10, keto tautomer), 49.56 (C-14), 43.58 (C-13), 41.19 (CH), 39.04 (CH), 36.52 (CH$_2$), 33.95 (CH$_2$), 30.69 (CH$_2$), 26.25 (CH$_2$), 26.17 (CH$_2$), 23.38 (CH$_2$), 11.20 (C-18). IR (ATR): ν_{max}/cm^{-1} = 2927, 2307, 1733, 1716, 1636, 1457, 1082 HRMS (EI): m/z = [M$^{\bullet+}$] calculated for C$_{15}$H$_{22}$O$_3$$^{\bullet+}$: 250.1563; found: 250.1563.

(4bS,6aS,7S,9aS,9bR)-2-Methoxy-6a-methyl-4b,6,6a,7,8,9,9a,9b,10,11-decahydro-5H-indeno[5,4-f]quinazolin-7-ol (**2**): Crude compound **17** (0.401 g, 1.60 mmol, 1.00 eq) was added to a round bottom flask and dissolved in 10 mL of dry methanol. Then, methyl carbamimidate sulfate (0.826 g, 4.80 mmol, 3.00 eq) and 3.2 mL of a freshly prepared solution of sodium methanolate in methanol (0.11 g of sodium in 3.2 mL of dry methanol, 4.80 mmol, 3.00 eq) were added to the flask and the mixture was refluxed for 8 h under a nitrogen atmosphere. After cooling to room temperature, water (100 mL) was added, and the mixture was extracted with ethyl acetate (3 × 50 mL). The combined organic layers were washed with water and brine and dried over anhydrous sodium sulfate. After filtration and evaporation of the solvent, the residue was purified by flash column chromatography (isohexane/ethyl acetate 2:1 with 1% triethylamine) to obtain compound **2** as a white solid (0.174 g, 0.603 mmol, 37.7%). m.p.: 179 °C $[\alpha]_D^{23}$ = 2.1° (CH$_2$Cl$_2$) ^{1}H NMR (400 MHz, CD$_2$Cl$_2$) δ/ppm = 8.31 (s, 1H, 1-H), 3.91 (s, 3H, OCH$_3$), 3.70 (t, 1H, J = 8.5 Hz, 17-H), 2.83 (m, 2H, 6-H), 2.29 (m, 1H, 11-H$_a$), 2.20 (m, 1H, 9-H), 2.08 (m, 1H, 16-H$_a$), 1.96 (m, 1H, 7-H$_a$), 1.92 (m, 1H, 12-H$_a$), 1.70 (m, 1H, 15-H$_a$), 1.48 (m, 1H, 11-H$_b$), 1.45 (m, 1H, 16-H$_b$), 1.42 (m, 1H, 8-H), 1.39 (m, 1H, 7-H$_b$), 1.36 (m, 1H, 15-H$_b$), 1.29 (m, 1H, 12-H$_b$), 1.18 (m, 1H, 14-H), 0.76 (s, 3H, 18-H) ^{13}C NMR (101 MHz, CD$_2$Cl$_2$) δ/ppm = 168.87 (C-5), 164.32 (C-3), 156.38 (C-1), 127.06 (C-10), 82.14 (C-17), 54.86 (OCH$_3$), 50.12 (C-14), 43.78 (C-13), 42.11 (C-9), 38.76 (C-8), 36.85 (C-12), 32.74 (C-6), 30.91 (C-16), 26.92 (C-7), 26.10 (C-11), 23.54 (C-15), 11.36 (C-18). IR (ATR): ν_{max}/cm^{-1} = 2943, 2866, 2307, 1734, 1654, 1587, 1546, 1467, 1389, 1323, 1034, 749 HRMS (ESI): m/z = [M + H]$^+$ calculated for C$_{17}$H$_{25}$N$_2$O$_2$$^+$: 289.1911; found: 289.1912 Purity (HPLC, acetonitrile/water 50:50): >96% (λ = 210 nm), >97% (λ = 254 nm).

3.2. Biological Testing

hTRPML1∆NC-YFP, a plasma membrane variant of wild-type TRPML1, was obtained from HEK293 cells stably expressing plasma membrane-targeted TRPML1 by trypsination and after resuspending in HEPES buffered solution. IC$_{50}$ values for TRPML1 inhibition were determined on a fluorescence imaging plate reader built into a robotic liquid handling station (Freedom Evo 150, Tecan, Mannedorf, Switzerland) using the calcium dye Fluo-4/AM (Invitrogen, Thermo Fisher Scientific, Waltham, MA, USA) according to the test procedure described in our previous work [13] in the section Compound screening and generation of concentration–response curves.

4. Conclusions

In conclusion, we have worked out straightforward chiral pool syntheses of the 4-aza (**1**) and 2,4-diaza analog (**2**) of the TRPML1 inhibitor estradiol methyl ether (**EDME**) starting with oxidative cleavage of ring A of the readily available steroid 19-nortestosterone (**3**) to provide ketocarboxylic acid **4** as the central intermediate for both target compounds. By utilizing carefully selected protective groups for the 17-OH group (benzyl in the pyridine synthesis, TBDS in the pyrimidine synthesis) and oxidants for dehydrogenation ($CuBr_2$/LiBr/methanesulfonic acid in the pyridine synthesis) and chain degradation (selenylation/selenoxide elimination/ozonolysis in the pyrimidine synthesis) both target compounds were obtained in 6 and 8 steps, respectively, and in acceptable overall yields (8.6%, 7.5%).

While the 4-aza analog **1** showed significant TRPML1-inhibitory activity (only factor <2 less potent than the gold standard **EDME**), the 2,4-diaza analog **2** significantly lost inhibitory potency, and the pyridone analog, obtained as an unexpected side product, was completely inactive. This leads to the conclusion that for the cation channel TRPML1, aza analogs are not promising bioisosteres of **EDME**.

References

1. Bargal, R.; Avidan, N.; Ben-Asher, E.; Olender, Z.; Zeigler, M.; Frumkin, A.; Raas-Rothschild, A.; Glusman, G.; Lancet, D.; Bach, G. Identification of the gene causing mucolipidosis type IV. *Nat. Genet.* **2000**, *26*, 118–122. [CrossRef]

2. Kasitinon, S.Y.; Eskiocak, U.; Martin, M.; Bezwada, D.; Khivansara, V.; Tasdogan, A.; Zhao, Z.; Mathews, T.; Aurora, A.B.; Morrison, S.J. TRPML1 Promotes Protein Homeostasis in Melanoma Cells by Negatively Regulating MAPK and mTORC1 Signaling. *Cell Rep.* **2019**, *28*, 2293–2305. [CrossRef] [PubMed]

3. Yin, C.; Zhang, H.; Liu, X.; Zhang, H.; Zhang, Y.; Bai, X.; Wang, L.; Li, H.; Li, X.; Zhang, S.; et al. Downregulated MCOLN1 Attenuates The Progression Of Non-Small-Cell Lung Cancer By Inhibiting Lysosome-Autophagy. *Cancer Manag. Res.* **2019**, *11*, 8607–8617. [CrossRef] [PubMed]

4. Xing, Y.; Sui, Z.; Liu, Y.; Wang, M.-m.; Wei, X.; Lu, Q.; Wang, X.; Liu, N.; Lu, C.; Chen, R.; et al. Blunting TRPML1 channels protects myocardial ischemia/reperfusion injury by restoring impaired cardiomyocyte autophagy. *Basic Res. Cardiol.* **2022**, *117*, 20. [CrossRef]

5. Santoni, G.; Maggi, F.; Amantini, C.; Marinelli, O.; Nabissi, M.; Morelli, M.B. Pathophysiological Role of Transient Receptor Potential Mucolipin Channel 1 in Calcium-Mediated Stress-Induced Neurodegenerative Diseases. *Front. Physiol.* **2020**, *11*, 251. [CrossRef] [PubMed]

6. Zhang, X.; Li, X.; Xu, H. Phosphoinositide isoforms determine compartment-specific ion channel activity. *Proc. Natl. Acad. Sci. USA* **2012**, *109*, 11384–11389. [CrossRef]

7. Chen, C.C.; Keller, M.; Hess, M.; Schiffmann, R.; Urban, N.; Wolfgardt, A.; Schaefer, M.; Bracher, F.; Biel, M.; Wahl-Schott, C.; et al. A small molecule restores function to TRPML1 mutant isoforms responsible for mucolipidosis type IV. *Nat. Commun.* **2014**, *5*, 4681. [CrossRef]

8. Shen, D.; Wang, X.; Li, X.; Zhang, X.; Yao, Z.; Dibble, S.; Dong, X.P.; Yu, T.; Lieberman, A.P.; Showalter, H.D.; et al. Lipid storage disorders block lysosomal trafficking by inhibiting a TRP channel and lysosomal calcium release. *Nat. Commun.* **2012**, *3*, 731. [CrossRef] [PubMed]

9. Spix, B.; Butz, E.; Chen, C.-C.; Scotto Rosato, A.; Tang, R.; Jeridi, A.; Kudrina, V.; Melzergeb Plesch, E.; Wartenberg, P.; Arlt, E.; et al. Lung emphysema and impaired macrophage elastase clearance in mucolipin 3 deficient mice. *Nat. Commun.* **2022**, *13*, 318. [CrossRef] [PubMed]

10. Wang, W.; Gao, Q.; Yang, M.; Zhang, X.; Yu, L.; Lawas, M.; Li, X.; Bryant-Genevier, M.; Southall, N.T.; Marugan, J.; et al. Up-regulation of lysosomal TRPML1 channels is essential for lysosomal adaptation to nutrient starvation. *Proc. Natl. Acad. Sci. USA* **2015**, *112*, E1373–E1381. [CrossRef]

11. Leser, C.; Keller, M.; Gerndt, S.; Urban, N.; Chen, C.C.; Schaefer, M.; Grimm, C.; Bracher, F. Chemical and pharmacological characterization of the TRPML calcium channel blockers ML-SI1 and ML-SI3. *Eur. J. Med. Chem.* **2021**, *210*, 112966. [CrossRef] [PubMed]

12. Kriegler, K.; Leser, C.; Mayer, P.; Bracher, F. Effective chiral pool synthesis of both enantiomers of the TRPML inhibitor trans-ML-SI3. *Arch. Pharm.* **2022**, *355*, e2100362. [CrossRef] [PubMed]

13. Rühl, P.; Rosato, A.S.; Urban, N.; Gerndt, S.; Tang, R.; Abrahamian, C.; Leser, C.; Sheng, J.; Jha, A.; Vollmer, G.; et al. Estradiol analogs attenuate autophagy, cell migration and invasion by direct and selective inhibition of TRPML1, independent of estrogen receptors. *Sci. Rep.* **2021**, *11*, 8313. [CrossRef]

14. Mayer, C.D.; Bracher, F. Cytotoxic ring A-modified steroid analogues derived from Grundmann's ketone. *Eur. J. Med. Chem.* **2011**, *46*, 3227–3236. [CrossRef] [PubMed]

15. Renard, D.; Perruchon, J.; Giera, M.; Müller, J.; Bracher, F. Side chain azasteroids and thiasteroids as sterol methyltransferase inhibitors in ergosterol biosynthesis. *Bioorg. Med. Chem.* **2009**, *17*, 8123–8137. [CrossRef]

16. Meanwell, N.A. Synopsis of some recent tactical application of bioisosteres in drug design. *J. Med. Chem.* **2011**, *54*, 2529–2591. [CrossRef] [PubMed]

17. Subbaiah, M.A.M.; Meanwell, N.A. Bioisosteres of the Phenyl Ring: Recent Strategic Applications in Lead Optimization and Drug Design. *J. Med. Chem.* **2021**, *64*, 14046–14128. [CrossRef]

18. Tse, E.G.; Houston, S.D.; Williams, C.M.; Savage, G.P.; Rendina, L.M.; Hallyburton, I.; Anderson, M.; Sharma, R.; Walker, G.S.; Obach, R.S.; et al. Nonclassical Phenyl Bioisosteres as Effective Replacements in a Series of Novel Open-Source Antimalarials. *J. Med. Chem.* **2020**, *63*, 11585–11601. [CrossRef]

19. Brill, Z.G.; Condakes, M.L.; Ting, C.P.; Maimone, T.J. Navigating the Chiral Pool in the Total Synthesis of Complex Terpene Natural Products. *Chem. Rev.* **2017**, *117*, 11753–11795. [CrossRef]

20. Holt, D.A.; Levy, M.A.; Brandt, M.; Metcalf, B.W. Inhibition of pyridine-nucleotide-dependent enzymes by pyrazoles. Synthesis and enzymology of A novel A-ring pyrazole steroid. *Steroids* **1986**, *48*, 213–222. [CrossRef]

21. Rasmusson, G.H.; Reynolds, G.F.; Utne, T.; Jobson, R.B.; Primka, R.L.; Berman, C.; Brooks, J.R. Azasteroids as inhibitors of rat prostatic 5 alpha-reductase. *J. Med. Chem.* **1984**, *27*, 1690–1701. [CrossRef] [PubMed]

22. Xia, P.; Yang, Z.-Y.; Xia, Y.; Zhang, H.-B.; Zhang, K.-H.; Sun, X.; Chen, Y.; Zheng, Y.-Q. Synthesis of N-Substituted 3-Oxo-17β-carboxamide-4-aza-5α-androstanes and the Tautomerism of 3-Oxo-4-aza-5-androstenes. *Heterocycles* **1998**, *47*, 703–716. [CrossRef]

23. Skaanderup, P.R.; Poulsen, C.S.; Hyldtoft, L.; Jørgensen, M.R.; Madsen, R. Regioselective Conversion of Primary Alcohols into Iodides in Unprotected Methyl Furanosides and Pyranosides. *Synthesis* **2002**, *2002*, 1721–1727. [CrossRef]

24. Poon, K.W.C.; Dudley, G.B. Mix-and-Heat Benzylation of Alcohols Using a Bench-Stable Pyridinium Salt. *J. Org. Chem.* **2006**, *71*, 3923–3927. [CrossRef] [PubMed]

25. Zhang, J.; Yan, Y.; Hu, R.; Li, T.; Bai, W.J.; Yang, Y. Enantioselective Total Syntheses of Lyconadins A-E through a Palladium-Catalyzed Heck-Type Reaction. *Angew. Chem. Int. Ed.* **2020**, *59*, 2860–2866. [CrossRef]

26. Fischer, D.F.; Sarpong, R. Total Synthesis of (+)-Complanadine A Using an Iridium-Catalyzed Pyridine C—H Functionalization. *J. Am. Chem. Soc.* **2010**, *132*, 5926–5927. [CrossRef]

27. Lee, A.S.; Liau, B.B.; Shair, M.D. A unified strategy for the synthesis of 7-membered-ring-containing Lycopodium alkaloids. *J. Am. Chem. Soc.* **2014**, *136*, 13442–13452. [CrossRef]

28. Wu, B.; Bai, D. The First Total Synthesis of (±)-Huperzine B. *J. Org. Chem.* **1997**, *62*, 5978–5981. [CrossRef]

29. King, A.O.; Anderson, R.K.; Shuman, R.F.; Karady, S.; Abramson, N.L.; Douglas, A.W. Iodotrimethylsilane-mediated 2-monohalogenation of 4-aza-5.alpha.-androstan-3-one steroids. *J. Org. Chem.* **1993**, *58*, 3384–3386. [CrossRef]

30. King, L.C.; Ostrum, G.K. Selective Bromination with Copper(II) Bromide1. *J. Org. Chem.* **1964**, *29*, 3459–3461. [CrossRef]

31. Sander, M.; Gries, J.; Schuetz, A. Method for Aromatizing 19-Norandrost-4-en-3-Ones to Estra-1,3,5(10)-Trienes. U.S. Patent Application WO 2009/074313 A1, 18 June 2009.

32. White, J.D.; Li, Y.; Kim, J.; Terinek, M. Cyclobutane Synthesis and Fragmentation. A Cascade Route to the Lycopodium Alkaloid (−)-Huperzine A. *J. Org. Chem.* **2015**, *80*, 11806–11817. [CrossRef] [PubMed]

33. Mandal, P.K.; McMurray, J.S. Pd—C-Induced Catalytic Transfer Hydrogenation with Triethylsilane. *J. Org. Chem.* **2007**, *72*, 6599–6601. [CrossRef] [PubMed]

34. Falck, J.R.; Barma, D.K.; Baati, R.; Mioskowski, C. Differential Cleavage of Arylmethyl Ethers: Reactivity of 2,6-Dimethoxybenzyl Ethers. *Angew. Chem. Int. Ed.* **2001**, *40*, 1281–1283. [CrossRef]

35. Aversa, R.J.; Burger, M.T.; Dillon, M.P.; Dineen, T.A., Jr.; Lou, Y.; Nishiguchi, G.A.; Ramurthy, S.; Rico, A.C.; Rauniyar, V.; Sendzik, M.; et al. Compounds and Compositions as Raf Kinase Inhibitors. U.S. Patent Application WO 2016/038582 2016, 11 September 2014.

36. Bertin, D.; Nedelec, L.; Pierdet, A. Diaza Steroids. FR 1481182, 19 May 1967.

37. Nomine, G. Derivatives of 7-oxo-1,2,3,4,5,6,7,8-Octahydronaphthalene. FR 1234734, 19 October 1960.

38. de Avellar, I.G.J.; Vierhapper, F.W. Novel Partial Synthetic Approaches to Replace Carbons 2,3,4 of Steroids. A Methodology to Label Testosterone and Progesterone with 13C in the Steroid A Ring. Part 1. *Tetrahedron* **2000**, *56*, 9957–9965. [CrossRef]

Supporting Information

Aza Analogs of the TRPML1 Inhibitor Estradiol Methyl Ether (EDME)

Philipp Rühl [1] and Franz Bracher [1],*

[1] Department of Pharmacy – Center for drug Research, Ludwig-Maximilians University, Munich, Germany; philipp.ruehl@cup.lmu.de (P.R.); franz.bracher@cup.uni-muenchen.de (F.B.)

*   Correspondence: franz.bracher@cup.uni-muenchen.de

Additional synthetic procedures
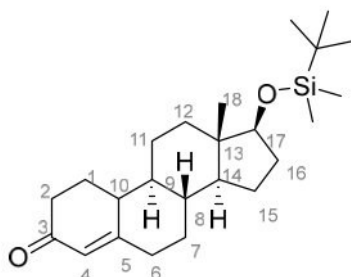
*(8R,9S,13S,14S,17S)-17-((tert-Butyldimethylsilyl)oxy)-13-methyl-1,2,6,7,8,9,10,11,12,13,14,15,16, 17-tetradecahydro-3H-cyclopenta[a]phenanthren-3-one (**S1**):* 19-Nortestosterone (**3**; 1.92 g, 7.00 mmol, 1.00 eq), *tert*-butyldimethylsilyl chloride (1.32 g, 8.75 mmol, 1.25 eq) and imidazole (1.19 g, 17.5 mmol, 2.50 eq) were combined in a round bottom flask. Dry dimethylformamide (20 mL) was added and the resulting reaction mixture stirred at room temperature for 7 h. It was diluted with diethyl ether (150 mL) and washed with 2M aqueous hydrochloric acid solution (3 x 50 mL), saturated aqueous sodium bicarbonate solution (3 x 50 mL) and water (30 mL). The organic layer was dried over anhydrous sodium sulfate and filtered. After evaporation of the solvent, the crude product was purified by flash column chromatography (isohexane/ ethyl acetate 4:1) to yield 2.60 g (6.69 mmol, 95.6 %) of the desired compound as a white solid. m.p.: 137 °C. ^{1}H NMR (400 MHz, CD$_2$Cl$_2$) δ/ppm = 5.75 (s, 1H, 4-H), 3.59 (dd, J = 8.8 Hz, 7.8 Hz, 1H, 17-H), 2.45 (ddd, J = 14.5 Hz, 4.0 Hz, 2.4 Hz, 1H, 6-H$_a$), 2.34 (m, 1H, 6-H$_b$), 2.28 (m, 1H, 2-H$_a$), 2.25 (m, 1H, 1-H$_a$), 2.22 (m. 1H, 2-H$_b$), 2.08 (m, 1H, 10-H), 1.90 (m, 1H, 16-H$_a$) 1.85 (m, 1H, 7-H$_a$ or 15-H$_a$), 1.81 (m, 1H, 7-H$_a$ or 15-H$_a$), 1.77 (m, 1H, 12-H$_a$), 1.59 (m, 1H, 11-H$_a$), 1.51 (m, 1H, 1-H$_b$), 1.45 (m, 1H, 16-H$_b$), 1.34 (m, 1H, 8-H), 1.29 (m, 1H, 11-H$_b$), 1.25 (m, 1H, 15-H$_b$), 1.06 (m, 1H, 12-H$_b$), 1.02 (m, 1H, 7-H$_b$), 0.97 (m, 1H, 9-H), 0.89 (s, 9H, (CH$_3$)$_3$), 0.82 (m, 1H, 14-H), 0.77 (s, 3H, 18-H) , 0.02 (s, 3H, dimethylsilyl$_a$), 0.01 (s, 3H, dimethylsilyl$_b$) ^{13}C NMR (101 MHz, CD$_2$Cl$_2$) δ/ppm = 199.74 (C-3), 167.24 (C-5), 124.62 (C-4), 82.11 (C-17), 50.20 (C-14), 49.79 (C-9), 43.74 (C-13), 43.00 (C-10), 40.92 (C-8), 37.28 (C-12), 36.96 (C-2), 35.90 (C-6), 31.24 (C-7 or C-16), 31.22 (C-7 or C-16), 27.10 (C-1), 26.62 (C-15), 26.02 ((CH$_3$)$_3$), 23.69 (C-11), 18.38 (tert-butyl, quaternary carbon), 11.50 (C-18), -4.39 (dimethylsilyl$_a$), -4.72 (dimethylsilyl$_b$) IR (ATR): v_{max}/cm^{-1} = 2929, 2856, 1667, 1616, 1457, 1249, 1140, HRMS (ESI): m/z = [M+H]$^+$ calculated for C$_{24}$H$_{41}$O$_2$Si$^+$: 389.2870; found: 389.2871.
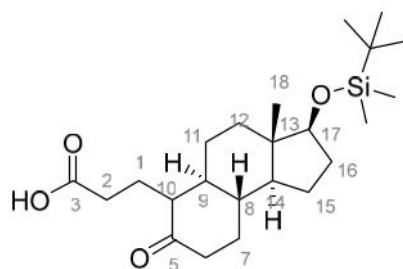
3-((3S,3aS,5aS,6R,9aR,9bS)-3-((tert-Butyldimethylsilyl)oxy)-3a-methyl-7-oxododecahydro-1H-cyclopenta[a]naphthalen-6-yl)propanoic acid (S2): To a solution of the above compound (2.60 g, 6.70 mmol, 1.00 eq) in 40 mL of *tert*-butanol were added 13.0 mL of a saturated aqueous Na_2CO_3 solution. The mixture was heated at reflux and a solution of $NaIO_4$ (14.3 g, 67.0 mmol, 10.00 eq) and $KMnO_4$ (80.0 mg, 0.500 mmol, 7.50 mol%) in water (40 mL) preheated to 80 °C was added via a dropping funnel over a time period of 30 min. After cooling, the reaction mixture was filtered and the filter cake was washed with 10 mL of water. The filtrate was acidified with 6M HCl to pH 2 and then extracted with dichloromethane (4 x 20 mL). The organic phase was washed with water (20 mL) and dried over anhydrous sodium sulfate. After filtration and removal of the solvent, the crude product was purified by column chromatography to yield a colorless oil (2.37 g, 5.81 mmol, 86.7%) ^{1}H NMR (400 MHz, DMSO-d6) δ/ppm = 11.98 (s, 1H, COOH), 3.58 (t, *J* = 8.1 Hz, 1H, 17-H), 2.41 (td, *J* = 13.7 Hz, 6.1 Hz, 1H, 6-H_a), 2.29 (m, 1H, 10-H), 2.20 (m, 1H, 6-H_b), 2.13 (m, 1H, 2-H_a), 2.07 (m, 1H, 2-H_b), 1.90 (m, 1H, 7-H_a or 16-H_a), 1.85 (m, 1H, 7-H_b or 16-H_a), 1.76 (m, 1H, 1-H_a), 1.69 (m, 1H, 15-H_a), 1.65 (m, 1H, 12-H_a), 1.61 (m, 1H, 1-H_b), 1.57 (m, 1H, 8-H), 1.51 (m, 1H, 11-H_a), 1.39 (m, 1H, 7H_b or 16-H_b), 1.32 (m, 1H, 15-H_b), 1.27 (m, 1H, 11-H_b), 1.15 (m, 1H, 7-H_b or 16-H_b), 1.06 (m, 1H, 12-H_b), 1.01 (m, 1H, 9-H), 0.94 (m, 1H, 14-H), 0.86 (s, 9H, $(CH_3)_3$), 0,74 (s, 3H, 18-H), 0.01 (s, 3H, dimethylsilyl$_a$), 0.00 (s, 3H, dimethylsilyl$_b$) ^{13}C NMR (101 MHz, DMSO-d6) δ/ppm = 211.39 (C-5), 174.61 (C-3), 81.01 (C-17), 52.77 (C-10), 49.50 (C-14), 47.40 (C-9), 43.00 (C-13), 41.15 (C-6), 40.15 (C-8), 36.18 (C-12), 30.91 (C-2), 30.70 (C-7 or C-16), 30.40 (C-7 or C-16), 26.50 (C-15), 25.75 ($(CH_3)_3$), 23.01 (C-11), 20,54 (C-1), 17.78 (*tert*-butyl, quaternary carbon), 11.30 (C-18), -4.51 (dimethylsilyl$_a$), -4.84 (dimethylsilyl$_b$) IR (ATR): v_{max}/cm^{-1} = 2927, 2856, 1715. 1558, 1541, 1418, 1249, 1199 HRMS (ESI): m/z = (M-H)$^-$ calculated for $C_{23}H_{39}O_4Si^-$: 407.2623; found: 407.2625.
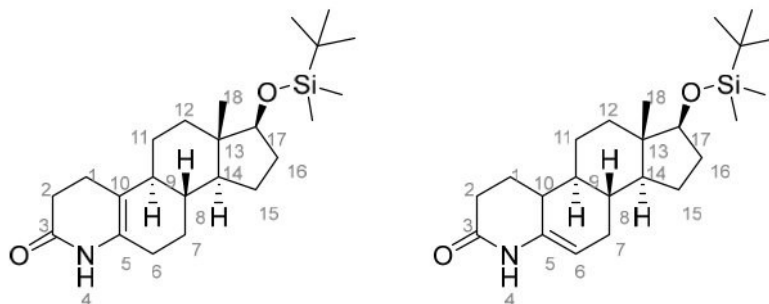
(4bS,6aS,7S,9aS,9bR)-7-((tert-Butyldimethylsilyl)oxy)-6a-methyl-1,3,4,4b,5,6,6a,7,8,9,9a,9b,10,11-tetradecahydro-2H-indeno[5,4-f]quinolin-2-one **(Δ5,10 isomer, S3a)** and *(4bS,6aS,7S,9aS,9bR)-7-((tert-butyldimethylsilyl)oxy)-6a-methyl-1,3,4,4a,4b,5,6,6a,7,8,9,9a,9b,10-tetradecahydro-2H-indeno[5,4-f]quinolin-2-one* **(Δ5,6 isomer, S3b)**: A mixture of the above ketocarboxylic acid (2.32
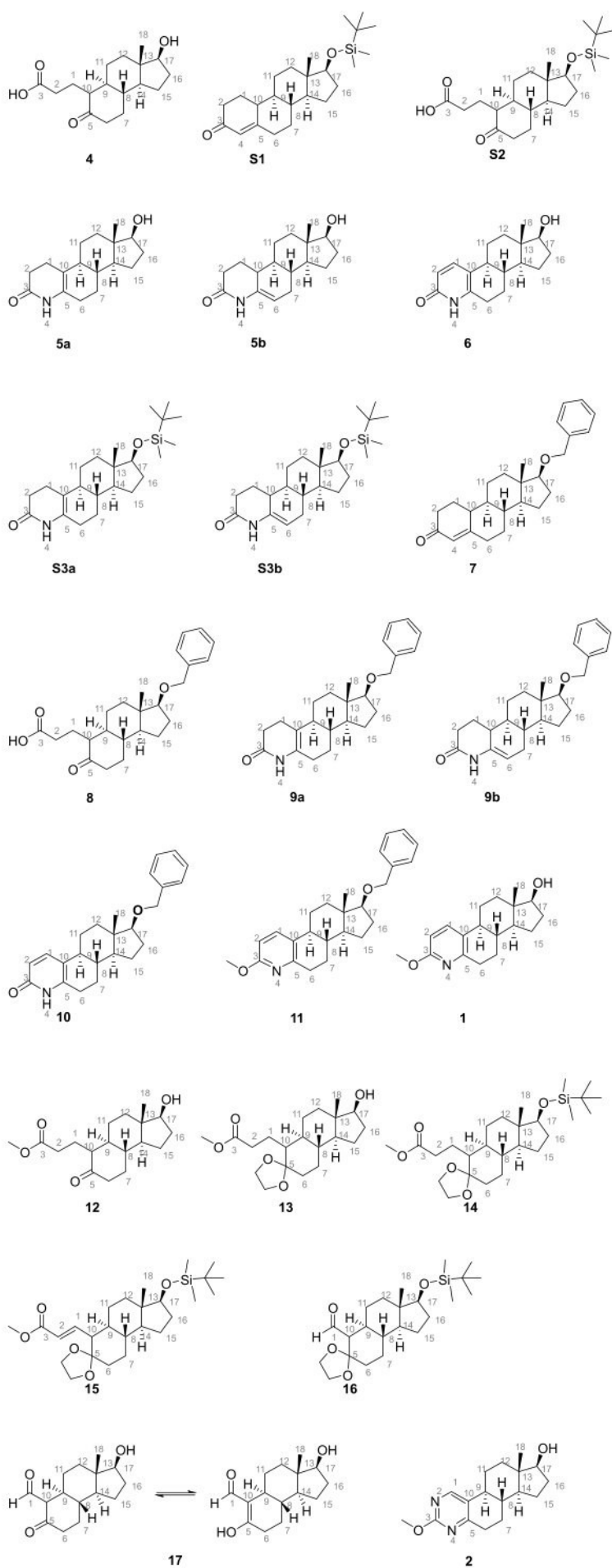
g, 5.70 mmol, 1.00 eq) and ammonium acetate (1.54 g, 19.9 mmol, 3.50 eq) in glacial acetic acid (45 mL) was stirred and heated at reflux for 4 h. After cooling, it was concentrated under reduced pressure and the remaining residue was poured into water. The precipitate was filtered, washed with water (20 mL) and dissolved in dichloromethane (40 mL). The resulting solution was washed with NaOH (1M, 3 x 20 mL), water (20 mL) and brine (20 mL), filtered over a hydrophobic filter and concentrated in vacuo. The crude product was purified by flash column chromatography (isohexane/ ethyl acetate 5:1) to yield 1.59 g (4.08 mmol, 71.6%) of a mixture of the two lactams (ratio: Δ5,10 isomer: Δ5,6 isomer: 15:85) as a beige solid.

Δ5,10 isomer S3a: ^{1}H NMR (500 MHz, CD$_2$Cl$_2$) δ/ppm = 3.62 (m, 1H, 17-H), 2.38 (m, 1H, 6-H$_a$), 2.31 (m, 1H, 1-H$_a$), 2.20 (m, 1H, 2-H$_a$), 2.12 (m, 1H, 1-H$_b$), 1.95 (m, 1H, 2-H$_b$), 1.91 (m, 1H, 16-H$_a$), 1.86 (m, 1H, 15-H$_a$), 1.81 (m, 1H, 12-H$_a$), 1.74 (m, 1H, 7-H$_a$), 1.68 (m, 1H, 9-H), 1.57 (m, 1H, 11-H$_a$), 1.50 (m, 1H, 15-H$_b$), 1.43 (m, 1H, 16-H$_b$), 1.36 (m, 1H, 11-H$_b$), 1.30 (m, 1H, 8-H), 1.26 (m, 1H, 6-H$_b$), 1.19 (m, 1H, 7-H$_b$), 1.10 (m, 1H, 14-H), 1.01 (m, 1H, 12-H$_b$), 0.88 (s, 9H, (CH$_3$)$_3$), 0.73 (s, 3H, 18-H), 0.02 (2s, 6H, dimethylsilyl) ^{13}C NMR (126 MHz, CD$_2$Cl$_2$) δ/ppm = 171.05 (C-3), 128.52 (C-5), 113.11 (C-10), 82.08 (C-17), 49.32 (C-14), 44.41 (C-9), 44.38 (C-13), 39.56 (C-8), 37.60 (C-12), 31.38 (C-6 or C-16), 31.10 (C-6 or C-16), 27.39 (C-2), 26.36 (C-7), 26.01 ((CH$_3$)$_3$), 25.75 (C-15), 23.45 (C-11), 22.21 (C-1), 18.38 (*tert*-butyl, quaternary carbon), 11.76 (C-18), -4.39 (dimethylsilyl$_a$), -4.72 (dimethylsilyl$_b$) IR (ATR): max/cm^{-1} = 32145, 2953, 2928, 1695, 1674, 1472, 1387, 1255, 1141, 1094, HRMS (EI): m/z = [M$^{•+}$] calculated for C$_{23}$H$_{39}$NO$_2$Si $^{•+}$: 389.2745; found: 389.2746.

Δ5,6 isomer S3b: ^{1}H NMR (500 MHz, CD$_2$Cl$_2$) δ/ppm = 7.58 (NH), 4.88 (dt, J = 5.1 Hz, 2.3 Hz, 1H, 6-H), 3.60 (t, J = 8.3 Hz, 1H, 17-H), 2.46 (ddd, J = 17.3 Hz, 5.0 Hz, 2.0 Hz, 1H, 2-H$_a$), 2.37 (m, 1H, 2-H$_b$), 2.11 (m, 1H, 1-H$_a$), 2.07 (m, 1H, 7-H$_a$), 1.95 (m, 1H, 10-H), 1.91 (m, 1H, 16-H$_a$), 1.89 (m, 1H, 11-H$_a$), 1.78 (m, 1H, 12-H$_a$), 1.64 (m, 1H, 7-H$_b$), 1.56 (m, 1H, 15-H$_a$), 1.44 (m, 1H, 16-H$_b$), 1.40 (m, 1H, 8-H), 1.31 (m, 1H, 1-H$_b$), 1.29 (m, 1H, 15-H$_b$, 1.27 (m, 1H, 11-H$_b$), 1.08 (m, 1H, 12-H$_b$), 1.00 (m, 1H, 9-H), 0.97 (m, 1H, 14-H), 0.88 (s, 9H, (CH$_3$)$_3$), 0.74 (s, 3H, 18-H), 0.02 (2s, 6H, Si(CH$_3$)$_2$) ^{13}C NMR (126 MHz, CD$_2$Cl$_2$) δ/ppm = 170.07 (C-3), 136.43 (C-5), 102.77 (C-6), 82.15 (C-17), 50.35 (C-14), 43.91 (C-9), 43.73 (C-13), 39.97 (C-10), 37.15 (C-8), 37.10 (C-12), 32.33 (C-2), 31.20 (C-16), 29.24 (C-7), 26.69 (C-11), 26.01 ((CH$_3$)$_3$), 25.27 (C-1), 23.63 (C-15), 18.38 (*tert*-butyl, quaternary carbon), 11.40 (C-18), -4.39 (dimethylsilyl$_a$), -4.72 (dimethylsilyl$_b$). IR (ATR): v$_{max}$/cm^{-1} = 32145, 2953, 2928, 1695, 1674, 1472, 1387, 1255, 1094 HRMS (EI): m/z = [M$^{•+}$] calculated for C$_{23}$H$_{39}$NO$_2$Si $^{•+}$: 389.2745; found: 389.2745.
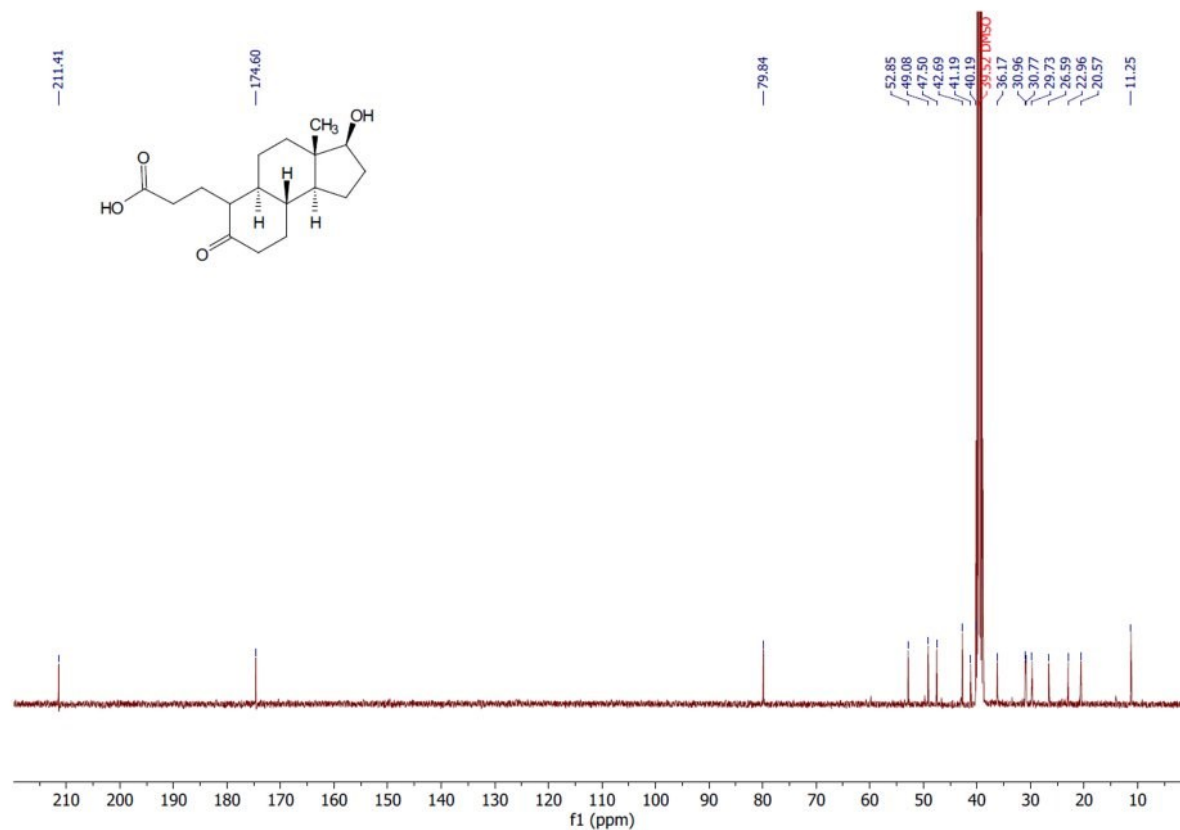
Figure S1: Numbering of the compounds (for assignment of NMR signals).

¹H- and ¹³C-NMR spectra
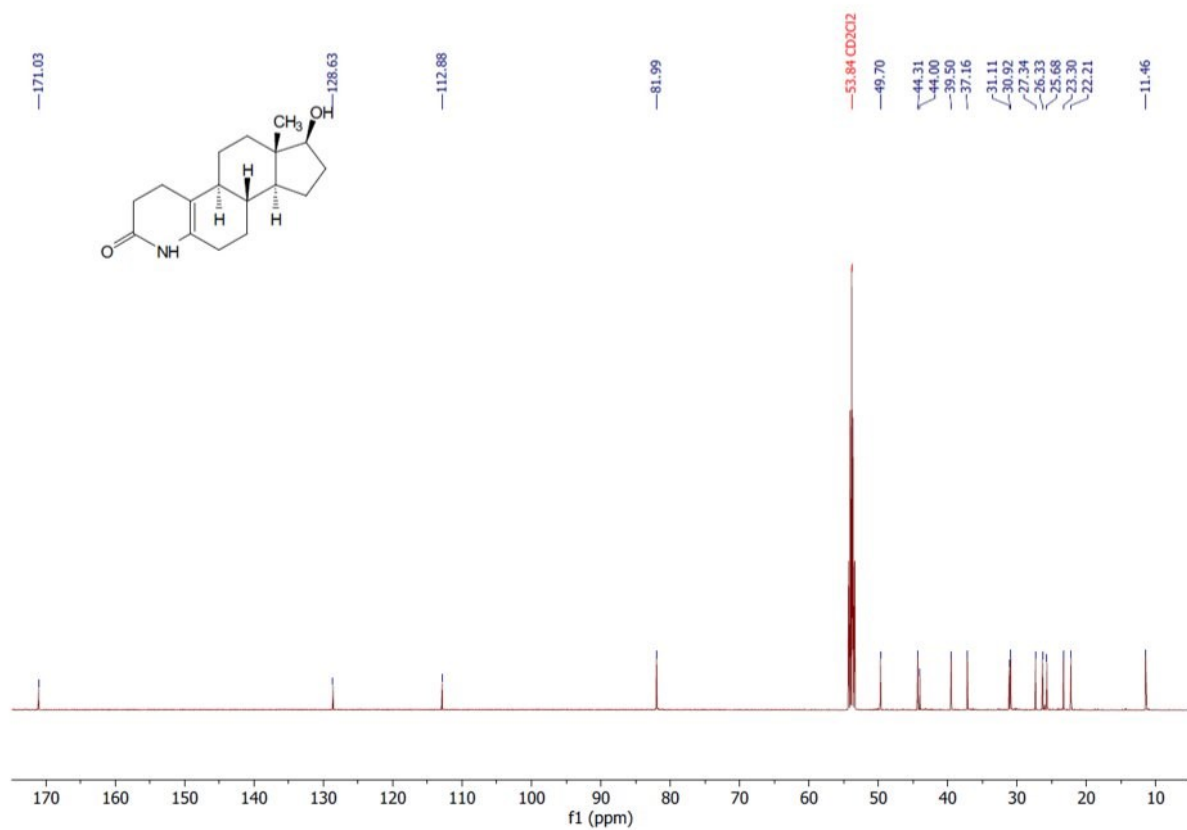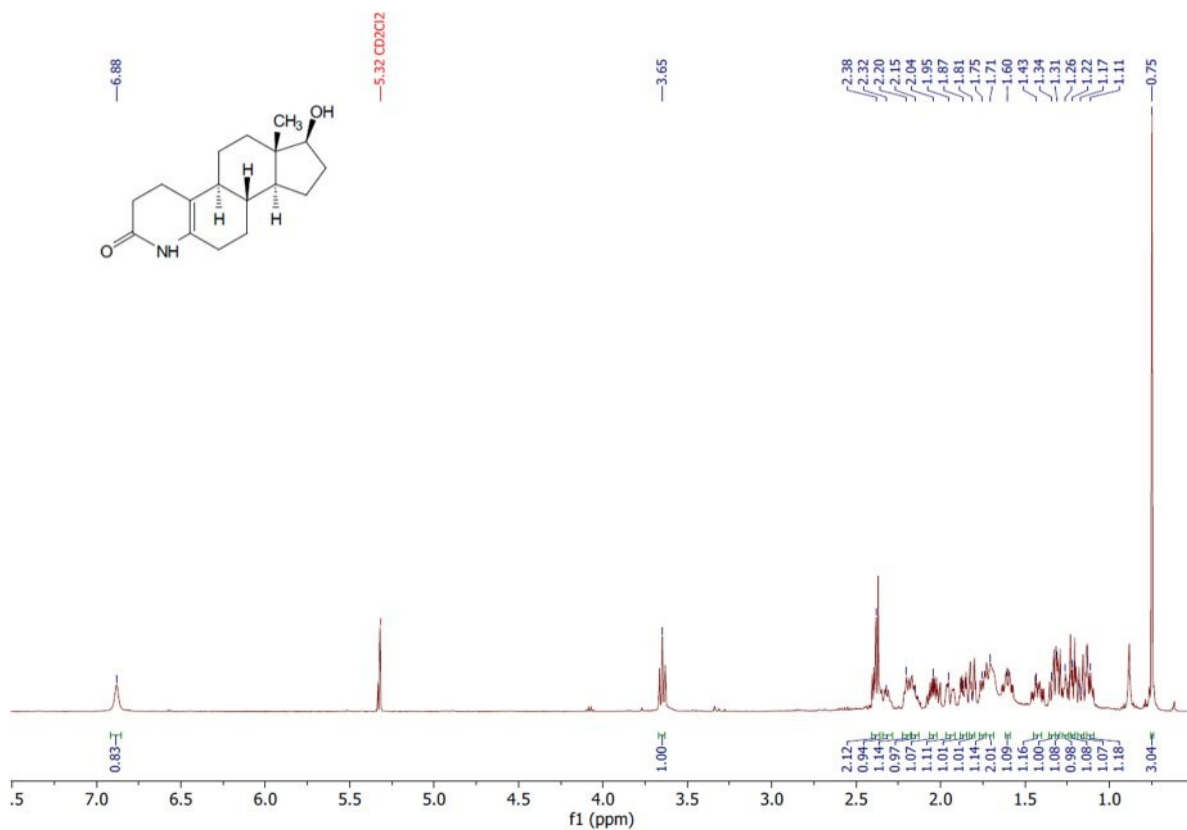
Compound 4

¹H-NMR spectrum

Peaks labeled: 11.95; 4.48; 3.45; 2.50 DMSO; 2.42; 2.28; 2.21; 2.17; 2.09; 1.88; 1.84; 1.63; 1.57; 1.52; 1.36; 1.30; 1.24; 1.22; 1.15; 1.03; 0.99; 0.95; 0.71

Integrations: 0.98; 0.95; 1.08; 1.03; 1.08; 1.02; 0.96; 1.04; 1.07; 0.99; 1.03; 0.96; 0.97; 1.05; 1.09; 1.06; 1.06; 0.99; 1.01; 1.05; 0.96; 3.00

f1 (ppm)

¹³C-NMR spectrum

Peaks labeled: 211.41; 174.60; 79.84; 52.85; 49.08; 47.50; 42.69; 41.19; 40.19; 39.52 DMSO; 36.17; 30.96; 30.77; 29.73; 26.59; 22.96; 20.57; 11.25
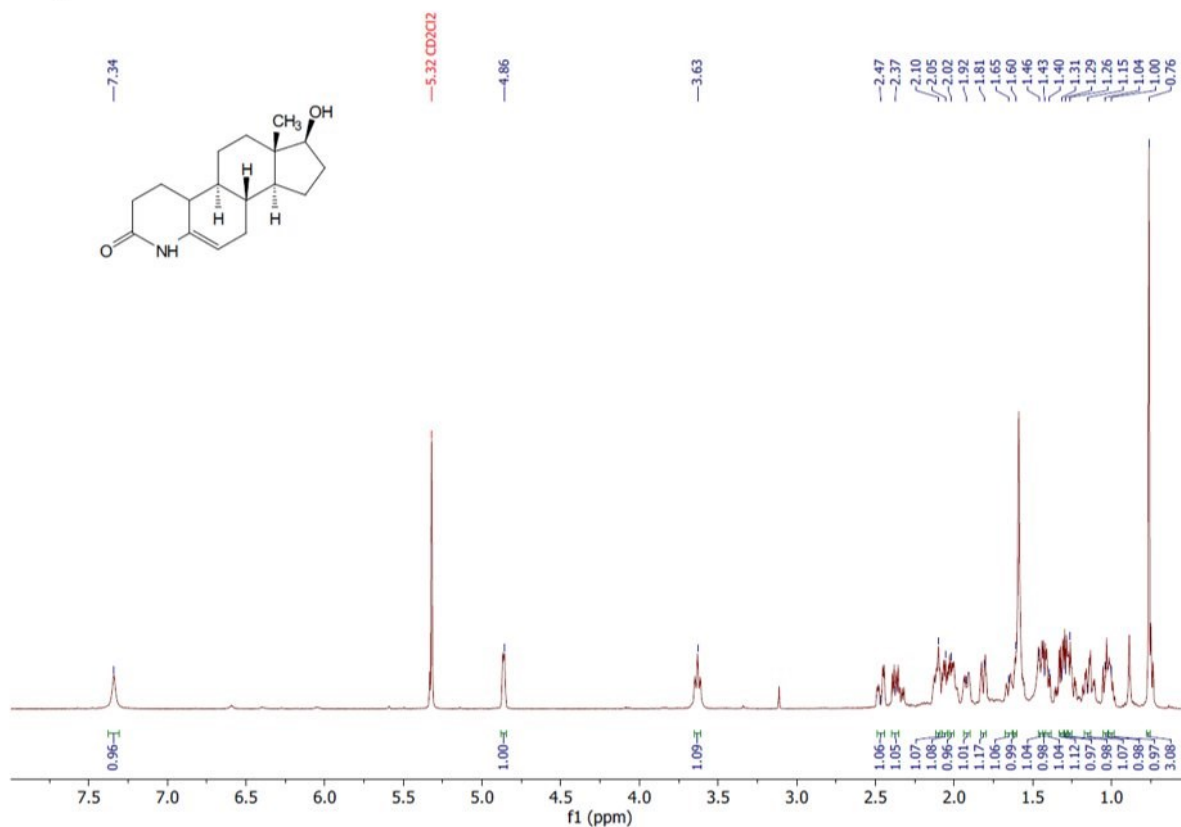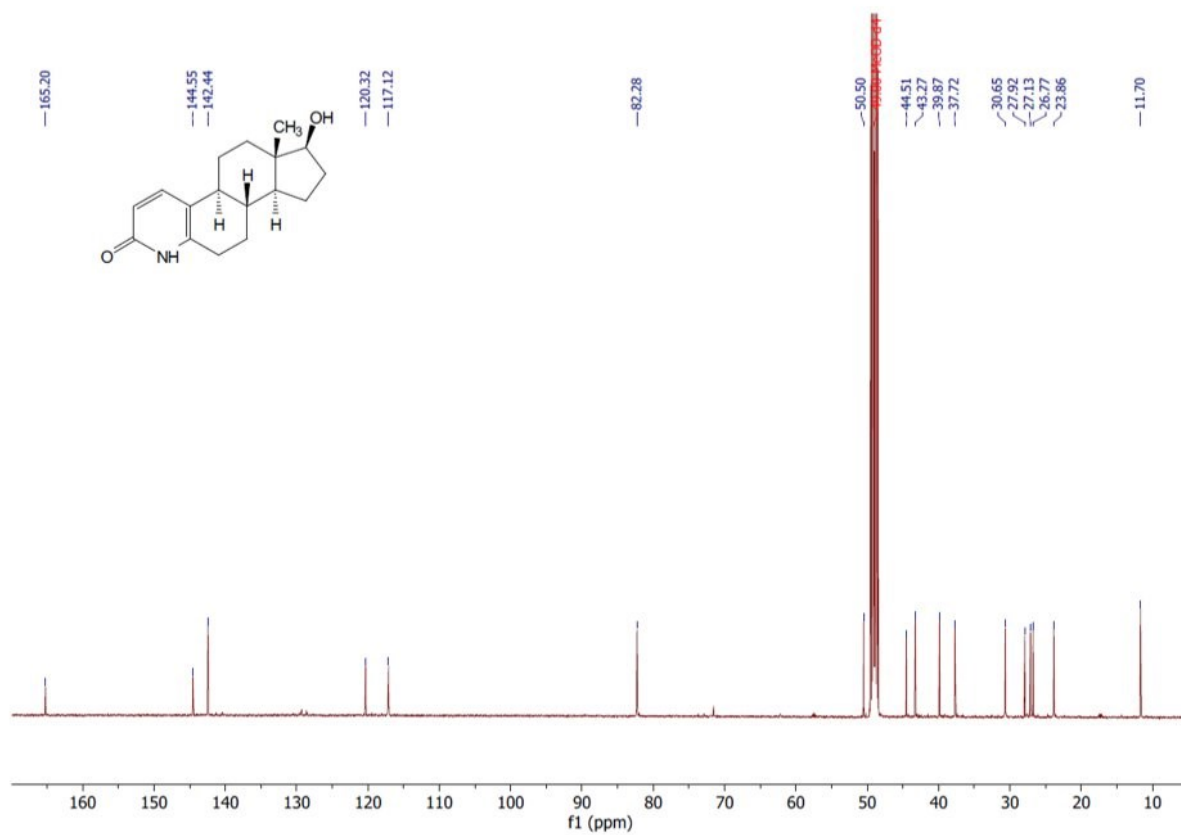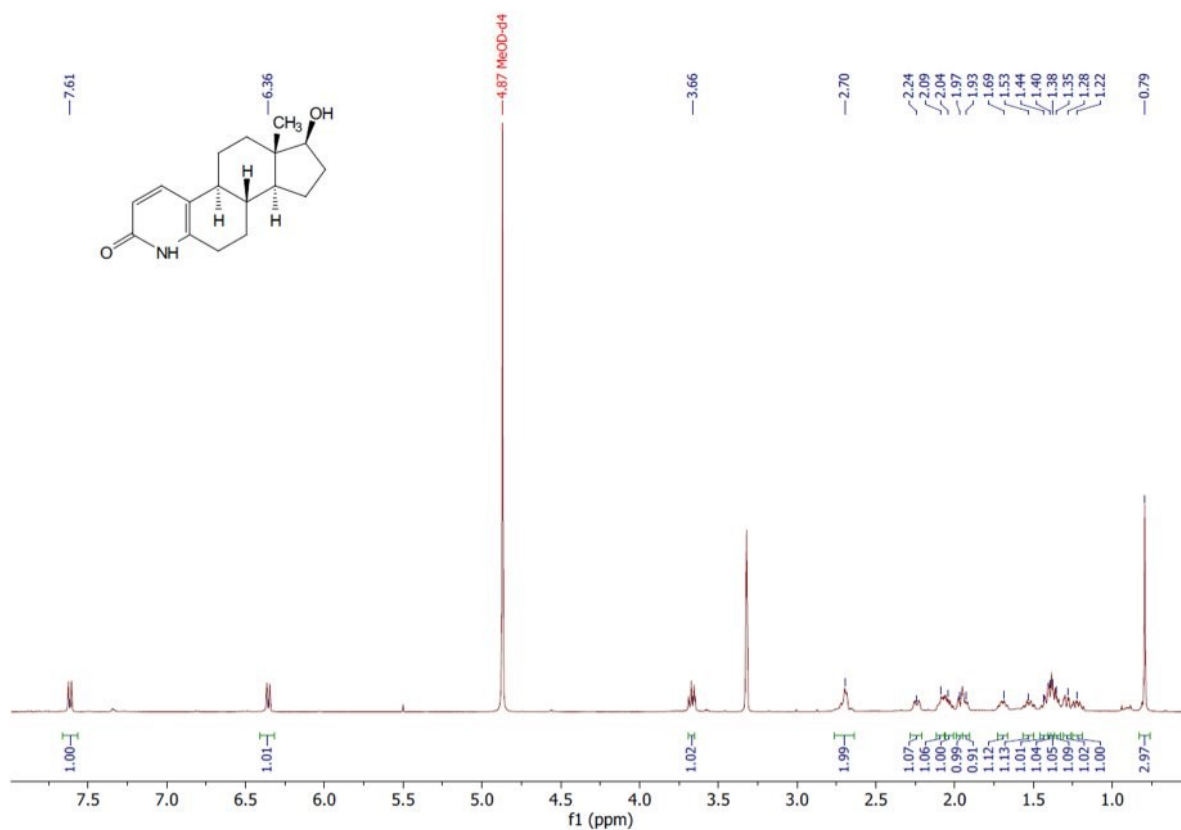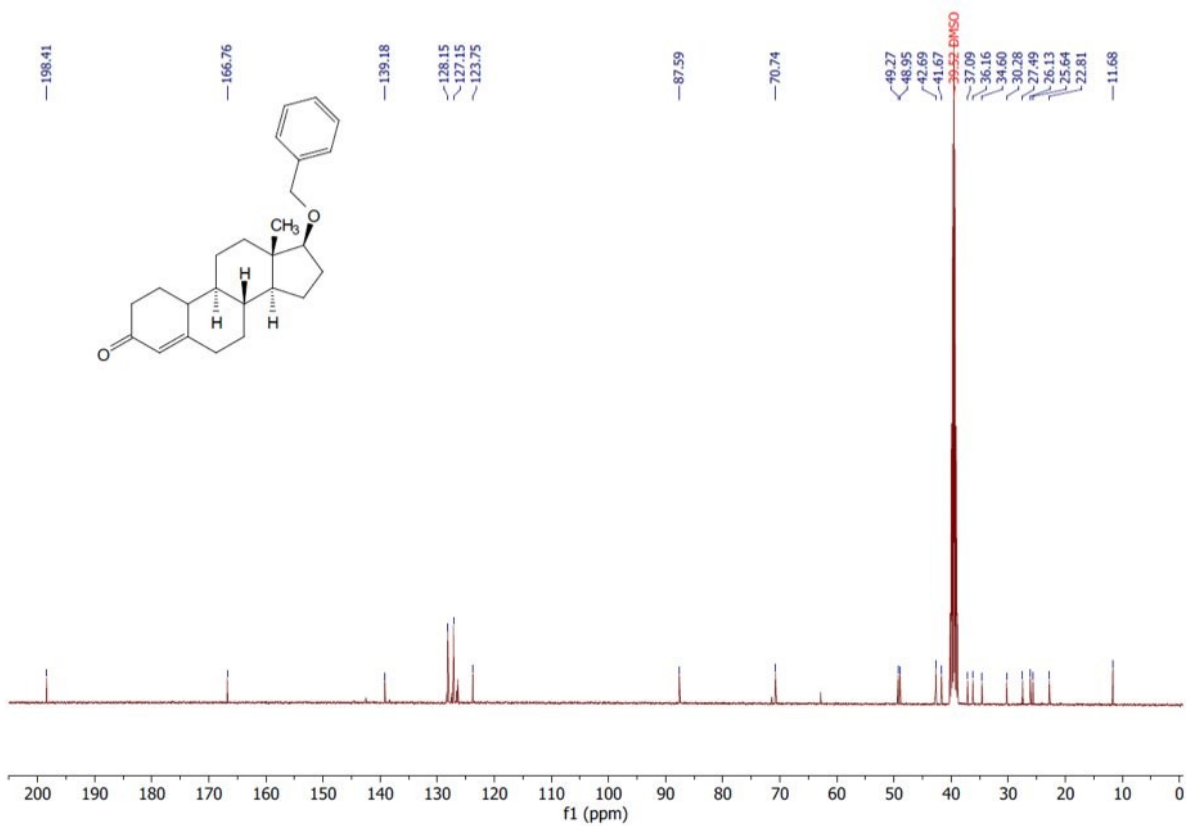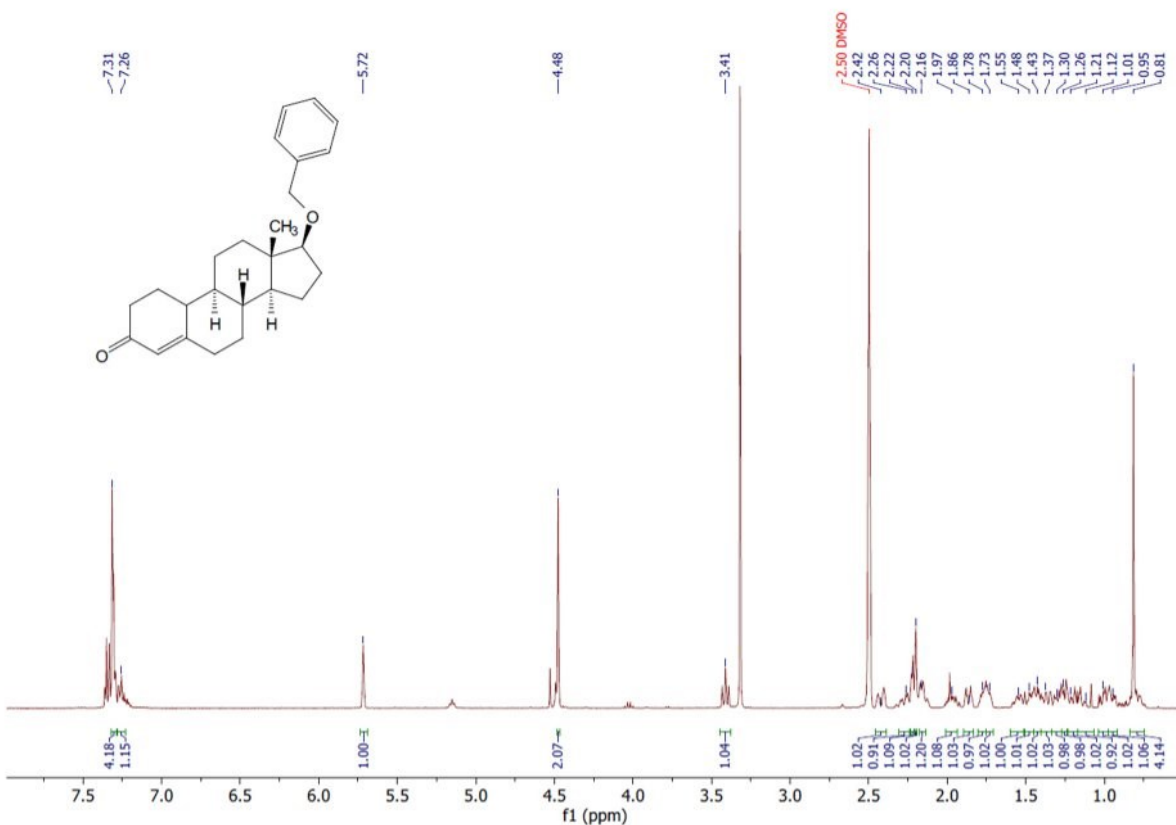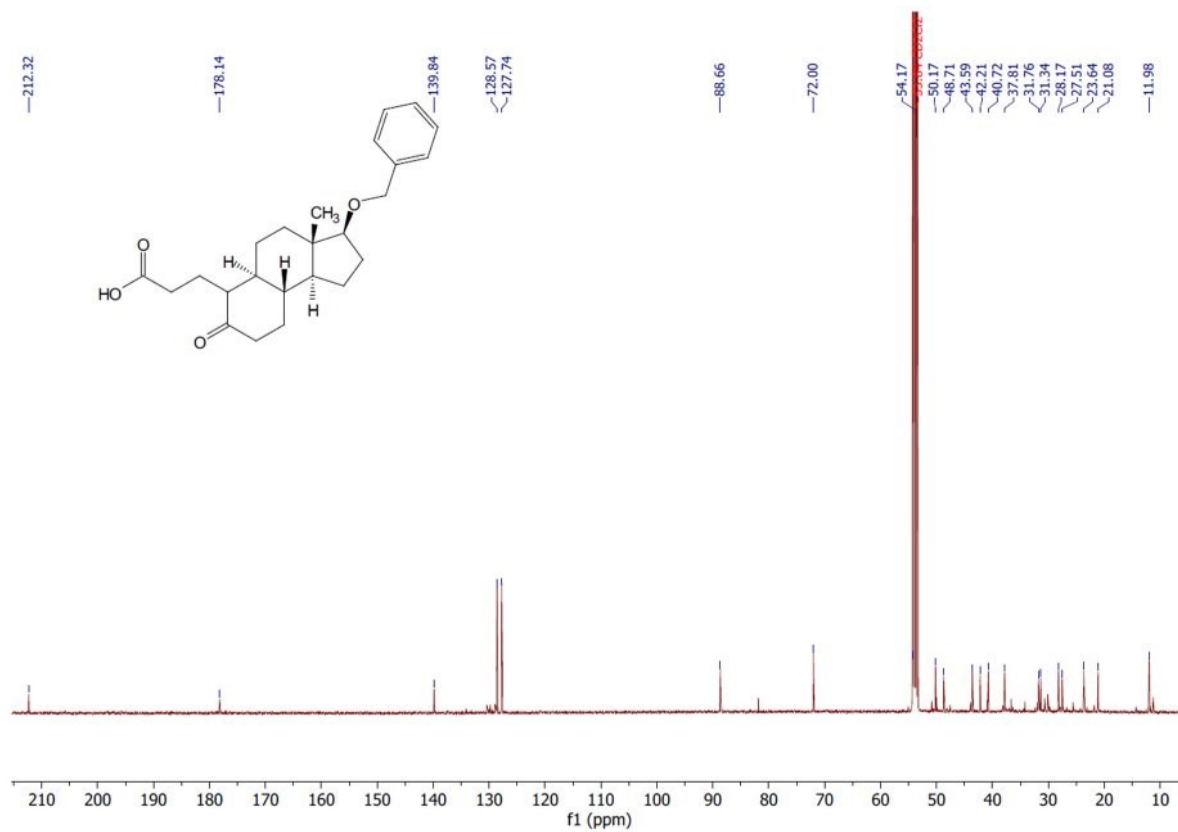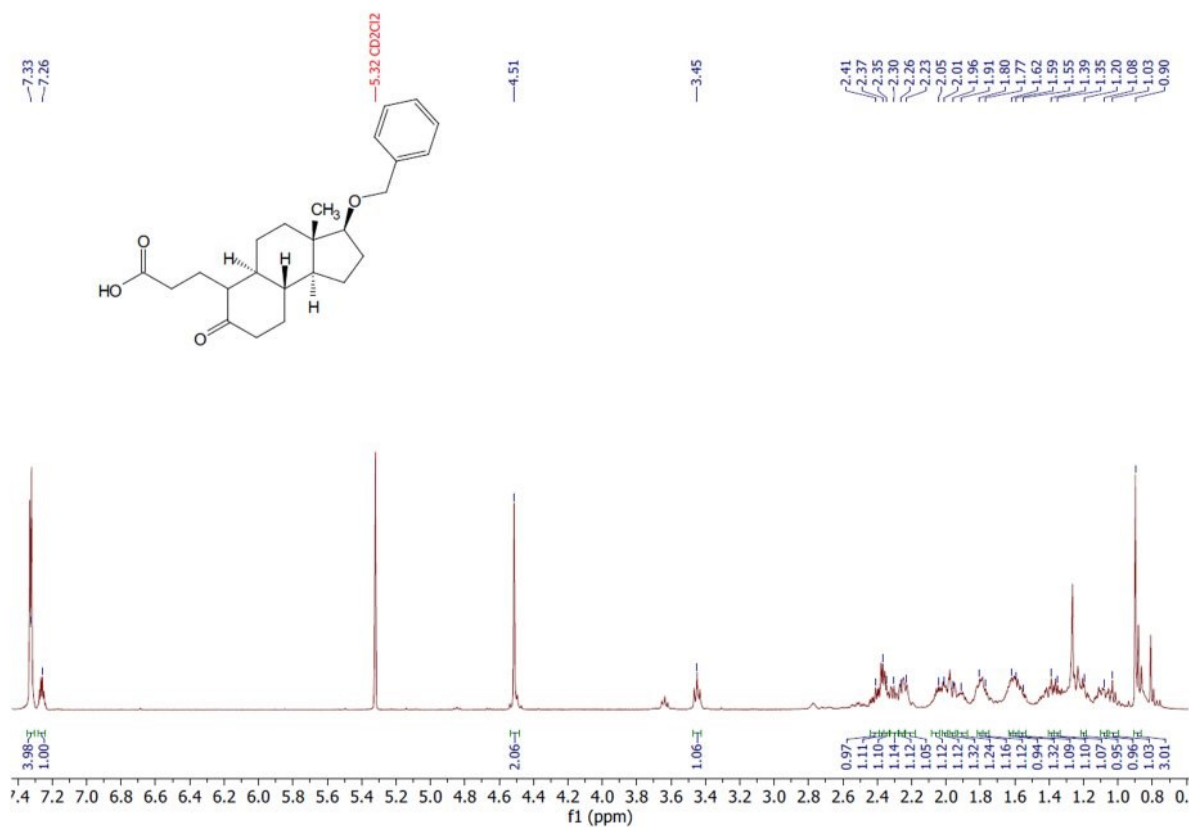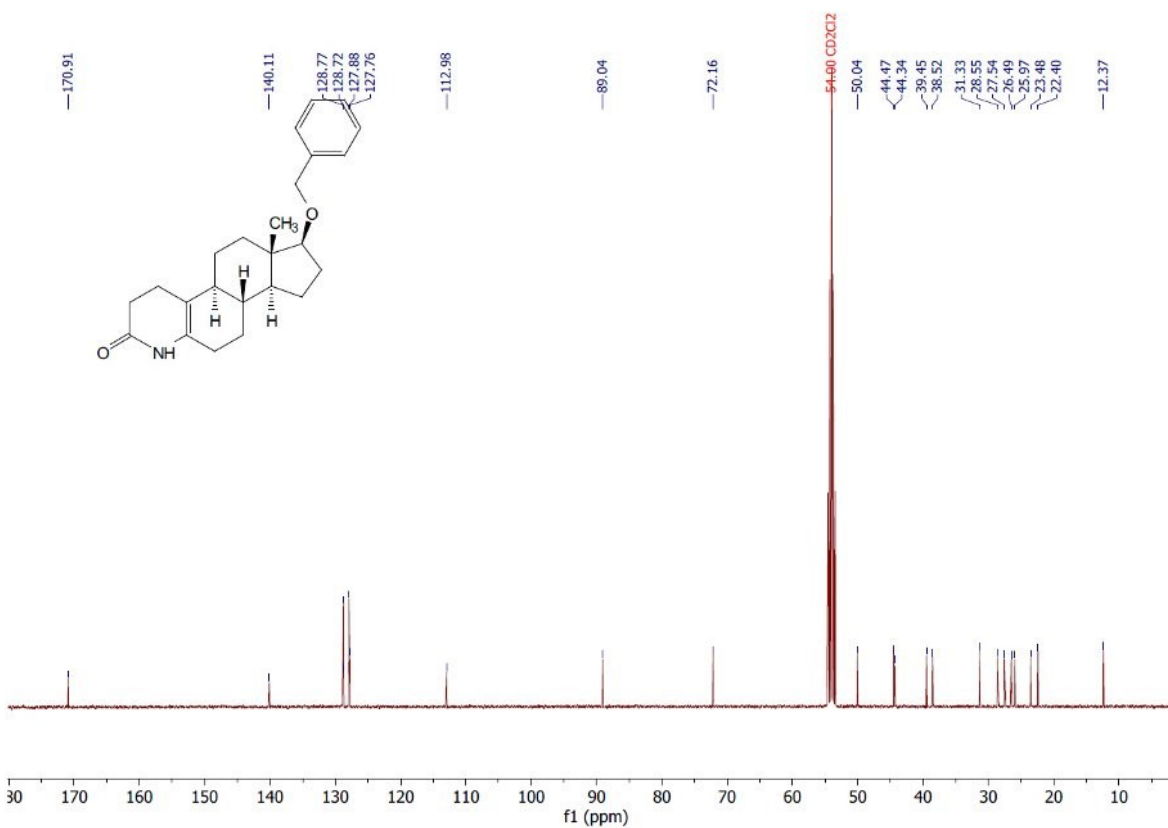
f1 (ppm)
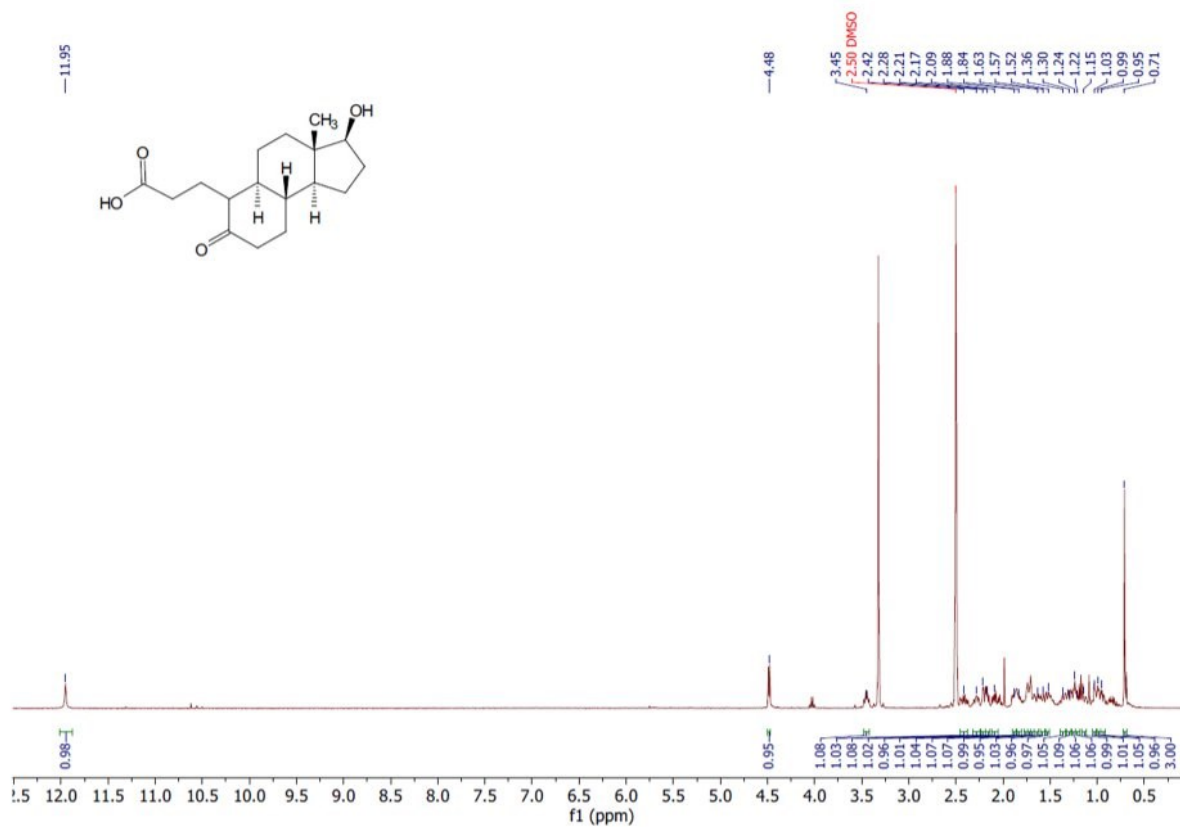
Compound 5a
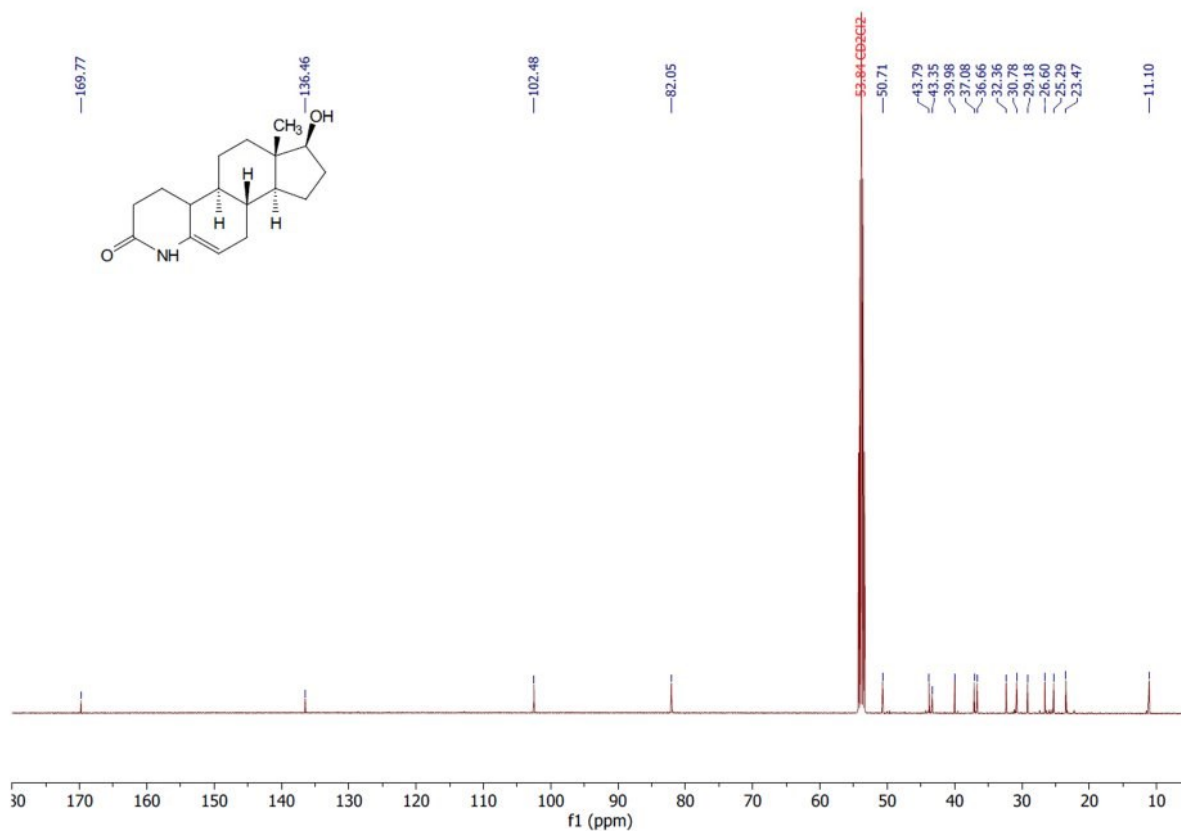
Compound 5b

Compound 6

Compound 7

Compound 8

Compound 9a

Compound 9b

Compound 10

Compound 11

¹H NMR peaks: 7.48, 7.34, 7.26, 6.49, 5.32 CD2Cl2, 4.54, 3.84, 3.52, 2.84, 2.23, 2.18, 2.10, 2.06, 1.95, 1.71, 1.59, 1.49, 1.44, 1.41, 1.39, 1.36, 1.22, 0.85

Integrations: 1.09, 4.04, 1.07, 1.09, 2.11, 2.98, 1.00, 2.03, 0.93, 1.12, 0.95, 1.10, 1.12, 1.15, 1.09, 1.06, 1.05, 0.98, 1.15, 1.09, 3.06

¹³C NMR peaks: 161.97, 154.62, 139.96, 136.57, 128.57, 128.21, 127.74, 127.61, 107.59, 88.93, 72.02, 53.84 CD2Cl2, 53.32, 50.36, 43.81, 43.67, 38.70, 38.17, 32.94, 28.33, 27.42, 26.77, 23.45, 12.00
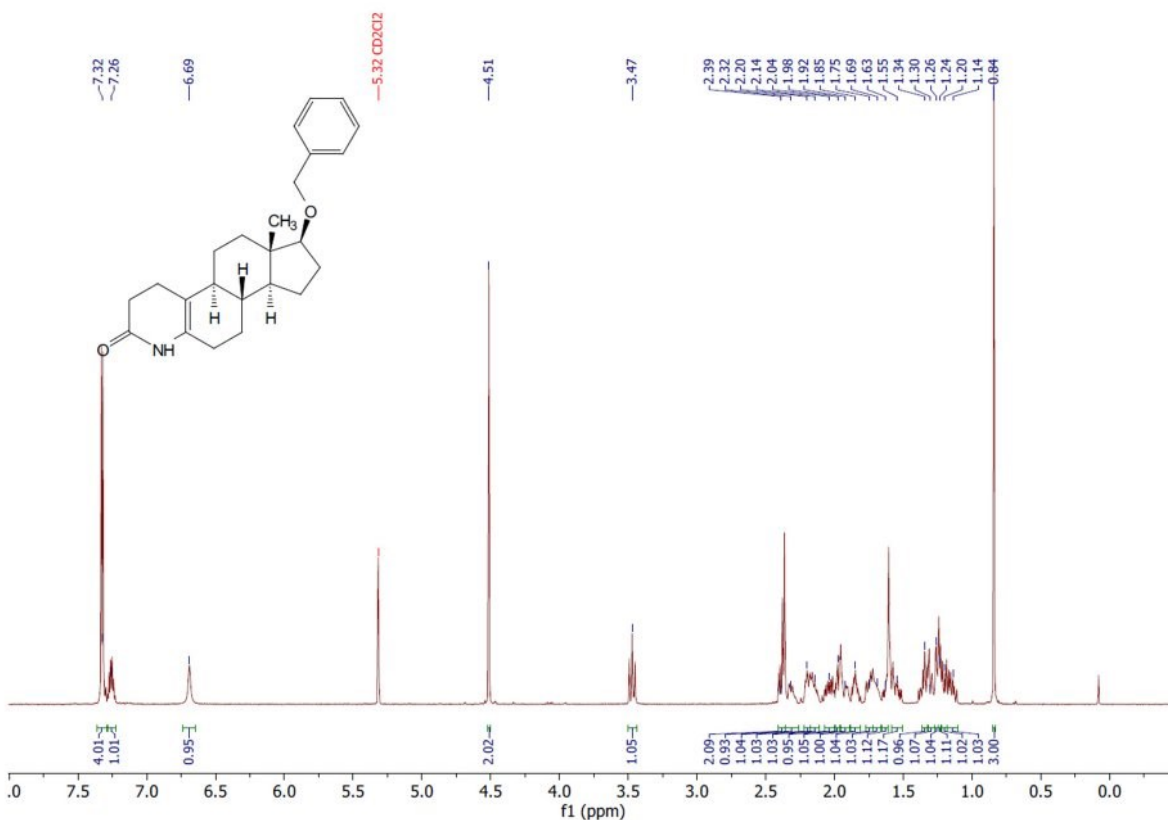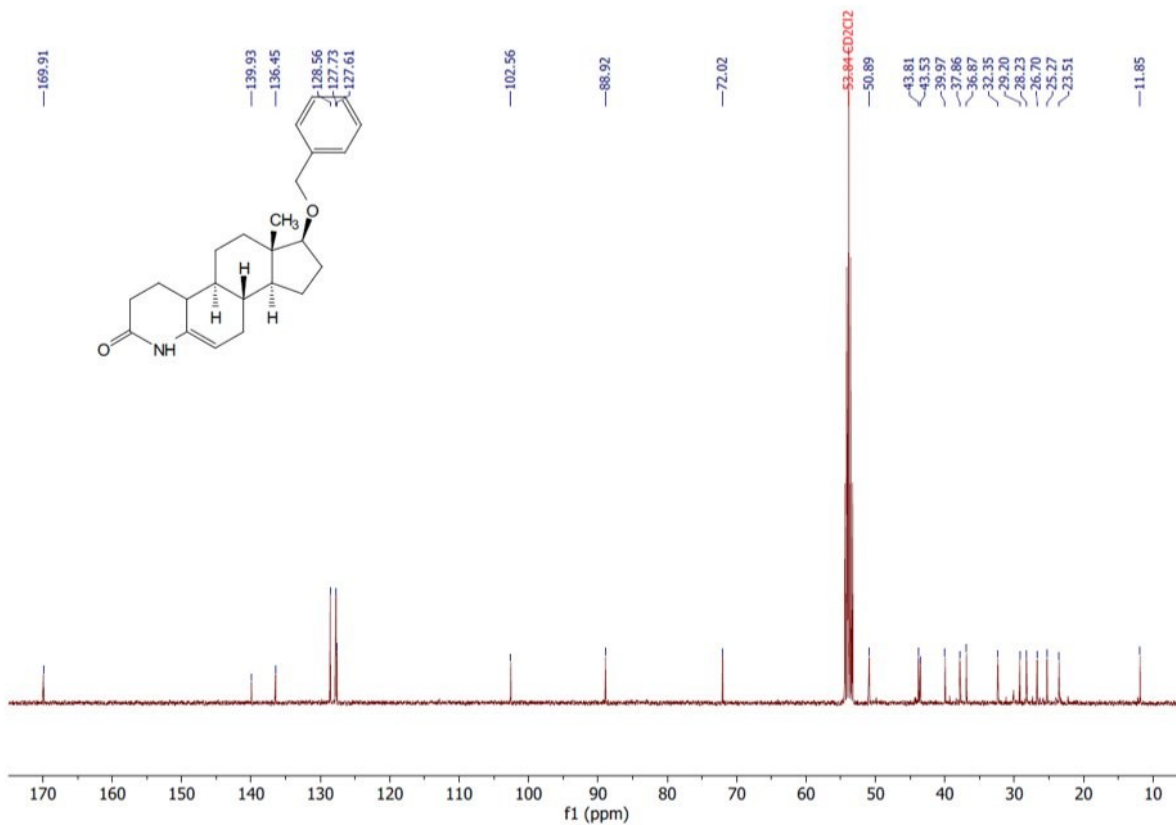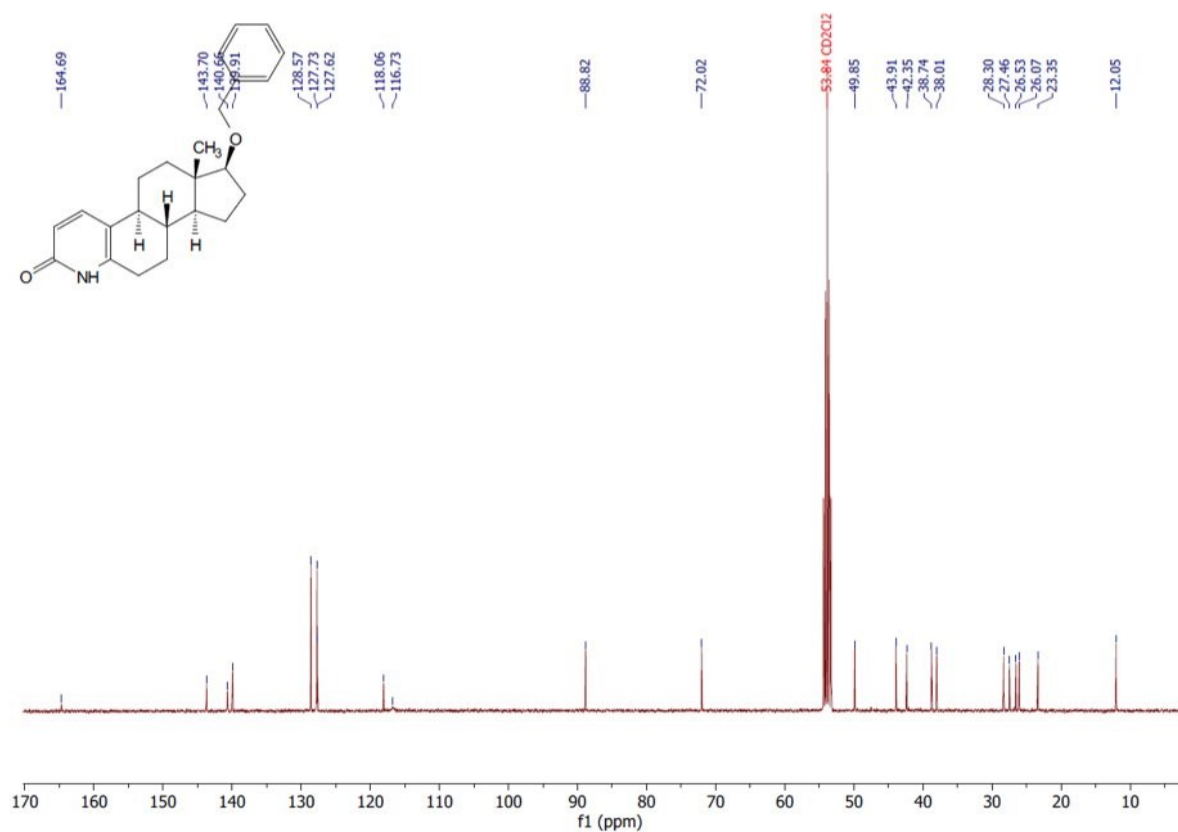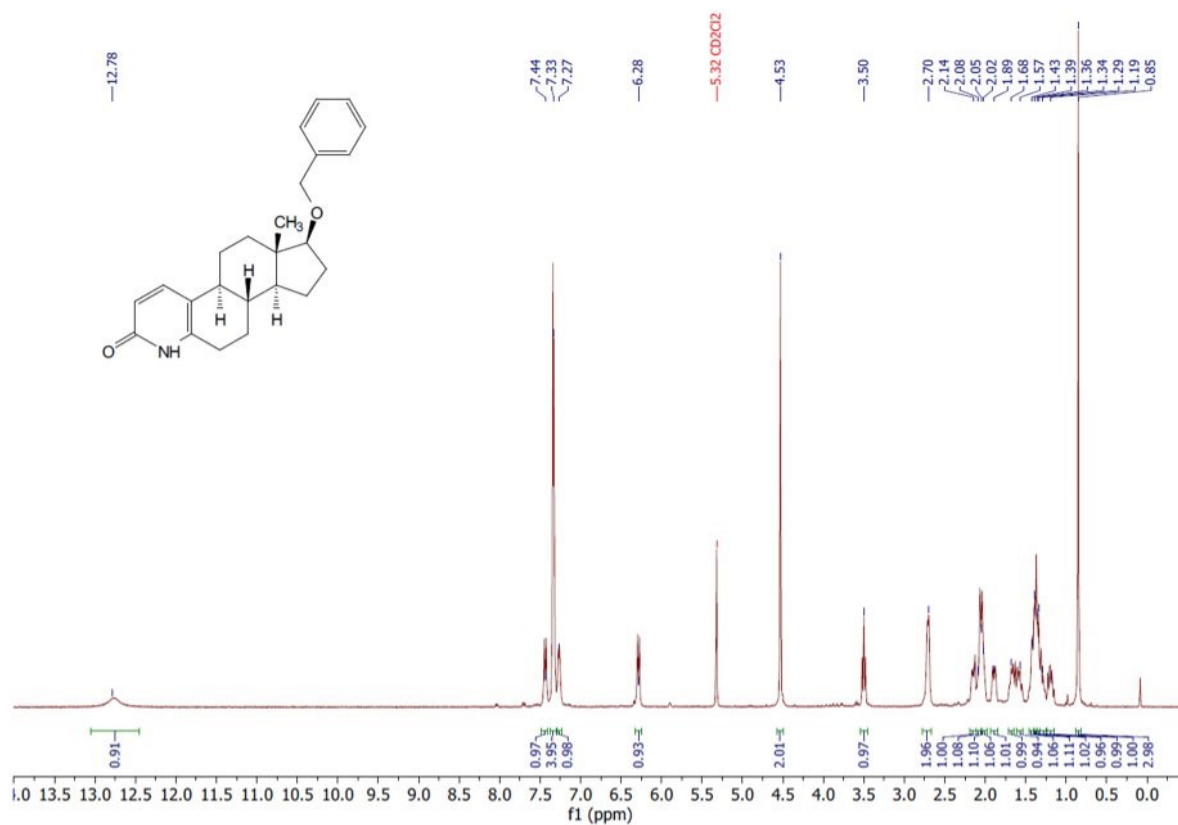
Compound 1

Compound 12

Compound 13

¹H NMR peaks: 4.44, 3.88, 3.81, 3.43, OH, CH₃, 2.59 DMSO, 2.38, 2.24, 1.82, 1.76, 1.70, 1.64, 1.61, 1.57, 1.47, 1.44, 1.38, 1.31, 1.21, 1.16, 1.13, 1.06, 1.01, 0.97, 0.94, 0.88

Integrations: 1.00, 2.01, 2.13, 3.16, 1.25, 1.14, 0.94, 1.04, 0.97, 1.10, 1.00, 1.04, 0.99, 1.00, 1.16, 1.06, 1.01, 1.00, 0.96, 1.03, 0.99, 1.01, 0.99, 1.01, 0.97, 2.97

f1 (ppm)

¹³C NMR peaks: 173.76, 110.55, 79.99, 63.88, 51.14, 49.41, 47.32, 44.90, 42.71, 36.58, 33.91, 32.68, 29.82, 27.17, 25.92, 22.93, 21.13, 11.35

f1 (ppm)

Compound 14

Compound 15

Compound 16

Compound 17
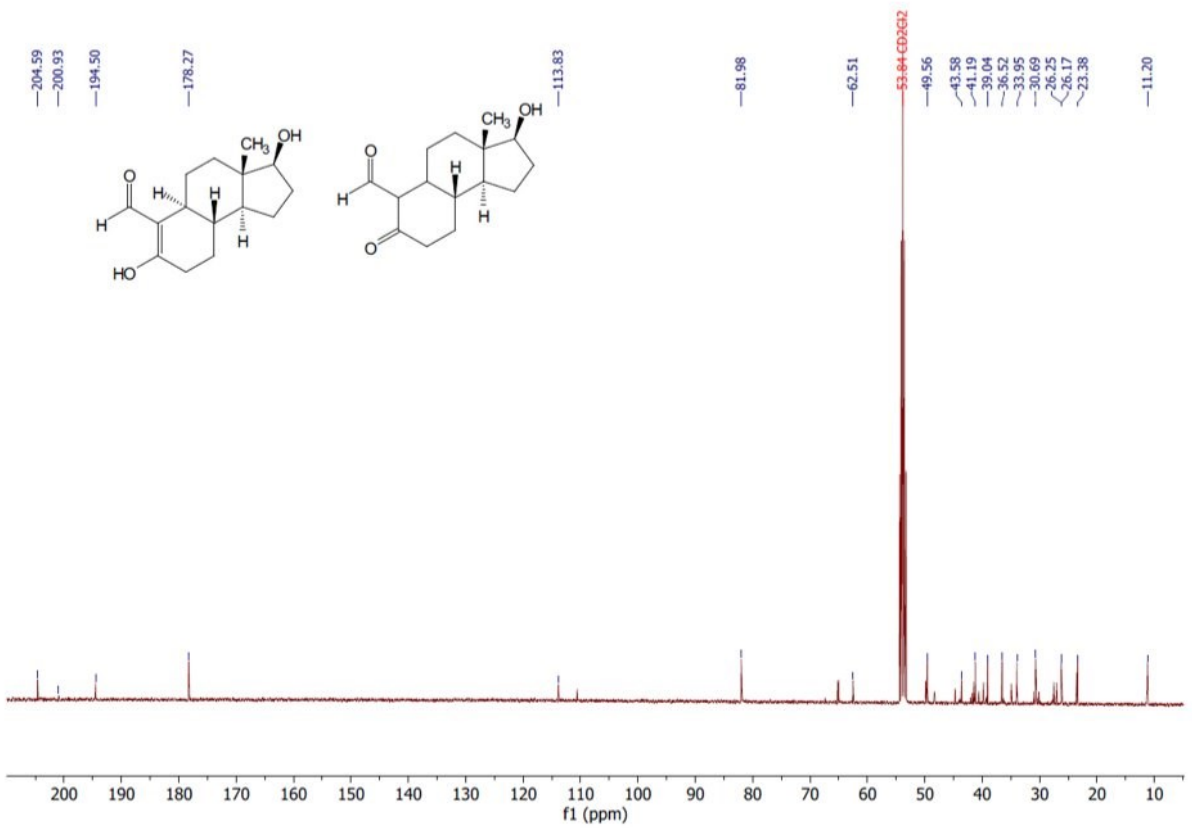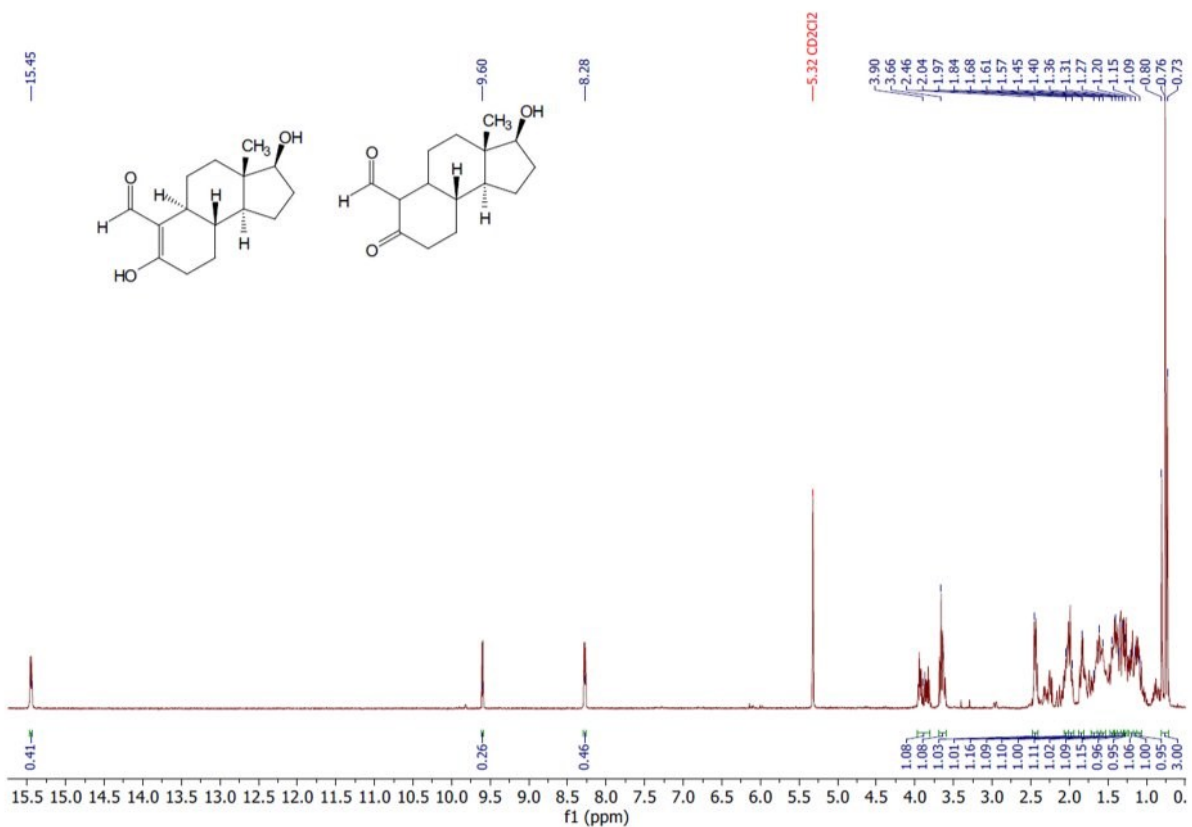
Compound 2

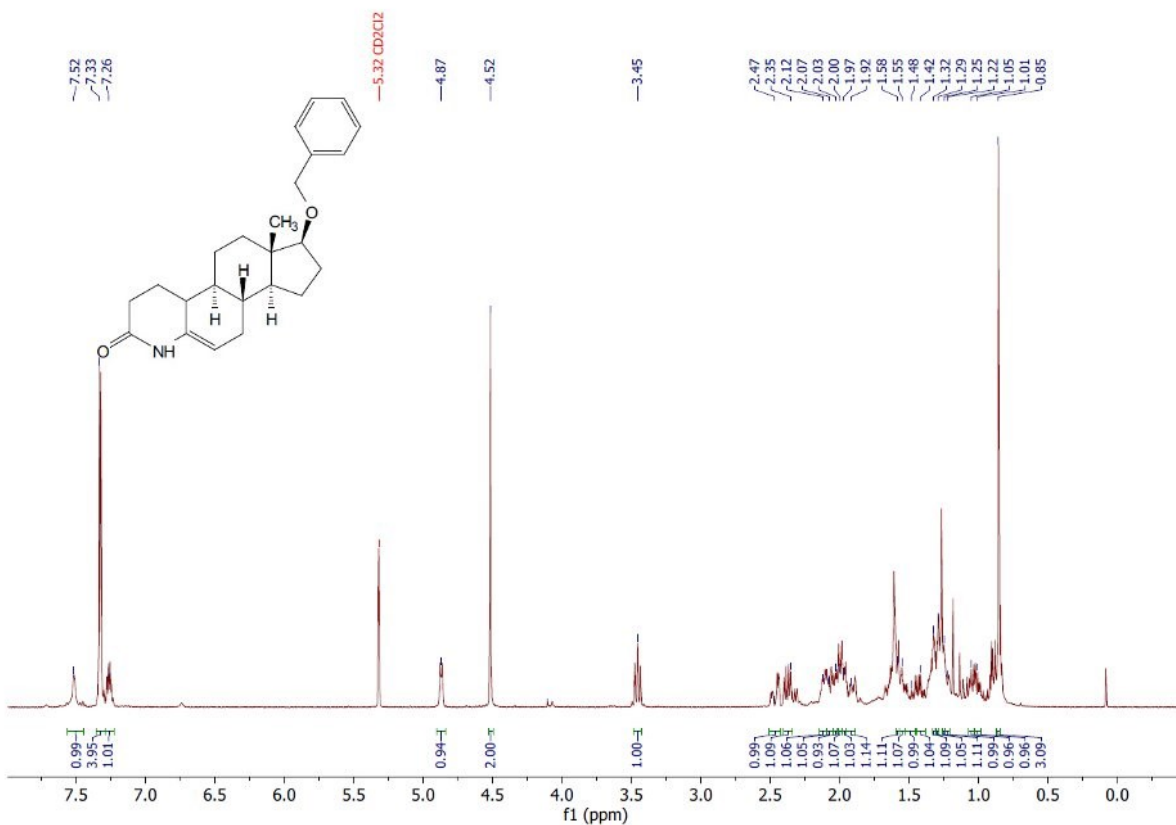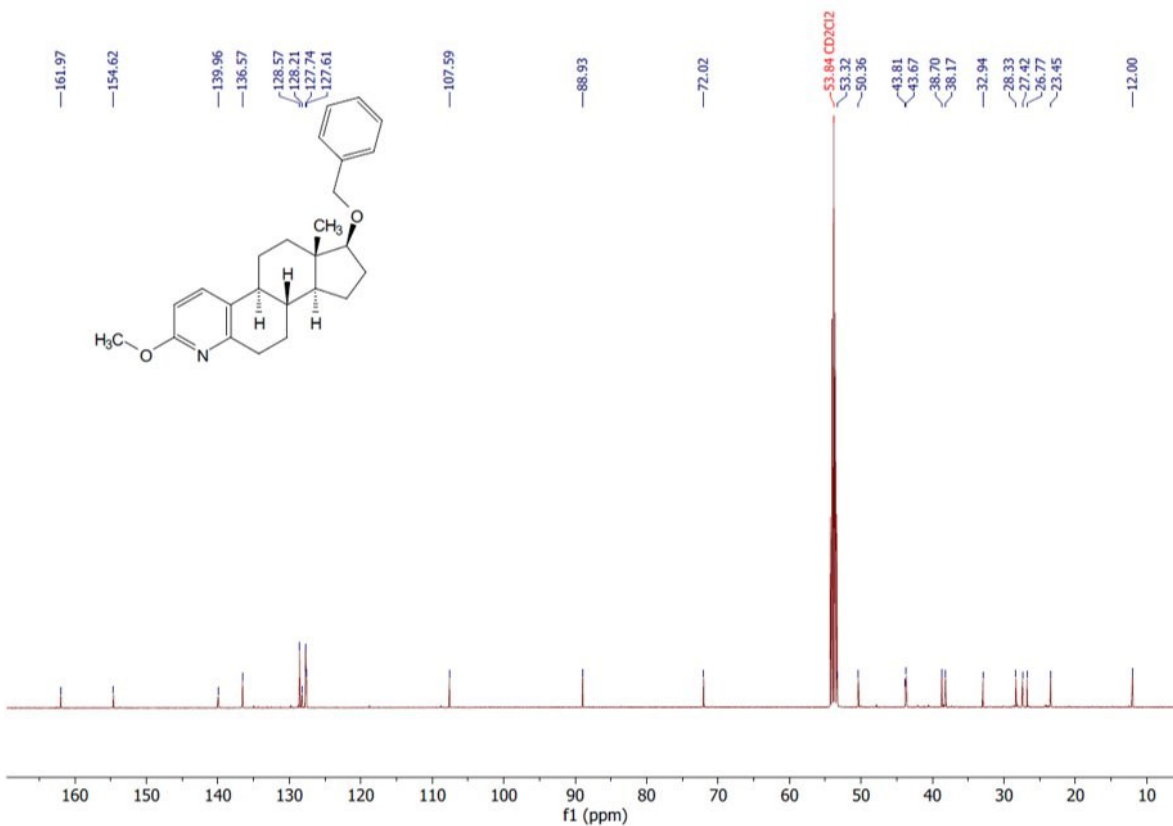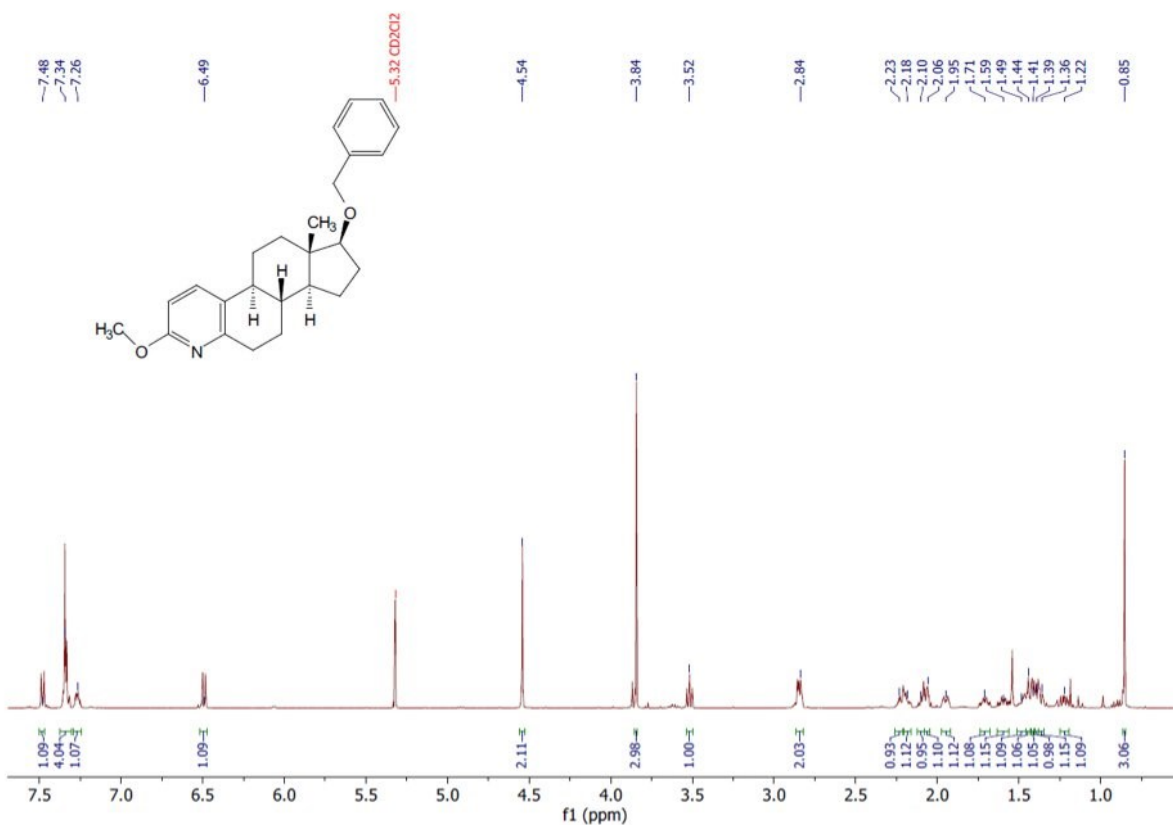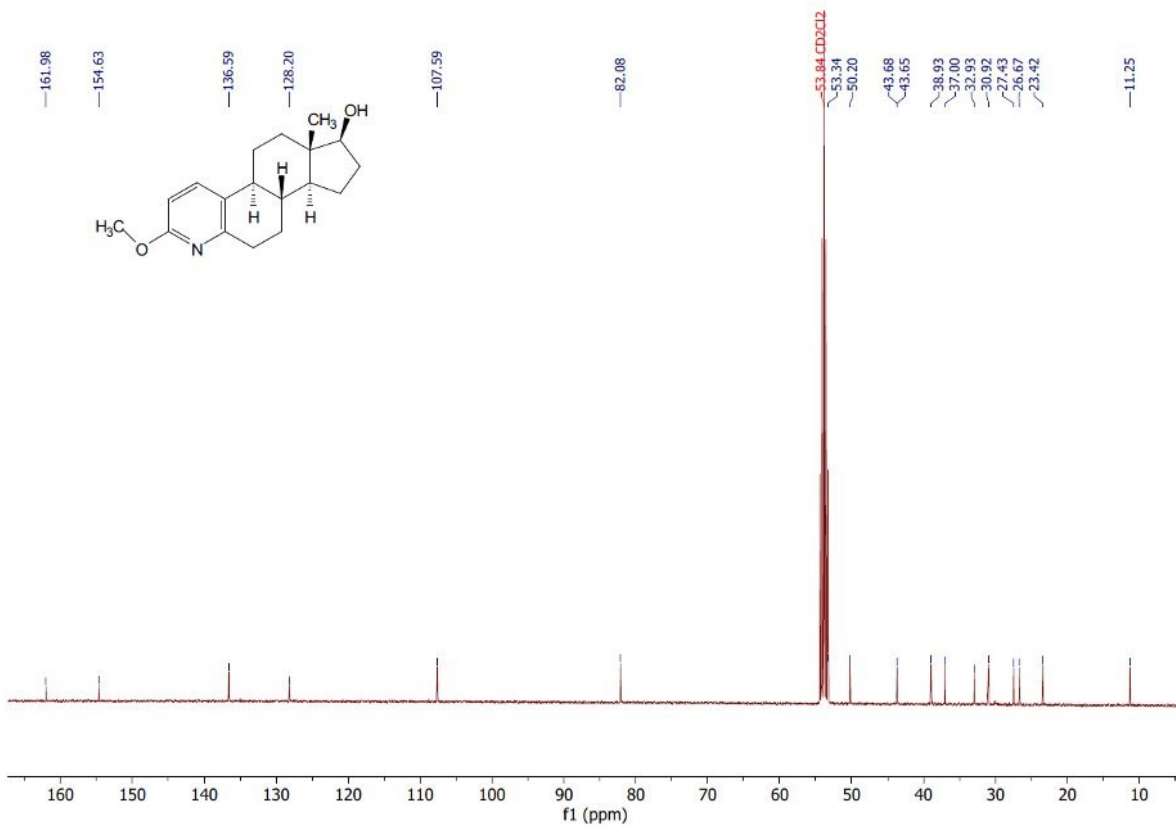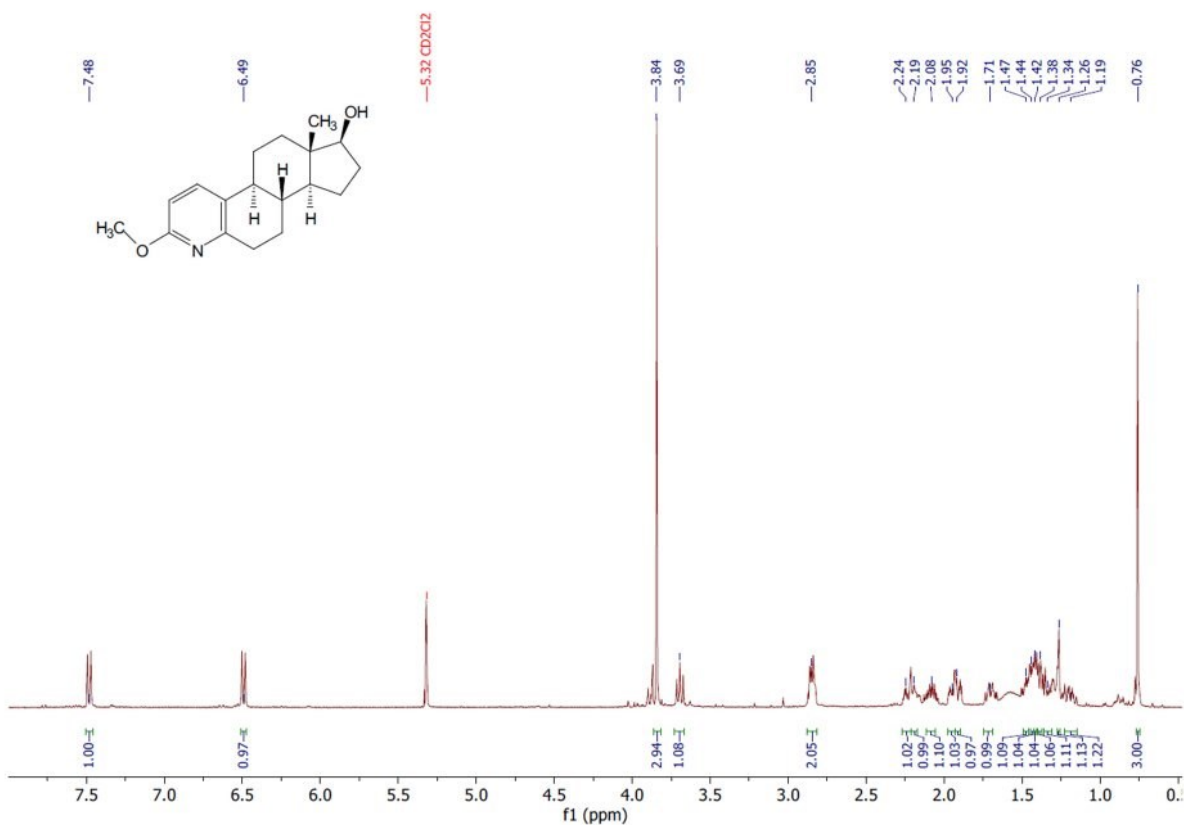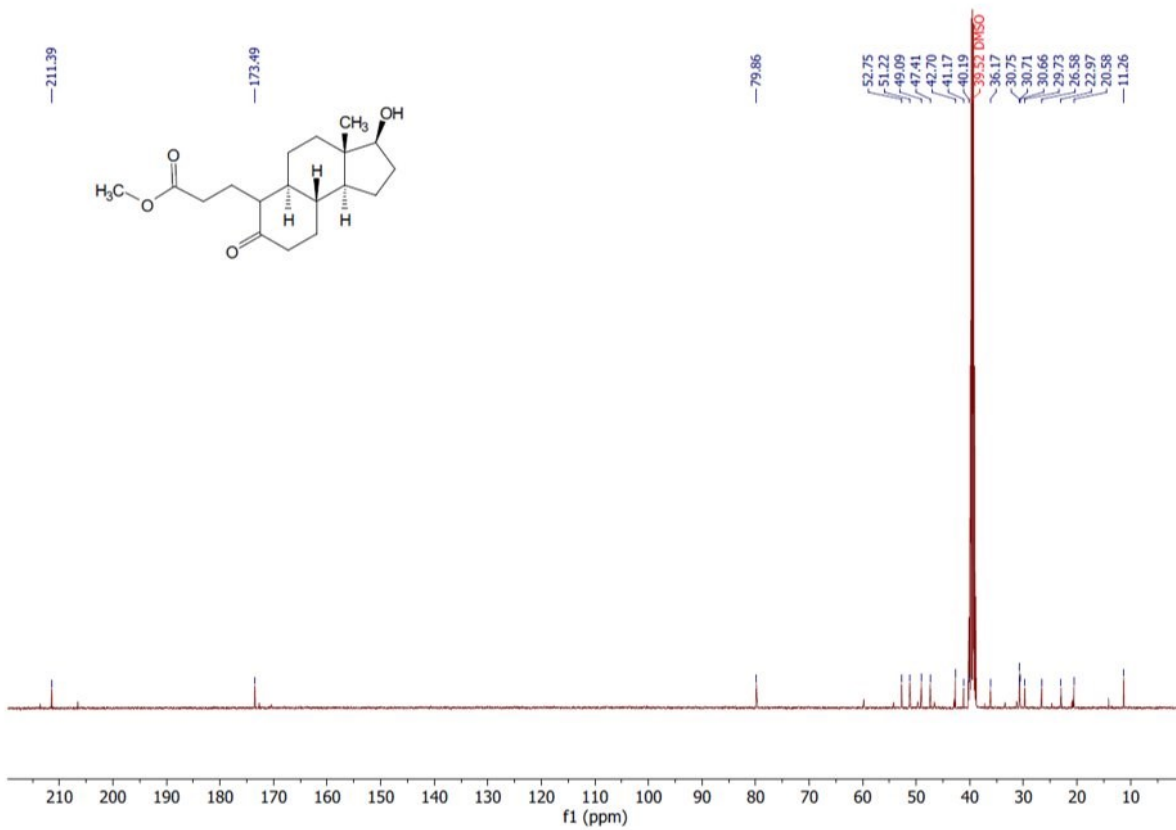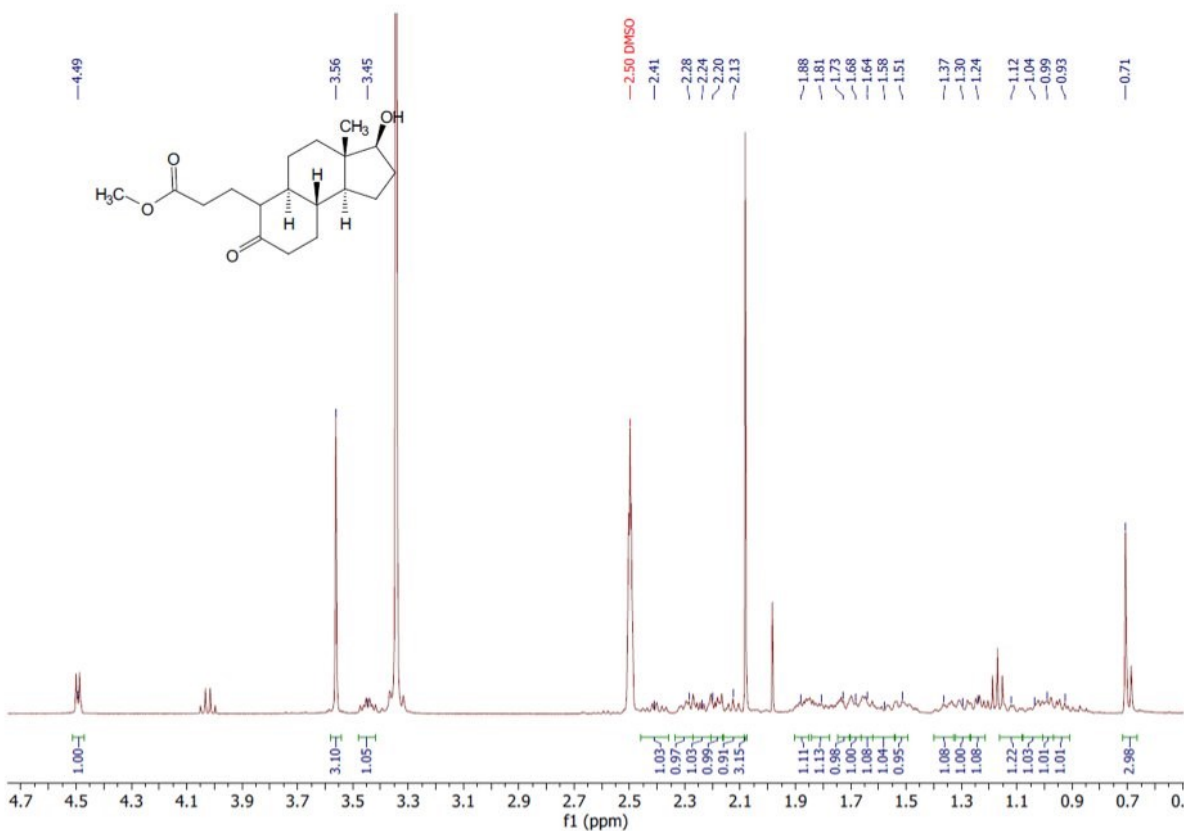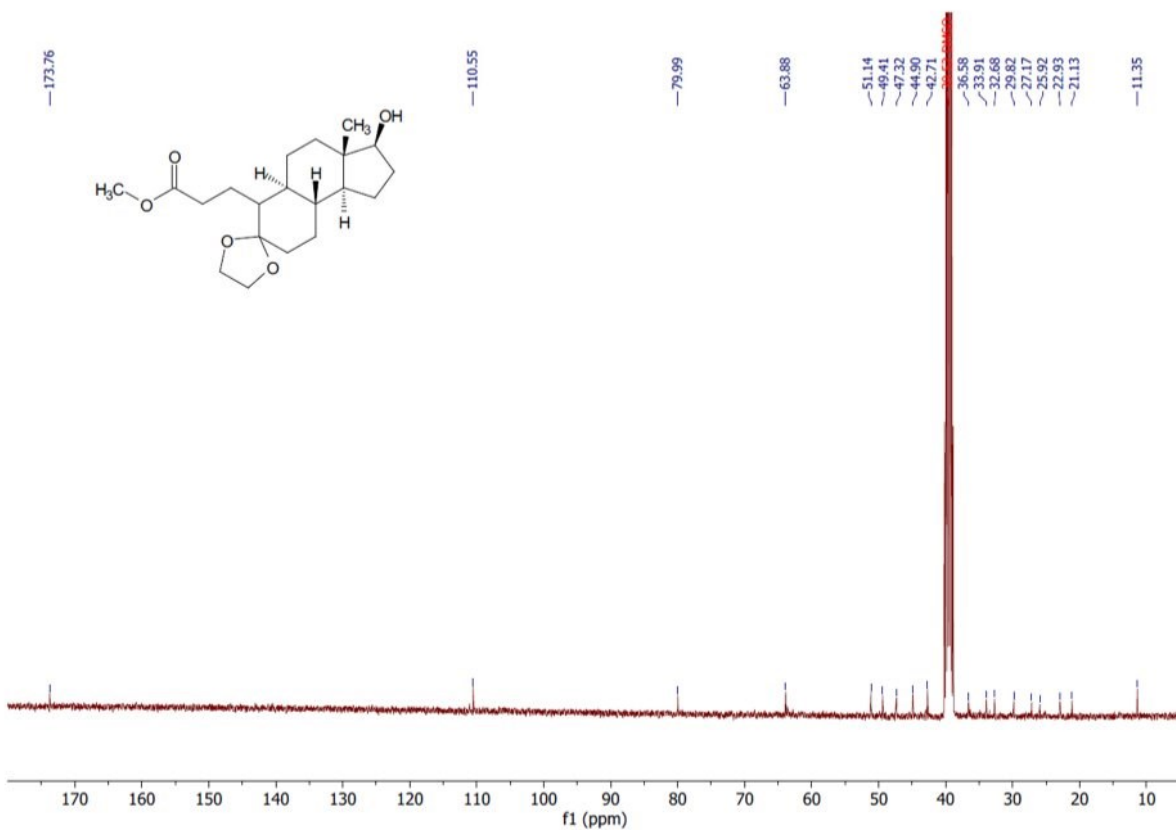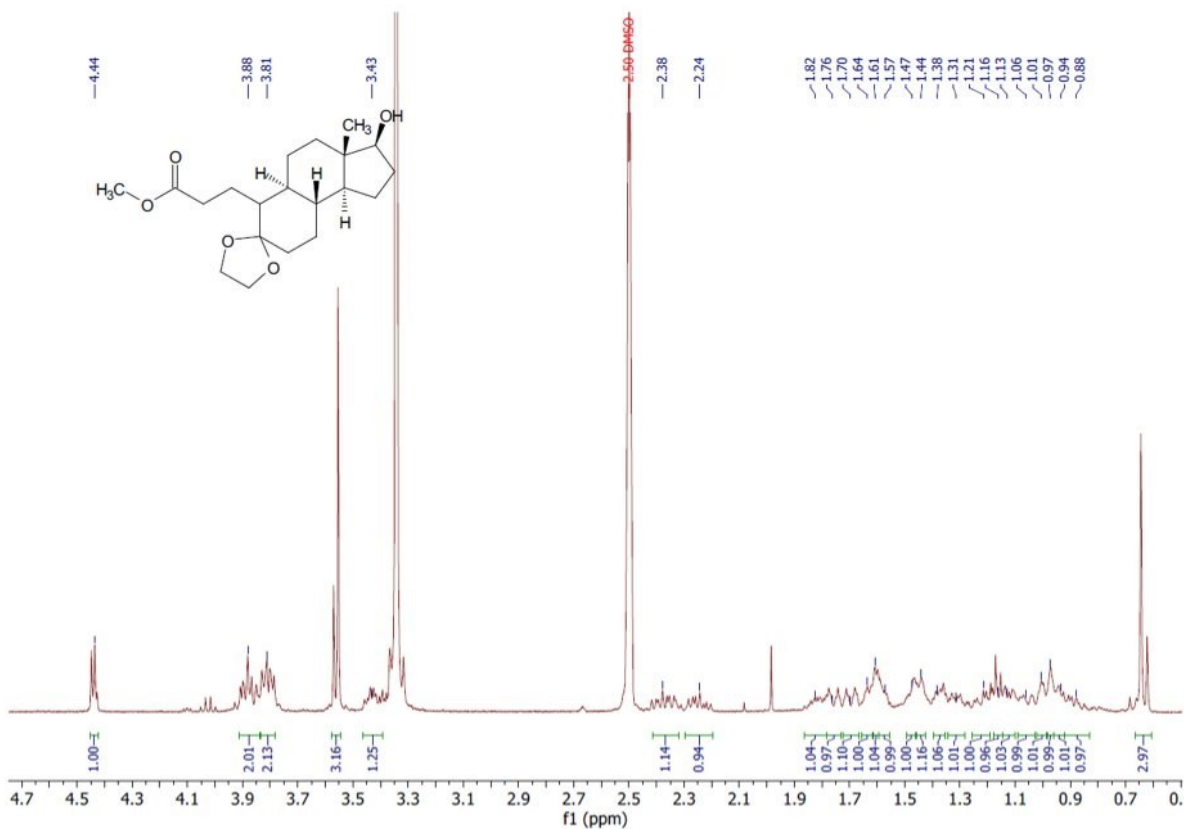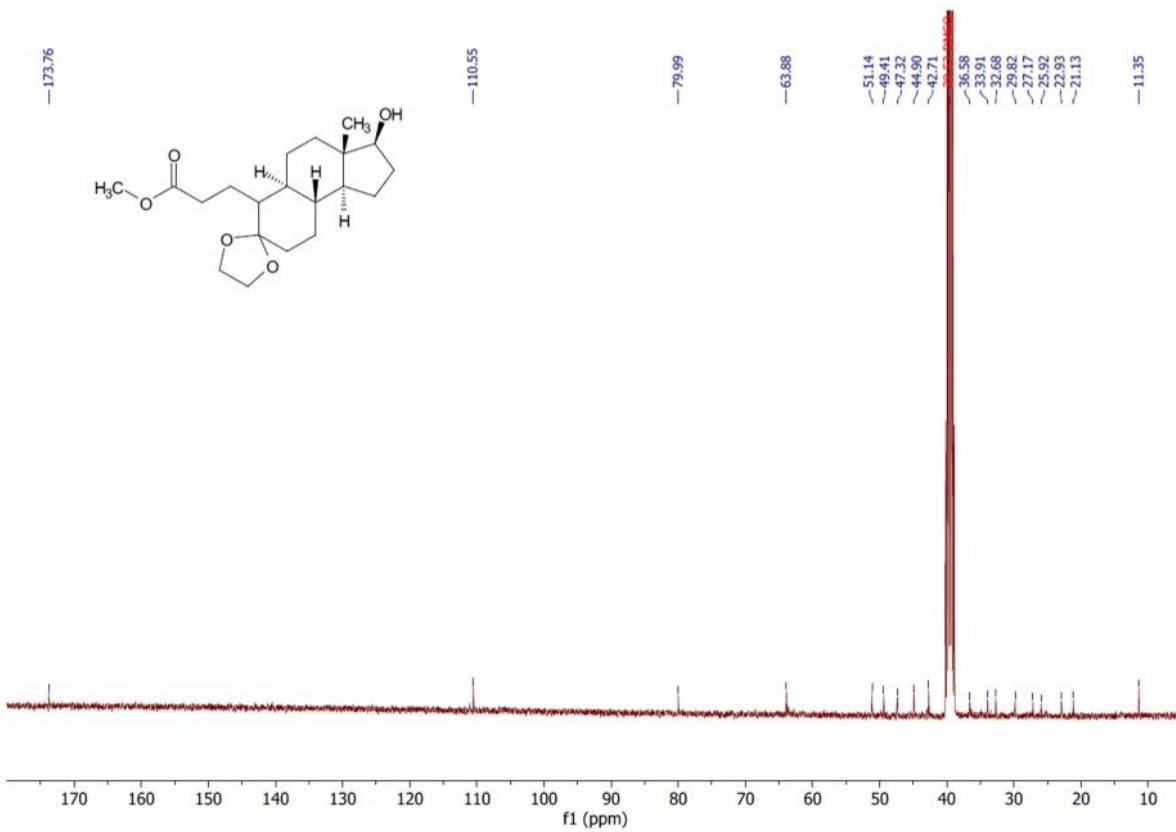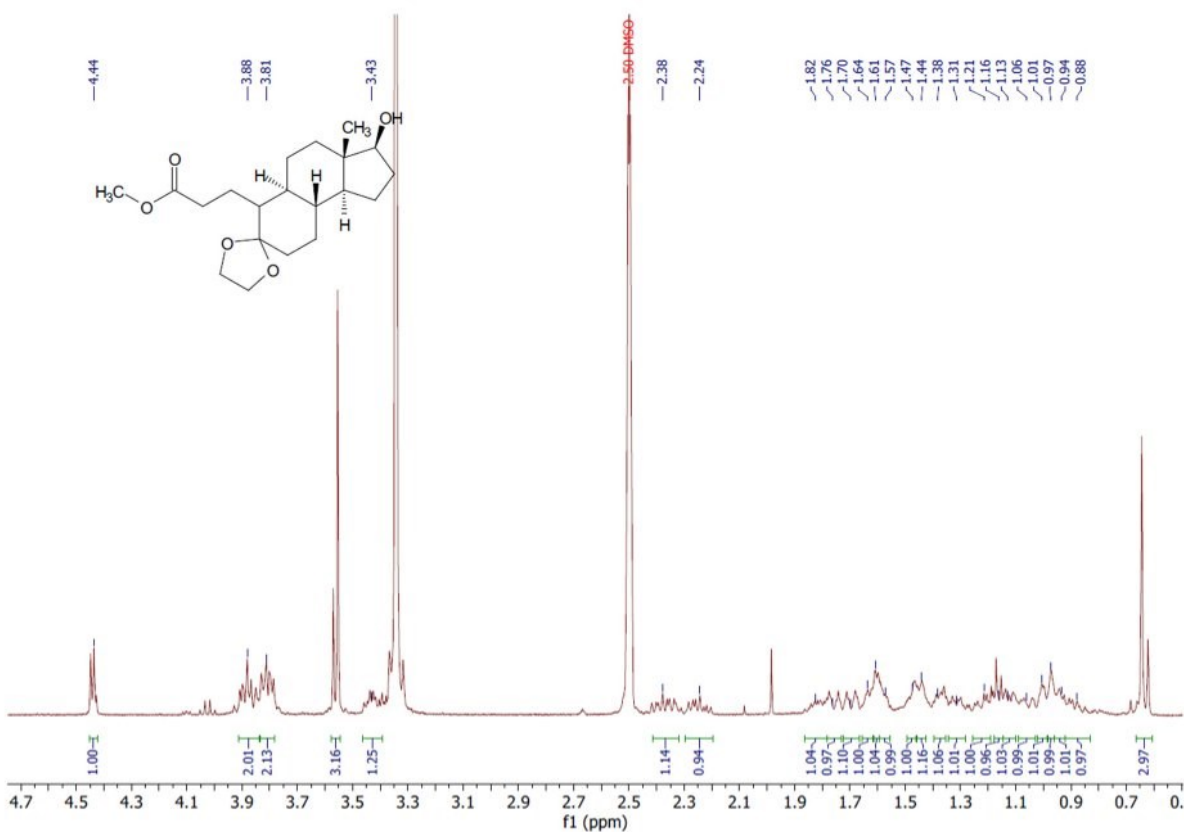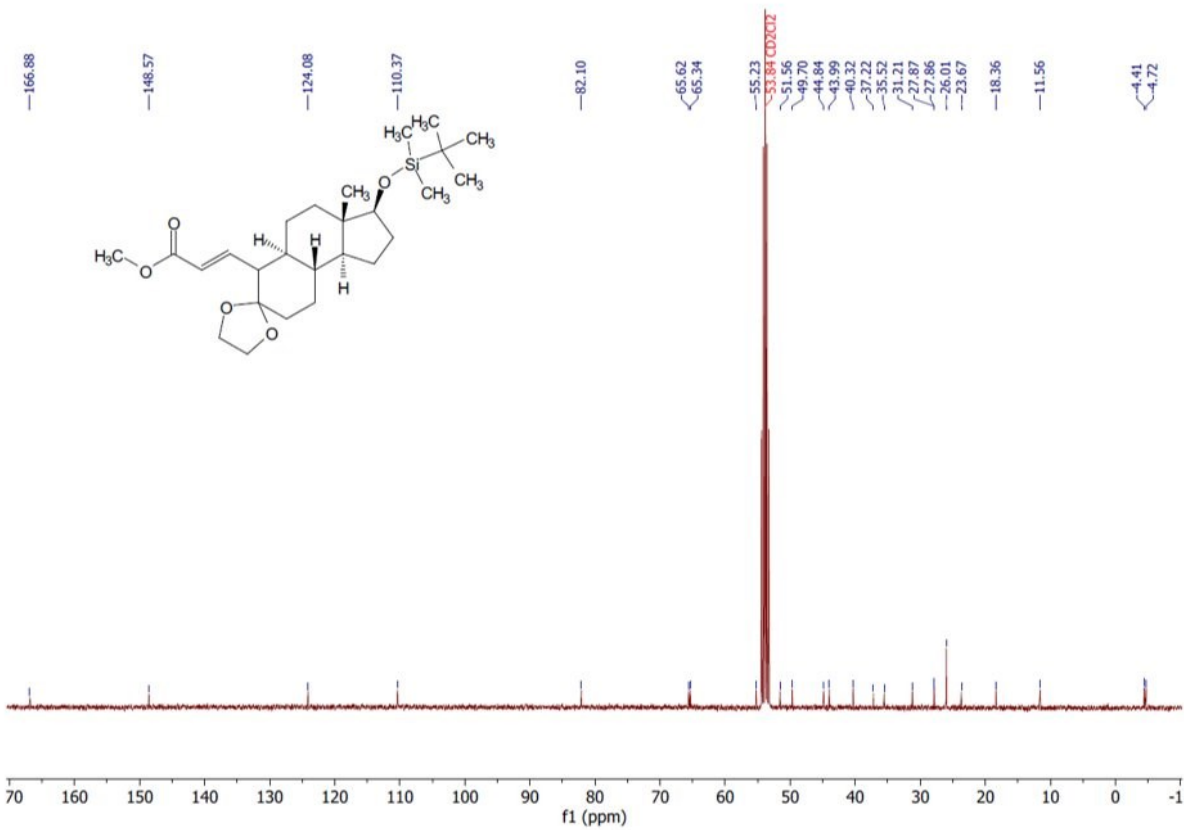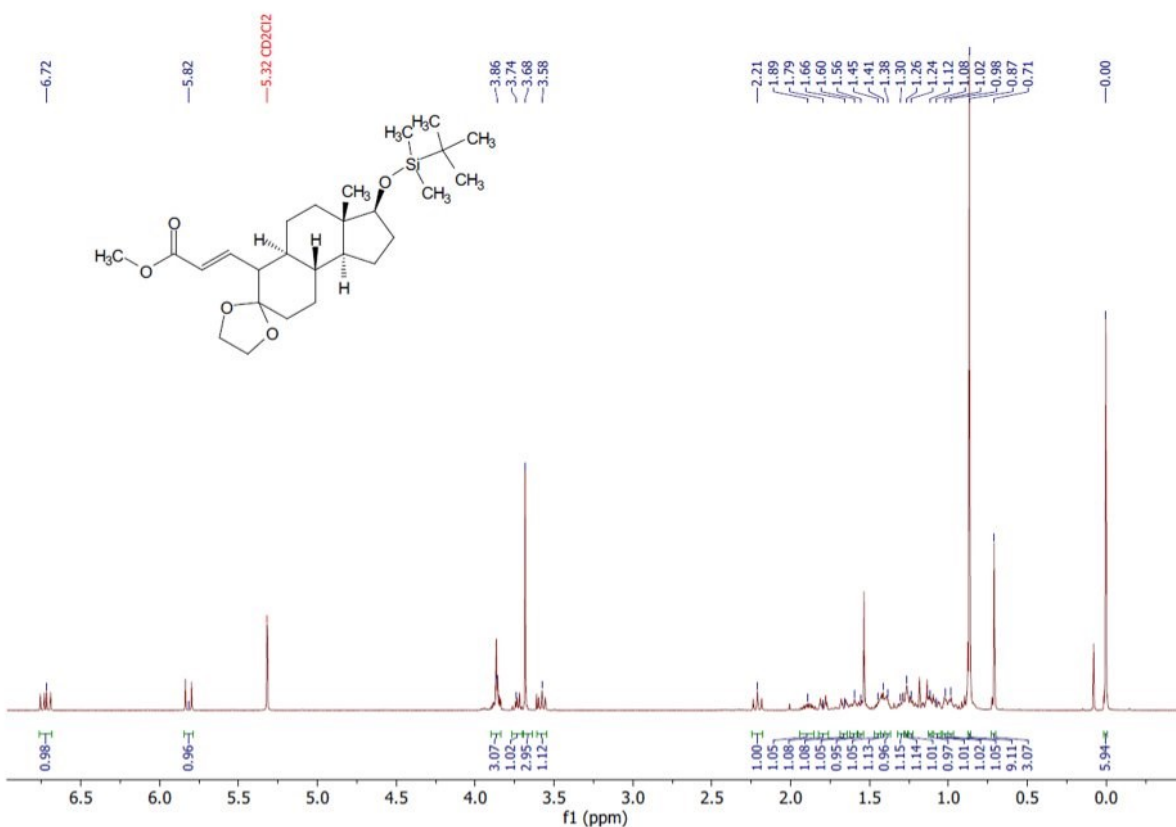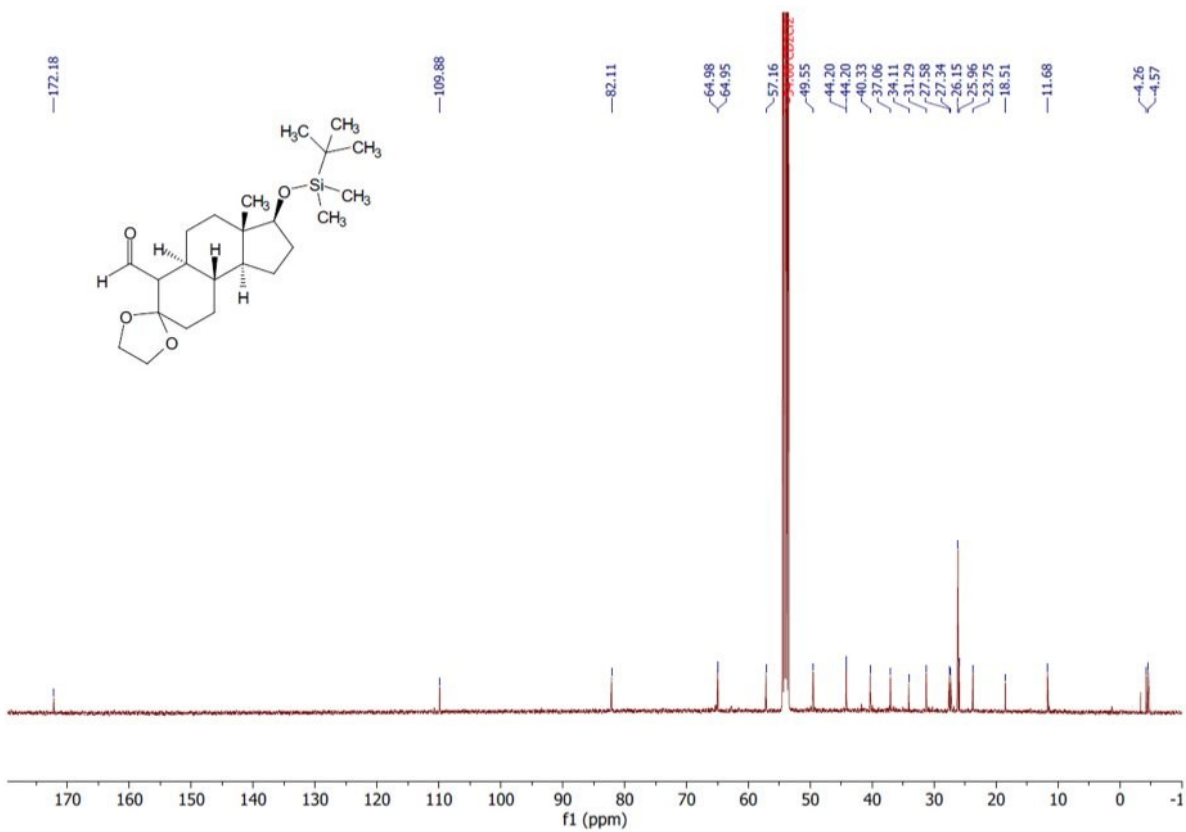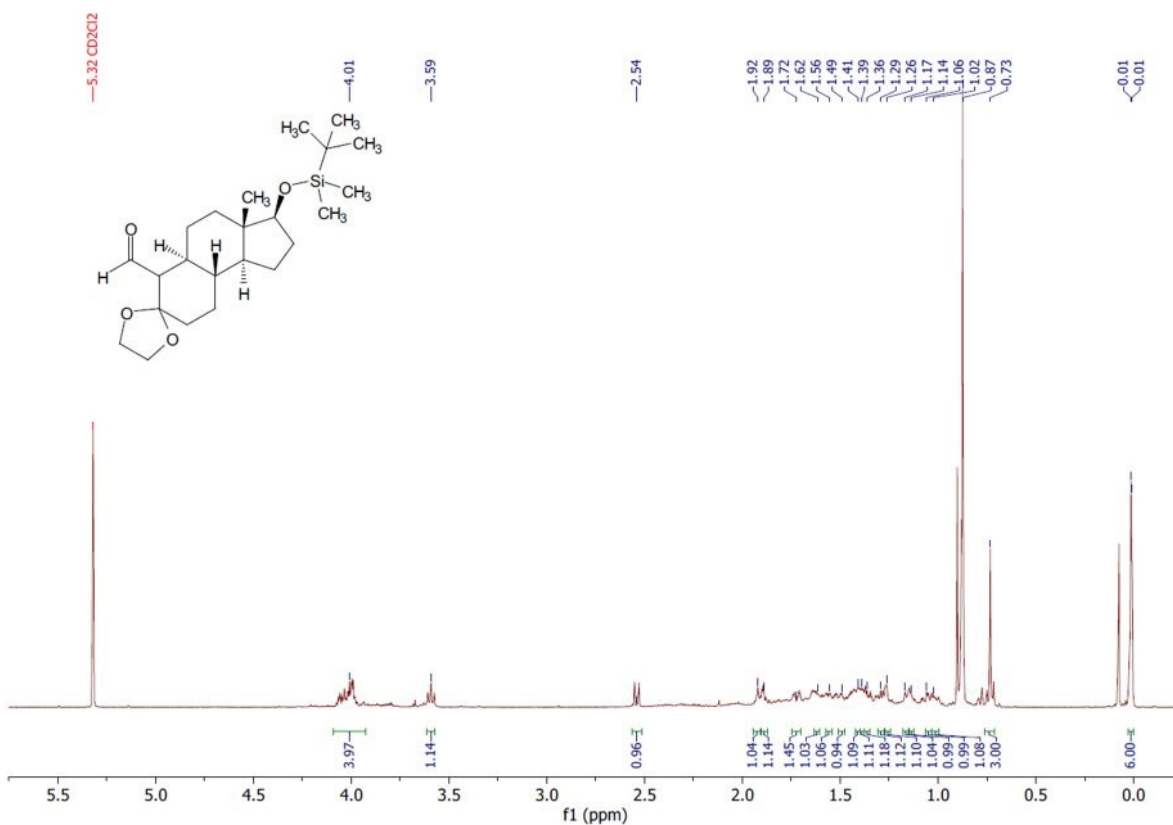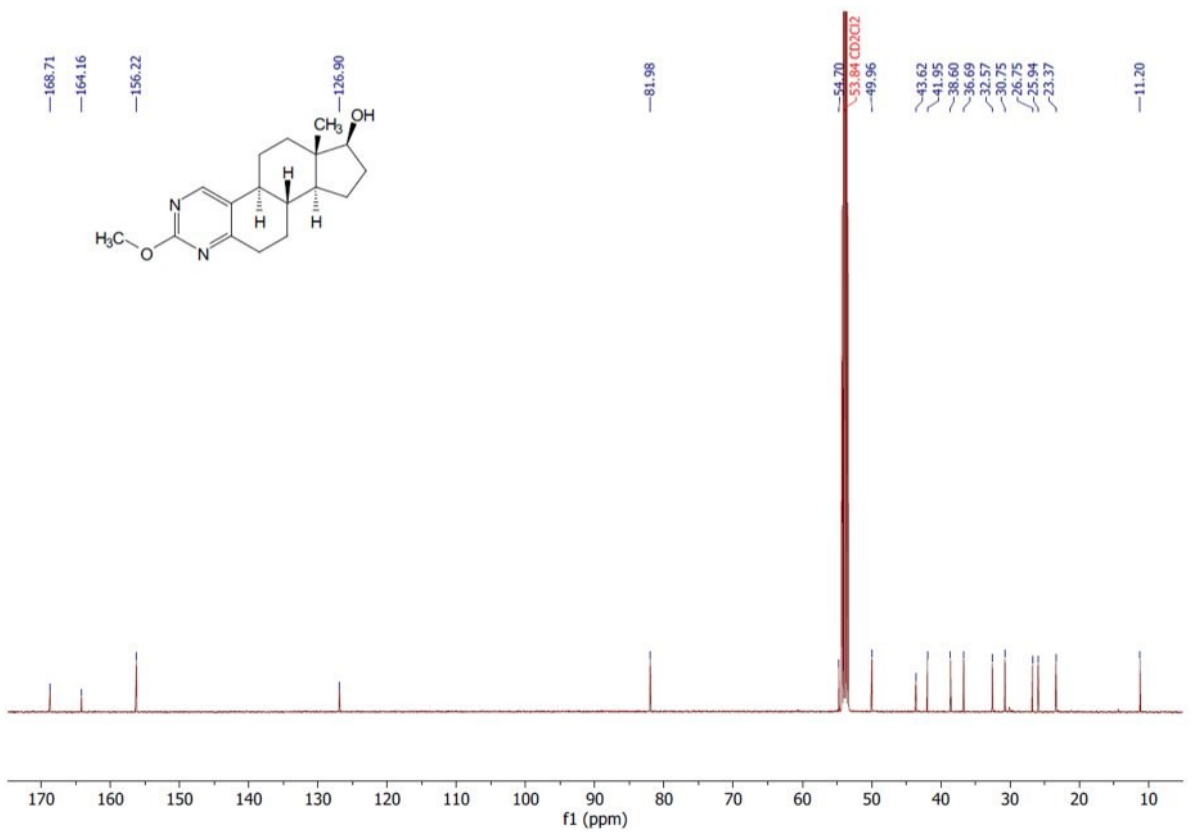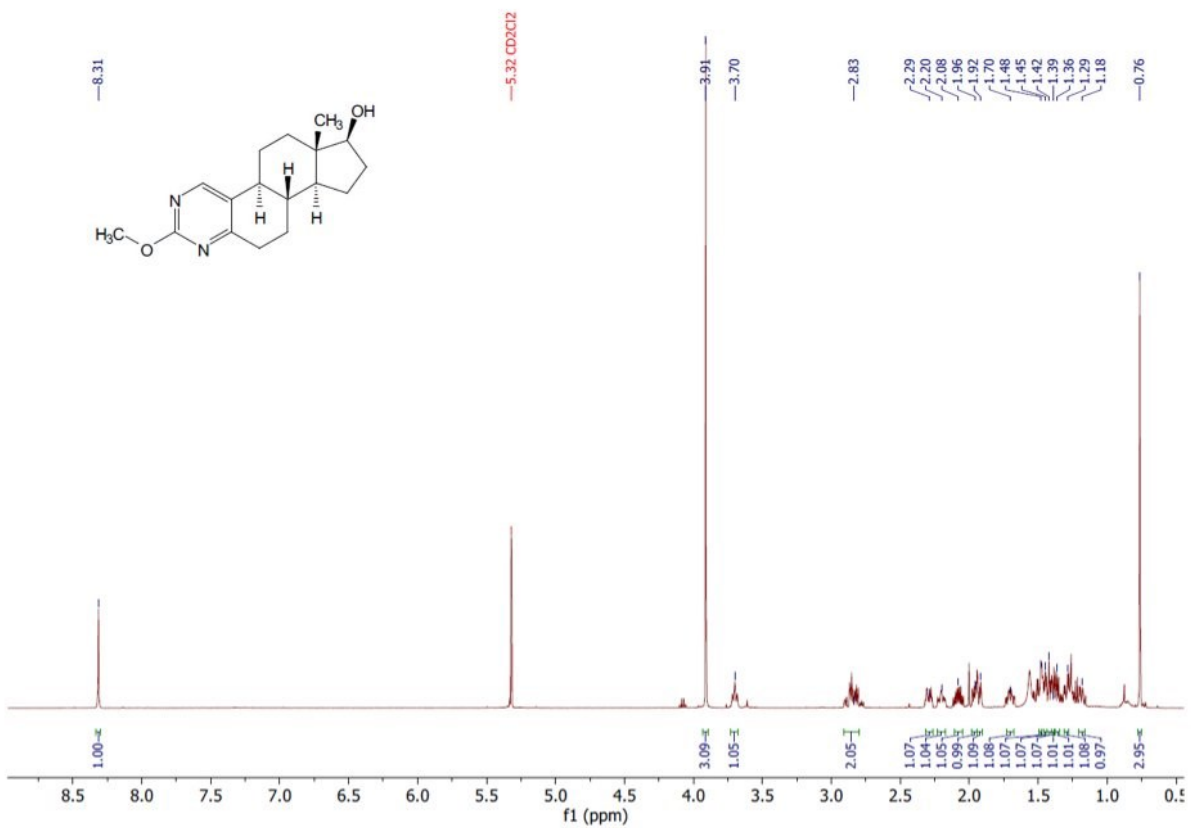# Compound S1
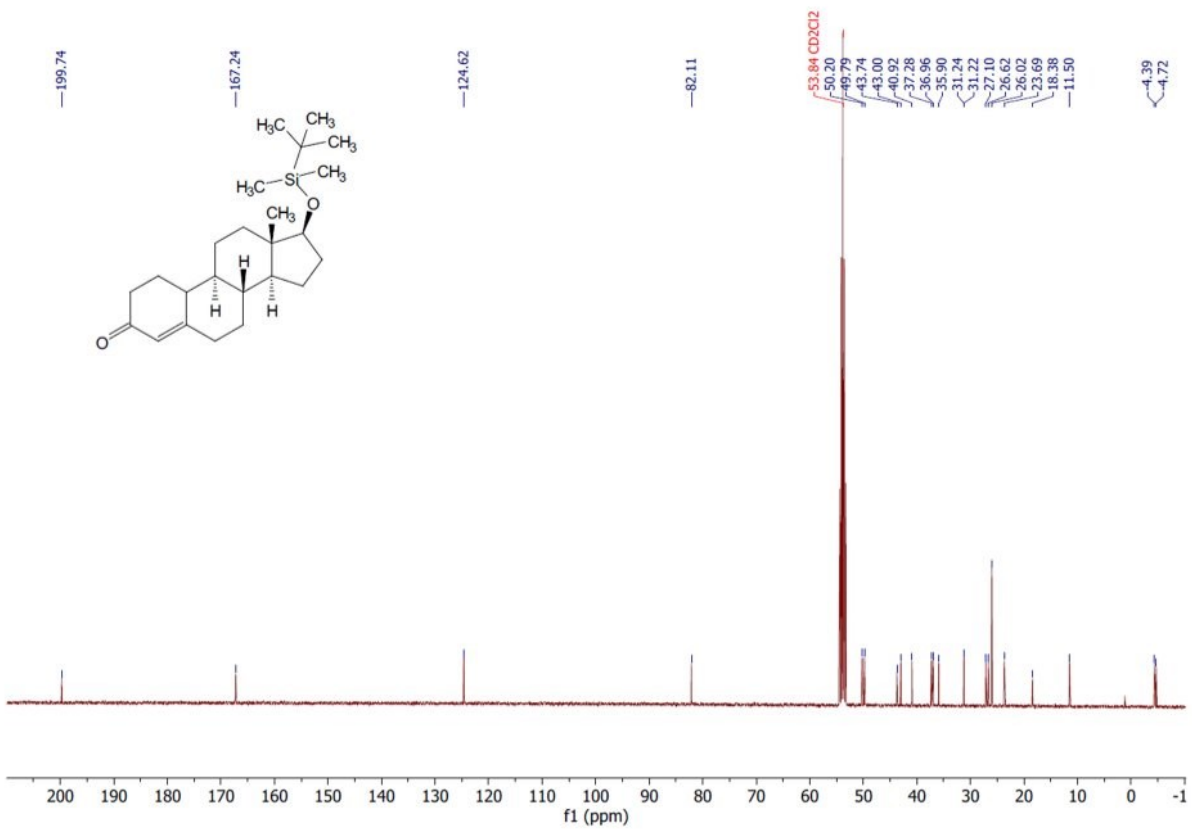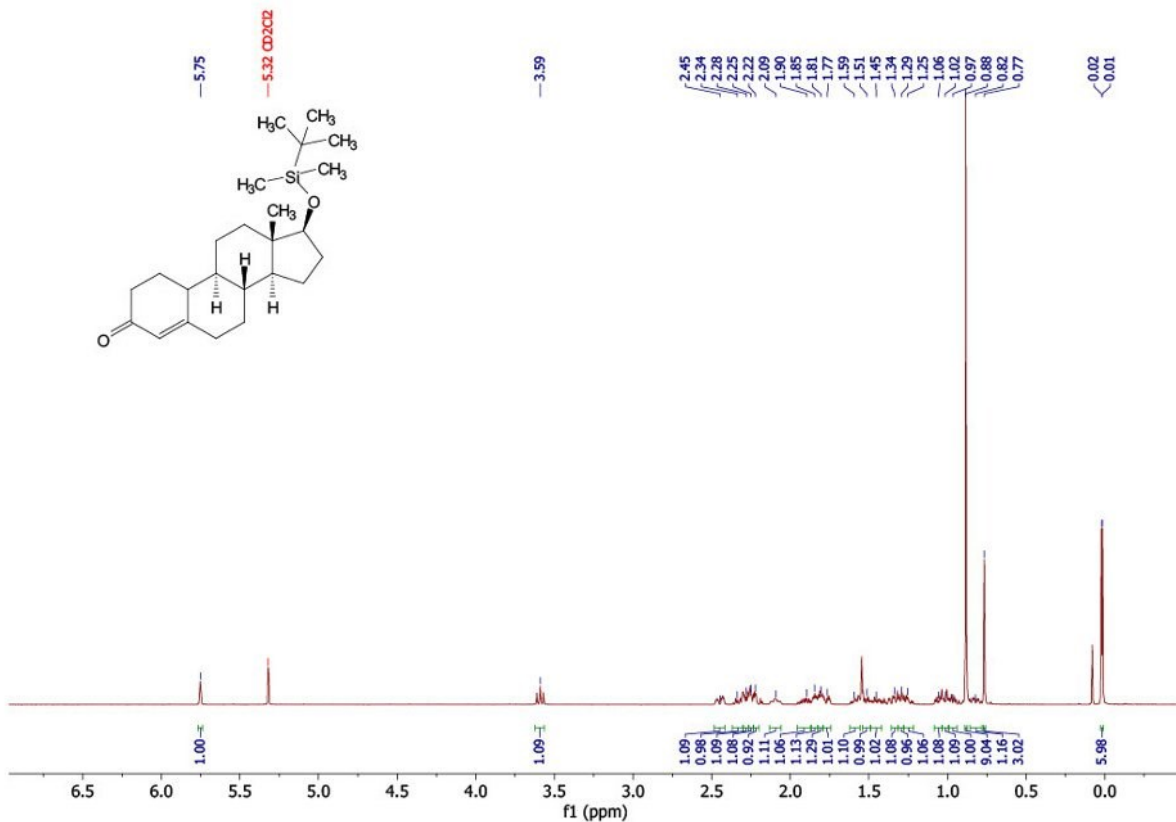
Compound S2
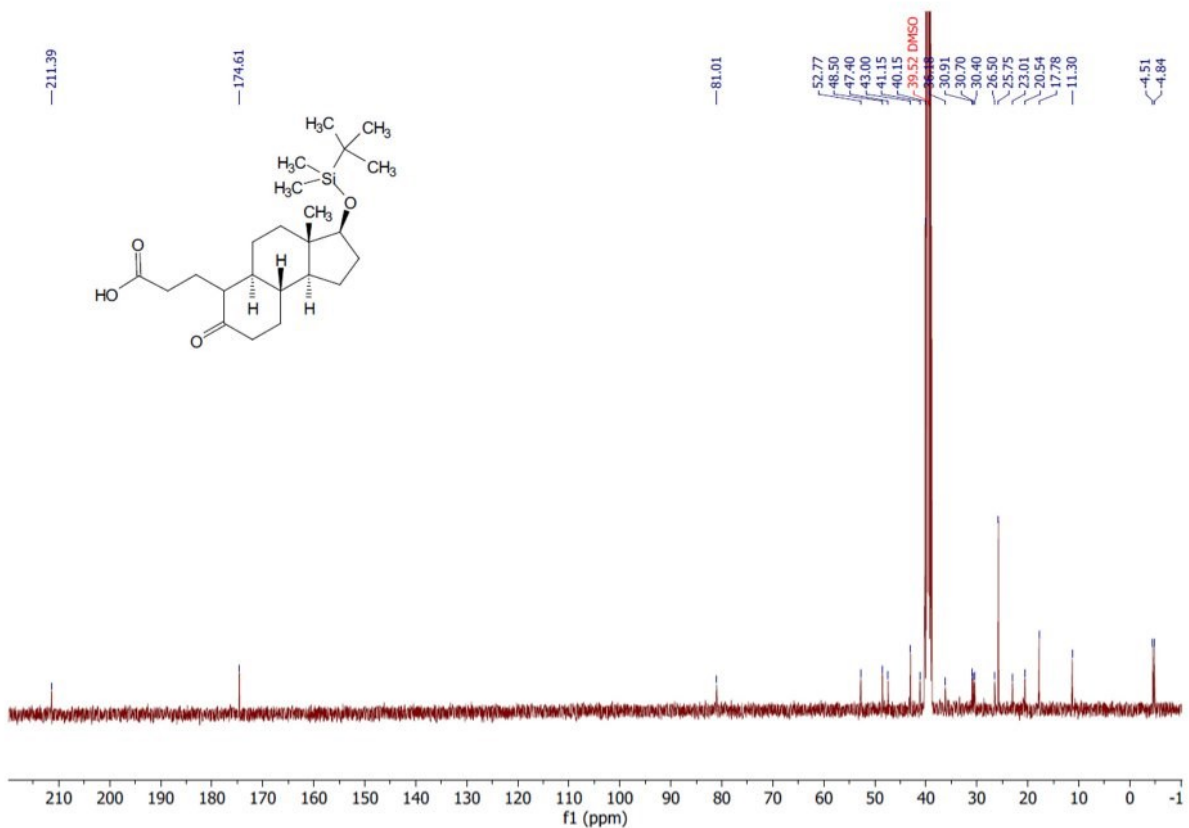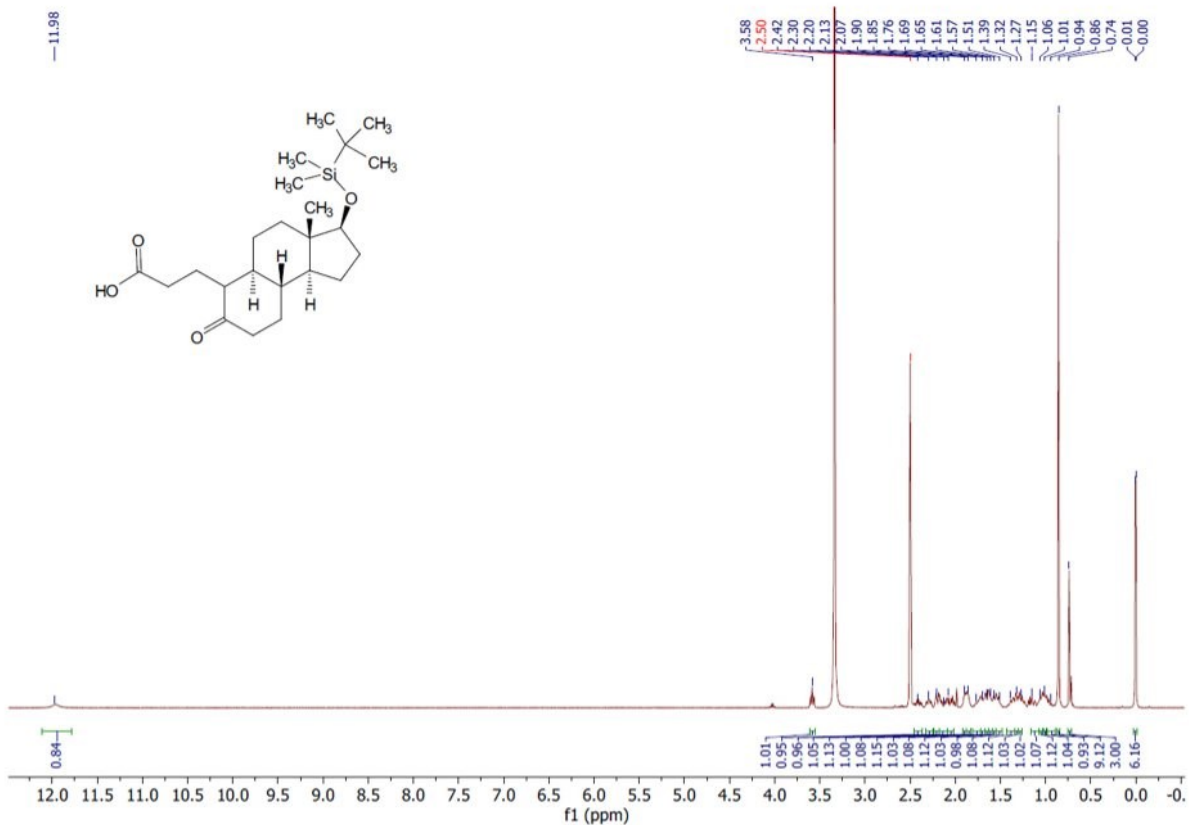
Compound S3a
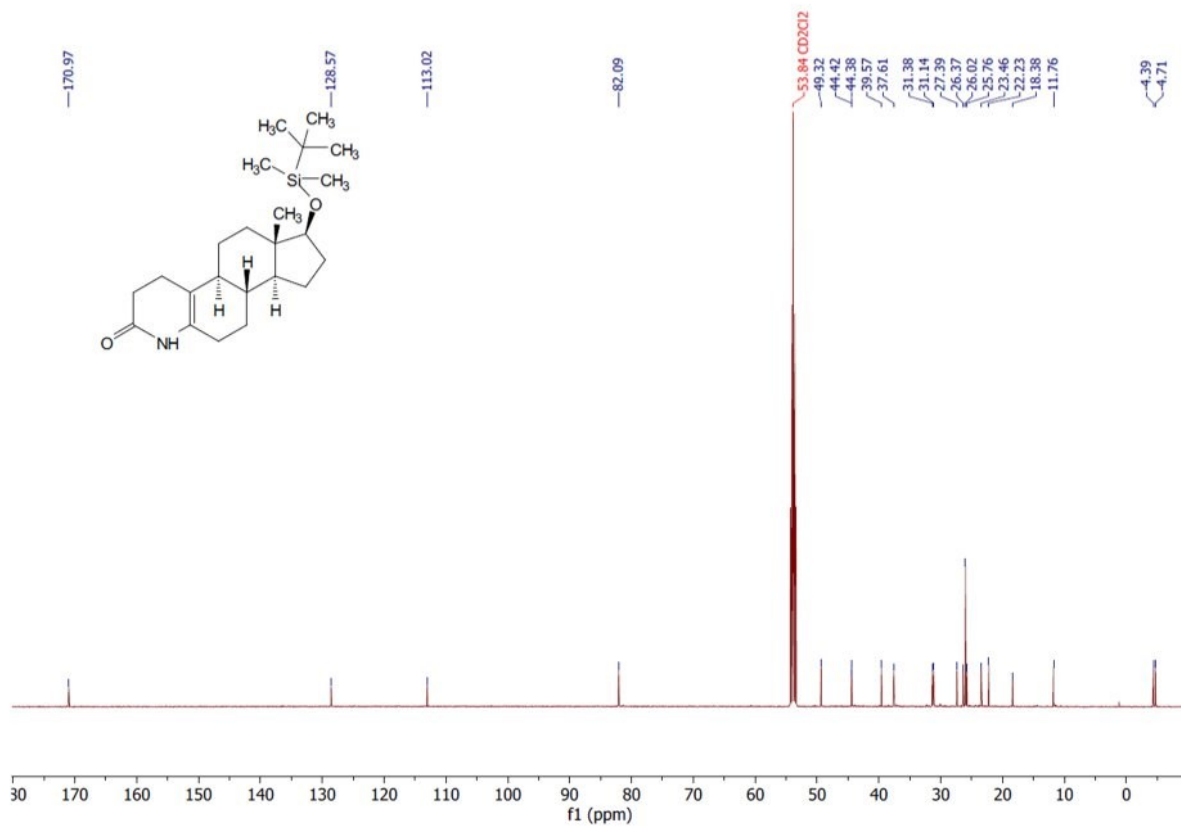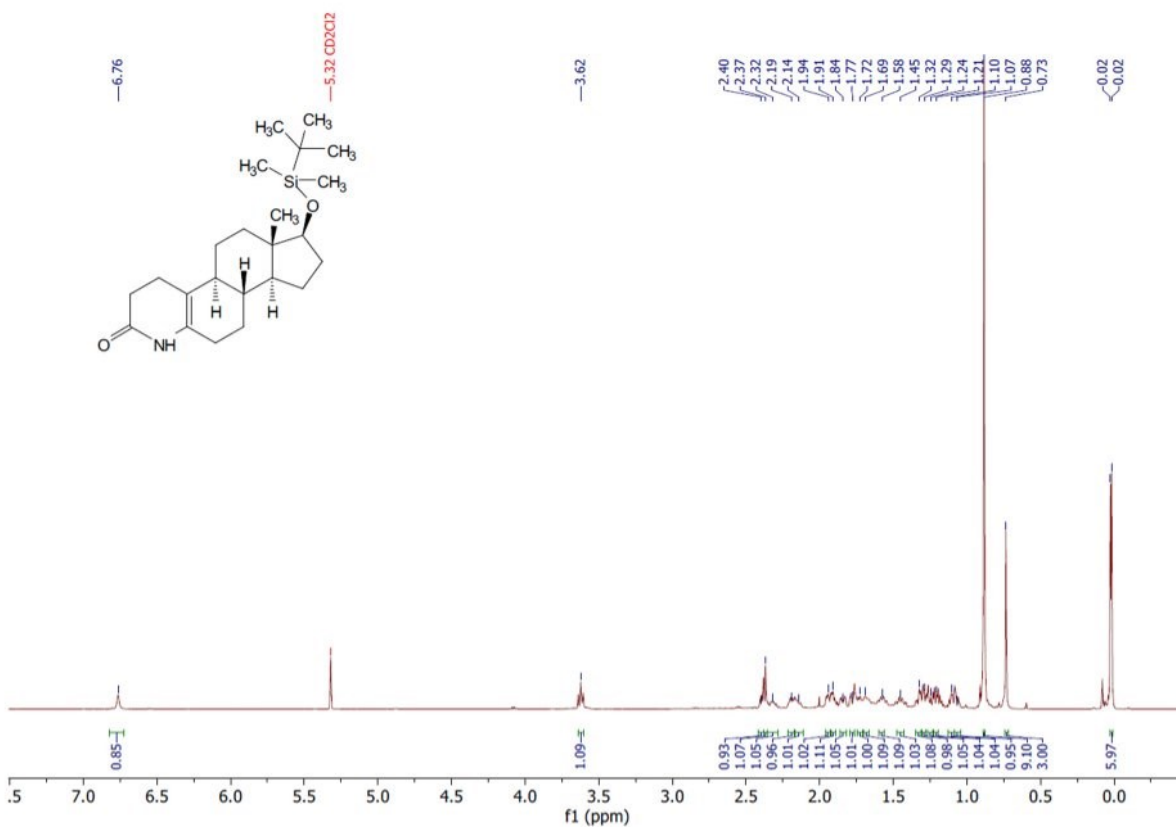
Compound S3b
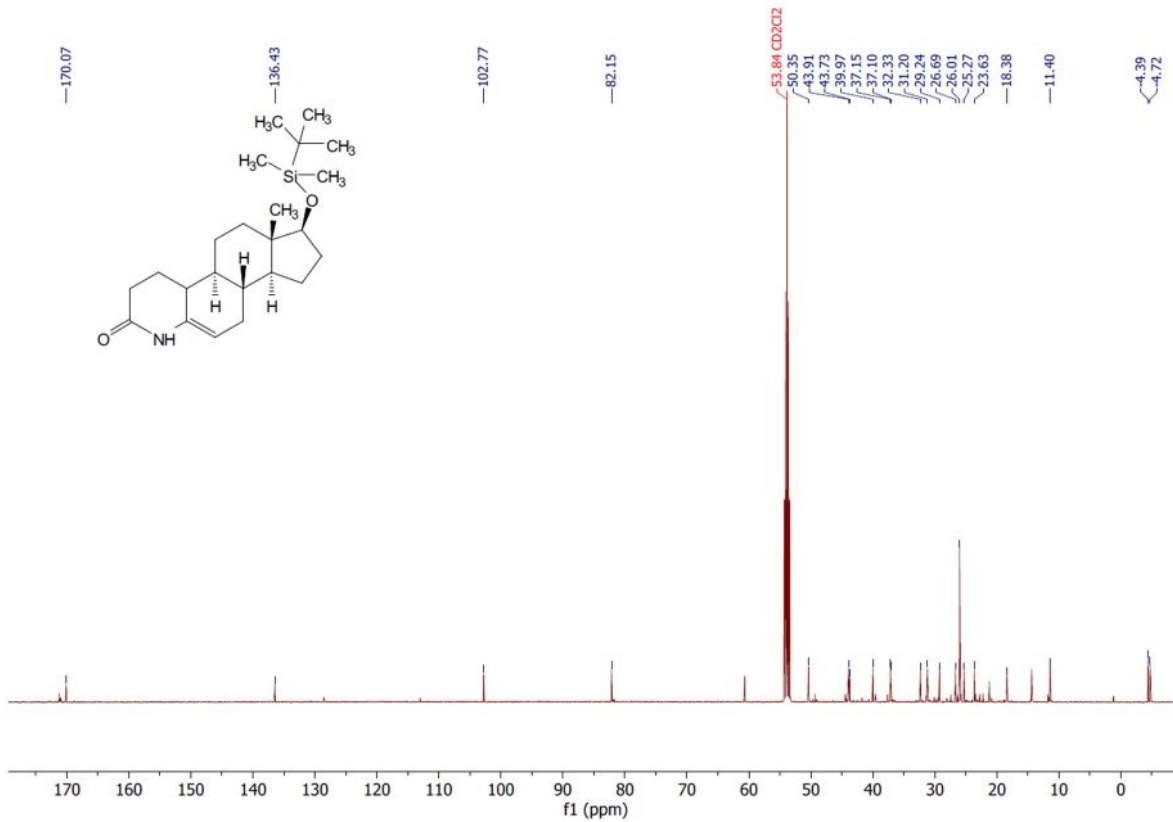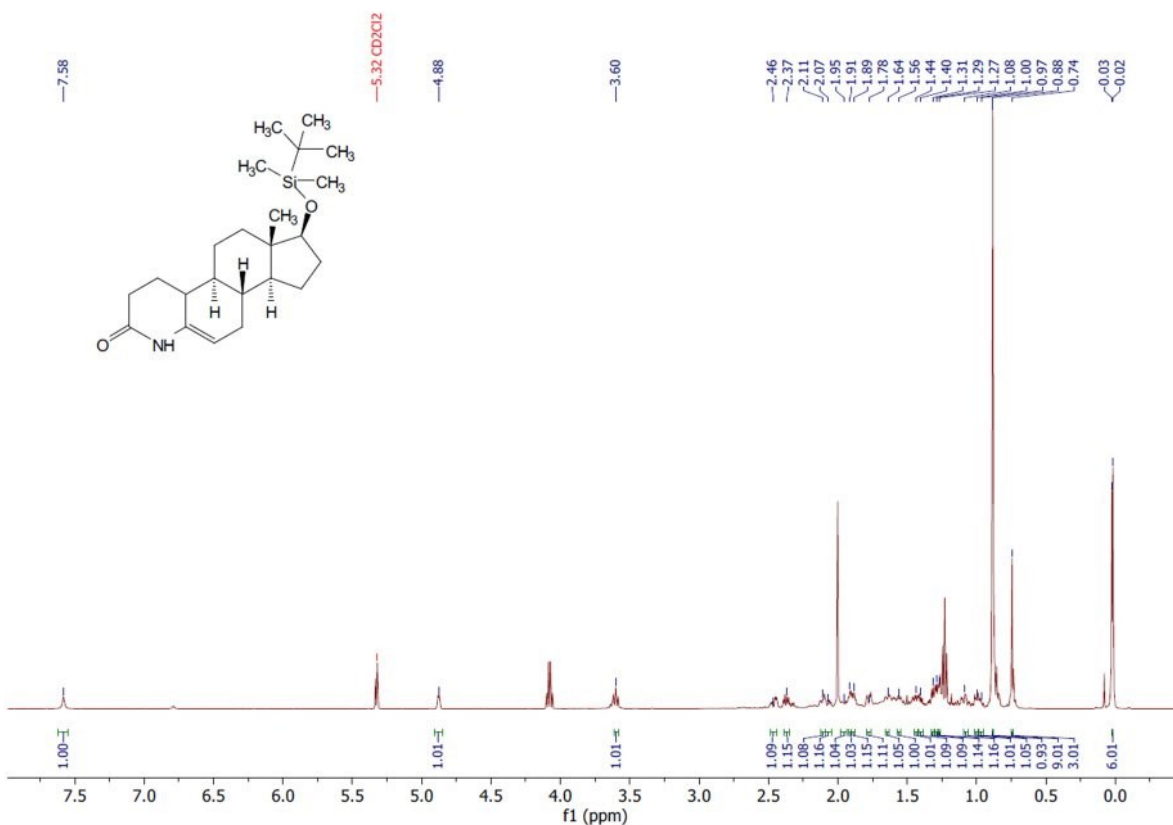
4.2 Biological evaluation

To characterize the pharmacological profile of the synthesized analogs, they were subjected to a profound biological evaluation. The main focus was on the determination of the inhibitory activity on the ion channel TRPML1 and the selectivity towards the two isoforms TRPML2 and TRPML3. As mentioned before, a major downside of the original screening hit **EDME** was the expectable estrogenic effect. Thus, examination of estrogenic effects of **EDME** and the consistently steroidal compounds synthesized throughout this work was another substantial subject. Consequently, the biological evaluation comprised four main aspects: Activity on TRPML1, selectivity within the TRPML subfamily, estrogenic effects and the obligatory test for cytotoxicity. Additionally, a screening for antimicrobial activity was performed using a standard agar diffusion (AD) assay, as this is part of the in-house routine of biological analysis in the BRACHER group.

All studies on ion channel activity were performed in close cooperation with the groups of Prof. Dr. MICHAEL SCHÄFER (Rudolf-Boehm-Institut in Leipzig) and Prof. Dr. Dr. CHRISTIAN GRIMM (Walther-Straub-Institut in Munich). Fluo-4 Ca^{2+} imaging experiments were performed by NICOLE URBAN from the group of Prof. Dr. MICHAEL SCHÄFER at the Rudolf-Boehm-Institut in Leipzig. For the first generation of analogs and the original screening hit **EDME**, Fura-2 Ca^{2+} imaging experiments were performed by myself in the lab of Prof. Dr. Dr. CHRISTIAN GRIMM at the Walther-Straub-Institut in Munich. Patch-clamp, cell invasion and migration as well as autophagy experiments for selected first-generation analogs were conducted by members of the group of Prof. Dr. Dr. CHRISTIAN GRIMM (see Chapter **4.1.1.3** for further details). The screening on estrogenic effects was conducted by Dr. SEBASTIAN DUNST and Dr. VERENA FETZ (Bundesinstitut für Risikobewertung, BfR, Berlin). MTT and AD assays were performed in-house by MARTINA STADLER from the BRACHER group.

4.2.1 TRPML1 inhibitory activity and isoform-selectivity

Activity of the final compounds on the desired target TRPML1 and selectivity over TRPML2 and TRPML3 were investigated by Ca^{2+} imaging experiments. For all assays, transfected HEK293 cells stably expressing the respective ion channel were used. In the cases of TRPML2 and TRPML3, the ion channel is located in the plasma membrane, hence HEK293 cells stably expressing hTRPML2-YFP and hTRPML3-YFP could be used. Since wild-type TRPML1 is not located in the plasma membrane, a mutant variant of TRPML1 that lacks the two late endosome/lysosome (LEL) directing di-leucine motifs (hTRPML1ΔNC-YFP) was used for transfection. Thereby, the channel is localized to the plasma membrane in the transfected cells[169], providing the desired HEK293 cells stably expressing plasma membrane-targeted TRPML1.

Ca²⁺ imaging is the optical measurement of calcium levels by quantification of calcium indicators. The cells are loaded with a fluorescent Ca²⁺ chelator, referred as calcium-dye. In most cases, binding of Ca²⁺ results in a measurable wavelength shift or increase of fluorescence intensity. To ensure membrane permeability of the dye, the respective lipophilic acetoxymethyl esters (AM) are used, which are finally converted into the active form by intracellular esterases (**Figure 19**).
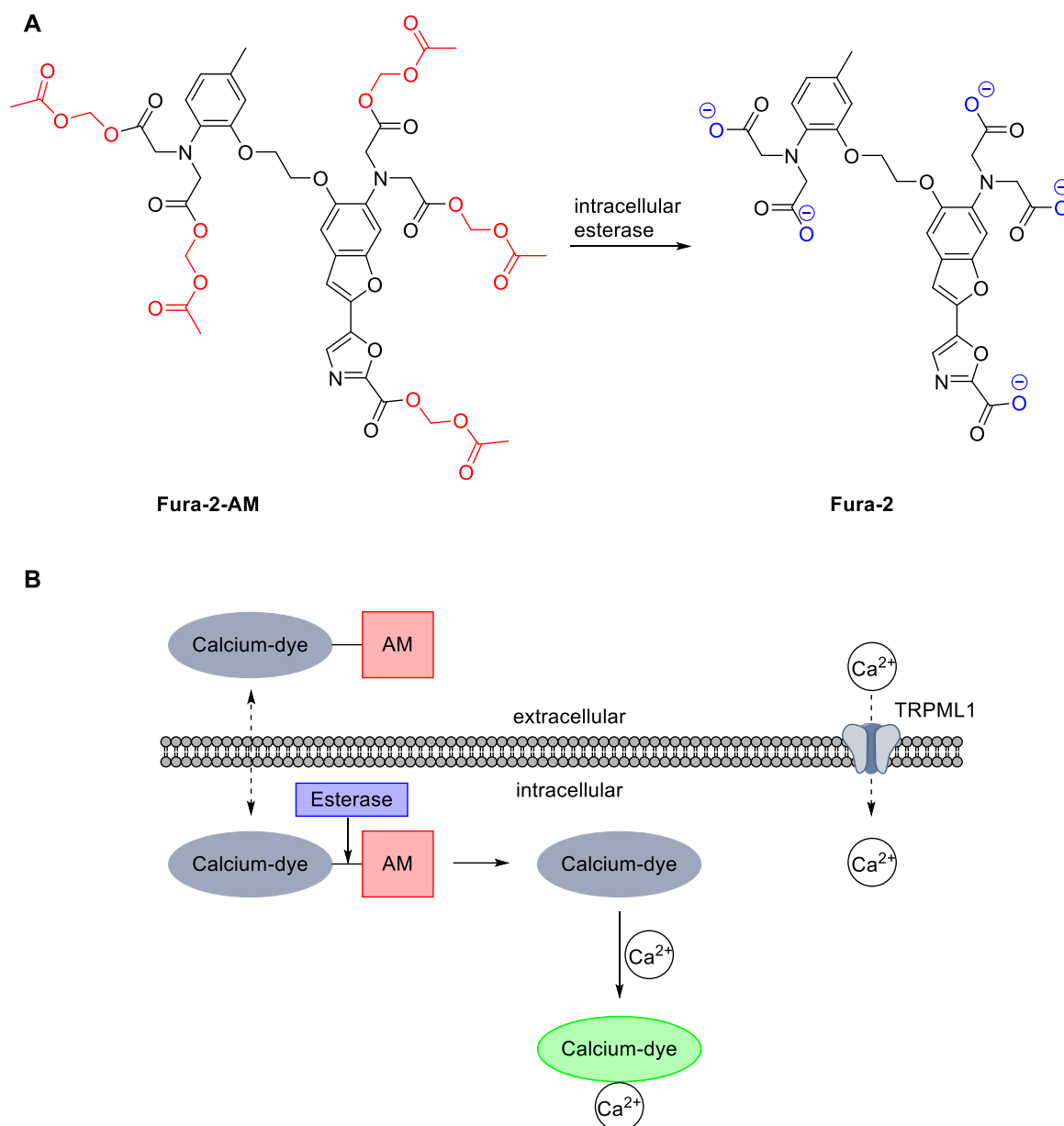
Figure 19: **A**: Fura-2-AM and conversion into the active form Fura-2, **B**: Principle of Ca²⁺ imaging using cells stably expressing membrane targeted TRPML1. Binding of Ca²⁺ leads to a shift of excitation wavelength or increased fluorescence at a defined wavelength

Two types of Ca²⁺ imaging assays were performed in the course of this work: Microscopic single cell Fura-2 Ca²⁺ imaging and fluorescence imaging plate reader (FLIPR) assisted Fluo-

4 Ca^{2+} imaging. While the Fura-2 Ca^{2+} imaging assay only allowed the measurement of one substance at a fixed concentration (in our case 10 µM), the Fluo-4 Ca^{2+} imaging assay enabled a large number of substances at different concentration to be analyzed simultaneously. Concentration-response measurements in the Fluo-4 routine also provided IC$_{50}$ values for each compound for all three TRPML channels.

The first generation of analogs was subjected to both single-cell Fura-2 and FLIPR assisted Fluo-4 Ca^{2+} imaging. The results of all these as well as patch-clamp, cell migration and invasion and autophagy experiments are depicted and analyzed in the publication in Scientific Reports in 2021[84] which is shown in Chapter **4.1.1.3**.

Since the Fura-2 Ca^{2+} imaging procedure we used only allowed investigation of effects at one single concentration (10 µM) and most of the compounds were already active in a lower concentration range the information content of these experiments was in our case limited for further research. For this and economic reasons, all analogs synthesized after this publication (referred as second generation of analogs) were solely subjected to the Fluo-4 Ca^{2+} imaging routine and tested by NICOLE URBAN from the group of Prof. Dr. MICHAEL SCHÄFER in the Rudolf-Boehm-Institut in Leipzig. The advantage of this procedure was that it could directly provide IC$_{50}$ values and selectivity data for each compound. **Figures 20** and **21** show the Fluo-4 Ca^{2+} imaging results of the final compounds of the second generation.
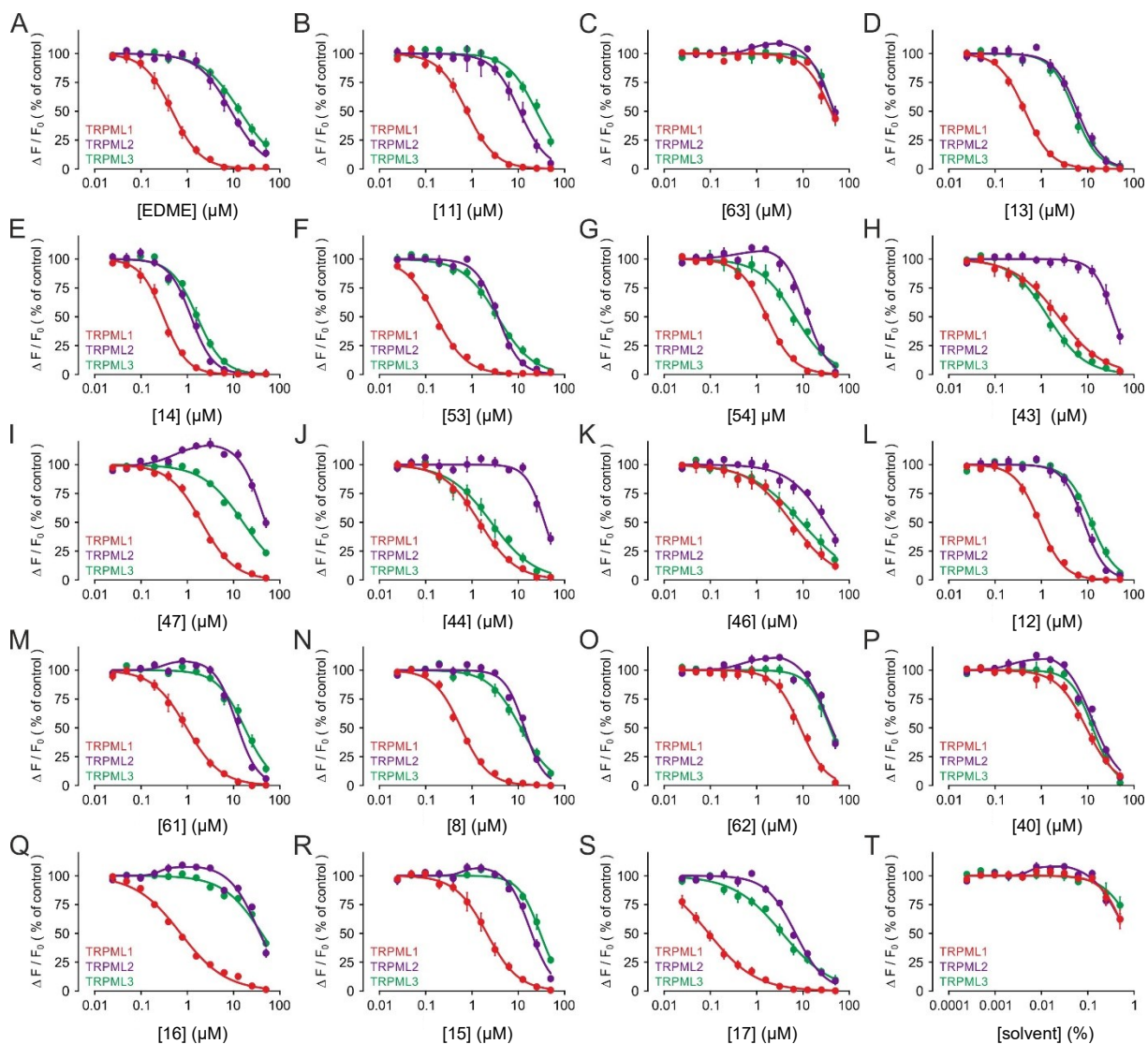
Figure 20: Activity and selectivity curves of the second-generation compounds generated by Fluo-4 Ca^{2+} imaging concentration-response experiments. Compound number in brackets. **A**: Original screening hit **EDME**, **B**-**S**: second-generation analogs. **T**: DMSO control, Compound number in brackets, Red: TRPML1, purple: TRPML2, green: TRPML3. Data are calculated from 3 to 5 independent experiments, each, and represented as means ± SEM. Cells were activated with **ML-SA1** (5 µM)

TRPML1 inhibition
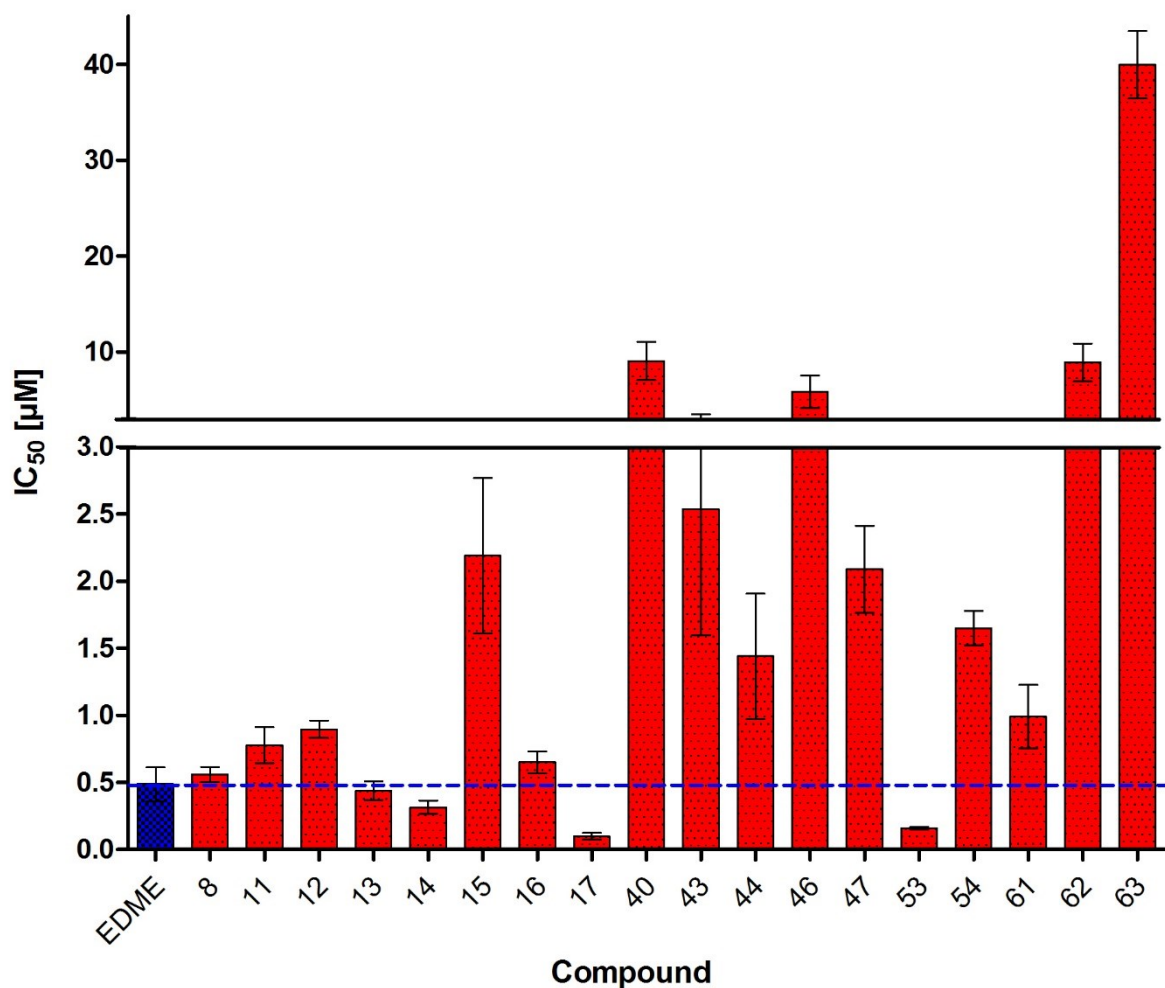
Figure 21: IC$_{50}$ values for TRPML1 inhibition of the second-generation compounds assessed with Fluo-4 Ca^{2+} imaging. Original screening hit **EDME** as a comparison is depicted in blue. Data are calculated from 3 to 5 independent experiments, each, and represented as means ± SEM. Cells were activated with **ML-SA1** (5 µM)
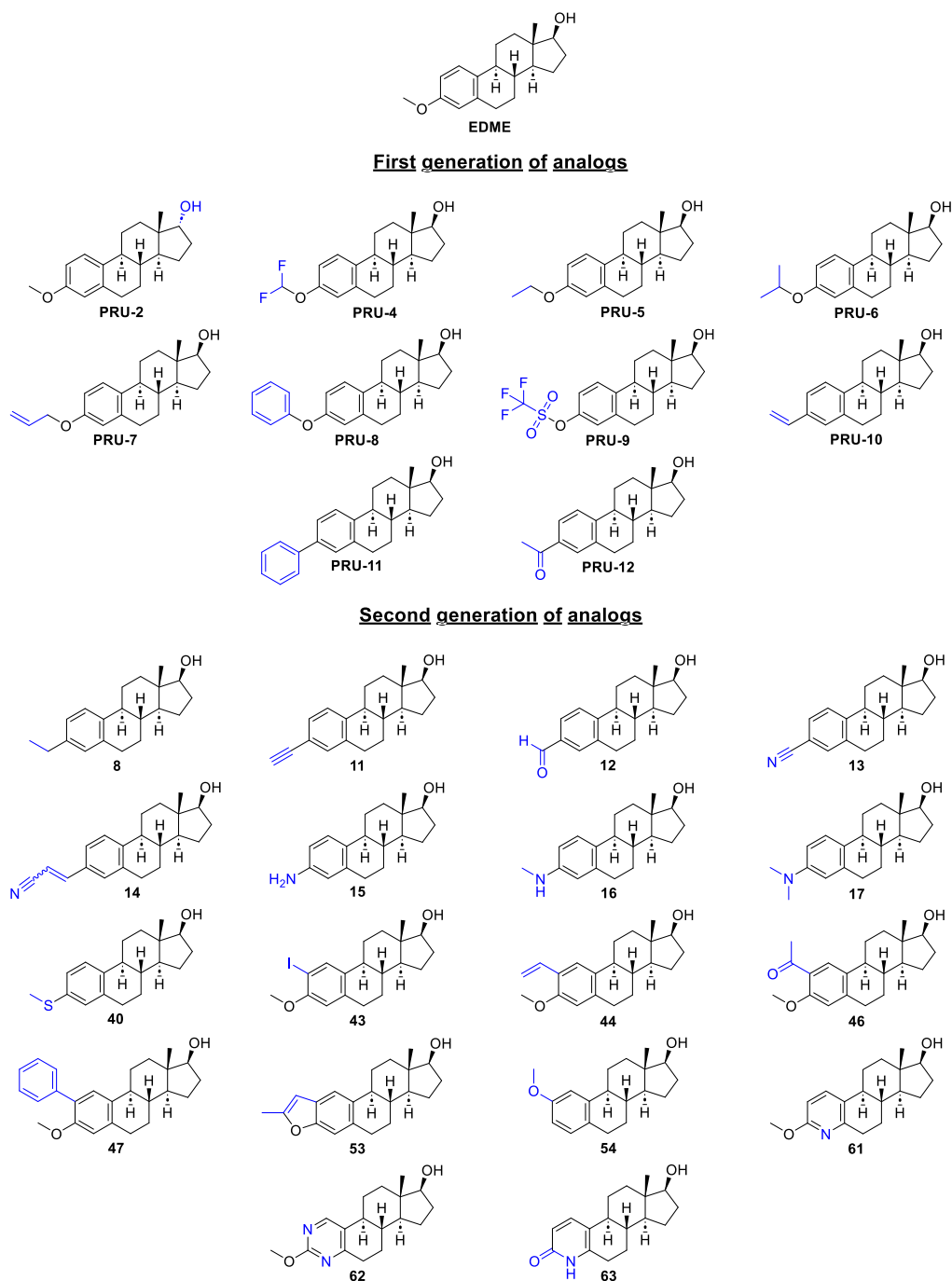
Figure 22: Overview of all synthesized analogs

All tested substances apart from the pyridone analog **63** are TRPML1 inhibitors. Except for the benzofuran analog **53**, the analogs carrying additional substituents at C-2 showed only poor activity. The pyrimidine analog **62**, the 3-methylthio analog **40** and the primary aromatic amine **15** also only exhibit a weak inhibitory effect. Nitriles **13** (IC$_{50}$: 0.4 μM) and **14** (IC$_{50}$: 0.3 μM), benzofuran analog **53** (IC$_{50}$: 0.2 μM) and *N,N*-dimethylamine analog **17** (IC$_{50}$: 0.1 μM) revealed lower IC$_{50}$ values than the original screening hit **EDME** (IC$_{50}$: 0.5 μM). The two most potent compounds are **53** and **17** with IC$_{50}$ values of 0.2 μM and 0.1 μM. The comparison of the three

3-amino analogs **15**, **16** and **17** indicates that deletion of methyl groups within this series is detrimental for TRPML1 inhibitory activity. While the *N,N*-dimethylamino analog **17** is highly potent, the activity of the *N*-monomethylamino analog **16** is lower, yet still moderate. Whereas primary aromatic amine **15** with an IC_{50} over 2 µM shows the weakest inhibition of these three compounds.

All analogs exhibiting moderate to good TRPML1 inhibitory activity (IC_{50} < 1.50 µM) possess a decent isoform-selectivity profile. Among them, acrylonitrile **14** (**Figure 20 E**) is the least selective with a 4.0-fold selectivity over TRPML2 and a 5.3-fold selectivity over TRPML3. The most potent TRPML1 inhibitors **53** (**Figure 20 F**) and **17** (**Figure 20 S**) show excellent isoform-selectivity concomitantly. Interestingly, 2-iodo analog **43** is more active on TRPML3 than on TRPML1. Unfortunately, it is not TRPML3 selective as the inhibitory curves for both these channels are in a similar concentration range (**Figure 20 H**).

Figure 23 and **Table 2** present the activity on TRPML channels for the first and the second generation of analogs together and thus provide an overview of the overall results:
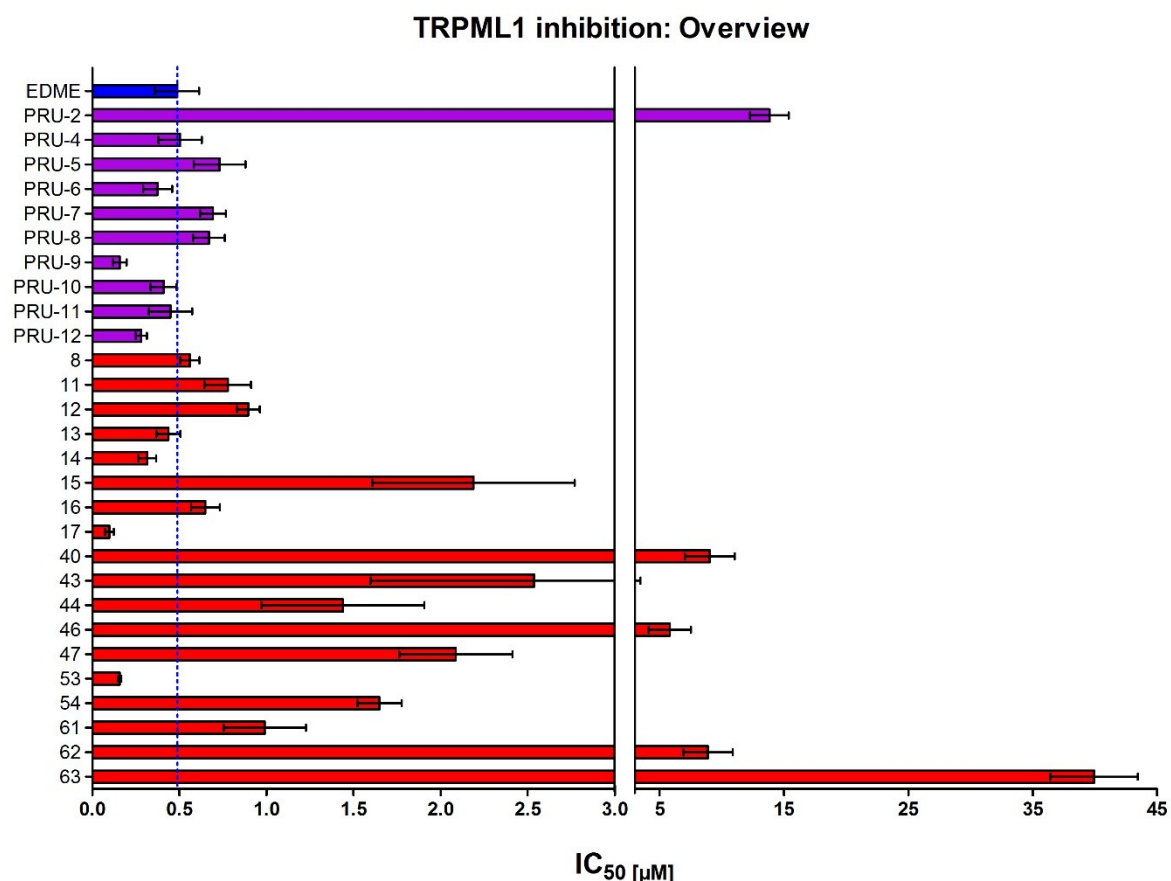
Figure 23: IC_{50} for TRPML1 inhibition of all compounds assessed with Fluo-4 Ca^{2+} imaging, blue: **EDME**, purple: first generation of analogs, red: second generation of analogs. Data are calculated from 3 to 5 independent experiments, each, and represented as means ± SEM. Cells were activated with **ML-SA1** (5 µM)

Compound	IC$_{50}$ TRPML1	IC$_{50}$ TRPML2		IC$_{50}$ TRPML3	
EDME	0.5	5.9	(9.8 fold)	20	(33 fold)
PRU-2	14	37	(2.6 fold)	> 50	(n.d.)
PRU-4	0.5	5.2	(10 fold)	4.8	(9.6 fold)
PRU-5	0.8	3.4	(4.3 fold)	15	(19 fold)
PRU-6	0.4	3.6	(9.0 fold)	7.9	(20 fold)
PRU-7	0.7	2.6	(3.7 fold)	15	(22 fold)
PRU-8	0.7	15	(22 fold)	39	(55 fold)
PRU-9	0.2	2.5	(13 fold)	6.0	(30 fold)
PRU-10	0.4	54	(135 fold)	16	(40 fold)
PRU-11	0.4	2.4	(6.0 fold)	32	(80 fold)
PRU-12	0.3	5.3	(18 fold)	14	(47 fold)
8	0.6	14	(23 fold)	11	(19 fold)
11	0.8	11	(13 fold)	25	(31 fold)
12	0.9	8.3	(9.2 fold)	12	(13 fold)
13	0.4	6.1	(15 fold)	5.2	(13 fold)
14	0.3	1.2	(4.0 fold)	1.6	(5.3 fold)
15	2.1	18	(8.5 fold)	30	(14 fold)
16	0.7	33	(47 fold)	41	(58 fold)
17	0.1	6.9	(69 fold)	3.6	(36 fold)
40	9.4	13	(1.3 fold)	13	(1.4 fold)
43	2.4	36	(n.d.)	1.4	(n.d.)
44	1.5	37	(25 fold)	2.6	(1.7 fold)
46	5.7	31	(5.4 fold)	9.5	(1.7 fold)
47	2.1	41	(20 fold)	16	(7.6 fold)
53	0.2	3.6	(18 fold)	3.6	(18 fold)
54	1.7	12	(6.8 fold)	6.0	(3.5 fold)
61	1.0	12	(12 fold)	17	(17 fold)
62	8.8	35	(3.9 fold)	38	(4.4 fold)
63	40	42	(n.d.)	45	(n.d.)

Table 2: Depiction of the IC$_{50}$ values of all final compounds at the three TRPML isoforms assessed by Fluo-4 Ca^{2+} imaging. In parentheses: fold selectivity at TRPML1 over the respective isoform, n.d.: not determined

The results of the Fluo-4 Ca^{2+} imaging can be resumed as follows: Triflate **PRU-9**, 3-vinylanalog **PRU-10**, 3-acetyl analog **PRU-12**, benzofuran analog **53** and *N,N*-dimethylamine analog **17** are the five best compounds as they are more potent than **EDME** and

simultaneously possess an excellent selectivity profile. Though it has to be mentioned, that triflate **PRU-9** can't be characterized as suitable chemical tool due to the instability of the molecule. Among these five top hits, **17** and **53** can be classified as the two most promising analogs as they have the lowest IC_{50} value for TRPML1 inhibition.
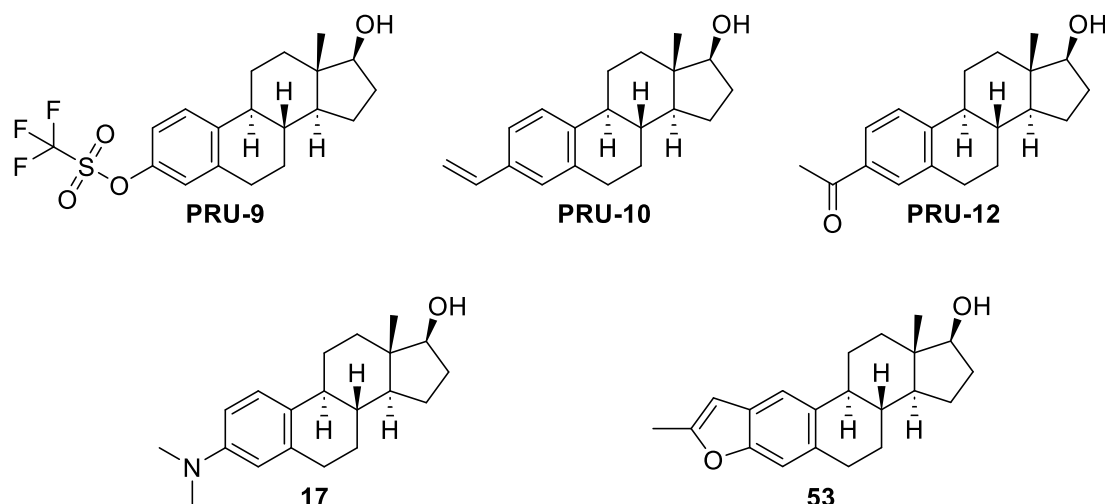
Figure 24: The five most potent TRPML1 inhibitors

4.2.2 Estrogenic effects

To assess estrogenic effects of **EDME** and all synthesized final compounds, they were subjected to the E-Morph screening assay[170]. The assay leverages an estrogen-dependent and clinically relevant phenotypic readout to measure ERα signaling activity in MCF-7 breast cancer cells *via* high-throughput confocal microscopy and automated image analysis[171-173]. In the E-Morph screening assay, MCF-7/E-Cad-GFP are treated with the antiestrogen fulvestrant (Fulv). This results in a profound restructuring of cell-cell contacts, such as altered E-Cadherin membrane distribution and increased E-Cadherin-GFP signal intensity (SI) within 48 h. This effect can be prevented by co-treatment of the cells with Fulv and estrogenic test substances like 17β-estradiol (E2) in a concentration-dependent manner. In brief, the cells were co-exposed with 10 nM Fulv and the respective compound at six different concentrations (0.001-100 µM). After 48 hours, the SI was measured and the EC_{50} values were determined with the help of the resulting concentration-response curves.

The results of the E-Morph screening assay for all final compounds are depicted in the following table:

Compound	Estrogenic effect EC$_{50}$ [µM]	Categorization
Estradiol (E2)	< 0.001	Positive control, strong
EDME	< 0.001	strong
PRU-5	< 0.001	strong
54	< 0.001	strong
PRU-6	< 0.001	strong
47	< 0.001	strong
PRU-7	< 0.001	strong
PRU-12	0.002	strong
16	0.01	strong
14	0.01	strong
17	0.02	strong
12	0.02	strong
8	0.03	strong
13	0.06	strong
15	0.07	strong
53	0.10	moderate
PRU-2	0.10	moderate
PRU-11	0.12	moderate
PRU-4	0.13	moderate
PRU-10	0.15	moderate
43	0.16	moderate
PRU-8	0.25	moderate
11	0.31	moderate
PRU-9	0.39	moderate
61	1.02	weak
44	1.45	weak
46	1.72	weak
40	2.76	weak
63	3.97	weak
62	11	weak

Table 3: Estrogenic effects of the synthesized compounds assessed with the E-Morph screening assay. Based on their respective EC$_{50}$ the compounds are categorized into the groups "strong" (< 0.1 µM), "moderate" (0.1 µM ≤ EC$_{50}$ < 1.0 µM) and "weak" (EC$_{50}$ ≥ 1.0 µM)

The original screening hit **EDME** exhibited a strong estrogenic effect in the assay. **EDME**, 2-methoxy estrane **53**, 2-phenyl analog **47** and the 3-phenolethers **PRU-5**, **PRU-6** and **PRU-7** lie in the same range as the positive control and endogenous ligand **E2**. They cannot be further distinguished as their EC_{50} is below the lowest applied concentration. The three amines **15**, **16** and **17** as well as the two nitriles **13** and **14** also displayed strong estrogenic effects. The benzofuran **53**, diphenylether **PRU-8**, biphenyl **PRU-11**, triflate **PRU-9** and vinyl analog **PRU-12** belong to the "moderate" group. The group of "weak" agonists comprises 2-vinyl compound **44**, 2-acetyl compound **46**, 3-methylthio analog **40** and the three azaanalogs **61**, **62** and **63**. Of all the tested substances, the pyrimidine **62** showed the weakest estrogenic effect with an EC_{50} of 11 μM.

Estrogenic effect
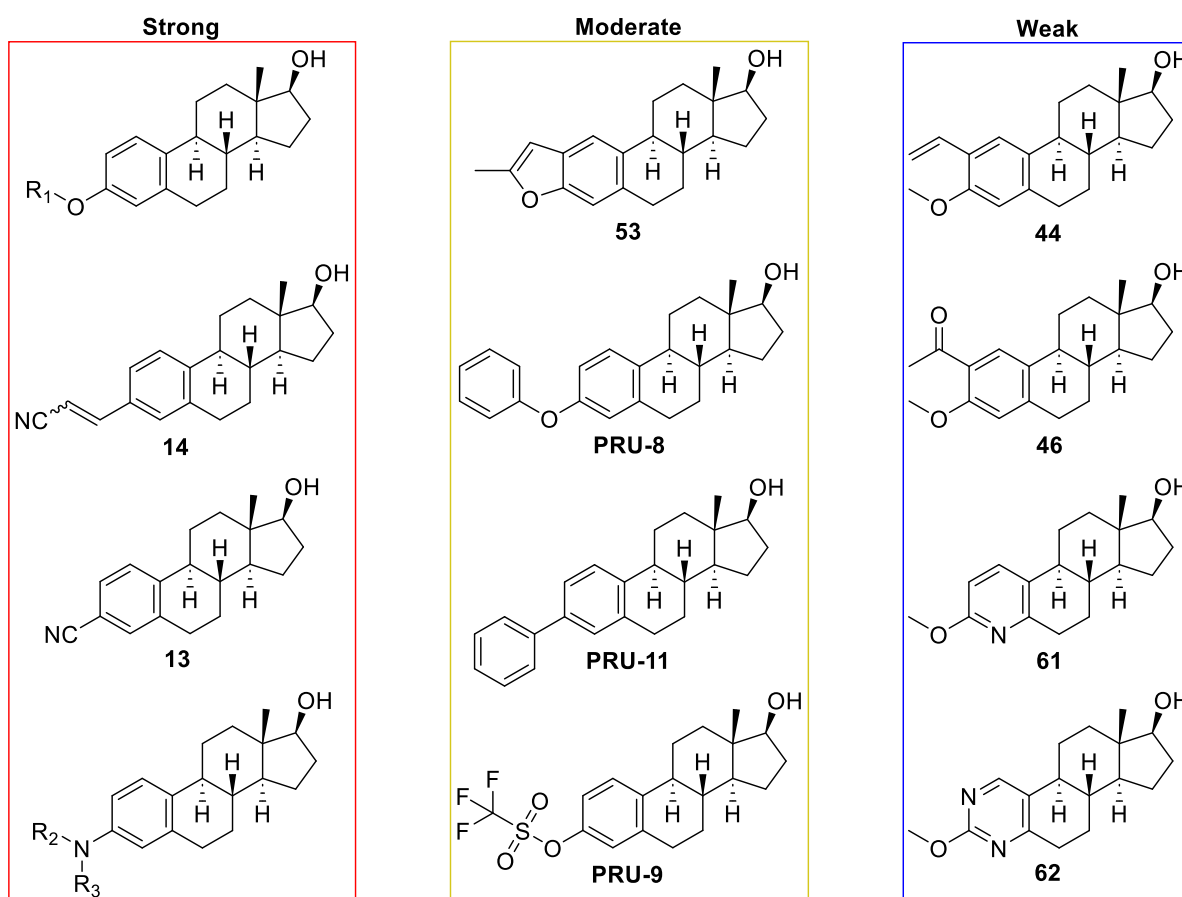
Figure 25: Selected compounds of the three groups. R_1=CH_3: **EDME**; R_1=C_2H_5: **PRU-5**; R_1=isopropyl: **PRU-7**; R_1=allyl: **PRU-8**; R_2=R_3=H: **15**; R_2=CH_3, R_3=H: **16**; R_2=R_3= CH_3: **17**

160

4.2.3 MTT assay

Since the synthesized substances were investigated using cell experiments, it was essential to evaluate their cytotoxicity. The results of these can only be correctly interpreted if the molecules do not exhibit noteworthy cytotoxicity in the used concentration range. Hence, all final compounds were subjected to a routine MTT assay according to a protocol of MOSMANN[174] performed by MARTINA STADLER from the BRACHER group. The assay was conducted in human leukemia cell line HL-60, Triton™ X-100 was used as positive control. It is based on the reduction of 3-(4,5-dimethylthiazol-2-yl)-2,5-diphenyltetrazolium bromide (MTT) to 5-(4,5-dimethylthiazol-2-yl)-1,3- diphenylformazan in living cells. More precisely, the soluble yellow tetrazolium salt MTT is converted into the insoluble blue formazan by dehydrogenases (**Scheme 49**). This reaction only occurs in metabolically active cells provided that NADH and NADPH are present.

MTT (yellow)   **formazan** (blue)
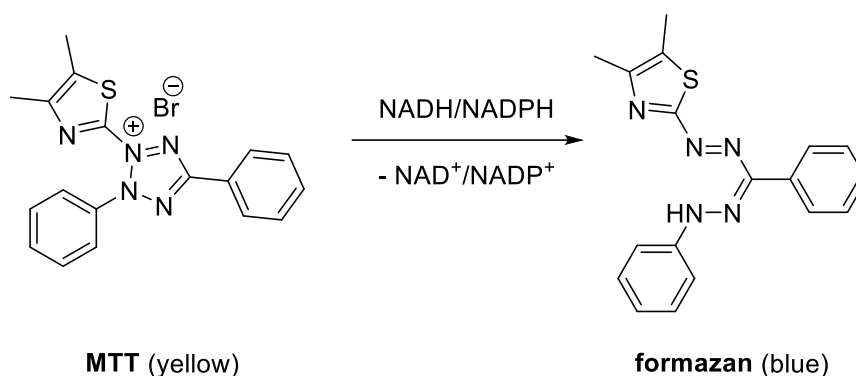
Scheme 49: Reduction of MTT to the formazan in living, metabolically active cells

Consequently, the amount of produced formazan, which can be measured photometrically correlates with cell viability. By means of concentration-response experiments, an IC_{50} value for cytotoxic activity can be determined for each compound.

Compound	IC_{50} [µM]	Compound	IC_{50} [µM]	Compound	IC_{50} [µM]
EDME	25	PRU-12	22	43	> 50
PRU-2	23	8	> 50	44	> 50
PRU-4	28	11	> 50	46	> 50
PRU-5	28	12	> 50	47	> 50
PRU-6	20	13	> 50	53	> 50
PRU-7	27	14	> 50	54	> 50
PRU-8	24	15	> 50	61	> 50
PRU-9	18	16	> 50	62	> 50
PRU-10	18	17	> 50	63	> 50
PRU-11	13	40	> 50		

Table 4: Cytotoxicity of all final compounds assessed with the MTT assay

161

For all the substances, the IC_{50} value for TRPML1 inhibition is far below the IC_{50} of the MTT assay. Thus, none of the compounds exhibits any significant toxicity in the employed concentrations.

4.2.4 Agar diffusion assay

To assess potential antimicrobial effects, all final compounds were submitted to a standard agar diffusion assay. The assay carried out by MARTINA STADLER of the BRACHER group included tests against Gram-positive (*Streptococcus entericus*, *Staphylococcus equorum*) and Gram-negative bacteria (*Escherichia coli*, *Pseudomonas marginalis*) as well as against fungi (*Yarrowia lipolytica*, *Saccharomyces cerevisiae*). As a reference, tetracycline was used for antibacterial activity and clotrimazole for antifungal activity as a positive control.

In none of the tests an inhibition zone could be observed for any of the compounds. Accordingly, no compound exhibits antimicrobial activity against any of the listed germs.

4.2.5 Conclusions for structure-activity relationships

For the concluding evaluation of the synthesized compounds, it is important to consolidate the information from the Fluo-4 Ca^{2+} imaging and the E-Morph assay. The combined results of the respective best compounds from both assays are depicted in the following table:

Entry	Compound	IC$_{50}$ TRPML1 [µM]	IC$_{50}$ TRPML2 [µM]	IC$_{50}$ TRPML3 [µM]	Estrogenic effect (EE) EC$_{50}$ [µM]	Relative activity (LogIC$_{50}$ TRPML1 - LogIC$_{50}$ EE)
1	EDME	0.5	5.9	19.5	< 0.001 (strong)	> 2.69
2	61	1.0	12	17	1.02 (weak)	-0.01
3	44	1.5	37	2.6	1.45 (weak)	0.01
4	46	5.7	31	9.5	1.72 (weak)	0.52
5	40	9.4	13	13	2.76 (weak)	0.53
6	63	40	42	45	4.0 (weak)	1.01
7	62	8.8	35	38	11 (weak)	-0.1
8	PRU-9	0.2	2.5	6.0	0.39 (moderate)	-0.29
9	PRU-10	0.4	54	16	0.15 (moderate)	0.43
10	53	0.2	3.6	3.6	0.10 (moderate)	0.30
11	PRU-12	0.3	5.3	14	0.002 (strong)	2.14
12	17	0.1	6.9	3.6	0.02 (strong)	0.72

Table 5: Combined results of the Fluo-4 Ca^{2+} imaging and the E-Morph assay. Entries 2-7 represent the substances that had the weakest effect in the E-Morph assay. Entries 8-12 represent the best hits in the Fluo-4 Ca^{2+} imaging. A negative relative activity suggests higher inhibitory activity on TRPML1 than agonistic activity in the E-Morph assay

From the group of weak ER agonists (EC$_{50}$ ≥ 1.0 µM), only the 2-vinyl analog **44** and pyridine **61** are moderate to decent TRPML1 inhibitors. While **44** is slightly more active on estrogen receptors (EC$_{50}$ = 1.45 µM vs IC$_{50}$ on TRPML1 = 1.5 µM), the effects of **61** in both assays were nearly balanced (EC$_{50}$ = 1.02 µM vs IC$_{50}$ on TRPML1 = 1.0 µM). Out of the top compounds of the Fluo-4 Ca^{2+} imaging, only **PRU-9** shows a negative relative activity, meaning that the ER agonistic effect in the E-Morph assay is lower than the inhibitory effect on TRPML1. The 3-vinyl analog **PRU-10** and the benzofuran **53** belong to the group of moderate ER agonists (0.1 µM ≤ EC$_{50}$ < 1.0 µM) but still exhibit a positive relative activity. The 3-acetyl analog **PRU-12** was strongly active in the E-Morph assay and thus showed the highest relative activity of this selection. The *N,N*-dimethylamino analog **17** as the most potent TRPML1 inhibitor also ranks among the strong ER agonists (< 0.1 µM) with an EC$_{50}$ value of 0.02 µM and a resulting relative activity of 0.72. Still, all the top compounds displayed significantly lower estrogenic effects than the original screening hit **EDME**.

In conclusion, none of the compounds is a potent TRPML1 inhibitor and at the same time shows weak or no estrogenic effects. Nevertheless, it was possible to synthesize isoform-selective analogs that show both higher activity at TRPML1 and lower estrogenic effects than **EDME**. The *N*,*N*-dimethylamino analog **17** and the benzofuran analog **53** all in all provided the best results and therefore represent the best TRPML1 inhibitors synthesized during this project.
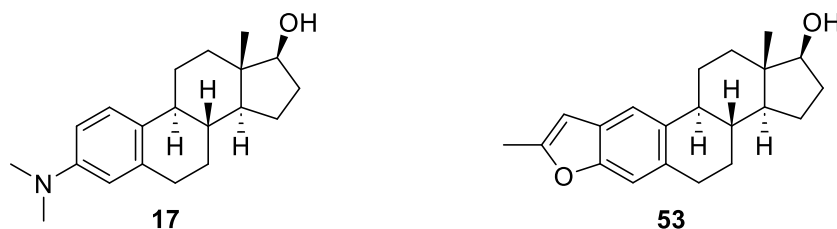
Figure 26: The two best TRPML1 inhibitors

Taking all data into account, several assertions can in general be drawn about structure-activity relationships.

<u>**Modifications at C-17:**</u>
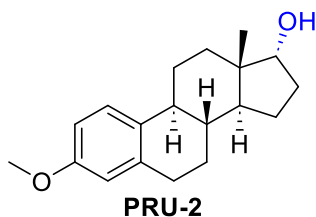
PRU-2

As discussed in the **Objectives** Chapter, the preliminary screening already indicated that alterations of functional groups at C-17 lead to a decrease in activity at the target ion channel TRPML1. Since the 17*α*-analog **PRU-2** was only marginally active, stereochemistry at this position also proved to be crucial for TRPML1 inhibitory activity and should definitely be conserved.

Modifications at C-3:
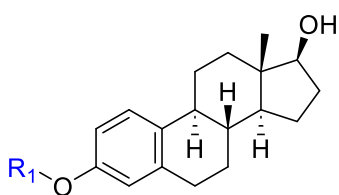
R$_1$= difluoromethyl, ethyl, isopropyl, allyl, phenyl
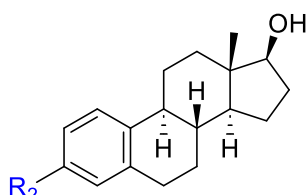
R$_2$= i.e. ethyl, ethinyl, vinyl, acetyl, phenyl, NH(CH$_3$), cyano
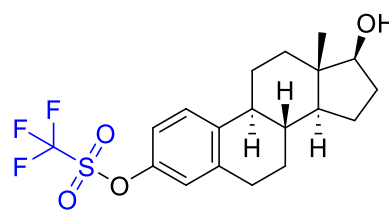
PRU-9
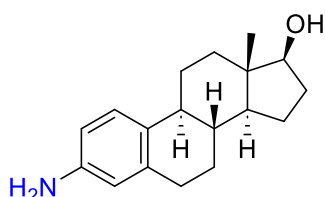
15
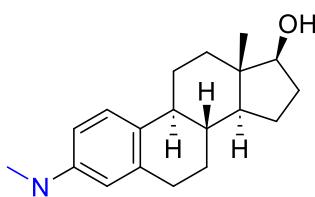
17
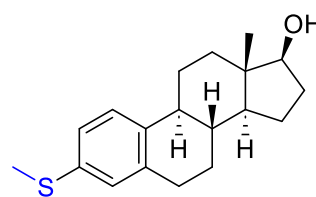
40

Replacement of the methyl ether by other substituents predominantly retained activity on TRPML1. Several different functional groups are tolerated, among them various ethers as well as compounds carrying a C-C bond, a C-N bond or a triflate at this position. The IC$_{50}$ values for TRPML1 inhibition of the substances of this series are in a range of 0.1 µM - 0.9 µM. The only two exceptions are the primary aromatic amine **15** (2.1 µM) and the 3-methylthio analog **40** (9.4 µM) which are only weak TRPML1 inhibitors. Regarding ER agonistic activity, the phenol ethers with aliphatic chains showed the strongest effect. Aromatic substituents or substituents bearing heteroatoms caused a decrease in estrogenic activity. The compounds with a C-C instead of a C-O bond at C-3 exhibited strong to moderate estrogenic effects and were all less active than the phenol ethers in the E-Morph assay.

Modifications at C-2:
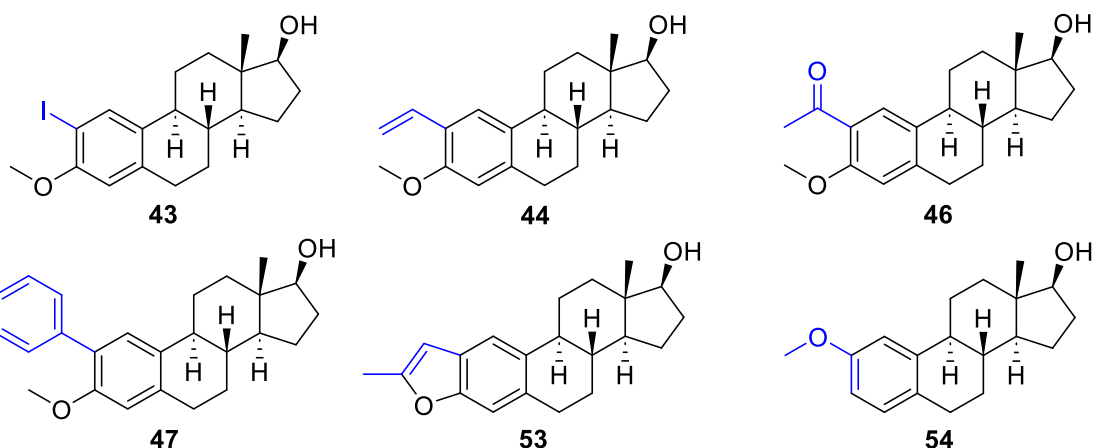
The insertion of an iodine, phenyl, vinyl or acetyl substituent at C-2 each led to a strong reduction in TRPML1 inhibitory activity. The 2-iodo analog **43**, the 2-vinyl analog **44** and the 2-acetyl analog **46** exhibited minor estrogenic effects, while the 2-phenyl analog **47** was highly estrogenic. The 2-methoxyestrane **54** showed a 2.8-fold lower inhibition of TRPML1 compared to its constitutional isomer **EDME**, but with an EC_{50} of < 0.001 a similarly strong activity in the E-Morph assay. In this group, solely the benzofuran analog **53** is superior to the original screening hit **EDME** as it is more active on TRPML1 and at the same time exerts a weaker estrogenic effect in the E-Morph assay.

Azaarenes:
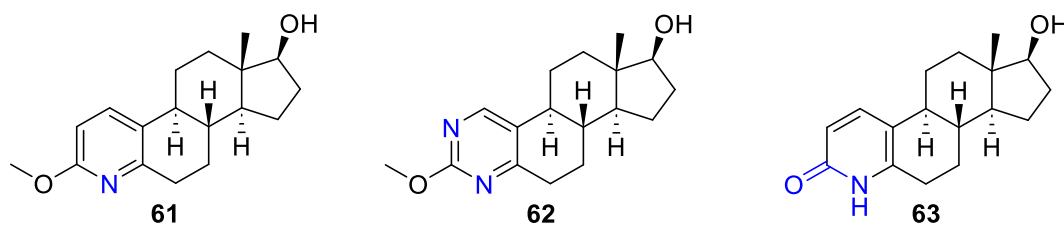
All three azaarenes are less active at TRPML1 but also have a much weaker estrogenic effect than **EDME**. While the pyrimidine **62** and the pyridone **63** do not even exhibit noteworthy TRPML1 inhibition, the pyridine **61** with an IC_{50} of 1.0 µM is still a decent TRPML1 inhibitor. As discussed above, this analog provides the most balanced profile between TRPML1 inhibition and estrogenic potential with a relative activity of -0.01. Referring to the results of the two bioisosteric analogs **61** and **62**, replacement of benzenoid ring A by the basic azaarenes pyridine and pyrimidine attenuates both the TPRML1 inhibitory activity and estrogenic effects.

5. Summary

This project was designed to develop new potent and selective inhibitors for the lysosomal cation channel TRPML1, which has emerged as a promising biological target, particularly in cancer research and in the study of neurodegenerative diseases. The basis for this work was a high-throughput screening of a substance library of 2430 drug-like small molecules carried out by our cooperation partners Prof. Dr. MICHAEL SCHAEFER, Prof. Dr. Dr. CHRISTIAN GRIMM and their respective groups, whereby the steroid 17β-estradiol methyl ether (**EDME**) was identified as the first highly potent and isoform-selective TRPML1 inhibitor. Due to its close structural similarity to natural estrogens and the derivable estrogenic potential as well as its metabolic lability, **EDME** itself as a chemical tool entails notable disadvantages and does not fulfill the criteria of a drug candidate for the desired target. The aim of this work was hence to synthetically modify **EDME** to generate and subsequently biologically evaluate various analogs. In this way, the structure-activity relationships should be elucidated and chemical tools be developed that are superior to the initial screening hit. The main objective of the synthetic approaches was to maintain or even increase potency and selectivity at TRPML1 and at the same time decrease the estrogenic effect.
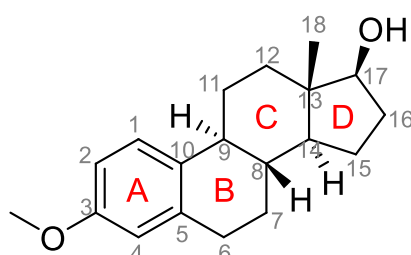
Figure 27: Screening hit **EDME**, numbering and ring annotation

In a consecutive screening campaign, which included several other pharmacologically active synthetic and natural steroidal compounds as well as synthetic estrogens and antiestrogens, a first framework of structure-activity relationships was established. The results indicated that the steroidal estrane scaffold had to be conserved and that exchange of the secondary alcohol at C-17 by a ketone or ester was detrimental for the activity at TRPML1.

The first envisaged analog was **PRU-2**, the 17α-epimer of **EDME**. The intention behind this structural modification was to investigate the importance of the stereochemistry at C-17. Since the 17α-epimer of estradiol (alfatradiol, **5**) is a significantly weaker estrogen than estradiol itself, this modification would represent a potential way to synthesize analogs with weaker estrogenic effects. **PRU-2** could be easily prepared from alfatradiol (**5**) *via* O-methylation at ring A with dimethyl sulfate under alkaline conditions (**Scheme 50**).
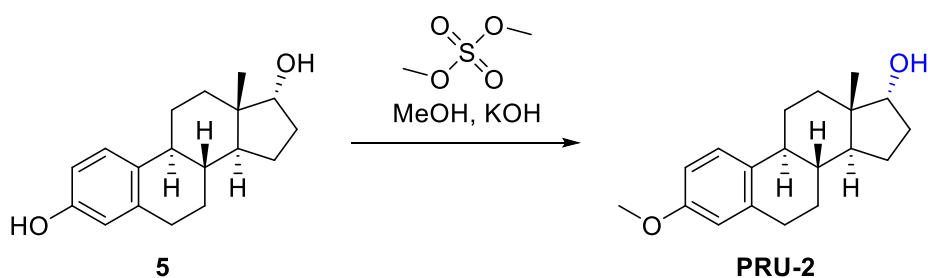
Scheme 50: Synthesis of 17α-epimer **PRU-2**

Because the phenol ether moiety of **EDME** is susceptible to metabolic cleavage by CYP enzymes, one aim was to replace this function with a metabolically stable bioisosteric group. To obtain difluoromethylether **PRU-4**, 17β-estradiol (**3**) was treated with potassium hydroxide and diethyl bromodifluoromethylphosphonate (**Scheme 51**).
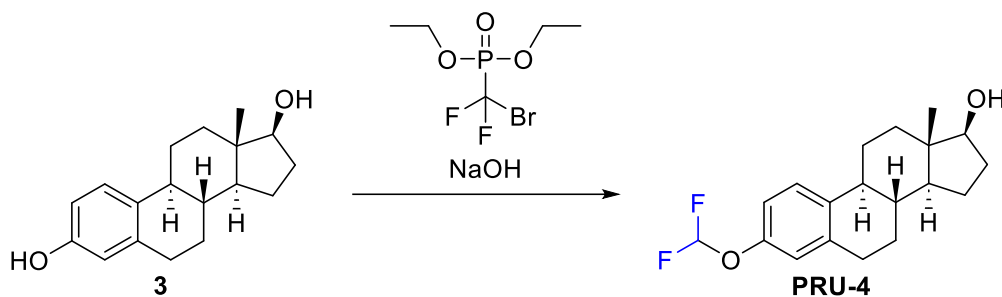
Scheme 51 Preparation of difluoromethyl ether **PRU-4**

The next consideration was to introduce a couple of different ethers at C-3 to investigate if other chain lengths and substituents are tolerated. Consequently, the three ether compounds **PRU-5** (ethyl), **PRU-6** (isopropyl) and **PRU-7** (allyl) were prepared from **3** by standard WILLIAMSON ether synthesis protocols. Diphenylether **PRU-8** was prepared from estradiol (**3**) by nucleophilic addition of benzyne, which was generated *in situ* from 2-(trimethylsilyl)phenyl trifluoromethanesulfonate and cesium fluoride. Treatment of **3** with 4-nitrophenyl trifluoromethanesulfonate and potassium carbonate allowed preparation of triflate **PRU-9** (**Scheme 52**).
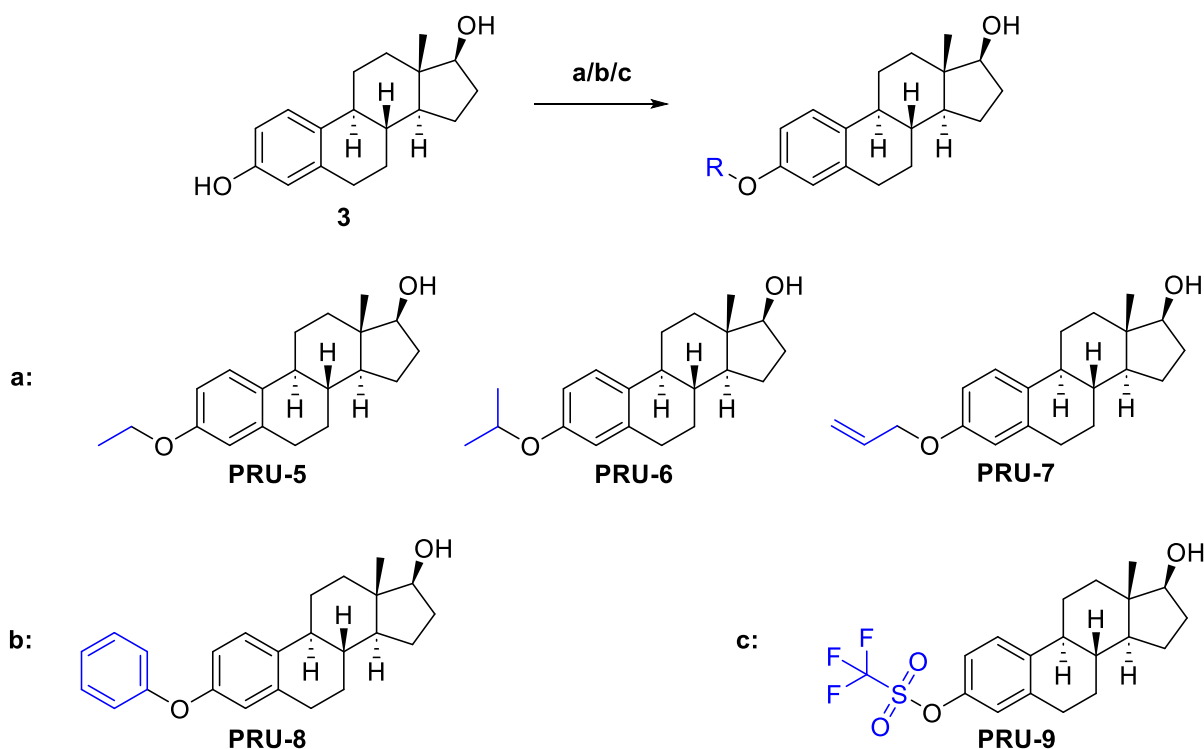
Scheme 52: Synthesis of **EDME** analogs by derivatization of estradiol (**3**), **a**: alkyl halide, base; **b**: 2-(trimethylsilyl)phenyl trifluoromethanesulfonate, CsF, **c**: 4-nitrophenyl trifluoromethanesulfonate, K_2CO_3

The next intention was to prepare analogs carrying a C-C bond instead of a C-O bond at C-3. This substitution should impede metabolic cleavage by CYP enzymes at this position and additionally after biological evaluation provide more profound information about SAR. Furthermore, these analogs were assumed to be less estrogenic, as the oxygen motif at this position is typical for estrogens. Hence, palladium-catalyzed coupling reactions were conducted with previously synthesized triflate **PRU-9**. The first three compounds derived from this synthesis strategy were the 3-vinyl analog **PRU-10**, the 3-phenyl estrane **PRU-11** and the 3-acetyl analog **PRU-12**. **PRU-10** and **PRU-12** were prepared by STILLE coupling under palladium catalysis: Reaction of **PRU-9** with tributyl(vinyl)tin provided **PRU-10**, whereas **PRU-12** was accessible *via* coupling of **PRU-9** with tributyl(1-ethoxyvinyl)tin and subsequent hydrolysis of the generated enol ether intermediate (**Scheme 53 A**). SUZUKI coupling of **PRU-9** with phenylboronic acid and K_3PO_4 afforded biphenyl **PRU-11**.

To gather information about the TRPML1 inhibitory activity of this first generation of compounds, the substances were tested by Fura-2 and Fluo-4 Ca^{2+} imaging assays. Furthermore, estrogenic effects were measured by a simple yeast estrogen screen (YES) assay. Since the 3-vinyl analog **PRU-10** and the 3-acetyl analog **PRU-12** delivered the best results, the successive synthetic approaches built on these data and focused on the replacement of the ether bond at C-3 through other functional groups.

The 3-ethyl analog **8** was easily accessible from **PRU-10** by catalytic hydrogenation on Pd/C. Analogous to the preparation of **PRU-10** and **PRU-12**, palladium catalyzed coupling procedures based on triflate **PRU-9** allowed for a number of additional variations (**Scheme 53 A**). A SONOGASHIRA like coupling reaction of **PRU-9** with trimethylsilylacetylene and subsequent cleavage of the trimethylsilyl group with TBAF afforded the 3-ethynyl analog **11**.

Aromatic aldehyde **12** was synthesized by a method for formylation of aryl triflates under palladium catalysis using *N*-formylsaccharine as a carbon monoxide surrogate. Nitrile **13** was obtained by palladium-catalyzed cyanation of **PRU-9** with KCN. A HECK-type reaction of **PRU-9** with acrylonitrile gave the vinylogous nitrile **14**. Aldehyde **12** and the two nitriles **13** and **14** were synthesized as potential reversible covalent inhibitors of TRPML1.

The three aromatic amines **15**, **16** and **17** could not be directly synthesized from **PRU-9** by BUCHWALD-HARTWIG coupling with amines. Instead, the C-17 alcohol of **PRU-9** had to be benzylated beforehand for this reaction to succeed. As conventional benzylation methods failed to furnish satisfactory results, it took several different approaches before benzylation with benzyloxy-1-methyl-pyridinium triflate was found to be the best method for this purpose. Thus, the desired benzyl-protected building block **23** could eventually be synthesized from **PRU-9** (**Scheme 53 B**). Based on this, the three amines could be prepared by BUCHWALD-HARTWIG coupling with benzylamine followed by sophisticated *N*-debenzylation and reductive *N*-alkyation sequences.
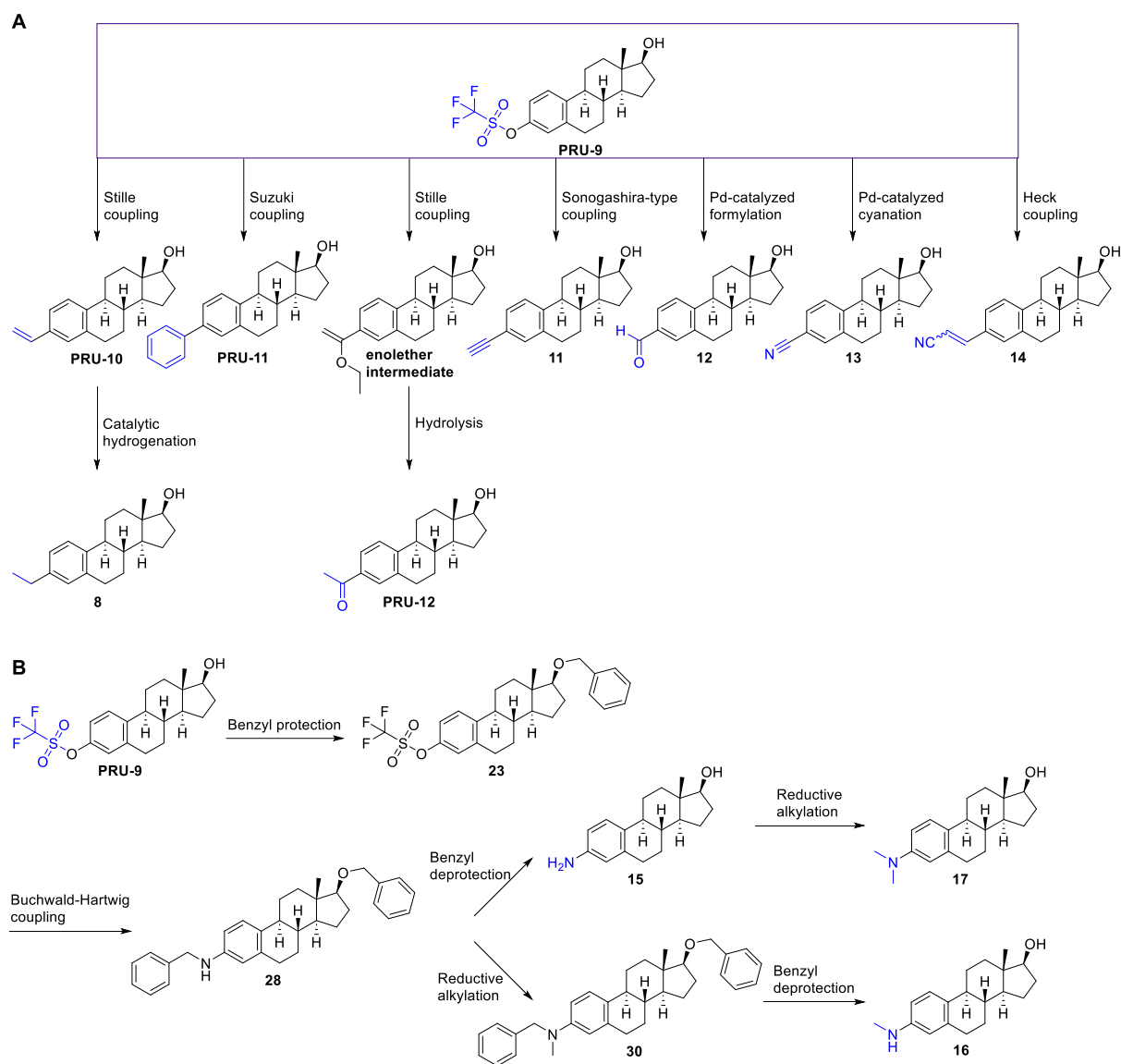
Scheme 53: Systematic variation of substituents at C-3 by palladium-catalyzed coupling reactions

As 3-methylthio analog **40** could not be prepared directly by a palladium-catalyzed coupling reaction, a palladium-catalyzed N\ *ewman*-K\ *wart* rearrangement procedure *via O*-aryl thiocarbamate **35** was conducted instead. Alkaline hydrolysis of the formed *S*-aryl thiocarbamate **38** followed by *S*-methylation with iodomethane and sodium hydride afforded the desired product **40** (**Scheme 54**).
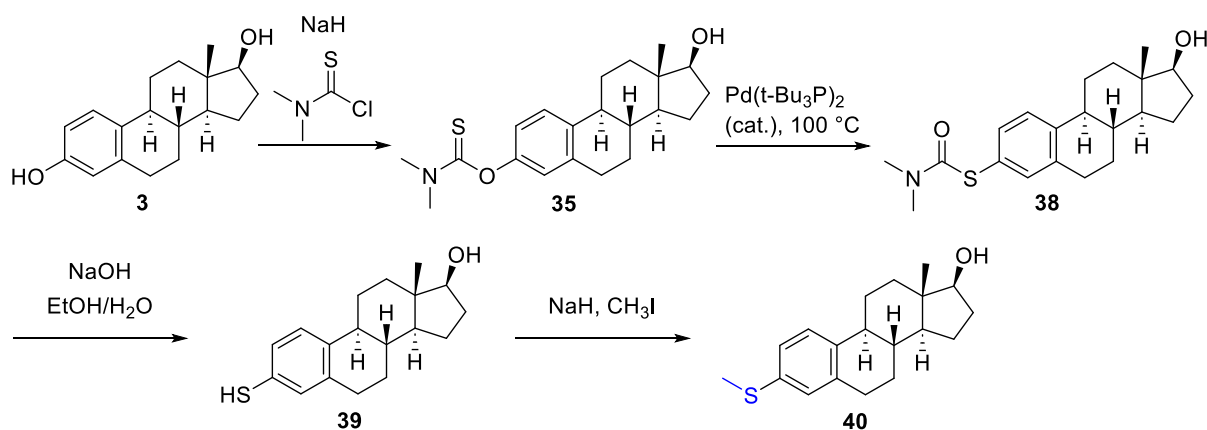
Scheme 54: Preparation of 3-methylthio analog **40**

To investigate the effect of substituents at C-2 of the estrane and thus expand knowledge about SAR, the next series of compounds was designed to vary this position. For this purpose, estradiol (**3**) was iodinated with NIS at C-2 with the aid of LEWIS acid Indium (III) triflate to give 2-iodoestradiol (**41**, **Scheme 55**). Subsequent methylation of the phenol group with iodomethane and cesium carbonate yielded the key intermediate **43**. Analogous to **PRU-9**, this building block could serve as a starting material for palladium-catalyzed coupling reactions. Hence, the 2-vinyl analog **44** and the 2-acetyl analog **46** were prepared by STILLE coupling, while 2-phenyl analog **47** could be obtained by SUZUKI coupling. Furthermore, 2-iodoestradiol (**41**) was also directly subjected to SONOGASHIRA coupling using a solution of propyne in DMF to receive 2-propynyl estrane **51**. Cyclization of this intermediate with NaOH in methanol yielded annulated benzofuran **53**.
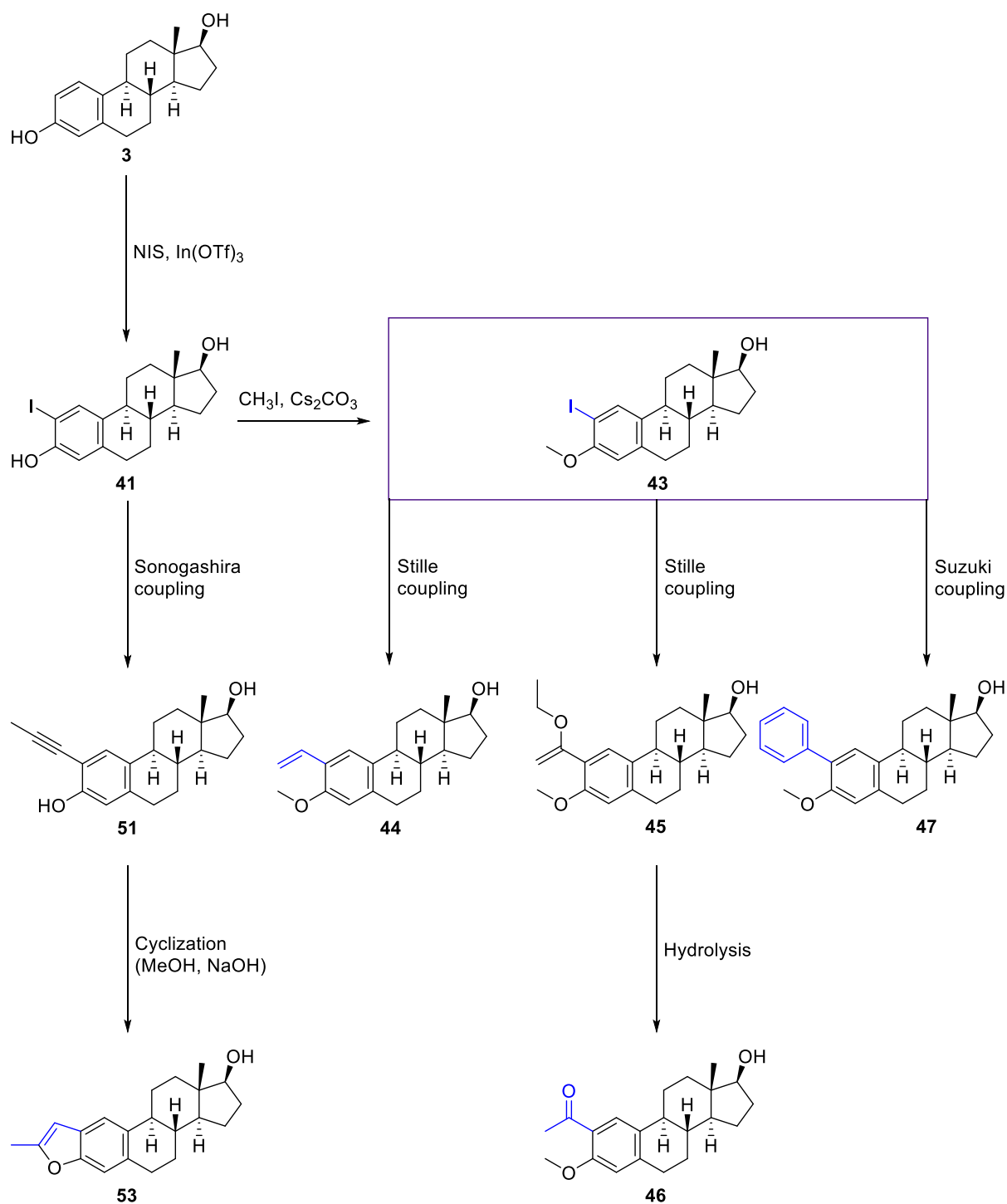
Scheme 55: Modifications at C-2 by means of iodination and subsequent palladium-catalyzed coupling reactions

Another envisaged analog was 2-methoxy estrane **54**, the constitutional isomer of **EDME** carrying the methoxy group at C-2. For the preparation of this compound, commercially acquired starting material 2-methoxyestradiol (**55**) was converted into triflate **60** using 4-nitrophenyl trifluoromethanesulfonate and potassium carbonate. Subsequent reductive

cleavage of the generated triflate with formic acid under palladium catalysis yielded the desired 2-methoxy analog **54** (**Scheme 56**).
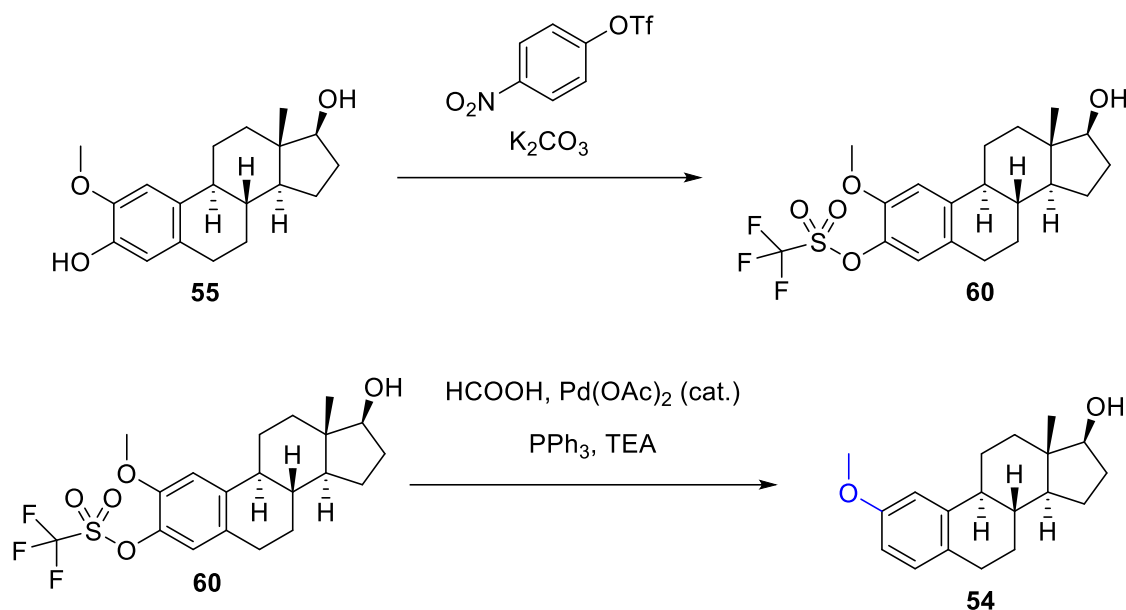
Scheme 56: Synthesis of 2-methoxy analog **54**

After modification of substituents at the aromatic ring A, another objective was to replace the benzenoid ring by suitable bioisosteres. Pyridine and pyrimidine were considered as promising candidates for this bioisosteric replacement as they would add new physicochemical properties to the molecule due to their basic nitrogen atoms and could thus impact interactions with the target protein and/or estrogen receptors. For both azaarenes, commercially available androgen 19-nortestosterone (**4**) was selected as starting material, as this homochiral compound already has the required configurations at the stereocenters in rings C and D and unlike related steroids lacks a methyl group at C-10, which would prevent aromatization of ring A after the preceding oxidative cleavage. In this way, the two azaarenes were successfully synthesized in 6 and 8 steps, respectively (**Scheme 57**).

For the synthesis of pyridine analog **61**, the previously shown benzylation method utilizing 2-benzyloxy-1-methyl-pyridinium triflate and magnesium oxide was applied to **4** to obtain benzyl protected steroid **A**. The introduction of a protective group at this position was crucial for the following reactions since the unprotected secondary alcohol was found to interfere with oxidants and other reagents used for dehydrogenation at a later stage. The benzyl group was selected as the preferred option as it is more resilient to acidic conditions than other protective groups, such as TBDMS ether, yet it can be deprotected selectively under relatively mild conditions. Oxidative cleavage of the cyclohexenone-type ring A with sodium periodate, potassium permanganate and potassium carbonate gave ketocarboxylic acid **B**, which was then recyclized with ammonium acetate in acetic acid to obtain a mixture of the two unsaturated

lactams **C1** and **C2**. The next step was the aromatization of these lactams. The lactam mixture was treated with copper (II) bromide, lithium bromide, 1,3-dimethoxybenzene and methanesulfonic acid to accomplish aromatization and yield pyridone **D** along with small amounts of the debenzylated pyridone compound **63**, which was generated as a side product. This reaction was the result of a comprehensive and laborious evaluation of numerous approaches for the dehydrogenation of lactams **C1** and **C2** including treatment with various oxidants and several published dehydrogenation protocols and reagents used for the synthesis of pyridones or related fields. Of all these experiments, only the method described above, which was originally used for a cyclohexenone-to-phenol conversion in 19-norandrost-4-en-3-ones, succeeded in producing the pyridone. To continue the route to azaarene **61**, the benzyl protected pyridone **D** was *O*-methylated utilizing silver (I) carbonate and iodomethane to give benzyl protected methoxy pyridine **E**. Deprotection of the benzyl group with boron trichloride finally yielded methoxy pyridine analog **61**.

The synthesis route to the pyrimidine analog **62** directly started with the oxidative cleavage of the cyclohexenone moiety of 19-nortestosterone (**4**) to obtain ketocarboxylic acid **F**. Intermediate **F** was converted into its methyl ester **G** using a standard methylation protocol with Cs_2CO_3 and iodomethane. After conversion of the keto group into the dioxolane **H**, the C-17 alcohol was converted into the TBDMS ether to give TBDMS protected seco-steroid **I**. In this case, the TBDMS ether was favored over the benzyl group since the deprotection of both the TBMDS group and the dioxolane could later be smoothly achieved in one single step. The TBDMS group was not introduced until this stage, as the preceding reactions did not require protection of the secondary alcohol, but the TBDMS ether could have been cleaved by the acidic conditions during the insertion of the dioxolane. The next step of the route involved the conversion of the methyl propionate side chain of **I** into the *α,β*-unsaturated ester **J** by a selenation-selenoxide elimination protocol including treatment with LDA/diphenyldiselenide and oxidation with H_2O_2. Two-carbon degradation to yield the aldehyde **K** was accomplished by ozonolysis. The treatment of **K** with acetic acid in THF/water resulted in simultaneous deprotection of the dioxolane and the TBDMS ether to provide the ketoaldehyde **L**. Finally, cyclization of **L** using *O*-methylisourea and sodium methoxide gave the target methoxy pyrimidine analog **62**.
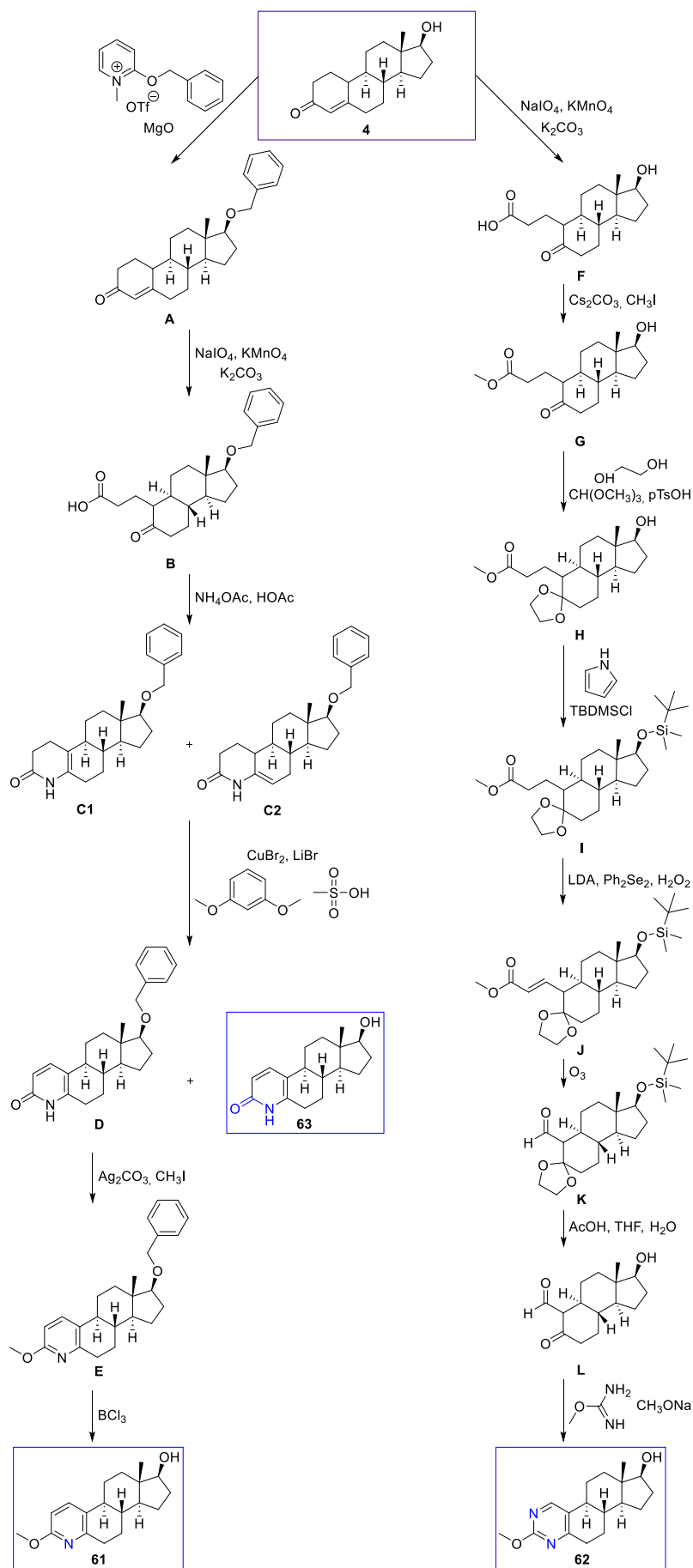
Scheme 57: Synthesis routes to the azaarene analogs of **EDME**

All **EDME** analogs were analyzed for their TRPML1 inhibitory activity, selectivity over the two isoforms TRPML2 and TRPML3, and for estrogenic effects. TRPML1 inhibitory activity as well as isoform-selectivity was determined by Fluo-4 Ca^{2+} imaging experiments performed by NICOLE URBAN from the group of Prof. Dr. MICHAEL SCHÄFER at the Rudolf-Boehm-Institut in Leipzig. Estrogenic effects were assessed by an E-Morph assay performed by Dr. VERENA FETZ and Dr. SEBASTIAN DUNST at the Bundesinstitut für Risikobewertung (BfR, Berlin). The IC_{50} values derived from Fluo-4 Ca^{2+} imaging showed that most of the analogs represent potent and selective TRPML1 inhibitors. Replacement of the ether moiety at C-3 by other functional groups led to minor changes in TRPML1 inhibitory activity but in all cases to a decrease of estrogenic effects. The only exception is 3-methylthio analog **40** which is a very weak TRPML1 inhibitor with an IC_{50} of 8.8 µM. The 3-vinyl analog **PRU-10** (IC_{50} for TRPML1 inhibition: 0.4 µM), the 3-acetyl analog **PRU-12** (IC_{50}: 0.3 µM) and the *N,N*-dimethylamine analog **17** (IC_{50} for TRPML1 inhibition: 0.1 µM) provided the best results of this group and were superior to the original screening hit **EDME** (IC_{50}: 0.5 µM). Triflate **PRU-9** showed an excellent activity and selectivity profile as well as a merely moderate estrogenic effect but is not considered a promising TRPML1 blocker since it is not drug-like due to the lability of the triflate group. Modifications at C-2 were detrimental for TRPML1 inhibitory activity, solely benzofuran analog **53** which comprises a modification of both C-2 and C-3 was highly active at TRPML1 (IC_{50}: 0.2 µM) and also only exhibited a moderate estrogenic effect. None of the azaarene analogs (pyridine **61**, pyrimidine **62**, pyridone **63**) is a highly potent TRPML1 inhibitor, but all of them showed comparably low estrogenic effects. With an IC_{50} of 1.0 µM, solely pyridine analog **61** exhibited noteworthy TRPML1 inhibition. Its ER agonistic activity was in the same concentration range (EC_{50}: 1.02 µM).

In summary, new potent and isoform-selective TRPML1 inhibitors have been successfully developed in this project. The original screening hit **EDME** was improved both in terms of its TRPML1 inhibitory activity, which was increased and its undesired estrogenic effect, which was decreased, through systematic structural variations and profound biological evaluation with the help of our cooperation partners. Furthermore, valuable information on SAR was gathered in this work. In particular, the *N,N*-dimethylamino analog **17** and the benzofuran analog **53** as the two best compounds represent promising chemical tools for the investigation of TRPML1 ion channels.
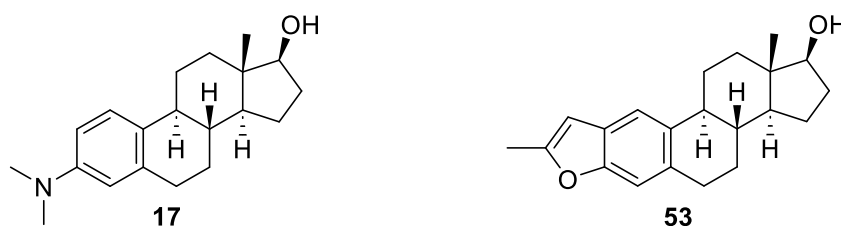
Scheme 58: The two best analogs of this work

However, it was not possible to synthesize an analog that combines a very weak or even no estrogenic effect with a high activity at TRPML1. The compounds that showed a weak estrogenic effect were in all cases found to have only a moderate or weak inhibition of TRPML1. Consequently, off-target effects on estrogen receptors remain to be considered in this structural class of TRPML1 inhibitors.

6. Experimental part

6.1 Biological methods

MTT assay

The MTT assay was performed by MARTINA STADLER (BRACHER group). HL-60 cells were maintained under standard cell culture conditions in RPMI 1640 medium supplemented with 10 % fetal bovine serum (FBS) without antibiotics. Cells were grown and incubated at 37 °C in a 5 % CO_2 atmosphere. HL-60 cells were seeded in 96-well plates at 9 x 104 cells/well and incubated for 24 h before treatment with test compounds for 24 h with a final well volume of 100 µL, 1 % DMSO; three technical replicates; the cosolvent control was treated with 1 % DMSO only. Triton-X 100 was used as a positive control. 3-[4,5-Dimethylthiazole-2-yl]-2,5-diphenyltetrazolium bromide (MTT; 5 mg in 1.0 mL PBS) was added to the cells for 2 h. Then DMSO (190 µL) was added. After 1 h, absorbance of the MTT metabolite formazan was measured at 570 nm using an MRX Microplate Reader (Dynex Technologies, Chantilly, USA). Absorbance data was averaged over the technical replicates, then normalised to viable cell count from the cosolvent control cells (% control) as 100 %, where 0 % viability was assumed to correspond to absorbance zero.

Agar diffusion assay

Agar diffusion tests were performed by MARTINA STADLER (BRACHER group). Solutions with 1 % (m/V) compound in DMSO were prepared. Of these solutions 3.0 µL were given on a test platelet (diameter 6 mm, Macherey-Nagel), equivalent to 30 µg substance. The same was done for the reference substances clotrimazole (antifungal) and tetracycline (antibacterial). A blind control was conducted with DMSO. The test platelets were then dried for 24 h at room temperature. Microorganisms were obtained from Deutsche Sammlung von Mikroorganismen und Zellkulturen GmbH (DSMZ) in Braunschweig and cultivated according to the DSMZ recommendations in liquid culture. For the agar diffusion assay, different agars were required. For *Candida glabrata* (DSM number: 11226), *Hyphopichia burtonii* (DSM number: 70663)*, Yarrowia lipolytica* (DSM number: 1345)*, Escherichia coli* (DSM number: 426), and *Pseudomonas marginalis* (DSM number: 7527) all-culture agar (AC-agar) of Sigma Aldrich was used. 35.2 g AC-agar and 20 g agar were suspended in 1.0 L water and autoclaved. For *Staphylococcus equorum* (DSM number: 20675) and *Streptococcus entericus* (DSM number: 14446) an agar is likewise prepared from 10.0 g casein peptone, 5.0 g yeast extract, 5.0 g glucose and 5.0 g sodium chloride in 1.0 L water. For *Aspergillus niger* (DSM number: 1988) 32 g potato dextrose agar and 20 g agar in 1.0 L water were used. After treatment in the autoclave, 15 mL each of the warm, liquid agar was filled into petri dishes under aseptic

conditions and cooled to 8 °C for 1 h. The germs were then brought onto the different agars using cotton swabs. The platelets containing the substances, the reference, and the blind control were put onto the agar. The agar plates were incubated for 36 h at 32 °C (bacteria) or 28 °C (yeasts). Then the diameters of growth inhibition were measured manually.

Yeast estrogen screen (YES) assay

Performed Prof. Dr. GÜNTHER VOLLMER as described in our publication[84]

E-Morph screening assay

The E-Morph Screening assay was performed by Dr. SEBASTIAN DUNST and Dr. VERENA FETZ (BfR, Berlin) as described in KLUTZNY et al., 2022[170]. A JANUS Automated Liquid Handling Workstation (PerkinElmer), customized treatment protocols written in WinPREP (PerkinElmer), and an ELx405 Select CW Microplate Washer (BioTek Instruments, Winooski, VT, USA) were used for all liquid handling procedures. MCF-7/E-Cad-GFP cells were coexposed with 10 nM Fulv in combination with the compounds at six different concentrations (0.001 - 100 µM) for 48 h and the SI (primary readout) at the cell membrane as a measure for the ER agonist activity of the test substances was measured. The potencies (half-maximal effective concentrations (EC_{50})) of the compounds were calculated by fitting the SI concentration-response curves for all non-cytotoxic concentrations using the non-linear fit algorithm (four parameters, variable hill slope). MCF-7/E-Cad-GFP cells were routinely maintained at 37 °C with 5% CO_2 in cell culture medium containing Dulbecco's modified Eagle's medium (DMEM, low glucose, pyruvate, no glutamine, no phenol red) (Gibco/Thermo Fisher Scientific, Waltham, MA, USA), 5% (v/Merck, Darmstadt, Germany), 2 mM stable glutamine (Gibco/Thermo Fisher Scientific), 100 µg/ml streptomycin / 100 U/ml penicillin (Biochrom/Merck), and 0.4 mg/ml geneticin (Gibco/Thermo Fisher Scientific). The final background estradiol concentration in the FBS-containing medium was 4.1 pM. For preparation of compound plates for the first range-finding run, 2 µl of a compound stock solution in DMSO (100 mM) were dissolved 1:100 in a 96-well microplate (Greiner Bio-One) containing 198 µl cell culture medium and the anti-estrogen fulvestrant (Fulv) (Sigma-Aldrich/Merck, Darmstadt, Germany) at 100 nM. From this start concentration (1 mM), a total of five serial dilutions (1,000 – 100 – 10 – 1 – 0.1 µM) were generated at a 1:10 ratio in 200 µl cell culture medium containing 100 nM Fulv (10X compound plates). For the second and third confirmatory runs, the compound stock solution was readjusted to 10 mM in DMSO to avoid precipitation in the cell culture medium and cytotoxic effects resulting in 10X compound plates containing serial compound dilutions of 100 – 10 – 1 – 0.1 – 0.01 µM.

For preparation of assay plates, 11,000 cells were seeded per well into PhenoPlate™ 384-well microplates (PerkinElmer, Waltham, MA, USA) in 90 µl cell culture medium and grown until 80-90% confluency for 24 h. Subsequently, 10 µl of the exposure medium containing the

diluted compounds (start concentrations: 1000 or 100 µM) were transferred from the compound plates to the assay plates containing 90 µl cell culture medium to achieve a final compound concentration series of 100 - 0.1 µM or 10 – 0.01 µM, a final Fulv concentration of 10 nM, and a maximal DMSO concentration of 0.1%. The exposure of cells with the compounds was performed with two technical replicates per plate for 48 h without an additional medium exchange.

Experimental controls included the solvent control (0.1% DMSO), the Fulv control containing 10 nM Fulv only, and the co-treatment (reactivity) control containing 10 nM Fulv + 100 nM 17β-estradiol (E2) (Sigma-Aldrich/Merck).

Single cell calcium imaging

Performed as described in our publication[84]

High-throughput screening (HTS)

Performed by NICOLE URBAN (Rudolf-Boehm-Institut, Leipzig) as described in our publication[84]

Fluo-4 calcium imaging (screening and concentration-response experiments)

Performed by NICOLE URBAN (Rudolf-Boehm-Institut, Leipzig) as described in our publication[84]

6.2 Instruments and materials

Solvents and reagents

All chemicals used were of analytical grade and were purchased from abcr (Karlsruhe, Germany), Fischer Scientific (Schwerte, Germany), Sigma-Aldrich (now Merck, Darmstadt, Germany), TCI (Eschborn, Germany) or Th. Geyer (Renningen, Germany). HPLC grade and dry solvents were purchased from VWR (Darmstadt, Germany) or Sigma-Aldrich, isohexane, ethyl acetate and methylene chloride were purified by distillation.

Microwave assisted synthesis

Microwave assisted synthesis was carried out in a Discover (S-Class Plus) SP (CEM, USA) microwave reactor.

Hydrophobic filters

Hydrophobic phase separation filters (MN 617 WA, 125 mm) were obtained from Macherey Nagel (Düren, Germany).

Thin layer chromatography (TLC)

All reactions were monitored by thin-layer chromatography (TLC) using pre-coated plastic sheets POLYGRAM® SIL G/UV254 from Macherey-Nagel (Düren, Germany) and detected by irradiation with UV light (254 nm or 366 nm) or visualized by staining with CAM (ceric ammonium molybdate), vanillin-sulfuric acid, DNPH (2,4-dinitrophenylhydrazine) or Dragendorff's reagent (K(BiI$_4$) solution in acetic acid/water).

Flash column chromatography (FCC)

Flash column chromatography was performed on Merck silica gel Si 60 (0.015 – 0.040 mm) if not otherwise stated. The used solvent systems are indicated in the synthesis details and analytical data section.

Nuclear magnetic resonance spectroscopy

All NMR spectra (^{1}H, ^{13}C, DEPT, H-H-COSY, HSQC, HMBC) were recorded at 23 °C on an Avance III 400 MHz Bruker BioSpin or Avance III 500 MHz Bruker BioSpin instrument. Chemical shifts δ are stated in parts per million (ppm) and are calibrated using residual protic solvents as an internal reference for proton (CDCl$_3$: δ = 7.26 ppm, CD$_2$Cl$_2$: δ = 5.32 ppm, CD$_3$OD: δ = 3.31 ppm, (CD$_3$)$_2$SO: δ = 2.50 ppm) and for carbon the central carbon resonance of the solvent (CDCl$_3$: δ = 77.16 ppm, CD$_2$Cl$_2$: δ = 53.84 ppm, CD$_3$OD: δ = 49.00 ppm, (CD$_3$)$_2$SO: δ = 39.52 ppm). Peak assignments were based on 2D NMR experiments using standard pulse programs (COSY, HSQC/HMQC, DEPT, HMBC). Multiplicity is denoted as s = singlet, d = doublet, t = triplet, q = quartet, m = multiplet. NMR spectra were analyzed with NMR software MestReNova, version 12.0.1-20560 (Mestrelab Research S.L.).

Mass spectrometry

High resolution mass spectra were performed by the LMU Mass Spectrometry Service applying a Thermo Finnigan MAT 95 or Joel MStation Sektorfeld instrument at a core temperature of 250 °C and 70 eV for EI or a Thermo Finnigan LTQ FT Ultra Fourier Transform Ion Cyclotron Resonance device at 250 °C for ESI. For reaction monitoring low resolution mass spectra were recorded on an expression LCMS device (Advion, USA) by atmospheric pressure solids analysis probe (ASAP) and atmospheric-pressure chemical ionization (APCI) for the analysis of samples in solution or neat solids. For the analysis of spots on a TLC plate, the measurement was carried out in combination with a Plate Express® TLC Plate Reader device (Advion, USA) using APCI or ESI ionization method.

Infrared spectroscopy

IR spectra were recorded on a Jasco FT/IR-4100 (type A) instrument (Jasco, Germany) equipped with a diamond ATR unit (Jasco PRO450-S) as neat materials. Absorption bands were reported in wave number (cm^{-1}) with ATR PRO450-S.

Melting points

Melting points were determined by the open tube capillary method on a Büchi melting point B-540 apparatus and are uncorrected.

High pressure liquid chromatography

HPLC purities were determined using an HP Agilent 1100 HPLC with a diode array detector. The substances (1.0 mg) were dissolved in ACN (1 mL) and diluted with ACN (1:10). HPLC purity measurements were performed by ANNA NIEDRIG from the BRACHER group and myself.

Method 1: Column InfinityLab Poroshell 120EC-C18 4,6x1000mm 2,7µm

a) Eluent ACN/H_2O: 70:30

b) Eluent ACN/0.1%TFA in H_2O: 50:50

c) Eluent ACN/H_2O: 80:20

d) Eluent ACN/H_2O: 50:50

e) Eluent: MeOH/phosphate buffer pH 9: 85:15

Method 2: Column Zorbax Eclipse Plus C18 4,6x150mm, 5µm, eluent ACN/H_2O: 70:30

Software

ChemDraw Professional® 16.0 (PerkinElmer, USA) was used for drawing structures or reaction schemes. MestReNova® 10.0 (Mestrelab Research, Spain) was used for processing and analysis of NMR spectra. GraphPad Prism® 5.0 and 8.4.3 (GraphPad Software Inc., USA) was used for data visualization and statistical analysis.

Numbering of the compounds

The numbering of atoms is based on the IUPAC nomenclature system of steroids. Atoms of secosteroids and derivatives thereof are numbered according to their initial position in the intact ring.

6.3 Synthesis details and analytical data

(8R,9S,13S,14S,17S)-3-Ethyl-13-methyl-7,8,9,11,12,13,14,15,16,17-decahydro-6H-cyclopenta[a]phenanthren-17-ol (8)
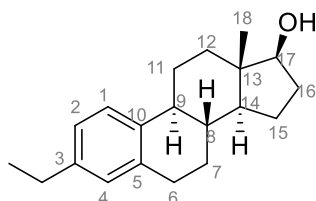
$C_{20}H_{28}O$

M_w: 284.44 g/mol

To 48.0 mg (0.170 mmol, 1.00 eq) of vinyl compound **PRU-10**, dissolved in 12.5 mL of ethanol, 9.05 mg (0.00850 mmol, 5 mol%) of Pd/C (10 %) was added under a nitrogen atmosphere. The flask was equipped with a rubber septum and a balloon, the system was purged with hydrogen and stirred at ambient temperature for 1 h. Then the reaction mixture was filtered through a pad of celite, which was washed with 10 mL of ethanol afterwards. The filtrate was concentrated *in vacuo* and the residue was purified by flash column chromatography to yield 46.0 mg (0.162 mmol, 95 %) of compound **8** as a colorless solid.

m.p.: 85 °C

¹H NMR (400 MHz, CD_2Cl_2) δ/ppm = 7.19 (d, J = 8.0 Hz, 1H, 1-H), 6.94 (dd, J = 8.2, 1.9 Hz, 1H, 2-H), 6.90 (s, 1H, 4-H), 3.69 (t, J = 8.4 Hz, 1H, 17-H), 2.83 (dd, J = 8.3 Hz, 2.8 Hz, 2H, 6-H), 2.55 (q, J = 7.6 Hz, 2H, ethyl CH_2), 2.33 (dq, J = 13.3 Hz, 3.9 Hz, 1H, 11-H_a), 2.20 (m, 1H, 9-H), 2.08 (dtd, J = 12.6 Hz, 9.2 Hz, 5.3 Hz, 1H, 16-H_a), 1.92 (ddd, J = 12.5 Hz, 3.9 Hz, 2.8 Hz, 1H, 12-H_a), 1.86 (m, 1H, 7-H_a), 1.69 (dddd, J = 12.5 Hz, 10.1 Hz, 6.7 Hz, 2.6 Hz, 1H, 15-H_a) 1.49 (m, 1H, 11-H_b), 1.46 (m, 1H, 16-H_b), 1.44 (m, 1H, 8-H), 1.36 (m, 1H, 15-H_b), 1.33 (m, 1H, 7-H_b), 1.29 (m, 1H, 12-H_b), 1.19 (t, J = 7.6 Hz, 3H, ethyl CH_3), 0.76 (s, 3H, 18-H)

¹³C NMR (101 MHz, CD_2Cl_2) δ/ppm = 141.80 (C-3), 138.09 (C-5 or C-10), 137.00 (C-5 or C-10), 128.71 (C-4), 125.59 (C-1), 125.44 (C-2), 82.17 (C-17), 50.54 (C-14), 44.71 (C-9), 43.60 (C-13), 39.23 (C-8), 37.18 (C-12), 30.95 (C-16), 29.94 (C-6), 28.69 (ethyl CH_2), 27.71 (C-7), 26.67 (C-11), 23.47 (C-15), 16.02 (ethyl CH_3), 11.25 (C-18)
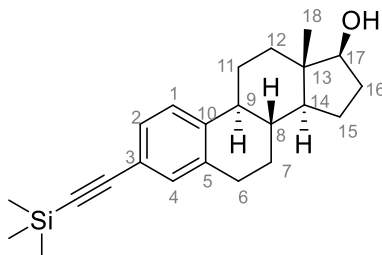
IR (ATR): $\tilde{v}_{max}$/cm⁻¹ = 3344, 2921, 2868, 1498, 1444, 1336, 1247, 1135, 1073, 886, 823

HRMS (EI): m/z = [M⁺] calcd. for $C_{20}H_{28}O$ ⁺: 284.2135; found: 284.2135

Purity (HPLC): > 97 % (λ = 210 nm) (Method 1a)

Literature known compound[97]

(8R,9S,13S,14S,17S)-13-Methyl-3-((trimethylsilyl)ethynyl)-7,8,9,11,12,13,14,15,16,17-decahydro-6H-cyclopenta[a]phenanthren-17-ol (10)

C$_{23}$H$_{32}$OSi

M$_w$: 352.59 g/mol

To a solution of triflate **PRU-9** (93.0 mg, 0.230 mmol, 1.00 eq) in 2.5 mL DMF in a round bottom flask were added triethylamine (0.192 mL, 1.38 mmol, 6.00 eq), ethynyltrimethylsilane (27.1 mg, 0.276 mmol, 1.20 eq) and Pd(PPh$_3$)$_2$Cl$_2$ (9.69 mg, 0.0138 mmol, 6 mol%). The flask was purged with nitrogen for three times and capped with a rubber septum. The resulting suspension was heated at 50 °C and stirred for 12 h under a nitrogen atmosphere. The reaction mixture was quenched with saturated aqueous ammonium chloride solution and extracted with dichloromethane (3 x 10 mL). The combined organic extracts were washed with water (20 mL) and brine (20 mL), dried over anhydrous sodium sulfate and concentrated *in vacuo*. The crude product was purified by flash column chromatography (isohexane/ethyl acetate 4:1) to yield compound **10** (70.0 mg, 0.199 mmol, 86 %) as a light yellow solid.

m.p.: 136 °C

^{1}H NMR (500 MHz, CD$_2$Cl$_2$) δ/ppm = 7.23 (d, *J* = 8.1 Hz, 1H, 1-H), 7.19 (d, *J* = 8.6 Hz, 1H, 2-H) 7.16 (s, 1H, 4-H), 3.69 (t, *J* = 8.5 Hz, 1H, 17-H), 2.82 (m, 2H, 6-H), 2.31 (dq, *J* = 13.2 Hz, 3,9 Hz, 1H, 11-H$_a$), 2.23 (td, *J* = 11.2 Hz, 4.3 Hz, 1H, 9-H), 2.08 (dtd, *J* = 12.7 Hz, 9.2 Hz, 5.5 Hz, 1H, 16-H$_a$), 1.93 (m. 1H, 12-H$_a$), 1.88 (m, 1H, 7-H$_a$), 1.70 (dddd, *J* = 12.4 Hz, 9.9 Hz, 7.0 Hz, 3.1 Hz, 1H, 15-H$_a$) 1.51 (m, 1H, 11-H$_b$), 1.47 (m, 1H, 16-H$_b$), 1.45 m, 1H, 8-H), 1.35 (m, 1H, 15-H$_b$), 1.31 (m, 1H, 7-H$_b$), 1.27 (m, 1H, 12-H$_b$), 1.19 (m, 1H, 14-H), 0.76 (s, 3H, 18-H), 0.23 (s, 9H, trimethylsilyl)

^{13}C NMR (126 MHz, CD$_2$Cl$_2$) δ/ppm = 141.91 (C-10), 137.45 (C-5), 132.62 (C-4), 129.24 (C-2), 125.73 (C-1), 120.38 (C-3), 105.77 (ethynyl, *α*-silyl), 93.32 (ethynyl, *α*-C-3), 82.09 (C-17), 50.55 (C-14), 44.88 (C-9), 43.54 (C-13), 38.82 (C-8), 37.08 (C-12), 30.92 (C-16), 29.60 (C-6), 27.41 (C-7), 26.39 (C-11), 23.45 (C-15), 11.22 (C-18), 0.07 (trimethylsilyl)

IR (ATR): ṽ$_{max}$/cm^{-1} = 2924, 1248, 1060, 865, 757

HRMS (EI): m/z = [M$^{•+}$] calcd. for C$_{23}$H$_{32}$OSi $^{•+}$: 352.2217; found: 352.2218

Literature known compound[102]

(8*R*,9*S*,13*S*,14*S*,17*S*)-3-Ethynyl-13-methyl-7,8,9,11,12,13,14,15,16,17-decahydro-6*H*-cyclopenta[*a*]phenanthren-17-ol (11)
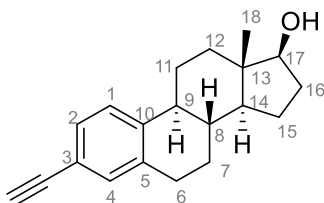
$C_{20}H_{24}O$

M_w: 280.4 g/mol

To a solution of silylated alkyne **10** (56.4 mg, 0.160 mmol, 1.00 eq) in THF (5 mL) was added TBAF·3 H_2O (55.5 mg, 0.176 mmol, 1.10 eq) at 0 °C. The mixture was allowed to come to room temperature and then stirred for 1h. Thereafter saturated aqueous ammonium chloride solution was added and the resulting mixture was extracted with dichloromethane (3 x 10 mL). The combined organic extracts were washed with water (20 mL), 1 M aqueous NaOH solution (20 mL) and brine (20 mL), dried over anhydrous sodium sulfate and concentrated *in vacuo*. The crude product was purified by flash column chromatography (isohexane/ethyl acetate 4:1) to yield compound **11** (32.0 mg, 0.114 mmol, 71 %) as a light yellow solid.

m.p.: 90 °C

¹H NMR (400 MHz, DMSO) δ/ppm = 7.28 (d, *J* = 8.2 Hz, 1H, 1-H), 7.19 (dd, *J* = 8.1 Hz, 1.9 Hz, 1H, 2-H) 7.15 (s, 1H, 4-H), 4,50 (d, *J* = 4,8 Hz, 1H, OH), 4.04 (s, 1H, alkyne CH), 3.52 (td, *J* = 8.4 Hz, 4.5 Hz, 1H, 17-H), 2.78 (m, 2H, 6-H), 2.28 (m, 1H, 11-H$_a$), 2.18 (m, 1H, 9-H), 1.89 (m, 1H, 16-H$_a$), 1.85 (m. 1H, 12-H$_a$), 1.81 (m, 1H, 7-H$_a$), 1.59 (m, 1H, 15-H$_a$) 1.38 (m, 1H, 16-H$_b$), 1.35 (m, 1H, 11-H$_b$), 1.32 m, 1H, 8-H), 1.26 (m, 1H, 7-H$_b$), 1.24 (m, 1H, 15-H$_b$), 1.17 (m, 1H, 12-H$_b$), 1.12 (m, 1H, 14-H), 0.66 (s, 3H, 18-H)

¹³C NMR (101 MHz, DMSO) δ/ppm = 141.33 (C-10), 136.84 (C-5), 131.88 (C-4), 128.80 (C-2), 125.58 (C-1), 118.72 (C-3), 83.70 (alkyne C-C), 79.97 (C-17), 79.79 (alkyne C-H), 49.57 (C-14), 43.92 (C-9), 42.73 (C-13), 38.03 (C-8), 36.50 (C-12), 29.85 (C-16), 28.57 (C-6), 26.50 (C-7), 25.60 (C-11), 22.75 (C-15), 11.19 (C-18)

IR (ATR): $\tilde{v}_{max}$/cm⁻¹ = 3298, 2925, 1692, 1602, 1493, 1249, 1053, 898

HRMS (EI): m/z = [M˙⁺] calcd. for $C_{20}H_{24}O$ ˙⁺: 280.1822; found: 280.1827

Purity (HPLC): > 95 % (λ = 210 nm), > 96 % (λ = 254 nm) (Method 2)

Literature known compound[175]

(8*R*,9*S*,13*S*,14*S*,17*S*)-17-Hydroxy-13-methyl-7,8,9,11,12,13,14,15,16,17-decahydro-6*H*-cyclopenta[*a*]phenanthrene-3-carbaldehyde (12)
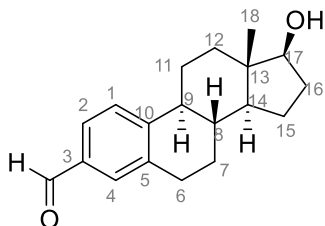
$C_{19}H_{24}O_2$

M_w: 284.40 g/mol

Palladium (II) acetate (11.2 mg, 0.0500 mmol, 5 mol%), 1,1′-bis(diphenylphosphino)ferrocen (dppf) (41.6 mg, 0.0800 mmol, 8 mol%), *N*-formylsaccharin (317 mg, 1.50 mmol, 1.50 eq) and acetonitrile (5.0 mL) were combined in a flame dried 25 mL round bottom flask equipped with a reflux condenser, a septum with a nitrogen balloon and a magnetic stirring bar. The system was purged with nitrogen for three times. Triflate **PRU-9** (404 mg, 1.00 mmol, 1.00 eq), triethylsilane (0.240 mL 1.50 mmol, 1.50 eq) and sodium carbonate (159 mg, 1.50 mmol, 1.50 eq) were added to the suspension under a nitrogen flow. The mixture was heated to 80 °C under stirring for 16 h. After cooling to room temperature, dichloromethane (5 mL) and water (5 mL) were added to the mixture and it was extracted with dichloromethane (3 x 5 mL). The combined organic extracts were washed with water (10 mL) and brine (10 mL), filtered through a hydrophobic filter and concentrated under reduced pressure. The crude product was purified by flash column chromatography (isohexane/ethyl acetate 2:1) to yield 57.1 mg (0.201 mmol, 20 %) of compound **12** as a colorless oil.

¹H NMR (500 MHz, DMSO) δ/ppm = 9.92 (d, *J* = 1.2 Hz, 1H, aldehyde), 7.64 (dd, *J* = 8.1 Hz, 1.8 Hz, 1H, 2-H), 7.58 (d, *J* = 1.9 Hz, 1H, 4-H), 7.51 (d, *J* = 8.1 Hz, 1H, 1-H), 4.52 (br s, 1H, OH), 3.53 (t, *J* = 8.5 Hz, 1H, 17-H), 2.89 (dd, *J* = 10.3, 6.6 Hz, 2H 6-H), 2.35 (dt, *J* = 13.2, 3.7 Hz, 1H, 11-H$_a$), 2.26 (m, 1H, 9-H), 1.88 (m, 1H, 16-H$_a$), 1.86 (m, 1H, 12-H$_a$), 1.83 (m, 1H, 7-H$_a$), 1.60 (dtd, *J* = 9.7 Hz, 7.2 Hz, 3.3 Hz, 1H, 15-H$_a$), 1.42 (m, 1H, 11-H$_b$), 1.38 (m, 1H, 8-H), 1.37 (m, 1H, 16-H$_b$), 1.31 (m, 1H, 7-H$_b$), 1.26 (m, 1H, 15-H$_b$), 1.22 (m, 1H, 12-H$_b$), 1.15 (m, 1H, 14-H), 0.67 (s, 3H, 18-H)

¹³C NMR (126 MHz, DMSO) δ/ppm = 192.84 (aldehyde), 147.55 (C-5), 137.47 (C-10), 133.85 (C-2), 129.98 (C-4), 126.63 (C-1 or C-2), 126.14 (C-1 or C-2), 79.96 (C-17), 49.63 (C-14), 44.39 (C-9), 42.71 (C-13), 37.86 (C-8), 36.51 (C-12), 29.85 (C-16), 28.75 (C-6), 26.41 (C-7), 25.62 (C-11), 22.78 (C-15), 11.18 (C-18)

IR (ATR): $\tilde{v}_{max}$/cm^1 = 3426, 2924, 2868, 1603, 1569, 1422, 1379, 1226, 1137, 1050, 1010

HRMS (EI): m/z = [M$^{•+}$] calcd. for $C_{19}H_{24}O_2^{•+}$: 284.1771; found: 284.1770

(8*R*,9*S*,13*S*,14*S*,17*S*)-17-Hydroxy-13-methyl-7,8,9,11,12,13,14,15,16,17-decahydro-6*H*-cyclopenta[*a*]phenanthrene-3-carbonitrile (13)
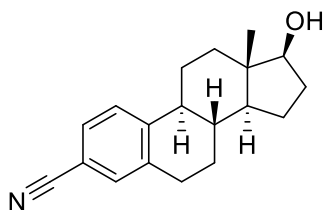
$C_{19}H_{23}NO$

M_w: 281.40 g/mol

404 mg (1.00 mmol, 1.00 eq) of triflate **PRU-9**, 130 mg (2.00 mmol, 2.00 eq) of potassium cyanide, 20.7 mg (0.0200 mmol, 2 mol%) of tris(dibenzylideneacetone) dipalladium (0)-chloroform adduct and 55.4 mg (0.100 mmol, 0.100 eq) of 1,1'-bis(diphenylphosphino) ferrocene (dppf) were combined in a round bottom flask. Then 0.5 mL of 1-methyl-2-pyrrolidinone was added and the resulting mixture was stirred at 60 °C for 6 h under a nitrogen atmosphere. After cooling, the mixture was filtered through a small pad of celite, evaporated to dryness and purified by flash column chromatography (isohexane/ethyl acetate 3:1) to yield 224 mg (0.796 mmol, 80 %) of compound **13** as a light yellow solid.

m.p.: 131 °C

H NMR (400 MHz, DMSO) δ/ppm = 7.55 (dd, *J* = 8.1 Hz, 1.9 Hz, 1H, 2-H), 7.52 (d, *J* = 1.6 Hz, 1H, 4-H) 7.47 (d, *J* = 8.1 Hz, 1H, 1-H), 4,52 (d, *J* = 4,8 Hz, 1H, OH), 3.53 (td, *J* = 8.5 Hz, 4.8 Hz, 1H, 17-H), 2.83 (m, 2H, 6-H), 2.32 (dq, *J* = 12.8 Hz, 3.7 Hz, 1H, 11-H$_a$), 2.24 (m, 1H, 9-H), 1.88 (m, 1H, 16-H$_a$), 1.85 (m. 1H, 12-H$_a$), 1.81 (m, 1H, 7-H$_a$), 1.60 (dddd, *J* = 12.0 Hz, 9.7 Hz, 6.8 Hz, 3.1 Hz, 1H, 15-H$_a$), 1.39 (m, 1H, 16-H$_b$), 1.36 (m, 1H, 11-H$_b$), 1.33 (m, 1H, 8-H), 1.28 (m, 1H, 7-H$_b$), 1.24 (m, 1H, 15-H$_b$), 1.18 (m, 1H, 12-H$_b$), 1.13 (m, 1H, 14-H), 0.67 (s, 3H, 18-H)

^{13}C NMR (101 MHz, DMSO δ/ppm = 146.16 (C-10), 138.15 (C-5), 132.24 (C-4), 129.11 (C-2), 126.47 (C-1), 119 (nitrile C),108.24 (C-3), 79.91 (C-17), 49.55 (C-14), 44.07 (C-9), 42.68 (C-13), 37.64 (C-8), 36.42 (C-12), 29.83 (C-16), 28.43 (C-6), 26.15 (C-7), 25.40 (C-11), 22.72 (C-15), 11.14 (C-18),

IR (ATR): $\tilde{v}_{max}$/cm^{-1} = 3507, 2865, 2229, 1602, 1248, 1138, 1058, 1002, 900, 782

HRMS (EI): m/z = [M$^{•+}$] calcd. for $C_{19}H_{23}NO$ $^{•+}$: 281.1774; found: 281.1775

Literature known compound[97]

(*E*/*Z*)-3-((8*R*,9*S*,13*S*,14*S*,17*S*)-17-Hydroxy-13-methyl-7,8,9,11,12,13,14,15,16,17-decahydro-6*H*-cyclopenta[*a*]phenanthren-3-yl)acrylonitrile (14)
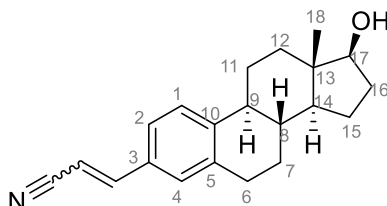
C$_{21}$H$_{25}$NO

M$_w$: 307.44 g/mol

A flame dried Schlenk flask was evacuated and backfilled with nitrogen three times prior to the addition of 283 mg (0.700 mmol, 1.00 eq) of triflate **PRU-9**, 0.07 mL (1.05 mmol, 1.50 eq) of 2-propenenitrile, 89.9 mg (2.10 mmol, 3.00 eq) of lithium chloride, 1.00 mg of 2,6-di-*tert*-butyl-4-methylphenol, 0.4 mL (0.280 mmol, 0.400 eq) of triethylamine and 2 mL of DMF. Then 49.1 mg (0.0700 mmol, 0.100 eq) of bis(triphenylphosphine)palladium dichloride was added under a nitrogen flow. The resulting suspension was then heated at 90 °C under a nitrogen atmosphere and stirred rapidly for 14 h. After cooling, the reaction mixture was extracted with ethyl acetate (3 x 10 mL) and the combined organic extracts were washed with brine (2 × 10 mL), dried over anhydrous sodium sulfate and concentrated *in vacuo*. The residue was purified by flash column chromatography to yield 72.0 mg (0.234 mmol, 34 %) of compound **14** as a mixture of *E*/*Z*-isomers.

m.p.: 170 °C

¹H NMR (500 MHz, CD$_2$Cl$_2$) δ/ppm = 7.61-7.08 (3H, 1-H, 2-H, 4-H; 1H, Ar-CH), 5.84 (d, *J* = 16.6 Hz, 0.53H, CH-CN E-isomer), 5.38 (d, *J* = 12.1 Hz, 0.46H, CH-CN Z-isomer), 3.70 (m, 1H, 17-H), 2.88 (m, 2H, 6-H), 2.34 (m, 1H), 2.25 (m, 1H), 2.08 (m, 1H), 1.95 (m, 1H), 1.90 (m, 1H), 1.80 (m, 1H), 1.50-1.42 (m, 3H), 1.38-1.29 (m, 3H), 1.18 (m, 1H, 12-H), 1.21 (m, 1H, 14-H), 0.76 (2s, 3H, 18-H)

¹³C NMR (126 MHz, CD$_2$Cl$_2$ δ/ppm = 150.96 and 148.98 (Ar-CH), 144.86 and 144.52 (C-10), 138.50 and 138.00 (C-5) 131.52 and 131.31 (C-3), 130.09-124.86 (6 peaks, C-1, C-4, C-2), 118.89 and 118.03 (CN), 95.38 and 94.33 (CH-CN), 82.05 (C-17), 50.54 (C-14), 45.06 (C-9), 43.53 (C-13), 38.78 (C-8), 37.06 (C-12), 30.90 and 30.09 (C-16), 29.77 (C-6), 27.35 (C-7), 26.41 (C-11), 23.44 (C-15), 11.20 (C-18)

IR (ATR): ṽ$_{max}$/cm^{-1} = 2853, 2215, 1738, 1616, 1453, 1261, 1054, 1022, 814, 788

HRMS (EI): m/z = [M$^{•+}$] calcd. for C$_{21}$H$_{25}$NO $^{•+}$: 307.1931; found: 307.1931

Purity (HPLC): > 95 % (λ = 210 nm), > 99 % (λ = 254 nm) (Method 2)

(8*R*,9*S*,13*S*,14*S*,17*S*)-3-Amino-13-methyl-7,8,9,11,12,13,14,15,16,17-decahydro-6*H*-cyclopenta[*a*]phenanthren-17-ol (15)
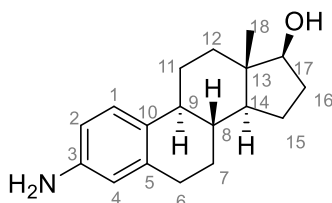
$C_{18}H_{25}NO$

M_w: 271.40 g/mol

Benzylamine **32** (97.6 mg, 0.270 mmol, 1.00 eq), Pd/C (10 %) (14.4 mg, 0.0135 mmol, 5 mol%) and methanol (1.2 mL) were combined in a flame dried flask under a nitrogen atmosphere. The resulting suspension was brought under a hydrogen atmosphere and stirred at room temperature for 6 h. The catalyst was removed by filtration through a small pad of celite and after evaporation of the solvent, the crude product was purified by flash column chromatography (isohexane/ethyl acetate 1:1 with 1 % triethylamine) to yield 66.0 mg (0.243 mmol, 90 %) of compound **15** as a white solid.

m.p.: 92 °C

¹H NMR (500 MHz, CD₃OD) δ/ppm = 7.06 (d, *J* = 8.3 Hz, 1H, 1-H), 6.57 (dd, *J* = 8.3 Hz, 2.5 Hz, 1H, 2-H), 6.51 (d, *J* = 2.4 Hz, 1H, 4-H), 3.66 (t, *J* = 8.7 Hz, 1H, 17-H), 2.77 (td, *J* = 9.7 Hz, 6.3 Hz, 2H, 6-H), 2.30 (dq, *J* = 13.3 Hz, 3.9 Hz, 1H, 11-Hₐ), 2.14 (m, 1H, 9-H), 2.04 (m, 1H, 16-Hₐ), 1.96 (m, 1H, 12-Hₐ), 1.88 (ddt, *J* = 12.5 Hz, 5.7 Hz, 2.5 Hz, 1H, 7-Hₐ), 1.71 (m, 1H, 15-Hₐ), 1.54 (m, 1H, 16-H_b), 1.43 (m, 1H, 11-H_b), 1.39 (m, 1H, 8-H), 1.35 (m, 1H, 15-H_b), 1.31 (m, 1H, 7-H_b), 1.26 (m, 1H, 12-H_b), 1.19 (m, 1H, 14-H), 0.78 (s, 3H, 18-H).

¹³C NMR (126 MHz, CD₃OD) δ/ppm = 144.61 (C-3), 138.38 (C-5), 132.59 (C-10), 126.97 (C-1), 117.57 (C-4), 115.25 (C-2), 82.52 (C-17), 51.33 (C-14), 45.44 (C-9), 44.39 (C-13), 40.60 (C-8), 38.05 (C-12), 30.71 (C-6 or C-16), 30.70 (C-6 or C-16), 28.58 (C-7), 27.58 (C-11), 24.04 (C-15), 11.69 (C-18).

IR (ATR): ṽ_max/cm⁻¹ = 3336, 2923, 1738, 1614, 1502, 1445, 1259, 816

HRMS (ESI): m/z = [M+H]⁺ calcd. for $C_{18}H_{26}NO^+$: 272.2009; found: 272.2010

Purity (HPLC): > 96 % (λ = 210 nm), > 96 % (λ = 254 nm) (Method 1d)

(8*R*,9*S*,13*S*,14*S*,17*S*)-13-Methyl-3-(methylamino)-7,8,9,11,12,13,14,15,16,17-decahydro-6*H*-cyclopenta[*a*]phenanthren-17-ol (16)
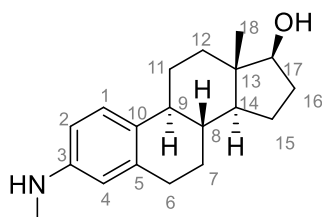
$C_{19}H_{27}NO$

M_w: 285.43 g/mol

Under a nitrogen atmosphere amine **31** (75.1 mg, 0.200 mmol, 1.00 eq) was dissolved in dichloromethane (4.0 mL) and cooled to -78 °C. Then boron trichloride solution (1 M in dichloromethane, 2.34 mL, 2.34 mmol, 3.00 eq) was added dropwise and the resulting solution was allowed to warm up to 0 °C and stirred at this temperature for 2 h. Thereafter the mixture was quenched with methanol (4 mL) and filtered through a small pad of celite. After evaporation of the solvent, the crude product was purified by flash column chromatography (isohexane/ethyl acetate 2:1 with 1 % triethylamine) to yield 40.4 mg (0.142 mmol, 71 %) of compound **16** as a white solid.

m.p.: 137 °C

¹H NMR (400 MHz, CD_2Cl_2) δ/ppm = 7.07 (d, *J* = 8.4 Hz, 1H, 1-H), 6.40, (dd, *J* = 8.4 Hz, 2.6 Hz, 1H, 2-H), 6.32 (d, *J* = 2.6 Hz, 1H, 4-H), 3.68 (dd, *J* = 9.0 Hz, 7.9 Hz, 1H, 17-H), 2.80 (m, 2H, 6-H), 2.77 (s, 3H, NCH₃), 2.28 (m, 1H, 11-H$_a$), 2.14 (m, 1H, 9-H), 2.05 (m, 1H, 16-H$_a$), 1.89 (m, 1H, 12-H$_a$), 1.84 (m, 1H, 7-H$_a$), 1.69 (m, 1H, 15-H$_a$), 1.47 (m, 1H, 16-H$_b$), 1.43 (m, 1H, 11-H$_b$), 1.41 (m, 1H, 8-H), 1.38 (m, 1H, 15-H$_b$), 1.30 (m, 1H, 7-H$_b$), 1.26 (m, 1H, 12-H$_b$), 1.17 (m, 1H, 14-H), 0.76 (s, 3H, 18-H)

¹³C NMR (101 MHz, CD_2Cl_2) δ/ppm = 147.80 (C-3), 137.82 (C-5), 129.80 (C-10), 126.29 (C-1), 112.72 (C-4), 110.84 (C-2), 82.21 (C-17), 50.44 (C-14), 44.39 (C-9), 43.65 (C-13), 39.58 (C-8), 37.17 (C-12), 31.17 (NCH₃), 30.96 (C-16), 30.23 (C-6), 27.83 (C-7), 26.86 (C-11), 23.46 (C-15), 11.28 (C-18)

IR (ATR): $\tilde{v}_{max}$/cm⁻¹ = 3393, 2923, 2847, 1613, 1505, 1452, 1349, 1262, 1092, 729

HRMS (ESI): m/z = [M+H]⁺ calcd. for $C_{19}H_{28}NO^+$: 286.2165; found: 286.2167

Purity (HPLC): > 98 % (λ = 210 nm), > 99 % (λ = 254 nm) (Method 1d)

Literature known compound[177]

(8*R*,9*S*,13*S*,14*S*,17*S*)-3-(*N,N*-Dimethylamino)-13-methyl-7,8,9,11,12,13,14,15,16,17-decahydro-6*H*-cyclopenta[*a*]phenanthren-17-ol (17)
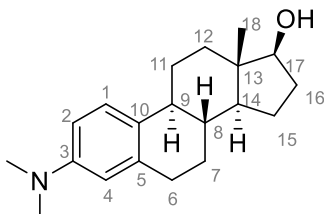
$C_{20}H_{29}NO$

M_w: 299.46 g/mol

To a solution of 16.3 mg (0.060 mmol, 1.00 eq) of primary amine **15** in 0.7 mL of acetonitrile, formaldehyde (37 % aqueous solution, 40 µL, 0.54 mmol, 9.0 eq), acetic acid (17 µL, 0.30 mmol, 5.0 eq) and sodium cyanoborohydride (19.8 mg, 0.300 mmol, 5.00 eq) were added and the resulting mixture was stirred for 1 h at ambient temperature. Thereafter the reaction was quenched with 1 mL of saturated aqueous sodium bicarbonate solution and the mixture extracted with ethyl acetate (3 x 2.5 mL). The combined organic phases were washed with water (5 mL) and brine (5 mL), filtered through a hydrophobic filter and evaporated to dryness. The crude product was purified by flash column chromatography (isohexane/ethyl acetate 2:1 with 1 % triethylamine) to yield 10.0 mg (0.0334 mmol, 56 %) of compound **17** as a white solid.

m.p.: 97 °C

¹H NMR (400 MHz, CD$_2$Cl$_2$) δ/ppm = 7.12 (d, *J* = 8.6 Hz, 1H, 1-H), 6.55 (dd, *J* = 8.6, 2.8 Hz, 1H, 2-H), 6.46 (s, 1H, 4-H) 3.68 (t, *J* = 8.3 Hz, 1H, 17-H), 2.86 (s, 6H, N(CH$_3$)$_2$), 2.80 (m, 2H, 6-H), 2.29 (dq, *J* = 13.2 Hz, 3.9 Hz, 1H), 2.29 (m, 1H, 11-H$_a$), 2.16 (m, 1H, 9-H), 2.07 (m, 1H, 16-H$_a$), 1.90 (m, 1H, 12-H$_a$), 1.85 (m, 1H, 7-H$_a$), 1.68 (m, 1H, 15-H$_a$), 1.45 (m, 1H, 16-H$_b$), 1.43 (m, 1H, 11-H$_b$), 1.39 (m, 1H, 8-H), 1.34 (m, 1H, 15-H$_b$), 1.29 (m, 1H, 7-H$_b$), 1.24 (m, 1H, 12-H$_b$), 1.18 (m, 1H, 14-H), 0.76 (s, 3H, 18-H)

¹³C NMR (101 MHz, CD$_2$Cl$_2$) δ/ppm = 149.38 (C-3), 137.55 (C-5), 129.47 (C-10), 126.16 (C-1), 113.57 (C-4), 111.31 (C-2), 82.22 (C-17), 50.46 (C-14), 44.34 (C-13), 43.67 (C-9), 41.08 (N(CH$_3$)$_2$), 39.60 (C-8), 37.19 (C-12), 30.96 (C-16), 30.43 (C-6), 27.90 (C-7), 26.83 (C-11), 23.47 (C-15), 11.29 (C-18)

IR (ATR): ṽ$_{max}$/cm^{-1} = 2923, 1974, 1665, 1610, 1509, 1422, 1352, 1208, 806

HRMS (ESI): m/z = [M+H]$^+$ calcd. for C$_{20}$H$_{30}$NO$^+$: 300.2322; found: 300.2324

Purity (HPLC): > 95 % (λ = 210 nm), > 97 % (λ = 254 nm) (Method 1d)

Literature known compound[178]

(8*R*,9*S*,13*S*,14*S*,17*S*,*E*)-17-Hydroxy-13-methyl-1,2,6,7,8,9,10,11,12,13,14,15,16,17-tetradecahydro-3*H*-cyclopenta[*a*]phenanthren-3-one oxime (18)
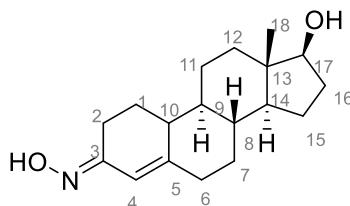
$C_{18}H_{27}NO_2$

M_w: 289.42 g/mol

(8*R*,9*S*,13*S*,14*S*,17*S*,*Z*)-17-Hydroxy-13-methyl-1,2,6,7,8,9,10,11,12,13,14,15,16,17-tetradecahydro-3*H*-cyclopenta[*a*]phenanthren-3-one oxime (19)
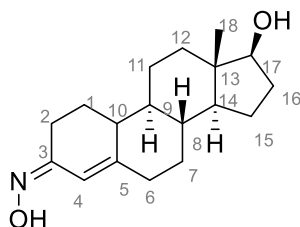
$C_{18}H_{27}NO_2$

M_w: 289.42 g/mol

19-Nortestosterone (**4**) (0.988 g, 3.60 mmol, 1.00 eq) and hydroxylamine hydrochloride (0.963 g, 13.9 mmol, 3.85 eq) were added to a round bottom flask and dissolved in a 20 mL of a mixture of pyridine and ethanol (1:1). The resulting solution was heated at reflux for 4 hours. Then the solvent was removed under reduced pressure and the residue was poured into water (50 mL). The precipitate was collected by filtration and dried *in vacuo*. The crude product was purified by flash column chromatography to yield 0.866 g (2.99 mmol, 83 %) of a mixture of partially separable *E*-(**18**) and *Z*-(**19**) oximes (ratio estimated on basis of NMR data: *E*:*Z* = 3:1) as a beige solid.

18:

m.p.: 168 °C

¹H NMR (400 MHz, DMSO) δ/ppm = 10.41 (s 1H, NOH), 5,78 (s, 1H, 4-H), 4.44 (d, *J* = 4,8 Hz, 1H, OH), 3.44 (td, *J* = 8.5 Hz, 4.4 Hz, 1H, 17-H), 2.86 (dt, *J* = 16.5 Hz, 4.2 Hz, 1H, 2-H$_a$), 2.34 (dt, *J* = 14.5 Hz, 3.2 Hz, 1H, 6-H$_a$), 2.14 (m, 1H, 6-H$_b$), 2.03 (m, 1H, 1-H or 15-H), 1.90 (m. 1H, 10-H), 1.86 (m, 1H, 2-H$_b$), 1.81 (m, 1H, 16-H$_a$) 1.76 (m, 1H, 1-H or 15-H), 1.72 (m, 1H, 12-H$_a$), 1.66 (m, 1H, 7-H$_a$), 1.49 (m, 1H, 11-H$_a$), 1.34 (m, 1H, 16-H$_b$), 1.26 (m, 1H, 8-H), 1.21 (m, 1H, 1-H or 15-H), 1.17 (m, 1H, 11-H$_b$), 1.14 (m, 1H, 1'-H), 0.98 (m, 1H, 12-H$_b$), 0.92 (m, 1H, 14-H) 0.84 (m, 1H, 7-H$_b$), 0.67 (s, 3H, 18-H), 0.64 (m, 1H, 9-H)

¹³C NMR (101 MHz, DMSO) δ/ppm = 154.40 (C-3), 148.35 (C-5), 118.63 (C-4), 80.01 (C-17), 49.42 (C-14), 49.27 (C-9), 42.61 (C-13), 41.37 (C-10), 40.10 (C-8), 36.42 (C-12), 34.36 (C-6), 30.63 (C-7), 29.79 (C-16), 25.84 (C1 or C-15), 25.73 (C1 or C-15), 22.92 (C-11), 20.72 (C-2), 11.22 (C-18)

IR (ATR): $\tilde{v}_{max}$/cm⁻¹ = 3269, 2922, 2861, 1641, 1446, 1347, 1132, 1053, 959, 711

HRMS (ESI): m/z = [M+H]⁺ calcd. for $C_{18}H_{28}NO_2^+$: 290.2115; found: 290.2116

19:

m.p.: 188 °C

¹H NMR (400 MHz, DMSO) δ/ppm = 10.15 (s 1H, NOH), 6.39 (s, 1H, 4-H), 4,44 (d, *J* = 4,8 Hz, 1H, OH), 3.44 (td, *J* = 8.7 Hz, 1H, 17-H), 2.34 (d, *J* = 14 Hz, 1H, 6-Ha), 2.23 (m. 1H. 1-H or 15-H), 2.15 (m, 1H, 6-Hb), 2.08 (m, 1H, 1-Ha or 15-Ha), 2.03 (m, 1H, 1-Ha or 15-Ha), 1.96 (m. 1H, 10-H), 1.83 (m, 1H, 16-Ha), 1.76 (m, 1H, 11-Ha), 1.73 (m, 1H, 12-Ha) 1.69 (m, 1H, 7-Ha), 1.49 (m, 1H, 2-Ha), 1.32 (m, 1H, 16-Hb), 1.24 (m, 1H, 8-H), 1.21 (m, 1H, 2-Hb or 1-Hb or 15-Hb), 1.18 (m, 1H, 2-Hb or 1-Hb or 15-Hb), 1.14 (m, 1H, 11-Hb), 0.98 (m, 1H, 12-Hb), 0.92 (m, 1H, 14-H) 0.86 (m, 1H, 7-Hb), 0.68 (s, 3H, 18-H), 0.65 (m, 1H, 9-H)

¹³C NMR (101 MHz, DMSO) δ/ppm = 152.24 (C-3), 151.33 (C-5), 111.61 (C-4), 79.98 (C-17), 49.56 (C-9), 49.35 (C-14), 42.62 (C-13), 42.45 (C-10), 39.94 (C-8), 36.38 (C-12), 35.03 (C-6), 30.89 (C-7), 29.79 (C-16), 27.16 (C1 or C-15), 27.00 (C1 or C-15), 25.65 (C-11), 22.91 (C-2), 11.22 (C-18)

IR (ATR): $\tilde{v}_{max}$/cm⁻¹ = 3206, 2913, 2861, 2360, 1631, 1429, 1336, 1277, 1054, 879

HRMS (ESI): m/z = [M+H]⁺ calcd. for $C_{18}H_{28}NO_2^+$: 290.2115; found: 290.2112

Literature known compounds[116]

(8*R*,9*S*,13*S*,14*S*,17*S*)-3-Acetamido-13-methyl-7,8,9,11,12,13,14,15,16,17-decahydro-6*H*-cyclopenta[*a*]phenanthren-17-yl acetate (20)
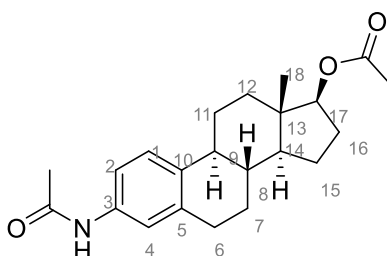
$C_{22}H_{29}NO_3$

A mixture of 0.269 g (0.930 mmol) of oximes **17** and **18** was dissolved in 5 mL of acetic anhydride under a nitrogen atmosphere. The resulting solution was stirred at 110 °C overnight. After cooling, the solvent was evaporated and the resulting dark oil was dissolved in a mixture of 3 mL of ethanol, 1.5 mL of water and 0.15 mL of acetic acid. This mixture was then heated at reflux for 15 hours. Thereafter it was cooled to room temperature, concentrated under reduced pressure and the resulting dark slurry was dissolved in dichloromethane (20 mL), washed with water (10 mL), 1 M aqueous NaOH (10 mL), again water (10 mL) and brine (10 mL). The solution was dried over anhydrous sodium sulfate, concentrated *in vacuo* and purified by flash column chromatography (isohexane/ethyl acetate 3:1) to yield 121 mg (0.340 mmol, 37 %) of compound **20** as a yellow solid.

m.p.: 200 °C

^{1}H NMR (500 MHz, DMSO) δ/ppm = 9.74 (s, 1H, NH), 7.28 (s, 1H, 4-H), 7.26 (m, 1H, 2-H) 7.16 (d, *J* = 8.4 Hz, 1H, 1-H), 4,60 (dd, *J* = 9,2 Hz, 7.7 Hz, 1H, 17-H), 2.76 (m, 2H, 6-H), 2.27 (m, 1H, 11-H$_a$), 2.15 (m, 1H, 9-H), 2.11 (m, 1H, 16-H$_a$), 2.01 (s, 3H, CH$_3$ at ester), 1.99 (s, 3H, CH$_3$ at amide), 1.81 (m. 1H, 7-H$_a$), 1.76 (m, 1H, 12-H$_a$), 1.67 (m, 1H, 15-H$_a$) 1.49 (m, 1H, 16-H$_b$), 1.37 (m, 1H, 15-H$_b$), 1.34 (m, 1H, 8-H), 1.33 (m, 1H, 12-H$_b$), 1.31 (m, 1H, 11-H$_b$), 1.28 (m, 1H, 7-H$_b$), 1.24 (m, 1H, 14-H), 0.78 (s, 3H, 18-H)

^{13}C NMR (126 MHz, DMSO δ/ppm = 170.37 (carbonyl of ester), 168.01 (carbonyl of amide), 136.84 (C-3), 136.32 (C-5 or C-10), 134.55 (C-5 or C-10), 125.42 (C-1), 119.11 (C-4), 116.66 (C-2), 81.89 (C-17), 49.09 (C-14), 43.42 (C-9), 42.51(C-13), 38.07 (C-8), 36.45 (C-12), 29.16 (C-6), 27.18 (C-16), 26.76 (C-7), 25.68 (C-11), 23.96 (CH$_3$ at amide), 22.79 (C-15), 20.90 (CH$_3$ at ester), 11.19 (C-18)

IR (ATR): ṽ$_{max}$/cm^{-1} = 3286, 2914, 2862, 2359, 1731, 1659, 1430, 1374, 1052, 878

HRMS (EI): m/z = [M$^{•+}$] calcd. for C$_{22}$H$_{29}$NO$_3$ $^{•+}$: 355.2142; found: 355.2142

Literature known compound[116]

(8*R*,9*S*,13*S*,14*S*,17*S*)-17-(Benzyloxy)-13-methyl-7,8,9,11,12,13,14,15,16,17-decahydro-6*H*-cyclopenta[*a*]phenanthren-3-yl trifluoromethanesulfonate (23)

$C_{26}H_{29}F_3O_4S$
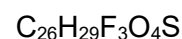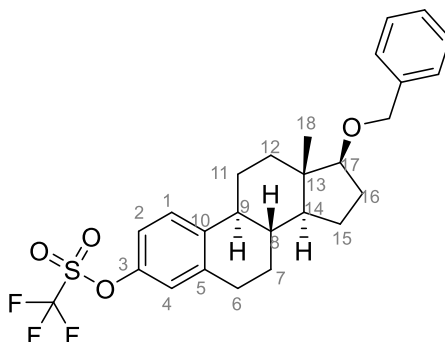
M_w: 494.57 g/mol

Triflate **PRU-9** (615 mg, 1.52 mmol, 1.00 eq), 2-benzyloxy-1-methylpyridinium triflate (1.06 g, 3.04 mmol, 2.00 eq) and magnesium oxide (vacuum dried, 126 mg, 18.0 mmol, 2.00 eq) were combined in a round bottom flask. Trifluoro toluene (5.0 mL) was added and the resulting suspension was heated at 83 °C under stirring for 24 h. After cooling to room temperature, the reaction mixture was diluted with dichloromethane (5 mL) and filtered through a small pad of celite. After evaporation of the solvent, the crude product was purified by flash column chromatography (isohexane/ethyl acetate 20:1) to yield 671 mg (1.36 mmol, 90 %) of compound **23** as a white solid.

m.p.: 63 °C

^{1}H NMR (400 MHz, CD_2Cl_2) *δ/*ppm = 7.36 (m, 1H, 1-H), 7.34 (m, 4H, benzyl aromatic ortho and meta Hs), 7.27 (ddt, *J* = 8.6, 5.6 Hz, 2.9 Hz, 1H, benzyl aromatic para H), 7.03 (dd, *J* = 8.7 Hz, 2.8 Hz, 1H, 2-H), 6.98 (d, *J* = 2.7 Hz, 1H, 4-H), 4.54 (s, 2H, benzyl CH_2), 3.52 (t, *J* = 8.3 Hz, 1H, 17-H), 2.88 (m, 2H, 6-H), 2.31 (m, 1H, 11-H$_a$), 2.24 (m, 1H, 9-H), 2.11 (m, 1H, 12-H$_a$), 2.06 (m, 1H, 16-H$_a$), 1.91 (m, 1H, 7-H$_a$), 1.71 (m, 1H, 15-H$_a$), 1.60 (m, 1H, 16-H$_b$), 1.55 (m, 1H, 11-H$_b$), 1.48 (m, 1H, 8-H), 1.43 (m, 1H, 12-H$_b$), 1.39 (m, 1H, 15-H$_b$), 1.36 (m, 1H, 7-H$_b$), 1.21 (m, 1H, 14-H), 0.86 (s, 3H, 18-H)

^{13}C NMR (101 MHz, CD_2Cl_2) *δ/*ppm = 147.84 (C-3), 141.71 (C-5 or C-10 or benzyl, quarternary carbon), 140.25 (C-5 or C-10 or benzyl, quarternary carbon), 139.92 (C-5 or C-10 or benzyl, quarternary carbon), 128.57 (C-1 or benzyl aromatic ortho or meta), 127.74 (C-1 or benzyl aromatic ortho or meta), 127.62 (benzyl, aromatic para), 121.43 (C-4), 118.39 (C-2), 1121.51-117.58 (qu, triflate), 88.85 (C-17), 72.03 (benzyl CH_2), 50.59 (C-14), 44.51 (C-9), 43.67 (C-13), 38.41 (C-8), 38.15 (C-12), 29.93 (C-6), 28.33 (C-16), 27.13 (C-7), 26.62 (C-11), 23.46 (C-15), 11.93 (C-18)

IR (ATR): $\tilde{v}_{max}$/cm^{-1} = 2935, 1486, 1402, 1250, 1137, 1080, 913, 838, 694

HRMS (EI): m/z = [M⁺] calcd. for $C_{26}H_{29}F_3O_4S$ ⁺⁺: 494.1733; found: 494.1733.

(8*R*,9*S*,13*S*,14*S*,17*S*)-17-Hydroxy-13-methyl-7,8,9,11,12,13,14,15,16,17-decahydro-6*H*-cyclopenta[*a*]phenanthren-3-yl *N,N*-dimethylcarbamate (24)
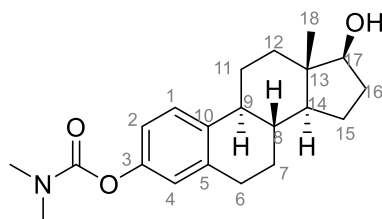
$C_{21}H_{29}NO_3$

M_w: 343.47 g/mol

5 mL of acetonitrile was added to a mixture of 501 mg (1.75 mmol, 1.00 eq) of 17*β*-estradiol (**3**) and 434 mg (2.63 mmol, 1.50 eq) of potassium carbonate in a round bottom flask. After addition of 0.24 mL (2.63 mmol, 1.50 eq) *N,N*-dimethylcarbamoyl chloride, the mixture was stirred for 3 h at 90 °C. It was then cooled to room temperature and concentrated *in vacuo*. Thereafter water (10 mL) was added and the resulting mixture was extracted with dichloromethane (3 × 10 mL). The combined organic extracts were washed with water (10 mL) and brine (10 mL), dried over anhydrous sodium sulfate and concentrated *in vacuo*. The crude product was purified by flash column chromatography (isohexane/ethyl acetate 3:1) to yield 600 mg (1.75 mmol, quant.) of compound **24** as a white solid.

m.p.: 188 °C

¹H NMR (500 MHz, CD₂Cl₂) *δ*/ppm = 7.26 (d, *J* = 8.5 Hz, 1H, 1-H), 6.83 (dd, *J* = 8.5 Hz, 2.5 Hz,1H, 2-H), 6.78 (d, *J* = 2.6 Hz, 1H, 4-H), 3.69 (t *J* = 8.5 Hz, 1H, 17-H), 3.06 (s, 3H, NCH₃), 2.95 (s, 3H, NCH₃'), 2.86 (m, 2H, 6-H), 2.33 (m, 1H, 11-Hₐ), 2.23 (td, *J* = 11.3 Hz, 4.3 Hz, 1H, 9-H), 2.08 (dtd, *J* = 12.5 Hz, 9.2 Hz, 5.4 Hz, 1H, 16-Hₐ), 1.93 (m, 1H, 12-Hₐ), 1.88 (m, 1H, 7-Hₐ), 1.70 (dddd, *J* = 12.4 Hz, 9.9 Hz, 7.0 Hz, 3.0 Hz, 1H, 15-Hₐ), 1.50 (m, 1H, 11-H_b), 1.48 (m, 1H, 8-H), 1.45 (m, 1H, 16-H_b), 1.36 (m, 1H, 15-H_b), 1.32 (m, 1H, 7-H_b), 1.28 (m, 1H, 12-H_b), 1.20 (m, 1H, 14-H), 0.77 (s, 3H, 18-H)

¹³C NMR (126 MHz, CD₂Cl₂) *δ*/ppm = 155.49 (carbonyl), 149.83 (C-3), 138.52 (C-5), 137.84 (C-10), 126.42 (C-1), 122.20 (C-4), 119.28 (C-2), 82.13 (C-17), 50.47 (C-14), 44.55 (C9), 43.57 (C-13), 39.00 (C-8), 37.12 (C-12) 36.84 (NCH₃), 36.62 (NCH₃'), 30.94 (C-16), 29.94 (C-6), 27.48 (C-7), 26.68 (C-11), 23.46 (C-15), 11.23 (C-18)

IR (ATR): $\tilde{v}_{max}$/cm⁻¹ = 2923, 1720, 1392, 1225, 1135, 1080. 1009, 886, 758

HRMS (EI): m/z = [M⁺] calcd. for $C_{21}H_{29}NO_3$ ⁺⁺: 343.2142; found: 343.2139

(8R,9S,13S,14S,17S)-17-(benzyloxy)-13-methyl-7,8,9,11,12,13,14,15,16,17-decahydro-6H-cyclopenta[a]phenanthren-3-yl N,N-dimethylcarbamate (25)
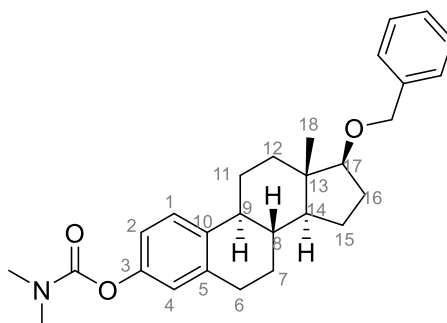
$C_{28}H_{35}NO_3$

M_w: 433.59 g/mol

Carbamate **24** (0.797 g, 2.32 mmol, 1.00 eq), Dudley Reagent (2-benzyloxy-1-methylpyridinium triflate) (1.62 g, 4.64 mmol, 2.00 eq) and magnesium oxide (vacuum dried, 0.190 g, 4.64 mmol, 2.00 eq) were combined in a round bottom flask. Trifluoro toluene (2.5 mL) was added and the resulting suspension was heated under stirring at 83 °C for 24 h. After cooling to room temperature, the reaction mixture was diluted with dichloromethane (10 mL) and filtered through a small pad of celite. After evaporation of the solvent, the crude product was purified by flash column chromatography (isohexane/ethyl acetate 20:1) to yield 0.577 g (1.33 mmol, 57 %) of compound **25** as a white solid.

m.p.: 169 °C

1H NMR (500 MHz, CD$_2$Cl$_2$) δ/ppm = 7.34 (m, 4H, benzyl aromatic ortho and meta Hs), 7.27 (m, 2H, benzyl aromatic para H and 1-H), 6.82 (dd, J = 8.5 Hz, 2.5 Hz, 1H, 4-H), 6.78 (d, J = 2.6 Hz, 1H, 2-H), 4.55 (s, 2H, benzyl CH$_2$), 3.52 (t, J = 8.3 Hz, 1H, 17-H), 3.06 (s, 3H, NCH$_3$), 2.96 (s, 3H, NCH$_3$'), 2.86 (m, 2H, 6-H), 2.31 (m, 1H, 11-H$_a$), 2.23 (td, J = 11.1, 4.1 Hz, 1H, 9-H), 2.10 (m, 1H, 12-H$_a$), 2.06 (m, 1H, 16-H$_a$), 1.89 (ddt, J = 12.1 Hz, 5.8 Hz, 2.7 Hz, 1H, 7-H$_a$) 1.70 (dddd, J = 12.3, 9.7, 7.0, 3.2 Hz, 1H, 15-H$_a$), 1.61 (m, 1H, 16-H$_b$), 1.56 (m, 1H, 11-H$_b$), 1.49 (m, 1H, 8-H), 1.43 (m, 1H, 12-H$_b$), 1.39 (m, 1H, 15-H$_b$), 1.35 (m, 1H, 7-H$_b$), 1.22 (m, 1H, 14-H), 0.86 (m, 1H, 18-H)

13C NMR (126 MHz, CD$_2$Cl$_2$) δ/ppm = 155.48 (carbamate, quarternary carbon), 149.82 (C-3), 139.99 (benzyl, quarternary carbon), 138.50 (C-5), 137.86 (C-10), 128.56((benzyl, aromatic para), 127.75 (2C, benzyl aromatic ortho or meta), 127.60 (2C, benzyl aromatic ortho or meta), 126.42 (C-1), 122.19 (C-2), 119.26 (C-4), 89.00 (C-17), 72.03 (benzyl CH$_2$), 50.65 (C-14),

44.55 (C-9), 43.75 (C-13), 38.78 (C-8), 38.32 (C-12), 36.82 (NCH$_3$), 36.64 (NCH$_3$'), 29.94 (C-6), 28.38 (C-16), 27.46 (C-7), 26.79 (C-11), 23.49 (C-15), 11.98 (C-18)

IR (ATR): $\tilde{v}_{max}$/cm^{-1} = 2932, 2869, 1711, 1493, 1453, 1384, 1226, 1121, 1027, 732, 694

HRMS (EI): m/z = [M$^{•+}$] calcd. for C$_{28}$H$_{35}$NO$_3{}^{•+}$: 433.2611; found: 433.2608

(8*R*,9*S*,13*S*,14*S*,17*S*)-*N*-Benzyl-17-(benzyloxy)-13-methyl-7,8,9,11,12,13,14,15,16,17-decahydro-6*H*-cyclopenta[a]phenanthren-3-amine (28)
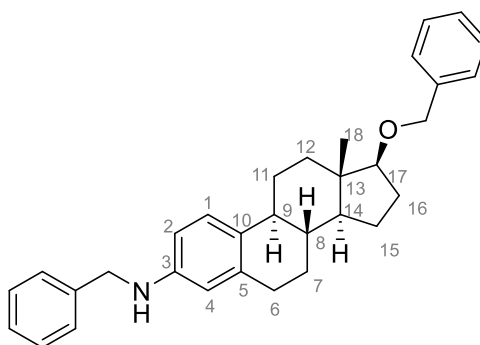
C$_{32}$H$_{37}$NO

M$_w$: 451.65 g/mol

Aryl triflate **23** (742 mg, 1.50 mmol, 1.00 eq), palladium (II) acetate (33.7 mg, 0.15 mL, 10 mol%), XPhos (71.5 mg, 0,150 mmol, 0.100 eq) and cesium carbonate (489 mg, 1.50 mmol, 1.00 eq) were combined in a flame dried Schlenk flask and suspended in toluene (4.5 mL). Benzylamine (0.246 mL, 241 mg, 2.25 mmol, 1.50 eq) was added and the suspension was heated at 100 °C under stirring for 24 h. After cooling to ambient temperature, water (2.5 mL) was added and the resulting mixture was extracted with ethyl acetate (3 x 5 mL). The combined organic phases were washed with water (10 mL) and brine (10 mL), filtered through a hydrophobic filter and evaporated to dryness. The crude product was purified by flash column chromatography (isohexane/ethyl acetate 10:1) to yield 458 mg (1.01 mmol, 68 %) of compound **28** as a white solid.

m.p.: 95 °C

¹H NMR (400 MHz, CDCl$_3$) δ*/*ppm = 7.34 (m, 8H, *N*-benzyl ortho and meta Hs, *O*-benzyl aromatic ortho and meta Hs), 7.28 (m, 1H, *O*-benzyl or *N*-benzyl aromatic para H), 7.25 (m, 1H, *O*-benzyl or *N*-benzyl aromatic para H), 7.10 (d, *J* = 8.4 Hz, 1H, 1-H), 6.46 (dd, *J* = 8.4 Hz, 2.6 Hz, 1H, 2-H), 6.39 (d, *J* = 2.5 Hz, 1H, 4-H), 4.57 (s, 2H, *O*-benzyl CH$_2$), 4.30 (s, 2H, *N*-benzyl CH$_2$), 3.49 (t, *J* = 8.3 Hz, 1H, 17-H), 2.79 (m, 2H, 6-H), 2.25 (m, 1H, 11-H$_a$), 2.14 (m, 1H, 9-H), 2.08 (m, 1H, 12-H$_a$), 2.04 (m, 1H, 16-H$_a$), 1.83 (m, 1H, 7-H$_a$),1.66 (m, 1H, 15-H$_a$),

1.59 (m, 1H, 16-H$_b$), 1.48 (m, 1H, 11-H$_b$), 1.43 (m, 1H, 8-H), 1.38 (m, 1H, 15-H$_b$), 1.32 (m, 1H, 12-H$_b$), 1.26 (m, 1H, 7-H$_b$), 1.17 (m, 1H, 14-H), 0.86 (s, 3H, 18-H)

^{13}C NMR (101 MHz, CDCl$_3$) δ/ppm = 146.23 (C-3), 139.90 (*O*-benzyl or *N*-benzyl, quarternary carbon), 139.52 (*O*-benzyl or *N*-benzyl, quarternary carbon), 137.72 (C-5), 129.98 (C-10), 128.73-127.28 (6 peaks, 8C, *O*-benzyl and *N*-benzyl aromatic C-Hs), 126.33 (C-1), 113.10 (C-4), 110.97 (C-2), 88.54 (C-17), 71.80 (*O*-benzyl CH$_2$), 50.38 (C-14), 48.72 (*N*-benzyl CH$_2$), 44.12 (C-9), 43.61 (C-13), 38.96 (C-8), 38.16 (C-12), 30.00 (C-6), 28.18 (C-16), 27.50 (C-7), 26.61 (C-11), 23.28 (C-15), 11.99 (C-18)

IR (ATR): ṽ$_{max}$/cm^{-1} = 2922, 2851, 2360, 1613, 1502, 1452, 1070, 1027, 734

HRMS (ESI): m/z = [M+H]$^+$ calcd. for C$_{32}$H$_{38}$NO$^+$: 452.2948; found: 452.2952

(8*R*,9*S*,13*S*,14*S*,17*S*)-*N*-Benzyl-17-(benzyloxy)-*N*,13-dimethyl-7,8,9,11,12,13,14,15,16,17-decahydro-6*H*-cyclopenta[*a*]phenanthren-3-amine (30)
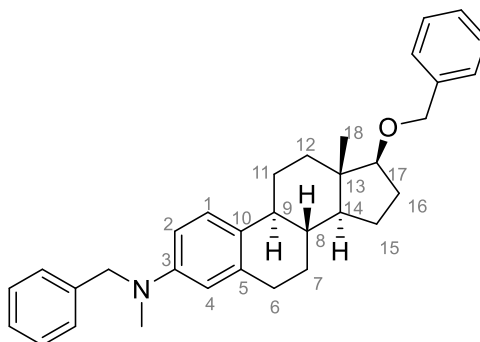
C$_{33}$H$_{39}$NO

M$_w$: 465.68 g/mol

To a solution of 203 mg (0.450 mmol) of amine **28** in 10 mL of acetonitrile formaldehyde (37 % aqueous solution, 0.124 mL, 4.50 mmol, 10.0 eq), acetic acid (0.371 mL, 6.48 mmol, 14.4 eq) and sodium cyanoborohydride (38.7 mg, 0.585 mmol, 1.30 eq) were added and the resulting mixture was stirred for 1 h at ambient temperature. After quenching with 1 mL of saturated aqueous sodium bicarbonate solution the mixture was extracted with ethyl acetate (3 x 5 mL). The combined organic phases were washed with water (10 mL) and brine (10 mL), filtered through a hydrophobic filter and evaporated to dryness. The crude product was purified by flash column chromatography (isohexane/ethyl acetate 10:1) to yield 110 mg (0.236 mmol, 53 %) of compound **30** as colorless oil.

^{1}H NMR (500 MHz, CD$_2$Cl$_2$) δ/ppm = 7.30 (m, 10H, *O*-benzyl and *N*-benzyl aromatic Hs), 7.09 (d, *J* = 8.6 Hz, 1H, 1-H), 6.54 (dd, *J* = 8.6 Hz, 2.7 Hz, 1H, 2-H), 6.47 (d, *J* = 2.8 Hz, 1H, 4-H), 4.54 (s, 2H, *O*-benzyl CH$_2$), 4.48 (s, 2H, *N*-benzyl CH$_2$), 3.51 (t, *J* = 8.3 Hz, 1H, 17-H), 2.96 (s,

3H, NCH$_3$), 2.78 (m, 2H, 6-H), 2.26 (m, 1H, 11-H$_a$), 2.15 (td, J = 10.8 Hz, 4.1 Hz, 1H, 9-H), 2.07 (m, 1H, 16-H$_a$), 2.05 (m, 1H, 12-H$_a$), 1.85 (ddt, J = 12.6 Hz, 5.8 Hz, 2.4 Hz, 1H, 7-H$_a$), 1.69 (dddd, J = 12.4 Hz, 9.7 Hz, 7.1 Hz, 3.2 Hz, 1H, 15-H$_a$), 1.59 (m, 1H, 16-H$_b$), 1.44 (m, 1H, 11-H$_b$), 1.41 (m, 1H, 8-H), 1.37 (m, 1H, 15-H$_b$), 1.32 (m, 1H, 7-H$_b$), 1.27 (m, 1H, 12-H$_b$), 1.20 (m, 1H, 14-H), 0.85 (s, 3H, 18-H)

^{13}C NMR (126 MHz, CD$_2$Cl$_2$) δ/ppm = 148.08 (C-3), 140.04 (*O*-benzyl or *N*-benzyl, quarternary carbon), 140.02, (*O*-benzyl or *N*-benzyl, quarternary carbon) 137.70 (C-5), 129.27 (C-10), 128.79-127.08 (6 peaks, 8C, *O*-benzyl and *N*-benzyl aromatic C-Hs), 126.27 (C-1), 113.02 (C-4), 110.86 (C-2), 89.08 (C-17), 72.02 (*O*-benzyl CH$_2$), 56.99 (*N*-benzyl CH$_2$), 50.63 (C-14), 44.33 (C-9), 43.85 (C-13), 39.36 (C-8), 38.94 (NCH$_3$), 38.41 (C-12), 30.46 (C-6), 28.39 (C-16), 27.86 (C-7), 26.93 (C-11), 23.48 (C-15), 12.04 (C-18)

IR (ATR): $\tilde{v}_{max}$/cm^{-1} = 2919, 2864, 1611, 1510, 1451, 1351, 1216, 1138, 1098, 956, 730

HRMS (ESI): m/z = [M+H]$^+$ calcd. for C$_{33}$H$_{40}$NO$^+$: 466.3104; found: 466.3094

(8*R*,9*S*,13*S*,14*S*,17*S*)-17-(benzyloxy)-*N*,13-dimethyl-7,8,9,11,12,13,14,15,16,17-decahydro-6*H*-cyclopenta[*a*]phenanthren-3-amine (31)
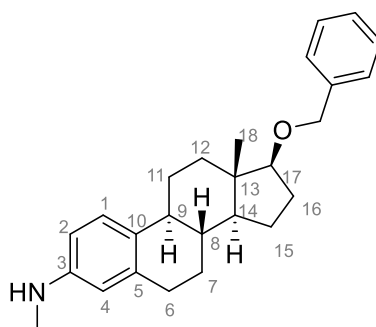
C$_{26}$H$_{33}$NO

M$_w$: 375.56 g/mol

Amine **30** (40.0 mg, 0.086 mmol, 1.00 eq), Pd/C (10 %); 4.58 mg, 0.00430 mmol, 5 mol%) and methanol (1.2 mL) were combined in a flame dried flask under a nitrogen atmosphere. The resulting suspension was brought under a hydrogen atmosphere and stirred at room temperature for 6 h. Thereafter the catalyst was removed by filtration through a small pad of celite and after evaporation of the solvent, the crude product was purified by flash column chromatography (isohexane/ethyl acetate 3:1 with 1 % triethylamine) to yield 29.1 mg (0.0775 mmol, 90 %) of compound **31** as a colorless oil.

^{1}H NMR (500 MHz, CD$_2$Cl$_2$) δ/ppm = 7.34 (m, 4H, benzyl aromatic ortho and meta Hs), 7.26 (td, J = 6.6 Hz, 6.1 Hz, 2.6 Hz, 1H, benzyl aromatic para H), 7.07 (d, J = 8.4 Hz, 1H, 1-H), 6.40 (dd, J = 8.5 Hz, 2.6 Hz, 1H, 2-H), 6.32 (d, J = 2.6 Hz, 1H, 4-H), 4.54 (s, 2H, benzyl CH$_2$), 3.51

(t, *J* = 8.3 Hz, 1H, 17-H), 2.77 (s, 3H, NCH$_3$), 2,77 (m, 2H, 6-H), 2.26 (dt, *J* = 11.5 Hz, 3.5 Hz, 1H, 11-H$_a$) 2.13 (m, 1H, 9-H), 2.07 (m, 1H, 16-H$_a$), 2.04 (m, 1H, 12-H$_a$), 1.85 (ddd, *J* = 12.8 Hz, 5.7 Hz, 2.8 Hz, 1H, 7-H$_a$), 1.69 (dddd, *J* = 12.4 Hz, 9.7 Hz, 7.1 Hz, 3.3 Hz, 1H, 15-H$_a$), 1.58 (m, 1H, 16-H$_b$), 1.46 (m, 1H, 11-H$_b$), 1.41 (m, 1H, 8-H), 1.37 (m, 1H, 15-H$_b$), 1.33 (m, 1H, 12-H$_b$), 1.29 (m, 1H, 7-H$_b$), 1.20 (m, 1H, 14-H), 0.85 (s, 3H, 18-H)

^{13}C NMR (126 MHz, CD$_2$Cl$_2$) δ/ppm = 147.79 (C-3), 140.03 (benzyl, quarternary carbon), 137.81 (C-10), 129.83 (C-5), 128.56 (2C, benzyl aromatic ortho or meta), 127.74 (2C, benzyl aromatic ortho or meta), 127.58 (benzyl aromatic para), 126.29 (C-1), 112.70 (C-4), 110.83 (C-2), 89.09 (C-17), 72.02 benzyl CH$_2$), 50.63 (C-14), 44.39 (C-9), 43.83 (C.13), 39.36 (C-8), 38.41 (C-12), 31.17 (NCH$_3$), 30.23 (C-6), 28.39 (C-16), 27.81 (C-7), 26.99 (C-11), 23.49 (C-15), 12.03 (C-18)

IR (ATR): 2919, 2864, 1611, 1510, 1451, 1351, 1098, 1070, 956, 861, 780, 730

HRMS (ESI): m/z = [M+H]$^+$ calcd. for C$_{26}$H$_{34}$NO$^+$: 376.2635; found: 376.2634

(8*R*,9*S*,13*S*,14*S*,17*S*)-3-(Benzylamino)-13-methyl-7,8,9,11,12,13,14,15,16,17-decahydro-6*H*-cyclopenta[*a*]phenanthren-17-ol (32)
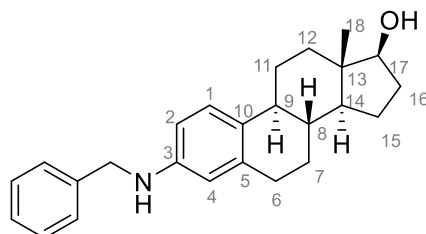
C$_{25}$H$_{31}$NO

M$_w$: 361.53 g/mol

Under a nitrogen atmosphere amine **28** (176 mg, 0.390 mmol, 1.00 eq) was dissolved in dichloromethane (7.8 mL) and cooled to -78 °C. Then boron trichloride solution (1 M in dichloromethane, 2.34 mL, 2.34 mmol, 3.00 eq) was added dropwise and the resulting solution was allowed to warm up to 0 °C and stirred at this temperature for 2 h. Thereafter the mixture was quenched with methanol (5 mL) and filtered through a small pad of celite. After evaporation of the solvent, the crude product was purified by flash column chromatography (isohexane/ethyl acetate 5:1) to yield 121 mg (0.335 mmol, 86 %) of compound **32** as a white solid.

m.p.: 145 °C

^{1}H NMR (400 MHz, CD$_2$Cl$_2$) δ/ppm = 7.34 (m, 4H, benzyl aromatic ortho and meta Hs), 7.26 (m, 1H, benzyl aromatic para H), 7.05 (m, 1H, 4-H), 6.42 (dd, *J* = 8.4 Hz, 2.7 Hz, 1H, 2-H),

6.36 (d, *J* = 2.6 Hz, 1H, 1-H), 4.30 (s, 2H, benzyl CH$_2$), 3.68 (t, *J* = 8.5 Hz, 1H, 17-H), 2.75 (m, 2H, 6-H), 2.26 (dq, *J* = 13.3 Hz, 4.0 Hz, 1H, 11-H$_a$), 2.13 (m, 1H, 9-H), 2.05 (m, 1H, 16-H$_a$), 1.89 (m, 1H, 12-H$_a$), 1.84 (m, 1H, 7-H$_a$), 1.68 (tdd, *J* = 10.1 Hz, 6.9 Hz, 2.8 Hz, 1H, 15-H$_a$), 1.44 (m, 1H, 16-H$_b$), 1.41 (m, 1H, 11-H$_b$), 1.38 (m, 1H, 8-H), 1.34 (m, 1H, 15-H$_b$), 1.30 (m, 1H, 7-H$_b$), 1.27 (m, 1H, 12-H$_b$), 1.16 (m, 1H, 14-H), 0.75 (s, 3H, 18-H)

^{13}C NMR (101 MHz, CD$_2$Cl$_2$) δ/ppm = 146.41 (C-3), 140.52 (benzyl, quarternary carbon), 137.92 (C-5), 130.18 (C-10), 128.87 (2C, benzyl aromatic ortho or meta), 127.77 (2C, benzyl aromatic ortho or meta), 127.37 (benzyl aromatic para), 126.36 (C-4), 113.34 (C-1), 111.16 (C-2), 82.19 (C-17), 50.43 (C-14), 48.63 (benzyl CH$_2$), 44.39 (C-9), 43.63 (C-13), 39.52 (C-8), 37.15 (C-12), 30.95 (C-16), 30.20 (C-6), 27.78 (C-7), 26.82 (C-11), 23.45 (C-15), 11.27 (C-18)

IR (ATR): $\tilde{v}_{max}$/cm^{-1} = 3402, 2919, 1614, 1505, 1451, 1261, 1053, 1021, 811, 737

HRMS (ESI): m/z = [M+H]$^+$ calcd. for C$_{25}$H$_{32}$NO$^+$: 362.2478; found: 362.2476

(8*R*,9*S*,13*S*,14*S*,17*S*)-17-(benzyloxy)-*N*,13-dimethyl-7,8,9,11,12,13,14,15,16,17-decahydro-6*H*-cyclopenta[*a*]phenanthren-3-amine (33)
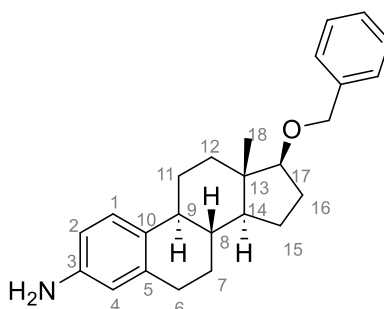
C$_{25}$H$_{31}$NO

M$_w$: 361.53 g/mol

Amine **28** (135 mg, 0.300 mmol, 1.00 eq), Pd/C (10 %) (16.0 mg, 0.0150 mmol, 5 mol%) and methanol (1.5 mL) were combined in a flame dried Schlenk flask under a nitrogen atmosphere. The flask was put in a dry ice/acetone bath until the solvent was frozen. The bath was removed and the headspace in the flask was evacuated until the solvent thawed. This process was repeated three times. The degassed suspension was then brought under a hydrogen atmosphere and stirred at room temperature for 6 h. Thereafter the catalyst was removed by filtration through a small pad of celite and after evaporation of the solvent, the crude product was purified by flash column chromatography (isohexane/ethyl acetate 3:1 with 1 % triethylamine) to yield 44.0 mg (0.122 mmol, 41 %) of compound **33** as a colorless oil.

¹H NMR (500 MHz, CD$_2$Cl$_2$) δ/ppm = 7.33 (m, 4H, benzyl aromatic ortho and meta Hs), 7.26 (ddd, J = 8.7 Hz, 5.5 Hz, 2.4 Hz, 1H, benzyl aromatic para H), 7.04 (d, J = 8.3 Hz, 1H, 1-H), 6.45 (dd, J = 8.3 Hz, 2.5 Hz, 1H, 2-H), 6.39 (d, J = 2.6 Hz, 1H, 4-H), 4.54 (s, 2H, benzyl CH$_2$), 3.51 (t, J = 8.3 Hz, 1H, 17-H), 2.75 (m, 2H, 6-H), 2.25 (dq, J = 12.3 Hz, 3.5 Hz, 3.1 Hz, 1H, 11-H$_a$) 2.12 (m, 1H, 9-H), 2.07 (m, 1H, 16-H$_a$), 2.04 (m, 1H, 12-H$_a$), 1.84 (ddt, J = 12.5 Hz, 5.8 Hz, 2.5 Hz, 1H, 7-H$_a$), 1.68 (dddd, J = 12.4 Hz, 9.7 Hz, 7.0 Hz, 3.3 Hz, 1H, 15-H$_a$), 1.59 (m, 1H, 16-H$_b$), 1.45 (m, 1H, 11-H$_b$), 1.39 (m, 1H, 8-H), 1.35 (m, 1H, 15-H$_b$), 1.30 (m, 1H, 12-H$_b$), 1.27 (m, 1H, 7-H$_b$), 1.20 (m, 1H, 14-H), 0.85 (s, 3H, 18-H)

¹³C NMR (126 MHz, CD$_2$Cl$_2$) δ/ppm = 144.67 (C-3), 140.03 (benzyl, quarternary carbon), 138.01 (C-5), 130.97 (C-10), 128.58 (2C, benzyl aromatic ortho or meta), 127.76 (2C, benzyl aromatic ortho or meta), 127.60 (benzyl aromatic para), 126.45 (C-1), 115.46 (C-4), 113.08 (C-2), 89.08 (C-17), 72.04 (benzyl CH$_2$), 50.64 (C-14), 44.40 (C-9), 43.83 (C-13), 39.28 (C-8), 38.40 (C-12), 30.05 (C-6), 28.40 (C-16), 27.74 (C-7), 26.95 (C-11), 23.50 (C-15), 12.04 (C-18)

IR (ATR): 2923, 2876, 1611, 1471, 1081, 1037, 956, 824, 739

HRMS (ESI): m/z = [M+H]$^+$ calcd. for C$_{25}$H$_{32}$NO$^+$: 362.2478; found: 362.2476

O-((8*R*,9*S*,13*S*,14*S*,17*S*)-17-Hydroxy-13-methyl-7,8,9,11,12,13,14,15,16,17-decahydro-6*H*-cyclopenta[*a*]phenanthren-3-yl) *N,N*-dimethylcarbamothioate (35)
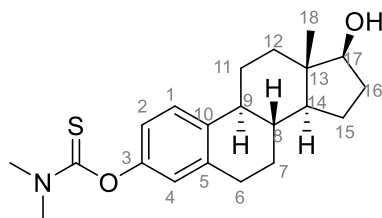
C$_{21}$H$_{29}$NO$_2$S

M$_w$: 359.53 g/mol

17*β*-Estradiol (**3**) (1.00 g, 3.67 mmol, 1.00 eq) was added to a flame dried round bottom flask and dissolved in 10 mL of dry DMF under a nitrogen atmosphere. The solution was cooled to 0 °C and sodium hydride (60 wt% in mineral oil, 147 mg, 3.67 mmol, 1.00 eq) was slowly added in portions under a continuous nitrogen flow. The flask was equipped with a rubber septum and a balloon and purged with nitrogen for three times. After 30 min of stirring at 0 °C, *N,N*-dimethylcarbamoyl chloride (499 mg, 4.04 mmol, 1.10 eq) was added *via* syringe. The reaction mixture was allowed to warm up to room temperature and then stirred for 2 h. Then the mixture was slowly poured in 0.1 M aqueous HCl (50 mL), followed by extraction with ethyl acetate (3 x 30 mL). The combined organic layers were washed with water (3 x 50 mL) and brine (25 mL), filtered through a hydrophobic filter and concentrated *in vacuo*. The crude product was purified

by flash column chromatography (isohexane/ethyl acetate 2:1) to yield 1.00 g (2.78 mmol, 76 %) of compound **35** as a white solid.

m.p.: 180 °C

^{1}H NMR (500 MHz, DMSO) δ/ppm = 7.27 (d, J = 8.6 Hz, 1H, 1-H), 6.78 (dd, J = 8.5 Hz, 2.5 Hz, 1H, 2-H), 6.72 (d, J = 2.6 Hz, 1H, 4-H), 4.51 (d, J = 4.8 Hz, 1H, OH), 3.53 (td, J = 8.5 Hz, 4.7 Hz, 1H, 17-H), 3.34 (s, 3H, NCH$_3$), 3.27 (s, 3H, NCH$_3$'), 2.78 (m, 2H, 6-H), 2.30 (dt, J = 12.5 Hz, 3.6 Hz, 1H, 11-H$_a$), 2.16 (td, J = 10.9 Hz, 10.5 Hz, 4.0 Hz, 1H, 9-H), 1.90 (m, 1H, 16-H$_a$), 1.85 (m, 1H, 12-H$_a$), 1.80 (m, 1H, 7-H$_a$), 1.59 (qt, J = 9.6, 7.4, 3.1 Hz, 1H, 15-H$_a$), 1.40 (m, 1H, 11-H$_b$), 1.37 (m, 1H, 16-H$_b$), 1.33 (m, 1H, 8-H), 1.27 (m, 1H, 7-H$_b$), 1.23 (m, 1H, 15-H$_b$), 1.18 (m, 1H, 12-H$_b$), 1.12 (m, 1H, 14-H), 0.68 (s, 3H, 18-H)

^{13}C NMR (126 MHz, DMSO) δ/ppm = 186.57 (C=S), 151.52 (C-3), 137.34 (C-5 or C-10), 137.31 (C-5 or C-10), 125.85 (C-1), 122.23 (C-4), 119.81 (C-2), 80.03 (C-17), 49.57 (C-14), 43.72 (C-9), 42.79 (C-13), 42.76 (NCH$_3$), 38.39 (NCH$_3$'), 38.28 (C-8), 36.57 (C-12), 29.89 (C-16), 28.97 (C-6), 26.66 (C-7), 25.89 (C-11), 22.79 (C-15), 11.25 (C-18)

IR (ATR): $\tilde{v}_{max}$/cm^{-1} = 3440, 2922, 2854, 1727, 1538, 1494, 1396, 1292, 1253, 1228, 1136, 1010, 818

HRMS (EI): m/z = [M$^{•+}$] calcd. for C$_{21}$H$_{29}$NO$_2$S $^{•+}$: 359.1914; found: 359.1913

Literature known compound[150]

S-((8*R*,9*S*,13*S*,14*S*,17*S*)-17-hydroxy-13-methyl-7,8,9,11,12,13,14,15,16,17-decahydro-6*H*-cyclopenta[*a*]phenanthren-3-yl) *N*,*N*-dimethylcarbamothioate (38)
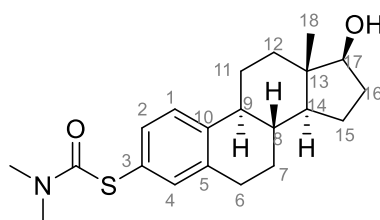
C$_{21}$H$_{29}$NO$_2$S

M$_w$: 359.53 g/mol

O-aryl thiocarbamate **35** (920 mg, 2.56 mmol, 1.00 eq) and dry toluene (5.0 ml) were combined in a flame dried tube with a magnetic stirring bar. The tube was closed with a rubber septum, a nitrogen balloon was added and the system was purged three times with nitrogen before it was placed in an oil bath preheated to 100 °C. After stirring for 5 minutes, the suspension turned into a yellow solution. Then bis(tri-tert-butylphosphin)palladium (0) (26.2 mg, 0.0512 mmol, 2 mol%) was added under a nitrogen flow. The reaction mixture was stirred at 100 °C

for 4 hours. After cooling to room temperature, the mixture was diluted with dichloromethane (5 mL) and filtered through a small pad of celite. The solvent was evaporated and the crude product was purified by flash column chromatography (isohexane/ethyl acetate 2:1) to yield *S*-aryl thiocarbamate **38** as a yellow solid (267 mg, 0.743 mmol, 29 %).

m.p.: 160 °C

^{1}H NMR (400 MHz, DMSO) δ/ppm = 7.30 (d, *J* = 8.2 Hz, 1H, 2-H), 7.15 (dd, *J* = 8.0 Hz, 2.0 Hz, 1H, 4-H), 7.10 (d, *J* = 1.9 Hz, 1H, 1-H), 4.51 (d, *J* = 4.8 Hz, 1H, OH), 3.53 (td, *J* = 8.5 Hz, 4.8 Hz, 1H,17-H), 3.01 (s, 3H, NCH$_3$), 2.91 (s, 3H, NCH$_3$'), 2.79 (dd, *J* = 8.6, 4.2 Hz, 2H, 6-H), 2.31 (dd, *J* = 13.4 Hz, 3.6 Hz, 1H, 11-H$_a$), 2.20 (t, *J* = 11.6 Hz, 1H, 9-H), 1.91 (m, 1H, 16-H$_a$), 1.85 (m, 1H, 12-H$_a$), 1.81 (m, 1H, 7-H$_a$), 1.58 (m, 1H, 15-H$_a$), 1.42 (m, 1H, 16-H$_b$), 1.37 (m, 1H, 8-H or 11-H$_b$), 1.33 (m, 1H, 8-H or 11-H$_b$), 1.29 (m, 1H, 7-H$_b$), 1.24 (m, 1H, 15-H$_b$), 1.18 (m, 1H, 12-H$_b$), 1.12 (m, 1H, 14-H), 0.67 (s, 3H, 18-H)

^{13}C NMR (101 MHz, DMSO) δ/ppm = 165.35 (C=O), 141.38 (C-10), 137.17 (C-5), 135.70 (C-1), 132.67 (C-4), 125.95 (C-2), 124.96 (C-3), 80.00 (C-17), 49.59 (C-4), 43.89 (C-9), 42.76 (C-13), 38.09 (C-8), 36.53 (C-12), 36.44 (2C, NCH$_3$, NCH$_3$'), 29.87 (C-16), 28.75 (C-6), 26.58 (C-7), 25.69 (C-11), 22.77 (C-15), 11.21 (C-18)

IR (ATR): $\tilde{v}_{max}$/cm^{-1} = 3477, 2917, 2863, 1652, 1361, 1096, 1073, 906, 688

HRMS (EI): m/z = [M$^{•+}$] calcd. for C$_{21}$H$_{29}$NO$_2$S $^{•+}$: 359.1914; found: 359.1912

Literature known compound[150]

(8*R*,9*S*,13*S*,14*S*,17*S*)-3-Mercapto-13-methyl-7,8,9,11,12,13,14,15,16,17-decahydro-6*H*-cyclopenta[*a*]phenanthren-17-ol (39)
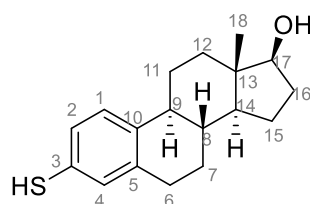
C$_{18}$H$_{24}$OS

M$_w$: 288.45 g/mol

A round bottom flask was charged with *S*-aryl thiocarbamate **38** (262 mg, 0.730 mmol, 1.00 eq), ethanol (30 mL) and a solution of sodium hydroxide (819 mg, 14.6 mmol, 20.0 eq) in water (3.6 mL). The flask was equipped with a reflux condenser, a rubber septum and a balloon and purged with nitrogen for three times. The resulting mixture was heated at reflux under a nitrogen atmosphere for 3 hours. After cooling to room temperature, 2 M aqueous hydrochloric

acid was added until pH 7 was reached. The mixture was concentrated under reduced pressure and the residue was poured into water (5 mL) and extracted with dichloromethane (3 x 5 mL). The combined organic layers were washed with water (10 mL) and brine (10 mL) and filtered through a hydrophobic filter. After evaporation of the solvent, the crude product was purified by flash column chromatography (isohexane/ethyl acetate 3:1) to yield 173 mg (0.600 mmol, 82 %) of compound **39** as a yellow solid.

m.p.: 85 °C

^{1}H NMR (500 MHz, CDCl$_3$) δ/ppm = 7.16 (d, J = 8.1 Hz, 1H, 1-H), 7.06 (dd, J = 8.1 Hz, 2.1 Hz, 1H, 2-H), 7.02 (d, J = 2.1 Hz, 1H, 4-H), 3.73 (t, J = 8.5 Hz, 1H, 17-H), 3.34 (s, 1H, SH), 2.81 (m, 2H, 6-H) , 2.30 (dtd, J = 13.4 Hz, 4.2 Hz, 2.7 Hz, 1H, 11-H$_a$), 2.19 (m, 1H, 9-H), 2.13 (m, 1H, 16-H$_a$), 1.95 (ddd, J = 12.6 Hz, 3.9 Hz, 2.7 Hz, 1H, 12-H$_a$), 1.88 (m, 1H, 7-H$_a$), 1.70 (m, 1H, 15-H$_a$), 1.49 (m, 1H, 11-H$_b$), 1.45 (m, 1H, 16-H$_b$), 1.40 (m, 1H, 8-H), 1.37 (m, 1H, 15-H$_b$), 1.33 (m, 1H, 7-H$_b$), 1.30 (m, 1H, 12-H$_b$), 1.19 (ddd, J = 12.2 Hz, 10.9 Hz, 7.3 Hz, 1H, 14-H), 0.78 (s, 3H, 18H)

^{13}C NMR (126 MHz, CDCl$_3$) δ/ppm = 138.34 (C-5 or C-10), 137.95 (C-5 or C-10), 130.27 (C-4), 127.23 (C-2), 127.11 (C-3), 126.36 (C-1), 82.01 (C-17), 50.22 (C-14), 44.24 (C-9), 43.36 (C-13), 38.70 (C-8), 36.79 (C-12), 30.73 (C-16), 29.47 (C-6), 27.19 (C-7), 26.22 (C-11), 23.25 (C-15), 11.18 (C-18)

IR (ATR): $\tilde{v}_{max}$/cm^{-1} = 2924, 1974, 1592, 1484, 1445, 1217, 1136, 815, 756

HRMS (EI): m/z = [M$^{\bullet+}$] calcd. for C$_{18}$H$_{24}$OS $^{\bullet+}$: 288.1542; found: 288.1542

Literature known compound[179]

(8R,9S,13S,14S,17S)-13-Methyl-3-(methylthio)-7,8,9,11,12,13,14,15,16,17-decahydro-6H-cyclopenta[a]phenanthren-17-ol (40)
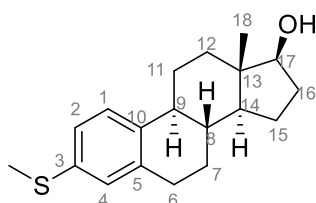
C$_{19}$H$_{26}$OS
M$_w$: 302.48 g/mol

Thiophenol **39** (121 mg, 0.420 mmol, 1.00 eq) was dissolved in 7.0 mL of dry DMF in a round bottom flask equipped with a rubber septum and a balloon filled with nitrogen. The flask was purged with nitrogen three times. A suspension of sodium hydride (60 wt% in mineral oil, 20.0

mg, 1.20 eq) in dry DMF (1 mL) was drawn up using a syringe with a 10 G cannula. The content of the syringe was slowly added to the flask. A further 0.3 mL of DMF were drawn up with the syringe to float up the remaining residue and the resulting suspension was again added through the septum. This step was repeated three times in order to transfer the entire amount of sodium hydride to the flask. After the evolution of hydrogen gas had ceased, the flask was cooled to 0 °C and iodomethane (80 µL, 0.50 mmol, 1.2 eq) was added. The resulting mixture was then allowed to warm to room temperature and stirred for 3 hours. Thereafter it was poured into 2 M aqueous NaOH (10 mL). Water (10 mL) was added and the mixture was extracted with ethyl acetate (3 x 10 mL). The combined organic layers were washed with water (3 x 10 mL) and brine (10 mL), filtered through a hydrophobic filter and concentrated *in vacuo*. The crude product was purified by flash column chromatography (isohexane/ethyl acetate 3:1) to yield 42.0 mg (0.139 mmol, 33 %) of compound **40** as a white solid.

m.p.: 121 °C

^{1}H NMR (500 MHz, CD_2Cl_2) δ/ppm = 7.21 (d, *J* = 8.2 Hz, 1H, 1-H), 7.02 (dd, *J* = 8.1 Hz, 2.1 Hz, 1H, 2-H), 6.97 (d, *J* = 2.4 Hz, 1H, 4-H), 3.69 (td, *J* = 8.5 Hz, 5.7 Hz, 1H, 17-H), 2.83 (m, 2H, 6-H), 2.44 (s, 3H, SCH$_3$), 2.31 (dtd, *J* = 13.3 Hz, 4.2 Hz, 2.8 Hz, 1H, 11-H$_a$), 2.20 (td, *J* = 11.1 Hz, 4.2 Hz, 1H, 9-H), 2.08 (dtd, *J* = 12.8 Hz, 9.1 Hz, 5.5 Hz, 1H, 16-H$_a$), 1.92 (m, 1H, 12-H$_a$), 1.88 (m, 1H, 7-H$_a$), 1.69 (m, 1H, 15-H$_a$), 1.46 (m, 1H, 11-H$_b$), 1.44 (m, 1H, 16-H$_b$), 1.42 (m, 1H, 8-H), 1.35 (m, 1H, 15-H$_b$), 1.31 (m, 1H, 7-H$_b$), 1.27 (m, 1H, 12-H$_b$), 1.19 (m, 1H, 14-H), 0.76 (s, 3H, 18-H)

^{13}C NMR (126 MHz, CD_2Cl_2) δ/ppm = 138.15 (C-5 or C-10), 138.01 (C-5 or C-10), 135.25 (C-3), 127.59 (C-4), 126.28 (C-1), 124.57 (C-2), 82.12 (C-17), 50.49 (C-14), 44.57 (C-13), 43.58 (C-9), 39.06 (C-8), 37.10 (C-12), 30.93 (C-16), 29.86 (C-6), 27.53 (C-7), 26.57 (C-11), 23.45 (C-15), 16.31 (SCH$_3$), 11.24 (C-18)

IR (ATR): $\tilde{v}_{max}$/cm^{-1} = 3323, 2921, 2867, 2362, 1485, 1438, 1262, 1136, 1055, 815

HRMS (EI): m/z = [M$^{•+}$] calcd. for $C_{19}H_{26}OS^{•+}$: 302.1699; found: 302.1698

Purity (HPLC): > 99 % (λ = 210 nm), > 99 % (λ = 254 nm) (Method 1e)

Literature known compound[180]

(8*R*,9*S*,13*S*,14*S*,17*S*)-2-Iodo-13-methyl-7,8,9,11,12,13,14,15,16,17-decahydro-6*H*-cyclopenta[*a*]phenanthrene-3,17-diol (41)
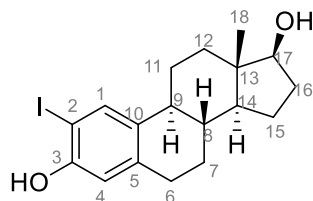
$C_{18}H_{23}IO_2$

M_w: 398.28 g/mol

17*β*-Estradiol (**3**) (2.18 g, 8.00 mmol, 1.00 eq), *N*-iodosuccinimide (2.04 g, 8.80 mmol, 1.10 eq) and indium (III) trifluoromethanesulfonate (450 mg, 0.800 mmol, 0.100 eq) were combined in a round bottom flask. Acetonitrile (40 mL) was added and the resulting mixture was stirred for 8 h at ambient temperature. The progress of the reaction was monitored by TLC control. After completion, the solvent was evaporated and dichloromethane (50 mL) and water (25 mL) were added. The organic layer was separated and washed with water (2 x 25 mL) and brine (25 mL). The crude product was purified by flash column chromatography (isohexane/ethyl acetate 4:1) to yield 2.00 g (5.02 mmol, 63 %) of compound **41** as a white solid and 323 mg (0.615 mmol, 8 %) of side product **42** (characterization shown in the next entry) as a yellow solid.

Characterization of **41**:

m.p.: 136 °C

¹H NMR (400 MHz, DMSO) *δ*/ppm = 9.87 (s, 1H, phenol), 7.45 (s, 1H, 1-H), 6.55 (s, 1H, 4-H), 4.49 (br s, 1h, OH), 3.52 (t, *J* = 8.5 Hz, 1H, 17-H) , 2.67 (dt, *J* = 8.4, 3.9 Hz, 2H, 6-H), 2.17 (dt, *J* = 13.3 Hz, 3.3 Hz, 1H, 11-H$_a$), 2.05 (m, 1H, 9-H), 1.88 (m, 1H, 16-H$_a$), 1.81 (m, 1H, 12-H$_a$), 1.75 (m, 1H, 7-H$_a$), 1.55 (m, 1H, 15-H$_a$), 1.37 (m, 1H, 16-H$_b$), 1.30 (m, 1H, 11-H$_b$), 1.25 (m, 1H, 8-H), 1.22 (m, 1H, 15-H$_b$), 1.19 (m, 1H, 7-H$_b$), 1.14 (m, 1H, 12-H$_b$), 1.06 (m, 1H, 14-H), 0.64 (s, 3H, 18-H)

¹³C NMR (101 MHz, DMSO) *δ*/ppm = 154.15 (C-3), 137.81 (C-10), 135.24 (C-1), 133.31 (C-5), 114.82 (C-4), 81.24 (C-2), 79.99 (C-17), 49.41 (C-14), 43.05 (C-9), 42.74 (C-13), 38.32 (C-8), 36.45 (C-12), 29.86 (C-16), 28.72 (C-6), 26.66 (C-7), 25.99 (C-11), 22.74 (C-15), 11.20 (C-18)

IR (ATR): *ṽ*$_{max}$/cm^{-1} = 3393, 2925, 2864, 1613, 1505, 1452, 1349, 1262, 1092, 863, 730

HRMS (EI): m/z = [M$^{•+}$] calcd. for $C_{18}H_{23}IO_2$$^{•+}$: 398.0737; found: 398.0744

Literature known compound[154]

(8*R*,9*S*,13*S*,14*S*,17*S*)-2,4-Diiodo-13-methyl-7,8,9,11,12,13,14,15,16,17-decahydro-6*H*-cyclopenta[*a*]phenanthrene-3,17-diol (42)

$C_{18}H_{22}I_2O_2$

M_w: 524.18 g/mol

Side product of the above procedure.

m.p.: 164 °C

¹H NMR (500 MHz, DMSO) *δ/*ppm = 9.20 (s, 1H, phenol), 7.59 (s, 1H, 1-H), 4.49 (br s, 1H,OH), 3.50 (m, 1H, 17-H), 2.69 (m, 2H, 6-H), 2.21 (dt, *J* = 12.2 Hz, 3.4 Hz, 1H, 11-H$_a$) 2.11 (m, 1H, 9-H), 1.90 (m, 1H, 16-H$_a$), 1.85 (m, 1H, 7-H$_a$), 1.81 (m, 1H, 12-H$_a$), 1.57 (m, 1H, 15-H$_a$), 1.37 (m, 1H, 16-H$_b$), 1.30 (m, 1H, 11-H$_b$), 1.25 (m, 1H, 15-H$_b$), 1.22 (m, 1H, 8-H), 1.19 (m, 1H, 7-H$_b$), 1.15 (m, 1H, 12-H$_b$), 1.07 (m, 1H, 14-H), 0.64 (s, 3H, 18-H)

¹³C NMR (126 MHz, DMSO) *δ/*ppm = 153.00 (C-3), 140.22 (C-5), 136.50 (C-10), 135.38 (C-1), 96.61 (C-4), 83.56 (C-2), 79.93 (C-17), 49.31 (C-14), 43.34 (C-9), 42.66 (C-13), 37.44 (C-8), 37.18 (C-6), 36.43 (C-12), 29.89 (C-16), 27.61 (C-7), 26.21 (C-11), 22.69 (C-15), 11.14 (C-18)

IR (ATR): $\tilde{v}_{max}$/cm⁻¹ = 3298, 2917, 2865, 2359, 1450, 1382, 1265, 1178, 1123, 1012, 746

HRMS (EI): m/z = [M⁺] calcd. for $C_{18}H_{22}I_2O_2$⁺: 523.9704; found: 523.9700

Literature known compound[181]

(8*R*,9*S*,13*S*,14*S*,17*S*)-2-Iodo-3-methoxy-13-methyl-7,8,9,11,12,13,14,15,16,17-decahydro-6*H*-cyclopenta[*a*]phenanthren-17-ol (43)

$C_{19}H_{25}IO_2$

M_w: 412.31 g/mol

Iodoestrane **41** (1.20 g, 3.00 mmol, 1.00 eq), cesium carbonate (1.96 g, 6.00 mmol, 2.00 eq) and acetonitrile (35 mL) were combined in a round bottom flask. Iodomethane (1.49 mL, 24.0 mmol, 8.00 eq) was added dropwise and the resulting mixture was stirred and heated at reflux for 2.5 h. After cooling to room temperature, the reaction mixture was poured into water and 2 M aqueous hydrochloric acid was added until pH 7 was reached. The mixture was extracted with ethyl acetate (3 x 20 mL) and the combined organic layers were washed with water (30 mL) and brine (30 mL). After filtration through a hydrophobic filter, the solvent was evaporated and the crude product was purified by flash column chromatography (isohexane/ethyl acetate 4:1) to yield 1.01 g (2.45 mmol, 82 %) of compound **43** as a colorless solid.

m.p.: 167 °C

^{1}H NMR (400 MHz, DMSO) δ/ppm = 7.55 (s, 1H, 1-H), 6.68 (s, 1H, 4-H), 4.49 (d, J = 4.8 Hz, 1H, OH), 3.76 (s, 3H, OCH$_3$), 3.51 (td, J = 8.4 Hz, 4.7 Hz, 1H, 17-H), 2.77 (m, 2H, 6-H), 2.20 (dd, J = 13.7 Hz, 3.3 Hz, 1H, 11-H$_a$), 2.09 (t, J = 11.2 Hz, 1H, 9-H), 1.89 (m, 1H, 16-H$_a$), 1.83 (m, 1H, 12-H$_a$), 1.79 (m, 1H, 7-H$_a$), 1.57 (m, 1H, 15-H$_a$), 1.37 (m, 1H, 16-H$_b$), 1.31 (m, 1H, 11-H$_b$), 1.26 (m, 1H, 8-H), 1.24 (m, 1H, 7-H$_b$ or 15-H$_b$), 1.21 (m, 1H, 7-H$_b$ or 15-H$_b$), 1.16 (m, 1H, 12-H$_b$), 1.12 (m, 1H, 14-H), 0.65 (s, 3H, 18-H)

^{13}C NMR (101 MHz, DMSO) δ/ppm = 155.46 (C-3), 138.22 (C-10), 135.56 (C-1), 134.75 (C-5), 111.75 (C-4), 82.57 (C-2), 79.98 (C-17), 56.20 (OCH$_3$), 49.41 (C-14), 43.10 (C-9), 42.76 (C-13), 38.25 (C-8), 36.47 (C-12), 29.87 (C-16), 29.11 (C-6), 26.61 (C-7), 25.97 (C-11), 22.74 (C-15), 11.21 (C-18)

IR (ATR): $\tilde{v}_{max}$/cm^{-1} = 3470, 2923, 2862, 1975, 1590, 1486, 1462, 1387, 1253, 1022, 879

HRMS (EI): m/z = [M$^{\bullet+}$] calcd. for C$_{19}$H$_{25}$IO$_2$$^{\bullet+}$: 412.0894; found: 412.0898

Purity (HPLC): > 95 % (λ = 210 nm), > 99 % (λ = 254 nm) (Method 2)

Literature known compound[182]

(8*R*,9*S*,13*S*,14*S*,17*S*)-3-Methoxy-13-methyl-2-vinyl-7,8,9,11,12,13,14,15,16,17-decahydro-6*H*-cyclopenta[*a*]phenanthren-17-ol (44)
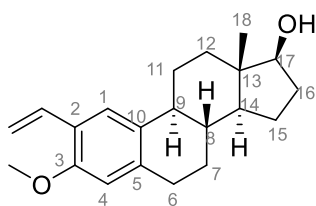
C$_{21}$H$_{28}$O$_2$

M$_w$: 312.45 g/mol

A flame-dried Schlenk flask was evacuated and backfilled with nitrogen five times prior to the addition of 206 mg (0.500 mmol, 1.00 eq) of iodoestrane **43**, 91.0 mg (2.13 mmol, 4.25 eq) lithium chloride, 1.10 mg (0.00500 mmol, 1 mol%) of 2,6-di-*tert*-butyl-4-methylphenol and 35.1 mg (0.0500 mmol, 0.100 eq) of bis(triphenylphosphine)palladium (II) chloride. The mixture was suspended in 3.0 mL DMF and 0.19 mL (206 mg, 0.650 mmol, 1.30 eq) tributyl(vinyl)tin were added dropwise. The resulting suspension was stirred for 4 h at 90 °C under a nitrogen atmosphere, then cooled to room temperature and treated with 0.2 mL of pyridine and 0.4 mL of hydrogen fluoride-pyridine (Olah's reagent). The resulting mixture was stirred at room temperature overnight and then diluted with 15 mL diethyl ether and filtered to remove the catalyst. The filtrate was washed with 10 mL of water, 10 mL of 2 M aqueous hydrochloric acid, again 10 mL of water and 10 mL of brine. The organic layer was dried over anhydrous sodium sulfate and concentrated under reduced pressure. The crude product was suspended in cold isohexane and cooled to 5 °C overnight. The precipitated solid was collected by filtration and purified by silica gel column chromatography (isohexane/ethyl acetate 4:1) to yield **44** as a colorless solid (120 mg, 0.384 mmol, 77 %).

m.p.: 186 °C

^{1}H NMR (500 MHz, DMSO) δ/ppm = 7.35 (s, 1H, 1-H), 6.88 (dd, J = 17.7 Hz, 11.3 Hz, 1H, vinyl CH), 6.66 (s, 1H, 4-H), 5.72 (dd, J = 17.8 Hz, 1.8 Hz, 1H, vinyl CH$_2$), 5.14 (dd, J = 11.2 Hz, 1.8 Hz, 1H, CH$_2$'), 4.50 (m, 1H, OH), 3.74 (s, 3H, OCH$_3$), 2.78 (dd, J = 8.9 Hz, 4.1 Hz, 2H, 6-H), 2.34 (dd, J = 13.8 Hz, 3.9 Hz, 1H. 11-H$_a$), 2.10 (t, J = 11.0 Hz, 1H, 9-H), 1.89 (m, 1H, 16-H$_a$), 1.85 (m, 1H, 12-H$_a$), 1.80 (m, 1H, 7-H$_a$), 1.59 (m, 1H, 15-H$_a$), 1.39 (m, 1H, 16-H$_b$), 1.34 (m, 1H, 11-H$_b$), 1.30 (m, 1H, 8-H), 1.27 (m, 1H, 7-H$_b$), 1.23 (m, 1H, 15-H$_b$), 1.19 (m, 1H, 12-H$_b$), 1.14 (m, 1H, 14-H), 0.67 (s, 3H, 18-H)

^{13}C NMR (126 MHz, DMSO) δ/ppm = 154.33 (C-3), 137.53 (C-5), 132.05 (C-10), 131.62 (vinyl CH), 123.09 (C-1), 122.93 (C-2), 113.45 (vinyl CH$_2$), 111.37 (C-4), 80.09 (C-17), 55.40 (OCH$_3$), 49.57 (C-14), 43.51 (C-9), 42.84 (C-13), 38.60 (C-8), 36.61 (C-12), 29.92 (C-16), 29.33 (C-6), 26.88 (C-7), 26.04 (C-11), 22.81 (C-15), 11.30 (C-18)

IR (ATR): $\tilde{v}_{max}$/cm^1 = 3448, 2924, 1738, 1647, 1602, 1494, 1264, 1227, 1134, 1076, 1010, 916

HRMS (EI): m/z = [M$^{•+}$] calcd. for C$_{21}$H$_{28}$O$_2$$^{•+}$: 312.2084; found: 312.2084

Purity (HPLC): > 96 % (λ = 210 nm), > 99 % (λ = 254 nm) (Method 2)

1-((8*R*,9*S*,13*S*,14*S*,17*S*)-17-Hydroxy-3-methoxy-13-methyl-7,8,9,11,12,13,14,15,16,17-decahydro-6*H*-cyclopenta[*a*]phenanthren-2-yl)ethan-1-one (46)

$C_{21}H_{28}O_3$

M_w: 328.45 g/mol

A flame dried Schlenk flask was evacuated and backfilled with nitrogen five times prior to the addition of 124 mg (0.300 mmol, 1.00 eq) of iodoestrane **43**, 38.5 mg (0.900 mmol, 3.00 eq) lithium chloride and 21.1 mg (0.0300 mmol, 0.100 eq) of bis(triphenylphosphine)palladium (II) chloride. The mixture was suspended in 3 mL of DMF and tributyl(1-ethoxyvinyl)tin (0.100 mL, 108 mg, 0.300 mmol, 1.00 eq) was added dropwise. The resulting suspension was stirred at 110 °C for 14 h under a nitrogen atmosphere. After cooling to room temperature, the mixture was treated with 5 mL of water and 5 mL of ethyl acetate. The organic phase was separated and washed with cold water (3 × 10 mL), brine (10 mL) and 1 M aqueous LiCl solution (10 mL), dried over anhydrous sodium sulfate and concentrated *in vacuo*. The crude product was suspended in cold isohexane and cooled to 5 °C overnight. Then the solid was collected by filtration and purified by silica gel column chromatography (isohexane/ethyl acetate 4:1) to yield 42.0 mg (0.128 mmol, 43 %) of compound **46** as a colorless solid.

m.p.: 179 °C

¹H NMR (500 MHz, CD₂Cl₂) δ/ppm = 7.64 (d, *J* = 1.2 Hz, 1H, 1-H), 6.70 (s, 1H, 4-H), 3.86 (s, 3H, OCH₃), 3.69 (t, *J* = 8.5 Hz, 1H, 17-H), 2.88 (m, 2H, 6-H), 2.54 (s, 3H, ketone CH₃), 2.37 (dtd, *J* = 13.4 Hz, 4.2 Hz, 2.7 Hz, 1H, 11-H$_a$), 2.17 (td, *J* = 10.9 Hz, 10.5 Hz, 4.0 Hz, 1H, 9-H), 2.07 (dtd, *J* = 12.9 Hz, 9.2 Hz, 5.6 Hz, 1H, 16-H$_a$), 1.93 (m, 1H, 12-H$_a$), 1.89 (m, 1H, 7-H$_a$), 1.69 (m, 1H, 15-H$_a$), 1.47 (m, 1H, 11-H$_b$), 1.43 (m, 1H, 16-H$_b$), 1.40 (m, 1H, 8-H), 1.36 (m, 1H, 15-H$_b$), 1.32 (m, 1H, 7-H$_b$), 1.27 (m, 1H, 12-H$_b$), 1.19 (m, 1H, 14-H), 0.75 (s, 3H, 18-H)

¹³C NMR (126 MHz, DMSO) δ/ppm = 199.35 (carbonyl), 157.43 (C-3), 144.01 (C-5), 133.12 (C-10), 127.68 (C-1), 125.90 (C-2), 112.24 (C-4), 82.07 (C-17), 55.82 (OCH₃), 50.39 (C-14), 44.14 (C-9), 43.58 (C-13), 39.16 (C-8), 36.98 (C-12), 32.08 (ketone CH₃), 30.87 (C-16), 30.39 (C-6), 27.39 (C-7), 26.69 (C-11), 23.42 (C-15), 11.22 (C-18)

IR (ATR): $\tilde{v}_{max}$/cm¹ = 3412, 2928, 2864, 1659, 1603, 1495, 1404, 1226, 1060, 1023, 864

HRMS (EI): m/z = [M˙⁺] calcd. for C₂₁H₂₈O₃˙⁺: 328.2033; found: 328.2032

Purity (HPLC): > 98 % (λ = 210 nm), > 95 % (λ = 254 nm) (Method 2)

(8*R*,9*S*,13*S*,14*S*,17*S*)-3-Methoxy-13-methyl-2-phenyl-7,8,9,11,12,13,14,15,16,17-decahydro-6*H*-cyclopenta[*a*]phenanthren-17-ol (47)

$C_{25}H_{30}O_2$

M_w: 362.51 g/mol

Method A: Iodoestrane **43** (219 mg, 0.530 mmol, 1.00 eq), phenylboronic acid (96.9 mg, 0.795 mmol, 1.50 eq), bis(triphenylphosphine)palladium (II) chloride (18.6 mg, 0.0265 mmol, 5 mol%), triethylamine (0.220 mL, 1.60 mmol, 3.00 eq) and DMF (2.0 mL) were combined in a flame dried Schlenk flask under a nitrogen atmosphere. The resulting suspension was heated at 80 °C and stirred at this temperature for 6 h. After cooling to room temperature, water (2 mL) was added and the mixture was extracted with dichloromethane (3 x 10 mL). The combined organic layers were washed with water (10 mL) and brine (10 mL), filtered through a hydrophobic filter and concentrated under reduced pressure. The crude product was purified by flash column chromatography (isohexane/ethyl acetate 4:1) to yield 37.0 mg (0.102 mmol, 19.3 %) of compound **47** as a colorless solid.

Method B: Biphenyl **48** (105 mg, 0.300 mmol, 1.00 eq), cesium carbonate (195 mg, 0.600 mmol, 2.00 eq) and acetonitrile (3.5 mL) were combined in a round bottom flask. Iodomethane (0.150 mL, 2.40 mmol, 8.00 eq) was added dropwise and the resulting mixture was stirred and heated at reflux for 2.5 h. After cooling to room temperature, the reaction mixture was poured into water and 2 M aqueous hydrochloric acid was added until pH 7 was reached. The mixture was extracted with ethyl acetate (3 x 5 mL) and the combined organic layers were washed with water (10 mL) and brine (10 mL). After filtration through a hydrophobic filter, the solvent was evaporated and the crude product was purified by flash column chromatography (isohexane/ethyl acetate 4:1) to yield 57.0 mg (0.157 mmol, 52.4 %) of compound **47** as a colorless solid.

m.p.: 105 °C

¹H NMR (500 MHz, CD₂Cl₂) *δ*/ppm = 7.48 (d, *J* = 1.5 Hz, 1H, phenyl, aromatic ortho or meta H), 7.46 (d, *J* = 1.2 Hz, 1H, phenyl, ortho or meta H), 7.37 (m, 2H, phenyl, ortho or meta Hs), 7.28 (td, J = 7.2 Hz, 1.4 Hz, 1H, phenyl, para H), 7.20 (s, 1H, 1-H), 6.71 (s, 1H, 4-H), 3.76 (s, 3H, OCH₃), 3.70 (t, *J* = 8.4 Hz, 1H, 17-H), 2.90 (m, 2H, 6-H), 2.33 (m, 1H, 11-Hₐ), 2.23 (td, *J* =

11.1 Hz, 4.2 Hz, 1H, 9-H), 2.09 (J = 12.4 Hz, 9.0 Hz, 5.2 Hz, 1H, 16-H_a), 1.92 (m, 1H, 12-H_a), 1.90 (m, 1H, 7-H_a), 1.71 (m, 1H, 15-H_a), 1.52 (m, 1H, 11-H_b), 1.48 (m, 1H, 16-H_b), 1.46 (m, 1H, 8-H), 1.38 (m, 1H, 15-H_b), 1.36 (m, 1H, 7-H_b), 1.29 (m, 1H, 12-H_b), 1.21 (m, 1H, 14-H), 0.79 (s, 3H, 18-H)

^{13}C NMR (126 MHz, CD_2Cl_2) δ/ppm = 154.65 (C-3), 139.52 (C-5), 137.79 (phenyl, quarternary carbon), 133.13 (C-10), 129.90 (2 C, phenyl, ortho or meta Cs or C-1), 128.24 (2C, phenyl, ortho or meta Cs or C-1), 128.23 (phenyl, ortho or meta C or C-1), 128.22 (C-2), 126.91 (phenyl, para C), 111.91 (C-4), 82.16 (C-17), 55.86 (OCH_3) 50.44 (C-14), 44.36 (C-9), 43.62 (C-13), 39.37 (C-8), 37.12 (C-12), 30.95 (C-16), 30.14 (C-6), 27.72 (C-7), 26.83 (C-11), 23.47 (C-15), 11.26 (C-18)

IR (ATR): $\tilde{v}_{max}$/cm^{-1} = 2925, 1963, 1738, 1610, 1486, 1444, 1218, 1132, 1053, 750

HRMS (EI): m/z = [M$^{•+}$] calcd. for $C_{25}H_{30}O_2$$^{•+}$: 362.2240; found: 362.2240

Purity (HPLC): > 92 % (λ = 210 nm), > 99% (λ = 254 nm) (Method 2)

(8*R*,9*S*,13*S*,14*S*,17*S*)-13-Methyl-2-phenyl-7,8,9,11,12,13,14,15,16,17-decahydro-6*H*-cyclopenta[*a*]phenanthrene-3,17-diol (48)
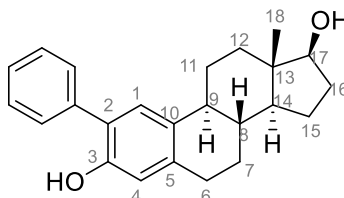
$C_{24}H_{28}O_2$

M_w: 348.49 g/mol

Iodoestrane **41** (482 mg, 1.21 mmol, 1.00 eq), phenylboronic acid (221 mg, 1.81 mmol, 1.50 eq) and potassium phosphate (771 mg, 3.63 mmol, 3.00 eq) were combined in a round bottom flask. Then 1,2-dimethoxyethane (20 mL), water (5 mL) and tetrakis-(triphenylphosphine)palladium (0) (69.9 mg, 0.0605 mmol, 5 mol%) were added and the resulting mixture was stirred at 50 °C for 24 hours under a nitrogen atmosphere. After cooling to room temperature, water (10 mL) was added and the mixture was extracted with ethyl acetate (3 x 20 mL). The combined organic layers were washed with saturated aqueous ammonium chloride solution, filtered through a hydrophobic filter and evaporated to dryness. The crude product was purified by flash column chromatography (isohexane/ethyl acetate 3:1) to yield 310 mg (0.890 mmol, 74 %) of compound **48** as a colorless solid.

m.p.: 111 °C

¹H NMR (400 MHz, CDCl₃) δ/ppm = 7.47 (m, 4H, phenyl ortho and meta Hs), 7.38 (m, 1H, aromatic para H), 7.17 (s, 1H, 1-H), 6.73 (s, 1-H, 4-H), 5.30 (s, 0.82H, methylene chloride), 5.05 (s, 0.86H, methylene chloride), 3.73 (m, 1H, 17-H), 2.88 (m, 2H, 6-H), 2.32 (m, 1H, 11-H$_a$), 2.23 (td, J = 11.0 Hz, 4.2 Hz, 1H, 9-H), 2.12 (m, 1H, 16-H$_a$), 1.95 (m, 1H, 12-H$_a$), 1.90 (m, 1H, 7-H$_a$), 1.72 (dddd, J = 12.3 Hz, 9.9 Hz, 7.0 Hz, 2.9 Hz, 1H, 15-H$_a$), 1.52 (m, 1H, 11-H$_b$), 1.49 (m, 1H, 16-H$_b$), 1.46 (m, 1H, 8-H), 1.38 (m, 1H, 15-H$_b$), 1.36 (m, 1H, 7-H$_b$), 1.27 (m, 1H, 12-H$_b$), 1.21 (m, 1H, 14-H), 0.79 (s, 3H, 18-H)

¹³C NMR (101 MHz, CDCl₃) δ/ppm = 150.30 (C-3), 138.19 (C-5), 137.66 (phenyl, quarternary carbon), 133.02 (C-10), 129.35 (2C, phenyl ortho or meta Cs), 129.24 (2C, phenyl ortho or meta Cs), 127.75 (phenyl, para C), 127.39 (C-1), 125.78 (C-2), 115.82 (C-4), 82.07 (C-17), 50.21 (C-14), 44.09 (C-9), 43.40 (C-13), 39.01 (C-8), 36.84 (C-12), 30.76 (C-16), 29.55 (C-6), 27.38 (C-7), 26.53 (C-11), 23.29 (C-15), 11.21 (C-18)

IR (ATR): $\tilde{v}_{max}$/cm⁻¹ = 2924, 1985, 1738, 1586, 1469, 1443, 1353, 1054, 750, 700

HRMS (EI)**:** m/z = [M˙⁺] calcd. for C₂₄H₂₈O₂˙⁺: 348.2084; found: 348.2085

Literature known compound[180]

(8*R*,9*S*,13*S*,14*S*,17*S*)-13-Methyl-2-(prop-1-yn-1-yl)-7,8,9,11,12,13,14,15,16,17-decahydro-6*H*-cyclopenta[*a*]phenanthrene-3,17-diol (51)

C₂₁H₂₆O₂
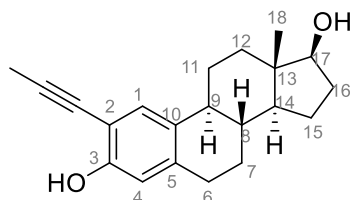
M$_w$: 310.44 g/mol

A flame dried round bottom flask was evacuated and backfilled with nitrogen three times prior to the addition of iodoestrane **41** (370 mg, 0.930 mmol, 1.00 eq), propyne (1 M in DMF, 0.974 mL, 0.974 mmol, 1.05 eq), diisopropylamine (0.390 mL, 2.79 mmol, 3.00 eq) and toluene (5.00 mL). Then copper (I) iodide (3.54 mg, 0.0186 mmol, 2 mol%) and bis(triphenylphosphine)palladium (II) dichloride (6.53 mg, 0.00930 mmol, 1 mol%) were added under a nitrogen flow. The mixture was stirred for 5 h at ambient temperature under a nitrogen atmosphere. Thereafter ethyl acetate (10 mL) was added and the organic layer was washed with water (3 x 10 mL) and brine (2 x 10 mL) and dried over anhydrous sodium sulfate. After evaporation of the solvent, the crude product was purified by flash column chromatography

(isohexane/ethyl acetate 4:1) to yield an inseparable mixture (270 mg) of reactant **41** and compound **51** as a yellow to orange solid.

m.p.: 149 °C (mixture)

IR (ATR): $\tilde{v}_{max}$/cm^{-1} = 2925, 2360, 1973, 1726, 1480, 1217, 1042 (mixture)

HRMS (EI): calcd. for $C_{21}H_{26}O_2$ (M) $^{+\cdot}$: 310.1927; found: not found due to superimposition or suppression by **41**

(1S,3aS,3bR,10bS,12aS)-8,12a-Dimethyl-2,3,3a,3b,4,5,10b,11,12,12a-decahydro-1H-cyclopenta[7,8]phenanthro[2,3-b]furan-1-ol (53)
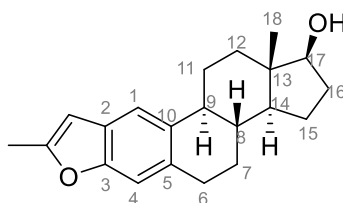
$C_{21}H_{26}O_2$

M_w: 310.44 g/mol

The above-described mixture of **51** and **41** (248 mg, 0.800 mmol (calculated as **51**, 1.00 eq) was dissolved in 4 mL methanol in a round bottom flask equipped with a magnetic stirring bar. Then a solution of KOH (135 mg, 2.40 mmol, 3.00 eq) in water (0.5 mL) was added. The resulting mixture was stirred overnight at room temperature. Thereafter it was concentrated *in vacuo*, ethyl acetate (10 mL) and water (10 mL) were added and the phases were separated. The aqueous phase was further extracted with ethyl acetate (2 x 10 mL). The combined organic layers were washed with brine (25 mL), dried over anhydrous sodium sulfate and evaporated to dryness. The crude product was purified by flash column chromatography (isohexane/ethyl acetate 3:1) to yield 134 mg (0.432 mmol, 36 % from **41** over two steps) of compound **53** as a yellow solid.

m.p.: 152 °C

^{1}H NMR (400 MHz, DMSO) δ/ppm = 7.38 (s, 1H, 1-H), 7.12 (s, 1H,4-H), 6.43 (s, 1H, furan H), 4.49 (d, J = 4.8 Hz, 1H, OH), 3.53 (td, J = 8.5, 4.8 Hz, 1H, 17-H), 2.89 (m, 2H, 6-H), 2.38 (s, 3H, furan CH$_3$), 2.34 (m, 1H, 7-H$_a$), 2.22 (m, 1H, 9-H), 1.90 (m, 1H, 16-H$_a$), 1.86 (m, 1H, 12-H$_a$), 1.81 (m, 1H, 7-H$_b$), 1.59 (m, 1H, 15-H$_a$), 1.44 (m, 1H, 11-H$_a$), 1.38 (m, 1H, 16-H$_b$), 1.33 (m, 1H, 8-H), 1.31 (m, 1H, 11-H$_b$), 1.26 (m, 1H, 15-H$_b$), 1.21 (m, 1H, 12-H$_b$), 1.13 (m, 1H, 14-H), 0.67 (s, 3H, 18-H)

¹³C NMR (101 MHz, DMSO) δ/ppm = 154.49 (furan, quarternary carbon), 152.73 (C-3), 134.92 (C-10), 132.05 (C-5), 126.66 (C-2), 116.25 (C-1), 109.65 (C-4), 102.54 (furan CH), 80.03 (C-17), 49.77 (C-14), 43.92 (C-9), 42.76 (C-13), 38.53 (C-8), 36.60 (C-12), 29.89 (C-16), 29.41 (C-6), 26.94 (C-11), 26.24 (C-7), 22.85 (C-15), 13.74 (furan CH$_3$), 11.23 (C-18)

IR (ATR): $\tilde{v}_{max}$/cm⁻¹ = 3479, 2938, 1601, 1467, 1262, 1052, 930, 810

HRMS (EI): m/z = [M$^{•+}$] calcd. for C$_{21}$H$_{26}$O$_2$$^{•+}$: 310.1927; found: 310.1929

Purity (HPLC): > 99 % (λ = 210 nm), > 99 % (λ = 254 nm) (Method 2)

Literature known compound[158]

(8*R*,9*S*,13*S*,14*S*,17*S*)-2-Methoxy-13-methyl-7,8,9,11,12,13,14,15,16,17-decahydro-6*H*-cyclopenta[*a*]phenanthren-17-ol (54)

C$_{19}$H$_{26}$O$_2$

M$_w$: 286.42 g/mol

Aryl triflate **60** (73.9 mg, 0.170 mmol, 1.00 eq), palladium (II) acetate (3.82 mg, 0.0170 mmol, 0.100 eq), formic acid (0.02 mL, 0.425 mmol, 2.50 eq), triethylamine (0.070 mL, 0.51 mmol, 3.0 eq), triphenylphosphine (8.92 mg, 0.0340 mmol, 0.200 eq) and DMF (0.8 mL) were combined in a flame dried Schlenk flask. The flask was purged with nitrogen three times and resulting mixture was stirred at 60 °C overnight under a nitrogen atmosphere. After cooling to room temperature, the mixture was concentrated *in vacuo* and water (5 mL) and saturated aqueous ammonium hydroxide solution were added to the residue until pH 9 was reached and the mixture was extracted with dichloromethane (3 x 5 mL). The combined organic layers were washed with water (3 x 5 mL) and brine (5 mL) and dried over anhydrous sodium sulfate. After evaporation of the solvent, the crude product was purified by flash chromatography (isohexane/ethyl acetate 3:1) to yield 27.7 mg (0.0967 mmol, 57 %) of compound **54** as a colorless solid.

m.p.: 133 °C

¹H NMR (400 MHz, DMSO) δ/ppm = 6.94 (d, *J* = 8.4 Hz, 1H, 4-H), 6.79 (d, *J* = 2.6 Hz, 1H, 1-H), 6.66 (dd, *J* = 8.3Hz, 2.6 Hz, 1H, 3-H), 4.50 (d, *J* = 4.9 Hz, 1H, OH), 3.69 (s, 3H, OCH$_3$), 3.52 (td, *J* = 8.4 Hz, 4.8 Hz, 1H, 17-H), 2.72 (m, 2H, 6-H), 2.27 (m, 1H, 11-H$_a$), 2.14 (t, *J* = 11.9

Hz, 1H, 9-H), 1.88 (m, 1H, 16-H$_a$), 1.86 (m, 1H, 12-H$_a$), 1.79 (m, 1H, 7-H$_a$), 1.58 (m, 1H, 15-H$_a$), 1.40 (m, 1H, 11-H$_b$), 1.34 (m, 1H, 16-H$_b$), 1.29 (m, 1H, 8-H), 1.26 (m, 1H, 15-H$_b$), 1.22 (m, 1H, 7-H$_b$), 1.19 (m, 1H, 12-H$_b$), 1.12 (m, 1H, 14-H), 0.67 (s, 3H, 18-H)

^{13}C NMR (101 MHz, DMSO) δ/ppm = 157.30 (C-2), 141.18 (C-10), 129.51 (C-3), 128.10 (C-5), 111.19 (C-4), 110.66 (C-1), 80.02 (C-17), 54.88 (OCH$_3$), 49.66 (C-14), 44.20 (C-9), 42.76 (C-13), 38.30 (C-8), 36.59 (C-12), 29.90 (C-16), 28.18 (C-6), 26.97 (C-7), 25.80 (C-11), 22.80 (C-15), 11.23 (C-18)

IR (ATR): $\tilde{v}_{max}$/cm^{-1} = 3298. 2932, 2850, 1743, 1604, 1575, 1497, 1242, 1057, 856, 802

HRMS (EI): m/z = [M$^{\bullet+}$] calcd. for C$_{19}$H$_{26}$O$_2$$^{\bullet+}$: 286.1927; found: 286.1917

Purity (HPLC): > 99 % (λ = 210 nm), > 99 % (λ = 254 nm) (Method 2)

Literature known compound[184]

(8*R*,9*S*,13*S*,14*S*,17*S*)-3-((*N,N*-Dimethylcarbamoyl)oxy)-13-methyl-7,8,9,11,12,13,14,15,16,17-decahydro-6*H*-cyclopenta[*a*]phenanthren-17-yl acetate (58)
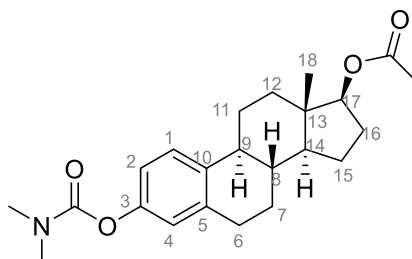
C$_{23}$H$_{31}$NO$_4$

M$_w$: 385.50 g/mol

501 mg (1.46 mmol, 1.00 eq) of carbamate **24** were dissolved in pyridine (3 mL). Then 0.27 mL (298 mg, 2.00 eq) of acetic anhydride were added and the resulting solution was stirred at 60 °C overnight. After cooling, the mixture was poured into ice-water (10 mL). The precipitate was collected by filtration and dissolved in ethyl acetate (30 mL). The resulting solution was washed with saturated aqueous CuSO$_4$ solution (2 x 20 mL), water (20 mL) and brine (20 mL), dried over anhydrous sodium sulfate and concentrated *in vacuo*. The residue was purified by flash column chromatography (isohexane/ethyl acetate 3:1) to yield compound **58** (423 mg, 1.10 mmol, 75 %) as a white solid.

m.p.: 188 °C

^{1}H NMR (500 MHz, CD$_2$Cl$_2$) δ/ppm = 7.25 (dd, *J* = 8.6 Hz, 1.1 Hz, 1H, 1-H), 6.82 (dd, *J* = 8.5, 2.6 Hz, 1H, 2-H), 6.79 (d, *J* = 2.6 Hz, 1H, 4-H), 4.66 (dd, *J* = 9.2, 7.8 Hz, 1H, 17-H), 3.06 (s, 3H, NCH$_3$), 2.95 (s, 3H, NCH$_3$'), 2.86 (td, *J* = 7.7, 7.1, 4.1 Hz, 2H, 6-H), 2.31 (m, 1H, 11-H$_a$),

2.25 (m, 1H, 9-H), 2.18 (m, 1H, 16-H$_a$), 2.02 (s, 3H, acetyl), 1.91 (m, 1H, 7-H$_a$), 1.87 (m, 1H, 12-H$_a$), 1.75 (dddd, J = 12.4 Hz, 9.8 Hz, 7.0 Hz, 3.1 Hz, 1H, 15-H$_a$), 1.53 (m, 1H, 16-H$_b$), 1.50 (m, 1H, 11-H$_b$), 1.45 (m, 1H, 8-H), 1.41 (m, 1H, 15-H$_b$), 1.38 (m, 1H, 12-H$_b$), 1.33 (m, 1H, 7-H$_b$), 1.28 (m, 1H, 14-H), 0.84 (s, 3H, 18-H)

^{13}C NMR (126 MHz, CD$_2$Cl$_2$) δ/ppm = 171.29 (carbonyl of ester), 155.47 (carbonyl of carbamate), 149.85 (C-3), 138.44 (C-5), 137.69 (C-10), 126.43 (C-1), 122.20 (C-4), 119.29 (C-2), 82.99 (C-17), 50.20 (C-14), 44.39 (C-9), 43.25 (C-13), 38.71 (C-8), 37.30 (C-12), 36.81 (NCH$_3$), 36.63 (NCH$_3$'), 29.90 (C-6), 27.96 (C-16), 27.45 (C-7), 26.57 (C-11), 23.58 (C-15), 21.31 (acetyl CH$_3$), 12.19 (C-18)

IR (ATR): $\tilde{v}_{max}$/cm^{-1} = 2952, 2929, 2856, 1666, 1462, 1360, 1248, 1138, 1082, 888, 831

HRMS (ESI): m/z = [M+H]$^+$ calcd. for C$_{23}$H$_{32}$NO$_4$$^+$: 386.2326; found: 386.2327

(8R,9S,13S,14S,17S)-17-Hydroxy-2-methoxy-13-methyl-7,8,9,11,12,13,14,15,16,17-decahydro-6H-cyclopenta[a]phenanthren-3-yl trifluoromethanesulfonate (60)
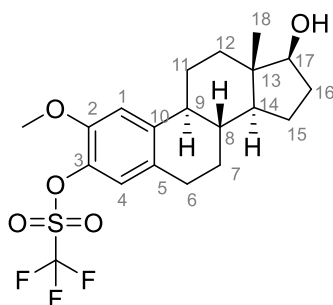
C$_{20}$H$_{25}$F$_3$O$_5$S

M$_w$: 434.47 g/mol

2-Methoxyestradiol (**55**) (96.8 mg, 0.320 mmol, 1.00 eq) was dissolved in DMF (1.5 mL). K$_2$CO$_3$ (106 mg, 0.640 mmol, 2.00 eq) was added, followed by 4-nitrophenyl trifluoromethanesulfonate (91.1 mg, 0.336 mmol, 1.05 eq) and the resulting suspension was stirred for 2 h at room temperature. Then water (5 mL) and diethyl ether (5 mL) were added and the aqueous layer was separated and extracted with diethyl ether (3 × 5 mL). The combined organic layers were washed with cold 1 M aqueous hydrochloric acid (5 mL), 1 M aqueous NaOH solution (3 × 5 mL), water (3 × 5 mL), brine (5 mL) and 1 M aqueous LiCl solution (5 mL) and then dried over anhydrous sodium sulfate. After evaporation of the solvent, the crude product was purified by flash column chromatography (isohexane/ethyl acetate 3:1) to yield 108 mg (0.247 mmol, 77 %) of compound **60** as a colorless solid.

m.p.: 184 °C

¹H NMR (500 MHz, DMSO) δ/ppm = 7.13 (s, 1H, 1-H), 7.07 (s, 1H, 4-H), 4.52 (d, J = 4.9 Hz, 1H, OH), 3.86 (s, 3H, OCH$_3$), 3.53 (td, J = 8.5 Hz, 4.8 Hz, 1H, 17-H), 2.75 (dt, J = 10.6 Hz, 4.6 Hz, 2H, 6-H), 2.37 (m, 1H, 11-H$_a$), 2.19 (td, J = 11.1 Hz, 4.2 Hz, 1H, 9-H), 1.91 (m, 1H, 16-H$_a$), 1.86 (m, 1H, 12-H$_a$), 1.80 (m, 1H, 7-H$_a$), 1.59 (m, 1H, 15-H$_a$), 1.44 (m, 1H, 11-H$_b$), 1.39 (m, 1H, 16-H$_b$), 1.35 (m, 1H, 8-H), 1.26 (m, 1H, 15-H$_b$), 1.22 (m, 1H, 7-H$_b$), 1.19 (m, 1H, 12-H$_b$), 1.12 (m, 1H, 14-H), 0.68 (s, 3H, 18-H)

¹³C NMR (126 MHz, DMSO) $δ$/ppm = 148.28 (C-2), 142.01 (C-10), 135.86 (C-3), 129.60 (C-5), 121.71 (C-4), 118.22 (q, triflate), 111.03 (C-1), 79.97 (C-17), 56.33, (OCH$_3$), 49.54 (C-14), 44.14 (C-9), 42.74 (C-13), 37.87 (C-8), 36.53 (C-12), 29.90 (C-16), 28.04 (C-6), 26.45 (C-7), 25.83 (C-11), 22.75 (C-15), 11.21 (C-18)

IR (ATR): $\tilde{v}_{max}$/cm^{-1} = 3186, 2915, 1991, 1606, 1513, 1422, 1259, 1205, 1098, 1058, 875, 803

HRMS (EI): calcd. for C$_{20}$H$_{25}$F$_3$O$_5$S (M) $^{·+}$: 434.1369, found: 434.1370

Literature known compound[185]

7. Appendices

7.1. Abbreviations

2,4-DTBP	2,4-Di-*tert*-butylphenol
Ac	acetyl
ACN	acetonitrile
AChE	acetylcholinesterase
AD	agar diffusion
AM	acetoxymethyl
APCI	atmospheric-pressure chemical ionization
aq.	aqueous
Ar	aryl
ASAP	atmospheric pressure solids analysis probe
ATP	adenosine triphosphate
ATR	attenuated total reflexion
BHT	butylated hydroxytoluene
BINAP	2,2′-bis(diphenylphosphino)-1,1′-binaphthyl
Bn	benzyl
CAL I	Calpain Inhibitor I
calcd.	calculated
CAM	cerium ammonium molybdate
cf.	confere
CLEAR	Coordinated Lysosomal Expression and Regulation
Cn	Calcineurin
CO	carbon monoxide
COMT	Catechol-O-methyltransferase

COSY	correlation spectroscopy
CYP	cytochrome P
d	doublet
DABCO	1,4-diazabicyclo[2.2.2]octane
dba	dibenzylideneacetone
DCM	dichloromethane
DEPT	Distortionless Enhancement by Polarization Transfer
DIPE	diisopropyl ether
DMF	dimethylformamide
DMSO	dimethyl sulfoxide
DNA	deoxyribonucleic acid
DNPH	2,4-dinitrophenylhydrazine
DPP IV	dipeptidyl peptidase 4
dppf	1,1′-bis(diphenylphosphino)ferrocene
EC_{50}	half maximal effective concentration
E-Cad	E-Cadherin
EDME	17β-estradiol methyl ether
EE	early endosome
e.g.	exempli gratia (for example)
EI	electron ionization
ELS	endolysosomal system
eq.	equivalents
ER	estrogen receptor
ERK2	extracellular signal-regulated kinase 2
ESI	electron spray ionization
Et	ethyl

EtOAc	ethyl acetate
EtOH	ethanol
FBS	fetal bovine serum
FCC	flash column chromatography
FDA	Food and Drug Administration
FLIPR	fluorescence imaging plate reader
FGFR4	fibroblast growth factor 4
FPT	Freeze-Pump-Thaw
Fulv	fulvestrant
GFP	green fluorescent protein
h	hour
HEK293	human embryonic kidney cells
HIV	human immunodeficiency virus
HOAc	acetic acid
HPLC	high-performance liquid chromatography
HRMS	high-resolution mass spectrometry
HMQC	heteronuclear multiple quantum correlation
HSQC	heteronuclear single quantum correlation
HRAS	Harvey Rat sarcoma virus
HTS	high-throughput screening
Hz	hertz
IC_{50}	half maximal inhibitory concentration
KO	knock-out
IDT	idiosyncratic drug toxicity
IR	infrared spectroscopy
LCMS	liquid chromatography mass spectrometry

LDA	lithium diisopropylamide
LE	late endosome
LEL	late endosome/lysosome
LiHMDS	lithium bis(trimethylsilyl)amide
lit	literature
m	meta
m	multiplet (NMR)
M	molar
MCF-7	breast cancer cell line
MCOLN1	Mucolipin-1
MDA-MB-231	breast cancer cell line
Me	methyl
MeOH	methanol
min	minutes
ML-IV	Mucolipidosis type VI
mmol	millimole
mol	mole
MOM	methoxy methyl
m.p.	melting point
mTORC1	mechanistic target of rapamycin complex 1
MTT	3-(4,5-dimethylthiazol-2-yl)-2,5-diphenyltetrazoliumbromid
M_w	molecular weight
mw	microwave
m/z	mass-to-charge ratio
NAD	nicotinamide adenine dinucleotide
NADP	nicotinamide adenine dinucleotide phosphate

NFSI	*N*-fluorobenzenesulfonimide
NIS	*N*-iodosuccinimide
NK	natural killer
NMP	*N*-methyl-2-pyrrolidinone
NaO*t*Bu	sodium *tert*-butoxide
n.d.	not determined
NMR	nuclear magnetic resonance
ns	not significant
NSAR	non-steroidal anti-inflammatory drug
o	ortho
OTf	triflate
p	para
PBS	phosphate buffered saline
PG	protective group
ph	phenyl
PhI(OAc)$_2$	iodobenzene diacetate
PhOH	phenol
PI(3,5)P$_2$	phosphatidylinositol 3,5-bisphosphate
PI(4,5)P$_2$	phosphatidylinositol 4,5-bisphosphate
pKa	acid dissociation constant
ppm	parts per million
pTsOH	p-Toluenesulfonic acid
q	quartet (NMR)
RBA	relative binding affinity
RE	recycling endosome
Rf	retardation factor

ROS	reactive oxygen species
RP	reversed phase
rt	room temperature
s	singlet (NMR)
SAR	structure-activity relationships
s-BuLi	*sec*-butyllithium
SEM	standard error of the mean
SI	signal intensity
TBAF	tetra-*n*-butylammonium fluoride
TBDMS	*tert*-butyldimethylsilyl
TEA	triethylamine
TFA	trifluoroacetic acid
TFAA	trifluoroacetic acid anhydride
TFEB	transcription factor EB
THF	tetrahydrofuran
TLC	thin-layer chromatography
TNBC	triple negative breast cancer
TRP	transient receptor potential
TRPA	transient receptor potential channel ankyrin
TRPC	transient receptor potential channel canonical
TRPM	transient receptor potential channel melastatin
TRPML	transient receptor potential cation channel
TRPN	transient receptor potential cation channel no mechanoreceptor potential C
TRPP	transient receptor potential cation channel polycystic
TRPV	transient receptor potential channel vanilloid
quant.	quantitative

UV	ultraviolet
VATPase	vacuolar-type ATPase
$\tilde{v}$	wavenumber
XPhos	2-(dicyclohexylphosphino)-2',4',6'-triisopropyl-1,1'-biphenyl
YES	yeast estrogen screen
YFP	yellow fluorescent protein

7.2. References

[1]   de Duve C, Pressman BC, Gianetto R, Wattiaux R, Appelmans F, *Biochemical Journal* **1955**, 60 (4) 604-17

[2]   Perera RM, Zoncu R, *Annual Review of Cell and Developmental Biology* **2016**, 32 (1) 223-53

[3]   Settembre C, Fraldi A, Medina DL, Ballabio A, *Nature Reviews Molecular Cell Biology* **2013**, 14 (5) 283-96

[4]   Mindell J.A., *Annual Review of Physiology* **2012**, 74 (1) 69-86

[5]   Trivedi P.C., Bartlett J.J., Pulinilkunnil T., Cells **2020**; 9(5), permission link http://creativecommons.org/licenses/by/4.0/

[6]   Ballabio A., Bonifacino J.S., *Nature Reviews Molecular Cell Biology* **2020**, 21 (2) 101-18

[7]   Gruenberg J., *Nature Reviews Molecular Cell Biology* **2001**, 2 (10) 721-30

[8]   Winckler B., Faundez V., Maday S., Cai Q., Guimas Almeida C, Zhang H, *J Neurosci* **2018**, 38 (44) 9364-74

[9]   Vidyadhara D.J., Lee J.E., Chandra S.S., *Journal of Neurochemistry* **2019**, 150 (5) 487-506

[10]   Andres-Alonso M., Kreutz M.R., Karpova A., *Cellular and Molecular Life Sciences* **2021**, 78 (6) 2621-39

[11]   Hansen M., Rubinsztein D.C., Walker D.W., *Nature Reviews Molecular Cell Biology* **2018**, 19 (9) 579-93

[12]   Kirkin V., *Journal of Molecular Biology* **2020**, 432 (1) 3-27

[13]   Aman Y., Schmauck-Medina T., Hansen M., Morimoto R.I., Simon A.K., Bjedov I., Palikaras, K., Simonsen, A., Johansen, T.,Tavernarakis, N.Rubinsztein, D.C.Partridge, L.Kroemer, G.Labbadia, J.Fang, E.F., *Nature Aging* **2021**, 1 (8) 634-50

[14]   Al Outa A., Hicks S., Thambawita V., Andresen S., Enserink J.M., Halvorsen P., Riegler, M.A., Knævelsrud, H., *Scientific Data* **2023**, 10 (1) 806, permission link http://creativecommons.org/licenses/by/4.0/

[15]   Aits S., Jäättelä M., *Journal of Cell Science* **2013**, 126 (9) 1905-12

[16]   Yang C., Wang X., *Journal of Cell Biology* **2021**, 220 (6) e202102001

[17]   Lawrence R.E., Zoncu R., *Nature Cell Biology* **2019**, 21 (2) 133-42

[18]   Mahapatra K.K., Mishra S.R., Behera B.P., Patil S., Gewirtz D.A., Bhutia S.K., *Cellular and Molecular Life Sciences* **2021**, 78 (23) 7435-49

[19]   Yang J., Zhao Z., Gu M., Feng X., Xu H., *Protein & Cell* **2019**, 10 (1) 8-19

[20]   Nakamura S., Yoshimori T., *Molecules and Cells* **2018**, 41 (1) 65-72

[21]   Wong S.Q., Kumar A.V., Mills J., Lapierre L.R., *Human Genetics* **2020**, 139 (3) 277-90

[22]   Onorati A.V., Dyczynski M., Ojha R., Amaravadi R.K., *Cancer* **2018**, 124 (16) 3307-18

[23]   Debnath J., Gammoh N., Ryan K.M., *Nat Rev Mol Cell Biol* **2023**, 24 (8) 560-75

[24]   Menzies F.M., Fleming A., Caricasole A., Bento C.F., Andrews S.P., Ashkenazi A, Füllgrabe J.,Jackson A., Jimenez Sanchez, M., Karabiyik C., Licitra, F., Lopez Ramirez A, Pavel M., Puri C., Renna M., Ricketts,T., Schlotawa L., Vicinanza M., Won H., Zhu Y., Skidmore J., Rubinsztein D.C., *Neuron* **2017**, 93 (5) 1015-34

[25]   Vargas J.N.S., Hamasaki M., Kawabata T., Youle R.J., Yoshimori T., *Nature Reviews Molecular Cell Biology* **2023**, 24 (3) 167-85

[26]   Settembre C., Di Malta C., Polito V.A., Garcia Arencibia M., Vetrini F., Erdin S., Erdin S.U., Huynh T., Medina, D.L., Colella P., Sardiello M., Rubinsztein D.C., Ballabio A. *Science* **2011**, 332 (6036) 1429-33

[27]   Palmieri M., Impey S., Kang H., di Ronza A., Pelz C., Sardiello M., Ballabio A., *Human Molecular Genetics* **2011**, 20 (19) 3852-66

[28]   Tan A., Prasad R., Lee C., Jho E-h., *Cell Death & Differentiation* **2022**, 29 (8) 1433-49

[29]   Napolitano G., Ballabio A., *Journal of Cell Science* **2016**, 129 (13) 2475-81

[30] Medina DL., Di Paola S., Peluso I., Armani A., De Stefani D., Venditti R., Montefusco S., Scotto Rosato A., Prezioso C., Forrester A., Settembre C., Wang W., Gao Qi., Xu H., Sandri M., Rizzuto R., De Matteis M.A., Ballabio A., *Nature Cell Biology* **2015**, 17 (3) 288-99

[31] Ballabio A., *EMBO Molecular Medicine* **2016**, 8 (2) 73-6-6, permission link https://creativecommons.org/licenses/by/4.0/

[32] Chen Q., She J., Zeng W., Guo J., Xu H., Bai X-c., Jiang Y., *Nature* **2017**, 550 (7676) 415-8

[33] Vergarajauregui S., Puertollano R., *Traffic* **2006**, 7 (3) 337-53

[34] Wu Y., Huang P., Dong X-P., *Cancers* **2021**; 13 (6), 1299, permission link http://creativecommons.org/licenses/by/4.0/

[35] Zhang X., Li X., Xu H., *Proc Natl Acad Sci U S A* **2012**, 109 (28) 11384-9

[36] Zhang X., Cheng X., Yu L., Yang J., Calvo R., Patnaik S., Hu X., Gao Q., Yang M., Lawas M., Delling M., Marugan J., Ferrer M., Xu H., *Nature Communications* **2016**, 7 (1) 12109

[37] Li M., Zhang W.K., Benvin N.M., Zhou X., Su D., Li H., Wang S., Michailidis I.E., Tong L., Li X., Yang J., *Nature Structural & Molecular Biology* **2017**, 24 (3) 205-13

[38] Dong X-P., Cheng X., Mills E., Delling M., Wang F., Kurz T., Xu H., *Nature* **2008**, 455 (7215) 992-6

[39] Xu H., Delling M., Li L., Dong X., Clapham D.E., *Proceedings of the National Academy of Sciences* **2007**, 104 (46) 18321-6

[40] Miedel M.T., Rbaibi Y., Guerriero C.J., Colletti G., Weixel K.M., Weisz O.A., Kiselyov K., *Journal of Experimental Medicine* **2008**, 205 (6) 1477-90

[41] Venkatachalam K., Long A.A., Elsaesser R., Nikolaeva D., Broadie K., Montell C., *Cell* **2008**, 135 (5) 838-51

[42] Wakabayashi K., Gustafson A.M., Sidransky E., Goldin E., *Molecular Genetics and Metabolism* **2011**, 104 (3) 206-13

[43] Xu H., Ren D., *Annual Review of Physiology* **2015**, 77 (1) 57-80

[44] Di Paola S., Medina D.L. *Calcium Signalling: Methods and Protocols* **2019**. p. 143-4.

[45] Li X., Rydzewski N., Hider A., Zhang X., Yang J., Wang W., Gao Q., Cheng X., Xu H., *Nature Cell Biology* **2016**, 18 (4) 404-17

[46] Li R-J., Xu J., Fu C., Zhang J., Zheng Y.G., Jia H., Liu J.O., *eLife* **2016**, 5 e19360

[47] Huang P., Dong R.Y., Wang P., Xu M., Sun X., Dong X-P., *Autophagy* **2024**, 1-2

[48] Scotto Rosato A., Montefusco S., Soldati C., Di Paola S., Capuozzo A., Monfregola J., Polishchuk E., Amabile A., Grimm C., Lombardo A., De Matteis M. A., Ballabio A., Medina D. L., *Nature Communications* **2019**, 10 (1) 5630

[49] Cheng X., Zhang X., Gao Q., Ali Samie M., Azar M., Tsang W.L., Dong, Libing Sahoo N., Li X., Zhuo Y., Garrity, A.G., Wang X., Ferrer M., Dowling J., Xu L., Han R., Xu, H., *Nature Medicine* **2014**, 20 (10) 1187-92

[50] Erkhembaatar M., Gu D.R., Lee S.H., Yang Y-M., Park S., Muallem S., Shin D.M., Kim M.S., *Journal of Bone and Mineral Research* **2017**, 32 (2) 385-96

[51] Bretou M., Sáez P.J., Sanséau D., Maurin M., Lankar D., Chabaud M., Spampanato C., Malbec O., Barbier L., Muallem S., Maiuri P., Ballabio A., Helft J., Piel M., Vargas P., Lennon-Duménil A-M.., *Science Immunology* **2017**, 2 (16) eaak9573

[52] Goodridge J.P., Jacobs B., Saetersmoen M.L., Clement D., Hammer Q., Clancy T., Skarpen E., Brech A., Landskron J., Grimm C., Pfefferle A., Meza-Zepeda L., Lorenz S., Wiiger M.T., Louch W.E., Ask E.H., Liu L.L., Oei V. Y. S., Kjällquist. U., Linnarsson S.,Patel S., Taskén K., Stenmark H., Malmberg, K.-J., *Nature Communications* **2019**, 10 (1) 514

[53] Spix B., Chao Y-K., Abrahamian C., Chen C-C., Grimm C., *Frontiers in Immunology* **2020**, 11 318

[54] Eichelsdoerfer J.L., Evans J.A., Slaugenhaupt S.A., Cuajungco M.P., *Journal of Biological Chemistry* **2010**, 285 (45) 34304-8

[55] Cuajungco M-P., Basilio L-C., Silva J., Hart T., Tringali J., Chen C-C., Biel M., Grimm C., *Traffic* **2014**, 15 (11) 1247-65

[56] Qi J., Xing Y., Liu Y., Wang M-M., Wei X., Sui Z., Ding L., Zhang Y., Lu C., Fei Y.-H., Liu N., Chen R., Wu M., Wang L., Zhong Z., Wang T., Liu Y., Wang Y., Liu J., Xu H., Guo F., Wang W., *Autophagy* **2021**, 17 (12) 4401-22

[57] Xu Y., Du S., Marsh J.A., Horie K., Sato C., Ballabio A., Karch C.M., Holtzman D.M., Zheng H., *Molecular Psychiatry* **2021**, 26 (10) 5925-39

[58] Somogyi A., Kirkham E.D., Lloyd-Evans E., Winston J., Allen N.D., Mackrill J.J., Anderson, K.E., Hawkins, Phillip T. Gardiner, S.E., Waller-Evans H., Sims R., Boland B., O'Neill C., *Journal of Cell Science* **2023**, 136 (6) jcs259875

[59] Tsunemi T, Perez-Rosello T, Ishiguro Y, Yoroisaka A, Jeon S, Hamada K,Rammonhan M., Wong Y.C., Xie Z., Akamatsu W., Mazzulli J.R., Surmeier, D.J.,Hattori N., Krainc D., *The Journal of Neuroscience* **2019**, 39 (29) 5760-72

[60] Khan N., Lakpa K.L., Halcrow P.W., Afghah Z., Miller N.M., Geiger J.D., Chen X., *Scientific Reports* **2019**, 9 (1) 12285

[61] Capurro M.I., Greenfield L.K., Prashar A., Xia S., Abdullah M., Wong H., Zhong X.Z., Bertaux-Skeirik N., Chakrabarti J., Siddiqui I., O'Brien C., Dong X., Robinson L., Peek Jr R.M., Philpott D.J., Zavros Y., Helmrath M., Jones N.L., *Nature Microbiology* **2019**, 4 (8) 1411-23

[62] Kasitinon S.Y., Eskiocak U., Martin M., Bezwada D., Khivansara V., Tasdogan A., Zhao Z., Mathews T., Aurora A.B., Morrison S.J., *Cell Reports* **2019**, 28 (9) 2293-305.e9

[63] Xu M., Almasi S., Yang Y., Yan C., Sterea A.M., Rizvi Syeda A.K., Shen B., Richard Derek C., Huang P., Gujar S., Wang J., Zong W.-X., Trebak M.,El Hiani Y., Dong X.-P., *Cell Calcium* **2019**, 79 80-8

[64] Pan Y., Zhao Q., He H., Qi Y., Bai Y., Zhao J., Yang Y., *Frontiers in Oncology* **2023**, 13

[65] Frey N., Ouologuem L., Blenninger J., Siow W-X., Thorn-Seshold J., Stöckl J., Abrahamian C.,Fröhlich T.,Vollmar A.M.,Grimm C., Bartel K., *Journal of Biological Chemistry* **2024**, 300 (1)

[66] Jung J., Cho K.J., Naji A.K., Clemons K.N., Wong C-O., Villanueva M., Gregory, Steven Karagas N.E., Tan L., Liang H., Rousseau M.A.,Tomasevich K.M., Sikora, A.G., Levental I., van der Hoeven D., Zhou Y., Hancock J. F., Venkatachalam K.., *EMBO reports* **2019**, 20 (4) e46685

[67] Morelli M.B., Amantini C., Tomassoni D., Nabissi M., Arcella A., Santoni G. *Cancers* **2019**; 11(4) 525

[68] Jung J., Venkatachalam K., *Channels* **2019**, 13 (1) 374-81

[69] Xu M., Dong X-P., *Biomolecules* **2021**; 11(1) 65

[70] Krogsaeter E., Scotto Rosato A., Grimm C., *Cell Calcium* **2022**, 103 102553

[71] Chen C-C., Keller M., Hess M., Schiffmann R., Urban N., Wolfgardt A., Schaefer M., Bracher F., Biel M,.Wahl-Schott C., Grimm C., *Nature Communications* **2014**, 5 (1) 4681

[72] Shen D., Wang X., Li X., Zhang X., Yao Z., Dibble S, Dong X.-p., Yu T., Lieberman A.P., Showalter, H.D., Xu H., *Nature Communications* **2012**, 3 (1) 731

[73] Spix B, Butz E.S., Chen C-C., Scotto Rosato A., Tang R., Jeridi A., Kudrina, Veronika Plesch E., Wartenberg P., Arlt E., Briukhovetska D., Ansari M., Günsel G.G., Conlon T.M., Wyatt A., Wetzel S., Teupser D., Holdt L.M.., Ectors F., Boekhoff I., Boehm U., García-Añoveros J., Saftig P., Giera M., Kobold S., Schiller H.B., Zierler S., Gudermann T., Wahl-Schott C., Bracher F., Yildirim A.Ö., Biel M., Grimm C., *Nature Communications* **2022**, 13 (1) 318

[74] Peng X., Holler C.J., Alves A-M.F., Oliviera M.G., Speake M., Pugliese A., Oskouei M.R., de Freitas I.D., Chen A.Y. P.,Gallegos R., McTighe S.M., Koenig G., Hurst R.S., Blain J.-F., Lanter J.C., Burnett D.A., *Bioorganic & Medicinal Chemistry Letters* **2024**, 98 129595

[75] Samie M., Wang X., Zhang X., Goschka A., Li X., Cheng X., Gregg E., Azar M., Zhuo Y., Garrity A.G., Gao Q., Slaugenhaupt S., Pickel J., Zolov S.N., Weisman L.S., Lenk G.M., Titus S., Bryant-Genevier M., Southall N., Juan M., Ferrer M., Xu H., *Developmental Cell* **2013**, 26 (5) 511-24

[76] Wang W., Gao Q., Yang M., Zhang X., Yu L., Lawas M., Li X., Bryant-Genevier M., Southall N.T., Marugan J., Ferrer M., Xu H., *Proceedings of the National Academy of Sciences* **2015**, 112 (11) E1373-E81

[77] Leser C., Keller M., Gerndt S., Urban N., Chen C-C., Schaefer M., Grimm C, Bracher, F., *European Journal of Medicinal Chemistry* **2021**, 210 112966

[78] Kriegler K., Leser C., Mayer P., Bracher F., *Archiv der Pharmazie* **2022**, 355 (2) 2100362

[79] Stresser D.M., Kupfer D., *Biochem Pharmacol* **1998**, 55 (11) 1861-71

[80] Brill Z.G., Condakes M.L., Ting C.P., Maimone T.J., *Chem Rev* **2017**, 117 (18) 11753-95

[81] Korenman S.G., *Steroids* **1969**, 13 (2) 163-77

[82] Zhu B.T., Han G-Z., Shim J-Y., Wen Y., Jiang X-R., *Endocrinology* **2006**, 147 (9) 4132-50

[83] Meanwell N.A., *J Med Chem* **2011**, 54 (8) 2529-91

[84]   Rühl P., Scotto Rosato A., Urban N., Gerndt S., Tang R., Abrahamian C., Leser C., Sheng J., Jha A., Vollmer G., Schaefer M., Bracher F., Grimm C., *Scientific Reports* **2021**, 11 (1) 8313

[85]   Pindur U., Schall T., *Archiv der Pharmazie* **1994**, 327 (10) 637-42

[86]   Muddana S.S., Price A.M., MacBride M.M., Peterson B.R., *Journal of Medicinal Chemistry* **2004**, 47 (21) 4985-8

[87]   Johnson B.M., Shu Y-Z., Zhuo X., Meanwell N.A., *Journal of Medicinal Chemistry* **2020**, 63 (12) 6315-86

[88]   Besset T., Jubault P., Pannecoucke X., Poisson T., *Organic Chemistry Frontiers* **2016**, 3 (8) 1004-10

[89]   Inoue M., Sumii Y., Shibata N., *ACS Omega* **2020**, 5 (19) 10633-40

[90]   Jeschke P., Baston E., Leroux R.F., *Mini-Reviews in Medicinal Chemistry* **2007**, 7 (10) 1027-34

[91]   Zhong D., Xie Z., Chen X., *Journal of Pharmacy and Pharmacology* **2005**, 57 (3) 341-9

[92]   Boland S., Alen J., Bourin A., Castermans K., Boumans N., Panitti L., Vanormelingen J., Leysen D., Defert O., *Bioorganic & Medicinal Chemistry Letters* **2014**, 24 (18) 4594-7

[93]   Cenacchi V., Battaglia R., Cinato F., Riccardi B., Spinabelli D., Brogin G., Puccini P., Pezzetta D., *Xenobiotica* **2015**, 45 (8) 693-710

[94]   Liu J-B., Chen C., Chu L., Chen Z-H., Xu X-H., Qing F-L., *Angewandte Chemie International Edition* **2015**, 54 (40) 11839-42

[95]   Matsuya Y., Sasaki K., Ochiai H., Nemoto H., *Bioorganic & Medicinal Chemistry* **2007**, 15 (1) 424-32

[96]   Zafrani Y., Sod-Moriah G., Segall Y., *Tetrahedron* **2009**, 65 (27) 5278-83

[97]   Shi Y., Koh J.T., *Journal of the American Chemical Society* **2002**, 124 (24) 6921-8

[98]   Cooper T., Novak A., Humphreys L.D., Walker M.D., Woodward S., *Advanced Synthesis & Catalysis* **2006**, 348 (6) 686-90

[99]   Talele T.T., *Journal of Medicinal Chemistry* **2020**, 63 (11) 5625-63

[100]   Subbaiah M.A.M., Meanwell N.A., *Journal of Medicinal Chemistry* **2021**, 64 (19) 14046-128

[101] Su L., Ren T., Dong J., Liu L., Xie S., Yuan L., Zhou Y., Yin S.-F., *Journal of the American Chemical Society* **2019**, 141 (6) 2535-44

[102] Wang H., Qiu S., Wang S., Zhai H., *ACS Catalysis* **2018**, 8 (12) 11960-5

[103] Shintaro N., Ryo A., Hideo T., Yoshimasa K., Atsushi K., Yoko N., Daisuke N., Osamu O., *Drug Metabolism and Disposition* **2009**, 37 (9) 1970

[104] Claxton A.J., Cramer J., Pierce C., *Clinical Therapeutics* **2001**, 23 (8) 1296-310

[105] Bauer R.A., *Drug Discovery Today* **2015**, 20 (9) 1061-73

[106] Singh J., *Journal of Medicinal Chemistry* **2022**, 65 (8) 5886-901

[107] De Cesco S., Kurian J., Dufresne C., Mittermaier A.K., Moitessier N., *European Journal of Medicinal Chemistry* **2017**, 138 96-114

[108] Johnson D.S., Weerapana E., Cravatt B.F., *Future Med Chem* **2010**, 2 (6) 949-64

[109] Ray S., Murkin A.S., *Biochemistry* **2019**, 58 (52) 5234-44

[110] Faridoon, Ng R., Zhang G., Li J.J., *Medicinal Chemistry Research* **2023**, 32 (6) 1039-62

[111] Fairhurst R.A., Knoepfel T., Buschmann N., Leblanc C., Mah R., Todorov M., Nimsgern P., Ripoche S., Niklaus M., Warin N., Luu V.H., Madoerin M., Wirth J., Graus-Porta D., Weiss A., Kiffe M., Wartmann M., Kinyamu-Akunda J., Sterker D., Stamm C., Adler F., Buhles A., Schadt H., Couttet P., Blank J., Galuba I., Trappe J., Voshol J., Ostermann N., Zou C., Berghausen J., Del Rio Espinola,A., Jahnke W., Furet P., *Journal of Medicinal Chemistry* **2020**, 63 (21) 12542-73

[112] Beck P., Dubiella C., Groll M., *Biological Chemistry* **2012**, 393 (10) 1101-20

[113] Konishi H., Kumon M., Yamaguchi M., Manabe K., *Tetrahedron* **2020**, 76 (48) 131639

[114] Au - Furigay M.H., Au - Boucher M.M., Au - Mizgier N.A., Au - Brindle C.S., *JoVE* **2018**, (134) e57639

[115] Jia Y., Wang K., Wang H., Zhang B., Yang K., Zhang Z., Dong H., Wang J., *Bioorganic & Medicinal Chemistry* **2022**, 74 117053

[116] Weidner J.J., Weintraub P.M., Schnettler R.A., Peet N.P., *Tetrahedron* **1997**, 53 (18) 6303-12

[117] Bauer L., Hewitson R.E., *The Journal of Organic Chemistry* **1962**, 27 (11) 3982-5

[118] Gawley R.E., *The Beckmann Reactions: Rearrangements, Elimination–Additions, Fragmentations, and Rearrangement–Cyclizations*, *Organic Reactions* **2004**, 1-420.

[119] Wang Z., *Comprehensive Organic Name Reactions and Reagents*, **2010**, 2552-5.

[120] Lezcano-González I., Boronat M., Blasco T., *Solid State Nuclear Magnetic Resonance* **2009**, 35 (2) 120-9

[121] McLeod D., McNulty J., *European Journal of Organic Chemistry* **2012**, 2012 (31) 6127-31

[122] Miki T., Kori M., Mabuchi H., Banno H., Tozawa R-i., Nakamura M., Itokawa S., Sugiyama Y., Yukimasa H., *Bioorganic & Medicinal Chemistry* **2002**, 10 (2) 401-14

[123] Templ J., Gjata E., Getzner F., Schnürch M., *Organic Letters* **2022**, 24 (40) 7315-9

[124] Guram A.S., Rennels R.A., Buchwald S.L., *Angewandte Chemie International Edition in English* **1995**, 34 (12) 1348-50

[125] Louie J., Hartwig J.F., *Tetrahedron Letters* **1995**, 36 (21) 3609-12

[126] Taeufer T., Pospech J., *The Journal of Organic Chemistry* **2020**, 85 (11) 7097-111

[127] Wentland M.P., Duan W., Cohen D.J., Bidlack J.M., *Journal of Medicinal Chemistry* **2000**, 43 (19) 3558-65

[128] Garzya V., Forbes I.T., Gribble A.D., Hadley M.S., Lightfoot A.P., Payne A.H., Smith A.B., Douglas S.E., Cooper D.G., Stansfield I.G., Meeson M., Dodds E.E., Jones D.N.C., Wood M., Reavill C., Scorer C.A., Worby A., Riley G., Eddershaw P., Ioannou C., Donati D., Hagan J.J., Ratti E.A., *Bioorganic & Medicinal Chemistry Letters* **2007**, 17 (2) 400-5

[129] Wolfe J.P., Wagaw S., Buchwald S.L., *Journal of the American Chemical Society* **1996**, 118 (30) 7215-6

[130] Hartwig J.F., *Accounts of Chemical Research* **2008**, 41 (11) 1534-44

[131] Surry D.S., Buchwald S.L., *Angewandte Chemie International Edition* **2008**, 47 (34) 6338-61

[132] Degli Innocenti M., Schreiner T., Breinbauer R., *Advanced Synthesis & Catalysis* **2023**, 365 (23) 4086-4120

[133] Green A.E., Agouridas V., Deniau E., *Tetrahedron Letters* **2013**, 54 (51) 7078-9

[134] Bouzide A., Sauvé G., *Tetrahedron Letters* **1997**, 38 (34) 5945-8

[135]   Koh P.F., Loh T.P., *Green Chemistry* **2015**, 17 (7) 3746-50

[136]   Eckenberg P., Groth U., Huhn T., Richter N., Schmeck C., *Tetrahedron* **1993**, 49 (8) 1619- 24

[137]   Paterson I., Yeung K-S., Watson C., Ward R.A., Wallace P.A., *Tetrahedron* **1998**, 54 (39)   11935-54

[138]   Skaanderup P.R., Poulsen C.S., Hyldtoft L., Jørgensen M.R., Madsen R., *Synthesis* **2002**,   2002 (12) 1721-7

[139]   Riaz M.T., Pohorilets I., Hernandez J.J., Rios J., Totah N.I., *Tetrahedron Letters* **2018**, 59 (29) 2809-12

[140]   Poon K.W.C., Dudley G.B., *The Journal of Organic Chemistry* **2006**, 71 (10) 3923-7

[141]   Rühl P., Bracher F., *Molecules* **2023**; 28 (21) 7428

[142]   Xie Q., Dong G., *Journal of the American Chemical Society* **2021**, 143 (36) 14422-7

[143]   Wang G-J., Wang L., Zhu G-D., Zhou J., Bai H-Y., Zhang S-Y., *Organic Letters* **2021**, 23 (21) 8434-8

[144]   Schön U., Messinger J., Buchholz M., Reinecker U., Thole H., Prabhu M.K.S., Konda A., *Tetrahedron Letters* **2005**, 46 (42) 7111-5

[145]   Song H., Liu Y., Wang Q., *Organic Letters* **2013**, 15 (13) 3274-7

[146]   Aversa RJB, M.T.; Dillon, M.P.; Dineen, T.A., Jr.; Lou, Y.; Nishiguchi, G.A.; Ramurthy, S.; Rico, A.C.; Rauniyar, V.;, Sendzik Mea, Compounds and Compositions as Raf Kinase Inhibitors, US WO2016/038582, **2016**

[147]   Mandal P.K., McMurray J.S., *The Journal of Organic Chemistry* **2007**, 72 (17) 6599-601

[148]   You X., Cai Y., Xiao C., Ma L., Wei Y., Xie T., Chen L., Yao H., *Molecules* **2022**, 27 (22) 7979

[149]   Rostrup-Nielsen J.R., *Sulfur Poisoning. Progress in Catalyst Deactivation*; **1982** Dordrecht: Springer Netherlands.

[150]   Broese T., Roesel A.F., Prudlik A., Francke R., *Organic Letters* **2018**, 20 (23) 7483-7

[151]   Lloyd-Jones G.C., Moseley J.D., Renny J.S., *Synthesis* **2008**, 2008 (05) 661-89

[152]   Pui-Kai L., Pillai R., Young B.L., Bender W.H., Martino D.M., Lin F-T., *Steroids* **1993**, 58 (3) 106-11

[153] Harvey J.N., Jover J., Lloyd-Jones G.C., Moseley J.D., Murray P., Renny J.S., *Angewandte Chemie International Edition* **2009**, 48 (41) 7612-5

[154] Zhou C-Y., Li J., Peddibhotla S., Romo D., *Organic Letters* **2010**, 12 (9) 2104-7

[155] Perreault M., Maltais R., Roy J., Dutour R., Poirier D., *ChemMedChem* **2017**, 12 (2) 177-82

[156] Carro L., Torrado M., Raviña E., Masaguer C.F., Lage S., Brea J., Loza M.I., *European Journal of Medicinal Chemistry* **2014**, 71 237-49

[157] Cockerill G.S., Easterfield H.J., Percy J.M., *Tetrahedron Letters* **1999**, 40 (13) 2601-4

[158] Cushman M., He H-M., Katzenellenbogen J.A., Varma R.K., Hamel E., Lin C.M., Ram S., Sachdeva Y.P., *Journal of Medicinal Chemistry* **1997**, 40 (15) 2323-34

[159] Tedesco R., Thomas J.A., Katzenellenbogen B.S., Katzenellenbogen J.A., *Chemistry & Biology* **2001**, 8 (3) 277-87

[160] Ohno S., Qiu J., Miyazaki R., Aoyama H., Murai K., Hasegawa J-y., Arisawa M., *Organic Letters* **2019**, 21 (20) 8400-3

[161] Dawling S., Roodi N., Mernaugh R.L., Wang X., Parl F.F., *Cancer Res* **2001**, 61 (18) 6716-22

[162] Ba M-Y., Xia L-W., Li H-L., Wang Y-G., Chu Y-N., Zhao Q., Hu C.-P., He X.-T., Li T-X., Liang K.-Y., Zhang, Y.-H.,Yang L., Xie W.-H., Yang H., Sun M.-R., *Steroids* **2019**, 146 99-103

[163] Yang X., Sun Y., Chen Z., Rao Y., *Advanced Synthesis & Catalysis* **2014**, 356 (7) 1625-30

[164] Akselsen Ø.W., Hansen T.V., *Tetrahedron* **2011**, 67 (40) 7738-42

[165] Ho A., Kim Y-e., Lee H-S., Cyrus K., Baek S-H., Kim K-B., *Bioorganic & Medicinal Chemistry Letters* **2006**, 16 (13) 3383-7

[166] Mun J., Voll R.J., Goodman M.M., *Journal of Labelled Compounds and Radiopharmaceuticals* **2006**, 49 (12) 1117-24

[167] Hostetler E.D., Jonson S.D., Welch M.J., Katzenellenbogen J.A., *The Journal of Organic Chemistry* **1999**, 64 (1) 178-85

[168] Csutoras C., Zhang A., Zhang K., Kula N.S., Baldessarini R.J., Neumeyer J.L., *Bioorganic & Medicinal Chemistry* **2004**, 12 (13) 3553-9

[169] Grimm C., Jörs S., Saldanha S.A., Obukhov A.G., Pan B., Oshima K., Cuajungco M.P., Chase P., Hodder P., Heller S., *Chemistry & Biology* **2010**, 17 (2) 135-48

[170] Klutzny S., Kornhuber M., Morger A., Schönfelder G., Volkamer A., Oelgeschläger M., Dunst S., *Environment International* **2022**, 158 106947

[171] Bischoff P., Kornhuber M., Dunst S., Zell J., Fauler B., Mielke T., Taubenberger A.V., Guck J., Oelgeschläger M., Schönfelder G., *iScience* **2020**, 23 (11) 101683

[172] Kornhuber M., Dunst S., Schönfelder G., Oelgeschläger M., *Environment International* **2021**, 149 106411

[173] Kornhuber M., Dunst S. *TGF-Beta Signaling: Methods and Protocols*. **2022**. p. 207-26.

[174] Mosmann T., *Journal of Immunological Methods* **1983**, 65 (1) 55-63

[175] Ouyang L., Liang Y., Wang S., Miao R., Liao J., Yang Z., Luo R., *Journal of Catalysis* **2023**, 427 115096

[176] Wang T., Stein P.M., Shi H., Hu C., Rudolph M., Hashmi A.S.K., *Nature Communications* **2021**, 12 (1) 7029

[177] Coutts I.G.C., Southcott M.R., *Journal of the Chemical Society, Perkin Transactions 1* **1990**, (3) 767-71

[178] Pappo R., Process and Intermediates for Manufacture of 19-Norsteroids, US3383384, **1968**

[179] Schwarz S., *Pharmazie* **1946**, 30

[180] Dutour R., Roy J., Cortés-Benítez F., Maltais R., Poirier D., *Journal of Medicinal Chemistry* **2018**, 61 (20) 9229-45

[181] Kometani T., Watt D.S., Ji T, Fitz T., *The Journal of Organic Chemistry* **1985**, 50 (25) 5384-7

[182] Sweet F., Patrick T.B., Mudd J.M., *The Journal of Organic Chemistry* **1979**, 44 (13) 2296-8

[183] Hoehn W.M., A-Ring acyclated Estrone Derivatives and corresponding Alcohols, their Esters, and Ethers, US2846453, **1958**

[184] Fishman J., Tomasz M., *The Journal of Organic Chemistry* **1962**, 27 (2) 365-8

[185] Fang Z., Agoston G.E., Ladouceur G., Treston A.M., Wang L., Cushman M., *Tetrahedron* **2009**, 65 (51) 10535-43